.

UNIVERSITÉ DU QUÉBEC
INSTITUT NATIONAL DE LA RECHERCHE SCIENTIFIQUE
CENTRE EAU TERRE ENVIRONNEMENT

Systèmes de biofiltres avancés pour l'élimination efficace de la microcystine-leucine arginine et les principaux polluants de l'eau

Par

Pratik Kumar

(M. Tech., Environmental Engineering)

Thèse présentée pour l'obtention du grade de
Philosophiae Doctor (Ph.D.)
en sciences de l'Eau

Jury d'évaluation

Président du jury et examinateur interne	Prof. Jean-François Blais INRS-ETE, Québec, Canada
Examinateur externe	Prof. Ahmed Eldyasti York University, Ontario, Canada
Examinateur externe	Prof. Manuel Rodriguez Laval University, Québec, Canada
Directeur de recherche	Prof. Satinder Kaur Brar INRS-ETE, Québec, Canada
Codirecteur de recherche	Dr. Maximiliano Cledon CIMAS-CONICET, UnComa, Argentine

Dédicace

This thesis is dedicated to my parents and teachers for their endless support and love.

"One act of obedience is better than one hundred sermons."……*Dietrich Bonhoeffer*

REMERCIEMENTS

I would like to express my humble gratitude to my Ph.D. supervisor, Professor Satinder Kaur Brar for her guidance, suggestions and valuable feedback during my doctoral training. Her constant motivation, support, and encouragement helped me to become more organized and creative, that allowed me to work with more freedom and passion. I want to equally express my regards to my project co-supervisor, Dr. Maximiliano Cledon who helped me in solving essential problems with multi-approach ideas.

I would also like to thank my examiners, Prof. Manuel Rodriguez, Prof. Ahmed Elsyadi, Prof. Jean-François Blais whose suggestions and recommendations helped in improving the quality of my thesis. I am sincerely thankful to ATRAPP for financing the project work. I would like to especially thanks Prof. Sébastien Sauvé for coordinating the work objectives in form of biannual meeting every year. I am very grateful to Prof. Rosa Galvez and Prof. Azadeh Kermanshahi-pour for their constant guidance and technical support.

I would like to thank all the laboratory personnel from INRS, especially Sebastian Duval for the instrument training. I would like to express my humble gratitude and genuinely like to thank my teammates who supported me throughout my Ph.D. study, especially, Dr. Sung Vo Duy, Dr. Krishnamoorthy Hegde, Dr. Rama Pulicharla, Dr. Linson Lonappan, Dr. Mehrdad Taheran, Dr. Vinayak Pachapur, Dr. Joanna Lecka, Dr. Naghdi Mitra, Dr. Gayatri Suresh, Dr. Agnieszka Cupryś, Lalit Ram Kumar, Joseph Sebastian, Carlos Osorio, Mariana Valdez, Mohammad Reza, Saba Miri, Rahul Saini, Dr. Sravan Kumar Yellapu, Dr. Rajwinder Kaur Sidhu, Ms Bharti Bhadana, Mr. Lalit Kumar, Dr. Saurabh Kumar Ram and Dr. Bikash Tiwari. A much and special thanks to Mona Chaali and Dr. Dany Roy to help me enormously with the French translation of my thesis. It would be incomplete without thanking my interns, Heidi Rubio Pascagaza, Hadji Rehab and Jose Alberto, who assisted me during the project.

Finally, I would like to give my sincerest thanks to my parents, my uncle, my grandfather, grandmother and my brother who constantly supported and motivated me.

RÉSUMÉ

La microcystine-LR (MC-LR) est la toxine provenant d'une algue la plus répandue dans l'écosystème aquatique. La MC-LR est principalement excrétée par l'espèce dominante *Microcystis aeruginosa* de manière extracellulaire pendant les fleurs d'eau (« bloom »). Les changements climatiques et l'intervention humaine permettent désormais le déclenchement des fleurs d'eau tout au longu de l'année, particulièrement durant les saisons d'été et d'automne. L'utilisation des eaux de surface en tant que source d'eau potable oblige maintenant les usines de filtration des eaux potables (UFE) à traiter la MC-LR afin d'éliminer les toxines de l'eau et la rendre sécutaire pour la consommation humaine. Plusieurs méthodes conventionnelles de traitement telles que l'ozonation et la chloration se sont montrées efficaces pour l'enlèvement de la MC-LR. Cependant, leur utilisation peut mener à la formation de sous-produits toxiques et ces méthodes sont sensibles aux différentes conditions d'opération, incluant le pH, et la présence de composés organiques naturels et d'autres polluants organiques. Une option prometteuse est l'utilisation des procédés biologiques. Ces procédés ont démontré la possibilité de produire une eau exempte de toxine MC-LR, mais les cinétiques de dégradation obtenues étaient lentes (de 10 à 100 µg MC-LR L^{-1} d^{-1} en présence d'un média en suspension). Dans cette étude, l'idée d'une méthode biologique par biofiltre (procédé par média fixé) utilisant un sable non-modifié et modifié comme média adsorbant pour éliminer la MC-LR et d'autres contaminants des eaux est explorée. La faisabilité des biofiltres à sable (« biosand filters ») pour l'enlèvement de la MC-LR a été explorée afin d'éviter la production de sous-produits toxiques et d'offrir une option de modernisation du procédé de traitement des UFE existantes.

Les communautés bactériennes indigènes (*Pseudomonas fragi* and *Chryseobacterium* sp., identifiées par « X ») ayant la capacité de dégrader la MC-LR ont été isolées à partir d'une unité de filtration de l'usine de filtration du Chemin Ste-Foy, Québec, Canada. Ces bactéries indigènes ont été individuellement cultivées en présences de 3 espèces de bactéries capables de dégrader la MC-LR (*Arthrobacter ramosus* (A), *Bacillus* sp. (B) *Sphingomonas* sp. (S)). Ensuite, chacune des co-cultures (X+A, X+B and X+S) a été mise à l'essai pour la biodégradation de la MC-LR et l'enlèvement d'autres contaminants des eaux avec deux configurations de biofiltre : a) filtre à sable (filtre statique), et a) réacteur à biofilm à lit mobile (« RBLM », filtre dynamique). Dans tous les cas, la concentration initiale en MC-LR était de 50 µg/L. Le RBLM a démontré un taux de

dégradation de la MC-LR significativement plus faible que le filtre à sable (>70% d'enlèvement en 36 heures), nécessitant d'important temps de rétention. De son côté, le biofiltre à sable a démontré un taux d'enlèvement <50% de la MC-LR avec un temps de rétention d'environ une heure (filtre témoin). De plus, >80% d'enlèvement de la MC-LR a été obtenue avec un biofiltre bioaugmenté avec la culture S+X. Cependant, ce filtre a démontré une plus faible activité biologique (par rapport à la formation du biofilm) à la surface des grains de sable et une percée prématurée du filtre (<1 semaine d'opération) par la MC-LR a été observée dans l'eau filtrée. Afin de contrer ce défi, l'activité bactérienne a été améliorée par l'utilisation de résidus d'agriculture (fibre de chanvre, boues de désencrage, boues de pâtes et papier déshydratées) comme matériaux filtrants de surface potentiels. Ces matériaux ont démontré desefficacité d'enlèvement de la MC-LR de >85%. Cependant, les longs temps de résidence (>2 heures) et les phénomènes de percée prématurée ont persisté et demeurent un défi. *Par conséquent, le sable adsorbant nécessite des améliorations dans sa porosité et la taille de sa surface spécifique afin d'atteindre des plus faibles temps de résidence et une formation efficace de biofilm, respectivement*. La grande taille de la surface de l'adsorbant modifié a également été supposée adsorber une plus grande quantité de MC-LR, ce qui permettrait de prolonger la période d'opération avant la percée. Par conséquent, le média de sable a été modifié paur un composite graphène-sable en utilisant une solution de sucre à faible coût (effluent de brasserie comme source de sucre ; GS1), sable de dioxide de manganèse (MN), et leur mélange (GS+MN). À titre de comparaison, le sucrose a été utilisé comme solution de sucre à haut coût pour graphiter le média de sable (GS2). Le GS2 s'est avéré dégrader 10-15% moins de MC-LR et des autres contaminants des eaux que le GS1. Un plus faible temps de résidence hydraulique (<0.75 heure) et des taux d'enlèvement de la MC-LR s'élevant jusqu'à 98% ont été observés avec le GS1. De plus, le GS1 a démontré un temps de percé jusqu'à 8 fois supérieur à celui du sable pur avec l'absence de lixiviation de la MC-LR pour une période d'opération de plus de 20 semaines. D'autres médias de filtration ont également été synthétisés pour relever les défis mentionnés dans les hypothèses ci-haut (en italique), incluant un sable enrobé d d'oxyde de graphène (GO), un sable enrobé de graphène réduit (rGO), un sable enrobé d'oxyde de Fe (Fe), et un mélange FeGO. Les biofiltre avec médias rGO et GO ont démontré des enlèvements de la MC-LR >85% avec des périodes de percé 5 semaines plus tôt que le biofiltre avec média GS1.

En général, le biofiltre avec media GS1 a été identifié comme étant le plus réalisable des filtres, offrant une solution durable à faibles coûts (avec l'utilisation d'effluents de brasseries), qui, en plus d'atteindre un enlèvement complet de la MC-LR, augmente l'enlèvement de 30-40% des autres contaminants retrouvés dans les eaux de surface par rapport aux filtres à sable conventionnels. Comme résultat, la faisabilité de la mise à l'échelle a été évaluée par l'utilisation de programmes informatiques de calcul de dynamique des fluides (Programme : ANSYS/CFX) et la taille minimale suggérée de la dimension du bioréacteur (« *minimum subjective bioreactor dimension* ») offrant la meilleure canalisation par rapport au régime d'écoulement a été comparée à celle du réacteur à l'échelle laboratoire.

L'eau d'un lac pollué a été utilisée comme alimentation pour des essais en laboratoire et analysée pour tous les paramètres importants de la qualité des eaux qui sont habituellement analysés dans les stations de filtration des eaux, incluant la MC-LR. Une simulation de station de filtration des eaux à l'échelle laboratoire, nommée SAP-1©, a été créée pour la mise à l'essai du média GS1. Les essais ont démontré un enlèvement complet de la MC-LR (<1 µg/L). Le module de traitement (Filtre GS1) peut offrir une solution à faible coût aux usines de filtration des eaux pour un enlèvement efficace des contaminants d'eaux de surface et pour l'enlèvement saisonnier ou à l'année des éclosions de MC-LR. Le module GS1 peut aussi agir comme unité de traitement individuelle à des fins domestiques.

Mots clés : Microcystine-LR, eau potable, biodégradation, adsorption, biofiltre, sable, graphène, sable enrobé, dynamique des fluides numérique, mise à l'échelle

ABSTRACT

Microcystin-LR (MC-LR) is the most prominent algal toxin prevalent in an aquatic ecosystem. MC-LR is excreted extracellularly by the cyanobloom dominated by *Microcystis aeruginosa*. Climate change and human intervention has triggered the cyanoblooms to break all year round, especially during the summer-autumn season. The use of surface water as a drinking water source has necessitated the drinking water treatment plant (DWTPs) operators to treat MC-LR in order to render and avail toxic-free drinking water for human consumption. Various conventional treatment methods such as ozonation and chlorination have shown effective MC-LR removal albeit formation of toxic by-products and found sensitive under various experimental parameters including pH, natural organic matter and other pollutants. On the other hand, biological process was found to undergo toxic-free MC-LR removal but the degradation kinetics were reported slow (from 10-100 µg MC-LR L^{-1} d^{-1} under suspended growth mechanism). Herein, this study explores the idea of biological method for the removal of MC-LR and other water quality parameters (WQPs) via biofilter (attached growth mechanism) using non-modified and modified sand as a cheap adsorbent media. The feasibility of MC-LR removal using biosand filters were explored to report no toxic by-products formation as well as quick treatment option to retrofit the research idea in an existing DWTP.

The native bacterial community (*Pseudomonas fragi* and *Chryseobacterium* sp. named: 'X') potent in degrading MC-LR was isolated from the filtration unit of a DWTP, Chemin Ste-Foy, Quebec City, Canada. These native bacteria ('X') were co-cultured with three known MC-LR-degraders individually (*Arthrobacter ramosus* (A+X), *Bacillus* sp. (B+X) *Sphingomonas* sp. (S+X)) and tested for MC-LR biodegradation and removal of other water contaminants (water quality parameters: WQPs) using two kinds of biofilter: a) sand filter (static bed filter) and b) moving bed biofilm reactor (MBBRs: dynamic bed filter). In all cases, the initial MC-LR concentration was 50 µg/L. The MBBRs showed a relative slower MC-LR degradation rate (>70% removal in 36 hours) along with a high retention time while the biosand filter showed <50% MCLR removal but with a better retention time (~1 hour: control filter (sand)). Moreover, >80% MC-LR removal was achieved for filter bioaugmented with S+X. However, lower bacterial activity (biofilm formed) over the sand surface and an early leaching/breakthrough (<1 week of filter operation) of MC-LR was observed in the filtered water. To counter this challenge, bacterial

activity was enhanced using agro-residues microfibers (hemp fiber, deinking sludge, pulp and paper dried sludge) as a potential 'filter-top' material that showed >85% MC-LR removal. However, high retention time (>2 hours) and early leaching phenomenon persisted and remained a challenge. *Hence, the sand adsorbent needed enhancement in its porosity and specific surface area to achieve lower retention time and effective biofilm formation, respectively. The high surface area of the modified adsorbent was also hypothesized to adsorb more MC-LR that could help in prolonging the leaching period.* Hence, sand media was modified to graphene sand composite using a low-cost sugar solution (brewery effluent as the sugar source: GS1), manganese dioxide sand (MN) and their mixture (GS+MN). As a comparison, sucrose was used as a high-cost sugar solution to graphitize the sand material (GS2) and was found to degrade 10%-15% less MC-LR and other WQPs than GS1. A lower retention time (< 0.75 hour) and high MC-LR removal up to 98% by GS1 was observed. Moreover, GS1 showed a breakthrough time up to 8 times more than the raw sand with no leaching phenomenon observed for over 20 weeks of filter operation. Some other filter media was also synthesized for the above-mentioned hypothesis (in italics) including graphene oxide coated-sand (GO), reduced graphene coated-sand (rGO), iron oxide coated sand (Fe), and FeGO. Biofilter rGO and GO showed >85% MC-LR removal with leaching period less (5 weeks) than GS1 biofilter.

Overall, GS1 biofilter was marked as the most feasible filter offering a low-cost sustainable solution (use of waste brewery effluent) that not only achieved a complete MC-LR removal but also an enhanced removal by up to 30%-40% for other WQPs as compared to raw sand. As a result, scale-up feasibility was introspected using the computational fluid dynamics (software: ANSYS/CFX) and '*minimum subjective bioreactor dimension*' was determined that offered better channelization of fluid regime as compared to the bench-scale filter. The polluted lake water was used as an influent and analyzed for all the important WQPs that are usually checked in a real DWTP, including MC-LR using scale-up GS1 biofilter. A simulated laboratory-scale DWTP micro-model named SAP-1© was created for the above purpose where complete MC-LR removal was observed (< 1 µg/L). The treatment module (GS1 filter) can offer a low-cost solution in a DWTP for an effective removal of WQPs and for the seasonal or year-round breakout of MC-LR in surface water which can also act as a stand-alone treatment module for household purposes.

Keywords: Microcystin-LR, Drinking water, Biodegradation, Adsorption, Biofilter, Sand, Graphene, coated sand, Computational Fluid Dynamics, Scale-up

PUBLICATIONS DE CETTE THÈSE

1. **Kumar P.**, Hegde K., Brar S.K., Cledon M., Kermanshahi-pour A., Roy-Lachapelle A., & Galvez-Cloutier R. (2018). Biodegradation of microcystin-LR using acclimatized bacteria isolated from different units of the drinking water treatment plant. **Environmental Pollution**, 242, 407-416. doi:10.1016/j.envpol.2018.07.008.

2. **Kumar P.**, Hegde K., Brar S.K., Cledon M., Kermanshahi-pour A., (2018). Physico-chemical treatment for the degradation of cyanotoxins with emphasis on drinking water treatment—How far have we come? **Journal of Environmental Chemical Engineering**, 6(4), 5369-5388. doi:10.1016/j.jece.2018.08.032.

3. **Kumar P.**, Hegde K., Brar S.K., Cledon M., Kermanshahi-pour A., Roy-Lachapelle A., & Galvez-Cloutier R. (2019). Novel fluidized-bed biofilm reactor for concomitant removal of microcystin-LR and organics. **Chemical Engineering Journal**, 359, 99-111. doi:10.1016/j.cej.2018.11.119.

4. **Kumar P.**, Hegde K., Brar S.K., Cledon M., Kermanshahi-pour A., (2019). Potential of biological approaches for cyanotoxin removal from drinking water: A review. **Ecotoxicology and Environment Saf**, 172, 488-503. doi:10.1016/j.ecoenv.2019.01.066.

5. **Kumar P.**, Rubio H.D.P., Hegde K., Brar S.K., Cledon M.K., Kermanshahi-pour A., Roy Lachapalle A., Sauve S., Galvez-Cloutier R. (2019). Agro-industrial residues as a unique support in a sand filter to enhance the bioactivity to remove microcystin-Leucine aRginine and organics. **Science of The Total Environment**, 670, 971-981. doi:10.1016/j.scitotenv.2019.03.260.

6. **Kumar, P.**, Hegde, K., Brar, S. K., Cledon, M., Kermanshahi-pour, A., Roy-Lachapelle, A., Galvez-Cloutier, R. (2019). Co-culturing of native bacteria from drinking water treatment plant with known degraders to accelerate microcystin-LR removal using biofilter. **Chemical Engineering Journal**. doi:10.1016/j.cej.2019.123090.

7. **Kumar, P.**, Rehab, H., Hegde, K., Brar, S. K., Cledon, M., Kermanshahi-pour, A., Duy S.V., Sauve S., Surampalli, R. Y. (2020). Physical and biological removal of Microcystin-LR and other water contaminants in a biofilter using Manganese Dioxide coated sand and Graphene sand composites. **Science of The Total Environment**, 703. doi:10.1016/j.scitotenv.2019.135052.

8. **Kumar, P.**, Brar, S. K., Surampalli, R. Y. Ozonation in Tandem with bio-sand filtration to assess the Removal efficiency of Microcystin-LR, **Journal of Environmental Engineering**, doi: 10.1061/(ASCE)EE.1943-7870.0001801

9. **Kumar, P.**, Alberto E.P.J., Cledon, M., Brar S.K., Kermanshahi-pour, A., Duy S.V., Sauve S., Removal of Microcystin-LR and other Water Quality Parameters using Sand Filter Media Coated with Bio-optimized Carbon Submicron particles: Graphene Oxide and reduced Graphene Oxide, **Journal of Chemical Engineering**, doi: 10.1016/j.cej.2020.125398

10. **Kumar P.**, Brar S.K., Cledon M., Can ANSYS-CFX be used to predict the scale-up dimension of a filter column? A computational fluid dynamics approach (Submitted).

11. **Kumar P.**, Brar S.K., Cledon M., A low-cost graphitized sand filter to deliver Microcystin-LR free potable water: Scale-up feasibility for household units (Submitted in Science of the Total Environment).

PUBLICATION EN DEHORS DE CETTE THÈSE

1. **Kumar P.**, Pulicherla R., Brar S.K., Kermanshahi-pour A., Surampalli R.Y. (2019). Techno-economic study of chlortetracycline removal from wastewater treatment plant: A simple approach, **Journal of Hazardous, Toxic and Radioactive Waste**, 10.1061/(ASCE)HZ.2153-5515.0000441.

2. Taheran, M., **Kumar, P.**, Naghdi, M., Brar, S. K., Knystautas, E. J., Verma, M., & Surampalli, R. Y. (2019). Development of an advanced multifunctional portable water purifier. **Nanotechnology for Environmental Engineering**, *4*(1). doi:10.1007/s41204-019-0054-6.

3. Sebastian J., Hegde K., **Kumar P**., Rouissi T., Brar S.K. (2019), Bioproduction of fumaric acid: An insight into microbial strain improvement strategies, **Critical Reviews in Biotechnology**, Doi: 10.1080/07388551.2019.1620677.

4. Bendourou F.B., Suresh G., Laadila A., **Kumar P.**, Rouissi T., Dhillon G.S., Zied K., Brar S.K., Galvez R., "Feasibility of the use of different types of enzymatically treated cellulosic fibres for polylactic acid (PLA) recycling", **Journal of Composites: A**, Applied Science and Manufacturing (Submitted).

5. Laadila M.A., Suresh G., Rouissi T, **Kumar P.**, Brar S.K., Cheikh R.B., Abokitse K., Galvez-Cloutier R., Jacob C., "Biocomposite fabrication from enzymatically treated nanocellulosic fibers and recycled polylactic acid", **Journal of Energies** (Submitted).

6. **Kumar, P.**, Brar, S. K., Cledon, M., Kermanshahi-pour, A., & Galvez-Cloutier, R. (2019). Dataset of breakthrough time for various modified sand materials using Rhodamine-B as an adsorbate. **Data in Brief**, *27*. doi:10.1016/j.dib.2019.104751

CONFÉRENCES

1. **Kumar P.**, Brar S.K., Cledon M. (2017). Microcystin-LR degradation by enriched bacteria isolated from different units of Drinking Water Treatment Plant. Réseau Environement Water Management Symposium, October 10-11, 2017, CentrEau Lévis Convention Center, Lévis, Quebec, Canada (Poster)

2. **Kumar P.,** Brar S.K., Cledon M., Galvez,R., Kermanshahi-pour A. (2017). Microcystin-LR degradation by enriched bacteria isolated from different units of Drinking Water Treatment Plant. 4th student symposium on "Green processes for the bioeconomy of tomorrow" CRIBIQ, September 25-26, 2017, Laval University, Quebec City, Quebec, Canada (Poster)

3. **Kumar P**., Hegde K., Brar S.K., Cledon M., Galvez, R., Kermanshahi-pour A. (2018). Biodegradation of microcystin-LR using acclimatized bacteria isolated from different units of the drinking water treatment plant. 53rd CENTRAL Canadian Symposium on Water Quality Research, February 22nd, 2018, University of Toronto, Toronto, Ontario, Canada (Oral)

4. **Kumar P**., Hegde K., Brar S.K., Cledon M., Galvez,R., Kermanshahi-pour A., Roy-Lachapelle A., Sauve S., Galvez R. (2018). Novel fluidized-bed bioreactor for concomitant removal of Microcystin-LR and organics. iCAMP, 2nd international conference on advanced materials and processes for environment, energy and health, 31st October-2nd November 2018, Montreal, Canada. (Poster)

5. **Kumar P**., Hegde K., Brar S.K., Cledon M., Galvez, R., Kermanshahi-pour A. (2019). Co-culturing of Native Bacteria from Drinking Water Treatment Plant with Known Degraders to Accelerate Microcystin Removal. 54th CENTRAL Canadian Symposium on Water Quality Research, February 27th, 2019, York University, Toronto, Ontario, Canada. (Oral).

6. **Kumar P**., Cuprys A., Miri S., Davoodi S.M. (2019). “Bioremediation”, Lassonde Research Day, 1st May, 2019, York University, Ontario, Canada (Poster)

7. **Kumar P**., Hegde K., Brar S.K., Cledon M., Galvez, R., Kermanshahi-pour A. (2019). Co-culturing of Native Bacteria from Drinking Water Treatment Plant with Known Degraders to Accelerate Microcystin Removal. ATRAPP - Algal blooms, treatment, risk assessment, prediction and prevention through genomics, troisième rencontre annuelle du projet atrapp, May 13th, 2019, University du Montreal, Montreal, Quebec, Canada. (Poster).

8. **Kumar P**., Brar S.K.,“Validité du filtre bio-sable par la dynamique des fluides à l'aide du solveur ANSYS-CFX », October 22-23, 2019, espace posters du symposium sur la gestion de l'eau, Montreal, Quebec, Canada (Poster).

9. **Kumar P.**, Brar S.K., Cledon M., (2020). Modelling and simulation of bench-scale filter to check scale-up modulation using ANSYS-CFX, 55th CENTRAL Canadian Symposium on Water Quality Research, February 20th, 2020, Ryerson University, Toronto, Ontario, Canada. (Oral).

10. **Kumar P.**, Tiwari, B., Brar S.K., Cledon M., (2020). Evaluating Microcystin-LR and other water quality parameters removal: A mass balance approach using laboratory-made Drinking Water Treatment Plant micro-model (SAP-1©), 55th CENTRAL Canadian Symposium on Water Quality Research, February 20th, 2020, Ryerson University, Toronto, Ontario, Canada. (Oral).

TABLE DES MATIÈRES

LIST OF TABLES

LIST OF FIGURES

LIST OF EQUATIONS

LISTE DES ABRÉVIATIONS

ARMs	Agro-residue materials
BET	Brunauer - Emmett - Teller
CCD	Central Composite Design
CHAB	Cyanobacteria harmful algal bloom
CFD	Computation Fluid Dynamics
CFU	Colony-forming unit
COD	Chemical Oxygen Demand
CV	Crystal Violet
CYN	Cylindrospermopsin
DMSO	Dimethyl sulfoxide
DO	Dissolved Oxygen
DOC	Dissolved Organic Carbon
DSF	Deinking sludge fiber filter
DWTP	Drinking Water Treatment Plant
EDX	Energy Dispersive X-ray
EPS	Extracellular polymeric substances
Fe/IOCS	Iron oxide coated sand
FeGO	Iron oxide coated over graphene oxide-coated sand
FTIR	Fourier-transform infrared spectroscopy
GAC	Granular Activated Carbon
GO	Graphene oxide or Graphene oxide -coated sand
GS1	Graphitized sand using brewery effluent sugar
GS1MN	GS1 coated with manganese dioxide
GS2	Graphitized sand using sucrose
GS2MN	GS2 coated with manganese dioxide
HFF	Hemp Fiber Filter
HPLC	High Performance Liquid Chromatography
MC-LR	Microcystin-Leucine-aRginine
MDI	Morrill Dispersion Index

MIB	Méthylisobornéol
MTT	3-(4,5-dimethylthiazol-2-yl)-2,5-diphenyltetrazolium bromide
NOM	Natural Organic Matter
NTU	Nephelometric Turbidity Unit
OD	Optical Density
OMS	Organisation Mondiale de la Santé
OUR	Oxygen Utilization Rate
PAC	Powdered Activated Carbon
PCA	Principal Component Analysis
PP1A	Protein Phosphatase 1A
PPF	Pulp and Paper fiber filter
PQE	Paramètre de Qualité de l'eau
rGO	Reduced graphene oxide or reduced graphene oxide-coated sand
RO	Reverse Osmosis
RS	Raw sand
RS	Raw sand
RSMN	Raw sand and manganese dioxide
SAP-1	Sudha Ashok Pratik/Satinder and Pratik -1
SEM	Scanning Electron Microscope
SFI	Sand filter inoculated
SSA	Specific Surface Area
STEP	Station de Traitement d'eau Potable
STX	Saxitoxin
SUVA	Specific ultraviolet absorbance
TOC	Total Organic Carbon
THM	Trihalomethanes
TP	Total Protein
TS	Total Saccharide
UF	Ultrafiltration
USEP	Usine de Production de l`eau Potable
UV254	Ultraviolet absorbance at wavelength of 254 nanometer

WHO	World Health Organization

CHAPTER ONE: SYNTHÈSE

PARTIE 1. INTRODUCTION

Les cyanotoxines sont produites par les cyanobactéries ou par des algues bleues. Les cyanobactéries sont connues comme étant le groupe de procaryotes photosynthétiques le plus primitif connu sur terre, datant depuis plus de 3,5 milliards d'années (Bullerjahn and Post, 2014). Leur croissance anormale entraîne la production d'une toxine mortelle appelée cyanotoxine et est néfaste pour les espèces aquatique. À ce jour, la cause des sécrétions de cyanotoxines par les cyanobactéries demeure inconnue. Cependant, de nombreux scientifiques croient que cela pourrait être dû à l'accumulation de conditions de stress ce qui favorisent la libération de toxines, alors que certaines théories affirment que les cyanobactéries sécrètent des toxines pour contrer la dominance compétitive d'autres espèces qui croissent dans leur milieu naturel.

La cyanotoxine la plus courante dans le biote aquatique est la microcystine-leucine-arginine (MC-LR) (McLellan and Manderville 2017). La cyanobactérie dominante sécrétant la MC-LR est *Microcystis aeruginosa*. Outre les organismes aquatiques, le MC-LR a également un impact profond sur la santé humaine. MC-LR est une hépatotoxine et attaque les cellules hépatiques, ce qui provoque des effets aigus à chroniques sur la santé, endommageant le système immunitaire, le foie, les reins et parfois une défaillance d'organes multiples. La présence de cyanotoxines pendant presque toute la saison estivale et automnale oblige l'utilisation d'une usine de production de l'eau potable (UPEP) afin de traiter l'eau de source provenant des lacs et des rivières. La recommandation de l'OMS pour le polluant MC-LR dans l'eau potable est de <1 µg/L. Afin d'éviter de retrouver cette toxine dans l'eau du robinet, des nombreuses méthodes de traitement efficaces ont été étudiées dans le passé, telles que la photocatalyse, l'ozonation, la chloration et le filtre à charbon actif (Pinkernell and von Günter, 2001, Jacobs et al. 2013, Pestana et al. 2015). Cependant, des difficultés opérationnelles, le coût élevé du traitement, l'utilisation de produits chimiques et la production de sous-produits toxiques ont restreint l'utilisation de ces technologies pour le traitement des eaux chargées de MC-LR dans les UPEP (Banker et al. 2001, Rodriguez et al. 2007, Al Momani et al. 2010). Par exemple, la dose d'oxydant dépend fortement de la concentration de MC-LR à traiter et dépend également du pH, de la matière organique naturelle et de la présence d'autres contaminants dans l'eau de source (Ma et al. 2012). Une concentration élevée de MC-LR exige un dosage d'oxydant plus élevé qui produit des sous-produits toxiques dans l'eau traitée après complexation avec les molécules MC-LR hydrolysées ou fragmentées. De plus, un temps de

contact plus long que la normale est nécessaire pour retirer complètement le MC-LR. Par conséquent, pour garder la dose sous réglementation et la toxicité sous contrôle, ainsi qu'un fonctionnement strict en temps de séjour, l'unité de traitement doit être moins dépendante des produits chimiques, moins énergivore et économique comme mentionné ci-dessus.

Le processus biologique a non seulement réussi à éliminer le MCLR, mais la toxicité résulte également de la formation de sous-produits. La combinaison des processus biologique aux unités basées sur le principe de l'adsorption peut être considérée comme une solution combinée pour contrer les problèmes susmentionnés liés à l'élimination des MC-LR (Manage et al. 2009, Yang et al. 2014). Un exemple de combinaison d'unités de traitement pourrait être un bio-filtre (procédé passif à faible coût énergétique) n'utilisant aucun produit chimique pour fonctionner (donc pas de sous-produits toxiques dus à la transformation). En fait, diverses études ont montré une élimination efficace des MC-LR à l'aide d'un bio-filtre utilisant du sable comme milieu adsorbant. Cependant, la lenteur de la filtration et l'adsorption partielle des MC-LR sur le sable limitent leur application, surtout lorsque d'autres polluants de l'eau sont présents en même temps (Grutzmacher et al. 2002, Wang et al. 2007, Terin et al. 2019).

Néanmoins, le milieu sableux est bon marché et toute modification à l'intérieur et autour de celui-ci pourrait quand même offrir une solution peu coûteuse pouvant être mise à l'échelle pour les UPEP. Les travaux de recherche présentés dans cette étude sont centrés sur l'aspect bio-augmentation dans le sable filtrant et sur la modification du milieu de filtration. Cette méthode de traitement pourrait éventuellement améliorer l'activité des bactéries fixées pouvant potentiellement aider à la biodégradation de la MC-LR et favoriser l'adsorption efficace d'autres contaminants des eaux de surface en améliorant la capacité d'adsorption du milieu filtrant.

Référence

Jacobs, L. C. V., Peralta-Zamora, P., Campos, F. R., & Pontarolo, R. (2013). Photocatalytic degradation of microcystin-LR in aqueous solutions. *Chemosphere, 90*(4), 1552-1557.

Pestana, C. J., Edwards, C., Prabhu, R., Robertson, P. K. J., & Lawton, L. A. (2015). Photocatalytic degradation of eleven microcystin variants and nodularin by TiO2 coated glass microspheres. *J Hazard Mater, 300,* 347-353. doi:10.1016/j.jhazmat.2015.07.016

Lenntech, Ozone applications drinking water, https://www.lenntech.com/library/ozone/drinking/ozone-applications-drinking-water.html, Date Accessed: 12th April, 2018

Pinkernell U, von Gunten U: Bromate Minimization during Ozonation: Mechanistic Considerations. *Environmental Science & Technology* 2001, 35:2525-2531.

Rodríguez E, Onstad GD, Kull TPJ, Metcalf JS, Acero JL, von Gunten U: Oxidative elimination of cyanotoxins: Comparison of ozone, chlorine, chlorine dioxide and permanganate. *Water Research* 2007, 41:3381-3393.

Al Momani, F. A., & Jarrah, N. (2010). Treatment and kinetic study of cyanobacterial toxin by ozone. *Journal of Environmental Science and Health, Part A, 45*(6), 719-731.

Banker, R., Carmeli, S., Werman, M., Teltsch, B., Porat, R., & Sukenik, A. (2001). Uracil Moiety is Required for Toxicity of the Cyanobacterial Hepatotoxin Cylindrospermopsin. *Journal of Toxicology and Environmental Health, Part A, 62*(4), 281-288. doi:10.1080/009841001459432

Bullerjahn, G. S., & Post, A. F. (2014). Physiology and molecular biology of aquatic cyanobacteria. *Front Microbiol, 5*. doi:10.3389/fmicb.2014.00359.

McLellan, N. L., & Manderville, R. A. (2017). Toxic mechanisms of microcystins in mammals. *Toxicology Research, 6*(4), 391-405. doi:10.1039/c7tx00043j

Miller TR, Beversdorf LJ, Weirich CA, Bartlett SL. Cyanobacterial Toxins of the Laurentian Great Lakes, Their Toxicological Effects, and Numerical Limits in Drinking Water. Mar Drugs. 2017;15(6)

Manage, P. M., Edwards, C., Singh, B. K., & Lawton, L. A. (2009). Isolation and Identification of Novel Microcystin-Degrading Bacteria. *Appl Environ Microbiol, 75*(21), 6924-6928.

Yang F, Neilan B Zhou Y, Yin L, Zhu G, Liang G, Pu Y: Microcystin-Degrading Activity of an Indigenous Bacterial Strain Stenotrophomonas acidaminiphila MC-LTH2 Isolated from Lake Taihu. *PLoS ONE* 2014, 9:e86216.

Wang, H. L. Ho, D.M. Lewis, J.D. Brookes, G. Newcombe, Discriminating and assessing adsorption and biodegradation removal mechanisms during granular activated carbon filtration of microcystin toxins, Water Res. 41 (18) (2007) 4262–4270, https://doi.org/10.1016/j.watres.2007.05.057.

Grutzmacher, G., Bottcher, I. Chorus, H. Bartel, Removal of microcystins by slow sand filtration, Environ. Toxicol. 17 (4) (2002) 386–394, https://doi.org/10.1002/tox.10062.

Terin, U.C., L.P. Sabogal-Paz, Microcystis aeruginosa and microcystin-LR removal by household slow sand filters operating in continuous and intermittent flows, Water Res. 150 (2019) 29–39, https://doi.org/10.1016/j.watres.2018.11.055

PARTIE 2. REVUE DE LITTÉRATURE

2.1. Que sont les cyanobactéries et les cyanotoxines?

Les cyanobactéries font partie du plus grand groupe de procaryotes photosynthétiques présents dans les milieux terrestres et aquatiques et sont capables de faire concurrence à d'autres algues et microorganismes présents dans les lacs, les réservoirs et les étangs. Dans des conditions environnementales favorables, les cyanobactéries fleurissent et couvrent toute la surface de l'eau, un phénomène communément appelé cyanobloom [1]. Ces floraisons sont une préoccupation mondiale et une menace pour le biote aquatique ainsi que pour la qualité de l'eau, car elles épuisent le niveau d'oxygène dissous, puis libèrent des cyanotoxines. Les scientifiques ne comprennent pas encore parfaitement " pourquoi ces cyanobactéries produisent des cyanotoxines ". Différentes théories affirment que les cyanobactéries produisent des cyanotoxines pour se nourrir lorsqu'elles sont stressées, et certaines théories affirment que la libération de toxines par les cyanobactéries vise à contrer la domination croissante de tout concurrent perçu (Tony Briscoe, 2019). D'après leurs différences structurelles, les cyanotoxines sont divisées en deux catégories principales : a) les peptides cycliques, b) les alcaloïdes. Les peptides cycliques comprennent la microcystine et la nodularine, tandis que les alcaloïdes comprennent la cylindrospermopsine, l'anatoxine et la saxitoxine. La cyanotoxine la plus répandue dans le milieu aquatique est la Microcystine-Leucine-aRginine (MC-LR), de sorte que l'analyse documentaire portera principalement sur la MC-LR et les méthodes de traitement de l'eau qui lui sont associées. La prochaine section traite de l'impact des cyanotoxines sur les plans d'eau de surface et des risques connexes pour la santé humaine.

2.2. Impact des cyanotoxines sur les eaux de surface et sur la santé publique

Un lac en Chine (le lac Taihu : troisième plus grand lac de Chine) a été touché par le phénomène de cyanobloom où des cyanotoxines dangereuses (surtout MC-LR) ont été libérées en quantité suffisante pour laisser plus de deux millions de personnes sans accès à l'eau potable pendant plus d'une semaine. Ainsi, lorsque ces cellules cyanobactériennes ou cyanotoxines dissoutes entrent dans la station de traitement d'eau potable (STEP) avec l'eau brute, leur traitement devient important. La Figure 1.1 présente quelques données récentes sur l'éclosion de cyanobactéries en Amérique du Nord. Au Canada, le lac Érié a été gravement touché, et les cyanotoxines libérées

par la prolifération de cyanobactéries menacent la santé publique, car elles polluent les eaux de surface.

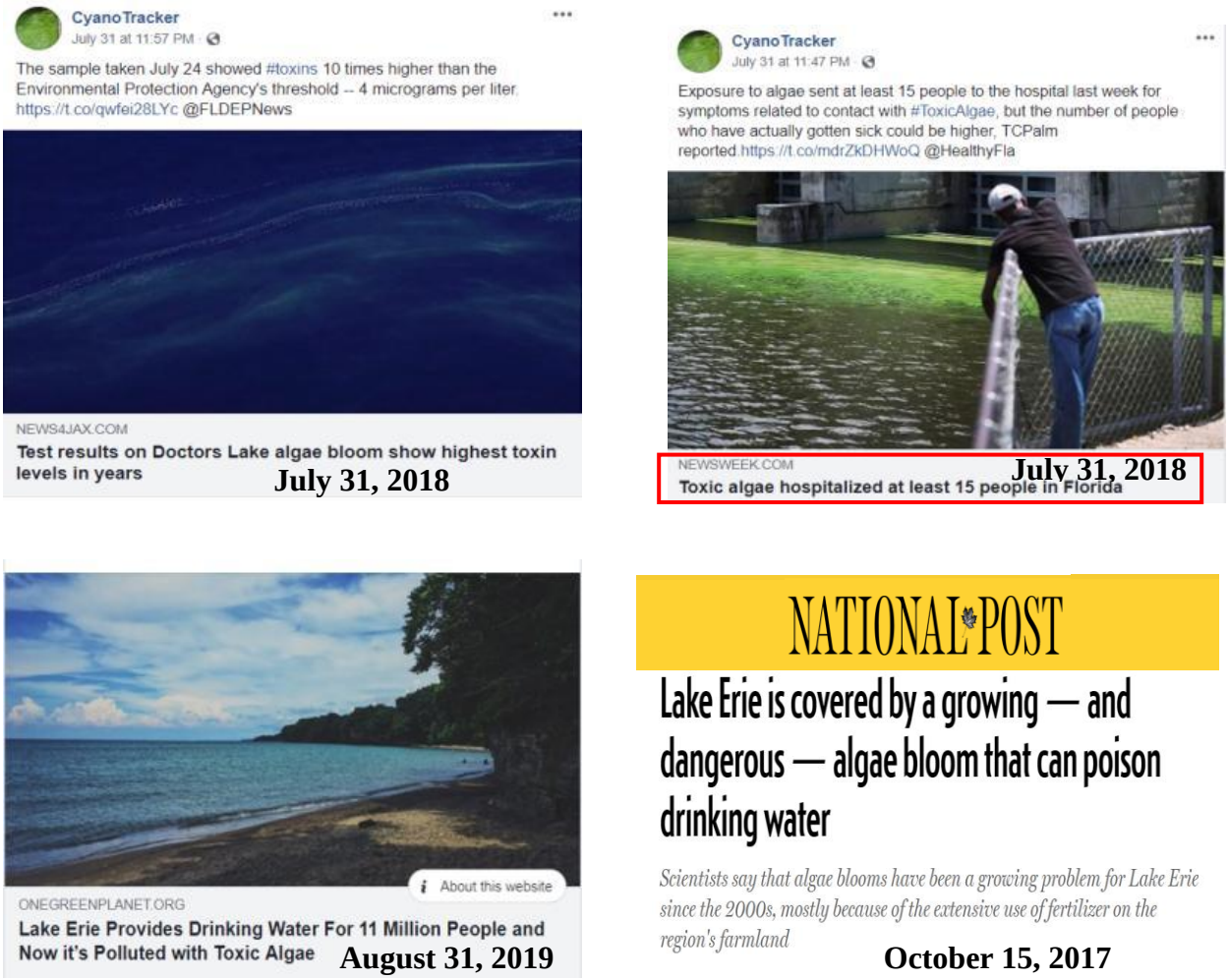

Figure 1.1: Recent news on the impact of cyanobloom and release of cyanotoxins in various environments

Selon les recommandations de l'OMS pour l'eau potable, la concentration critique de certaines cyanotoxines telles que les MC-LR doit être <1 µg/L (OMS, 2009). Les cyanotoxines et leurs métabolites sont persistants dans l'environnement et peuvent donc entrer directement dans la STEP. Par exemple, la demi-vie de la MC-LR (sécrétée par *Microcystis aeruginosa*) est d'environ 90 jours et est connue pour être l'une des cyanotoxines les plus toxiques présentes dans le milieu naturel [2]. La demi-vie d'autres cyanotoxines, comme la saxitoxine (produite par *Anabaena sp.*), est d'environ 9 à 28 jours. Certains de leurs sous-produits (comme les gonyautoxines) ont une demi-vie encore plus longue, soit >90 jours [3]. Outre les organismes aquatiques, les problèmes

de santé graves associés à ces cyanotoxines s'étendent également aux humains, allant des effets aigus (irritation de la peau, gastro-intestinal) aux effets chroniques (lésions rénales, lésions hépatiques, cancérogènes possibles) [4]. Le Tableau 1.1 présente diverses cyanotoxines produites par différents genres de cyanobactéries ainsi que leurs valeurs de DL_{50}. L'absorption continue d'eau de source non traitée utilisée pour l'eau potable peut atteindre la dose létale dans le corps humain en raison d'une bioaccumulation prolongée (Tableau 1.1). Il est donc nécessaire d'éliminer efficacement les cyanotoxines dans les STEP afin d'éviter tout problème éventuel pour l'utilisateur (eau du robinet). La section suivante porte sur les méthodes de traitement qui ont été étudiées pour l'élimination des cyanotoxines.

Table 1.1: Groups of cyanotoxin, cyanobacterial genera and their geographical distribution

Cyanotoxin	LD_{50} (µg kg^{-1}) [5]	Years to reach LD_{50} value in human body **	Genera	Geographical distribution	Reference
Microcystin	25-60	16	Anabaena, Microcystis, Planktothrix(oscillatoria)	Australia, Canada, China, Europe, Japan, South Africa, UK, USA	[6-7]
Nodularin	60	38	Nodularia	USA, Canada, Oceania	[8]
Anatoxin-a	200-250	128	Planktothrix, Anabaena, Aphanizomenon	Finland, Japan, Ireland, Germany, Canada, Denmark	[9]
Aplysiatoxin	20	12	Lyngbya, Schizothrix, Planktothrix (Oscillatoria)	NA	--
Cylindrospermopsin	300	191	Cylindrospermopsis, Aphanizomenon, Umezakia	Israel, Australia, Hungary, Japan	[10,11]
Saxitoxin	10	6	Anabaena, Aphanizomenon,	Australia, USA, Brazil	[12]

LD_{50}: Lethal Dose at which 50% of test population dies

2.3. Traitement physico-chimique

Différents procédés de traitement physico-chimique, dont l'opération photo-catalytique, la séparation par membrane, l'ozonation et la chloration, ont été appliqués avec succès pour l'élimination des toxines extracellulaires ainsi que des toxines entrantes. Un DWTP typique

consiste en l'ozonation et la chloration comme principales unités de traitement d'oxydation et donc la discussion sur leur rôle dans l'élimination du MC-LR et d'autres cyanotoxines a été traitée dans la section suivante. La méthode photocatalytique est une technologie de traitement avancée qui n'a pas été très couramment appliquée dans un DWTP. Cependant, leurs avantages et leurs limites ont également été discutés. L'utilisation d'un procédé de traitement par adsorption impliquant du charbon actif en poudre et une filtration à base de charbon actif granulaire a également été discutée, en particulier pour l'élimination du MC-LR. La discussion est passée du processus de traitement avancé (processus photocatalytique) au processus de traitement couramment appliqué (oxydation et adsorption). Le Tableau 1.2 présente diverses méthodes de traitement classiques et avancées utilisées pour le traitement de différentes cyanotoxines (principalement les MC-LR) ainsi que leurs principales lacunes et leur efficacité d'élimination.

2.3.1 Méthode photo-catalytique

L'élimination rapide et efficace des cyanotoxines peut être obtenue par la méthode photo-catalytique qui est répandue dans les stations d'épuration modernes. En fait, l'oxydation photo-catalytique à l'échelle du laboratoire a fait ses preuves pour l'élimination de diverses cyanotoxines, comme la microcystine, l'anatoxine et la cylindrospermopsine (CYN). La Figure 1.2 montre différents cas de traitement photo-catalytique illustrant le TiO_2 comme photo-catalyseur et le MC-LR comme molécule représentative de cyanotoxine, sans condition de dopage (Figure 1.2 (A)), la présence d'oxydants (Figure 1.2 (B)), la présence du MnO à pH = 7 et à pH < 7 (Figure 1.2 (C) et (D), respectivement) et le scénario du TiO_2 dopé au métal (Figure 1.2 (E)).

D'après les études signalées (Tableau 1.2), on peut voir que la présence du MnO est principalement tenue comme étant responsable d'une élimination inefficace de la toxine, car le procédé de traitement exige une énergie supplémentaire pour éliminer la cyanotoxine dans un délai donné. Les Figures 1.2 (C) et (D) montrent l'effet des MnO dans différentes conditions de pH où les particules de MnO absorbent la lumière UV et agissent comme un piégeur du radical hydroxyle (responsable de la dégradation de la cyanotoxine). Sous un pH faible, l'effet de l'adsorption de surface des MnO inhibe l'interaction de la molécule MC-LR avec la surface du catalyseur. Par conséquent, outre l'action de piégeage (qui se produit dans une plage de pH plus large), l'adsorption de composés étrangers sous forme de MnO et d'autres oxydants, comme les molécules de peroxyde (Figure 1.2 (B)), interfère avec la surface du photocatalyseur et, par conséquent, affecte

l'élimination des molécules de cyanotoxine. Les molécules de cyanotoxines restent donc stables plus longtemps, ce qui exige plus de temps de fonctionnement et donc plus d'investissement en énergie.

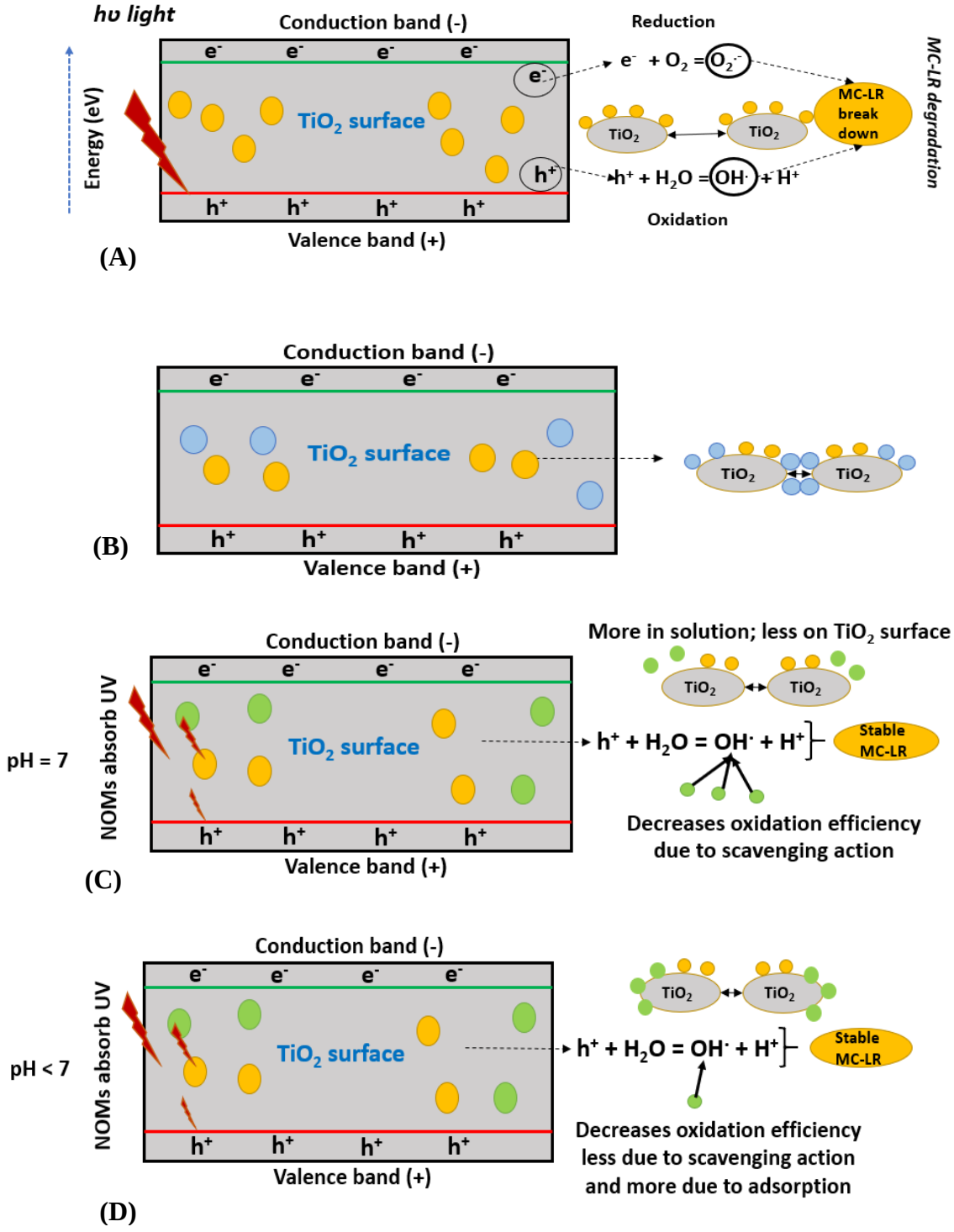

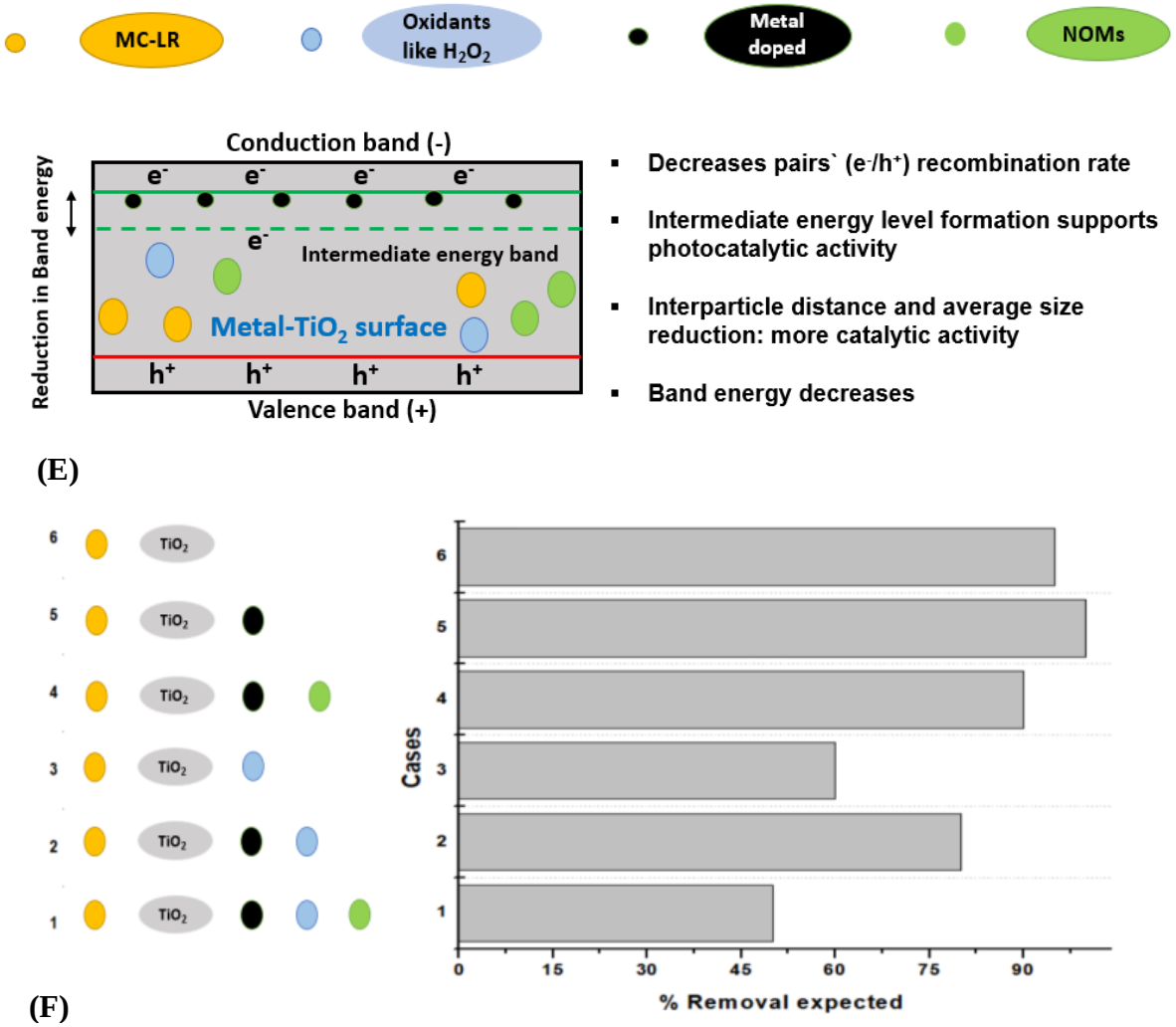

Figure 1.2: (A) A photocatalytic surface (TiO_2) with Microcystin-LR (MC-LR) molecule showing effective interaction; (B) Oxidants (H_2O_2) with TiO_2 and MC-LR molecules; (C) NOM interaction with TiO_2 and MC-LR at pH=7; (D) NOM interaction with TiO2 and MC-LR at pH < 7; (E) Metal doped TiO_2 interaction with MC-LR, oxidants and NOMs (explained more in text); (F) Overall comparative degradation efficiency analysis for various cases [14-17].

D'après le Tableau 1.2, on peut également observer que toutes les études ont été réalisées à l'échelle de laboratoire avec un volume opérationnel < 20 ml, ce qui pourrait être trop faible pour permettre d'appliquer les résultats à l'échelle pilote. De plus, la préparation de la surface du catalyseur qui peut être devenue résistante (persiste pendant une période prolongée) est discutable, car aucune étude n'a été effectuée pour justifier la longévité des catalyseurs utilisés. En outre, il faut également suivre de temps en temps la consommation d'énergie et l'efficacité obtenue, ce qui peut en soi ajouter une charge opérationnelle pour l'exploitant de l'installation.

Le processus photo-catalytique pour l'élimination des cyanotoxines est fortement influencé par la modification du pH du milieu environnant. Par exemple, Zhang et al. (2014) [13] ont obtenu un

taux maximal de dégradation des MC-LR (concentration initiale : 9 mg/L) pour un pH de 5,01 (système de photocatalyseurs Ag_3PO_4 ; dose 26,6 ppm) avec une pseudo constante cinétique du premier ordre, une valeur *k* de 1,52 h^{-1} et une efficacité d'élimination de 99,98 % en 5 h. La constante cinétique et la dégradation globale ont encore diminué, passant respectivement à 0,18 h^{-1} et 59,19 % lorsque le pH a été porté à 11,96. Tout changement de pH influence l'hydrophobicite des cyanotoxines, telles que les MC-LR, qui augmente avec une diminution du pH, permettant activement à ces composés de se déplacer vers la surface du catalyseur à partir de la solution mère. D'autre part, dans des conditions basiques, les MC-LR ont montré une très faible adsorption à la surface du catalyseur. Ceci explique le fait que le pH influence l'activité photocatalytique et la solubilité des cyanotoxines, ce qui, en fin de compte, entrave l'ensemble de l'opération de photocatalyse. Pour contrer ces difficultés, la STEP pourrait devoir mettre en place un réservoir de neutralisation juste avant la chambre photocatalytique pour avoir un traitement efficace des cyanotoxines. Ainsi, les problèmes liés à la variation du pH peuvent être résolus, mais la présence d'autres substances, telles que les MnO et autres matières organiques, peut encore diminuer l'efficacité de l'élimination des cyanotoxines. De plus, les coûts opérationnels supplémentaires ainsi que le fardeau supplémentaire du maintien du débit (requis pour le bassin de neutralisation) peuvent affecter le processus de traitement intermédiaire, causant une élimination non uniforme des MC-LR ou d'autres cyanotoxines. Ces incohérences dans l'efficacité de l'élimination et la formation de sous-produits toxiques pendant la photocatalyse remettent également en question sa viabilité commerciale.

Table 1.2: Various conventional and alternative treatment methods for cyanotoxins removal

Methods		**Type of cyanotoxins**	**Results**	**Shortcomings**	**Reactor volume**	**Ref**
	(TiO2/ZnO)	Microcystin-LR	100% removal in 5 minutes	----------	250 mL	[18]
	NF-TiO2	Microcystin-LR, -RR, -LA, -YR and CYN	100% removal in 2 hours	Presence of NOM reduced rate of degradation; Overall, process is pH dependent	10 mL	[19]
			Removal decreased from			

Methods		Type of cyanotoxins	Results	Shortcomings	Reactor volume	Ref
Photocatalysis	UV-C LEDs/UV-C LED/H_2O_2	Anatoxin-a	97% to 77% by addition of H_2O_2 and for 97% to 72% when DOC was at 1.4 mg/L (lake water)	Presence of NOMs decreased efficiency significantly (by around 20%)	5 mL	[20]
	UV LED/TiO_2 Using Photospheres ™	Nodularin and microcystin variants	All cyanotoxin removed in less than 6 minutes (nodularin being least adsorbed due to darkness)	Further research is necessary to crosscheck result on more complex matrix, amino group affects results.	3 mL	[21]
	TiO_2	Microcystin-LR and Cylindrosperm opsin (CYN)	MC-LR achieved significant removal but No CYN adsorption	Requires high solar exposure time to achieve high degradation	20 L	[22]
	UV/TiO_2/Hi O_2	MC-LR 100%	100% removal within 60 min at pH 3.5	Requires upscale evaluation	100 mL	[23]
Photocatalysis	NF-TiO2 PF-TiO2 and S-TiO2	CYN (6-HOMU), model compound for CYN	100% (2hr),100% (4hr) and 80% (4hr) removal in NF-TiO2, PF-TiO2 and S-TiO2 respectively		100 mL	[24]
	Graphene Oxide- TiO_2 (doped)	Microcystin-LR	97% removal	Process was highly pH dependent	20 mL	[25]
	RO Membrane	Microcystin-LR and microcystin-RR	>95% retention rate achieved for salt and tap water	Retention of toxic particles need safe disposal; membrane fouling	Flow rate: 250 L/h	[26]

Methods		Type of cyanotoxins	Results	Shortcomings	Reactor volume	Ref
Membrane techniques	NF membrane (Two flat-sheet filtration membranes, NF-270 and NF-90)	Saxitoxin and congeners	<20% removal of neoSTX, dcSTX and STX from NF-270 and 100 % from NF-90	Specificity is required for the removal of the main toxin and congeners.	Flux (NF 270): 250 L/m2/h	[27]
	Gravity-driven membrane (GDM)	Microcystin-LR	100% in 10 days of bioflm growth over membrne	Biofilm increased from day 1 to day 10 and flux rate decreased from >4 L m−2 h−1 to around 1 L m−2 h−1	mean flux of 4.7 L m−2 h−1	[28]
Chlorination		Microcystin-LR	Can be ineffective process sometimes; generally, >95% removal	pH dependent; production of harmful by-product	300 mL	[16]
		NOD	Effective in removal (almost 95%)	pH dependent, mechanism of degradation not known	50 mL	[29]
		CYN	Complete CYN degradation in <20 min	pH dependent, one new unidentified by-product which could be toxic.	<15 ml	[30]
		Saxitoxins	>99.1 % removal at higher pH (8)	pH dependent kinetics behaviour (oxidation being more effective at pH values over 6.5)	250 mL	[30]
		Anatoxin	<10% removal was achieved (poor oxidation)	pH dependent and high chlorine dose required than normal; high chlorine dose require hence high TTHM formation	5 mL	[32]
		Microcystis bloom toxins	100% removal mostly	By-product characterization difficult	1.5 L	[33]

Methods	Type of cyanotoxins	Results	Shortcomings	Reactor volume	Ref
Ozonation	Saxitoxin and their by-products	O3 dose (continuous) removed 31% of GTX-5, and 77% of STX	Some unidentified peaks were deciphered which could be toxic	50 mL	[34]
	CYN	CYN IC50 at 24 incubations (MTT assay) 64.1 µM,; ozonation products of CYN shows no measurable cytotoxicity to human cells (HepG2 cells)	More than 32 by-products formed which requires further study	ND; ozone doses (0−62.5 µM) Initial CYN: 20.0 µM	[35]
Permanganate (Potassium)	Microcystin-LR	95% removal in just 30 mins	Little known about any by-products, their character and nature	100 mL	[36]
	Anatoxin and MC-LR	Both are removed at higher concentration (>90%)	At lower concentration (2-10 µg/L), high permanganate is required (>6mg/L) which is unacceptable owing to guidelines	<50 mL	[37]
Hydrogen peroxide	Microcystin	Ineffective in removal (to as low as 17%)	Reaction kinetics are quite unfavourable for microcystin removal	100 mL	[38]
	CYN (through UV/H_2O_2, $UV/S_2O_8^{2-}$, and UV/HSO5)	Presence of metal ions in tap water enhanced degradation (almost 100%)	Depends on metal ion concentration and NOM present in raw water	<50 mL	[39]

ND: not detected

<u>DÉDUCTION 1 :</u> La méthode photocatalytique est efficace. Cependant, elle est très sensible au traitement lorsqu'elle est soumise à des changements de pH et de MnO. Elle implique des coûts élevés et est énergivore.

2.3.2. Ozonation

L'utilisation d'oxydants chimiques tels que l'ozone, le chlore, le dioxyde de chlore, les chloramines et le permanganate ont été efficaces pour la plupart des cyanotoxines (en particulier les MC-LR) [16]. Une étude d'ozonation pour l'élimination de différentes cyanotoxines, notamment les MC-LR, les CYN et les anatoxines, a permis d'obtenir une oxydation d'environ 95 % à des doses de 0,25 mg/L, 0,38 mg/L et 0,75 mg/L d'ozone, respectivement [32]. Ces concentrations étaient inférieures à la concentration à laquelle les sous-produits nocifs ont été détectés. Cette dose d'ozone est également compatible avec le fonctionnement de la STEP, car elle se situe dans les plages de doses sécuritaires (0,4 mg/L à un faible niveau de MnO est considéré comme sécuritaire pour le prétraitement de l'eau brute dans les STEP) [40]. Certaines études ont même montré la non-formation de bromure (Bromure : non acceptable dans le traitement de l'eau potable) même dans l'eau exempte d'ammoniac, ce qui renforce l'utilisation de l'ozonation dans les STEP pour l'élimination des cyanotoxines. Généralement, la teneur en bromure dans les sources d'eau naturelle varie entre 10 et 100 µg/L et, ainsi, elle peut être problématique pour la santé humaine si l'eau n'est pas traitée adéquatement (recommandation de l'OMS de max 25 ug/L). Différents sous-produits de bromure lié à la matière organique peuvent être générés et peuvent être néfastes pour la santé humaine [46]. Le traitement à l'ozone est largement utilisé dans les STEP et est également considéré comme une bonne option pour l'élimination des cyanotoxines, car il présente l'avantage supplémentaire de ne pas permettre la libération de toxines par les cellules cyanobactériennes à faible dose d'ozone (jusqu'à 0,6 mg/L) [41]. Une dose d'ozone inférieure à 1 mg/L est assez courante dans les STEP, comme nous l'avons déjà mentionné. Dans un autre cas, Liu et al. (2010) [132] ont étudié l'élimination du MC-LR (concentration initiale de 100 µg/L) avec un traitement UV pendant une durée de 5 minutes (2,6 mW/cm^2) suivi d'une dose d'ozone de 0,2 mg/L où ils ont

atteint une concentration finale de MC-LR de 1 µg/L. Avec une dose d'ozone plus élevée de 0,5 mg/L, la concentration de MC-LR a encore diminué pour atteindre 0,1 µg/L (< valeur recommandée par l'OMS). Cependant, la dose était plus faible que la dose d'ozone généralement appliquée dans les STEP.

Cependant, l'ozonation entraîne la formation de sous-produits toxiques sous forme de formaldéhydes, d'autres aldéhydes et de cétones. L'efficacité élevée de dégradation des MC-LR est obtenue par une force ou un potentiel d'oxydation plus important sous la forme de H_2O_2 en même temps que la dose d'ozone appliquée (H_2O_2/O_3 : > 90 % en <1 min alors que seulement O_3 : 60 % en 30 min) mais au détriment de la production de sous-produits toxiques [38]. Il a été observé qu'à un rapport molaire plus faible de l'ozone et du MC-LR (40:1), le traitement H_2O_2/O_3 produisait une biotoxicité équivalente à une concentration de Zn^{2+} de 0,04 ppm par rapport à 0,008 ppm lorsque seul le traitement O_3 était suivi. Cette tendance n'a pas beaucoup changé à un rapport plus élevé, où le dernier a montré une biotoxicité de 0,01 ppm de concentration de Zn^{2+} alors que le premier a montré 0,05 ppm. Par conséquent, il faut surveiller étroitement l'équilibre entre la dégradation effective des MC-LR (ou d'autres cyanotoxines) et le niveau de biotoxicité pendant l'exploitation de la STEP. Chang et al. (2015) [135] ont également montré une élimination efficace du MC-LR par traitement UV/O_3. À faible niveau d'ozone (48 µg/L) et à une dose élevée (76 µg/L), l'inclusion des UV a amélioré l'élimination des MC de >40% et >20%, respectivement. Cette étude a démontré (preuve avec spectres de masse) un clivage complet de la molécule de chaîne latérale Adda (représente la toxicité) et contredit donc l'étude discutée précédemment. De plus, le traitement O_3/UV a montré une performance stable d'élimination des MC en présence de NOM à teneurs élevées (>4 mg/L) à environ 85% contre 60% lorsque seule l'ozone était utilisée comme traitement. Cela pourrait s'avérer très efficace, pratique et apte à traiter les cyanotoxines (MC en particulier) en présence de NOM, car il s'agit du défi le plus courant et le plus important pour tous les procédés de traitement physico-chimique. L'eau brute (à NOM et MC élevés) entrant dans l'unité de prétraitement (préozonation) sera traitée efficacement dans une STEP et garantira un rejet d'eau non toxique vers les unités opérationnelles en aval. La formation de sous-produits intermédiaires au cours de chaque étape de la réaction s'est avérée toxique, ce qui nécessite un traitement supplémentaire pour leur élimination [33, 43, 44]. La molécule de fragment Adda est une partie caractéristique des microcystines et les phosphates protéiques sont inhibés par ces molécules. Ainsi, les molécules de sous-produits comprenant le fragment « Adda » sont un signe

de métabolites toxiques [134]. Les métabolites toxiques sont principalement constitués de masses de fragments Adda de valeurs m/z: 192, 208, 232, 248 et certaines masses moléculaires supérieures de 796 et 836 [133].

En outre, la présence de MnO élevées dans l'eau brute non traitée a été un défi majeur pour le système d'ozonation en raison de sa nature compétitive pour réagir avec la molécule d'ozone [45]. Tout comme le processus de photocatalyse, l'ozonation est également sensible au pH du milieu environnant. Par exemple, dans des conditions alcalines, l'ozone a un potentiel d'oxydation plus faible (1,24 V) que dans des conditions acides (2,07 V), ce qui permet au radical hydroxyle de décomposer les molécules d'ozone dans les conditions basiques et donc, agit comme un radical inhibiteur pour l'élimination des cyanotoxines. L'augmentation de la décomposition de l'ozone dans une courte fenêtre de pH comprise entre 7,5 et 9 peut même faire dévier le résultat de 45 % (de MC-LR non oxydés) en solution [33]. Ainsi, pour les sources d'eau potable contenant des cyanotoxines, l'ozonation n'est pas toujours une option variable et peut poser de grands défis si l'équilibre global n'est pas atteint.

2.3.3 Chloration

La chloration montre également l'élimination efficace des cyanotoxines en présence d'une dose allant jusqu'à 3 mg/L qui entraîne une dégradation complète des MC-LR [46]. Cependant, l'élimination varie pour les autres cyanotoxines, en particulier les anatoxines, alors que dans une étude, on a constaté que seulement 15 % des anatoxines étaient oxydées pour le même apport de chlore. La formation de sous-produits de désinfection à une dose élevée de chlore peut rendre l'élimination globale des cyanotoxines encore plus inefficace (car la dose habituelle est absorbée par la présence de MnO). Par conséquent, les STEP qui traitent l'anatoxine pourraient devoir choisir une autre solution que la chloration (ou même l'ozonation, comme nous l'avons vu plus tôt). D'autres oxydants tels que le chlore, les chloramines et les dioxydes de chlore se sont également avérés inefficaces pour certaines variétés de cyanotoxines, en particulier l'anatoxine, dont le pH dépend fortement à un moment donné du traitement [47]. De plus, le chlore et la chloramine ont montré une efficacité d'élimination variable pour différentes cyanotoxines. Cependant, les chloramines présentent un avantage par rapport au chlore utilisé dans la STEP (en particulier dans les eaux à forte teneur en MnO), car ces dernières forment des sous-produits de désinfection comparativement plus importants que le premier. L'utilisation des chloramines réduit

la concentration de THM et d'autres analogues chloro/bromo et assure une meilleure sécurité pour le public. Cependant, Nicholson et al. (1994) [29] ont constaté que l'utilisation de 20 mg/L de monochloramine ne permettait d'éliminer que 17 % des extraits de cyanotoxines (de *M. aeruginosa* : surtout des MC-LR) en 5 jours, alors que la chloration révélait une concentration non détectable d'extrait de cyanotoxine (MC-LR) à une dose de 2 ppm et un temps de contact de 30 minutes. Les chloramines ont un potentiel oxydant plus faible que l'ion acide hypochloreux/hypochlorite et procèdent généralement avec la vitesse cinétique plus lente pour les MC-LR, CYN ou les anatoxines (< 1 M-1 s^{-1}) surtout lorsque l'MnO est dans le fond [32]. De plus, l'utilisation des chloramines peut exiger un rapport molaire plus important pour le traitement des cyanotoxines. Par exemple, Banker et al. (2001) [48] ont montré que le chlore exigeait un rapport molaire moins élevé (CYN : chlore = 1:1) que la chloramine (CYN : chloramine = 1:2) pour éliminer le niveau de toxicité de la CYN, qui a été dûment déterminé par la formation de 5-chloro-cylindrospermopsine (non toxique).

D'autres cyanotoxines, telles que l'anatoxine-a et les saxitoxines, sont résistantes à la chloration. Ceci peut être principalement attribué aux différences de structure entre les différentes cyanotoxines [49]. Même après 30 minutes de contact et des changements de pH, elles n'ont montré aucun effet. Une autre étude de Rodriguez et al. (2007) [32] a montré qu'une dose de chlore d'environ 1,5 mg/L était suffisante pour une oxydation complète de la cylindrospermopsine (CYN), alors que 3 mg/L de chlore ne permettaient d'éliminer que 8 % d'anatoxine. Par conséquent, la chloration n'est pas efficace pour traiter toute la variété de cyanotoxines et une dose élevée (> 2-3 mg/L) pourrait être nécessaire, ce qui risque de dépasser la recommandation du traitement de l'eau potable. De plus, l'oxydation des CYN par le chlore s'accompagne de la formation de trihalométhanes (THM) à une concentration détectable de 150 µg/L. Ces niveaux de THM sont supérieurs aux recommandations de l'UE de 1998 (100 µg/L) et peuvent donc être préjudiciables à la santé humaine s'ils sont présents dans l'eau potable.

Ainsi, la variation de l'efficacité d'élimination et du taux de dégradation pose un défi pour l'élimination des cyanotoxines par chloration dans la station de traitement de l'eau. De plus, l'accumulation de divers sous-produits oxydants formés au cours de la réaction chimique nécessite un traitement supplémentaire et n'est pas souhaitable sur le plan économique. Ces sous-produits non traités, lorsqu'ils sont rejetés dans les plans d'eau, affectent la santé des organismes aquatiques

[50]. Les sous-produits sous forme de trihalométhane et d'acides haloacétiques sont valorisés, notamment en raison de la présence de faibles teneurs en matière organique naturelle (MnO), ce qui est assez courant dans plus de 90 % des STEP. Un temps de contact (TC) plus élevé dans le traitement par chloration entraîne une meilleure élimination de la toxine, mais au détriment de la formation de THM et d'acide haloacétique. Il a été démontré que l'interaction des cyanotoxines, comme les MC-LR, avec le chlore ou d'autres agents chlorés entraîne la formation de dichloro-microcystine suivie d'un hydroxylation, ce qui entraîne la formation de dihydroxy-microcystine. Les sous-produits de la microcystine chlorée pourraient être plus toxiques que leur composé d'origine [16]. Un inconvénient majeur de l'utilisation de la chloration, outre la formation de sous-produits nocifs, réside également dans les difficultés opérationnelles, car plusieurs paramètres, tels que la dose optimale de chlore, le temps de contact et le pH, doivent être optimisés, ce qui est difficile à réaliser compte tenu de la variété des cyanotoxines et des différents taux de dégradation [22].

DÉDUCTION 2 : **L'ozonation et la chloration sont efficaces pour éliminer la MC-LR. Cependant, la toxicité posée par les sous-produits et l'exigence d'une dose d'entrée élevée de produits chimiques (ozone et chlore) par rapport aux directives suggérées, limitent son utilisation dans la STEP.**

2.3.4. Procédés physiques d'adsorption

Le procédé de filtration sur charbon actif en poudre (PAC) et sur charbon actif en granulés (GAC) est basé sur le mécanisme d'adsorption physique et fait l'objet de recherches depuis quelques décennies pour l'élimination des cyanotoxines. L'efficacité de la filtration dépend principalement du matériau filtrant utilisé [51]. De nombreux chercheurs ont montré que les médias filtrants affectent la dégradation des cyanotoxines [52]. Le potentiel de dégradation des cyanotoxines dépend également de la texture de ces matériaux, en dehors des différents médias de lit utilisés. Par exemple, Miller et Fallonfield (2001) [51] ont observé que dans le cas d'un sol à forte teneur en sable (98,5 % de sable), la dégradation de la microcystine est plus faible que dans le cas d'un

sol argileux (16,1 % d'argile) où un sol à teneur maximale en carbone organique (2,9 %) a été utilisé. De telles modifications du milieu filtrant ont également une incidence sur la dose, ce qui modifie le temps de contact nécessaire à l'élimination efficace de la cyanotoxine. Donati et ses collaborateurs (1994) [53] ont signalé qu'une augmentation de la dose des PAC à l'aide de différents médias filtrants (de 25 mg/L dans le cas du carbone à base de bois à 50 mg/L dans le cas du carbone à base de mousse de tourbe) avait une incidence significative sur l'efficacité de la dégradation des MC-LR (élimination de 98 % dans le premier cas contre 60 % dans le second) (Tableau 1.3). Dans une autre étude de Vlad et al. (2015) [54], l'élimination des saxitoxines a été évaluée à l'aide de PAC, de bois, de noix de coco et de charbon ; les PAC ont été éliminées à 100 % par rapport aux autres matériaux. Cela indique que l'origine de la poudre de carbone joue également un rôle essentiel dans l'élimination des cyanotoxines. Peu ou pas d'études ont été rapportées à ce jour sur l'élimination des cyanotoxines par les PAC. Cependant, quelques études ont montré qu'une dose élevée de PAC est nécessaire pour l'élimination des cyanotoxines, ce qui dépend également de la source d'où provient la PAC. Par exemple, Ho et al. (2008) [55] ont constaté que pour éliminer seulement 5 µg/L de CYN, il faut environ 25 mg/L de PAC à une période de contact élevée (60 minutes), avec une différence d'efficacité constatée pour les PAC obtenus de différentes sources. En fait, l'effet des MnO ont également joué un rôle important dans l'élimination du CYN, car la compétition d'adsorption entre les métabolites cyanobactériens augmente avec le pic de concentration des MnO. Ainsi, la PAC finit par perdre son efficacité d'adsorption en raison du mécanisme de blocage des pores, ce qui est également valable pour d'autres cyanotoxines [56].

Table 1.3: Different cyanotoxin (microcystin, anatoxin, and saxitoxin) removal using powdered activated carbon

Case	Cyanotoxins removed	PAC/GAC concentration	Initial concentration of toxin	Removal efficiency	References
1	Freeze dried cyanobacterial material (PAC)	20 mg/L	15 µg/L	90 %	[33]
2	Microcystin-LR (PAC)	>20 mg/L	40 µg/L	85%	[57]
3	Microcystin-LR (PAC)	25 mg/L	50 µg/L	98%	[53]

Case	Cyanotoxins removed	PAC/GAC concentration	Initial concentration of toxin	Removal efficiency	References
4	Microcystin-LR (PAC)	50 mg/L	50 µg/L	60%	[53]
5	Microcystin-LR (PAC)	12 mg/L	50 µg/L	95%	[58]
6	Microcystin-LR (PAC)	30 mg/L	0.5 µg/L	82%	[59]
7	Microcystin-LR (PAC)	100 mg/L	22 µg/L	86.4%	[52]
8	Microcystin-LR (GAC)	100 mg/L	9 to 47 µg/L	100%	
9	Anatoxin-a (GAC)	10 mg/L; 30 mg/L	<10 µg/L	60-90%; 50-90%	[60]
10	Anatoxin-a (PAC)	50 mg/L	100 µg/L	100%	[61]
11	decarbomoyl saxitoxin (dc-STX); STX (GAC)	3 mg/10 mL	10.5 µg/L and 60.4 µg/L	>90%	[62]
12	Saxitoxin (PAC)	1-90 mg/L	25 µg/L	100% at pH 10.2 and almost no removal at pH 5.7	[63]

PAC: Powder activated carbon; GAC: Granular activated carbon

Le Tableau 1.3 montre l'élimination des cyanotoxines (surtout les MC-LR), avec la concentration initiale de la toxine et la dose de PAC. Le facteur de dose devient une préoccupation dans les scénarios de la vie réelle, où la teneur en matières organiques dissoutes présente un comportement compétitif avec les MC-LR et fluctue avec le temps. Dans ces scénarios, le filtre PAC nécessiterait un dosage élevé, ce qui pourrait remettre en question l'économie globale du procédé. De plus, le changement fréquent de la concentration de cyanotoxines sur un mois ou deux peut exiger une vérification périodique plus fréquente. Parfois, la dose requise suit une relation exponentielle avec la quantité de toxine éliminée. Par exemple, les toxines cyanobactériennes lyophilisées ont été éliminées jusqu'à 90 % à la dose de 20 mg/L de PAC. Cependant, l'élimination complète nécessitait une dose de 100 à 200 mg/L de poudre de carbone, ce qui rendait le processus global non rentable. Cependant, ces problèmes peuvent être surmontés en combinant un ou plusieurs procédés de

traitement avec la méthode d'adsorption des PAC. Par exemple, la coagulation à l'alun combinée à l'opération PAC a montré une meilleure élimination des cyanotoxines [33]. L'ajout d'une dose plus faible de poudre de charbon actif (5 mg/L) pendant la coagulation a montré une élimination efficace de certaines hépatotoxines et de plus de 50 % de l'anatoxine-a. Ainsi, l'exécution d'une étape de prétraitement de l'eau contaminée qui passe dans le filtre PAC peut potentiellement réduire la dose plus élevée requise de charbon actif [64]. Le Tableau 1.3 présente certaines options de traitement réussies à l'aide des PAC.

Cependant, cela n'est pas toujours vrai. Dans l'une des études, Lee et Walker (2006) [65] ont étudié l'élimination des MC-LR à l'aide de PAC/UF et de PAC seuls. On a observé que la cinétique d'adsorption (cycle de 1 heure) des PAC/UF était inférieure à celle du processus de PAC. Même avec une dose élevée de PAC (10 mg/L), la même tendance a été observée avec l'avantage d'une concentration normalisée plus faible à la fin de l'expérience d'adsorption (1 % et 2,5 % de la concentration normalisée à la dose de 10 mg/L par rapport à 10,5 % et 16 % de la valeur lorsque la dose de PAC). De plus, le système combiné PAC/UF en présence de MnO n'a pas réussi à éliminer les MC-LR à un niveau inférieur à 1 µg/L (ligne directrice de l'OMS) [66]. Cependant, la concentration initiale plus faible de MC-LR (dans la plage de 5,3-7,4 µg/L), a montré une concentration finale de <1 µg/L en présence de 2,5-5,0 mg/L de MnO, mais au détriment de la dose élevée de PAC (15 mg/L). Par contre, les doses de PAC de 5 mg/L et de 10 mg/L étaient insuffisantes pour éliminer les MC-LR à un niveau inférieur à 1 µg/L. Entre-temps, à une dose de 17,1-23,2 µg/L de MC-LR_{eq}, même une dose de 15 mg/L de PAC s'est avérée insuffisante pour éliminer les microcystines à un niveau inférieur à 1 µg/L.

Il a été démontré que l'élimination par sorption d'autres cyanotoxines, comme la saxitoxine, dépend des interactions électrostatiques et non électrostatiques. Ces interactions électrostatiques ont été causées par la gamme de pH étudiée (de 5,7 à 10,2), la sorption maximale étant atteinte à un pH de 10,2. Pour un pH de 10,2, une dose de 1 à 40 mg/L de PAC a éliminé plus de 99 % de la saxitoxine, tandis qu'à un pH de 5,7, on n'a observé pratiquement aucune élimination (sorption) de la saxitoxine pour une dose de PAC comprise entre 1 et 40 mg/L. Ces observations suggèrent une sorption efficace des molécules de cyanotoxine dans des conditions alcalines, qui sont quelque peu irrationnelles si elles sont appliquées dans une STEP. De plus, la dose de PAC varie beaucoup en fonction de l'efficacité du traitement requis. De plus, il a été démontré que la présence de MnO

diminuait le comportement de sorption de la PAC pour la saxitoxine éliminée et qu'une dose plus élevée de PAC était donc nécessaire pour l'adsorber efficacement [63].

En général, le fonctionnement des PAC est considéré comme plus rentable que celui des GAC, en termes de coûts d'investissement et de fonctionnement [67]. Comme pour les PAC, l'élimination des cyanotoxines par les GAC dépend aussi de la répulsion électrostatique entre la molécule de cyanotoxine qui aide à leur élimination globale. Par exemple, dans une étude récente de Silva et al. (2015) [62], dans un traitement par filtre GAC, la saxitoxine et la décarbomoyl saxitoxine (dc-STX) ont montré une nature cationique (entre mono-cationique et di-cationique) dans leur structure moléculaire en raison de la présence du groupe amine à un pH neutre, ce qui a encore aidé ces molécules à être éliminées en raison de la répulsion électrostatique. Cependant, ces répulsions électrostatiques peuvent varier entre les différentes cyanotoxines en fonction de la taille et des charges. Par exemple, Wang et al. (2007) [68] ont trouvé que le facteur de répulsion électrostatique diminuait l'élimination des microcystines dans une colonne de filtre GAC (plus grande en taille par rapport à la saxitoxine). Dans une autre étude, cependant, une tentative a été faite pour réduire la répulsion en augmentant la force ionique de la solution contenant la microcystine, ce qui a entraîné une meilleure élimination de la microcystine [69].

> ***DÉDUCTION 3 :*** ***Le média filtrant PAC est un moyen économique de traiter les cyanotoxines. Cependant, le fonctionnement du procédé dépend des MnO et de la concentration initiale de cyanotoxines ainsi que des problèmes courants des filtres : étouffement et percée précoce.***

Ainsi, la taille de la molécule et l'hydrophobicite des cyanotoxines influencent également la propriété de la GAC à les traiter. Une hydrophobicité plus élevée d'un composé est souvent associée à des taux élevés d'adsorption physique dans le processus de filtration. Cependant, la molécule de microcystine-LA (MC-LA), qui est plus petite et plus hydrophobe que la MC-LR, a montré un taux d'élimination relativement plus faible sur le filtre de la GAC (tous deux dopés à la concentration initiale de 10 µg/L) [70]. Ainsi, parmi les variantes d'une même cyanotoxine, l'efficacité d'élimination peut varier en raison de la nature variée de la structure moléculaire. L'adsorption étant le principal mécanisme, le problème de la percée précoce se pose en raison d'une

diminution de l'adsorption au fil du temps [47]. De plus, le problème de colmatage dû à une forte teneur en matière organique réduit la filtrabilité du lit et affecte donc l'efficacité globale du filtre.

2.4. Dégradation biologique des cyanotoxines

Le traitement biologique des cyanotoxines a pris beaucoup d'importance au cours des dernières décennies et promet de fonctionner en coordination avec divers traitements physico-chimiques. Le procédé biologique présente des avantages par rapport aux traitements physico-chimiques, en étant plus économique, plus efficace (bio-adsorption) et surtout en produisant moins de sous-produits toxiques. La toxicité des sous-produits devient très importante par rapport au traitement de l'eau potable. Dans la prochaine section, le mécanisme de biodégradation de la cyanotoxine la plus courante : MC-LR est discuté.

2.4.1 Mécanisme de biodégradation: MC-LR

La Figure 1.3 montre la structure chimique de la molécule de microcystine-LR où sont numérotées toutes les petites structures peptidiques formant le composé. La première étape de la biodégradation de cette structure complexe est l'hydroxylation, suivie de la linéarisation (Figure 1.3). Le mécanisme de dégradation biologique comprend la linéarisation de la structure complexe de la cyanotoxine (en particulier, la microcystine et la nodularine) en une série de produits oxydants simples par l'intermédiaire de gènes codant pour les protéines, ce qui rend la dégradation globale non toxique. Par exemple, l'hydroxylation suivie de la linéarisation du composé de microcystine se produit après le clivage de la liaison Adda (peptide toxique)-Arg. La molécule du fragment Adda est une partie caractéristique de la MC-LR et les phosphates protéiques sont inhibés par ces molécules. Ainsi, les molécules de sous-produits comprenant le fragment "Adda" sont un signe de métabolites toxiques [43]. Les métabolites toxiques sont principalement constitués de masses de fragments adda de valeurs m/z : 192, 208, 232, 248 et quelques masses moléculaires supérieures de 796 et 836 [44].

La biodégradation des MC-LR (par *Sphingomonas sp.* ACM-3962) et la formation subséquente des métabolites ont été signalées à la suite d'une hydrolyse enzymatique séquentielle des liaisons peptidiques [71,72]. Le groupe de gènes *mlr* (*mlrA, mlrB, mlrC, mlrD*) joue un rôle essentiel dans ce mécanisme séquentiel, en formant au moins trois enzymes intracellulaires. Le gène *mlrA* code pour une enzyme qui est responsable de la rupture de la structure cyclique de MC-LR, qui coupe

la liaison peptidique Adda-Arg (Figure 1.3 flèche en pointillé). Le gène *mlrB* code une sérine peptidase putative, qui est responsable de la dégradation de la molécule MC-LR linéaire en tétrapeptide H-Adda-Glu-Mdha-Ala-OH, formé après l'étape d'hydrolyse par les gènes *mlrA*. D'autre part, le gène *mlrC* est responsable de la décomposition ultérieure des tétrapeptides en Adda ou en acides aminés plus petits, tandis que le gène *mlrD* code pour les protéines de transport, qui permettent l'absorption de MC dans la cellule [73]. La nodularine a une structure chimique similaire à celle de la MC-LR avec un pentapeptide ajouté [cyclo-(D-MeAsp-L-Arg-Adda-D-Glu-Mdha)]. Ainsi, en général, les bactéries qui dégradent les MC-LR sont également de bons dégradants de la nodularine, probablement en raison du codage des gènes mlrA responsables de l'activité enzymatique hydrolytique [73]. Le mécanisme de biodégradation des cyanotoxines comme la CYN a été difficile à généraliser et est principalement inconnu, peut-être parce qu'elles subissent une voie enzymatique spécifique [74].

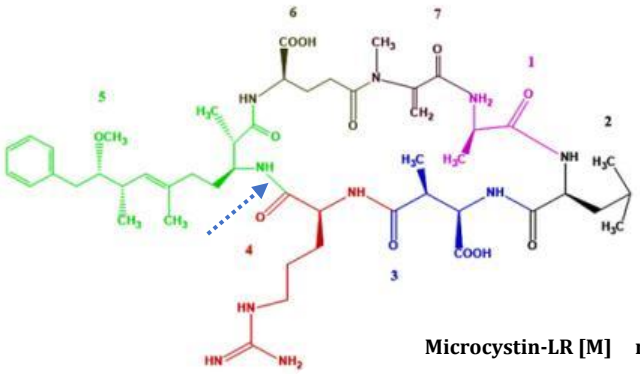

Microcystin-LR [M] m/z = 995

After Hydrolysis
+ H_2O

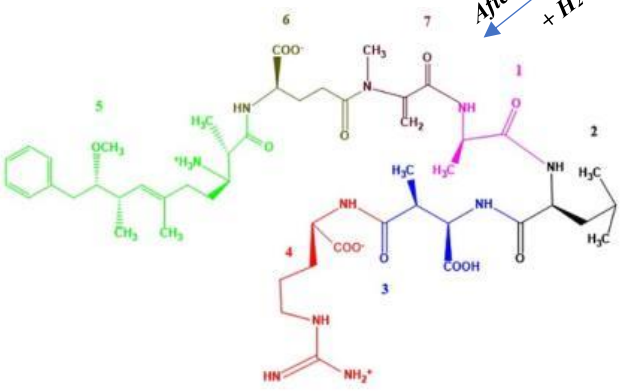

m/z =1013 [M + H_2O + H+] = M_1

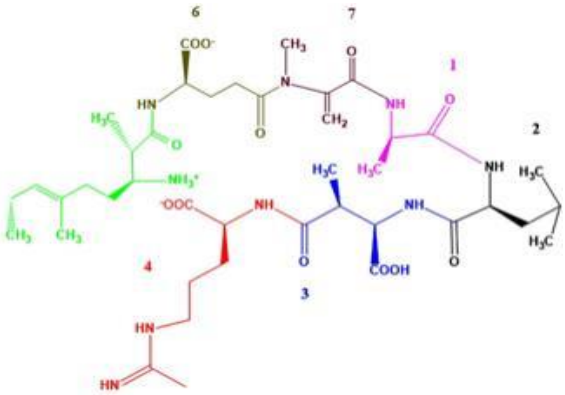

m/z =862.5 [M_1 – NH_2 – $PhCH_2CHOMe$ + H^+]

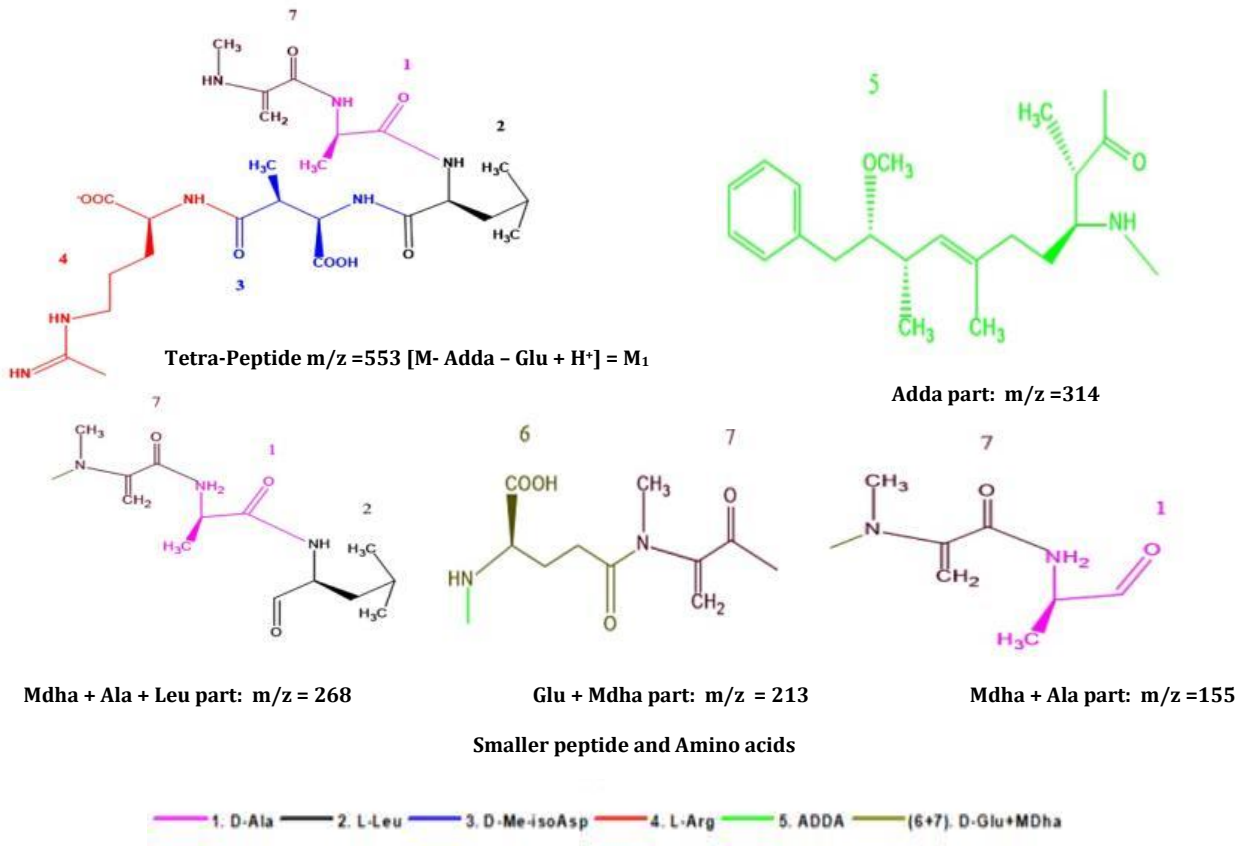

Figure 1.3: Proposed degradation pathways (based on mass spectra) for the breakdown of MC-LR by the co-culture bacterial community isolated from Top-sand filtration sand Unit (Kumar et al. 2018) [61].

Cependant, pour une élimination réussie des MC-LR, il n'est pas nécessaire que le gène mlrA soit codé dans les souches. Comme l'a montré l'étude de Manage et al. (2009) [80], les souches bactériennes : *Arthrobacter sp. , Brevibacterium sp.* et *Rhodococcus sp.* ont presque complètement éliminé les MC-LR en 2 jours (2500 µg/l/jour). De plus, l'étude de Yang et al. (2014) [81] a montré que la souche bactérienne : *Stenotrophomonas acidaminiphila* MC-LTH2 a éliminé le MC-LR complet à un taux de dégradation similaire (3000 µg/l/jour). En fait, ces taux de dégradation sont plus élevés que ceux de la plupart des études présentées au Tableau 1.4. Toutefois, la toxicité de l'échantillon dégradé n'a pas été signalée dans les études susmentionnées. Néanmoins, le taux de biodégradation était assez prometteur.

<u>DÉDUCTION 4 :</u> Les espèces bactériennes n'ont pas besoin de coder les gènes mlrA pour dégrader les MC-LR et présentent en fait une meilleure cinétique de dégradation. Toutefois, la toxicité pourrait-elle être problématique

2.4.2 Importance de la concentration initiale de MC-LR pendant la biodégradation

Différents types de cyanotoxines ont besoin de paramètres différents pour être optimisés en vue de leur dégradation accrue. Par exemple, la concentration initiale de ces toxines pour l'étude de la dégradation des lots par une culture bactérienne spécifique est l'un des facteurs les plus cruciaux (Tableau 1.4) qui influent sur le taux de dégradation (mesuré en cyanotoxines dégradées/L/jour). Plus la concentration initiale de la toxine est élevée, plus le taux de dégradation est élevé, comme le montrent diverses études [77, 78, 79]. On a signalé des taux de biodégradation de différentes microcystines allant de 2,99 mg/L/j pour la microcystine-RR lorsque la concentration initiale était de 3 000 µg/L [77] à moins de 0,00125 mg/L/j pour la CYN pour une concentration initiale de 300 µg/L [78]. Ces taux de biodégradation sont beaucoup plus lents que la dégradation des cyanotoxines par le processus d'oxydation au chlore, où le taux de dégradation a atteint jusqu'à 80 000 mg/L/j [82]. Cependant, l'utilisation du chlore est mise à l'épreuve par la production de sous-produits toxiques [83]. Le Tableau 1.4 présente certaines études où le taux de dégradation peut être lié à la concentration initiale de diverses cyanotoxines. On s'attend à un taux de biodégradation plus élevé à une concentration initiale plus élevée de cyanotoxines en raison d'une augmentation des gènes *mlrA* (dans le cas des MC), qui sont les principaux responsables de la dégradation de la toxine [50]. Smith et al. (2008) [77] ont poussé plus loin cette compréhension et ont déclaré qu'une concentration plus élevée de toxines agit comme un inducteur qui active les gènes responsables de la synthèse des enzymes impliquées dans la dégradation. Pour appuyer cette hypothese, une étude de Mohamed et al. (2012) [78], où la dégradation du CYN par le *Bacillus* sp. (Isolé du lac qui a connu une prolifération d'algues) a été étudiée. À une concentration initiale de CYN de 10-300 µg/L, le taux de biodégradation le plus élevé (50 µg/L/d) a été obtenu à 300 µg/L et le plus faible (1,25 µg/L/jour) à la plus faible concentration de toxine (10 µg/L). Comme on peut le voir au Tableau 1.4, différentes cyanotoxines sous des espèces bactériennes distinctes ont répondu de façon variable en termes de taux de dégradation en fonction de la concentration initiale de cyanotoxines (en raison des différents gènes impliqués dans chacune d'elles : *mlrA, nda, stx, cyn* pour la microcystine, la nodularine, les saxitoxines et la cylindrospermopsine, respectivement).

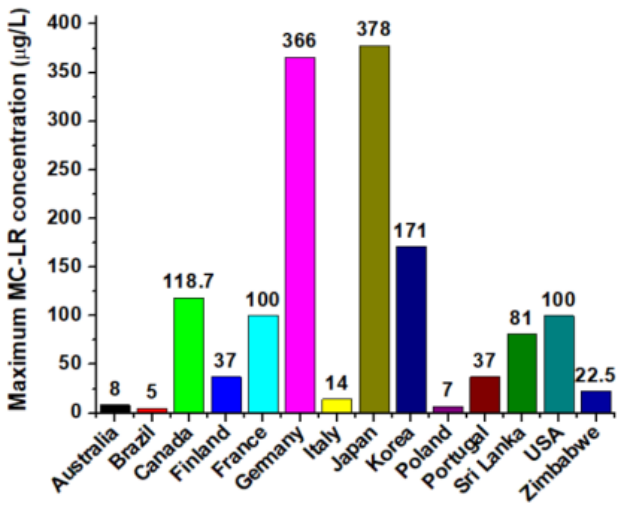

Figure 1.4: Highest recorded Microcystin-LR concentration across the globe [50]

La concentration initiale de cyanotoxine devient un critère important, surtout en ce qui concerne le traitement de l'eau potable. Sachant que la concentration élevée (> 300 µg/L) de cyanotoxine présente dans l'eau de source se dégrade plus rapidement (comme nous l'avons vu plus haut), une telle concentration n'est pas prévue dans un scénario réel. La plupart du temps de l'année, même dans les conditions de pointe été-automne, la concentration atteint à peine 30 µg/L [85]. La Figure 1.4 présente un graphique à barres indiquant la concentration maximale de MC-LR relevée dans divers pays. Une étude mondiale a révélé que la concentration maximale de MC-LR dans les sources d'approvisionnement en eau se situe entre 5 et 378 µg/L, alors que la concentration maximale de MC-LR signalée au Canada était d'environ 120 µg/L. *En tenant compte de tous les aspects, on a choisi 50 µg/L comme concentration initiale de MC-LR dans toutes les études effectuées dans le cadre de ce projet de recherche, sauf l'acclimatation des bactéries isolées qui a été étudiée à l'aide de 200 µg/L de MC-LR.*

> ***<u>DÉDUCTION 5:</u> Une concentration initiale élevée de MC-LR est favorable à la dégradation bactérienne des MC-LR. Cependant, dans le scénario réel, la concentration de la STEP est souvent inférieure à 50 µg/L.***

2.4.3 Importance des espèces bactériennes in situ pour la biodégradation des cyanotoxines

Des progrès récents en écologie microbienne moléculaire ont montré que des souches bactériennes du genre *Sphingomonas* sp., *Sphingosinicella* sp., *Arthrobacter* sp. , *Brevibacterium sp.* ,

Rhodococcus sp. et bien d'autres sont capables de dégrader différentes cyanotoxines en l'espace de quelques heures à quelques jours [86, 87]. Il y a une preuve que des membres spécifiques des bactéries planctoniques, y compris les *Myxophyceae, Cyanophyta,* qui sont capables de dégrader les cyanotoxines, deviennent plus efficaces en présence des fleurs d'eau cyanobactériennes toxiques [88]. Ceci simule les microorganismes dégradant les cyanotoxines présents (bactéries in situ) dans divers plans d'eau [75,76]. Cela pourrait être dû à une augmentation du nombre de gènes dégradant les cyanotoxines. Les bactéries, isolées des sédiments ou d'autres matières particulaires présentes dans les plans d'eau, où des proliférations de cyanobactéries se sont produites dans le passé, peuvent en fait biodégrader les toxines extracellulaires et intracellulaires [89,90]. Ishii et ses collègues (2000) [91] ont étudié la biodégradation de la microcystine en incubant de l'eau de lac (lac Suwa, Nagano, Japon), qui s'était déjà avérée contaminée par des cyanobactéries. Une dégradation complète de la microcystine (50 mL en mode discontinu avec une concentration initiale de 20 µg/mL) a été constatée après l'ajout de sédiments de lit (en mettant directement de la boue) provenant du lac. On a également signalé que les bactéries isolées des plans d'eau naturels (eau du lac), dont on savait auparavant qu'elles étaient contaminées par des cyanotoxines (microcystine provenant principalement de *Microcystis sp.*), biodégradaient les CM sans présenter de phase de latence [92]. De plus, de multiples souches bactériennes isolées des sédiments lacustres se sont avérées capables de dégrader la microcystine et d'autres cyanotoxines [93]. Même la communauté bactérienne (contenant *Sphingomonas sp.* ACM-3926) obtenue à partir de l'unité de biofiltration de l'anthracite (de la station de traitement des eaux usées) a montré une élimination de plus de 80 % des MC-LR en 9 à 10 jours après le processus d'enrichissement [94]. Ces résultats peuvent potentiellement conduire à une étude de la communauté bactérienne in situ ou native capable de dégrader les cyanotoxines. Plusieurs espèces bactériennes capables de biodégradation des cyanotoxines ont été identifiées dans divers plans d'eau, ce qui prouve que le traitement biologique in situ des cyanotoxines est prometteur. De plus, la formation de métabolites toxiques est moins importante que dans le cas des technologies de traitement physico-chimique [95, 77, 78]. En ce qui concerne les STEP, l'étude d'une communauté bactérienne isolée de la couche supérieure de l'unité de filtration (sur sable) pourrait fournir de plus amples renseignements sur la présence de grappes de gènes, leur activité enzymatique et le mécanisme de réaction possible qui peut confirmer la dégradation des cyanotoxines avec des métabolites non toxiques.

DÉDUCTION 6 : ***Les espèces bactériennes in situ/indigènes conviennent mieux à l'élimination améliorée des MC-LR et, si elles sont acclimatées dans un environnement de MC-LR avant de commencer la biorestauration peuvent-elles donner de meilleurs résultats***

Table 1.4: Biodegradation performance of different cyanotoxins

Cyanotoxin	Bacteria	Lag period; Initial concentration	Half-life of toxin	Full degradation period	Degradation efficiency	Ref.
	Sphingopyxis sp. USTB-05	1d; 50mg/L	2d	3d	100%	[96]
MC-RR	*Bacillus flexus* SSZ01	NSD; 10mg/L	1.7 days	5d	100%	[97]
MC-LR	*Sphingomonas isolate NV-3*	NSD; 25 µg/mL	<1 d	3 d	100 %	[98]
MC-RR	*Sphingomonas* CBA4	200 µg /L	18h	36h	100%	[99]
MC-LR	*S. acidaminiphila* MC-LTH2	NSD; 21.2 mg/L	5.5 d	7 d	100 %	[81]
MC-RR	*S. acidaminiphila* MC-LTH2	3 d; 39.2 mg/L	5.5 d	7 d	100 %	[81]
MC-LR	Bacillus sp.	NSD; 2.15 mg/L	18h	24h	100%	[77]
MC-LR	Particulate attached bacteria (PAB)	4-6d; 10 µg/L	5.4d	14d	100%	[95]
MC-LR	(No PAB presence)	12d; 10 µg/L	14.6d	24d	100%	
Sludge	(PAB)	<2d; 10 µg/L	2.7d	19d	100%	
MC-LR	(No PAB presence)	6d; 10 µg/L	8.8d	21d	100%	
MC-YR	(PAB)	4-6d; 10 µg/L	5.4d	14d	100%	
MC-YR	(No PAB presence)	12d;10 µg/L	13.9d	24d	100%	
MC-YR	(PAB)	<2d;10 µg/L	2.3d	19d	100%	
MC-YR	(No PAB presence)	6d; 10 µg/L	8.5d	21d	100%	
MC-LY	(PAB)	4-6d;10 µg/L	8.5d	8.5d	100%	
MC-LY	(No PAB presence)	12d;10 µg/L	------	----	-----	

Cyanotoxin	Bacteria	Lag period; Initial concentration	Half-life of toxin	Full degradation period	Degradation efficiency	Ref.
	Sphingopyxis sp. USTB-05	1d; 50mg/L	2d	3d	100%	[96]
MC-LY	(PAB)	<2d;10 µg/L	2.8d	19d	100%	
MC-LY	(No PAB presence)	6d; 10 µg/L	-----	-----	-----	
MC-LW	(PAB)	4-6d;10 µg/L	8.8d	8.8d	100%	
MC-LW	(No PAB presence)	12d ;10 µg/L	----	----	------	
MC-LW	(PAB)	<2d; 10 µg/L	3.4d	19d	100%	
MC-LW	(No PAB presence)	6d; 10 µg/L	-----	-----	------	
MC-LF	(PAB)	4-6d; 10 µg/L	8.3d	8.3d	100%	
MC-LF	(No PAB presence)	12d ; 10 µg/L	---	---	------	
MC-LF	(PAB)	<2d; 10 µg/L	3d	19d	100%	
MC-LF	(No PAB presence)	6d; 10 µg/L	----	----	-----	
CYN	(PAB)	4-6d; 3 µg/L	---	---	-----	
CYN	(No PAB presence)	12d; 3.25 µg/L	---	---	------	
CYN	(PAB)	<2d; 3 µg/L	6.1d	17d	Approx 95%	
CYN	(No PAB presence)	6d; 4.25 µg/L	---	---	----	
MC-LR	*Stenotrophomonas sp.*	NSD; 700 µg/L	13 h	24 h	100%	[100]
MC-RR	*Stenotrophomonas sp.*	NSD; 1700 µg/L	11 h	24 h	100 %	[100]
MC-LR	L.Rhamnosus LC-705	NSD;100 µg/L	15h	24h	Approx 60	[101]
MC-LR	B.Longum 46	NSD;100 µg/L	12h	24h	Approx 70	[101]
MC-LR	*Bacillus sp.*	NSD; 100 µg/L	2d	4d	100 %	[102]
MC-LR	*Bacillus sp.*	2-7 d; 220 µg/L	2d	12 d	>74 %	[102]
		NSD; 100 µg/L	4d	7d	100%	
		NSD 100 µg/L	6d	8d	100%	

Cyanotoxin	Bacteria	Lag period; Initial concentration	Half-life of toxin	Full degradation period	Degradation efficiency	Ref.
	Sphingopyxis sp. USTB-05	1d; 50mg/L	2d	3d	100%	[96]
MC-LR	Sphingopyxis genes (isolate LH21)	NSD; 25 µg/L	>10d	12d	100%	[103]
		NSD; 10 µg/L	3d	4d	100%	
		NSD; 3 µg/L	1d	2d	100%	
	Sphingomonas ACM-3962	NSD; 25 µg/L	12d	15d	100%	
		NSD; 10 µg/L	4d	7d	100%	
MC-LA	Sphingopyxis genes	NSD; 30 µg/L	11d	12d	100%	
		NSD; 10 µg/L	3d	4d	100%	
		NSD; 5 µg/L	1d	2d	100%	
	Sphingomonas ACM-3962	NSD; 30 µg/L	14d	15d	100%	
		NSD; 10 µg/L	7d	9d	100%	
MC-LR	*Microbacterium, Ochrobactrum anthropi*	NSD; 250 µg/L	10 d	>30 d	84%	[104]
NOD^^	Natural microbial population	4-5d; 1 µg/mL	15d	15d	100%	[105]
MC-LR	*Pseudomonas aeruginosa*	< 1d; 1 µg/L	>15 d	24 d	100 %	[104]
MC-LR and MC-LA	Sphinopyxis sp.	NSD; 2.17 mg/L(MC-LR) and 3.27 mg/L(MC-LA)	<2 d (both) (8d)	8d	100%	[106]
MC-LR	Morganella morganii	NSD; 20 µg/L	6d	9d	100%	[94]
MC-LR	*Arthrobacter spp.,*	ND; 5 µg/mL	ND	3 d	84% (2 days), 100% (3 days)	[87]
MC-LR	*Brevibacterium sp.*	ND; 5 µg/mL	ND	3 d	23% (2 days); 100 % (3 days)	[87]

Cyanotoxin	Bacteria	Lag period; Initial concentration	Half-life of toxin	Full degradation period	Degradation efficiency	Ref.
	Sphingopyxis sp. USTB-05	1d; 50mg/L	2d	3d	100%	[96]
MC-LR	Stenotrophomonas maltophilia	NSD; 5 µg/mL	5 d	10 d	100% (10 days)	[107]
MC-LR	*Ralstonia solanacearum*	1d; >25 mg/L	2 days	3 d	100 % (3 days)	[108]
MC-LR	*Rhodococcus sp.*	ND; 5 µg/mL	ND	3 d	64% (2 days); 99 % (3 days)	[87]
CYN	*Bacillus* strain (AMRI-03)	NSD; 300 µg/L NSD; 100 µg/L NSD; 10 µg/L	3.5 d 3.75 d 5.5 d	6 days 7 days 8 days	100 %	[78]
CYN	*Aeromonas* sp.	1 d; 3000 µg/L	13d	14 days study (<50% degradation)	<50%	[74]
CYN	Aphanizomenon ovalisporum UAM 290	100 µg/L	----	40 days (almost no degradation)	<5 %	[109]

***probiotic bacterial cells; #enzymatic presence shown faster degradation than probiotic bacterial cells; PAB particulate attached bacteria; ^^ one of the many results database; NSD: No significant delay**

2.4.4 Bioadsorption with respect to MC-LR removal

De nombreuses expériences à l'échelle du laboratoire ont été menee jusqu'à présent (Tableau 1.4) comprenant diverses cyanotoxines et les espèces bactériennes impliquées dans leur dégradation. Cependant, le traitement biologique n'a pas été exploré à l'échelle pilote ou à l'échelle réelle, ce qui peut être dû aux connaissances limitées sur la cinétique et le mécanisme de dégradation des toxines et sur leur interaction avec différentes espèces bactériennes. La commercialisation d'un système de traitement biologique exige une compréhension de la biodégradation des cyanotoxines ainsi qu'une innovation dans la conception des technologies de traitement. Il est donc important d'étudier le mécanisme de biodégradation et le taux d'élimination des cyanotoxines dans le cadre d'une approche systématique afin de comprendre les paramètres qui les influencent. Toutefois, contrairement au traitement chimique, les processus biologiques progressent à un rythme cinétique

beaucoup plus lent, principalement en raison d'une période d'apparition plus longue (phase de latence élevée). En fait, plus de 90 % des études rapportées sur la dégradation biologique des cyanotoxines sont basées sur le mode de suspension (mécanisme de croissance en suspension). Le mode de croissance en suspension limite la cinétique de transfert de masse en raison de la présence d'ions métalliques, de MnO, d'autres matières oxydables, ce qui prolonge encore la phase de latence et rend les processus biologiques non toxiques bien que moins efficaces. L'importance du mécanisme de croissance attaché ou du traitement par biofilm promet non seulement un traitement sans toxicité mais aussi une meilleure biodégradation. Dans la section suivante, les deux modes de dégradation biologique sont examinés dans le contexte de l'élimination des cyanotoxines.

2.4.5 Biodegradation of cyanotoxin: Attached growth vs Suspended growth

Le procédé de croissance en suspension et le procédé de croissance en milieu fixe peuvent tous deux être utilisés dans une opération de bioréacteur pour l'élimination des cyanotoxines [110, 111]. Le succès du traitement biologique est influencé par la gestion de la microflore, le type de substrat dans le système, le besoin d'entretien énergétique, la stabilité pour résister à la charge de choc et la capacité de la biomasse à dégrader le composé d'intérêt (cyanotoxines) dans un bioréacteur [112,113]. La Figure 1.5 présente une conceptualisation du mécanisme de croissance en suspension et fixée des cellules bactériennes pour l'élimination des cyanotoxines. En phase de croissance en suspension, les bactéries sont censées obtenir de la nutrition et de l'oxygène de leur environnement de croissance où elles sont exposées à un grand rapport volume/surface moyen (liquide), qui est généralement insuffisant et essentiel pour la dégradation du substrat. D'autre part, le mécanisme de croissance attaché établit une surface optimale pour la croissance des bactéries, l'apport de nourriture/nutrition dans et autour d'une zone définie proche de leurs micro-colonies (comme le suppose la Figure 1.5). De cette façon, il assure un équilibre facile entre l'espace où les bactéries se développent et la facilité à effectuer leur activité métabolique [113].

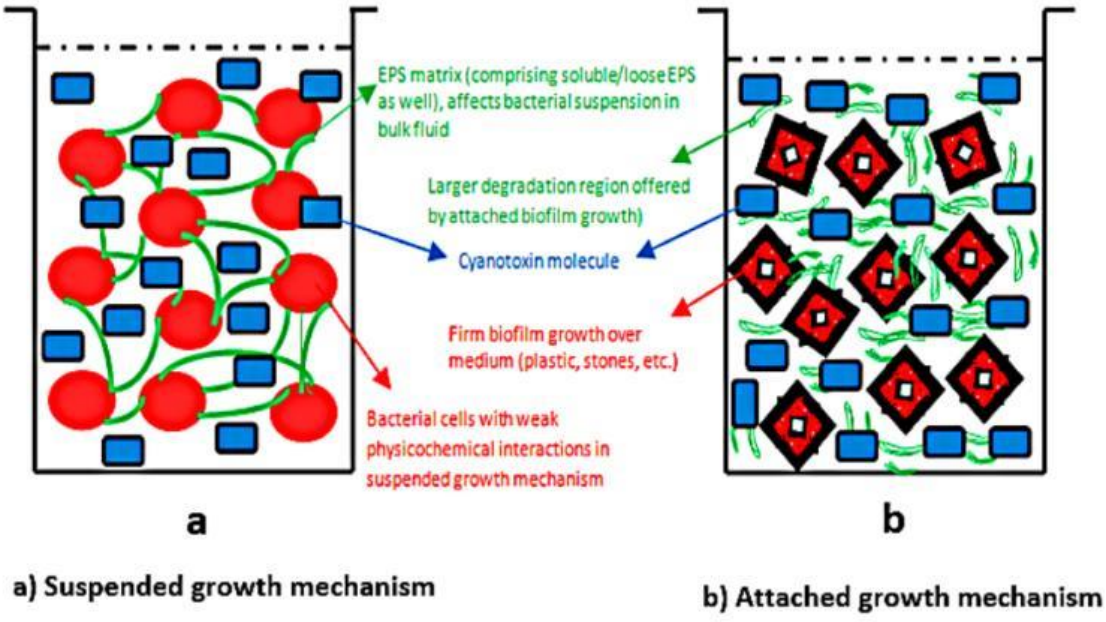

Figure 1.5: a) suspended vs. b) attached growth bacterial processes for the removal of cyanotoxins (Hypothetical picturization)

La couleur verte de la Figure 1.5 (a) représente le lien matriciel de la substance polymère extracellulaire (SPE) ou relié à deux ou plusieurs cellules bactériennes (exagérées) (couleur rouge) dans un mécanisme de croissance en suspension. On peut s'attendre à ce que l'espace vide soit plus grand entre ces liaisons et que la participation des molécules de cyanotoxines soit insuffisante. Par contre, la Figure 1.5 (b) représente le mécanisme de croissance attaché où la région/zone du biofilm devrait faire participer les molécules de cyanotoxines efficacement et en association avec la dégradation. On peut s'attendre à un espace vide relativement plus faible entre deux supports de milieu (couleur rouge) entre ces zones d'influence (indiquées en vert) créées par l'attachement bactérien. En outre, la dégradation de ces molécules devrait être affectée principalement par : a) la résilience au cisaillement de la matrice de substance polymérique extracellulaire (SPE) (qui se forme pendant la croissance bactérienne en utilisant le substrat), b) la surface d'adhésion (pour une croissance bactérienne initiale appropriée et la résilience pour contrer les charges de choc) et c) la zone de dégradation offerte par la communauté bactérienne.

Certaines études sur le biofilm suggèrent que le mécanisme d'assemblage et l'exportation de la SPE sont relativement préservés et nécessitent de la copolymérase de polysaccharides et d'autres protéines de ce type, qui peuvent être obtenues par les cyanobactéries présentes dans et autour des bactéries en cours de dégradation. Ceci libère de la cyanotoxine en conséquence [114]. Ces

copolymérases peuvent influencer la matrice de la SPE pendant la croissance bactérienne, de sorte que leur formation est soutenue par d'autres nutriments disponibles autour du biofilm (adaptés aux biofilms de croissance attachés). Une des études a également révélé que la présence et l'absence de ces nutriments (azote, phosphore, métaux traces) influencent la production des gènes *mlrA* dans la dégradation des cyanotoxines [115]. Le processus de croissance attaché où les biofilms sont principalement composés de cellules microbiennes, de SPE (constituant 50%-90% du carbone organique total des biofilms) [116], et de matrice de la SPE (avec une présence de copolymérase, d'autres sources de nutriments). On peut comprendre que le concept de bactérie de croissance attaché dans un bioréacteur a la possibilité de jouer un rôle important dans la dégradation des cyanotoxines. De plus, on s'attend à ce que le processus de croissance attaché subisse un taux de dégradation plus rapide que le mécanisme de croissance en suspension [116,117].

Le rôle de l'activité biologique accompagnée de l'adsorption a montré des améliorations dans l'élimination des cyanotoxines. De nombreuses études ont montré une augmentation de l'élimination des cyanotoxines en raison de l'inclusion de l'activité biologique sur les milieux GAC. La bioaugmentation dans les milieux a également montré une élimination accrue des cyanotoxines. Cependant, on n'a pas signalé beaucoup de cas de filtration avec du sable pour l'élimination des cyanotoxines jusqu'à présent. De plus, le sable est le média filtrant le plus largement utilisé dans les stations de traitement d'eau potable (STEP) et le plus important est la période opérationnelle qui dure habituellement de 10 à 30 minutes pour un filtre à sable rapide ou un filtre à sable supra-rapide. Cependant, la présence de divers polluants tels que les métaux, la matière organique naturelle, le carbone organique total, l'ammoniac ou des micropolluants comme la Microcystine-LR (MC-LR), limitent sa résistance en tant qu'adsorbant. Par conséquent, le concept de biofilm ou de biofiltre peut être exploré pour obtenir une solution rapide, non toxique et économique.

DÉDUCTION 7 : ***Le mode de croissance attaché permet une meilleure disponibilité des nutriments, un transfert de masse et une capacité à résister aux charges de choc comme on peut s'y attendre en raison de la présence de cyanotoxines et d'autres polluants pendant le traitement.***

2.4.6. Biofilter operation for cyanotoxins removal

Le biofiltre fonctionne principalement selon deux principes : l'adsorption et la dégradation. Il a été démontré que l'interférence biologique (cellules bactériennes ou formation d'un biofilm sur le média porteur) augmente la propriété d'adsorption d'un média filtrant. Par exemple, dans une étude pilote, l'activité biologique sur le GAC a favorisé l'élimination des anatoxines, non seulement en prouvant l'adsorption, mais aussi le processus biologique étant un aspect important dans la réalisation de la dégradation globale des toxines [118]. De nombreux auteurs ont signalé la polyvalence du filtre biologique basé sur la GAC qui a montré une dégradation réussie des MC [119,120]. Newcombe et al. (2002) [121] ont noté que la biodégradation dans les filtres à base de GAC entraînait une élimination importante des microcystines (>80 %). L'influence biologique sur l'adsorption physique a amélioré l'efficacité des filtres à éliminer les cyanotoxines. Par exemple, Wang et al. (2007) [119] ont constaté que la colonne de GAC stérile pouvait éliminer les MC- LR et les MC- LA à seulement 70 % et 40 % environ, respectivement. Mais plus tard, avec l'intrusion de la bioactivité, c'est-à-dire la croissance des cellules bactériennes sur la GAC, on a constaté une augmentation de leur élimination globale jusqu'à 90 % et 70 %, dans les 38 jours de fonctionnement, respectivement. L'élimination de la microcystine par un filtre à sable rapide a également été examinée, et on a constaté que la dégradation biologique était le principal mécanisme d'élimination plutôt que l'adsorption physique [119].

Une évaluation à l'échelle du laboratoire de l'élimination des cyanotoxines de la microcystite et du planktothrix a été étudiée à l'aide d'un filtre à sable lent, où l'on a constaté une élimination de 80 % et de 30 à 65 %, respectivement. Comme on ne peut s'attendre à ce que le filtre seul élimine toute la toxine extracellulaire, la biosorption avec une certaine biotransformation pourrait être le mécanisme dominant pendant le processus [122]. Bourne et al. (2006) [110] ont étudié la dégradation des MC-LR à 50 µg/L (mode de fonctionnement continu où l'eau décantée d'un volume de 20 L était transférée quotidiennement) dans six filtres à sable lents à l'échelle pilote. Après avoir inoculé le filtre avec *Sphingomonas sp.* , on a obtenu une élimination complète des MC-LR en 6 jours avec un taux de dégradation plus rapide que celui des filtres non inoculés.

En ce qui concerne les STEP (sable), l'unité de filtration est la seute étape de traitement possible où le système biologique peut être introduit. De plus, il a été prouvé que la dégradation biologique subit un traitement de l'eau sans toxines par rapport aux autres traitements physico-chimiques. Cependant, les études susmentionnées n'ont pas respecté la période de traitement. Dans une STEP, le temps de séjour de 15 à 25 minutes est généralement respecté pour le fonctionnement de l'unité de filtration. En raison de cette contrainte, il peut être difficile pour les microorganismes fixés de disposer d'un temps de contact suffisant entre eux et la molécule de cyanotoxine.

Cet aspect de l'approche hybride (physique et biologique) peut encore être amélioré si le milieu adsorbant est modifié. Une telle amélioration des médias filtrants largement utilisés (principalement le sable et le charbon actif) peut être improvisée pour fournir une surface plus efficace permettant une dégradation biologique accrue en éliminant la limitation posée par la phase de latence. De plus, les bactéries dégradant les cyanotoxines doivent avoir le potentiel de former un biofilm stable à long terme. Pour un processus de croissance attaché, il est essentiel d'évaluer le comportement d'adsorption avant de les appliquer dans un bioréacteur. Ho et ses collaborateurs (2006) [123] ont évalué la filtration biologique sur sable (biofilm fixé) dans une colonne de laboratoire pour l'élimination des MC-LR et des microcystines-LA à une concentration initiale de 20 µg/L. La biodégradation s'est avérée être le principal mécanisme (l'élimination par adsorption était secondaire). Les bactéries présentes dans le biofilm (formé par l'eau du réservoir alimenté en continu sur le sable prélevé dans la STEP) ressemblaient à celles de la *Sphingopyxis sp.* C- 1 (numéro d'ordre du NCBI AB161685) et à celles de la Sphingomonas sp. ACM-3962 (numéro d'ordre du NCBI AF411068), toutes deux codant pour les gènes *mlrA*. Bien que la période de latence ait duré 3 jours, une biodégradation complète a été obtenue en 4 jours environ. Avec une amélioration supplémentaire du processus par la réduction de la période de latence grâce à l'enrichissement de la culture cellulaire, l'élimination des cyanotoxines peut être rapide ou être étudiée de manière appropriée avec des surfaces adsorbantes plus efficaces (comme la bentonite, l'argile ou le charbon actif). Dans le passé, la communauté bactérienne native (dominante) des genres *Chryseobacterium* et *Pseudomonas* a également démontré sa capacité à éliminer d'autres métabolites cyanobactériens secondaires, notamment la géosmine et le 2-méthylisobornéol (MIB) [125-127]. Certaines études se sont révélées prometteuses pour le traitement biologique d'autres cyanotoxines que les CM,

notamment la cylindrospermopsine et la nodularine par l'intermédiaire des genres bactériens *Arthrobacter*, *Bacillus* et *Sphingomonas* [78, 128, 129]. Le potentiel de ces trois bactéries énumérées (non pathogènes pour l'homme également) peut être exploré et étudié en conjugaison avec les bactéries indigènes identifiées et dominantes résidant dans l'unité de filtration de la STEP. Cela pourrait renforcer le potentiel des genres bactériens mentionnés ci-dessus lorsqu'ils sont combinés avec des espèces bactériennes indigènes pour accélérer l'élimination des MC-LR. Par conséquent, à l'avenir, une méthode d'ensemencement appropriée de ces dégradants MC-LR (également capables de manipuler d'autres cyanotoxines) peut être réalisée pour s'attaquer à l'effet de toxicité posé par diverses cyanotoxines. Les exploitants de STEP peuvent également utiliser le lavage à contre-courant pour faire recirculer les dégradants MC-LR comme technique d'ensemencement afin de relever le défi de l'élimination des MC qui se produit pendant une période plus courte de l'année [131]. Le Tableau 1.5 présente certaines études de colonnes de filtration qui ont été réalisées pour l'élimination de la microcystine. Les genres bactériens : *Sphingomonas* s'est avéré être un dégradant potentiel des CM pour les études de filtration biologique active [123, 103, 110]. Cependant, la période de biodégradation était encore plus longue, ce qui limite la possibilité de moderniser ou de remplacer l'unité de filtration de la STEP existante.

Table 1.5: Various studies reported for the sand filter for the microcystin removal

Filter type	Filter specification	Cyanotoxin studied	Removal %	Initial toxin	Degradation period	Bacteria inoculated	Ref
Biologically active sand filter	0.5 ml/min, sand size: 0.5 mm, height=1 m; Diameter 3.5cm*	[Dha^7] microcystin-LR	100 %	5000 µg/L	7 d EBCT: not mentioned	*Novosphingobium* sp. KKU15 (bacterial concentration of 1.6×10^7CFU/cm^3 of sand)	[98]
Slow sand and bank filtration	0.8 m-1.3 m sand height, 0.6 m/d-2.4m/d (filter rate)	Microcystin	62% - 78%	6-10 µg/L	8h-24h*	NA	[78]
Biologically active sand filter	height 30 cm, internal diameter 2.5 cm; Flow	MC-LR and MC-LA	> 95 %	20-25 µg/L	(EBCT: 7.5-30 min)	*Sphingopyxis* sp. C1 (NCBI accession number	[123]

Filter type	Filter specification	Cyanotoxin studied	Removal %	Initial toxin	Degradation period	Bacteria inoculated	Ref
	rate: 0.3-1.2 m/h					AB161685); Sphingomonas sp. ACM-3962	
Biologically active slow sand filters	0.5m sand and 0.3 m water; PVC piping, 100mm in diameter; sand size: 0.20–0.40mm	MC-LR	> 75 %	50 µg/L	1d; EBCT: NA	*Sphingomonas* sp (5×10^8 cells (in a volume of 10 ml)	[110]
Biological Sand Filters	length of 30 cm, inner diameter of 2.5 cm at a bed height of 15 cm; flow rate: 0.6 m/h	MC-LR	100 %	3-20 µg/L	4d; 15 min EBCT	*Sphingopyxis* sp. C-1 (NCBI accession number AB161685)	[103]
Household slow Sand filter	Bed depth: 55 cm; sand size: 0.153 mm, diameter: 250 mm	MC-LR	>75 %	5.5 µg/L	Intermittent flow (2.95 m^3 m^{-2}/d) and continuous flow (1.22 m^3 m^{-2}/d); EBCT: 6 hours*	NA	[130]

***Values calculated based on the information available in the article; #Breakthrough of MC-LR occurred after backwashing and after 8-week study**

Le problème du temps de traitement des eaux avec un débit faible ou vide (EBCT) peut être résolu en diminuant la concentration de l'inoculum afin de contrôler la croissance excessive de la biomasse qui obstrue le milieu de sable (diminution du débit). Une telle stratégie pourrait éventuellement aider à éliminer les MC-LR dans la période de rétention de 15-25 min. De plus, l'exploration d'autres dégradeurs de MC-LR ainsi que d'autres souches bactériennes indigènes isolées de l'unité de filtration d'autres STEP peut aider les opérateurs de la station à atteindre le degré de traitement MC requis. De plus, il est possible de modifier davantage les milieux adsorbants peu coûteux, comme le sable, afin de les rendre plus rugueux et de leur donner une

plus grande surface, ce qui permet la formation d'un biofilm à long terme qui pourrait favoriser la bioadsorption des MC-LR.

> ***DÉDUCTION 8 :*** ***Les biofiltres peuvent s'avérer être une solution efficace pour le traitement des cyanotoxines. Le sable comme média filtrant peut rendre le procédé économique et rapide, ce qui devient pertinent pour les opérations de STEP et facile à mettre à niveau. Cependant, le faible capacité d'adsorption du sable peut poser des défis pour l'élimination d'autres contaminants et l'étude de la formation de biofilms devra être bien caractérisée.***

Référence

1. Saha, R., Liu, D., Hoynes-O'Connor, A., Liberton, M., Yu, J., Bhattacharyya-Pakrasi, M., Pakrasi, H. B. (2016). Diurnal Regulation of Cellular Processes in the CyanobacteriumSynechocystissp. Strain PCC 6803: Insights from Transcriptomic, Fluxomic, and Physiological Analyses. *MBio, 7*(3), e00464-00416.

2. Welker, M., & Steinberg, C. (2000). Rates of Humic Substance Photosensitized Degradation of Microcystin-LR in Natural Waters. *Environ Sci Technol, 34*(16), 3415-3419.Jones, G. J., & Negri, A. P. (1997). Persistence and degradation of cyanobacterial paralytic shellfish poisons (PSPs) in freshwaters. *Water Research, 31*(3), 525-533.

3. Jones, G. (1994). Release and degradation of microcystin following algicide treatment of a Microcystis aeruginosa bloom in a recreational lake, as determined by HPLC and protein phosphatase inhibition assay. *Water Research, 28*(4), 871-876.

4. Zanchett, G., & Oliveira-Filho, E. (2013). Cyanobacteria and Cyanotoxins: From Impacts on Aquatic Ecosystems and Human Health to Anticarcinogenic Effects. *Toxins (Basel), 5*(10), 1896-1917.

5. Kaebernick, M., Dittmann, E., Borner, T., & Neilan, B. A. (2002). Multiple Alternate Transcripts Direct the Biosynthesis of Microcystin, a Cyanobacterial. *Appl Environ Microbiol, 68*(2), 449-455.

6. Valério, E., Chaves, S., & Tenreiro, R. (2010). Diversity and Impact of Prokaryotic Toxins on Aquatic Environments: A Review. *Toxins (Basel), 2*(10), 2359-2410.

7.Kurmayer, R., Blom, J. F., Deng, L., & Pernthaler, J. (2014). Integrating phylogeny, geographic niche partitioning and secondary metabolite synthesis in bloom-forming Planktothrix. *The ISME Journal, 9*(4), 909-921. doi:10.1038/ismej.2014.189

8. Fewer, D. P., Jokela, J., Rouhiainen, L., Wahlsten, M., Koskenniemi, K., Stal, L. J., & Sivonen, K. (2009). The non-ribosomal assembly and frequent occurrence of the protease inhibitors spumigins in the bloom-forming cyanobacteriumNodularia spumigena. *Mol Microbiol, 73*(5), 924-937.

9. Humpage, A. R., Magalhaes, V. F., & Froscio, S. M. (2010). Comparison of analytical tools and biological assays for detection of paralytic shellfish poisoning toxins. *Anal Bioanal Chem, 397*(5), 1655-1671.

10. Liu, H., & Scott, P. M. (2011). Determination of the cyanobacterial toxin cylindrospermopsin in algal food supplements. *Food Additives & Contaminants: Part A, 28*(6), 786-790.

11. Moreira, C., Azevedo, J., Antunes, A., & Vasconcelos, V. (2013). Cylindrospermopsin: occurrence, methods of detection and toxicology. *J Appl Microbiol, 114*(3), 605-620.

12. Al-Tebrineh, J., Mihali, T. K., Pomati, F., & Neilan, B. A. (2010). Detection of Saxitoxin-Producing Cyanobacteria and Anabaena circinalis in Environmental Water Blooms by Quantitative PCR. *Appl Environ Microbiol, 76*(23), 7836-7842

13. Zhang, Y., Sui, X., Wang, X., Huang, H., Peng, G., Wang, S., & Fan, Z. (2014). A Novel Photocatalytic Material for Removing Microcystin-LR under Visible Light Irradiation: Degradation Characteristics and Mechanisms. *PLoS One, 9*(4), e95798.

14. El-Sheikh SM, Zhang G, El-Hosainy HM, Ismail AA, O'Shea KE, Falaras P, Kontos AG, Dionysiou DD: High performance sulfur, nitrogen and carbon doped mesoporous anatase–brookite TiO2 photocatalyst for the removal of microcystin-LR under visible light irradiation. *Journal of Hazardous Materials* 2014, 280:723-733.

15. Pelaez M, Falaras P, Kontos AG, de la Cruz AA, O'Shea K, Dunlop PSM, Byrne JA, Dionysiou DD: A comparative study on the removal of cylindrospermopsin and microcystins from water with NF-TiO2-P25 composite films with visible and UV–vis light photocatalytic activity. *Applied Catalysis B: Environmental* 2012, 121-122:30-39.

16. Lawton, L. A., & Robertson, P. K. J. (1999). Physico-chemical treatment methods for the removal of microcystins (cyanobacterial hepatotoxins) from potable waters. *Chemical Society Reviews, 28*(4), 217-224

17. De Freitas, A. M., Sirtori, C., Lenz, C. A., & Peralta Zamora, P. G. (2013). Microcystin-LR degradation by solar photo-Fenton, UV-A/photo-Fenton and UV-C/H_2O_2: a comparative study. *Photochem. Photobiol. Sci., 12*(4), 696-702.

18. Jacobs, L. C. V., Peralta-Zamora, P., Campos, F. R., & Pontarolo, R. (2013). Photocatalytic degradation of microcystin-LR in aqueous solutions. *Chemosphere, 90*(4), 1552-1557.

19. Pelaez, M., de la Cruz, A. A., O'Shea, K., Falaras, P., & Dionysiou, D. D. (2011). Effects of water parameters on the degradation of microcystin-LR under visible light-activated TiO2 photocatalyst. *Water Research, 45*(12), 3787-3796.

20. Verma, S., & Sillanpää, M. (2015). Degradation of anatoxin-a by UV-C LED and UV-C LED/H2O2 advanced oxidation processes. *Chemical Engineering Journal, 274*, 274-281. doi:10.1016/j.cej.2015.03.128

21. Pestana, C. J., Edwards, C., Prabhu, R., Robertson, P. K. J., & Lawton, L. A. (2015). Photocatalytic degradation of eleven microcystin variants and nodularin by TiO2 coated glass microspheres. *J Hazard Mater, 300*, 347-353. doi:10.1016/j.jhazmat.2015.07.016

22. Pinho LX, Azevedo J, Brito Â, Santos A, Tamagnini P, Vilar VJP, Vasconcelos VM, Boaventura RAR: Effect of TiO2 photocatalysis on the destruction of Microcystis aeruginosa cells and degradation of cyanotoxins microcystin-LR and cylindrospermopsin. *Chemical Engineering Journal* 2015, 268:144-152.

23. Li, W. y., Liu, Y., Sun, X. l., Wang, F., Qian, L., Xu, C., & Zhang, J. p. (2015). Photocatalytic degradation of MC-LR in water by the UV/TiO2/H2O2 process. *Water Science and Technology: Water Supply, 16*(1), 34-43.

24. Zhao, C., Pelaez, M., Dionysiou, D. D., Pillai, S. C., Byrne, J. A., & O'Shea, K. E. (2014). UV and visible light activated TiO2 photocatalysis of 6-hydroxymethyl uracil, a model compound for the potent cyanotoxin cylindrospermopsin. *Catalysis Today, 224*, 70-76.

25. Liang, Y., He, X., Chen, L., & Zhang, Y. (2014). Preparation and characterization of TiO2–Graphene@Fe3O4magnetic composite and its application in the removal of trace amounts of microcystin-LR. *RSC Adv., 4*(100), 56883-56891.

26. Neumann, U., & Weckesser, J. r. (1998). Elimination of microcystin peptide toxins from water by reverse osmosis. *Environmental Toxicology and Water Quality, 13*(2), 143-148.

27. Coral LA, Proença LAdO, de Jesus Bassetti F, Lapolli FR: Nanofiltration membranes applied to the removal of saxitoxin and congeners. *Desalination and Water Treatment* 2011, 27:8-17.

28. Misra, R., Kohler, E., Villiger, J., Posch, T., Derlon, N., Shabarova, T., . . . Blom, J. F. (2014). Biodegradation of Microcystins during Gravity-Driven Membrane (GDM) Ultrafiltration. *PLoS One, 9*(11), e111794. doi:10.1371/journal.pone.0111794

29. Nicholson, B. C., Rositano, J., & Burch, M. D. (1994). Destruction of cyanobacterial peptide hepatotoxins by chlorine and chloramine. *Water Research, 28*(6), 1297-1303

30. Bláha, L., Babica, P., & Maršálek, B. (2009). Toxins produced in cyanobacterial water blooms - toxicity and risks. *Interdisciplinary Toxicology, 2*(2).

31. Zamyadi, A., Ho, L., Newcombe, G., Daly, R. I., Burch, M., Baker, P., & Prévost, M. l. (2010). Release and Oxidation of Cell-Bound Saxitoxins during Chlorination ofAnabaena circinalisCells. *Environ Sci Technol, 44*(23), 9055-9061. doi:10.1021/es102130b

32. Rodríguez E, Onstad GD, Kull TPJ, Metcalf JS, Acero JL, von Gunten U: Oxidative elimination of cyanotoxins: Comparison of ozone, chlorine, chlorine dioxide and permanganate. *Water Research* 2007, 41:3381-3393.

33. Keijola, A. M., Himberg, K., Esala, A. L., Sivonen, K., & Hiis-Virta, L. (1988). Removal of cyanobacterial toxins in water treatment processes: Laboratory and pilot-scale experiments. *Toxicity Assessment, 3*(5), 643-656.

34. Orr, P. T., Jones, G. J., & Hamilton, G. R. (2004). Removal of saxitoxins from drinking water by granular activated carbon, ozone and hydrogen peroxide—implications for compliance with the Australian drinking water guidelines. *Water Research, 38*(20), 4455-4461. doi:10.1016/j.watres.2004.08.024

35. Yan, S., Jia, A., Merel, S., Snyder, S. A., O'Shea, K. E., Dionysiou, D. D., & Song, W. (2016). Ozonation of Cylindrospermopsin (Cyanotoxin): Degradation Mechanisms and Cytotoxicity Assessments. *Environ Sci Technol, 50*(3), 1437-1446. doi:10.1021/acs.est.5b04540

36. Rositano, J., Nicholson, B. C., & Pieronne, P. (1998). Destruction of Cyanobacterial Toxins By Ozone. *Ozone: Science & Engineering, 20*(3), 223-238.

37. Hall, T., Hart, J., Croll, B., & Gregory, R. (2000). Laboratory-Scale Investigations of Algal Toxin Removal by Water Treatment. *Water and Environment Journal, 14*(2), 143-149. doi:10.1111/j.1747-6593.2000.tb00241.x

38. M. Drikas, *Control and/or removal of toxins,* in *Toxic Cyanobacteria: Current Status of Research and Management*, Eds: D. A. Steffensen and B. C. Nicholson, Australian Centre for Water Quality, Salisbury, Australia, 1994, p. 93.

39. He, X., de la Cruz, A. A., & Dionysiou, D. D. (2013). Destruction of cyanobacterial toxin cylindrospermopsin by hydroxyl radicals and sulfate radicals using UV-254nm activation of hydrogen peroxide, persulfate and peroxymonosulfate. *Journal of Photochemistry and Photobiology A: Chemistry, 251*, 160-166. doi:10.1016/j.jphotochem.2012.09.017.

40. Lenntech, Ozone applications drinking water, https://www.lenntech.com/library/ozone/drinking/ozone-applications-drinking-water.html, Date Accessed: 12th April, 2018

41. Hart, J, Fawell, J.K and Croll, B. (1997) The fate of both intra and extracellular toxins during drinking water treatment. Special subject No. 18, SS18-1-6, IWSA World Congress, Blackwell Science, Oxford.

42. Lu, S., Wang, N., & Wang, C. (2018). Oxidation and biotoxicity assessment of microcystin-LR using different AOPs based on UV, O3 and H2O2. *Frontiers of Environmental Science & Engineering, 12*(3). doi:10.1007/s11783-018-1030-2

43. Zong, W., Wang, X., Du, Y., Zhang, S., Zhang, Y., & Teng, Y. (2017). Molecular Mechanism for the Regulation of Microcystin Toxicity to Protein Phosphatase 1 by Glutathione Conjugation Pathway. *Biomed Res Int, 2017*, 1-10. doi:10.1155/2017/9676504

44.Al Momani, F., Smith, D. W., & Gamal El-Din, M. (2008). Degradation of cyanobacteria toxin by advanced oxidation processes. *J Hazard Mater, 150*(2), 238-249

45. Al Momani, F. A., & Jarrah, N. (2010). Treatment and kinetic study of cyanobacterial toxin by ozone. *Journal of Environmental Science and Health, Part A, 45*(6), 719-731.

46.Pinkernell U, von Gunten U: Bromate Minimization during Ozonation: Mechanistic Considerations. *Environmental Science & Technology* 2001, 35:2525-2531.

47. Carlile, P.R. 1994 *Further Studies to Investigate Microcystin-LR and Anatoxin-a Removal from Water.* Report No. 0458, Foundation for Water Research, Marlow, UK.

48. Banker, R., Carmeli, S., Werman, M., Teltsch, B., Porat, R., & Sukenik, A. (2001). Uracil Moiety is Required for Toxicity of the Cyanobacterial Hepatotoxin Cylindrospermopsin. *Journal of Toxicology and Environmental Health, Part A, 62*(4), 281-288. doi:10.1080/009841001459432

49. Rositano, J., Newcombe, G., Nicholson, B., & Sztajnbok, P. (2001). Ozonation of nom and algal toxins in four treated waters. *Water Research, 35*(1), 23-32. doi:10.1016/s0043-1354(00)00252-9

50. Carrière, A., Prévost, M., Zamyadi, A., Chevalier, P., & Barbeau, B. (2010). Vulnerability of Quebec drinking-water treatment plants to cyanotoxins in a climate change context. *J Water Health, 8*(3), 455-465. doi:10.2166/wh.2009.207

51. Miller, M. J., & Fallowfield, H. J. (2001). Degradation of cyanobacterial hepatotoxins in batch experiments. *Water Sci Technol, 43*(12), 229-232.

52. Drogui P, Daghrir R, Simard M-C, Sauvageau C, Blais JF: Removal of microcystin-LR from spiked water using either activated carbon or anthracite as filter material. *Environmental Technology* 2012, 33:381-391.

53. Donati, C., Drikas, M., Hayes, R., & Newcombe, G. (1994). Microcystin-LR adsorption by powdered activated carbon. *Water Research, 28*(8), 1735-1742.

54. Vlad, S. (2015). *Treatment of the Cyanotoxin Anatoxin-a via Activated Carbon Adsorption.* UWSpace. Retrieved from http://hdl.handle.net/10012/9392

55. Ho, L., Slyman, N., Kaeding, U., & Newcombe, G. (2008). Optimizing PAC and chlorination practices for cylindrospermopsin removal. *Journal - American Water Works Association, 100*(11), 88-96. doi:10.1002/j.1551-8833.2008.tb09776.x

56. Cook, D., Newcombe, G., Sztajnbok, P., 2001. The application of powdered activated carbon for MIB and geosmin removal: predicting PAC doses in four raw waters. Water Research 35, 1325e1333.

57. Hart, J. and Stott, P. 1993 *Microcystin-LR Removal from Water*. Report FR 0367, Foundation for Water Research, Marlow, UK.

58. Bernezeau, F. 1994 Can microcystins enter drinking water distribution systems, In: D.A. Steffensen and B.C. Nicholson [Eds] *Toxic Cyanobacteria, Current Status of Research and Management.* Proceedings of an International Workshop, Adelaide, Australia, American Water Works Association Research Foundation, Australian Centre for Water Quality Research, Centre for Water Research, Belgium, 115-118.

59. Lambert, T. W., Holmes, C. F. B., & Hrudey, S. E. (1996). Adsorption of microcystin-LR by activated carbon and removal in full scale water treatment. *Water Research, 30*(6), 1411-1422.

60. Ho, L., Tanis-Plant, P., Kayal, N., Slyman, N., & Newcombe, G. (2009). Optimising water treatment practices for the removal of Anabaena circinalis and its associated metabolites, geosmin and saxitoxins. *J Water Health, 07*(4), 544. doi:10.2166/wh.2009.075

61. Kumar, P., Hegde, K., Brar, S. K., Cledon, M., Kermanshahi-pour, A., Roy-Lachapelle, A., & Galvez-Cloutier, R. (2018). Biodegradation of microcystin-LR using acclimatized bacteria isolated from different units of the drinking water treatment plant. *Environmental Pollution, 242*, 407-416. doi:10.1016/j.envpol.2018.07.008

62. Silva Buarque, N. M., de Brito Buarque, H. L., & Capelo-Neto, J. (2015). Adsorption kinetics and diffusion of Saxitoxins on granular-activated carbon: influence of pore size distribution. *Journal of Water Supply: Research and Technology—AQUA, 64*(3), 344. doi:10.2166/aqua.2015.140

63. Shi, H., Ding, J., Timmons, T., & Adams, C. (2012). pH effects on the adsorption of saxitoxin by powdered activated carbon. *Harmful Algae, 19*, 61-67. doi:10.1016/j.hal.2012.05.008

64. Minatol, W., Jones G., Craig, K. and Naylor, R. (1993), Removal of low level cyanobacterial peptide toxins from drinking water using powdered and granular activated carbon and chlorination — Results of laboratory and pilot plant studies. Proceedings of the 15th Federal Convention of the Australian Water and Wastewater Association, April 18–23, 1993, Gold Coast, Queensland, Australia. Vol. 2. Australian Water and Wastewater Association. pp. 339–346

65. Lee, J., & Walker, H. W. (2006). Effect of Process Variables and Natural Organic Matter on Removal of Microcystin-LR by PAC−UF†. *Environ Sci Technol, 40*(23), 7336-7342.

66. World Health Organisation. Public Health and the Environment. WHO; Geneva: 2009. Guidelines for drinking water quality policies and procedures used in updating the WHO Guidelines for Drinking Water Quality

67. Gray, N. F. (2008). *Drinking Water Quality: Problems and Solutions*: Cambridge University Press.

68. Wang, H., Ho, L., Lewis, D. M., Brookes, J. D., & Newcombe, G. (2007). Discriminating and assessing adsorption and biodegradation removal mechanisms during granular activated carbon filtration of microcystin toxins. *Water Research, 41*(18), 4262-4270

69. Newcombe, G., Cook, D., Brooke, S., Ho, L., & Slyman, N. (2008). Treatment options for microcystin toxins: Similarities and differences between variants. *Environ Technol, 24*(3), 299-308. doi:10.1080/09593330309385562

70. Gimbel, R., Graham, N., & Collins, M. R. (2006). *Recent Progress in Slow Sand and Alternative Biofiltration Processes*: Chapter 19, Biofiltration of cyanotoxins toxin: an Australian perspective, IWA Publishing.

71. Imanishi, S., Kato, H., Mizuno, M., Tsuji, K., & Harada, K.-i. (2005). Bacterial Degradation of Microcystins and Nodularin. *Chemical Research in Toxicology, 18*(3), 591-598.

72. Zhang, Y., Wei, H., Xin, Q., Wang, M., Wang, Q., Wang, Q., & Cong, Y. (2016). Process optimization for microcystin-LR degradation by Response Surface Methodology and mechanism analysis in gas–liquid hybrid discharge system. *J Environ Manage, 183*, 726-732.

73. Edwards, C., & Lawton, L. A. (2009). Chapter 4 Bioremediation of Cyanotoxins. *67*, 109-129.

74. Dziga, D., Kokocinski, M., Maksylewicz, A., Czaja-Prokop, U., & Barylski, J. (2016). Cylindrospermopsin Biodegradation Abilities of Aeromonas sp. Isolated from Rusałka Lake. *Toxins (Basel), 8*(3), 55.

75. Mazur-Marzec H, Toruńska A, Błońska MJ, Moskot M, Pliński M, Jakóbkiewicz-Banecka J, Węgrzyn G: Biodegradation of nodularin and effects of the toxin on bacterial isolates from the Gulf of Gdańsk. *Water Research* 2009, 43:2801-2810.

76. Feng N, Yang F, Yan H, Yin C, Liu X, Zhang H, Xu Q, Lv L, Wang H: Pathway for Biodegrading Nodularin (NOD) by Sphingopyxis sp. USTB-05. *Toxins* 2016, 8:116.

77. Hu, L., Zhang, F., Liu, C., & Wang, M. (2012). Biodegradation of Microcystins by Bacillus sp. strain EMB. *Energy Procedia, 16*, 2054-2059.

78. Mohamed, Z. A., & Alamri, S. A. (2012). Biodegradation of cylindrospermopsin toxin by microcystin-degrading bacteria isolated from cyanobacterial blooms. *Toxicon, 60*(8), 1390-1395.

79. Saito, T., Sugiura, N., Itayama, T., Inamori, Y., & Matsumura, M. (2003). Biodegradation of microcystis and microcystins by indigenous nanoflagellates on biofilm in a practical treatment facility. *Environ Technol, 24*(2), 143-151.

80. Manage, P. M., Edwards, C., Singh, B. K., & Lawton, L. A. (2009). Isolation and Identification of Novel Microcystin-Degrading Bacteria. *Appl Environ Microbiol, 75*(21), 6924-6928.

81. Yang F, Neilan B Zhou Y, Yin L, Zhu G, Liang G, Pu Y: Microcystin-Degrading Activity of an Indigenous Bacterial Strain Stenotrophomonas acidaminiphila MC-LTH2 Isolated from Lake Taihu. *PLoS ONE* 2014, 9:e86216.

82. Tsuji, K., Setsuda, S., Watanuki, T., Kondo, F., Nakazawa, H., Suzuki, M., & Harada, K.-I. (1996). Microcystin levels during 1992-95 for lakes sagami and tsukui-japan. *Natural Toxins, 4*(4), 189-194.

83. Kull, T. P. J., Backlund, P. H., Karlsson, K. M., & Meriluoto, J. A. O. (2004). Oxidation of the Cyanobacterial Hepatotoxin Microcystin-LR by Chlorine Dioxide: Reaction Kinetics, Characterization, and Toxicity of Reaction Products. *Environ Sci Technol, 38*(22), 6025-6031.

84. Lezcano, M., J. Morón-López, R. Agha, I. López-Heras, L. Nozal, A. Quesada and R. El-Shehawy (2016). "Presence or Absence of mlr Genes and Nutrient Concentrations Co-Determine the Microcystin Biodegradation Efficiency of a Natural Bacterial Community." Toxins 8(11): 318

85. Shang, L., Feng, M., Xu, X., Liu, F., Ke, F., & Li, W. (2018). Co-Occurrence of Microcystins and Taste-and-Odor Compounds in Drinking Water Source and Their Removal in a Full-Scale Drinking Water Treatment Plant. *Toxins (Basel), 10*(1), 26. doi:10.3390/toxins10010026

86. Kormas, K. A., & Lymperopoulou, D. S. (2013). Cyanobacterial Toxin Degrading Bacteria: Who Are They? *Biomed Res Int, 2013*, 1-12.

88. Kulasooriya, S. A. (2012). Emeritus Professor of Botany, University of Peradeniya, Peradeniya, Sri Lanka and Visiting Professor Institute of Fundamental Studies, Kandy. *Ceylon Journal of Science (Biological Sciences), 40*(2).

89. Bourne, D. G., Jones, G. J., Blakeley, R. L., Jones, A., Negri, A. P., & Riddles, P. (1996). Enzymatic pathway for the bacterial degradation of the cyanobacterial cyclic peptide toxin microcystin LR. *Appl Environ Microbiol, 62*(11), 4086-4094.

90. Cousins, I. T., Bealing, D. J., James, H. A., & Sutton, A. (1996). Biodegradation of microcystin-LR by indigenous mixed bacterial populations. *Water Research, 30*(2), 481-485.

91. Ishii H, Abe T. Release and biodegradation of microcystins in blue-green algae, Microcystis PCC7820. Journal of the School of Marine Science and Technology Tokai University 2000;49: 143–157

92. Christoffersen, K., Lyck, S., & Winding, A. (2002). Microbial activity and bacterial community structure during degradation of microcystins. *Aquatic Microbial Ecology, 27*, 125-136.

93. Rapala, J., Lahti, K., Sivonen, K., & Niemelä, S. I. (1994). Biodegradability and adsorption on lake sediments of cyanobacterial hepatotoxins and anatoxin-a. *Lett Appl Microbiol, 19*(6), 423-428.

94. Eleuterio, L., & Batista, J. R. (2010). Biodegradation studies and sequencing of microcystin-LR degrading bacteria isolated from a drinking water biofilter and a fresh water lake. *Toxicon, 55*(8), 1434-1442.

95. Maghsoudi, E., Fortin, N., Greer, C., Duy, S. V., Fayad, P., Sauvé, S., Dorner, S. (2015). Biodegradation of multiple microcystins and cylindrospermopsin in clarifier sludge and a drinking water source: Effects of particulate attached bacteria and phycocyanin. *Ecotoxicol Environ Saf, 120*, 409-417.

96. Zhang, M., Pan, G., & Yan, H. (2010). Microbial biodegradation of microcystin-RR by bacterium Sphingopyxis sp. USTB-05. *J Environ Sci (China), 22*(2), 168-175.

97. Alamri, S. A. (2012). Biodegradation of microcystin-RR by Bacillus flexus isolated from a Saudi freshwater lake. *Saudi Journal of Biological Sciences, 19*(4), 435-440.

98. Somdee, T., Thunders, M., Ruck, J., Lys, I., Allison, M., & Page, R. (2013). Degradation of [Dha7]MC-LR by a Microcystin Degrading Bacterium Isolated from Lake Rotoiti, New Zealand. *ISRN Microbiology, 2013*, 1-8.doi:10.1155/2013/596429

99. Valeria, A. M., Ricardo, E. J., Stephan, P., & Alberto, W. D. (2006). Degradation of Microcystin-RR by Sphingomonas sp. CBA4 isolated from San Roque reservoir (Córdoba – Argentina). *Biodegradation, 17*(5), 447-455.

100. Chen J, Hu LB, Zhou W, Yan SH, Yang JD, Xue YF, Shi ZQ: Degradation of Microcystin-LR and RR by a Stenotrophomonas sp. Strain EMS Isolated from Lake Taihu, China. *International Journal of Molecular Sciences* 2010, 11:896-911.

101. Nybom, S. M. K., Dziga, D., Heikkilä, J. E., Kull, T. P. J., Salminen, S. J., & Meriluoto, J. A. O. (2012). Characterization of microcystin-LR removal process in the presence of probiotic bacteria. *Toxicon, 59*(1), 171-181.

102. Kansole M, Lin T-F: Microcystin-LR Biodegradation by Bacillus sp.: Reaction Rates and Possible Genes Involved in the Degradation. *Water* 2016, 8:508

103. Ho, L., Hoefel, D., Saint, C. P., & Newcombe, G. (2007). Isolation and identification of a novel microcystin-degrading bacterium from a biological sand filter. *Water Research, 41*(20), 4685-4695.

104. Ramani, A., Rein, K., Shetty, K. G., & Jayachandran, K. (2011). Microbial degradation of microcystin in Florida's freshwaters. *Biodegradation, 23*(1), 35-45.

105. Edwards, C., Graham, D., Fowler, N., & Lawton, L. A. (2008). Biodegradation of microcystins and nodularin in freshwaters. *Chemosphere, 73*(8), 1315-1321.

106. Ho, L., Gaudieux, A.-L., Fanok, S., Newcombe, G., & Humpage, A. R. (2007). Bacterial degradation of microcystin toxins in drinking water eliminates their toxicity. *Toxicon, 50*(3), 438-441.

107. Idroos, F. S., De Silva, B., & Manage, P. M. (2017). Biodegradation of microcystin analogues by Stenotrophomonas maltophilia isolated from Beira Lake Sri Lanka. *Journal of the National Science Foundation of Sri Lanka, 45*(2), 91. doi:10.4038/jnsfsr.v45i2.8175

108. Zhang, M. L., Yan, H., & Pan, G. (2011). Microbial degradation of microcystin-LR byRalstonia solanacearum. *Environ Technol, 32*(15), 1779-1787. doi:10.1080/09593330.2011.556148

109. Wormer, L., Cirés, S., Carrasco, D., & Quesada, A. (2008). Cylindrospermopsin is not degraded by co-occurring natural bacterial communities during a 40-day study. *Harmful Algae, 7*(2), 206-213.

110. Bourne, D. G., Blakeley, R. L., Riddles, P., & Jones, G. J. (2006). Biodegradation of the cyanobacterial toxin microcystin LR in natural water and biologically active slow sand filters. *Water Research, 40*(6), 1294-1302.

111. Kayal, N., Newcombe, G., & Ho, L. (2008). Investigating the fate of saxitoxins in biologically active water treatment plant filters. *Environ Toxicol, 23*(6), 751-755.

112. H. J. Yeon , D. Chang, D. W. Kim, B. K. Kim, J. K. Choi, S. Y. Lim, C. Y. Yoon, D. J. Son, W. Y. Kim Comparison of Attached Growth Process with Suspended Growth Process World Academy of Science, Engineering and Technology 60 2011

113. Comparison of Suspended Growth and Attached Growth Wastewater Treatment Process: A Case Study of Wastewater Treatment Plant at MNIT, Jaipur, Rajasthan, India Neetu Dabi, European Journal of Advances in Engineering and Technology, 2015, 2(2): 102-105

114. Cassier-Chauvat, C., Veaudor, T., & Chauvat, F. (2016). Comparative Genomics of DNA Recombination and Repair in Cyanobacteria: Biotechnological Implications. *Front Microbiol, 7*.

115. Lezcano, M., Morón-López, J., Agha, R., López-Heras, I., Nozal, L., Quesada, A., & El-Shehawy, R. (2016). Presence or Absence of mlr Genes and Nutrient Concentrations Co-Determine the Microcystin Biodegradation Efficiency of a Natural Bacterial Community. *Toxins (Basel), 8*(11), 318.

116. Carrasco, D., Moreno, E., Sanchis, D., Wörmer, L., Paniagua, T., Del Cueto, A., & Quesada, A. (2006). Cyanobacterial abundance and microcystin occurrence in Mediterranean water reservoirs in Central Spain: microcystins in the Madrid area. *European Journal of Phycology, 41*(3), 281-291.

117. Stewart, P. S. (2003). Diffusion in Biofilms. *J Bacteriol, 185*(5), 1485-1491.

118. UK WIR, 1995 *GAC Tests to Evaluate Algal Toxin Removal.* Report DW-07/C, UK Water Industry Research Ltd., London.

119. Wang, H., Ho, L., Lewis, D. M., Brookes, J. D., & Newcombe, G. (2007). Discriminating and assessing adsorption and biodegradation removal mechanisms during granular activated carbon filtration of microcystin toxins. *Water Research, 41*(18), 4262-4270.

120. Ho, L., & Newcombe, G. (2007). Evaluating the adsorption of microcystin toxins using granular activated carbon (GAC). *Journal of Water Supply: Research and Technology—AQUA, 56*(5), 281.

121. Newcombe, G. (2002). Removal of algal toxins from drinking water using ozone and GAC. American Water Works Association Reseach Foundation and American Water Works Association, Denver, Colorado

122. Keijola, A. M., Himberg, K., Esala, A. L., Sivonen, K., & Hiis-Virta, L. (1988). Removal of cyanobacterial toxins in water treatment processes: Laboratory and pilot-scale experiments. *Toxicity Assessment, 3*(5), 643-656.

123. Ho, L., Meyn, T., Keegan, A., Hoefel, D., Brookes, J., Saint, C. P., & Newcombe, G. (2006). Bacterial degradation of microcystin toxins within a biologically active sand filter. *Water Research, 40*(4), 768-774.

124. Tony Briscoe (2019), "Drinking water supplying Great Lake turns toxic" weblink: stuff.co.nz/environment/117561856/drinking-water-supplying-great-lake-turns-toxic (Accessed: 10th January, 2020).

125. Egashira, K., Ito, K., & Yoshiy, Y. (1992). Removal of Musty Odor Compound in Drinking Water by Biological Filter. *Water Science and Technology, 25*(2), 307-314. doi:10.2166/wst.1992.0066

126. Eaton, R. W., & Sandusky, P. (2009). Biotransformations of (+/−)-geosmin by terpene-degrading bacteria. *Biodegradation, 21*(1), 71-79. doi:10.1007/s10532-009-9282-y

127. Zhou, B., Yuan, R., Shi, C., Yu, L., Gu, J., & Zhang, C. (2011). Biodegradation of geosmin in drinking water by novel bacteria isolated from biologically active carbon. *J Environ Sci (China), 23*(5), 816-823.

128. Kato, H., Imanishi, S. Y., Tsuji, K., & Harada, K.-i. (2007). Microbial degradation of cyanobacterial cyclic peptides. *Water Research, 41*(8), 1754-1762. doi:10.1016/j.watres.2007.01.003

129. Lawton, L. A., Welgamage, A., Manage, P. M., & Edwards, C. (2011). Novel bacterial strains for the removal of microcystins from drinking water. *Water Science and Technology, 63*(6), 1137-1142. doi:10.2166/wst.2011.352

130. Sathishkumar, M., Pavagadhi, S., Vijayaraghavan, K., Balasubramanian, R., & Ong, S. L. (2011). Concomitant uptake of microcystin-LR and -RR by peat under various environmental conditions. *Chemical Engineering Journal, 172*(2-3), 754-762. doi:10.1016/j.cej.2011.06.058

131. Jayathilake, P. G., Jana, S., Rushton, S., Swailes, D., Bridgens, B., Curtis, T., & Chen, J. (2017). Extracellular Polymeric Substance Production and Aggregated Bacteria Colonization Influence the Competition of Microbes in Biofilms. *Front Microbiol, 8*. doi:10.3389/fmicb.2017.01865

132. Liu, X., Chen, Z., Zhou, N., Shen, J., & Ye, M. (2010). Degradation and detoxification of microcystin-LR in drinking water by sequential use of UV and ozone. *J Environ Sci (China), 22*(12), 1897-1902.

133.Al Momani, F., Smith, D. W., & Gamal El-Din, M. (2008). Degradation of cyanobacteria toxin by advanced oxidation processes. *J Hazard Mater, 150*(2), 238-249

134. Zong, W., Wang, X., Du, Y., Zhang, S., Zhang, Y., & Teng, Y. (2017). Molecular Mechanism for the Regulation of Microcystin Toxicity to Protein Phosphatase 1 by Glutathione Conjugation Pathway. *Biomed Res Int, 2017*, 1-10. doi:10.1155/2017/9676504

135. Chang, J., Chen, Z.-l., Wang, Z., Kang, J., Chen, Q., Yuan, L., & Shen, J.-m. (2015). Oxidation of microcystin-LR in water by ozone combined with UV radiation: The removal and degradation pathway. *Chemical Engineering Journal, 276*, 97-105. doi:10.1016/j.cej.2015.04.070

PARTIE 3: PROBLÉMATIQUE

Sur la base de la revue de la littérature, les problématiques suivantes ont été définies et doivent être abordes avant de formuler les hypothèses et les objectifs des travaux.

3.1 Risques associés aux voies physiques et chimiques pour l'élimination du MC-LR et l'importance de la biodégradation

Les processus de traitement physico-chimiques tels que la photocatalyse, l'ozonation et la chloration génèrent des **sous-produits toxiques**. En plus, l'utilisation de **doses élevées de réactifs** est nécessaire pour remédier aux contraintes opérationnelles courantes telles qu'un changement soudain de pH, la présence de matière organique naturelle ainsi que la présence de cyanotoxine (ex. : MC-LR). L'utilisation à grande échelle de réactifs chimiques implique un énorme capital et des coûts opérationnels élevés. L'ozonation et la chloration nécessitent un dosage chimique élevé (ozone et produits chlorés) en plus de former des sous-produits qui ne sont pas faciles à identifier. La plupart du temps, ces processus sont inefficaces et seule **une élimination partielle de MC-LR** est obtenue. Étant donné que les processus de traitement mentionnés ci-dessus constituent un aspect du prétraitement (pré-oxydation) d'une UPEP typique, l'élimination de la MC-LR résiduelle est assumée par l'unité de filtration où le sable de quartz est le média filtrant le plus couramment utilisé. Contrairement au processus physico-chimique, le processus de biodégradation produit peu ou pas de sous-produits toxiques et l'hydroxylation MC-LR rompt la liaison Adda-Arg de la structure multi-peptide MC-LR, menant à une minéralisation efficace. L'ozonation est préférée à la chloration ces jours-ci en raison de la faible production d'éléments dangereux et sa réactivité non spécifique par rapport à la matière organique naturelle et la MC-LR. **Cependant, la forte dose d'ozone reste une préoccupation dans les UPEP.** *Par conséquent, un processus hybride impliquant l'ozonation et le biofiltre devrait être étudié pour réduire la dose d'oxydant et éliminer le MC-LR sans formation de sous-produits toxiques.*

3.2 Processus biologique : vitesse de dégradation lente

Le système basé sur du **biofilm adsorbé à la surface** d'un matériau inerte **ne permet pas de s'adapter au temps de rétention** de l'unité de filtration (généralement 0,5 heure-1 heure) due à une plus faible vitesse de dégradation des contminants. Par conséquent il est nécessaire

d'augmenter **la cinétique de biodégradation du processus d'adsorption**. Comme mentionné dans la revue de la littérature, les bactéries natives exposées aux cyanotoxines (MC-LR) se comportent bien en améliorant la cinétique de dégradation. Les bactéries adaptées à un environnement contenant de la MC-LR (par exemple, les bactéries présentes dans le biofilm de l'unité d'adsorption GAC) favorise l'élimination du MC-LR.

3.3 Biodégradation MC-LR insuffisante dans les biofiltres en raison du type d'espèces bactériennes formant le biofilm et de la faible activité biologique associée

Dans la plupart des systèmes de filtration, le temps de rétention typique varie entre 15 et 45 minutes. Par conséquent, **les espèces bactériennes natives attachées au matériau adsorbant (biofilm) pourraient s'avérer non efficaces et, par conséquent, la MC-LR pourraient ne pas être éliminés d'une façon efficace de l'eau**. Le rôle des espèces bactériennes appropriées est non seulement crucial dans la biodégradation du MC-LR, mais également dans la formation d'un biofilm efficace et actif sur de longues périodes. Par conséquent, **l'activité biologique prévalant dans les biofiltres à lit statique (comme le filtre biosable) peut limiter la capacité de biodégradation des micro-organismes en raison de la faible surface spécifique de l'adsorbant (sable)**. De plus, en raison de la présence d'autres polluants de l'eau, la faible activité biologique pourrait ne pas être suffisante pour éliminer la MC-LR étant donné qu'il ne s'agit pas d'une source de carbone préférentielle pour les bactéries formant le biofilm.

3.4 Faible capacité d'adsorption du sable, inefficacité au niveau de l'élimination du MC-LR

Les milieux sableux représentent une famille d'adsorbants à faibles propriétés absorbantes et ne garantissent pas l'élimination totale des polluants présents dans l'eau, en particulier les micropolluants et les contaminants émergents. Les directives de l'OMS pour la plupart des polluants, y compris pour la MC-LR (<1 µg / L), peine à être respectées à cause de l'utilisation des systèmes de filtres basé sur le système bio-sable. De plus, la capacité de saturation du sable de quartz est faible, ce qui se traduit par l'inefficacité de l'élimination du MC-LR et plusieurs autres macro-polluants, notamment des ions métalliques et les composés organiques dissous dans l'eau filtrée.

3.5 Défis lors de la mise en échelle du système de filtre bio-sable

Les paramètres hydrodynamiques tels que la pression à l'alimentation et la vitesse d'écoulement influencent le fonctionnement global du filtre. **Dans un filtre à l'échelle pilote, les effets de paroi et le garnissage de la surface jouent un rôle important qui influence le degré de liberté (DL) du fluide (pour trouver son chemin le moins résistif). Ainsi, la contrainte de cisaillement à laquelle sont exposés les contaminants adsorbés sur la surface du sable est plus élevée**. Au même moment, un plus faible DL dans les colonnes à l'échelle laboratoire **augmente la perte de pression** dans les filtres, **diminuant ainsi le taux de filtration (augmentant ainsi le temps de résidence hydraulique) et favorisant l'élimination des contaminants**. Par conséquent, à l'échelle pilote, l'efficacité d'élimination des contaminants de l'eau est surestimée. De ce fait, il est nécessaire de trouver la dimension minimale de mise en échelle qui permet d'éliminer les effets possibles du court-circuit et donc de favoriser un régime d'écoulement plus fluide.

PARTIE 4. HYPOTHÈSE

Le présent travail de recherche comprend les hypothèses suivantes:

1.) Hypothèse 1 au problème 3.1: La formation de sous-produits toxiques lors du traitement de l'eau par ozonation pourrait être résolue en hybridant l'ozonation avec l'unité de biofiltre. *Un traitement à l'ozone plus contrôlé, utilisant une plus faible dose d'ozone (tel que pratiqué dans les UPEP) pourrait éventuellement réduire la formation de sous-produits toxiques.* La MC-LR résiduelle obtenue suite à l'ozonation «contrôlée» peut être alimentée directement dans le biofiltre qui peut être bioaugmenté avec des dégradeurs MC-LR connus pour obtenir une élimination complète du MC-LR. L'eau traitée ainsi obtenue présenterait une toxicité réduite.

2.) Hypothèse 2 du problème 3.2: Il a été largement démontré dans la littérature que les bactéries indigènes isolées de diverses sources telles que les lacs, les rivières, les étangs et d'autres écosystèmes aquatiques où les cyanobactéries ont poussé dans le passé, ont la capacité à dégrader la MC-LR. Cependant, ils prennent plus de temps pour obtenir une dégradation complète de MC-LR que le temps de séjour d'une unité de filtration dans un UPEP. Par conséquent, une bonne acclimatation des bactéries isolées pourrait aider à améliorer la dégradation du MC-LR. Cela peut empêcher les bactéries de subir un choc toxique (effets dus à une exposition soudaine au MC-LR) pendant l'opération. *En outre, l'utilisation de bactéries indigènes, telles que celles présentes dans les unités UPEP, peut être explorée compte tenu de leur adaptabilité rapide qui pourrait améliorer le taux de dégradation de MC-LR. Par conséquent, les bactéries de différentes unités de la station d'épuration peuvent être isolées et évaluées pour leurs performances en termes d'élimination du MC-LR et, si possible, peuvent être acclimatées dans un environnement MC-LR pour offrir une meilleure élimination.* Ces bactéries, si elles présentent une résilience dans un environnement MC-LR, peuvent être très avantageuses car elles seront mieux adaptées, fiables et autosuffisantes.

3.) Hypothèse 3 (a) au problème 3.3: Application de biofiltre sur lit statique : Le potentiel de dégradation lente de MC-LR d'espèces bactériennes indigènes pourrait être accéléré en les co-cultivant avec des dégradeurs MC-LR connus dans le biofiltre (bioaugmentation). Les espèces bactériennes formant un biofilm et dérivées des sédiments précédemment exposés aux cellules cyanobactériennes dans la colonne d'eau des lacs, des étangs, etc., ont en fait montré une meilleure

capacité à dégrader le MC-LR. *Ainsi, ces dégradeurs MC-LR connus sous forme d'Arthrobacter ramosus, Bacillus sp. Et Sphingomonas sp. pourraient être explorés comme une potentialité de les co-cultiver individuellement avec les bactéries natives isolées de l'unité de filtration de UPEP (aide rapide à la formation de biofilm).* Cela pourrait aider à déchiffrer le comportement de ces bactéries natives avec les bactéries dégradant le MC-LR pour améliorer la biodégradation du MC-LR dans un filtre bio-sable (lit statique).

4.) Hypothèse 3 (b) du problème 3.3: Application d'un biofiltre à lit dynamique: divers microorganismes se développant en mode de croissance suspendu ou attaché ont montré un potentiel de dégradation du MC-LR. Par conséquent, la combinaison de ces deux aspects dans un seul réacteur sous la forme d'un réacteur à biofilm à lit fluidisé (biofiltre dynamique) pourrait améliorer le transfert de masse global (cinétique) qui peut effectivement décomposer plus de molécules MC-LR par rapport à la pratique uniquement du mécanisme de croissance suspendu. De tels réacteurs fonctionnent de manière à ce que le biofilm développé sur les milieux appropriés (bioporteurs), soit en mouvement fluidisé constant via l'aération. *Ce mode de fonctionnement devrait fournir un bon environnement oxydant dans et autour du biofilm développé où le MC-LR est diffusé et oxydé.* On peut également penser que cette application traite les boues d'eau potable présentes dans le réservoir de sédimentation (< 3 g/L de solides en suspension) contenant des cellules cyanobactériennes coagulées au fond du réservoir qui pourraient libérer périodiquement de la cyanotoxine. *Ces mélanges de boues pourraient améliorer la formation de biofilms sur les bioporteurs et simultanément pourraient également aider à éliminer la cyanotoxine libérée des cellules cyanobactériennes lysées.* Non seulement cela, mais la cyanotoxine présente dans le surnageant du réservoir de sédimentation peut également être considérée comme une option de traitement possible.

5.) Hypothèse 4 au problème 3.3: La limitation posée par la faible surface des adsorbants de sable ne permet pas une formation rapide de biofilm et si elle se forme, perd rapidement son attachement à cause de la morphologie de la raboteuse. De plus, le fait que l'activité majeure du biofilm dans un filtre à bio-sable prolifère dans les 10% supérieurs de la hauteur de la colonne, *la bio-activité de cette zone pourrait être augmentée et prolongée en posant un matériau composite «de couverture supérieure» stable qui pourrait faciliter un support ambiant pour la formation du*

biofilm. Certains des agro-résidus tels que la fibre de chanvre, les boues de désencrage et les fibres de papier et de pâte à papier ont une surface élevée et résistante à une biodégradation facile et pourraient donc rester stables pendant une longue période. Ces supports peuvent également fournir les nutriments essentiels pendant la croissance du biofilm, ce qui pourrait favoriser une population dominante de dégradeurs MC-LR bioaugmentés.

6.) Hypothèse 5 du problème 3.4: La modification du milieu d'adsorption (sable) peut améliorer l'adsorption du MC-LR et d'autres contaminants de l'eau présents à côté. Une courte période de percée est un problème courant d'un adsorbant dans un système de filtration qui sature la surface de l'adsorbant favorisant la lixiviation des polluants dans l'eau filtrée. La modification du milieu de sable peut augmenter la surface spécifique et la rugosité, retardant ainsi le phénomène de lixiviation. *L'adsorption de MC-LR peut être élevée à la surface du sable en la rendant a) plus électropositive (car le MC-LR possède une charge négative à une plage de pH de 3,5 à 10,4), b) en créant des surfaces fonctionnalisées plus hydrophiles et en c) en créant une surface mésoporeuse en revêtement thermique de divers composés sur les grains de sable.* L'utilisation de particules submicroniques de carbone telles que l'oxyde de graphène (GO) et l'oxyde de graphène réduit (rGO) peut fortifier les grains de sable (revêtement thermique) en fournissant une surface spécifique élevée, des sites actifs améliorés et de grands systèmes à électrons π délocalisés. *Ces particules de carbone submicroniques (sous forme de GO et de rGO) en raison de leur capacité d'adsorption élevée pourraient adsorber un MC-LR élevé, offrant une période de percée plus longue que le sable (non revêtu).* Pour émettre l'hypothèse de l'adsorption de MC-LR sur une surface plus électropositive, le sable pourrait être recouvert d'oxyde de fer (Fe) ou d'oxyde de fer recouvert de sable recouvert de GO/rGO (Fe + GO / rGO) qui pourrait également être supposé adsorber plus de MC- LR et autres contaminants de l'eau, lorsqu'ils sont présents ensembles. De plus, afin de fournir une fixation de biocellule efficace sur l'adsorbant de sable recouvert de GO/rGO, la surface pourrait être bio-optimisée pour sa dose de revêtement car GO et rGO sont antibactériens à haute concentration.

7.) Hypothèse 6 du problème 3.4: La fourniture d'un revêtement de sucre graphène (pas d'atome d'oxygène comme GO ou rGO, mais uniquement du carbone) sur les grains de sable peut également être supposée pour faire ressortir la même modification que celle discutée ci-dessus

(hypothèse 5). *Le sable de sucre de graphène peut offrir une interaction π – π de grande surface qui pourrait fournir une meilleure longévité et une meilleure capacité d'adsorption de saturation que les particules submicroniques de graphène recouvrant les grains de sable. En outre, la source de sucre pourrait être dérivée des effluents de la brasserie usagée, ce qui fournira une solution durable à la synthèse de sable de graphène* par rapport à une préparation plus coûteuse de sable d'oxyde de graphène utilisant des flocons de graphite (hypothèse 5). Une source de sucre à haute stabilité chimique sera plus adaptée pour adsorber une gamme de polluants chimiques. Cela garantira en outre si l'hydrophilie de l'adsorbant joue vraiment un rôle important dans l'adsorption de MC-LR ou est-ce uniquement dû à la surface de carbone mésoporeuse (pas d'atomes d'oxygène) qui facilite l'adsorption de contaminants élevés, y compris MC-LR.

8.) Hypothèse 7 au problème 3.5: Pour contrer ce problème (voir problème 3.5), le filtre à l'échelle du banc pourrait être modélisé et analysé en fonction de la propriété intrinsèque du milieu poreux: coefficient de perte et constante de perméabilité. À cette fin, le solveur ANSYS-CFX peut être utilisé et le comportement de mise à l'échelle de la colonne de filtre à l'échelle du banc peut être obtenu en fonction des conditions aux limites, de la relation pression-vitesse, des études de perte de charge et d'autres dynamiques d'écoulement. Cela peut aider à déchiffrer la « dimension d'échelle subjective minimale » où le régime d'écoulement devrait être plus radial et canalisé, ce qui pourrait minimiser la possibilité d'un phénomène de court-circuit pendant le fonctionnement du filtre. Ensuite, le filtre de dimension dérivée « échelle subjective minimale » dérivé pourrait enfin être utilisé pour valider les performances de mise à l'échelle de l'adsorbant le plus performant (jugé sur la base de l'élimination du MC-LR et d'autres polluants de l'eau en utilisant l'analyse des composants principaux). Une approche de bilan massique pourrait alors être utilisée (micro-modèle DWTP fabriqué au laboratoire nommé SAP-1 ©) pour mieux comprendre la faisabilité de la modernisation du biofiltre en DWTP.

PARTIE 5. OBJECTIFS

L'objectif global de ce travail de recherche consiste en l'élimination du MC-LR et d'autres polluants de l'eau en utilisant le mécanisme de cultures attachées qui combine, à la fois, des processus physiques et biologiques (bioadsorption). Les objectifs spécifiques de ce projet sont les suivants :

Objectifs 1: Traitement à l'ozone en tandem avec un filtre à bio-sable afin d'évaluer l'élimination du MC-LR présent dans la source de l'eau potable.

Objectifs 2: Étudier la biodégradation du MC-LR en utilisant des bactéries acclimatées, isolées de différentes unités de l'usine de traitement des eaux.

Objectifs 3: Étudier l'application d'un réacteur à biofilm à lit fluidisé et explorer un module de traitement compact pour l'élimination concomitante de MC-LR et d'autres polluants des eaux.

Objectifs 4: Étudier l'aspect de la co-culture des bactéries natives isolées à partir de l'unité de traitement des eaux avec des dégradeurs connus pour accélérer l'élimination du MC-LR par l'utilisation d'un filtre bio-sable

Objectifs 5: Étudier la faisabilité des résidus agro-industriels comme support unique de « couche supérieure » dans un filtre à sable pouvant améliorer la bioactivité pour éliminer le MC-LR et d'autres polluants des eaux.

Objectifs 6: Étudier l'élimination physique et biologique du MC-LR et d'autres contaminants de l'eau dans un biofiltre en utilisant du sable recouvert de dioxyde de manganèse et des composites de sable graphène

Objectifs 7: Étudier l'élimination du MC-LR par l'utilisation de sable recouvert de composés submicroniques de carbone biooptimisés : oxyde de graphène, oxyde de graphène réduit, oxyde de fer et oxyde de fer-oxyde de graphène

Objectifs 8 : **a)** Étudier la faisabilité du biofiltre à grande échelle en utilisant la modélisation et la simulation des paramètres de filtre à l'échelle du banc par le biais de la dynamique des fluides numérique

b) Evaluer la microcystine-LR et d'autres paramètres d'élimination de la qualité de l'eau par l'utilisation d'un filtre à grande échelle : une approche de bilan massique utilisant un micro-modèle d'usine de traitement des eaux élaboré au laboratoire (SAP-1 ©).

Un aperçu des objectifs plus intégré pour les objectifs définis ci-dessus peut être classé en quatre parties.

Objectifs majeurs	Titre mondial pour différents objectifs majeurs	Numéro de chapitre dans cette thèse	Objectifs marqués tels que présentés dans la Partie 5
1	Importance de la bioaugmentation dans un filtre utilisant des bactéries natives isolées du DWTP	Chapitre 2	Objectif 1,2
2	Co-culture de bactéries in situ et de dégradeurs MC-LR en lit mobile et biofiltre à lit fixe	Chapitre 3	Objectif 3-5
3	Modification du milieu de sable pour améliorer sa capacité d'adsorption et son temps de percée	Chapitre 4	Objectif 6,7
4	Étude de mise à l'échelle en utilisant les médias filtrants les plus performants	Chapitre 5	Objectif 8

PARTIE 6. ORIGINALITÉ

En se basant sur les hypothèses et les objectifs proposés, l'originalité de ce projet de thèse de doctorat repose sur les points suivants :

6.1 L'approche hybride de l'ozonation-biofiltre utilisant des dégradeurs de MC-LR permettra de comprendre l'importance et la faisabilité de l'application d'une dose de « faible ozone » dans un STEP (prévention de la surdose) et contribuera également à l'élimination des sous-produits toxiques et MC-LR résiduel.

6.2 Autrefois, les bactéries isolées de diverses sources telles que les rivières, les lacs et les étangs ont été étudiées pour la dégradation de MC-LR. Cependant, pour la première fois, des bactéries in situ ou natives isolées de « différentes unités » des STEP ont été étudiées de manière comparative afin d'évaluer la dégradation de MC-LR après les avoir acclimatées dans un environnement MC-LR. Cette étude a permis de découvrir deux nouvelles bactéries indigènes, à savoir: *Pseudomonas fragi* et *Chryseobacterium sp*.. Ces dernières ont été étudiées pour la première fois dans le but de rapporter la biodégradation du MC-LR.

6.3 La co-culture des dégradeurs MC-LR connus et des espèces bactériennes indigènes (après les avoir rendu plus résilientes dans un environnement MC-LR) a été étudiée pour la première fois ou bioaugmentée dans un biofiltre pour l'élimination du MC-LR, offrant ainsi un scénario plus réaliste et une approche de solution en ce qui concerne le STEP.

6.4 Le création d'un montage expérimental exclusif afin d'évaluer la formation de biofilm et de sélectionner les meilleurs dégradeurs MC-LR pour chaque adsorbant utilisé dans la présente étude.

6.5 L`utilisation des résidus agroindustriels pour la première fois en tant que matériau de filtre « couvercle supérieur " (adsorbant) en général et aussi (spécifiquement) afin d'étudier l'élimination du MC-LR dans un biofiltre, ce qui contribuera à augmenter la bioactivité dans un filtre en fournissant ainsi une meilleure plateforme pour la prolifération des cellules bactériennes et la formation d'un biofilm.

6.6 L'utilisation de particules submicroniques de carbone bio-optimisées (sous forme d'oxyde de graphène et d'oxyde de graphène réduit) pour recouvrir le grain de sable permettra la formation d'un biofilm efficace par les dégradeurs natifs et MC-LR et aidera, également et à la fois, d'obtenir une MC élevée -Adsorption LR en fournissant ainsi une surface rugueuse, hydrophile, mésoporeuse et électropositive.

6.7 L'utilisation d'une source de sucre durable et à faible coût sous forme d'effluents de déchets de brasserie pour la synthèse d'un « sable Graphene-sucre » adsorbant MC-LR très efficace.

6.8 Utilisation du solveur ANSYS-CFX pour modéliser, simuler et prédire la dimension de « mise à l'échelle minimale subjective » en fonction des performances du filtre à l'échelle du banc utilisant des paramètres hydrodynamiques dérivés.

6.9 La création d'un micro-modèle DWTP inventé et élaboré à l'échelle du laboratoire (SAP-1 ©) comprenant un filtre de grande échelle pour étudier l'élimination du MC-LR et d'autres polluants de l'eau. L'utilisation de « sable Graphène-sucre » comme milieu filtrant a également mis en évidence l'importance du module d'unité de filtration dans la chaîne DWTP (micro-modèle: SAP-1 ©).

Dans l'ensemble, l'originalité du travail de recherche proposé consiste principalement sur « **le développement d'un système de biofiltration avancé utilisant des bactéries potentiellement biofilmogènes, tirées des sources naturelles dans l'objectif de l'élimination du MC-LR et d'autres polluants des eaux**».

PARTIE 7 : MÉTHODOLOGIE GÉNÉRALE

Cette section décrit la méthodologie générale utilisée lors des expériences. La légende de toutes les figures utilisées dans cette section est restée la même que celle mentionnée dans la section article.

Réactifs et produits chimiques

La microcystine-LR (MC-LR) a été achetée auprès de Cayman Chemicals (Ann Arbor, Michigan, USA). Le $MgSO_4.7H_2O$, $ZnSO_4.\ 7H_2O$, $Na_2MoO_4.2H_2O$, KH_2PO_4, $Na_2HPO_4.7H_2O$, $CaCl_2$ et $FeCl_3$ ont été achetés auprès de Fisher Scientific (Ontario, Canada). Le chlorure de sodium (NaCl), la peptone et l'extrait de levure ont également été achetés auprès de Fisher Scientific (Ottawa, ON, Canada) et utilisés pour préparer le milieu LB pour la culture bactérienne et l'inoculation des bactéries isolées. Pour le test de toxicité, une solution tampon Tris-HCl (pH 7,5) a été préparée en utilisant du tampon Tris et du HCl 6N (Merck, US). Du bromure de 3- (4, 5-diméthylthiazol-2-yl) -2, 5-diphényltétrazolium (MTT), acheté auprès de Sigma Aldrich (Ontario, Canada), a été utilisé pour mesurer la viabilité cellulaire.

Microorganismes

Les espèces *Sphingomonas* sp. (NRRL B-59555) et *Rhizobium meliloti* (NRRL L-84) ont été achetées auprès de la collection de cultures NRRL de l'*Agricultural Research Service* (ARS). Elles ont respectivement été utilisées comme contrôle positif dans l'étude de la dégradation des MC-LR (Ishii et al., 2004) et comme bio-indicateur pour déterminer la toxicité du bouillon biodégradé (Botsford et al., 1997).

Étude de croissance bactérienne et test de viabilité dans un environnement de MC-LR

Les caractéristiques de croissance des bactéries ont été étudiées jusqu'à ce que la phase stationnaire soit atteinte, où la densité optique à X_{max} = 600 nm (DO 600) a été déterminée en fonction de l'heure de croissance. Les paramètres de croissance, tels que le temps de doublement, la phase de latence, la phase logarithmique (non représentée) et la relation entre la viabilité cellulaire et la densité optique A600 nm (UV-VIS Cary-50), ont été déterminées pour diverses variétés bactériennes. Le dénombrement viable (dénombrement cellulaire) a été mesuré en comptant les colonies sur une plaque de pétri LB-agar, le résultat étant exprimé en CFU/mL. Toutes ces expériences de dénombrement cellulaire ont été principalement réalisées en triplicata, sinon en

duplicata. Les conditions opératoires étaient généralement une température de 28 ± 2 °C et une vitesse de rotation de 150 tr/min.

Biodégradation de la MC-LR et analyse des sous-produits

Les échantillons de MC-LR ont été analysés après filtration à l'aide d'un filtre stérile de 0,45 µm, recouverts de tubes de microcentrifugation de couleur noire (BCCT) pour éviter leur photodégradation et stockés à -20 ºC, jusqu'à leur analyse par chromatographie liquide à haute performance (HPLC) selon le protocole proposé par Fayad et al. (2015). En bref, un aliquot d'échantillon de 20 µL a été analysé par chromatographie liquide à ultra-haute performance couplée à une spectrométrie de masse à haute résolution (Thermo Q-Exactive Orbitrap) (HPLC-MS), où l'ionisation est effectuée par électronébulisation. La colonne chromatographique était de marque Thermo Hypersil Gold avec une sélectivité C18 (100 x 2,1 mm, taille de particule 1,9 µm). La MC-LR a été détectée en mode MS à balayage complet et quantifiée par rapport à l'eau distillée. La méthode analytique a été validée pour la linéarité, l'exactitude et la précision; la performance était conforme aux critères d'acceptation (Roy-Lachapelle et al., 2019). La limite de quantification de la méthode (LQM) a été fixée au niveau de concentration le plus bas de la courbe d'étalonnage (soit 0,1 µg/L). À la fin de 6 semaines d'analyse de la MC-LR, une concentration moyenne finale de 8 255 µg/L a été obtenue à partir d'une culture de 150 mL, ce qui était suffisant pour préparer 2 litres d'eau de lac à une concentration de MC-LR finale de 50 µg/L en diluant environ d'un facteur dix.

Les fragments de sous-produits formés pendant la dégradation ont été analysés par spectroscopie de masse. Environ 1 mg/L de microcystine-LR a été utilisé comme standard interne avec une phase mobile de 50:50 (v/v) MeOH :H_2O avec 0,1% d'acide formique. Les paramètres finaux utilisés pour maximiser l'intensité du signal étaient une température capillaire de 350 °C, une température du vaporisateur de 450 °C et une pression de gaz de gaine, de gaz auxiliaire et de gaz de balayage ionique de 35, 10 et 0 unités arbitraires respectivement. Le temps de balayage a été ajusté à 0,02 s, où le premier et troisième quadripôles ont été opérés à la résolution unitaire avec une pression de gaz de collision quadripolaire de 1,5 mTorr. Dans l'ensemble, il s'agit d'une méthode chromatographique rapide optimisée utilisant une extraction en phase solide couplée à une analyse par HPLC-MS pour la détermination de sept cyanotoxines différentes, y compris la MC-LR.

Évaluation de la toxicité des échantillons/bouillons de MC-LR dégradés à l'aide de *Rhizobium meliloti*

La toxicité du bouillon de biodégradation a été examinée à l'aide d'un bio-indicateur, soit le *Rhizobium meliloti*. Le milieu du sol a été utilisé pour la culture de *R. meliloti* comme mentionné dans Surange et al. (1997) avec quelques modifications. La solution a été complétée à 1 litre et a été autoclavée à 121 ± 1 °C pendant 20 minutes. La souche de *R. meliloti* lyophilisée a été cultivée dans le milieu du sol et conservée pendant 24 à 36 h dans un incubateur à secousses à raison de 150 tr/min et à une température de 30 ± 1 °C. Ensuite, elle a été successivement repiquée deux fois (5% v/v) et striée sur une plaque de type LB-agar (1,8%) pour en obtenir des colonies pures.

Le protocole de toxicité décrit par Botsford et al (1999) a été suivi avec quelques modifications. Un ml de tampon Tris-HCl (pH 7,5), un échantillon toxique (DMSO et de la MC-LR à différentes concentrations) et une suspension de cellules bactériennes (*R. meliloti*) ont été mélangés dans un tube à essai en verre et laissés au repos pendant 60-120 secondes. Ce laps de temps a permis une exposition suffisante pour une mortalité partielle ou totale de la culture cellulaire en fonction du degré de toxicité du composé (MC-LR et DMSO testés). Par la suite, environ 350 µL de solution de colorant MTT ((3- (4,5-diméthylthiazol-2-yl) -2,5-diphényltétrazolium) (7 mg/10 mL) ont été ajoutés au mélange, ce qui converti la couleur de la solution initiale de jaune à bleu (les cellules viables, s'il en reste, meurent et forment du formazan (précipité bleu). Une étude plus spécifique pour évaluer la période d'incubation critique du bioindicateur a été réalisée à trois périodes (10, 16 et 24 h). Il a été constaté que la période d'incubation d'une nuit (10 h) était la période la plus critique, comme l'ont également observé Bodsford et al. (1999). Cette période (10 h) permet notamment d'obtenir le graphique d'absorbance le plus adapté à diverses concentrations de produits chimiques toxiques, c'est-à-dire sans ambiguïté dans la tendance (graphique des différentes périodes d'incubation non inclus). Pour le produit chimique de référence, trois composés ont été sélectionnés, à savoir le méthanol, l'éthanol et le diméthylsulfoxyde (DMSO). Parmi ces composés, le DMSO a finalement été choisi en fonction de l'uniformité du test d'absorbance. La relation entre la quantité de MC-LR (concentration allant de 92 µg/L à 1 470 µg/L) et DMSO (10% -100% v/v) a ensuite été établie pour signaler la toxicité du bouillon biodégradé en termes de DMSO équivalent (% v/v) concentration.

L'évaluation de la toxicité était basée sur la mesure de l'absorbance à 550 nm (spectrophotomètre UV-VIS Cary 50) après le changement de couleur (jaune à bleu) en raison de l'ajout du colorant MTT. Après l'addition de colorant MTT (0,350 ml) combiné avec du tampon Tris, de l'échantillon toxique et la suspension de cellules bactériennes (mélange total de 3,350 ml), les tubes à essai en verre ont été bouchés et incubés pendant 1,5 à 2,5 h à 35 ± 1 °C. Tous les tests ont été effectués en triplicata.

Identification des espèces bactériennes par séquençage ribosomique

L'isolement de l'ADN génomique a été effectué en utilisant le kit d'ADN bactérien E.Z.N.A.® (Omega Bio-Tek, USA) selon les instructions du fabricant. L'ADN isolé a été amplifié par PCR en utilisant une amorce directe 27F (5'-AGAGTTTGATCCTGGCTCAG) et une amorce inverse 1492R (5'-GGTTACCTTGTTACGACTT). L'amplicon de PCR a été séquencé pour l'identification de l'ADNr 16s de la souche bactérienne (service de séquençage du Centre d'innovation Génome Québec). La séquence identifiée a été analysée en utilisant le service NCBI BLAST pour identifier la souche bactérienne. L'ADNr 16aS identifié a par la suite été déposée dans la GenBank, au Centre national pour l'information biotechnologique (NCBI).

Analyses statistiques

Une analyse statistique liée aux paramètres analysés tels que l'écart-type, le test *t* de Student, une valeur de *p* de tous les ensembles de données et d'autres présentations graphiques ont été effectuées à l'aide du logiciel ORIGIN (version 8.5; OriginLab).

Culture et croissance de *Microcystis aeruginosa*

L'espèce *Microcystis aeruginosa* a été fournie par le Dr Jérome Compte (professeur, INRS-ETE, Québec, Canada) dans un tube de culture de 30 ml. Le milieu BG-11 a été utilisé pour cultiver *M. aeruginosa* comme mentionné par Rippka et al. (1979). Une lumière fluorescente a été installée pour fournir une source de lumière constante (8h/16h; phase claire/sombre) à la culture en croissance. Chaque semaine jusqu'à 12 semaines, 10 mL de milieu BG-11 préparé ont été ajoutés à la culture en croissance dans un erlenmeyer de 250 mL et la densité optique à λmax = 700 nm a été notée (valeurs non montrées ici). Après 12 semaines de croissance de culture et jusqu'à 6 semaines supplémentaires, la toxine MC-LR a été analysée dans le milieu de culture. Pour cela, 3 mL de culture ont été filtrés en utilisant un filtre HA de 0,45 µm où les cellules ont été retenues

sur le filtre et le filtrat a ensuite été utilisé pour l'analyse de MC-LR (seul la MC-LR extracellulaire a été analysée) en utilisant la méthode HPLC adaptée de Roy-Lachapelle et al. (2019).

Culture et formation de biofilms de dégradeurs de MC-LR sur des filtres à sable

Les dégradeurs de MC-LR, soit *Arthrobacter ramosus*, *Bacillus* sp. et *Sphingomonas* sp., ont été utilisés à des fins de criblage pour tous les matériaux adsorbants préparés lors de cette thèse. Ils ont été testés individuellement pour la bioaugmentation à l'aide de filtres à sable/sable modifié. Ces souches bactériennes ont été cultivées et rincées avec le tampon phosphate (pH = 7,21) pour obtenir des culots cellulaires. Selon la relation entre OD600 et la viabilité cellulaire (cellules/mL), les cellules ont été inoculées selon les détails fournis en tant qu'exigences spécifiques à l'aide d'une pompe de dosage automatique pendant une période de 11 jours (se référer séparément au matériel et aux méthodes pour chaque objectif). Cela a permis une formation rapide de biofilms dans le filtre à sable (pour plus de détails voir section 2.5). L'eau du lac a été utilisée comme matrice pour le fonctionnement du filtre.

La formation de biofilms a été contrôlée à travers trois paramètres: la viabilité cellulaire, la biomasse cellulaire et la concentration en protéines. Environ 0,1 à 0,2 gramme de sable a été recueilli de la couche supérieure de la colonne de sable, puis a été suspendu dans du tampon phosphate (1,5 mL à 2,0 mL). Le mélange a subi une courte rotation pour relâcher les cellules bactériennes attachées et la biomasse en suspension. Par la suite, la suspension cellulaire obtenue a été ensemencée dans une plaque à 96 puits pour le cristal violet (CV) et le test MTT tel que décrit dans une de nos études précédentes (Kumar et al. 2019) pour estimer la biomasse cellulaire et la viabilité cellulaire, respectivement. Pour la détermination des protéines, la suspension cellulaire a été analysée en utilisant le test de Bradford (Bradford et al. 1976).

Évaluation de la toxicité des échantillons à l'aide du test Protein Phosphatase 1A

Le test PP1A a largement été utilisé par de nombreux chercheurs pour étudier l'effet toxique de la MC-LR résiduelle dans l'échantillon d'eau. La PP1 appartient à la classe des protéines sérine/thréonine phosphatases et est responsable du contrôle du métabolisme du glycogène. La MC-LR étant une hépatotoxine, attaque les cellules hépatiques et inhibe l'activité cinétique de la PP1. Ainsi, le dosage de la PP1A est très significatif et spécifique en ce qui concerne l'évaluation de la toxicité de la MC-LR.

Le test a été effectué sur une plaque à 96 puits où les deux premières lignes et colonnes n'ont pas été utilisées en raison de l'effet de paroi et des différences de température signalées dans ces puits. Un volume de 300 µL, constitué de 20 µL de MC-LR à différentes concentrations (diluée dans le tampon de réaction), 40 µL de PP1 (solution mère diluée dans un tampon enzymatique selon les spécifications du fabricant: concentration finale du puit: 0,8 U/mL), 240 µL de Du pNPP (substrat: concentration finale du puit de 120 mM) a été mélangé pour initier la réaction colorimétrique. Le blanc a été préparé avec les concentrations standards sans MC-LR (blanc de substrat). Le blanc de substrat représentait l'activité de base de PP1 qui a été normalisée pour chaque puit exposé à l'activité de PP1 afin de déterminer l'effet de la MC-LR sur l'activité de PP1. Le taux d'activité (hydrolyse du pNPP basé sur le changement de couleur) a été déterminé et calculé sur la base de la densité optique d'absorbance colorimétrique (DO à λmax: 405 nm et 32 ± 3 °C) en utilisant le mini spectrophotomètre Biotek toutes les 2 minutes pendant 1 heure. Un taux linéaire (changement de DO/min) a été obtenu 1020-3520 secondes où le taux du blanc de substrat était au plateau après 1020 secondes. Plus l'hydrolyse du substrat de pNPP par l'enzyme PP1A sera faible, plus l'inhibition PP1A rapportée sera faible et vice-versa. Ainsi, plus le % d'activité rapporté est grand, moins est l'inhibition de PP1A par la MC-LR. Pour signaler les échantillons d'eau, un échantillon de 20 µL à la place de MC-LR a été mélangé dans les puits avec l'enzyme PP1A et le substrat de pNPP comme indiqué ci-dessus. L'activité a été signalée et comparée pour évaluer le changement de toxicité dû à la MC-LR résiduelle dans l'échantillon avant et après filtration. Tous les échantillons ont été analysés en triplicata.

Criblage des souches bactériennes

Un criblage des souches bactériennes (généralement trois d'entre elles: *Arthrobacter ramosus*, *Bacillus sp.* et *Sphingomonas sp.)* a été effectué pour étudier leur capacité à former un biofilm sur le milieu de sable. La Figure 3 montre la représentation schématique de la configuration préparée pour cet objectif (configuration en laboratoire illustrée à la figure C1, annexe C, pour chaque objectif, reportez-vous à la section matériel et méthode). Un modèle de réacteur en matière plastique composé d'un milieu de sable de 10 g a été placé dans une réplique pour chaque source d'inoculum (Figure 3.2.1 et Figure C1). Toutes les 4 h, 20 mL (volume de charge supérieur à l'espace des pores) d'inoculum (6 x 10^7 cellules/ml) sont passés dans les réacteurs modèles préréglés par la pompe doseuse automatique. L'eau nutritive à forte demande chimique en oxygène

(800 mg/L) a servi de matrice à l'inoculum (pour aider à la formation rapide et active de biofilm). L'opération a été poursuivie en mode recirculation pendant 10 à 19 jours (selon les adsorbants) pour atteindre la formation de biofilm mature. Les résultats du test ont été comparés au contrôle négatif (sans cellules inoculées) et au contrôle positif (*Staphylococcus epidermidis* reconnu pour être un bon formateur de biofilm).

Figure 4.1.0: Installation pour le criblage de dégradeurs de MC-LR via la formation de biofilm

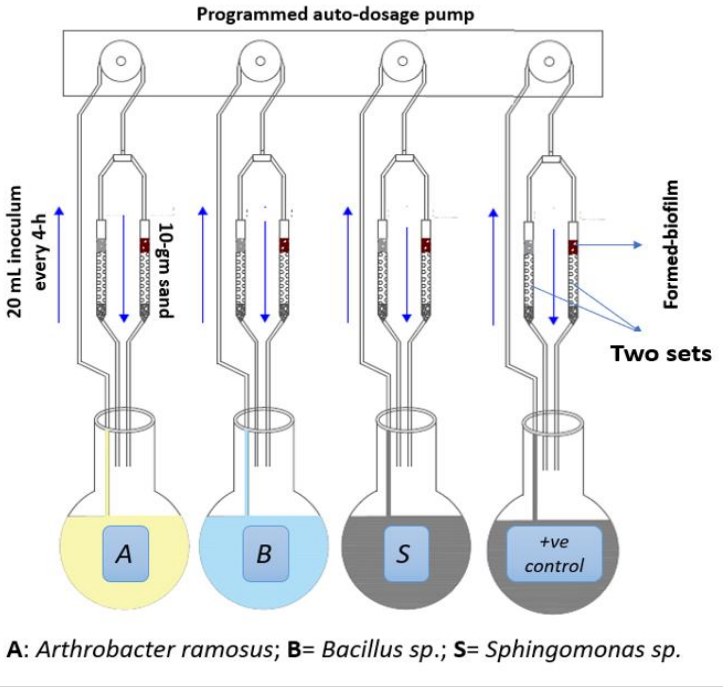

Figure 3.2.1: Montage pour étudier le criblage des bactéries formant un biofilm

Après tous les 3, 7, 11, 16 et 19 jours (selon l'adsorbant testé), une petite portion de milieu de sable (environ 0,3 g) a été prélevée sur la couche supérieure et a été suspendue dans 1,5 mL d'eau du robinet puis vortexée (jusqu'à extraire les cellules bactériennes attachées et la biomasse dans la solution). Par la suite, la portion liquide a été prélevée dans un volume de 200 µL pour ensemencer les puits d'une plaque à 96 puits (6 puits par échantillon). La biomasse de trois puits a été colorée en utilisant 100 µL de cristal violet (CV) à 0,1% (p/v) et 100 µL de solution de MTT (7 mg/10 mL) ont été injectés dans les trois puits restants. De même, le processus a été effectué pour les échantillons d'autres souches. Ensuite, la plaque a été incubée pendant une nuit à 35 ± 2 °C pour le dosage du cristal violet (CV) et 4 h à 35 ± 2 °C pour le test MTT. Pour le test CV, les puits ont été soigneusement lavés avec une solution tampon phosphate (pH 7,4) pour éliminer toute biomasse attachée de manière lâche, puis 300 µL de solution de diméthylsulfoxyde (DMSO) a été ajoutée pour solubiliser la biomasse colorée. Pour le test MTT, le précipité formé (formazan de couleur bleue) après séchage a été dissout en utilisant 300 µL de solution de DMSO. La lecture spectrophotométrique a été prise respectivement à 550 nm et 590 nm pour le test MTT et CV afin de quantifier la viabilité cellulaire (test MTT) et la biomasse cellulaire (test CV). Ces expériences ont fourni plus d'informations pour évaluer la capacité de la souche bactérienne à former un biofilm

et non directement le biofilm formé sur le grain de sable. Une représentation graphique de la séquence d'échantillonnage est présentée à l'annexe C (Figure C2).

Optimisation des paramètres d'entrée à l'aide d'une conception composite centrale

Avant le début du fonctionnement du filtre, une expérience d'optimisation a été réalisée pour comprendre la résistance et les meilleures conditions des supports de filtre à sable. Les paramètres physiques comprenant la turbidité initiale, le pH, la période de veille critique (temps de rétention) du fonctionnement du filtre et la température. Trois/quatre niveaux d'entrée ont été conçus pour chaque paramètre: pH de 6, 7 et 8; turbidité initiale de 10 NTU, 20 NTU et 30 NTU; température de 10 °C, 20 °C et 30 °C et période critique de veille (CSTI) de 1h, 2h, 3h et 4h. L'eau du lac (lac Sainte-Anne (47.262879N, -71.665158W) a été utilisée comme matrice de solution avec des ajustements appropriés de la turbidité (imitant avec une suspension d'argile turbide-hydratée maintenue pendant la nuit), du pH (acide chlorhydrique/hydroxyde de sodium) et de la température (chauffage). Le Tableau 3.2.1 répertorie les détails et les informations nécessaires relatifs à l'expérience d'optimisation. Puisque le nombre de colonnes de verre disponibles était limité, l'ensemble de l'expérience d'optimisation a été divisé en deux parties: a) 3 niveaux de température et 3 niveaux de pH (9 combinaisons); b) turbidité initiale à 3 niveaux et période de charge de temps critique à 4 niveaux (12 combinaisons). Par conséquent, 21 combinaisons de paramètres initiaux ont été conçues au total.

Pour optimiser ces conditions initiales, les paramètres de sortie (analysés pour les échantillons filtrés) ont été déterminés. Ceux-ci incluent l'élimination totale des coliformes, l'élimination de la turbidité, les essai MC-LR (détermination de la toxicité), l'élimination de l'oxygène dissous et du carbone (DOC), le débit, le changement de pH, l'oxygène dissous et la conductivité électrique. L'importance pondérée de chaque paramètre de sortie a été fixée selon l'objectif expérimental visé. Par exemple, le test MC-LR, l'élimination totale des coliformes, l'élimination de DOC et l'élimination de la turbidité ont été fixés à des poids de priorité élevée de 5, 5, 4 et 4, respectivement (les autres paramètres étant fixés à 2 ou 3 en fonction de l'importance). À l'aide de la conception composite centrale (Design-Expert 7.0) et de l'importance pondérée de tous les paramètres de sortie, une solution définitive et critique (en valeur codée), à savoir la valeur optimisée de la turbidité initiale, de la température, du pH et de la période d'attente du filtre a été déterminée. Cette méthodologie a subi quelques modifications en fonction des adsorbants utilisés pour les différentes

expériences. Par conséquent, les lecteurs sont invités à se référer à la section matériel et méthode de chaque chapitre pour obtenir l'information spécifique.

Expériences sur colonnes de sable et entretien du filtre

Cette section traite du montage de l'expérience sur colonnes de sable et des procédures de fonctionnement et de maintenance du filtre liées au Chapitre 3, Partie 2. Par conséquent, les lecteurs sont invités à lire les sections spécifiques relatives aux différents adsorbants utilisés dans cette thèse. Après le test de dépistage et l'expérience d'optimisation, les colonnes de verre ont été installées selon un arrangement d'écoulement de haut en bas comme le montre la Figure 3.2.2. Le sable provient de l'unité de filtration de l'usine de traitement d'eau potable (Chemin Ste-Foy, Québec, Canada). Au total, huit colonnes de verre (diamètre: 25 mm, épaisseur 2 mm, hauteur: 650 mm) ont été installées et remplies de particules de sable broyé de diamètre effectif D10 = 180 μm et de coefficient d'uniformité Cu = 2,32 pour une hauteur d'environ 490 mm. Le nombre de colonnes dépend des différents objectifs (voir sections spécifiques). Environ 40 mm de sable de drainage ont été ajoutés en utilisant une granulométrie de sable d'environ 2-4 mm. Un espace de 120 mm a été conservé au sommet de la colonne pour permettre à l'eau d'affluer. L'analyse de la distribution granulométrique et les calculs associés aux particules de sable sont détaillés dans le fichier en Annexe (Figure C3, Annexe C).

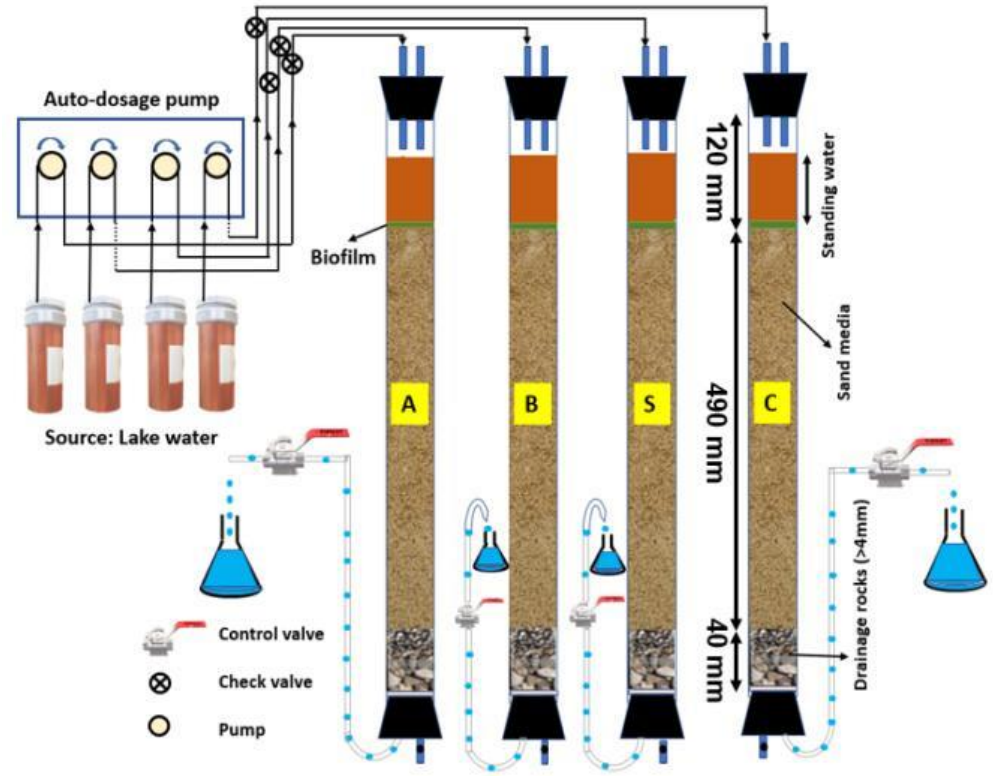

Figure 3.2.2: Représentation schématique détaillée du montage des colonnes de sable

Le Tableau 3.2.2 montre les détails des souches utilisées dans les filtres à colonnes et les caractéristiques de la source d'eau utilisée. Un bon filtre doit être capable de gérer d'autres paramètres de qualité de l'eau en plus des MC. Chaque filtre a été étudié afin d'évaluer le potentiel des dégradeurs de MC-LR de manière individuelle de même que lorsqu'ils sont co-cultivés avec les souches bactériennes natives (X) présentes dans l'unité de filtration du STEP, d'éliminer la MC-LR et d'évaluer d'autres paramètres de qualité de l'eau (WQP). Un filtre à colonne a été utilisé comme contrôle négatif (sans aucune souche bactérienne, filtre de contrôle C) pour différencier l'élimination de la MC-LR due à l'adsorption et à la biodégradation (Tableau 3.2.2). Connaissant l'importance du filtre de contrôle, une seconde colonne a également été installée en parallèle afin d'éliminer toute erreur expérimentale ambiguë (sur/sous-estimation des résultats). De plus, un filtre inoculé avec les souches bactériennes natives isolées de l'unité de filtration STEP (filtre X) a été simulé pour représenter un filtre à sable STEP. Le résultat obtenu à partir de ce filtre (X) a en outre permis d'évaluer la différence de dégradation de la MC-LR et des autres WQP lorsque X était co-cultivé avec des dégradeurs de la MC-LR (A + X, B + X et S + X).

Avant le fonctionnement du filtre, la condition d'écoulement en bouchon était assurée (pas de bulle d'air ni de perte de charge initiale) en déterminant l'indice de dispersion Morrill (tous les filtres présentaient un MDI proche de 2,5). Chaque filtre a été inoculé séparément avec les souches respectives pendant une période continue de 2 semaines (Tableau 3.2.2). L'inoculum a été préparé dans l'eau nutritive de 800 mg/L-DCO (détails de cette eau fournis dans le Chapitre 2 Partie 1) pour permettre une mise en place rapide du biofilm sur le milieu de sable (comme pour le test de dépistage). Environ 50 mL d'inoculum ont été passés toutes les 4 h (en mode recirculation) permettant un temps de contact substantiel entre les bactéries et le milieu de sable pour former des microcolonies rapidement. L'inoculum a été reconstitué avec des nutriments tous les deux jours, réduisant chaque fois la DCO de 100 mg/L pour obtenir 190 mg/L au jour 12. Par rapport au modèle de réacteur utilisé pour le criblage, l'inoculation lors du fonctionnement de la colonne de filtration a été réalisée avec une concentration 10 fois plus élevée de biocellules, soit 6 x 108 cellules/mL (car 10 fois plus de milieu de sable a été utilisé).

Le biofilm formé sur le milieu sableux a été périodiquement analysé selon divers paramètres tels que le débit, l'élimination du COD, la concentration en protéines et la viabilité cellulaire. Après la formation du biofilm, les huit filtres ont fonctionné en continu pendant 8 cycles, chaque cycle comprenant 7 jours toujours en utilisant l'eau du lac. Le débit a été mesuré en maintenant une hauteur constante de 5 cm d'eau stagnante à chaque fois que la mesure était enregistrée. La concentration en protéines a été déterminée par une méthode similaire à l'analyse CV, sauf que l'échantillon de sable a été vortexé dans le tampon de lyse cellulaire pour en extraire la protéine complète. L'échantillon a été centrifugé à 10 000 x g pendant 2 min puis le surnageant a été mesuré pour la concentration en protéines selon le test de Bradford [23]. La viabilité cellulaire a quant à elle été mesurée par test MTT comme mentionné dans la section précédente.

Aucun antécédent de microcystine ou de prolifération cyanobactérienne n'a été signalé pour l'eau du lac (les détails des résultats des diverses analyses de microcystine et d'autres cyanotoxines sont fournis à l'Annexe C: Tableau C1). Le Tableau 3.2.2 présente les paramètres environnementaux de l'eau du lac. Sur la base du temps de contact sur un volume de lit nul (EBCT), tous les filtres ont fonctionné en continu pendant la journée et le soir (de 9 h à 22 h). Pendant la nuit (de 23 h à 8 h), l'absorption des affluents a été auto-programmée de telle sorte qu'à tout moment, l'écart entre

deux charges d'affluents n'a pas dépassé la période de charge critique du filtre ou CSTI (2,16 h ~ 135 min), selon les résultats obtenus à partir de l'expérience d'optimisation.

L'opération de lavage à contre-courant a été effectuée une fois, après la fin du 4e cycle, à 10% d'expansion du volume de lit pendant 5 min. Cela a été réalisé pour simuler les filtres STEP qui sont régulièrement lavés à contre-courant pour éliminer toute croissance d'algues et la présence de bulles d'air (ce qui peut augmenter la perte de charge et ainsi l'élimination des contaminants). Tous les tuyaux et connecteurs ont été lavés tous les 2 cycles pour éliminer les particules/biofilms déposés.

Élimination des coliformes, élimination de la turbidité, élimination du COD, nitrate, nitrite et ammoniac

Dans cette section, différents paramètres de qualité de l'eau (PQE) ont été discutés. Les lecteurs sont invités à passer par la méthodologie spécifique à cet adsorbant car cette section démontre l'analyse des WQP pour l'objectif où l'adsorbant de sable a été utilisé (Chapitre 3, Partie 2). Il faut cependant noter que la procédure de base reste la même.

Les coliformes totaux dans l'effluent d'eau filtrée ont été déterminés en utilisant la technique de filtration sur membrane tous les 3 jours (deux fois/cycle) selon les méthodes standard (APHA, 1998) [24]. Le nombre de coliformes présents dans l'effluent de chaque filtre a été rapporté en CFU/100 mL puis comparé au coliformes totaux présents dans l'eau affluente (eau du lac). L'UFC moyenne/100 mL observée pour la source d'eau (moyenne de 9 échantillons) était de 2401 ± 312 UFC/100 mL. Le pourcentage d'élimination des coliformes totaux a été calculé par l'Équation 8 comme suit:

$$\frac{((2401 \pm 312\ \text{CFU/100 mL} - \text{Total coliform in filtered water sample/ 100 mL})}{(2401 \pm 312\ \text{CFU/100 mL})} \times 100 \quad \text{Équation 8}$$

La turbidité de l'eau filtrée a été déterminée chaque jour à l'aide du turbidimètre portable HACH 2100. Pour imiter la condition de turbidité initiale optimisée (13 NTU selon l'étude d'optimisation), l'eau du lac a été mélangée de manière appropriée en utilisant une concentration trouble de solution d'argile hydratée comme décrit par Asrafuzzaman et al. (2011). Il faut noter que la turbidité initiale de l'eau du lac était inférieure (6 NTU) à la valeur de turbidité optimisée (13 NTU). La turbidité

moyenne de l'effluent filtré pour chaque cycle a été rapportée en NTU et l'élimination a été calculée selon l'Équation 9:

((13 ±2.2 NTU –turbidité de l'effluent filtré (NTU))/(13 ±2.2 NTU) x 100 Équation 9

Environ 30 mL de l'échantillon avant et après filtration ont été filtrés à l'aide d'un filtre en fibre de verre de 0,45 µm. La COD de la solution résultante a été déterminée en utilisant un analyseur Shimadzu 5000A (Shimadzu, Japon). La COD a été estimée deux fois par cycle et a été rapportée en mg/L. Sur la base de la valeur DOC et de la valeur UV 254 (UVA), une valeur d'absorbance UV spécifique appelée SUVA a été rapportée (UVA 254/DOC) pour donner une estimation indirecte de l'élimination des NOM.

Le nitrate, le nitrite et l'ammoniac ont été déterminés dans l'échantillon selon la méthode décrite par Naghdi et al. (2017). Une solution d'eau de lac affluente a été préparée pour contenir 100 mg/L de nitrate, 10 mg/L de nitrite et 2 mg/L d'ammoniac-N à la fin de chaque cycle, où l'échantillon filtré a été déterminé pour le nitrate, le nitrite et ammoniac-N. Avant la préparation de la solution pour la concentration initiale requise, le nitrate, le nitrite et l'ammoniac ont été déterminés dans l'eau du lac.

pH, oxygène dissous, conductivité

Le pH a été mesuré tous les deux jours (trois fois par cycle) et la valeur moyenne de chaque cycle a été rapportée pour chaque filtre. De plus, de l'oxygène dissous a été signalé tous les deux jours (trois fois par cycle) à l'aide d'une sonde portable F4-Standard (Mettler Toledo Inc) pour vérifier la qualité de l'eau (pas d'accumulation de condition anoxique). La conductivité électrique de l'effluent filtré a été mesurée tous les deux jours à l'aide du conductimètre SevenCompact ™ Mettler Toledo ™ S230.

Débit

Le débit de chaque filtre a été rapporté en m/h (ou $m^3/m^2/h$) après la fin de chaque cycle. Le lavage en contre-courant a été effectué après la fin du 4e cycle lorsque le débit a été réduit à au moins 35% par rapport au 1er cycle. La hauteur de l'eau stagnante pendant la mesure du débit a été maintenue constante à environ 115 mm.

Bio-profilage des filtres à colonnes et imagerie SEM

Après la fin de 8 cycles de fonctionnement du filtre (7 jours/cycle), le sable de chaque filtre à colonne a été soigneusement déposé par gravité et recueilli tous les 5 cm. Pour chacun de ces échantillons de sable recueillis, le biofilm a été quantifié en termes de bioactivité (quantifiée en tant que viabilité cellulaire) et de biomasse en utilisant respectivement le test MTT et le test CV. Avant et après la formation du biofilm sur le milieu de sable, des micrographies SEM ont été réalisées à une tension d'accélération de 10 kV (Zeiss EVO ® 50 Smart SEM system).

Analyse des substances extra-polymères (EPS) et des protéines

Dans cette section, différentes quantifications d'EPS et de protéines ont été discutées. Les lecteurs sont invités une fois de plus à relire la méthodologie spécifique au matériau agro-résiduel car la présente section a utilisé cet adsorbant pour couvrir la partie supérieure du filtre à sable (Chapitre 3, Partie 3). Il faut cependant noter que la procédure de base reste la même.

La quantification de l'EPS dans le biofilm formé sur l'agro-résidu a été effectuée (après le cycle 7 et avant le démontage de la colonne) par la méthode de précipitation à l'éthanol comme décrit précédemment par Boon et al. (2008). En bref, les 10 premiers mL ou environ 2 g de l'agro-matériau (sable en cas de SFI) ont été soigneusement retirés du filtre à colonne et suspendus dans 10 mL d'eau du robinet pour initier la lyse cellulaire (choc cellulaire). Une solution tampon de lyse cellulaire a été ajoutée (5 mL) pour lyser davantage les cellules. Par la suite, la solution a été vortexée pendant 2-3 min et centrifugée à 7000 x g à température ambiante pendant 20 min. Le surnageant a été mélangé avec deux parts d'éthanol (environ 25 ml) et maintenu à -20 °C pendant une nuit. L'EPS précipité a été rapporté en µg/mg de la masse sèche du matériau agro-résiduel prélevé initialement.

Pour l'analyse des protéines, environ 0,1 g d'agro-résidu en haut de chaque filtre de colonne (DSF, HFF, PPF) a été soigneusement prélevé et mis en suspension dans 1,5 mL d'eau distillée (tube de microcentrifugeuse). Après 2 min de vortex et de centrifugation (8000 x g) à température ambiante pendant 3 min, le surnageant a été analysé pour les protéines totales selon le dosage Bradford et rapporté en µg/mL (Bradford, 1976).

Études d'adsorption des métaux

Les composites de sable préparés ont été analysés pour leur potentiel d'élimination des cations métalliques divalents communs que l'on trouve habituellement dans les sources d'eau potable. Pour l'expérience d'adsorption des métaux, des colonnes modèles de 15 cm^3 chacune ont été utilisées. Une solution de cuivre, de magnésium et de fer (cations métalliques divalents) à différentes concentrations initiales de 5, 10, 50, 100, 200, 250, 300 et 350 mg/L a été ajoutée à chaque colonne. La concentration d'équilibre finale de cuivre, de magnésium et de fer dans l'échantillon filtré a été déterminée par spectrophotométrie comme détaillé par Mehlig et al. (1941), Tesfaldet et al. (2004) et Fortune et al. (1938), respectivement. Dans ces études, le modèle d'isotherme d'adsorption qui s'adaptait le mieux aux valeurs observées (discuté en détail dans la section résultats) était l'isotherme de Langmuir. Ce modèle suppose que l'adsorption monocouche s'effectue sur une surface qui contient un nombre fini de sites d'adsorption en supposant qu'il n'y a pas de transmigration de l'adsorbat dans la surface plane (Hameed et al. 2007). L'isotherme est représentée par l'Équation 11 comme suit:

$$Ce/qe = 1/bqmax + Ce/qmax \qquad \text{Équation 11}$$

Le tracé linéaire de *(Ce/qe)* versus *qe* (représenté par l'Équation 11) obéit au modèle de Langmuir où les constantes *b* et *qmax* obtenues à partir de l'interception et de la pente représentent l'énergie d'adsorption et la capacité d'adsorption maximale, respectivement. À partir de l'isotherme d'adsorption de Langmuir, l'affinité sorbat-sorbant peut être prédite en utilisant une constante sans dimension, RL (facteur de séparation). Ceci est exprimé par l'Équation 12 suivante:

$$R_L = 1/(1+bCi) \qquad \text{Équation 12}$$

où *Ci* est la concentration initiale du sorbat. La forme de l'isotherme et la nature de l'adsorption sont indiquées par la plage de valeurs RL présentée ci-dessous:

RL> 1, défavorable; RL = 1 linéaire; 0 <RL <1, favorable; RL = 0, irréversible

Études de régénération et de réutilisation

La régénération et la réutilisabilité de la colonne sont un aspect important pour comprendre le comportement du média adsorbant et la faisabilité économique globale de la colonne. Pour cela, la solution de Rhodamine-B a été utilisée comme modèle de colorant-adsorbat (concentration initiale, Co: 1 mg/L) pour chaque adsorbant (divers composites de sable). Un débit continu de 4

ml/min a été choisi pour un volume de lit de matériau de 7,5 cm. Après chaque volume de débit de 40 ml, l'OD550 a été déterminée (en utilisant une plaque à 96 puits) en triplicata afin de quantifier la quantité de Rhodamine-B adsorbée sur le matériau. Après l'épuisement du matériau du lit (C/Co ~ 1), les adsorbants ont été régénérés via une solution d'acétone et réutilisés pendant un total de trois cycles pour comprendre le potentiel de réutilisabilité de l'adsorbant. La capacité d'adsorption saturée (Wsat: mg/g) de chaque matériau a été calculée en utilisant l'Équation 13:

$$Wsat = (\int(U_o\ C_o)\ (1\text{-}c/c0\ ))/\ (g\text{-adsorbant}) \qquad \text{Équation 13}$$

Où *Uo* est la vitesse d'écoulement en L/min, *Co* est la concentration initiale d'adsorbat en mg/L et *t* (intégré de 0 à *t*) est le temps de percée en min.

Caractérisation des matériaux synthétisés et des grains de sable enrobés

Des micrographies électroniques à balayage (SEM) du GO/rGO synthétisé, de tous les matériaux de sable graphitisés (Chapitre 4, Partie 1 et Partie 2) et de tous les autres matériaux de sable revêtus préparés ont été enregistrés à l'aide du système Zeiss Evo®50 Smart SEM entre 5 et 15 kV. De plus, les données de spectroscopie infrarouge à transformée de Fourier (FTIR) ont été enregistrées en utilisant un instrument Perkin Elmer, Spectrum RXI, FT-IR équipé d'un détecteur au tantalate de lithium (LiTaO3). Une analyse par rayons X à dispersion d'énergie (EDX) a été effectuée pour confirmer le pourcentage atomique d'oxygène et d'atomes de carbone dans le GO/rGO synthétisé et pour déterminer la proportion de fer, de carbone et d'oxygène dans la surface de sable revêtue de Fe et FeGO. Le potentiel zêta des grains enrobés obtenus a été comparé aux grains de sable non enrobés afin d'indiquer le degré de surface électro-positive relative (par rapport aux grains de sable non enrobés) obtenue après le processus d'enrobage. Les grains de sable pulvérisés (enrobés et non enrobés) ont été suspendus en utilisant de l'eau ultrapure dans des cellules jetables DTS1060 à potentiel zêta (Malvern Instruments).

Indice de dispersion Morrill (MDI)

L'indice de dispersion Morrill (MDI) est un indice largement utilisé pour déterminer la quantité ou le degré de diffusion et de mélange dans le système de contact (Teixeira et do Nascimento, 2008). Il a été calculé sur la base de l'analyse de la distribution du temps de séjour où le KCl a été utilisé comme composé traceur. 200 mg/L de KCl ont été trouvés équivalents à 67,7 µS/cm. Le MDI a été calculé sur la base de l'équation suivante:

$$MDI = T_{90}/T_{10} \qquad \text{Équation 15}$$

Où *T90* est le temps nécessaire pour atteindre 90% de la valeur de conductivité (proportionnel à la concentration de l'élément traceur) et *T10* est le temps nécessaire pour atteindre 10% de la valeur de conductivité (proportionnel à la concentration de l'élément traceur).

Une valeur MDI proche de 1 définit une condition d'écoulement de bouchon parfaite tandis qu'une valeur de 23 définit un réacteur complètement mélangé/agité (Fia et al. 2016). Par conséquent, pour une colonne à lit poreux, une valeur plus proche de 1 sera plus souhaitable. Pour cela, les filtres aux deux échelles ont été alimentés à travers le milieu poreux en continu à une vitesse égale afin de maintenir la condition de bord à chaque fois.

Préparation de l'eau du lac

Cette section traite des étapes de préparation de l'eau du lac pour affluer vers les filtres. À titre de démonstration, la discussion est spécifique à l'objectif du Chapitre 5, Partie 2. Les lecteurs sont invités à se référer aux différents chapitres et à ses parties pour tout objectif expérimental spécifique. L'eau du lac Sainte-Anne (47,262879N, -71,665158W) a été utilisée comme solution affluente. Les contaminants ont été ajoutés pour atteindre la concentration finale suivante: NH4-N: 5 mg/L, Cu^{2+}: 20 mg/L, Fe^{2+} 10 mg/L et MC-LR: 50 µg/L (à la fois commercialle et un rejeté) de la biomasse d'algues cultivées en laboratoire). Avant d'ajouter les contaminants ci-dessus, la concentration initiale de chaque polluant a été déterminée, puis en conséquence, la solution finale a été préparée.

La trousse pour tester l'eau douce API®-800 a été utilisée pour l'étalonnage de l'ammoniac-N, Cu^{2+} et Fe^{2+} et l'expérience d'analyse des échantillons. La couleur produite par le réactif de la trousse et celle de l'échantillon a été calibrée par spectrophotométrie où l'absorbance a été mesurée à la longueur d'onde caractéristique, obtenue à partir de la cinétique de balayage en utilisant un instrument spectrophotomètre UV Cary 300. Le sulfate d'ammonium a été utilisé comme source d'ammoniac-N et a été ajouté à l'eau du lac selon les calculs stoechiométriques pour préparer une concentration finale de 5 mg/L NH4 + -N (volume final: 2 L). Le carbone organique dissous (COD) a été calculé à l'aide de l'analyseur Shimadzu 5000A (Shimadzu, Japon). En bref, environ 50 mL d'échantillon de l'effluent ont été filtrés à l'aide d'un filtre en fibre de verre de 0,45 µm et analysés pour le COD. La valeur de COD moyenne dans l'eau du lac s'est avérée être de 4,1 ± 0,6 mg/L, ce

qui a été augmenté à 14,8 ± 1,1 mg/L en utilisant du dextrose (la relation entre la dose de dextrose et la COD est mentionnée dans la section supplémentaire). En général, la valeur de COD dans l'eau du lac reste <6 mg/L, mais dans cette étude, le niveau de COD a été augmenté pour mieux représenter l'eau de source pendant la saison du mousson.

Les coliformes totaux ont été déterminés par la technique de filtration sur membrane selon la méthode standard APHA (1998). Les coliformes totaux moyens dans l'eau du lac étaient de 121 ± 37 UFC/100 mL. Les ions métalliques Fe^{2+} et Cu^{2+} ont été choisis comme indicateur d'ions métalliques dans l'eau du lac où $FeSO_4.7H_2O$ et $CuSO_4.5H_2O$ ont été utilisés comme source de métal respectivement. Une concentration initiale de Fe^{2+} et Cu^{2+} de 10 mg/L et 20 mg/L a été choisie sur la base de l'équivalent stœchiométrique des sources métalliques (comme mentionné ci-dessus) et la mesure a été effectuée par spectrophotométrie. La concentration initiale d'ammoniac-N et de Cu^{2+} dans l'eau du lac variait de 0,1 à 0,3 mg/L et de 1,3 à 2,3 mg/L et la concentration de cuivre ainsi préparée de 20 mg/L (enrichie) ne formait pas de complexe ammoniac-Cu en quantité significative et vice versa. Ainsi, uniquement pour l'analyse de l'ammoniac-N (pour la concentration initiale: 5 mg/L), il a été vérifié que l'eau brute (eau de lac préparée) ne contient pas d'ions de cuivre enrichis et vice-versa, sinon, elle aurait pu interférer dans l'analyse colorimétrique. Par conséquent, deux affluents d'eau de lac distincts ont été préparés où le deuxième lot a été utilisé chaque jour uniquement pour l'analyse de Cu^{2+}/NH_4-N. Enfin, la turbidité de l'eau du lac préparée a été mesurée à l'aide des instruments HACH 2100A qui étaient en moyenne de 42,5 ± 5,2 NTU.

PARTIE 8. SOMMAIRE DES DIFFÉRENTS VOLETS DE RECHERCHE EFFECTUÉS DANS CETTE ÉTUDE

8.1 Importance de la bioaugmentation dans un filtre à sable et nécessité d'une approche de co-culture utilisant des bactéries indigènes isolées de la STEP

Le communautés bactériennes isolées de différentes unités d'une station de traitement de l'eau potable (STEP), y compris l'unité de pré-ozonation (UPO), le mélange boues-effluents de l'unité de sédimentation (USE) et l'échantillon de biofilm de la couche supérieure de sable de l'unité de filtration (USF) ont été acclimatése séparément dans un'environnement riche en MC-LR pour évaluer la biodégradation des MC-LR. La biodégradation MC-LR la plus élevée a été mise en évidence avec une communauté bactérienne isolée sous forme unité supérieure de filtre à sable, où le taux d'élimination de MC-LR a augmenté de 1,5 fois (19,5 µg / L / jour) pour les cas acclimatés par rapport aux conditions non acclimatées (12,5 µg / L /jour). L'analyse de toxicité effectuée pour le bouillon de dégradation par utilisation d'un bioindicateur (*Rhizobium meliloti*) ainsi que le dosage de PP1A a révélé une toxicité moindre que l'échantillon initial (chapitre 2, partie 1).
Dans une autre expérience (chapitre 2, partie 2), les dégradeurs MC-LR connus, *Arthrobacter ramosus* (A) et *Bacillus sp.* (B) ont été bioaugmenté individuellement dans un filtre à sable. Ces filtres biosable étaient alimentés avec de l'eau de lac traitée à l'ozone qui comprenait 50 µg / L de MC-LR. Ces dégradeurs MC-LR connus se sont révélés efficaces pour une dégradation supplémentaire de MC-LR de 10% à 20%. La co-culture de A ou B avec X (A + X et B + X), a encore renforcé l'activité PP1A à plus de 60%. Ceci a démontre une moindre toxicité dans l'échantillon dégradé en utilisant la méthode de co-culture par rapport à une bioaugmentation de bactéries individuelles.

8.2. Co-culture de bactéries indigènes et de MC-LR-dégradeurs connus dans un biofiltre dynamique et statique

Dans d'autres travaux de recherche, des combinaisons des dégradeurs MC-LR connus (*Arthrobacter ramosus* (A*), Bacillus* sp. (B) ou *Sphingomonas* sp. (S)) et la culture bactérienne native (X): A + X, B + X et S + X, ont été explorés pour l'élimination du MC-LR et d'autres polluants de l'eau. L'implication positive de la bioaugmentation de la co-culture dans un filtre à sable a été bien démontreé dans l'expérience précédente. L'application de la technique de co-

culture a été étudiée pour l'élimination du MC-LR en utilisant un lit dynamique ainsi qu'un biofiltre en lit statique (chapitre 3, partie 1 et chapitre 3, partie 2). Le filtre à lit dynamique (réacteur à biofilm à lit mobile) a montré un taux d'élimination très lent de 94% d'élimination en 6 jours (concentration initiale: 50 µg / L), tandis qu'une élimination maximale de plus de 85% (cas S + X) a été observée en utilisant un filtre à sable à lit statique. Cependant, le problème commun de la percée précoce du MC-LR dans l'eau filtrée persistait. La performance du filtre biosable s'est améliorée en termes de bioactivité et d'élimination du MC-LR par utilisation des matériaux agro-résiduels (fibres de chanvre, boues de désencrage, pulpe et boues séchées sur papier) comme matériau adsorbant de la "couche supérieure du filtre" sur le sable (chapitre 3, partie 3). L'élimination du MC-LR et d'autres polluants de l'eau a été améliorée de seulement 5% à 10%. De plus, le problème de percée précoce du MC-LR persistait toujours.

8.3. Modification du milieu sableux pour améliorer sa capacité d'adsorption et son temps de passage

Le phénomène de percée précoce du MC-LR et la mauvaise propriété d'adsorption des milieux filtrants (sable) demeure un défi, comme mentionné dans la section 7.2. Pour faire face à ce problème, la surface du sable a été modifiée (en termes d'hydrophilie, de rugosité et de surface spécifique) en utilisant la méthode de revêtement thermique. Pour ce faire, des particules de carbone submicroniques sous forme d'oxyde de graphène (GO) et d'oxyde de graphène réduit (rGO) ont été utilisées pour recouvrir les grains de sable. Étant donné que le MC-LR porte une charge négative sous une solution à pH neutre, la surface du sable a été modifiée en une surface plus électropositive en la recouvrant d'oxyde de fer (Fe) et d'oxyde de fer sur du sable recouvert d'oxyde de graphène réduit (Fe + rGO). La plus forte élimination des MC-LR, soit 91 %, a été obtenue lors de la phase de biodégradation (6 semaines de fonctionnement du biofiltre) en utilisant du sable recouvert de rGO qui a montré une augmentation de 47,2 % de l'élimination des MC-LR par rapport à la phase d'adsorption physique (6 semaines de fonctionnement). De façon surprenante, le filtre à Fe a été moins performant dans l'élimination des MC-LR (max : 33,6 %) pour les deux phases de fonctionnement du filtre que le filtre à sable (max : 54,7 %) (chapitre 4, partie1).

Dans une autre expérience (chapitre 4, partie 2), les grains de sable ont été modifiés par graphitisation. Pour assurer une graphitisation complète, une solution de sucre a été utilisée (0,1 g / g de sable) pour recouvrir les grains de sable. L'utilisation d'effluents de brasserie (contenant du sucre) a constitué la base d'une approche durable (sable graphité 1: GS1) afin d'atteindre l'objectif ci-dessus, tandis que du saccharose commercial a été utilisé pour préparer la solution de sucre témoin (sable graphité 2: GS2). Pour une meilleure amélioration de la surface de sable graphité, le di-oxyde de manganèse a été recouvert par chauffage thermique (GS1M et GS2M). GS1 et GS2 utilisés comme milieux filtrant, ont amélioré l'élimination du MC-LR de 50%. La lixiviation MC-LR dans la solution filtrée n'a pas été observée pendant 16 semaines de fonctionnement du filtre en utilisant l'adsorbant GS1 comme milieux filtrant. Après trois cycles de régénération et de réutilisation du filtre GS1, une diminution de seulement 14% de la capacité d'adsorption saturante a indiqué son aspect de réutilisation élevée.

Dans l'ensemble, le filtre GS1 a obtenu les meilleures performances parmi tous les filtres testés dans le cadre de ce projet, non seulement en ce qui concerne l'élimination des MC-LR et autres polluants de l'eau, mais aussi en termes de période de percée élevée. Une analyse détaillée des composantes principales est présentée au chapitre 4, partie 3.

8.4. Mise à l'échelle en utilisant les médias filtrants les plus performants

Après une adsorption réussie du MC-LR sur le milieu de sable graphité (GS1) et l'observation d'aucun phénomène de percée du MC-LR même après 16 semaines de fonctionnement du filtre, l'étape suivante a consisté à évaluer les paramètres hydrodynamiques du filtre à l'échelle du banc pour éviter tout phénomène de court-circuit qui pourrait affecter le régime d'écoulement pendant la mise à l'échelle. Le régime d'écoulement a été compris par la modélisation et la programmation intégrée à l'aide du solveur ANSYS-CFX utilisant le concept de la dynamique des fluides numérique. L'échelle minimale subjective de 9 cm x 9 cm avec une hauteur de 30 cm a été déchiffrée pour fournir un régime d'écoulement à vitesse radiale pour le plan orthogonal à la vitesse d'écoulement linéaire (chapitre 5, partie 1).

L'étude du bilan massique a été réalisée à l'aide du filtre 'subjectif à échelle minimal', dans le cadre de la configuration du modèle de la STEP en laboratoire appelé SAP-1© : SAP-1©. En plus du modèle MC-LR, divers autres paramètres de qualité de l'eau (" PQE ") ont été étudiés, notamment

les ions métalliques, les coliformes totaux, la turbidité et le carbone organique dissous, afin de rendre compte de l'efficacité de l'élimination de ces contaminants dans différentes unités de traitement. L'étude sur l'élimination des MC-LR a été réalisée pour une concentration initiale de 50 µg/L en utilisant deux sources de MC-LR : a) les MC-LR commerciales, b) les MC-LR sécrétés par la biomasse algale (*Microcystis aeruginosa*). De plus, une concentration initiale de 50 µg/L de MC-LR provenant des deux sources de MC-LR a été directement acheminée à travers le filtre, ce qui a permis de constater la présence de <0,7 µg/L de MC-LR dans l'effluent du filtre, conformément aux directives de l'OMS (< 1 µg/L). Cela suggère également une application du filtre GS1 de mise à l'échelle au niveau des ménages (chapitre 5, partie 2).

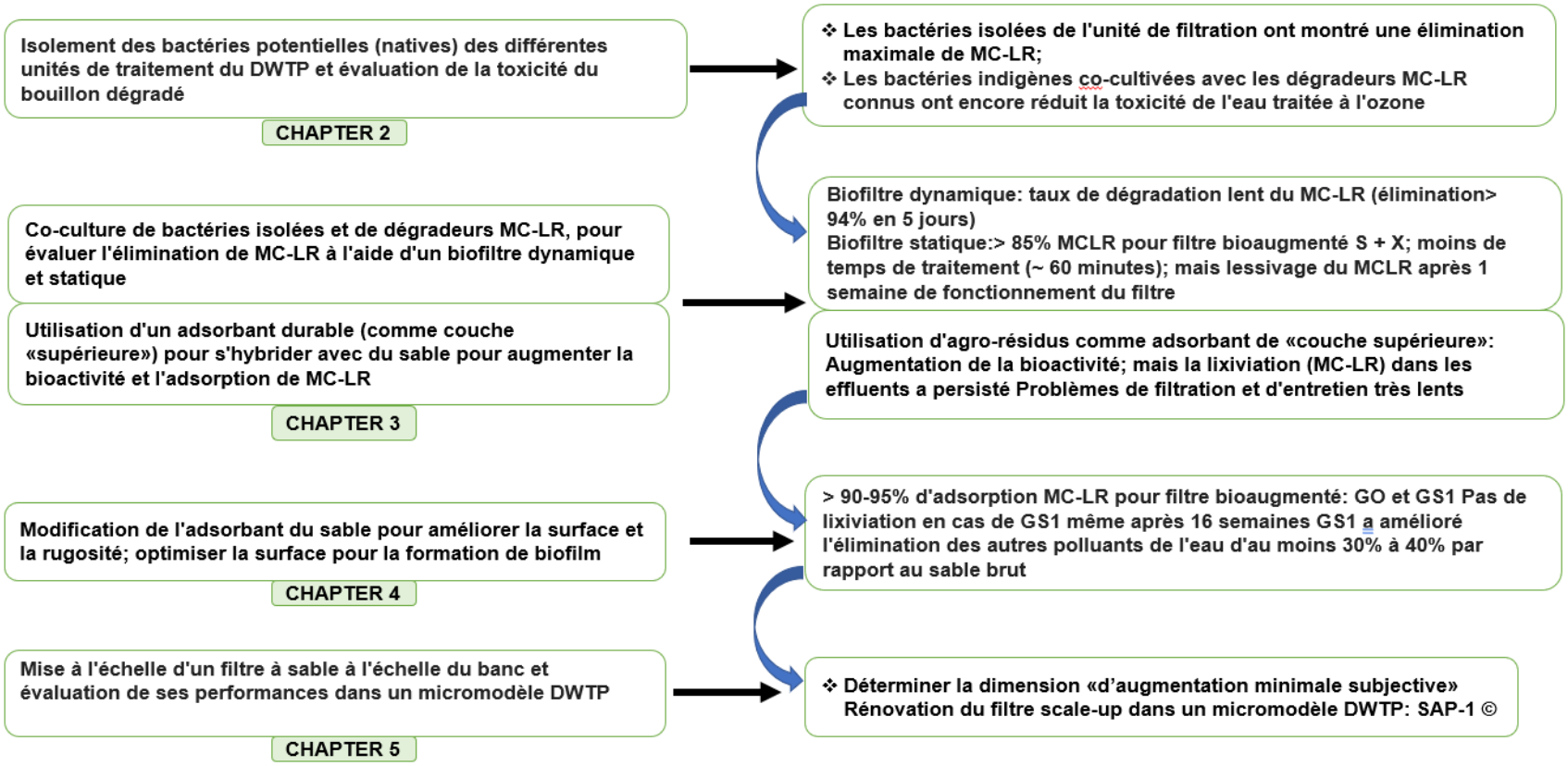

Figure 1.6: Schematic of objectives (left) and a brief summary (right)

CHAPTER 2: Significance of bioaugmentation in a filter using native bacteria isolated from DWTP

PART 1

Biodegradation of microcystin-LR using acclimatized bacteria isolated from different units of the Drinking Water Treatment Plant

Pratik Kumar [a], Krishnamoorthy Hegde [a], Satinder Kaur Brar [a*], Maximiliano Cledon[b], Azadeh Kermanshahi-pour[c], Audrey Roy-Lachapelle[d,e], Rosa Galvez-Cloutier[f]

[a] - INRS-ETE, Université du Québec, 490, Rue de la Couronne, Québec, Canada G1K 9A9

[b] - Instituto de Investigaciones Marinas y Costeras (IIMyC-CONICET), Funes 3350, Mar del Plata 7600, Argentina

[c] – Biorefining and Remediation Laboratory, Department of Process Engineering and Applied Science, Dalhousie University, 1360 Barrington Street, Halifax, Nova Scotia B3J 1Z1, Canada

[d]- Department of Chemistry, Université de Montréal, Montréal, QC, Canada

e- Environment and Climate Change Canada, 105 rue McGill, H2Y 2E7, Montréal, QC, Canadas

f- Faculté des Sciences et Génie, Département de génie civil et génie des Eaux, Université Laval, Québec (Québec), Canada.

[*]- Corresponding author, E-mail: satinder.brar@ete.inrs.ca (S.K. Brar)

***Environmental Pollution*, 242, 407-416 (2018); DOI: 10.1016/j.envpol.2018.07.008**

Résumé

Les communautés bactériennes isolées de différentes unités d'une usine de traitement d'eau potable (STEP), y compris l'unité de pré-ozonation (POU), le mélange effluent-boue de l'unité de sédimentation (ESSU) et l'échantillon d'eau de la couche de sable supérieure de l'unité de filtration (TSFU) ont été acclimatées séparément dans un environnement riche en MC-LR pour évaluer la biodégradation de MC-LR. L'efficacité de biodégradation maximale de 97,2 ± 8,7% a été atteinte par la communauté bactérienne acclimatée-TSFU suivie de 72,1 ± 6,4% et 86,2 ± 7,3% par la communauté bactérienne acclimatée-POU et acclimatée-ESSU, respectivement. De même, la communauté bactérienne non acclimatée a montré une efficacité de biodégradation similaire de 71,1 ± 7,4%, 86,7 ± 3,2% et 94,4 ± 10,6% pour TSFU, ESSU et POU, respectivement, par rapport à celles acclimatées. Cependant, le taux de biodégradation a augmenté de 1,5 fois pour une condition acclimatée par rapport à une condition non acclimatée. Les études de spectrométrie de masse sur la dégradation du MC-LR ont montré une linéarisation hydrolytique du MC-LR cyclique ainsi que la formation de petits fragments peptidiques comprenant une molécule «adda» liée à la toxicité réduite (analyse qualitative de la toxicité). Cela a été confirmé en outre quantitativement en utilisant *Rhizobium meliloti* comme bioindicateur. La communauté bactérienne TSFU acclimatée comprenait de nouvelles souches dégradantes de MC-LR, *Chryseobacterium* sp. et *Pseudomonas fragi,* tel confirmé par le séquençage de l'ARNr 16S.

Mots-clés: Bactéries acclimatées, microcystine, voie de dégradation, eau potable, toxicité

Abstract

Bacterial community isolated from different units of a Drinking Water Treatment Plant (DWTP) including pre-ozonation unit (POU), the effluent-sludge mixture of the sedimentation unit (ESSU) and top-sand layer water sample from the filtration unit (TSFU) were acclimatized separately in the MC-LR-rich environment to evaluate MC-LR biodegradation. Maximum biodegradation efficiency of 97.2 ± 8.7% was achieved by the acclimatized-TSFU bacterial community followed by 72.1 ± 6.4 % and 86.2 ± 7.3 % by acclimatized-POU and acclimatized-ESSU bacterial community, respectively. Likewise, the non-acclimatized bacterial community showed similar biodegradation efficiency of 71.1 ± 7.37 %, 86.7 ± 3.19 % and 94.35 ± 10.63 % for TSFU, ESSU and POU, respectively, when compared to the acclimatized ones. However, the biodegradation rate increased 1.5-folds for acclimatized condition as compared to non-acclimatized condition. The mass spectrometry studies on MC-LR degradation depicted hydrolytic linearization of cyclic MC-LR along with the formation of small peptide fragments including 'adda' molecule that is linked to the reduced toxicity (qualitative toxicity analysis). This was further confirmed quantitatively by using *Rhizobium meliloti* as a bioindicator. The acclimatized-TSFU bacterial community comprised of novel MC-LR degrading strains, *Chryseobacterium sp.* and *Pseudomonas fragi* as confirmed by 16S rRNA sequencing.

Keywords: Acclimatized bacteria, microcystin, degradation pathway, drinking water, toxicity

Introduction

The occurrence of cyanobacterial harmful algal bloom (CHABs) affects fresh and marine ecosystems (O`Neil et al. 2012). It is also a matter of public health concern, as the standard water treatments are not designed to target the removal of such compounds. (Hitzfeld et al. 2000). An algal bloom is a global issue, where CHAB genera, such as *Anabaena, Cylindrospermopsis, Nodularia, Microcystis* and other benthic species produce a variety of cyanotoxins, namely, cylindrospermopsin, nodularin, saxitoxin, microcystins (MCs), among others, affecting water quality (Carey et al. 2013). Among all, MCs are known to be stable in the natural aquatic environment due to their cyclic structure (Somdee et al. 2013). There are many variants of microcystin (MCs) produced by *Microcystis sp.*, such as MC-LR, MC-RR, MC-YR, MC-WR, MC-LA, MC-LY, MC-LW, MC-LF, depending on the position of different peptide groups in the cyclic structure. Among all, MC-LR, produced by *Microcystis aeruginosa* is known to be one of the deadliest cyanotoxins, commonly found in an aquatic ecosystem. Further, the WHO recommends that the microcystin present in drinking water should not exceed 1 µg/L (WHO, 1999).

When microcystins enter the DWTPs (at concentrations above 10 µg/L), conventional treatment options, such as ozonation, chlorination, coagulation/flocculation, become ineffective in the long run due to the periodic change in the parameters such as pH, temperature, among others. They sometimes produce toxic byproducts too (Gagala et al. 2012). Also, the advanced methods of cyanotoxin treatment, such as photodegradation and RO membrane technique are not cost-effective and are energy intensive. On the other hand, the biological approach is not only promising in degrading various cyanotoxins, but it is also sustainable, less energy-intensive and known to produce less toxic end-products than the parent compound (up to 160-fold less) (Somdee et al. 2013).

Many studies have reported biodegradation of MC-LR by native bacterial species isolated from various water streams, such as rivers, lakes, ponds, and sediments (Neilan et al. 2014; Chen et al. 2010). However, their applicability in DWTP is limited, given the fact that only a few studies have been reported on the interaction of MCs with the *in-situ* bacterial community present within the DWTP units. Hence, it is important to explore and compare the capability of such *in-situ*, naturally occurring microorganisms present in the DWTPs units for MC-LR degradation. These

acclimatized microorganisms have the advantage of natural growth and therefore could be utilized without any modification in the existing treatment units. For example, the sand filtration system can be modified into a bio-sand filter to effectively degrade microcystins.

This study investigates the role of bacterial community, isolated from three distinct units of DWTP comprising samples before pre-ozonation step (POU) in the form of raw water, the effluent-sludge mixture from the sedimentation unit (ESSU) and top layer-sand particles from the filtration unit (TSFU). The degradation efficiency and rate of these bacterial communities were compared before and after acclimatization in the presence of MC-LR. Also, the toxicity test for the biodegraded broth was performed using a bioindicator. To the best of our knowledge, this is the first report exploring the ability of microcystin-acclimatized indigenous bacterial communities isolated from "*different units of the DWTP*" to degrade MC-LR.

Material and methods

Reagents and chemicals

Microcystin-LR was purchased from Cayman Chemicals, (Ann Arbor, Michigan, USA). $MgSO_4 \cdot H_2O$, $ZnSO_4 \cdot H_2O$, $Na_2MoO_4 \cdot 2H_2O$, KH_2PO_4, $Na_2HPO_4 \cdot 7H_2O$, $CaCl_2$ and $FeCl_3$ *was bought from Fisher Scientific, (*Ontario, Canada*).* Millipore system (Milford, MA, USA) Milli-Q/Milli-RO was used to prepare mineral salt media (MSM) solutions spiked with MC-LR. Sodium chloride (NaCl), peptone and yeast extract were purchased from Fisher Scientific (Ottawa, ON, Canada) and used to prepare Luria-Bertani medium for bacterial culture and inoculation of the isolated bacteria. For the toxicity assay: Tris-HCl buffer (pH 7.5) was prepared using Tris-buffer and 6N HCl (Merck, US) and 3-(4, 5-dimethylthiazol-2-yl)-2, 5-diphenyltetrazolium bromide (MTT) was used for measuring cell viability, bought from Sigma Aldrich, (Ontario, Canada).

Microorganisms

Sphingomonas sp. (NRRL B-59555) and *Rhizobium meliloti* (NRRL L-84) were purchased from NRRL Agricultural Research Service (ARS) culture collection. They were respectively used as the positive control in studying MC-LR degradation (Ishii et al. 2004) and as a bioindicator for determining the toxicity of the biodegraded broth (Botsford et al. 1997).

Water sample collection for bacterial isolation

In total three unit operations of the DWTP at Chemin Ste-Foy, (Quebec City, Canada) were chosen for the water sample collection. The water sample from three different treatment stages *viz*., (1) influent stream (before pre-ozonation (POU) treatment), (2) effluent-sludge mixture from the sedimentation unit (ESSU) and, (3) top-sand water sample (biofilm+sand+water) from the filtration unit (TSFU) were collected for the microbial isolation. Henceforth, the study pertaining to these samples will be referred to as Unit-1, Unit-2, and Unit-3, respectively. Around 30 mL of the sample collected from Unit-1 was filtered using glass fiber filter (pore size: 0.45 µm) to separate out any solid particles and use filtrate as an inoculum for microbial culture. Likewise, around 30 mL of effluent-sludge collected from Unit-2 and sand biomass sample from Unit-3 was centrifuged at 8000 x g for 30 minutes and the supernatant was used as an inoculum.

Bacterial Isolation

Enriched culture method was used for culturing and isolation of bacteria from the water sample (Manage et al. 2009). In brief, 15 mL of a filtered water sample from Unit-1, Unit-2, and Unit-3 were individually added to 75 mL of Luria-Bertani (LB) media in 250 mL Erlenmeyer flask. The flasks were incubated at 30 ± 1 ºC and 150 rpm for 2 days. A 15 mL of enriched culture broth was sub-inoculated into the freshly prepared LB media (75 mL total). The procedure was repeated three times. The resulting culture broth (100 µl) was streaked on LB-agar plate and incubated at 30 ± 1 ºC for 2-3 days. The heterogeneous colonies (based on colour, morphology, and dominance) for each of the three units were isolated and serially streaked onto the LB-agar plates. In brief, a total of six bacteria was isolated. One from (INRSW1; Unit-1 bacterial community), two from ESSU (INRSW2+INRSY1= Unit-2 bacterial community) and three from TSFU (INRSW3+INRSY2+INRSB1 = Unit-3 bacterial community) where W, Y, and B stands for white, yellow and brown colour, respectively.

Bacterial growth study and viability test under MC-LR environment

Growth characteristics of all the six isolated bacteria were studied individually for three cases viz. a) without the presence of MC-LR; b) with a lower dose of MC-LR (10 µg/L) and; c) with a higher dose of MC-LR (100 µg/L). Growth parameters, such as doubling time, lag phase, log phase (not shown) and the relation between cell viability vs optical density: A_{600nm} (UV-VIS Cary-50) were determined for each bacterial variety. The viable cell count was determined by colony forming

unit (CFU) through serial dilution method as described by Gargouri et al, (2015) and its relationship to A_{600nm} was established. The viable count was measured by counting the colonies on LB-agar Petri plate, expressing the result as CFU/mL. All experiments were performed in triplicates. The experimental procedure and operating conditions were similar as described in section 2.4 for the growth study.

Viability count test on LB-agar plate was performed for four exponential points (i.e. one early, two mid and one late exponential point). The sum of viable colonies of all the four exponential points was considered to determine viability variations. The control was assigned a value of 100 (case a: control) and thus normalized values were reported to study the change in viability that occurred both at lower (10 µg/L) and higher MC-LR (100 µg/L) concentration.

Acclimatization and post-acclimatization biodegradation study of MC-LR

Bacterial community derived from Unit-1, Unit-2 and Unit-3 were acclimatized using 200 µg/L MC-LR and their degradation potential were evaluated. This study was performed to enrich the bacterial community and acclimatize them under MC-LR environment (Bourne et al. 2001). After acclimatization, the culture media (200 µL) was plated on LB-agar to isolate the enriched bacteria (2^{nd} generation bacteria) individually. Both acclimatization and post-acclimatization of MC-LR degradation studies were carried out in MSM, as suggested by Valeria et al. (2006), with some modifications as follows. The composition of the media per litre included 100 mg $MgSO_4 \cdot H_2O$, 5 mg $ZnSO_4 \cdot H_2O$, 2.5 mg $Na_2MoO_4 \cdot 2H_2O$, 300 mg KH_2PO_4, 650 mg $Na_2HPO_4 \cdot 7H_2O$, 20 mg $CaCl_2$ and 0.15 mg $FeCl_3$ as the nutrient and MC-LR as the sole carbon and nitrogen source.

Approximately, a 6 $x10^6$ cells/mL (exponential phase bacteria) were spiked to study MC-LR degradation for bacterial community derived from Unit-1, Unit-2, and Unit-3. For example, 6 $x10^6$ cells/mL of INRSW1 bacterial cells isolated from unit-1 sample, $3x10^6$ bacterial cells/mL each of INRSW2 and INRSY1 isolated from Unit-2 sample and $2x10^6$ bacterial cells/mL each of INRSW3, INRSY2, and INRSB1 from Unit-3 sample, were spiked in MSM to study MC-LR degradation. Hence, three flask studies were performed. Before spiking these bacterial cells, culture media (containing LB medium and bacterial cells) were centrifuged at 8000 rpm at room temperature for 30 minutes to obtain the bacterial pellets. These bacterial pellets were further rinsed and centrifuged twice with phosphate buffer (pH 6.91) to remove any residual carbon present in the

solution (due to LB medium in the previous step). MSM solution (60 mL) containing 200 µg/L MC-LR was then spiked with bacterial pellets of known cell concentration (co-culture combination as discussed above), shaken well and incubated at 30 ± 1 ºC and 150 rpm.

The degradation study for the acclimatization (non-enriched bacteria) and post-acclimatization phase were carried out for 15 days and 10 days respectively using same experimental condition (30 ± 1 °C;150 rpm, 200 µg/L MC-LR) and same co-culture cell suspension concentration (6 x 106 cells/mL). *Sphingomonas sp.* (NRRL B-59555) was spiked in MSM containing 200 µg/L MC-LR with the same cell suspension (6 x 10^6 cells/mL) as the positive control, which was previously reported to degrade MC-LR (Ishii et al. 2004; Valeria et al. 2006). In addition, MSM media with 200 µg/L MC-LR without any bacteria was taken as the negative control.

Kinetics test was performed for the degradation study by following two equations given below. Equation 1 shows zero-order kinetics relation between substrate concentration (MC-LR here) and time whereas equation 2 fits into the first order kinetics relation.

$C_o - C_t = kt$ Equation 1

$C_t = C_o . e^{-kt}$ Equation 2

Putting log on both sides and on rearranging the parameters, we get:

$\ln C_o - \ln C_t = kt$ Equation 3

Where C_o= Initial substrate concentration; C_t = Substrate concentration at time t and k= kinetics constant.

MC-LR biodegradation and by-products analysis

The MC-LR was analyzed in samples collected after 5 days, 9 days, 12 days, and 15 days for acclimatization-degradation study and after 2 days, 5 days, 8 days, and 10 days for post-acclimatized degradation study. These samples (3 mL) were centrifuged at 10,000 x g for 15 minutes at 20 ± 1 ºC. The supernatant was extracted and filtered using 0.45 µm sterile filter, capped in black-coloured microcentrifuge tubes (BCCT) to avoid MC-LR photodegradation and stored at -20 ºC, until High-Performance Liquid Chromatograph (HPLC) analysis following protocol as discussed in Fayad et al (2015).

By-product fragments formed during degradation were analyzed by mass spectroscopy. Around 1 mg/L of microcystin-LR was used as an internal standard along with mobile phase of 50:50 (v/v) MeOH (A) and water (B) with 0.1% formic acid. The final parameters used to maximize the signal intensity were: capillary temperature: 350°C, vaporizer temperature. 450°C, sheath gas pressure, aux gas pressure and ion sweep gas pressure: 35, 10 and 0 arbitrary units, respectively. The scan time was adjusted to 0.02 sec, where the first and third quadrupoles were operated at the unit resolution with second quadrupole collision gas pressure at 1.5 mTorr. Overall, this method presents an optimized rapid chromatographic method using an on-line solid-phase extraction coupled to ultra-HPLC tandem mass spectrometry for the determination of seven different cyanotoxins including microcystin-LR.

Toxicity assessment of the degraded MC-LR samples/broth

The toxicity of biodegradation broth (biodegraded sample obtained for the 10^{th} day) for all three units (Unit-1, Unit-2, and Unit-3) were examined using a bio-indicator: *Rhizobium meliloti* . Soil media was used for the culture of *R. meliloti* as mentioned in Surange et al. (1997) with some modifications.. Finally, the solution was made up to 1 litre and was autoclaved at 121 ± 1 °C for 20 minutes. Lyophilized *R. meliloti* strain was cultured in the soil media and kept for 24-36 h in a shaking incubator at 150 rpm and 30 ± 1°C. Afterwards, they were successively sub-cultured two times (5% v/v) and streaked on the LB-agar plate (1.8%) to obtain the pure colonies.

Toxicity-protocol described by Botsford et al (1999) was followed with some modifications as follows. A 1 mL each of Tris-HCl buffer (pH 7.5), toxic sample (DMSO and MC-LR at different concentrations) and bacterial cell suspension (*R.meliloti*) were mixed in a glass test tube and allowed to stand for 60-120 seconds. This time lapse allowed sufficient exposure for partial or total mortality of the cell culture depending on the degree of toxicity of the compound (MC-LR and DMSO tested). Later, around 350 µL of MTT ((3-(4,5-dimethylthiazol-2-yl)-2,5-diphenyltetrazolium bromide) dye solution (7 mg/10 mL) was added to the mixture which converted the solution from initial yellow to blue precipitate (viable cells, if left any, dies and forms formazan (blue precipitate). A special study to evaluate the critical incubation period for the bioindicator was performed. at three-time periods (10h, 16h, and 24h). It was found that the overnight incubation (10h) time period was the most critical time period, as also observed by Bodsford et al. (1999) to obtain the most fitted absorbance trend graph with various concentrations

of toxic chemicals, i.e., without any ambiguity in the trend (graph not included for different time periods of incubation). For the reference toxic chemical, three compounds were selected viz. methanol, ethanol and dimethyl sulfoxide (DMSO). Among these compounds, DMSO was finally chosen based on the uniformity in absorbance test achieved and devoid of any ambiguous observation in absorbance values. The relationship between MC-LR (concentration ranging: 92 µg/L to 1470 µg/L) and DMSO (10%-100% v/v) was then established to report toxicity of the biodegraded broth in terms of equivalent DMSO (% v/v) concentration.

The toxicity assessment was based on the absorbance measurement at 550 nm (UV-VIS Cary 50 Spectrophotometer) post colour change from yellow to blue due to the addition of MTT dye. After addition of MTT dye (0.350 mL) in combination with Tris-buffer, the toxic sample and bacterial cell suspension (total 3.350 mL mixture), the glass test tubes were capped and incubated for 1.5-2.5 h at 35 ± 1 °C. All the tests were done in triplicates.

Bacterial species identification by ribosomal sequencing

Out of the three DWTP units viz. Unit-1, Unit-2 and Unit-3, the bacterial community, which showed the highest MC-LR degradation was selected to undergo the MC-LR degradation test (performed individually on each of its comprising isolates). Bacterial species were further identified by ribosomal sequencing.

The genomic DNA isolation was performed using E.Z.N.A.® Bacterial DNA Kit (Omega Bio-Tek, USA) as per manufacturer's instructions. The isolated DNA was PCR amplified using a 27F forward primer (5'-AGAGTTTGATCCTGGCTCAG) and 1492R reverse primer (5'-GGTTACCTTGTTACGACTT). The PCR amplicon was further sequenced for 16s rDNA identification of the bacterial strain (sequencing service from Génome Québec Innovation Centre). The identified sequence was analyzed using NCBI BLAST service to identify the bacterial strain. The identified 16aS rDNA is deposited in NCBI GenBank.

Statistical Analysis

Statistical analysis related to the analyzed parameters such as standard deviation, student t-test, a p-value of all the data sets and other graphical presentations were performed in ORIGIN software (Version 8.5; OriginLab).

Results and discussion

Bacterial Culture and Isolation

Samples obtained from three different units of the DWTP were cultured and heterogeneous bacterial growth was obtained over the LB-agar plate for each case as discussed in later section. The dominant bacteria as observed based on the colour was chosen as the representative of the bacterial culture community for each of the three units. INRSW1 from Unit-1 with white colour, INRSW1 and INRSY1 from Unit-2 with white and yellow colour, respectively and INRSW1, INRSY2 and INRSB1 from Unit-3 with white, yellow and brown colour respectively, were isolated. Each of these bacteria was further studied for their growth behaviour under various conditions as discussed in the next section. However, the degradation study was carried out as a microbial community as discussed in later section.

Bacterial growth study and viability test under MC-LR environment

Figure 2.1.1 (A, B, C, D) shows the growth curve (48 h period) for all the six bacteria isolated from different units of the DWTPs studied for four cases viz. a) in absence of MC-LR (Fig 1A), b) with 10 µg/L MC-LR (Fig 1B), c) with 100 µg/L MC-LR (Fig 2.1.1 (C)) and, d) acclimatized bacteria (2^{nd} generation) without MC-LR.

The growth characteristics were measured as lag phase and doubling time (time needed to double the bacterial cells during exponential phase). Their ability to grow under the MC-LR environment (case “b” and “c”) were judged based on the change observed in lag phase and doubling time. It was found that the doubling time and lag phase increased for all the bacteria except for the yellow isolates (INRS Y1 and INRS Y2) and INRSB1 (Figure 2.1.1).

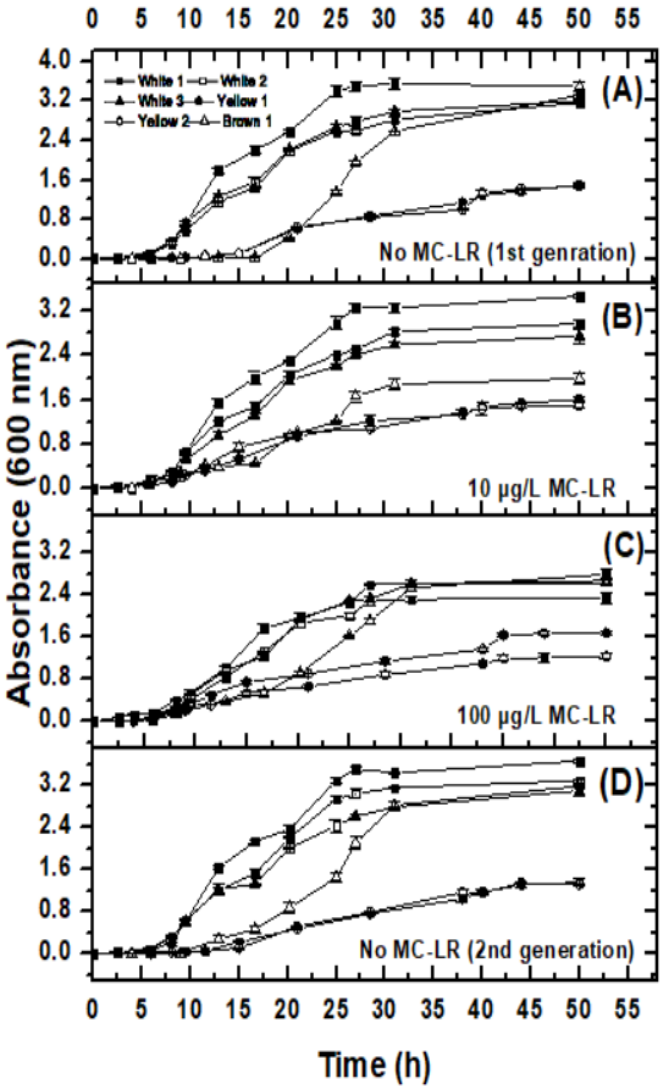

Figure 2.1.1: Growth curve for all six bacteria isolated from different units of drinking water treatment plant (DWTP) with (A) No MC-LR;(B) 10 µg/L MC-LR;(C) 100 µg/L MC-LR and; (D) No MC-LR (2nd generation)

This showed that the viable bacterial population under MC-LR environment decreased but continued their natural growth. However, from student`s t-test analysis which was carried out for all six bacteria to compare their growth under MC-LR (in terms of A_{600}) to case "a" (no MC-LR), it was found that there was no significant difference (p-value greater than t-value) between the case "a" and "b" (average p-value 0.73 as compared to a t-value of 0.33 for all six bacteria) and "a" and "c" (averaging p-value 0.98 as compared to a t-value of 0.02 for all six bacteria). This signifies that the growth characteristics did not change in response to the presence of MC-LR even at 100 µg/L.

To further confirm these observations qualitatively, the sum of viable cells (CFU/mL) of four exponential points (one early, two mid and one late exponential points) for the case "b" and "c" were compared to the case "a" (no-MC-LR; control and assigned value 100). Figure A1 (Appendix A) shows the bar graph for the survival test of these bacteria under MC-LR environment. It was found that sum of viable cells decreased (normalized value<100) for all the six bacteria showing an overall obvious maximum effect at 100 µg/L (case c). Even the worst viability among all the six variety of bacteria was shown to be above 75% (77% for INRS W2) (also proved statistically as discussed in the previous paragraph) This indicates the bacterial potential to survive even in presence of high MC-LR concentration.

Acclimatized bacteria (case "d") showed a decrease in doubling time for all bacteria when compared with the case "a" (non-acclimatized without MC-LR) except INRS W3 (which anyways showed minor change). This indicated that after acclimatization, the growth rate (slope of exponential part of the growth curve) and also the maximum growth of bacteria (represented by saturated optical density: $\lambda_{600\ nm}$ value) gets enhanced. A study by Hu et al. (2009) indicated that MCs degradation by *Methylobacillus sp.,* (isolated from cyanobacteria-salvaged sludge) required initial lag period which after acclimatization accelerated MC-LR degradation without any lag phase, even when new MCs extract was added (highlighting the importance of acclimatization). Table A1 (Appendix A) shows the relationship between viable cells (CFU/mL) and A_{600} for acclimatized bacteria. This relationship helped in obtaining the known concentration of bacterial cells for the degradation study (discussed in the next section).

Acclimatization biodegradation study of MC-LR

Degradation ability of co-cultured bacterial mix as found in Unit-1 (INRS W1), Unit-2 (INRS W2 + INRS Y1) and Unit-3 (INRS W3 + INRS Y2 + INRSB1) were tested with 200 µg/L MC-LR for both non-acclimatized bacteria (no previous MC-LR exposure) and acclimatized bacteria (previous exposure with MC-LR; case "d" as discussed in later section). Figure 2.1.2 (A) shows the degradation study of MC-LR for non-acclimatized bacterial culture for each unit: Unit-1, Unit-2, and Unit-3 along with the trend for the cell viability. Total MC-LR degradation achieved by bacterial community mixture derived from POU (Unit-1), ESSU (Unit-2) and TSFU (Unit-3) was observed to be 71.1 ± 7.4 %, 86.7 ± 3.2 % and 94.3 ± 10.6 %, respectively after 15 days. As depicted in Figure 2.1.2 (A), the heterogeneous bacterial cell count decreased from initial count of

6 x 10^6 CFU/mL to 5.2 x 10^6, 5.7 x 10^6 and 5.3 x 10^6 CFU/mL for Unit-1, Unit-2 and Unit-3 respectively after 15 days. The viable cell count decreased after 5 days followed by attaining maximum viability of 7.8 x 10^6, 7.2 x 10^6, 7.8 x 10^6 CFU/mL on the 9th day for Unit-1, Unit-2, and Unit-3, respectively (Figure 2.1.2 (A)). The initial decrease in cell count might be due to the toxic-shock of MC-LR to the bacterial community, which gradually recovered later, by metabolizing MC-LR (present as the sole carbon and nitrogen source in MSM). Kansole et al (2016) reported degradation of MC-LR (100 µg/L: by *Bacillus sp.* for 12 days) with a continuous decrease in bacterial population from 85 x 10^5 CFU/mL to 8 x 10^5 CFU/mL. However, in the present study, the decrease did not persist longer and after 5 days, the bacterial population increased 1.25 folds than the starting cell count (as discussed above), clearly showing the positive sign of bacterial adaptation utilizing MC-LR to maintain their metabolic activity.

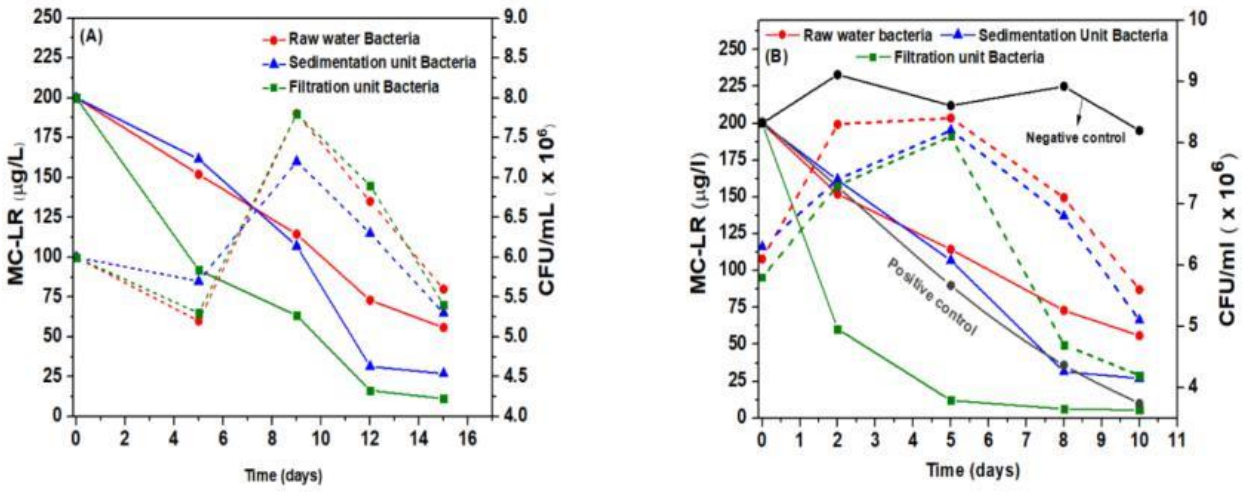

Figure 2.1.2: Drawdown curve of MC-LR and cells viability trend for: (A) pre-acclimatization phase and; (B) Post-acclimatization phase

Post-acclimatization biodegradation study of MC-LR

Figure 2.1.2 (B) shows the MC-LR degradation profile for the post-acclimatization phase (2nd generation bacteria) along with the cell viability tested between 2 to 10 days. The final MC-LR degradation efficiency was similar to the degradation in acclimatization phase. Acclimatized-TSFU (Unit-3) bacterial community achieved the highest degradation efficiency of 97.2 ± 8.7 % followed by ESSU (Unit-2) (86.2 ± 7.3 %) and POU (Unit-1) (72.1 ± 6.4 %) acclimatized bacterial

community. However, steady state was achieved after 10 days (as compared to 15 days for the non-acclimatized case) where corresponding degradation rate increased to 14.46 µg/L/day,17.32 µg/L/day,19.45 µg/L/day for Unit-1, Unit-2 and Unit-3, respectively (Table 2.1.1). These degradation rates were around 1.5-fold higher than the degradation under the non-acclimatized bacterial case. The degradation rates were higher than some previously reported studies on microcystin variants (MC-LR/MC-RR) with the same growth medium (MSM) used as shown in Table 1.4.

Table 2.1.1: Degradation efficiency and degradation rate for pre-acclimatization and post-acclimatization phase

Case	Degradation rate [µg/L/day]	Removal efficiency	Kinetics constant	Degradation rate [µg/L/day]	Removal efficiency	Kinetics constant
	Before acclimatization			After acclimatization		
Raw water	9.46	71.1 ± 7 %	9.74 µg/L/day	14.46	72.1 ± 6 %	14.07 µg/L/day
Sedimentation unit	11.56	86.7 ± 3 %	12.32 µg/L/day	17.32	86.2 ± 7 %	20.81 µg/L/day
Filtration unit	12.58	94.3 ± 11 %	0.184/day	19.45	97.2 ± 9 %	0.443/day

19.38 µg/L/day is kinetics zero-order constant for positive control

Table 2.1.1 shows the comparison between pre-acclimatization and post-acclimatization degradation study in terms of kinetics constant, degradation efficiency and overall degradation rate for all the three units. Zero-order reaction was obtained for Unit-1 (14.07 µg/L/day) and Unit-2 bacterial community (20.81 µg/L/day). However, first order reaction was observed for the Unit-3 bacterial community (0.443/day). The kinetic constant for acclimatized bacterial community showed an increase of 44.4%, 68.9% and 140.7% for Unit-1, Unit-2, and Unit-3, respectively as compared to the non-acclimatized case. This indicated that the metabolic activity of this *in-situ* bacterial community enhanced through acclimatization. Also, it signified that the bacterial community derived from Unit-3 holds better potential as compared to Unit-1 and Unit-2 bacterial community in effectively metabolizing MC-LR. Under similar experimental conditions, the first order kinetic constant for both acclimatized and non-acclimatized bacterial community present in Unit-3 was found to be higher than the study by Kansole et al. (2016) (0.180/day for the non-acclimatized case (this study) and 0.443/day (this study) for the acclimatized case as compared to k= 0.026/day). These differences might be due to isolated bacteria utilized in the non-acclimatized-

form as compared to our study which utilized bacterial isolates in the acclimatized-form. Some studies even reported incomplete degradation of microcystin variants. Ramani et al. (2011) reported incomplete degradation of both MC-LR (84%) and MC-RR (63.28%) at the end of 30 days with enriched bacteria (unidentified) in MSM. Kansole et al. (2016) also reported an incomplete MC-LR degradation study after 12 days (around 74%) with *Bacillus sp.* in autoclaved Hulupi Lake water. This may be due to the involvement of different bacterial degradation mechanisms for the effective breakdown of microcystin (Neilan et al. 2014). Further, in some cases, certain conditions favour the production of the *mlrA* gene (gene responsible for microcystin breakdown) (Dexter et al. 2018), such as supportive metabolites, and by-products, etc. indicating the complete death of toxins in some cases. Other studies, where MSM media was used for evaluating MC-LR degradation with bacteria, such as *Sphingomonas isolate NV-3* (Somdee et al. 2013) and *Pseudomonas aeruginosa (Lemes et al. 2015), achieved 100% degradation in 3 days and 24 days, respectively. However, their degradation rate of 8.33* µg/L/day *for Sphingomonas isolate NV-3* and 0.05 µg/L/day for *Pseudomonas aeruginosa was lower than the biodegradation rate of 20* µg/L/day using bacteria derived from Unit-3 *in this study* as mentioned in Table 1.4*).*

On another note, Kang et al. (2012) reported a degradation rate of 2.2 µg/L/day using 10^5 cells/mL of Pseudomonas aeruginosa. Likewise, this study maintained the cell viability > 10^6 cells/mL (comprising a bacterial strain: INRS W3, a *Pseudomonas* member too) till the end and enhanced MCs degradation rate by 9 times (19.5 µg/L/day). This further highlights the importance of acclimatization for achieving effective MC-LR degradation. Thus, the acclimatization of in-situ bacterial community present in the DWTPs unit is key to degrade MC-LR effectively and faster.

Contrary to the non-acclimatization degradation phase, an increase in the cell viability was observed during the initial period (5 days) for all the three unit study (increasing from approx. 6 x 10^6 CFU/mL to a minimum of 8 x 10^6 CFU/mL. However, the viability decreased for all of them after 5 days of degradation, which can be linked to the decrease in the substrate concentration (MC-LR) that happened with time. This increasing trend followed by a decrease in the bacterial population was also observed by Lemes et al. (2015) who studied MC-LR degradation with bacteria isolated from the beach sediment, where highest bacterial growth occurred after 12 days of degradation (117×10^5 CFU/mL) that lasted for 24 days. The final viability count after 24 days was 80 x 10^5 cells/mL when compared with the initial cell viability of 71 x 10^5 cells/mL. Similar

findings were observed in the present study (started from 6 x 10^6 cells/mL and ended at 4.25 x 10^6, 5.0 x 10^6 and 5.5 x 10^6 cells/mL for Unit-1, Unit-2 and Unit-3, respectively). However, the initial increase in cell viability of MC-LR-degrading bacteria can be related to the enhancement of energy metabolism (by the acclimatized bacteria) that helped to break down the complex, stable and cyclic microcystin-LR molecule. This might be a reason for the significant increase in the degradation rate as discussed above (1.5-fold). Likewise, this fact can also be attributed to the increase in the kinetic constant values in comparison to pre-acclimatization degradation phase.

By-product fragments analysis

The highest MC-LR degradation of 97.2 ± 8.7 % was achieved by the acclimatized-TSFU bacterial community (Unit-3). Thus, the qualitative toxicity assessment which depends on the formed by-products, their characterization (in terms of m/z value and change of chemical bond in structure) was needed. Figure A2 (Appendix A) illustrates the chromatograms for zero day, 2nd day and 5th day of MC-LR degradation by the Unit-3 bacterial community. The intensity (measured in absolute value) decrease with time corresponded to 69.75% and 94% degradation after day 2 and day 5, respectively. The other peaks observed are degradation by-products (Bourne et al. 1996). These by-products were further analyzed using mass spectra, which revealed several accompanied ions at m/z= 155.99, 162.9, 213.14, 268.24, 292.84, 315.19, 332.93, 375.25, 398.18, 470.29, 507.31, 553.29, 571.27, 599.34 and 862.48. Among them, m/z value of 862.5, 507.31, 571.27, 599.34 were identified as the biotransformed products, namely, $[M - NH_2 - PhCH_2CHOMe + H]^+$, $[M + H_2O + 2H]^{2+}$, [Mdha-Ala-Leu-Masp-Arg + H]+, and $[M^{\#} - NH2 + H]$+ respectively, where M is a cyclo MC-LR Adda-Glu-Mdha-Ala-Leu-Masp-Arg-OH and M# is tetrapeptide Adda-Glu-Mdha-Ala-OH (Bourne et al. 1996). Also, smaller m/z value of 332.93 and 315.19 were identified as the biotransformed products as $[M^*+ H]^+$ and $[M^* - NH_3 + H]$+ respectively where M* = Adda molecule (Figure 2.1.3). Figure 2.1.3 shows the proposed and hypothesized mechanism for the breakdown of the MC-LR compound by the bacterial community derived from Unit-3.

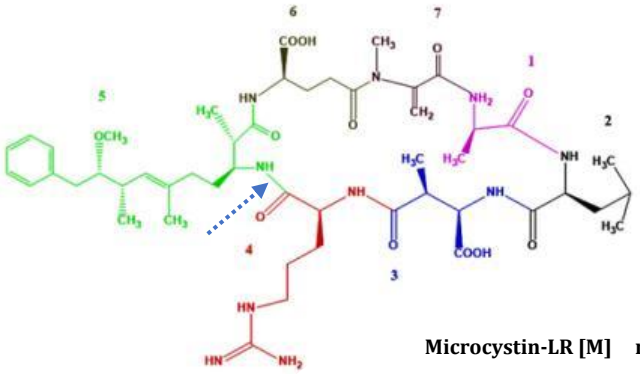

Microcystin-LR [M] m/z = 995

After Hydrolysis
+ H_2O

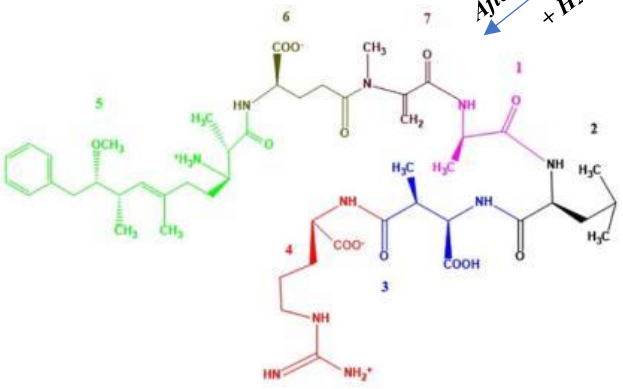

m/z =1013 [M + H_2O + H+] = M_1

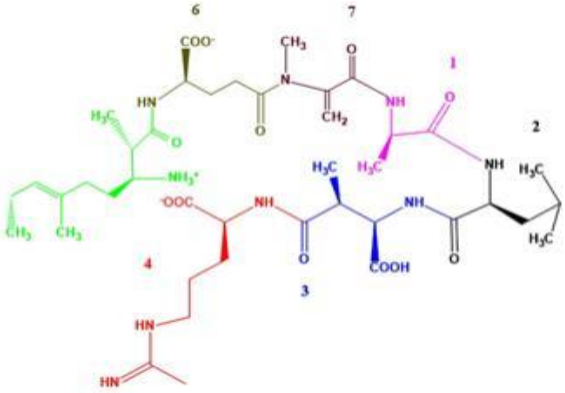

m/z =862.5 [M_1 – NH_2 – $PhCH_2CHOMe$ + H^+]

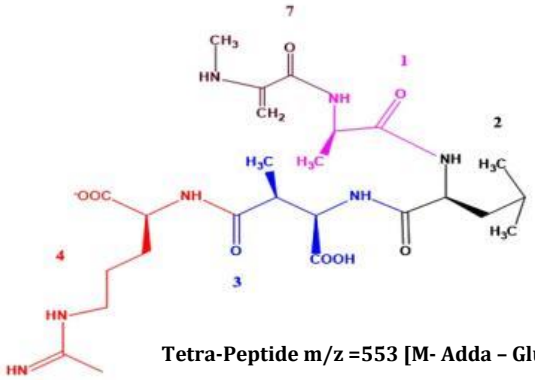

Tetra-Peptide m/z =553 [M- Adda – Glu + H^+] = M_1

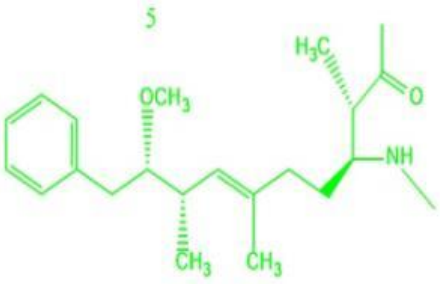

Adda part: m/z =314

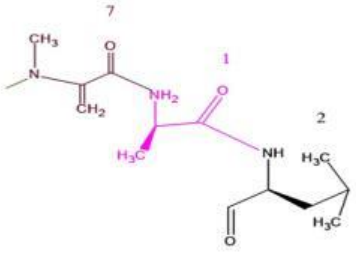

Mdha + Ala + Leu part: m/z = 268

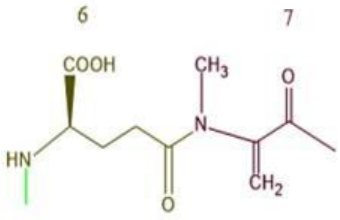

Glu + Mdha part: m/z = 213

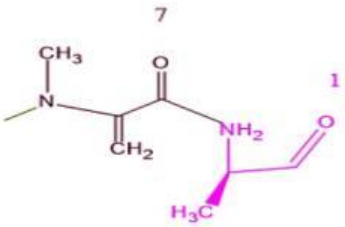

Mdha + Ala part: m/z =155

Smaller peptide and Amino acids

Figure 2.1.3: Proposed degradation pathway of MC-LR by the co-culture bacterial community isolated from Top-sand filtration sand Unit (TSFU)

The hypothesis predicts that the linearization of closed and complex MC-LR structure occurred after the formation of a biotransformed product having m/z value of 862.5. This linearization was due to the elimination of the terminal phenylethylmethoxy group and NH_2 group from Adda group through radical fragmentation (N-terminal Adda) (Bourne et al. 1996; Imanishi et al. 2005).Adda is one of the constituent amino acid compounds and is considered essential for the characteristic biological activity of microcystins as the toxicity disappears due to oxidation of Adda portion. It has been also reported that Adda is non-toxic up to 10 mg/kg in mice and it did not exhibit protein phosphate inhibition even at 10mM (Schmidt et al. 2014; Fujiki et al. 1996).

From Figure 2.1.3, a fragment with m/z value of 553 showed the presence of carboxy-terminal arginine similar to the fragment ion with m/z value of 571(Mdha-Ala-Leu-Masp-Arg-OH + 2H) and 488 (Ala-Leu-Masp-Arg-OH + 2H) as determined by Bourne et al. (1996) which corresponded to the C-C fragmentation at the N-terminal Adda representing tetrapeptide fragments. These tetrapeptides were further known to be cleaved by *mlrB* and *mlrC* genes into smaller peptides (as shown in Figure 2.1.3; m/z= 268, 213,155 and found in our study too). From mass spectra analysis, Adda fragment (m/z= 314) was formed for all the three biodegraded broths (Unit-1, Unit-2 and Unit-3) followed by these small peptide fragments indicating further oxidation of Adda might have occurred leading to non-toxicity.

Generally, hydrolysis of MC-LR is responsible for the linearization of the structure where m/z value increases by 18 (i.e. 995 (basic $[M+H]^+$ value) +18 $[H_2O]$=1013) (Figure 2.1.3). However, Edwards et al. (2008) and Dziga et al. (2012) indicated that further loss from hydrolyzed state due to loss of a portion from Adda group and amino groups incurs a total loss of 151 in m/z value resulting in a product with m/z value of 862 (Figure 2.1.3). This by-product is also related to the hydrolysis of parent ions by a *mlrA* gene which further suggested that the bacterial community present in TSFU (Unit-3) might contain *mlrA* gene which is responsible for the biotransformation of the cyclic and complex MC-LR compound. However, this hydrolyzed product was found in all the three units (Unit-1, Unit-2, and unit-3 bacterial community), which could be due to the induction of certain genes, such as *mlrA* as discussed above. Further, the *mlrA* has also been known

to detect the presence of MC-degrading bacteria (Saito et al. 2003; Hoefel et al. 2009). Some researchers also showed that MC-LR degrading bacteria containing microcysatinase *mlrA* encodes a hydrolytic enzyme capable of initiating MCs degradation by cleaving the Adda-arg peptide bond (shown by the dashed arrow in Figure 2.1.3) (Bourne et al. 2001). Moreover, these hydrolyzed linear by-products formation is also linked to the reduced toxicity (Hoefel et al. 2009) which is quantitatively studied using a bioindicator in the next section.

Toxicity assessment of the degraded MC-LR samples

The qualitative toxicity analysis based on mass spectra results depicted the formation of small peptide fragments and amino groups, thereby suggesting the non-toxicity nature of the degraded samples/broth. However, quantitative toxicity assay was also performed using a bioindicator: *Rhizobium meliloti* to confirm the findings. Figure 2.1.4 (A) shows the absorbance (at 550 nm) vs concentration graph for the reference toxic solution, i.e., dimethyl sulphoxide (DMSO) ranging from 10%-100% (v/v) at critical time-period of 10 h using *Rhizobium meliloti* as a bioindicator. As the DMSO concentration increased from 10% (v/v) to 100%, (v/v), a decrease in absorbance was observed. This is because all survived bacterial cells, after getting exposed to DMSO (a toxic substance) precipitated to blue colour (formazan) post MTT (yellow colour dye) addition. If the cell viability increased (less toxic compound), more precipitate would have been formed (hence more absorption value) and vice-versa, as reported by Botsford et al. (1997) too. In this study, a similar toxicity behaviour trend was observed for MC-LR also. The colour of the solution remained mostly yellow even at least MC-LR concentration tested (92 µg/L) which indicated the toxic behaviour of MC-LR. The trend followed a good quadratic curve fit with R^2 value 0.9591 for the critical incubation period of 10 h (not shown here). Figure 2.1.4 (B) shows the equivalent DMSO concentration (% v/v) for the various MC-LR concentrations (92 to 1470 µg/L) being studied. Based on the absorbance values obtained for the biodegraded broth, their equivalent DMSO concentration has been plotted. The equivalent DMSO concentration (% v/v) is the value proportional to the absorbance shown by various MC-LR concentrations when compared to the DMSO absorbance (shown in Figure 2.1.4 (A)). Hence, DMSO acted as a surrogate reference toxic solution to simulate MC-LR toxicity in the biodegraded broth.

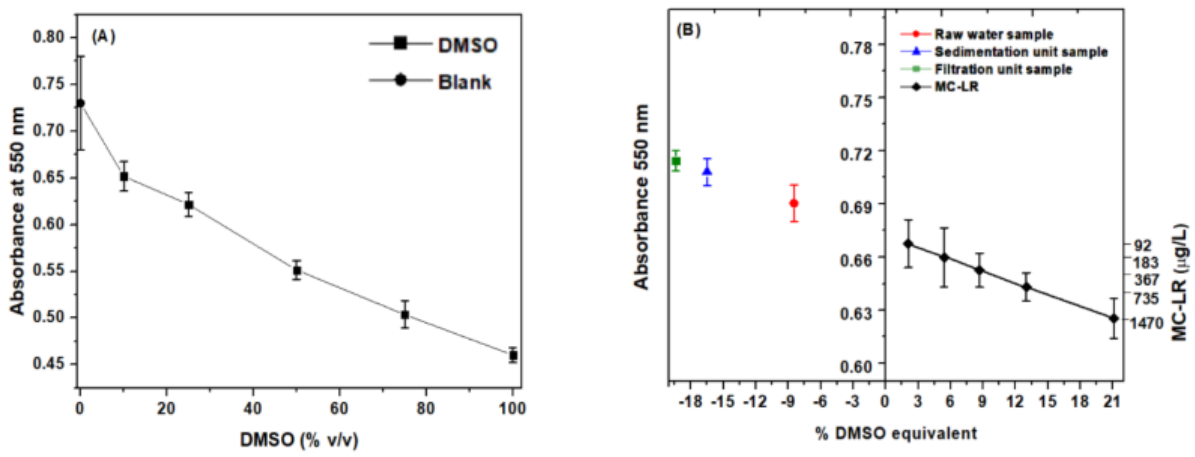

Figure 2.1.4: (A) Toxicity assay colorimetric test for various concentration of DMSO (% v/v) vs absorbance at 550 nm and; (B) Equivalent Dimethyl sulfoxide (DMSO) (% v/v) for microcystin-LR compound and biodegraded broth

Equivalent DMSO toxicities of the biodegraded broth for all three cases studied viz. Unit-1, Unit-2 and Unit-3 were found to be –8.4 (% v/v), -16.5 (% v/v) and -19.37 (% v/v), respectively. Negative concentration means the biodegraded broth was safe enough to be compared with DMSO potential toxicity. The blue colour observed for three samples illustrated non-toxicity and unchanged yellow colour illustrated toxicity for DMSO sample, as tested.

Many researchers have used DMSO as the reference solution to observe the toxic effects on various human cells as well as other species. For example, *in vitro* toxicity in a retinal neuronal cell line from rats was observed at DMSO concentration higher than 1% (v/v) (Galvao et al. 2013). DMSO was also shown to affect red blood cells, platelets and vascular endothelial cells *in vitro* at a concentration > 0.6% v/v and bacterial strains, such as *S.epidermidis* and *S.paratyphia* at a concentration >5% (v/v) (Yi et al. 2017). Another study revealed that DMSO with 0.5%– 2% v/v significantly suppressed the expression of many pro-inflammatory cytokines/chemokines (Proost et al. 2016). In fact, at 0.1-1.0 % v/v, it not only affected the phenotypic characteristics but also induced a significant alteration in the gene expression, protein content, and functionality of the differentiated hepatic cells. As compared to the literature, the biodegraded broth in the present study showed equivalent DMSO toxic level that did not affect any living cells.

Bacterial species identification by ribosomal sequencing

The best MC-LR degrading bacterial community was found to be from TSFU (listed in Table A1, Appendix A) which comprises three bacterial strains: INRSW3, INRSY2, and INRSB1. Before their identification, MC-LR degradation potential was evaluated for each of them individually (Appendix A: Figure A5). Results showed maximum degradation of 85.3% and 84.6% for INRSW3 and INRSY2, respectively and thus was further screened for identification through 16S rRNA PCR sequencing.

The BLAST analysis of the 16S rDNA sequencing of INRSW3 strain showed 99% homology to the *Pseudomonas fragi* and the INRSY2 strain showed 99% homology to the *Chryseobacterium sp.* The nucleotide sequence of 16S rDNA of the identified INRSW1 and INRSY2 bacterial strains has been deposited in NCBI with Acc. No. MH150821 and MH150822, respectively. However, it is interesting to note that there are very few literature reports available on the microcystin degradation studies from *Pseudomonas fragi sp*. However, there are no reports available on the degradation of microcystin by *Chryseobacterium sp*. Nevertheless, the present study showed that *Chryseobacterium sp*. and *Pseudomonas fragi sp*. degrade microcystin at 250 µg/L that is remarkably more than the other microorganisms in our study (more than 80%:). As shown in Table 1.4, some studies on MC-LR degradation achieved lower degradation rate than our study. Most importantly, they have been characterized for their toxicity and this suggests that the by-products formed are non-toxic. Thus, these microorganisms could be of interest for efficient degradation of microcystin. Further studies on phylogenetic analysis and in-silico identification of gene cluster responsible for degradation of microcystin in these organisms would shed more light on their genetic characteristics with respect to microcystin degradation. This will aid in cloning and characterization of microcystin degrading enzymes from *Chryseobacterium* sp. and *Pseudomonas fragi* sp.

Conclusion

The microcystin-LR-enriched bacterial community showed enhanced degradation rate as compared to the non-acclimatized (no-MCLR enrichment) bacterial community isolated from different units of the drinking water treatment plants viz. raw water entering the pre-ozonation unit (POU), effluent-sludge sedimentation unit (ESSU) and top-sand filtration unit (TSFU).

Acclimatized-TSFU bacterial community showed the best result achieving 97.2 ± 8.7% MCLR degradation. Based on the best MC-LR degradation results, two strains comprising TSFU community revealed over 99% homology to *Pseudomonas fragi* and *Chryseobacterium spp.* and were found to be novel MC-LR degrading species. Mass spectra result depicted hydrolysis of complex MCLR molecule into smaller peptide molecules along with Adda molecule formation (m/z= 314) which qualitatively suggested decreased toxicity of the final biodegraded broth. Furthermore, *Rhizobium meliloti* used as a bioindicator qualitatively confirmed these by-products as non-toxic. This study gives a lead to utilize these identified novel strains in DWTP for effective degradation of MC-LR ensuring safe and toxin-free drinking water.

Conflict of interest: None

Acknowledgment

The authors are sincerely thankful to the Natural Sciences and Engineering Research (Discovery Grant 23451), Genome Québec, Genome Canada) and ATRAPP (Algal blooms, treatment, risk assessment, prediction, and prevention) for financial support. Special thanks to Prof. Sébastien Sauvé for allowing the sample receipt and analysis in his laboratory. Authors would also like to thank the team for constant support and timely suggestions. We would like to thank Genome Quebec for timely sequencing for the bacterial identification. The views or opinions expressed in this article are exclusively those of the authors.

References

Botsford JL: A simple method for determining the toxicity of chemicals using a bacterial indicator organism. *Environmental Toxicology* 1999, 14:285-289.

Botsford JL: A simple, rapid, inexpensive assay for toxic chemicals using a bacterial indicator. 1997, 66:429-443.

Bourne, D. G., Jones, G. J., Blakeley, R. L., Jones, A., Negri, A. P., & Riddles, P. (1996). Enzymatic pathway for the bacterial degradation of the cyanobacterial cyclic peptide toxin microcystin LR. *Appl Environ Microbiol, 62*(11), 4086-4094.

Bourne, D. G., Riddles, P., Jones, G. J., Smith, W., & Blakeley, R. L. (2001). Characterisation of a gene cluster involved in bacterial degradation of the cyanobacterial toxin microcystin LR. *Environ Toxicol, 16*(6), 523-534.

Carey, R. O., Hochmuth, G. J., Martinez, C. J., Boyer, T. H., Dukes, M. D., Toor, G. S., & Cisar, J. L. (2013). Evaluating nutrient impacts in urban watersheds: Challenges and research opportunities. *Environmental Pollution, 173*, 138-149. doi:10.1016/j.envpol.2012.10.004

Chen, J., Hu, L. B., Zhou, W., Yan, S. H., Yang, J. D., Xue, Y. F., & Shi, Z. Q. (2010). Degradation of Microcystin-LR and RR by a Stenotrophomonas sp. Strain EMS Isolated from Lake Taihu, China. *Int J Mol Sci, 11*(3), 896-911. doi:10.3390/ijms11030896

Dexter, J., Dziga, D., Lv, J., Zhu, J., Strzalka, W., Maksylewicz, A., . . . Fu, P. (2018). Heterologous expression of mlrA in a photoautotrophic host – Engineering cyanobacteria to degrade microcystins. *Environmental Pollution*. doi:10.1016/j.envpol.2018.01.071

Dziga, D., Wladyka, B., Zielińska, G., Meriluoto, J., and Wasylewski, M. (2012) Heterologous expression and characterization of microcystinase. Toxicon 59, 578−586.

Edwards, C., Graham, D., Fowler, N., and Lawton, L. A. (2008) Biodegradation of microcystins and nodularin in freshwaters. Chemosphere 73, 1315−1321.

Fayad, P. B., Roy-Lachapelle, A., Duy, S. V., Prévost, M., & Sauvé, S. (2015). On-line solid-phase extraction coupled to liquid chromatography tandem mass spectrometry for the analysis of cyanotoxins in algal blooms. *Toxicon, 108*, 167-175. doi:10.1016/j.toxicon.2015.10.010

Fujiki, H., Sueoka, E., Suganuma, M., 1996. Carcinogenesis of microcystins. In: Watanabe, M.F., Harada, K.-I., Carmichael, W.W., Fujiki, H. (Eds.), Toxic Microcystis, CRC Press, Boca Raton, FL, pp. 203–232.

Gagala I, Mankiewicz-Boczek J (2012) The Natural Degradation of Microcystins (Cyanobacterial Hepatotoxins) in Fresh Water - the Future of Modern Treatment Systems and Water Quality Improvement. Pol J Environ Stud 21: 1125–1139.

Galvao J, Davis B, Tilley M, Normando E, Duchen MR, Cordeiro MF: Unexpected low-dose toxicity of the universal solvent DMSO. *The FASEB Journal* 2013, 28:1317-1330.

Gargouri, B., Mhiri, N., Karray, F., Aloui, F., & Sayadi, S. (2015). Isolation and Characterization of Hydrocarbon-Degrading Yeast Strains from Petroleum Contaminated Industrial Wastewater. *Biomed Res Int, 2015*, 1-11. doi:10.1155/2015/929424

Hitzfeld, B. C., Hoger, S. J., & Dietrich, D. R. (2000). Cyanobacterial toxins: removal during drinking water treatment, and human risk assessment. *Environ Health Perspect, 108 Suppl 1*, 113-122.

Ho, L., Hoefel, D., Saint, C. P., & Newcombe, G. (2007). Isolation and identification of a novel microcystin-degrading bacterium from a biological sand filter. *Water Research, 41*(20), 4685-4695. doi:10.1016/j.watres.2007.06.057

Hoefel, D., Adriansen, C. M. M., Bouyssou, M. A. C., Saint, C. P., Newcombe, G., & Ho, L. (2009). Development of an mlrA Gene-Directed TaqMan PCR Assay for Quantitative Assessment of Microcystin-Degrading Bacteria within Water Treatment Plant Sand Filter Biofilms. *Appl Environ Microbiol, 75*(15), 5167-5169. doi:10.1128/aem.00036-09

Hu, L. B., Yang, J. D., Zhou, W., Yin, Y. F., Chen, J., & Shi, Z. Q. (2009). Isolation of a Methylobacillus sp. that degrades microcystin toxins associated with cyanobacteria. *N Biotechnol, 26*(3-4), 205-211. doi:10.1016/j.nbt.2009.09.001

Imanishi, S., Kato, H., Mizuno, M., Tsuji, K., & Harada, K.-i. (2005). Bacterial Degradation of Microcystins and Nodularin. *Chemical Research in Toxicology, 18*(3), 591-598

Ishii, H., Nishijima, M., & Abe, T. (2004). Characterization of degradation process of cyanobacterial hepatotoxins by a gram-negative aerobic bacterium. *Water Research, 38*(11), 2667-2676. doi:10.1016/j.watres.2004.03.014

Kang, Y.-H., Park, C.-S., & Han, M.-S. (2012). *Pseudomonas aeruginosa* UCBPP-PA14 a useful bacterium capable of lysing Microcystis aeruginosa cells and degrading microcystins. *Journal of Applied Phycology, 24*(6), 1517-1525. doi:10.1007/s10811-012-9812-6

Kansole M, Lin T-F: Microcystin-LR Biodegradation by Bacillus sp.: Reaction Rates and Possible Genes Involved in the Degradation. *Water* 2016, 8:508.

Lemes G, Kist LW, Bogo MR, Yunes JS: Biodegradation of [D-Leu1] microcystin-LR by a bacterium isolated from sediment of Patos Lagoon estuary, Brazil. *Journal of Venomous Animals and Toxins including Tropical Diseases* 2015, 21:4.

Manage PM, Edwards C, Singh BK, Lawton LA: Isolation and Identification of Novel Microcystin-Degrading Bacteria. *Applied and Environmental Microbiology* 2009, 75:6924-6928.

Manage, P. M., Edwards, C., Singh, B. K., & Lawton, L. A. (2009). Isolation and Identification of Novel Microcystin-Degrading Bacteria. *Appl Environ Microbiol, 75*(21), 6924-6928. doi:10.1128/aem.01928-09

Neilan, B., Yang, F., Zhou, Y., Yin, L., Zhu, G., Liang, G., & Pu, Y. (2014). Microcystin-Degrading Activity of an Indigenous Bacterial Strain Stenotrophomonas acidaminiphila MC-LTH2 Isolated from Lake Taihu. *PLoS One, 9*(1), e86216. doi: 10.1371/journal.pone.0086216

O'Neil, J. M., Davis, T. W., Burford, M. A., & Gobler, C. J. (2012). The rise of harmful cyanobacteria blooms: The potential roles of eutrophication and climate change. *Harmful Algae, 14*, 313-334. doi:10.1016/j.hal.2011.10.027

Proost P, Elisia I, Nakamura H, Lam V, Hofs E, Cederberg R, Cait J, Hughes MR, Lee L, Jia W, et al.: DMSO Represses Inflammatory Cytokine Production from Human Blood Cells and Reduces Autoimmune Arthritis. *Plos One* 2016, 11:e0152538.

Ramani A, Rein K, Shetty KG, Jayachandran K: Microbial degradation of microcystin in Florida's freshwaters. *Biodegradation* 2011, 23:35-45.

Saito, T., Okano, K., Park, H. D., Itayama, T., Inamori, Y., Neilan, B. A., . Sugiura, N. (2003). Detection and sequencing of the microcystin LR-degrading gene, mlrA, from new bacteria isolated from Japanese lakes. *FEMS Microbiol Lett, 229*(2), 271-276.

Schmidt, J., Wilhelm, S., & Boyer, G. (2014). The Fate of Microcystins in the Environment and Challenges for Monitoring. *Toxins (Basel), 6*(12), 3354-3387. doi:10.3390/toxins6123354

Somdee, T., Thunders, M., Ruck, J., Lys, I., Allison, M., & Page, R. (2013). Degradation of [Dha7]MC-LR by a Microcystin Degrading Bacterium Isolated from Lake Rotoiti, New Zealand. *ISRN Microbiology, 2013*, 1-8. doi:10.1155/2013/596429

Surange, S., Wollum Ii, A. G., Kumar, N., & Nautiyal, C. S. (1997). Characterization of Rhizobium from root nodules of leguminous trees growing in alkaline soils. *Can J Microbiol, 43*(9), 891-894. doi:10.1139/m97-130

Valeria AM, Ricardo EJ, Stephan P, Alberto WD. Degradation of microcystin-RR by *Sphingomonas*sp. CBA4 isolated from San Roque reservoir (Cordoba—Argentina) Biodegradation. 2006;17:447–455.

World Health Organization. Toxic cyanobacteria in water: a guide to their public health consequences, monitoring and management. I. Chorus and J. Bartram (eds.). E & FN Spon, London, UK (1999)

Yi X, Liu M, Luo Q, Zhuo H, Cao H, Wang J, Han Y: Toxic effects of dimethyl sulfoxide on red blood cells, platelets, and vascular endothelial cells in vitro. *FEBS Open Bio* 2017, 7:485-494.

BRIDGE-1

BRIDGE: A successful bacterial isolation from the filtration unit of the DWTP was done and results assured their potential to degrade MC-LR under a high MC-LR environment. The next step was to check the feasibility of this bacterial culture to remove MC-LR, by bioaugmenting them in a sand filter. The purpose of combining the ozonation process with biofilter was to reduce the necessity of ozone dose (practiced in a DWTP) and to reduce the toxic by-product formation, where residual MC-LR obtained after ozone treatment can be biodegraded using biosand filter to further assure a toxic-free filter water. Also, the toxicity of the filtered water was evaluated when the sand filter was bioaugmented with and without the co-culture of isolated native bacteria with known MC-LR-degraders.

From here on, "Bridge" means: Link between the previous study and the next study.

PART 2

Ozonation in tandem with bio-sand filter to assess the removal of Microcystin-LR in drinking water

Pratik Kumar [a], Satinder Kaur Brar [a,b*], Rao Y. Surampalli[c]

[a-] INRS-ETE, Université du Québec, 490, Rue de la Couronne, Québec, Canada G1K 9A9

[b-] Department of Civil Engineering, Lassonde School of Engineering, York University, North York, Toronto M3J 1P3, Ontario, Canada

[c-] Dept. of Civil Engineering, University of Nebraska–Lincoln, N104 SEC PO Box 886105, Lincoln, NE 68588-6105

[*]Corresponding author, E-mail: satinder.brar@ete.inrs.ca; satinder.brar@lassonde.yorku.ca (S.K. Brar)

Corresponding author. Tel.: +1 418 654 3116; Fax: +1 418 654 2600.

Journal of Environmental Engineering **DOI**: **10.1061/(ASCE)EE.1943-7870.0001801**

Résumé

La pré-oxydation sous forme d'ozonation est plus répandue que la chloration dans la plupart des usines de traitement de l'eau potable (DWTP) compte tenu de l'efficacité de l'oxydation et de l'impact sur la santé des humains par les premières. Dans cette étude, une approche hybride de l'ozonation et de la biofiltration a été évaluée pour comprendre l'exigence et la concentration de la dose d'ozone pour l'élimination du micropolluant: MC-LR. Pour simuler une eau réellement polluée, trois niveaux de matière organique naturelle (NOMs: 1 mg / L, 2 mg / L et 5 mg / L) et cyanobloom (intensité faible, moyenne et élevée) sous deux temps d'exposition à l'ozone différents (C1 : 0,8 mg / L.min et C2: 1,6 mg / L.min) ont été étudiés (18 combinaisons). Dans les DWTP, l'unité de traitement la plus courante et successive (après coagulation et sédimentation) à la pré-ozonation est le filtre à sable. Par conséquent, la faisabilité de la bioaugmentation du filtre (inoculation des biocellules) est également discutée et comparée avec le filtre à sable non inoculé (contrôle), pour signaler toute différence dans l'élimination du MC-LR après le traitement à l'ozone. Pour la bioaugmentation, deux dégradeurs MC-LR: *Arthrobacter ramosus* (Filter FA) et *Bacillus* sp. (Filtre: FB) ont été choisis. Les trois filtres (y compris le contrôle: pas d'inoculation: FC) ont montré une corrélation négative (FA: -0,987; FB: -0,973 et FC: -0,977) entre «l'ozone résiduel» et «l'élimination du MC-LR due à l'ozonation». Arthrobacter ramosus (Filtre FA) a montré une forte résistance à l'ozone résiduel (0,1 à 0,4 mg / L) et n'a pas affecté l'élimination du MC-LR en raison de la filtration autant qu'il a affecté le filtre FB et FC. Seul le filtre FA a montré une différence significative (valeur de p: 0,047) entre l'état de floraison et l'élimination du MC-LR en raison de l'ozonation. L'analyse statistique a également suggéré une forte influence des NOMs sur les performances du filtre pour l'élimination du MC-LR. Dans l'ensemble, la bioaugmentation du filtre à sable (filtre FA et FB) a amélioré les performances du filtre de 19,5% et 10,5% pour les échantillons C1s et 6% et 2% pour les échantillons C2s. Le test de toxicité PP1A a signalé une formation de sous-produits toxiques moins importante lorsque des bactéries indigènes ont été co-cultivées et inoculées avec des dégradeurs de MC-LR connus dans un filtre à sable.

Mots-clés: Biofiltre, Microcystine, Étude de cas, Analyse technico-économique, ozonation, contaminant émergent.

Abstract

Pre-oxidation in the form of ozonation is more prevalent than chlorination in most of the drinking water treatment plants (DWTPs) considering the oxidation efficiency and health impact on humans by the former. In this study, a hybrid approach of ozonation and biofiltration was evaluated to understand the requirement and concentration of ozone dose for the removal of micropollutant: MC-LR. To simulate a real polluted water, three levels of natural organic matter (NOMs: 1 mg/L, 2 mg/L and 5 mg/L) and cyanobloom (low, mid and high intensity) under two different ozone-exposure times (C1: 0.8 mg/L.min and C2: 1.6 mg/L.min) were studied (18 combinations). In DWTPs, the most common and successive treatment unit (after coagulation and sedimentation) to pre-ozonation is sand filter. Hence, the feasibility of filter bioaugmentation (biocells inoculation) is also discussed and compared with non-inoculated sand filter (control), to report for any enhanced removal of MC-LR after the ozone treatment. For bioaugmentation, two MC-LR-degraders: *Arthrobacter ramosus* (Filter FA) and *Bacillus* sp. (Filter: FB) were chosen. All three filters (including control: no inoculation: FC) showed a negative correlation (FA: -0.987; FB: -0.973 and FC: -0.977) between the 'residual-ozone' and 'MC-LR removal due to ozonation'. *Arthrobacter ramosus* (Filter FA) showed a strong resilient towards the residual ozone (0.1- 0.4 mg/L) and did not affect the MC-LR removal due to filtration as much as it affected filter FB and FC. Only filter FA showed a significant difference (p-value: 0.047) between bloom condition and MC-LR removal due to ozonation. Statistical analysis also suggested strong influence of NOMs on filter performance for the MC-LR removal. Overall, bioaugmentation of sand filter (filter FA and FB) enhanced the filter performance by 19.5% and 10.5% for C1s samples and 6% and 2% for C2s samples. PP1A toxicity assay reported lesser toxic by-products formation when native bacteria were co-cultured and inoculated with known MC-LR-degraders in a sand filter.

Keywords: Biofilter, Microcystin, Case study, Techno-economic analysis, ozonation, emerging contaminant.

Introduction

Drinking water sources, such as lakes, rivers, and ponds are increasingly affected by the presence of emerging contaminants even at a very low concentration (1-100 µg/L) (Petrovic et al. 2004). In general, drinking water treatment plant (DWTP) lacks potential in complete removal of these contaminants where conventional treatment units or processes are found to beless effective (Petrovic et al. 2003). The co-occurrence of macro-pollutants in the form of metal ions, natural organic matter, and recalcitrant substances renders partial removal of these emerging contaminants. This necessitates a choice of high input dosage of oxidants (chlorine and ozone) during the pre-treatment steps. These chemical oxidants have been widely applied for the water treatment for over a century, primarily for disinfection and later for the abatement of inorganic and organic contaminants. The main challenges involve the formation of toxic by-products and other (eco)toxicological consequences (von Gunten, 2018). The pretreatment methods, such as pre-chlorination and pre-ozonation applied in a DWTP is very common, especially the former. However, various health risk factors or issues have been reported so far due to pre-chlorination practice (Brown, 2016). Moreover, the presence of residual chlorine triggers the formation of disinfection by-products, such as trihalomethanes and brominated compounds (Li and Mitch 2018). On the other hand, in a pre-ozonation treatment unit, a lower oxidant (ozone) dose (<3 mg/L) and lower exposure time (<4 min as compared to >25 min for chlorination) make it a rapid and effective option than the latter.. Pre-ozonation plays an important role in breaking the recalcitrant and complex organic matter which is then subsequently removed by the coagulation and filtration unit (Cui et al. 2014, Zoumpouli et al. 2019).

However, the practiced ozone dose in a DWTP, may not be enough for complete removal of both macro-and micropollutants, especially when pre-ozonation is practiced before sedimentation and filtration. An enhanced dose is required, if complex matrix is encountered, such as natural organic matter (NOMs), cyanobacterial bloom and other organic compounds (Goel et al. 1995; De Vera et al. 2015). However, various questions arise::a) “how much dose is optimum?” b)“what about the ecotoxicological consequences due to the toxic by-products generated from ozonation; and c) how efficient is the successive treatment unit, such as filtration in tackling it”. Some researchers studied and highlighted the importance of inoculated filters (biofilter) which enhanced the removal of unconventional and recalcitrant pollutants such as N,N-diethyl-meta-toluamide (DEET), naproxen

and ibuprofen (Hallé et al. 2015). Some pollutants are even recalcitrant to further degradation and may include their by-products as well (Schlüter-Vorberg et al. 2015). Ozonation is usually combined with biofiltration steps such as sand filtration to remove the biodegradable organic carbon and break down the transformed by-products (Gerrity et al. 2018). Zoumpouli et al. (2019) studied the ozonation-biofilter combination of water treatment using five trace organic contaminants: acesulfame, carbamazepine, diclofenac, dimethylsulfamide and fluoxetine. The complex transformed by-products from ozonation such as *N*-nitrosodimethylamine (NDMA) and an acesulfame product was removed from the biofilter while the recalcitrant oxidation products such as trifluoroacetic acid (TFA) and two products from diclofenac were removed partially. Thus, the ozonation-biofilter combination can form an effective tool in the removal of cyanotoxins as well.

However, the bioactivity in the filters can be inhibited by influent laden with the toxic by-products, formed due to the practice of higher ozone dose than normal. Hence, the residual ozone from the ozonation unit may affect the biofilter operation. For this reason, 'residual ozone' is hypothesized as an important parameter as an excess oxidant level may stress and kill the inoculated microorganism during the biofilter operation which can subsequently lower the removal efficiency of micropollutants and other organic matter. However, the ozone half-life in pure water can range anywhere between 20 minutes to an hour, depending on pH, temperature and other environmental factors (Gardoni et al. 2012). Thus, these factors must be considered as well, while studying the effect of residual ozone on biofilter.

In the present study, three levels of NOMs (1 mg/L, 2 mg/L and 5 mg/L), algal bloom intensity (low, mid and high) were studied along with a model micropollutant (emerging contaminants) in the form of Microcystin-LR (MC-LR): a very common algal toxin present in drinking water sources. Two distinct dose-exposure times was also studied (0.8 mg.min/L and 1.6 mg.min/L) for the ozonation experiment. In addition, two biosand filters inoculated individually with the MC-LR-degraders (*Arthrobacter ramosus* and *Bacillus* sp.) were operated in tandem with the ozone treatment experiment. Almost every DWTPs has a filtration unit in succession to a pre-oxidation treatment unit (pre-chlorination or pre-ozonation) where sand is used as a common adsorbing media. Hence, a hybrid operation of ozonation and filtration was evaluated to understand the level of ozone treatment (in terms of exposure time at a given ozone dose) that is required for a maximum MC-LR removal from the polluted source water. The toxicity of the filtered water was

further checked by the PP1A inhibition assay where the significance of co-culturing aspect in a biosand filter operation for the MC-LR removal (biodegradation) is discussed. To the best of the author`s knowledge, this is the first study discussing the MC-LR removal with the above hypothesis where the performance of ozonation and biofilter is evaluated in tandem.

Material and Methods

Chemicals and reagents

Microcystin-LR (MC-LR) was purchased from Cayman Chemicals (Ann Arbor, Michigan, MI, USA) and a stock solution of 50 mg/mL was made by diluting 100 μg lyophilized film of MC-LR (as supplied) using 2 mL of methanol, stored at -20 °C. Crystal violet and 3-(4, 5-dimethylthiazol-2-yl)-2,5-diphenyltetrazolium bromide (MTT) were purchased from Sigma Aldrich, (Ontario, Canada). Quartz sand was obtained from Chemin Ste-Foy DWTP, Quebec City, Canada. MC-degraders: *Arthrobacter ramosus* (NRRL B-3159 and *Bacillus* sp. (NRRL B-14393) were purchased from NRRL Agricultural Research Service (ARS) culture collection. All the analytical reagents used in preparing nutrient and culture media, LC-MS grade solvents and reagents used to prepare analytical mobile phases, were purchased from Fisher Scientific, (Ontario, Canada).

Culture and growth of Microcystis Aeruginosa

A 5-ml culture of *Microcystis Aeruginosa* was a kind gift from Dr. Jerome Compte (Assistant Professor, INRS-ETE, Quebec City, Canada). It was sub-cultured multiple times in BG-11 media discussed elsewhere (Khong et al. 2019) to finally obtain 2.5 liters of the culture stock. A relationship between the optical density at λ_{700nm} and cell concentration was found. The cell count was performed using the hemocytometer after a brief sonication of the culture to release any colony attachment in suspension.

Sample preparation for ozone treatment

A total of three variables were studied namely: ozone dose-exposure time (2 levels), the intensity of cyanobloom (3 levels) and NOMs (3 levels). Hence, a total of 18 combinations were studied. Lake Sainte-Anne (47.262879N, -71.665158W) water was used as the matrix for the sample preparation. Around 50 mL was prepared (more than one-bed volume for filter) for every 18

combinations in 125 mL Erlenmeyer flasks. For the ozone treatment, the ozone was produced by a module Ozonair EMO3-131® (EMO3, Avenue Newton, Quebec City, Quebec, G1P 4M3), with a flow of 47.195 L/s and a minimum rate of conversion of 0.02 ppm.

Humic acid was used as the representative chemical to mimic NOMs at three different concentrations: 1 mg/L (N1), 2 mg/L (N2) and 5 mg/L (N3). The drinking water plant operator of Chemin Ste-Foy, Quebec City informed about the ozone input dose which varies in the range 0.6-1.0 mg/L for a retention time of 2-3 minutes. This meant that the concentration x time value for ozone dose is in the range: 1.2 to 3 mg.min/L. Also, the fact that the present study discusses the significance of the ozone by-product effect on biofilter performance, the need for lower range value is considered. Based on this fact, a low (C1: 0.8 mg.min/L) and a high (C2: 1.6 mg.min/L) ozone dose-contact time (CT: multiple of concentration and time), was tested. Three bloom conditions based on the intensity: OD values of 0.2 (B1: low bloom intensity), 0.5 (B2: medium bloom intensity) and 1.0 (B3: high bloom intensity) were prepared corresponding to 1.9×10^6 cells/mL, 4.3×10^6 cells/mL and 8.4×10^6 cells/mL, respectively. The *Microcystis aeruginosa* culture used to mimic the bloom condition was also tested for any production of cyanotoxin. A total of 12 different variety of toxins were checked and none were found at any stage of their growth. Hence, to simulate the cyanotoxin presence in the sample, commercial MC-LR was externally added to provide an initial MC-LR concentration of 50 µg/L in each of the 18 samples.

Culture and biofilm formation of MC-LR-degraders over sand filters

Two MC-LR-degraders: *Arthrobacter ramosus* and *Bacillus* sp. were tested individually for the bioaugmentation in the sand filter (Filter FA and Filter FB, respectively). Both these bacterial strains were cultured and rinsed with the phosphate buffer (pH = 7.21) to obtain cell pellets. OD_{600} of 0.7 and OD_{600} of 0.9 represents 3×10^6 cells/mL for *Arthrobacter ramosus* and *Bacillus* sp., respectively. According to the relationship between OD_{600} and cell viability (cells/mL), 3×10^6 cells/mL was inoculated every 3 hours to the sand filter (more detail in section 2.5) using an auto-dosage pump for a period of 11 days. This allowed fast biofilm formation in the sand filter (more detail in section 2.5). Lake water was used as the matrix for the filter operation.

Biofilm formation was monitored through three parameters: cell viability, cell biomass and protein concentration. Around 0.2 grams of sand was collected from the top layer of the sand column followed by its suspension in phosphate buffer (2.0 mL). The mixture was given a short spin to

loosen the attached bacterial cells and biomass (both) in suspension. Afterward, the obtained cell suspension was seeded in a 96-well plate for crystal violet (CV) and MTT assay as described in our previous study (Kumar et al. 2019) to estimate the cell biomass and cell viability, respectively. For protein determination, the cell suspension was analyzed using the Bradford assay (Bradford et al. 1976).

Experimental set-up and filter operation

Figure 2.2.1 shows the schematic overview of the filters used in the study. In total, three filters were used as shown. Two filters were bioaugmented with *Arthrobacter ramosus* (FA) and *Bacillus* sp. (FB) for the formation of the biofilm and one filter represented the control (FC) where no biocell was inoculated. The control filter represented the case of a DWTP filter where no MC-LR degrader was inoculated and hence the obtained results from filter FA and FB were compared with this filter to understand the need and importance of sand filter bioaugmentation. All three column filters were made up of a glass of external diameter 22 mm and thickness 1 mm, with a total height of 650 mm (490 mm for sand media, 40 mm for drainage material and 120 mm headspace for standing water/sample). The sand media was formulated based on previously reported work by the research team (Kumar et al. 2019). The effective diameter of the sand particle was 0.22 mm and the coefficient of uniformity was 2.3.

After a mature biofilm formation (more details in section 3.1), the ozone-treated samples (18 combinations and two different CTs, 9 samples each), were discharged through each filter post-ozonation. After the passage of every sample (low-intensity bloom samples preferred first), the filters were primed with lake water to minimize the carryover effect of the previous sample. After every three combination is being sampled (in triplicates), i.e., the filtration had been performed, the sand media was washed, dried and prepared for fresh filter operation to further minimize the error due to an effect of the earlier samples.

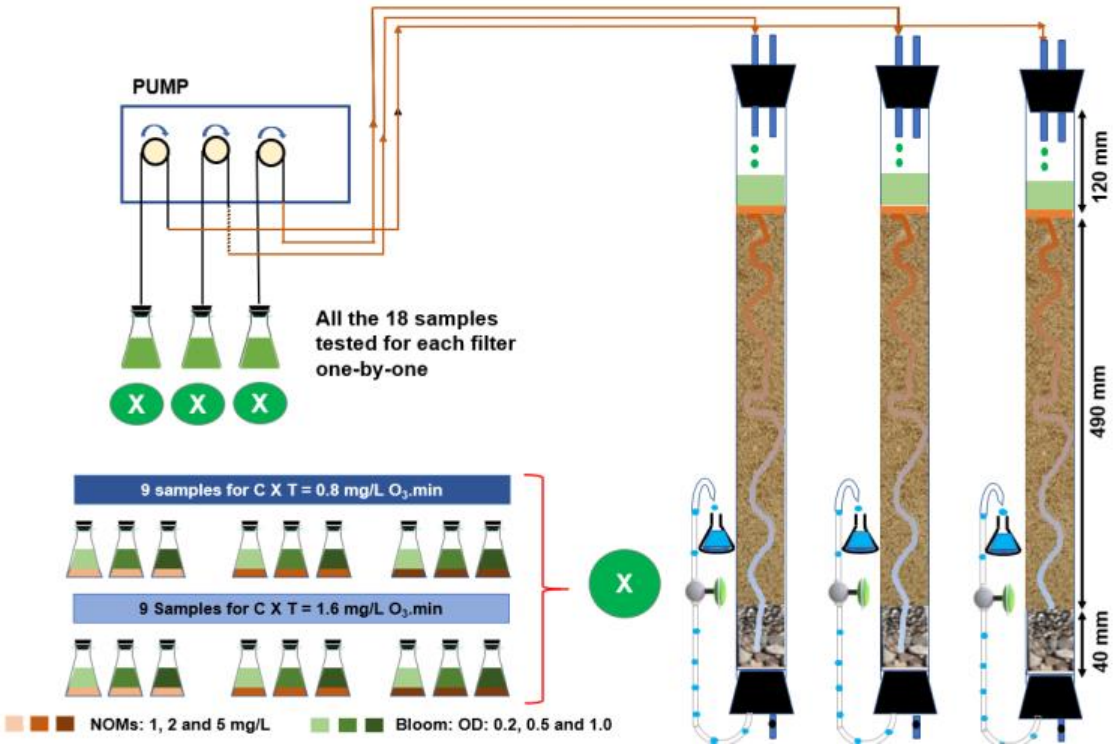

Figure 2.2.1: Schematic representation of filter operation for the ozone-treated samples

MC-LR analysis and residual ozone determination

The MC-LR was analyzed at two instances for each sample. Once after the ozonation and another after the samples were passed through the sand filter. The calculation of undegraded or residual MC-LR after hybrid ozonation-(bio)-filter treatment was calculated using Equation 4 as follows:

$$\frac{(\text{Initial MC-LR} - \{(\text{MC-LR removed after ozonation}) - (\text{MC-LR removed after filtration})}{50\ \mu g/L} \times 100 \quad \text{Equation 4}$$

The protocol used for the MC-LR analysis is discussed in Fayad et al. (2015). Briefly, a 20-µL sample aliquot was analyzed by ultra-high-performance liquid chromatography coupled to a Thermo Q-Exactive Orbitrap mass spectrometer through a positive electrospray ionization source. In full scan MS mode (resolution set at 70,000 FWHM at 200 m/z), MC-LR was detected and quantified against a matrix-matched lake water calibration curve. The method limit of quantification (LOQ) was set at the lowest concentration level of the calibration curve (i.e., 1 µg/L).

The residual ozone concentration in a treated sample was determined by the Indigo method as discussed in Bader et al. (1981). In brief, 1mM (0.62 gram) stock solution of Indigo Reagent was prepared by mixing it with 20 mM phosphoric acid (1 liter). After the ozone treatment of each sample for a given dose (0.8 mg/L O_3) and contact time (1 min for 0.8 mg/L O_3.min and 2 min for 1.6 mg/L O_3.min), the indigo solution was spiked continuously using burette (0.1 mL least graduation) until the Indigo color changes to colorless or a bit yellowish in texture. This change in color indicated a complete quenching of the residual ozone in the sample.

The experiment was carried out in two matrices: a) tap water, b) combination of medium bloom intensity (B2: OD_{700} of 0.5) and medium NOM concentrated sample (N2: 2 mg/L). Tap water was preferred over the deionized water because of the possible high reporting of the residual ozone in the sample (due to the latter) and hence to reduce the overestimation and positive error in interpretation of the result. The idea was to not overestimate the residual ozone concentration in the real matrix (bloom + NOM cases) as compared to the tap water (clear) where the former is expected to consume a part of the dissolved ozone because of the NOM and cyanobacterial cell inclusion. Also, since the color of the real matrix was light brownish green in color and to make the distinction clear between the indigo color changing into colorless, it was controlled bypassing the matrix using glass fiber filter (pore size: 0.45 μm). Then, the residual ozone concentration was determined as discussed earlier. The effect of the glass fiber filter adsorbing residual ozone was normalized by filtering the tap water sample while preparing the calibration curve.

A relationship between different contact times and Indigo solution added (to quench the ozone) was established. This relationship was determined for both the matrices. The residual ozone concentration in the sample post-ozone treatment was determined using Dissolved Ozone Testing Visual Kit that measures ozone in the range 0-2 mg/L (color coding for ozone concentration: 0.1, 0.2, 0.3, 0.4, 0.8, 1.0, 1.25, 1.50 and 2.00). Once the calibration curve was established, Indigo solution was used for the determination of residual ozone concentration to avoid the use of the expensive kit.

Toxicity assessment of the samples before and after biofiltration

PP1A assay has been widely used by many researchers to study the toxic effect of residual MC-LR in the water sample. PP1 belongs to protein serine/threonine phosphatases class and is responsible for the control of glycogen metabolism. MC-LR being a hepatotoxin, the compound

attacks the liver cells and inhibits the kinetic activity of PP1. Thus, PP1A assay is very significant and specific pertaining to the MC-LR toxicity assessment.

The assay was performed in a 96-well plate where the first two rows and columns were not used due to reported wall effect and temperature differences in these wells. A 300 µL consisting of 20 µL of MC-LR for different concentration (diluted in reaction buffer), 40 µL of PP1 (stock solution diluted in enzyme buffer according to manufacturer specification: final well concentration: 0.8 U/mL), 240 µL of pNPP (substrate: final well concentration of 120 mM), were mixed to initiate the colorimetric reaction. Blank was prepared along with the standard concentrations without MC-LR (substrate blank). The substrate blank represented the baseline activity of PP1 that was normalized for each well exposed to PP1 activity to determine for the effect of MC-LR in PP1 activity. The activity rate (hydrolysis of pNPP based on color change) was determined and calculated based on colorimetric absorbance optical density (OD at λmax: 405 nm and 32 ± 3°C) using Biotek mini spectrophotometer after every 2 minutes for 1 hour. A linear rate (change in OD/min) was obtained between the timeline: 1020-3520 seconds where the substrate blank rate was plateau after 1020 seconds. More the hydrolysis of pNPP substrate by PP1A enzyme less will be the OD value and hence less will be the reported PP1A inhibition and vice-versa. Thus, more % activity reported, less is the PP1A inhibition by MC-LR. For reporting the water samples, a 20 µL sample in place of MC-LR was mixed in wells along with PP1A enzyme and pNPP substrate as reported above, and the activity was reported and compared to assess the toxicity change due to residual MC-LR in the sample before and after filtration. All the samples were run in triplicates. An ozone-treated (CT: 0.8 mg.min/L) sample (500 mL) spiked at an initial MC-LR concentration of 50 µg/L was prepared as an influent to filters for this particular experiment. All three filters (FA, FB and FC) were primed using ozone-treated water (40 mL bed volume) and the effluent was measured for the % PP1A activity to determine the toxicity level in the residual MC-LR. The result was also compared to the then and another on-going project where co-culturing of known MC-LR-degraders (*Arthrobacter ramosus* or *Bacillus* sp.) and native bacteria.

Statistical analysis and graphics

All statistical analyses comprising standard deviation, average, student t-test, p-value comparison, principal component analysis (PCA) and all graphical presentations were performed in ORIGIN software (Version 8.5; OriginLab).

Results and Discussions

Monitoring biofilm growth in the filter

The biofilm monitoring was performed for 11 days. Figure 2.2.2 (A), (B), (C) and (D) represents the biofilm monitored in terms of Protein concentration, crystal violet (CV) assay (biomass quantification), filter flow rate and MTT assay (cell viability), respectively.

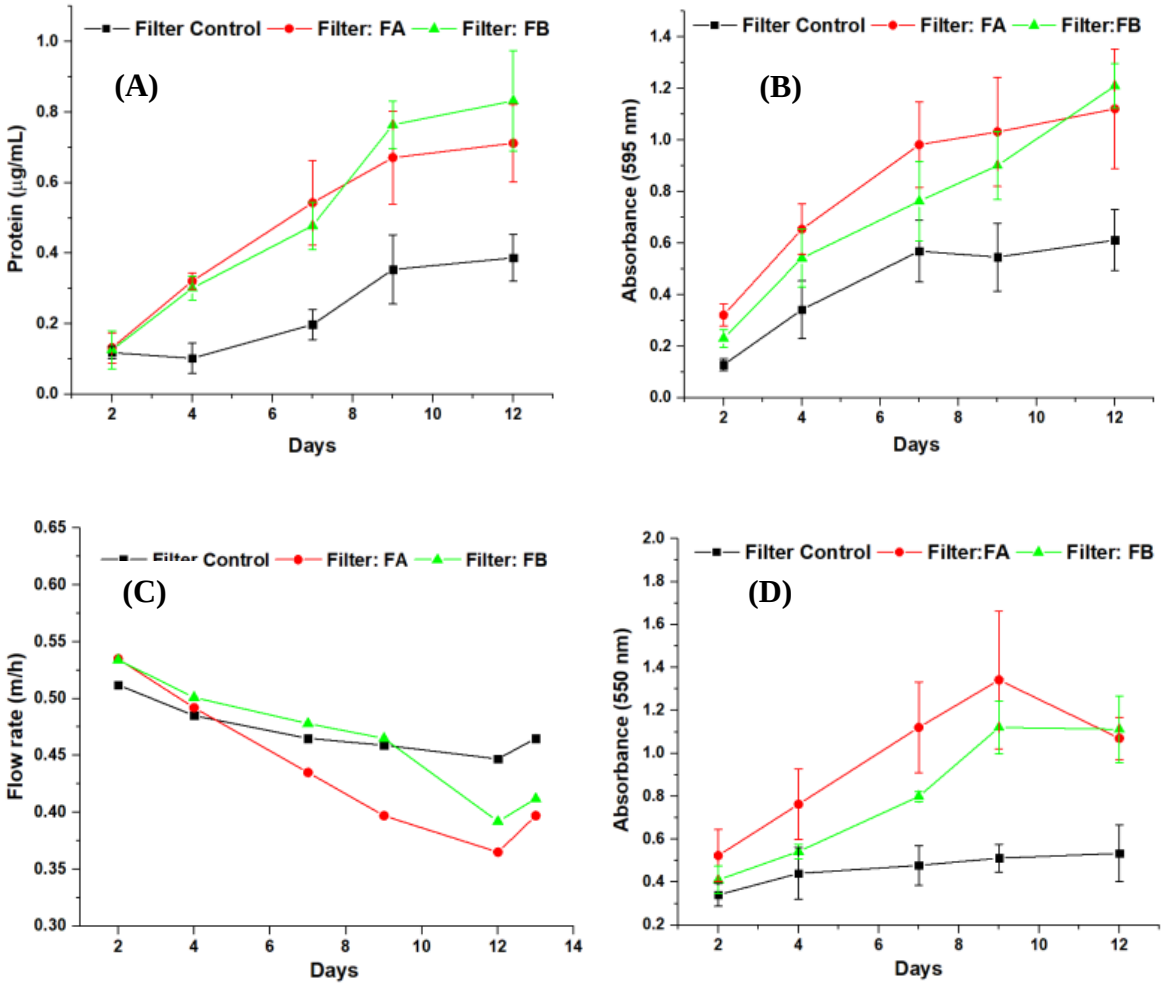

Figure 2.2.2: Biofilm quantification using: (A) Bradford assay (protein), (B) Crystal Violet assay, (C) Flow rate and, (D) Cell viability

As the biofilm started forming, the protein concentration, cell biomass, and cell viability increased while the flow rate decreased (due to biomass formation which promoted clogging). The protein concentration for filter FC, FA and FB increased from 0.118 µg/mL to 0.387 µg/mL, 0.132 µg/mL to 0.712 µg/mL and 0.126 µg/mL to 0.832 µg/mL, respectively while the highest absorbance value

of MTT assay (day 9) for filter FA and FB was recorded 2.5-fold and 2.1-fold more than the control filter (0.534). Akin to MTT assay, the CV assay showed the same trend where the highest absorbance value of filter FA and FB was found to be almost 2-fold as compared to the control filter.

The initial flow rate for all three filters was similar (0.52 m/h) and decreased as time progressed. The flow rate was determined by maintaining an influent head of 7.5 cm, measured from the top of the sand media and collecting at least a volume of 40 mL with the recorded time. A larger decrease in flow rate for filter FA, FB, and control as compared to the phase before bacterial cell inoculation was recorded to be: 25.8%, 22.8%, and 9.2%, respectively. A relatively higher decrease in flow rate for filter FA and FB was attributed to progressive biomass and viability of bacterial cells attached to the sand adsorbents affecting the tortuosity of the fluid flow. The nearly stable output of cell biomass, viability and protein concentration after day 10 indicated a fair and stable biofilm formation in the sand filters (FA and FB). Considering this stability, the ozone-treated samples were passed until day 11.

Residual ozone concentration in the ozone-treated sample and PCA analysis

The relationship between the residual ozone concentration and volume of Indigo solution required, for both the matrices is presented in Figure 2.2.3 (A) and (B). The volume of Indigo reagent required to quench residual ozone was slightly higher for the tap water matrix as compared to the NOM + bloom matrix. However, for obvious reason, the calibration curve for the latter matrix was used for estimating the residual ozone concentration in the ozone-treated samples. Overall, the quenching process did not take more than 1 minute for the sample (more for more dose and vice-versa) and thus any possibility of Indigo reagent reacting with the NOM present in the sample was inferred to be minimum.

Tap water matrix reported 25-30% higher residual ozone for the same Indigo reagent volume used and hence, an overestimation could have been reported had the medium bloom+medium NOM matrix was chosen. Figure 2.2.4 shows the bar chart for the residual ozone present in the sample after ozone treatment.

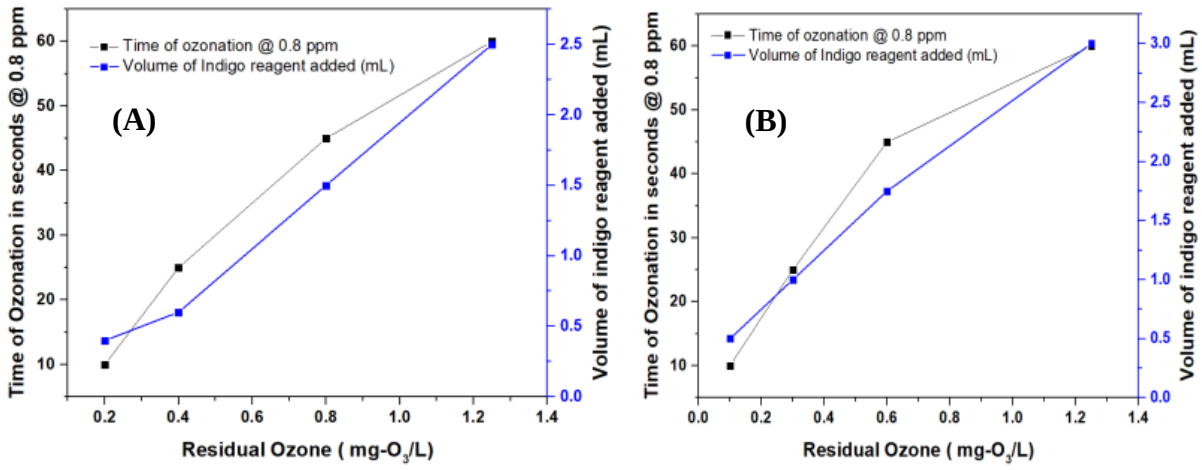

Figure 2.2.3: Residual ozone and contact time vs volume of Indigo solution used to quench the residual ozone in two matrices: A) NOM+ bloom condition, and B) Tap water

For all the three filters, there existed a negative correlation between the 'residual ozone' and the 'MC-LR removal due to ozonation'. The correlation factor of -0.987, -0.973 and -0.977 was found for control filter, FA and FB, respectively. This can be observed from the Principal Component Analysis (PCA, more detail in a later section) where the eigenvector of the two variables: 'MC-LR_ozone' and 'Res-Ozone' was found to be on the diametrically opposite side of the biplot axis (nearly 180° angle). This signifies that higher the residual ozone (obtained after ozonation), lesser was the participation/interaction of ozone with MC-LR compound during the ozonation. This trend can be related to the ozone molecules utilized in the oxidation of the MC-LR compound and the excess ozone left in the form of residual ozone which eventually became a direct marker for the undegraded MC-LR in the sample solution. Except for the case of N2B2C2 and N2B3C2, all other samples showed this phenomenon (represented in red arrow: Figure 2.2.4). Also, the combination which showed the best and worst increase in MC-LR removal with an increase in the ozone dosage was N1B2C2 (+ 67%) and N3B3C2 (+ 16%), respectively. This abnormal behavior can be explained by the fact that under higher bloom (B3: OD_{700} of 1.0) and NOM condition (N3: 5 mg/L), the ozone is also utilized for the degradation of NOM and cyanobacterial biomass before oxidizing the MC-LR compound. Hence, the residual ozone is left unreacted with the MC-LR molecule within a given contact time and shows lower removal (following the negative correlation).

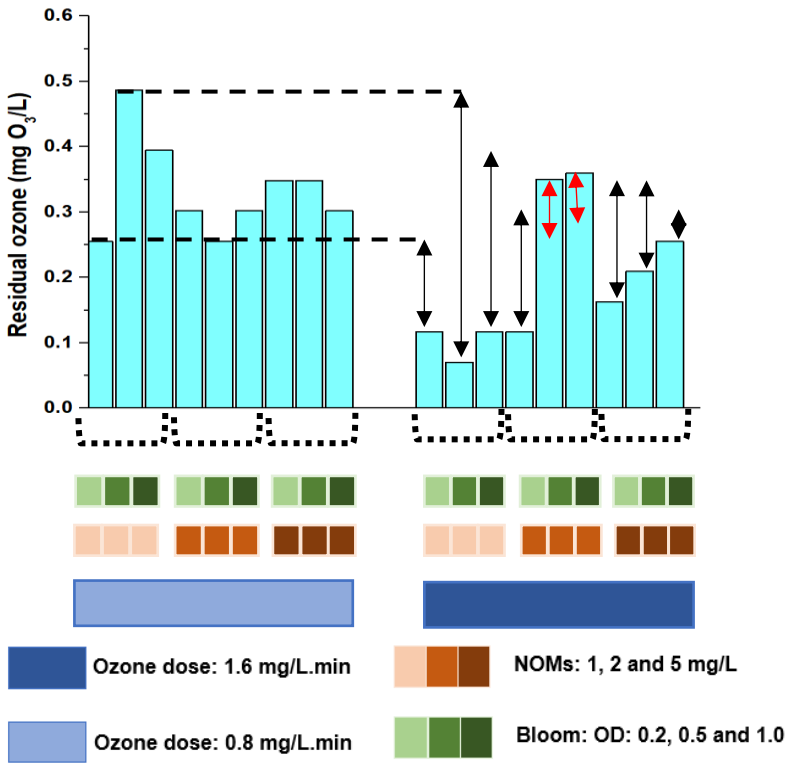

Figure 2.2.4: Bar graph showing residual ozone concentration for each sample tested

Significance of PCA analysis

Before discussing the PCA biplot results, it is important to outline the main reasons for using this multivariate tool to investigate the performance of the ozonation and biofilter operation for the removal of MC-LR. Some important outlines are as follow:

a) Understanding the effect of the residual ozone concentration on the MC-LR-degraders, bioaugmented in a sand filter for the removal of MC-LR.

b) Understanding the efficiency of ozonation and biofiltration for the removal of MC-LR, under the effect of environmental factors such as NOMs, bloom intensity and ozone dose-time

Figure 2.2.5 shows the PCA for control filter, FA and FB, respectively. In the PCA biplot, combinations of various environmental factors as stated above were the observation variables

while different factors such as MC-LR_ozone, MC-LR filter and res_ozone were considered as the main variables.

From the PCA analysis, a low correlation factor of 0.25 and 0.42 between 'Res_ozone' and 'MC-LR_filter' for control filter and filter FB was found that provided a strong evidence that residual ozone present in the sample (as an influent to the filters) did not affect the MC-LR removal in the control filter and filter inoculated with *Bacillus* sp.. However, for the FA filter, it showed a high correlation factor of 0.78 suggesting a strong impact of the residual ozone in MC-LR removal due to biofilter. Such a strong positive correlation (0.78) indicates good MC-LR removal despite a high residual ozone concentration. This further illustrates the stronger resistance potential of *Arthrobacter ramosus* than *Bacillus* sp. to residual ozone (0.1-0.4 mg/L: Figure 2.2.4). Hence, different MC-LR-degraders can behave differently from the residual ozone in a biofilter. However, the above results were interpreted considering limited variables (NOMs, bloom intensity and ozone dose) as discussed before. Hence, other critical variables, such as consistency in the bioactivity in the filter was missing. This could result in a possible dominance of the heterotrophic bacteria over MC-LR-degraders which can judge long-term biofilter operation for consistent MC-LR removal.

In order to understand the balance between the MC-LR removal due to ozonation and filtration, eigenvectors for variables: 'MC-LR_Ozone' and 'MC-LR_filter', were analyzed using PCA as shown in Figure 2.2.5 (A), (B) and (C) for control filter, FA and FB, respectively. Before discussing the results of PCA for all the three filters, notation N1, N2 and N3 represents the three-level of NOMs (1 mg/L, 2 mg/L and 5 mg/L), B1, B2 and B3 represents the three bloom intensity as discussed in the previous section while C1 and C2 represent the ozone-contact time dose value: 0.8 mg.min/L and 1.6 mg.min/L, respectively. For control filter, combinations: N1B1C2, N3B1C2, N1B2C2, N3B2C2 can be seen clustered together near the 'MC-LR_ozone' vector explaining that the MC-LR removal occurred mainly due to ozonation. A higher ozone concentration (C2) has shown favoring MC-LR removal even at the moderate bloom level B2 and NOM level N3. In contrast, no combination was found near the 'MC-LR_filter' vector. This clearly indicates that the control filter (without MC-LR-degraders) does not play an important role in the MC-LR degradation. Also, only one combination, i.e., N2B3C2 was closely aligned with the median vector drawn between the two vector variables: 'MC-LR_Ozone' and 'MC-LR_filter'. This further points out that the control filter is not suitable for an effective MC-LR removal in the tandem or hybrid

process of ozonation and filtration. For filter FA, combinations N2B1C2, N1B1C2, N1B2C2, N1B3C2 and for filter FB, combinations N1B2C2, N2B1C2, N1B1C2, N1B3C2 were found to be clustered together around the 'MC-LR_Ozone' vector.

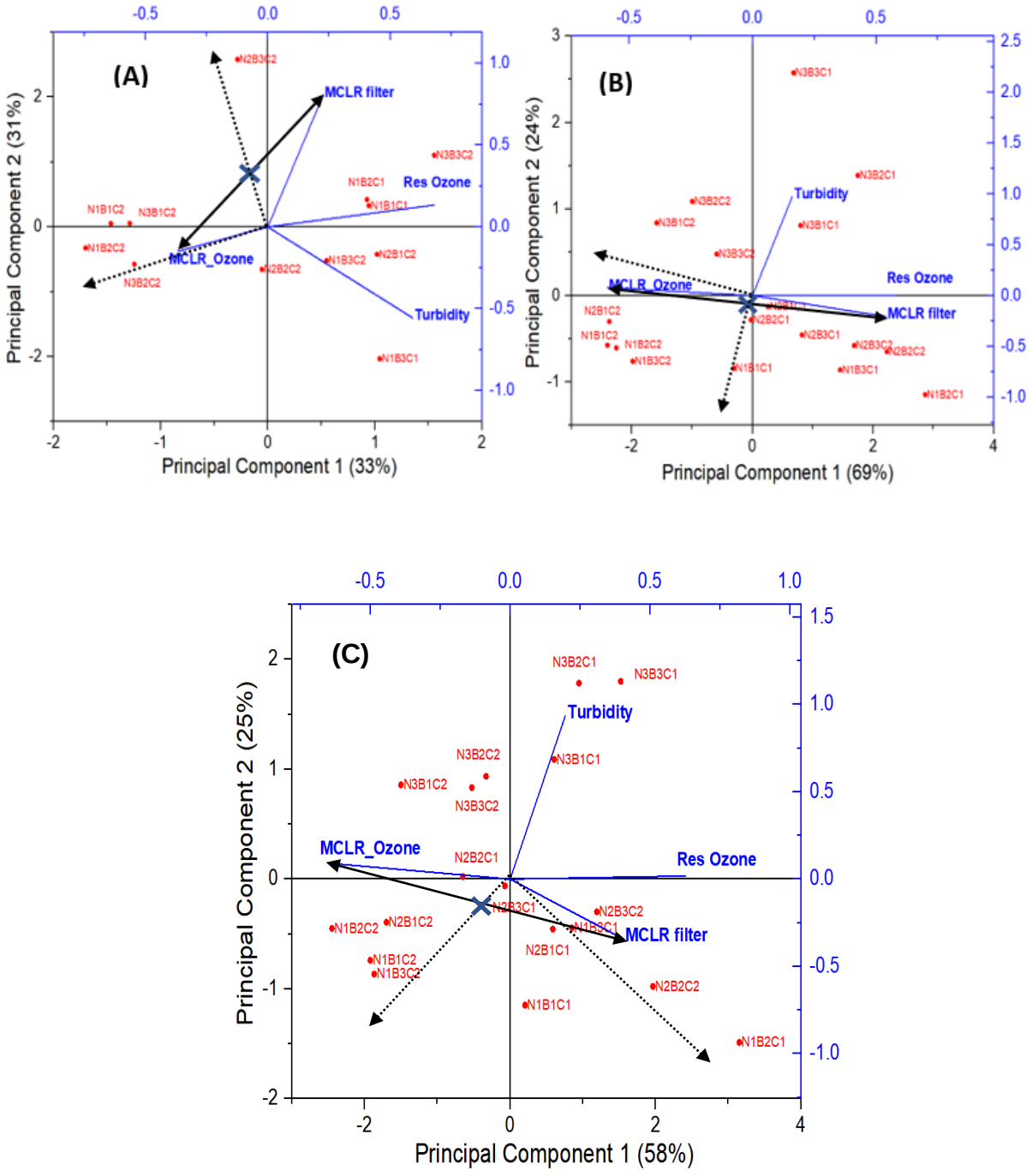

Figure 2.2.5: Principal Component Analysis biplot for A) Control filter, B) filter FA and C) filter FB

On the other hand, combinations: N2B3C1, N2B3C2, N1B3C1, N2B2C2, N1B2C1, and combinations: N2B1C1, N1B1C1, N2B2C2, N1B2C1 were found to be closely aligned towards the vector variable: 'MC-LR_filter' for filter FA and FB, respectively. This suggested that the biofilter worked effectively for the MC-LR removal as compared to the control filter where no combination showed close association or proximity with the 'MC-LR_filter' vector. Also, filter FA was found to be suitable for MC-LR removal even under high bloom (B3) and NOM conditions (N2B3C1, N2B3C2, N2B2C2, N1B2C1). The combination which worked closely in tandem for filter FA was N1B1C1 (rightly lying in the median vector: Figure 2.2.5 (B)) and N1B1C2, N1B3C2 for filter FB, respectively (Figure 2.2.5 (C)). This further states that the combined ozonation-biofilter process works better for the combination with lower NOM level (N1s) for both the biofilters: FA and FB.

MC-LR removal

Ozonation: In general, the residual ozone concentration for the C2s sample was found to be lower than C1s samples. However, for N2B2C2 and N2B3C2 (both C2s), the residual ozone was higher than their C1s counterpart (as shown by the red arrow in Figure 2.2.4). Hence, in general, it can be inferred that the MC-LR removal for low ozone concentration (C1s) is lower as compared to the higher ozone concentration (C2s). It may be due to less participation of ozone molecule with the MC-LR compound for the above two exceptional combinations, which might have resulted in a lesser MC-LR degradation as compared to their lower input ozone concentration counterparts (C1s: N2B2C1 and N2B3C1). The rest of the samples followed a general trend, i.e., more MC-LR removal for more ozone concentration input.

The relation between the ozone dose (C1 and C2), bloom conditions (B1, B2, and B3) and NOM concentrations (N1, N2 and N3) with MC-LR removal was also determined statistically and is presented in Table 2.2.1. The paired t-test and p-value showed a significant difference between the ozone dose and MC-LR for the control filter (p-value: 0.041) while biofilter FA and FB showed an obvious no significant difference (p-value: 0.36 and 0.23, respectively) because of the pivot significance of the biodegradation in MC-LR removal. On the other hand, only filter FA showed a significant difference between the bloom condition (B1 and B2) and the MC-LR removal. This could possibly be because of the more *M. aeruginosa* cells in the sample that may have been responsible for hindering the MC-LR removal by decreasing the activity of the MC-LR-degrader:

A. ramosus. The same opinion holds between B1 and B3 (Table 1) but there did not exist any significant difference between these bloom levels. Filters FA and FB showed a comparatively lower p-value: 0.41, 0.18, 0.22 & 0.29, 0.36, 0.27 for N1_N2, N2_N3 and N3_N1, respectively as compared to control filter (p-value: > 0.8 for all three cases). This suggests that the MC-LR removal is affected more (less removal) in the presence of the NOMs for the biofilters than non-bioaugmented filter (Filter FC). It can be related to the scavenging action between the NOMs and the oxidants formed during the oxidation reaction (Kumar et al. 2018). These reaction mechanisms has been reported to decrease the reaction rate by >50% (Verma et al. 2015). Also, the effect of two variables (bloom level/NOM or NOM/Ozone or Ozone/bloom level) on MC-LR removal is presented in Table 2.2.1 via 2-way ANOVA tests. The two variables are mainly affecting the FA filter as shown by the low p-values in the comparison table (Table 1) presenting the effect of two variables on MC-LR removal.

Table 2.2.1: ANOVA for all the three filters: a comparative analysis of the variables

Variable factors			**Filter 1 (Control)**	**Filter 2 (*Arthrobacter ramosus*)**	**Filter 3 (*Bacillus* sp.)**
Comparison	**Factor/s**	**Level of factor/s**	**p-value (paired t-test)**	**p-value (paired t-test)**	**p-value (paired t-test)**
Ozone Dose vs Microcystin-LR	Ozone dose	2	0.041 (OD1_OD2)	0.36 (OD1_OD2)	0.23 (OD1_OD2)
Bloom condition vs Microcystin-LR	Bloom condition	3	0.29 (LB_MB); 0.51 (LB_HB); 0.89 (MB_HB)	0.047 (LB_MB); 0.16 (LB_HB); 0.21 (MB_HB)	0.66 (LB_MB); 0.41 (LB_HB); 0.69 (MB_HB)
NOM vs Microcystin-LR	NOM	3	0.84 (N1_N2); 0.95 (N2_N3); 0.96 (N3_N1)	0.41 (N1_N2); 0.18 (N2_N3); 0.22 (N3_N1)	0.29 (N1_N2); 0.36 (N2_N3); 0.27 (N3_N1)
	NOM		1.00 (N1_N2); 1.00 (N2_N3); 1.00 (N3_N1)	0.98 (N1_N2); 0.68 (N2_N3); 0.59 (N3_N1)	0.85 (N1_N2); 0.93 (N2_N3); 0.65 (N3_N1)

Variable factors			Filter 1 (Control)	Filter 2 (*Arthrobacter ramosus*)	Filter 3 (*Bacillus* sp.)
Comparison	**Factor/s**	**Level of factor/s**	**p-value (paired t-test)**	**p-value (paired t-test)**	**p-value (paired t-test)**
NOM and Ozone dose vs Microcystin-LR	Ozone dose	3 and 2	0.045 (OD1_OD2)	0.76 (OD1_OD2)	0.44 (OD1_OD2)
Ozone Dose and Bloom condition vs Microcystin-LR	Ozone Dose	2 and 3	0.033 (OD1_OD2)	0.034 (OD1_OD2)	0.45 (OD1_OD2)
	Bloom condition		0.49 (LB_MB); 1.00 (LB_HB); 1.00 (MB_HB)	0.047 (LB_MB); 0.39 (LB_HB); 0.89 (MB_HB)	1.00 (LB_MB); 1.00 (LB_HB); 1.00 (MB_HB)
NOM and Bloom condition vs Microcystin-LR	NOM	3 and 3	0.76 (LB_MB); 1.00 (LB_HB); 1.00 (MB_HB)	0.032 (LB_MB); 0.21 (LB_HB); 0.46 (MB_HB)	0.95 (LB_MB); 1.00 (LB_HB); 1.00 (MB_HB)
	Bloom condition		1.00 (N1_N2); 1.00 (N2_N3); 1.00 (N3_N1)	0.98 (N1_N2); 0.44 (N2_N3); 0.54 (N3_N1)	1.00 (N1_N2); 1.00 (N2_N3); 1.00 (N3_N1)

NOM: Natural Organic Matter, N1, N2 and N3 are three levels of NOMs, LB, MB and HB represent intensity of bloom, OD: ozone dose (refer text for more detail)

Biodegradation: Bioaugmentation of the sand filter with MC-LR-degraders: *Arthrobacter ramosus* (Biofilter: FA), *Bacillus* sp. (Biofilter: FB) enhanced the MC-LR removal. Figure 2.2.6 (A), (B) and (C) shows the bar chart representing MC-LR removal % for each combination of samples for filter FC, FA, and FB, respectively. A total of 14 out of 18 combinations each for filter FA and FB showed an improvement in MC-LR degradation as compared to the results of filter FC (Figure 2.2.6 (A), (B)). Since most of the MC-LR removal occurred during the higher ozone concentration case 59.9 ± 19.9% (C2s) as compared to the lower concentration one 38 ± 12% (C1s), the biodegradation was mostly visible in the C1 samples.

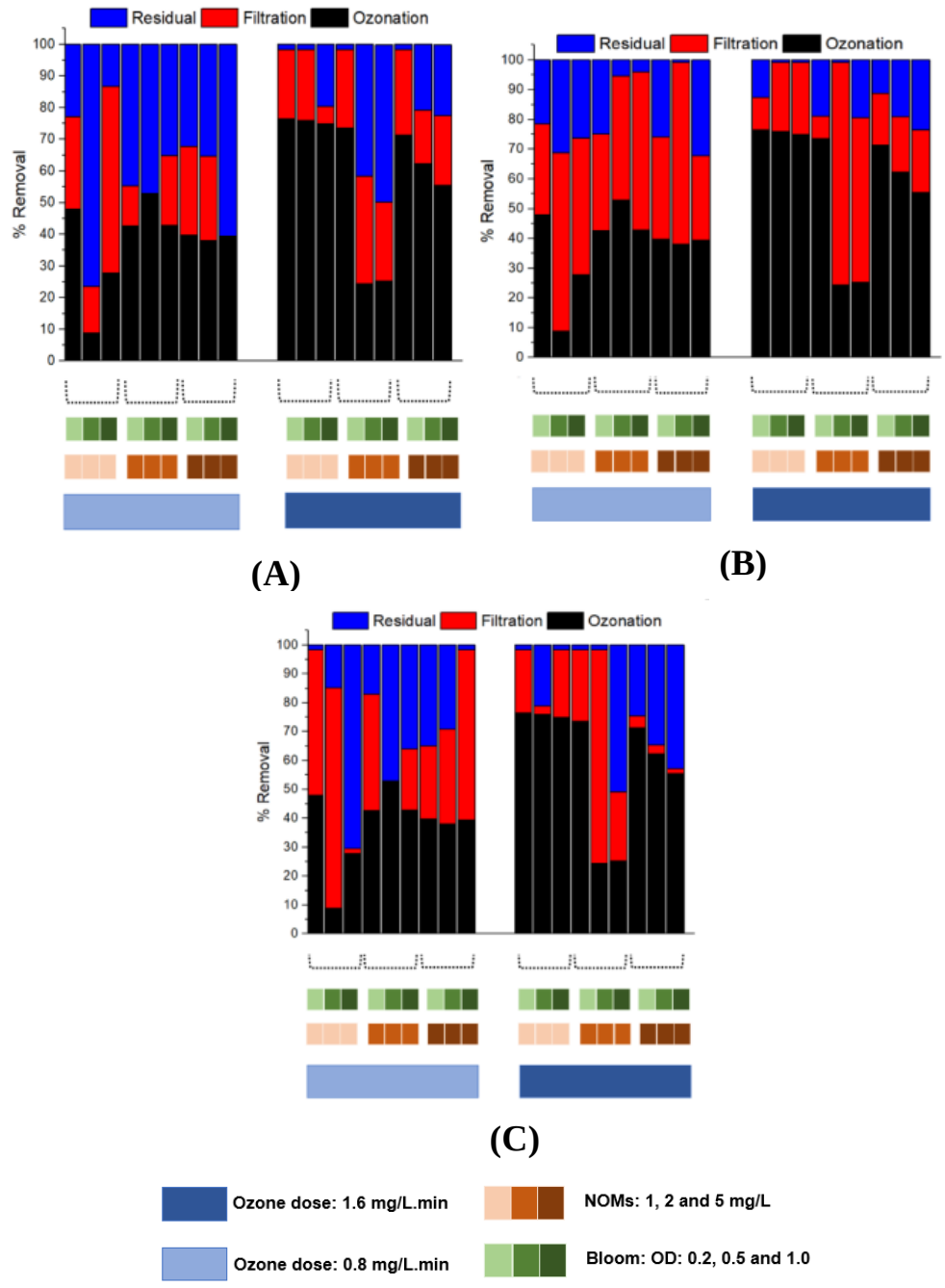

Figure 2.2.6: Bar graph showing the % removal of MC-LR for all the 18 combination samples for filter: (A) FC: Control filter; (B) Filter FA; (C) Filter FB.

On an average, bioaugmentation of *Arthrobacter ramosus* (filter FA) and *Bacillus* sp. (filter FB) enhanced the filter performance (compared to control) by 19.5% and 10.5% for C1s and 6% and 2% for C2s, respectively, when compared to filter FC. This seems obvious as more ozone concentration projects more residual concentration in the treated sample which eventually becomes

the part of influent to the biofilters affecting the physiological condition of the bacteria and their viability. Hence, MC-LR removal was relatively lower for C2s (more residual ozone affected biocells) than lower applied ozone concentration case (C1s).

Toxicity assessment of the ozone-treated sample using known MC-LR-degraders and native bacterial community isolated from DWTP

Figure 2.2.7 represents the standard activity curve for the PP1A enzyme (reported in %) vs. an increase in MC-LR concentration. For comparison, the PP1A % activity was also tested for the treated samples from biofilters inoculated (co-culturing) with native bacteria (*Chryseobacterium* sp. and *Pseudomonas fragi*) isolated from the filtration unit of the DWTP (Kumar et al. 2018) with known MC-LR-degraders: *Arthrobacter ramosus* and *Bacillus* sp.

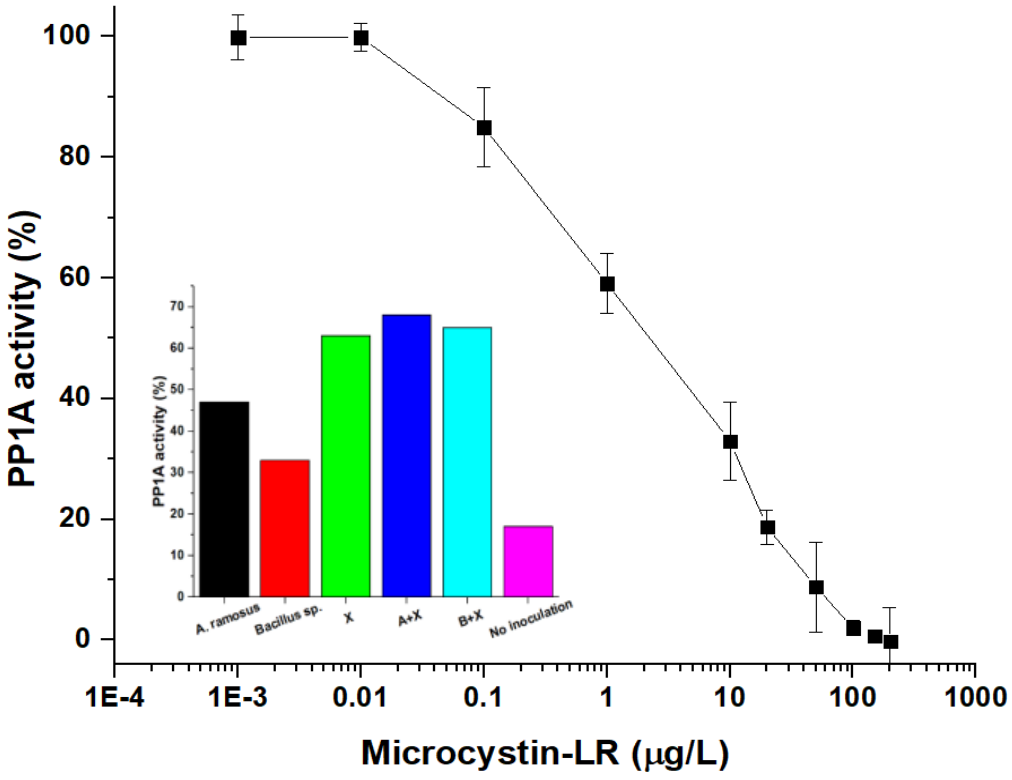

Figure 2.2.7: Standard curve showing relationship between % PP1A activity vs Microcystin-LR concentration and PP1A % activity for various bioaugmented case (inset). Bioaugmentation in a sand filter using: *Arthrobacter ramosus* (A), *Bacillus* sp. (B), native bacterial community (named 'X' = *Pseudomonas fragi* and *Chryseobacterium* sp.), A+X, B+X.

The % PP1A activity of 15% was reported for the influent (ozone-treated sample, dose: 0.8 mg.min/L) while 17% for the effluent obtained from filter FC (initial MC-LR: 50 µg/L). This result points to an important conclusion that though the MC-LR concentration reduces by 30-50% using

sand as the adsorbing media, but the % change in PP1A activity was reported just 2%. This can be attributed to the toxicity posed by other toxic-by products present in the filtered effluent. These toxic by-products generated after the ozone treatment or transformed after the filtration, might be responsible for the PP1A activity inhibition. However, the % PP1A activity increased to 33% and 47% for FB and FA filtered samples, respectively. This attributed to a decrease in MC-LR concentration and the related reduced toxicity due to formed and persistent by-products from ozonation or bio-transformed product post-filtration. From the earlier section, the enhanced MC-LR removal was observed for the bioaugmented sand filter (at C1 ozone dose) as 10.5% and 19.5% higher for filter FB and filter FA, respectively. Also, filters FA and FB reported 16% and 30% higher PP1A activity at the same ozone dose (C1), could possibly suggest that the (bio)transformed products (parent by-product generated from ozonation) decreased proportionally and remained independent of the type of MC-LR-degraders. Nevertheless, the results showed evidence on lesser toxic compounds present in the filtered water obtained from bioaugmented filters as compared to just sand filter. A detailed mass spectra analysis could possibly suggest more clarity on the nature of by-products transformed as a result of biodegradation.

In comparison to the results reported by the individual bacteria (as discussed above), the inoculation of the native bacteria (X) alone enhanced the % PP1A activity to 63%. Co-culturing X with *Arthrobacter ramosus* and *Bacillus* sp. further increased the % PP1A activity by 2%-5% to 65% and 68%, respectively. Though not as significant change, still the prospects of exploring co-culturing and native bacterial community for the MC-LR removal were open to decrease MC-LR residual and toxicity in the filtered water. Also, the population of the bacterial community in the bioaugmented sand filter can change over long-term water treatment. Thus, in the future, investigation on the microbial community is essential to ascertain the credibility, working and performing the techno-economic evaluation of the filter.

Conclusion

Ozone-Biofilter hybrid treatment of a model emerging contaminant: Microcystin-LR was evaluated using two different dose-contact times (CT): 0.8 mg.min/L and 1.6 mg.min/L. In addition, three distinct levels of natural organic matter (NOMs: 1 mg/L, 2 mg/L, and 5 mg/L) and three cyanobacterial bloom levels (low, mid and high) were tested for these two CTs. Two MC-LR-degraders: *Arthrobacter ramosus* (FA) and *Bacillus* sp. (FB) inoculated in a sand filter

performed differently in removing MC-LR after the samples were treated with ozone. A strong negative correlation (< -0.97) was shown by all three filters (including control) for the residual ozone concentration and the MC-LR removal due to ozonation. *Arthrobacter ramous* showed more resilience towards the residual ozone (0.1-0.4 mg/L) as compared to the *Bacillus* sp. for the MC-LR removal. Statistical analysis suggested strong influence on the biofilters towards the MC-LR removal due to cyano bloom level and NOM presence. Biofilter performed better than just the sand filter (no MC-LR-degraders inoculated) as the MC-LR removal efficiency for filter FA and FB improved by 19.5% and 10.5% for CT: 0.8 mg/L.min and 6% and 2% for CT: 1.6 mg.min/L, respectively. PP1A toxicity assay suggested the evidence of lower toxic by-products formation when native bacteria were co-cultured and inoculated with known MC-LR-degraders in a sand filter.

Acknowledgment

The authors are sincerely thankful to the Natural Sciences and Engineering Research (Discovery Grant 23451). A Special thanks to the plant operator Mr. Guy Desgroseilliers, Ville de Quebec for availing the quartz sand from the filtration unit of the drinking water treatment plant, Chemin Ste-Foy, Quebec City, Canada. The authors are also thankful to Dr. Jerome Compte for providing the *Microcystis Aeruginosa* culture. Authors are thankful to Mr. Dave Gilbert, President, and CEO, EMO3 for availing the ozone generator.

Conflict of interest

None

References

Bijan, L. and M. Mohseni (2005). "Integrated ozone and biotreatment of pulp mill effluent and changes in biodegradability and molecular weight distribution of organic compounds." Water Research **39**(16): 3763-3772.

Bradford, M. M. (1976). "A rapid and sensitive method for the quantitation of microgram quantities of protein utilizing the principle of protein-dye binding." Analytical Biochemistry **72**(1-2): 248-254.

Brown, LeAnn L., "Human Health Risks from Tap Water Chlorine Disinfection Byproducts: An Ohio Study" (2016). *Williams Honors College, Honors Research Projects*. 283.

Chu, W., D. Yao, Y. Deng, M. Sui and N. Gao (2017). "Production of trihalomethanes, haloacetaldehydes and haloacetonitriles during chlorination of microcystin-LR and impacts of pre-oxidation on their formation." Journal of Hazardous Materials **327**: 153-160.

Cui, Y., Wu, Q., Xiao, S., An, X., Sun, J., & Cui, F. (2014). Optimum Ozone Dosage of Preozonation and Characteristic Change of Refractory Organics in Landfill Leachate. *Ozone: Science & Engineering, 36*(5), 427-434. doi:10.1080/01919512.2013.874276

De Vera, G. A., D. Stalter, W. Gernjak, H. S. Weinberg, J. Keller and M. J. Farré (2015). "Towards reducing DBP formation potential of drinking water by favouring direct ozone over hydroxyl radical reactions during ozonation." Water Research **87**: 49-58.

Fayad, P. B., A. Roy-Lachapelle, S. V. Duy, M. Prévost and S. Sauvé (2015). "On-line solid-phase extraction coupled to liquid chromatography tandem mass spectrometry for the analysis of cyanotoxins in algal blooms." Toxicon **108**: 167-175.

Gardoni, D., Vailati, A., & Canziani, R. (2012). Decay of Ozone in Water: A Review. *Ozone: Science & Engineering, 34*(4), 233-242. doi:10.1080/01919512.2012.686354

Gerrity, D., Arnold, M., Dickenson, E., Moser, D., Sackett, J. D., & Wert, E. C. (2018). Microbial community characterization of ozone-biofiltration systems in drinking water and potable reuse applications. *Water Research, 135*, 207-219. doi:10.1016/j.watres.2018.02.023

Goel, S., R. M. Hozalski and E. J. Bouwer (1995). "Biodegradation of NOM: effect of NOM source and ozone dose." Journal - American Water Works Association **87**(1): 90-105.

Hallé, C., P. M. Huck and S. Peldszus (2015). "Emerging Contaminant Removal by Biofiltration: Temperature, Concentration, and EBCT Impacts." Journal - American Water Works Association **107**(7): E364-E379.

Helmy E.G. (2015), "Using ozone instead of chlorine in a typical water treatment plant in egypt: a case study", Fourteenth International Water Technology Conference, IWTC 14 2010, Cairo, Egypt.

Keijola, A.M., Himberg, K., Esala, A.L., Sivonen, K., Hiis-Virta, L, Removal of cyanobacterial toxins in water treatment processes: laboratory and pilot-scale experiments, Toxic. Assess. 3 (5) (1988) 643–656.

Khong, N. M. H., Khaw, Y. S., Nazarudin, M. F., & Yusoff, F. M. (2019). *Microcystis aeruginosa* grown in different defined media leads to different cultivable heterotrophic bacteria composition that could influence cyanobacterial morphological characteristics and growth properties. *bioRxiv*, 721175. doi:10.1101/721175

Kumar, P., Hegde, K., Brar, S. K., Cledon, M., Kermanshahi-pour, A., Roy-Lachapelle, A., & Galvez-Cloutier, R. (2018). Biodegradation of microcystin-LR using acclimatized bacteria

isolated from different units of the drinking water treatment plant. *Environmental Pollution, 242*, 407-416. doi:10.1016/j.envpol.2018.07.008

Kumar, P., H. D. P. Rubio, K. Hegde, S. K. Brar, M. Cledon, A. Kermanshahi-pour, S. Sauvé, A. Roy-Lachapelle and R. Galvez-Cloutier (2019). "Agro-industrial residues as a unique support in a sand filter to enhance the bioactivity to remove microcystin-Leucine aRginine and organics." Science of The Total Environment **670**: 971-981.

Kumar, P., K. Hegde, S. K. Brar, M. Cledon and A. Kermanshahi pour (2018). "Physico-chemical treatment for the degradation of cyanotoxins with emphasis on drinking water treatment—How far have we come?" Journal of Environmental Chemical Engineering **6**(4): 5369-5388.

Li, X.-F. and W. A. Mitch (2018). "Drinking Water Disinfection Byproducts (DBPs) and Human Health Effects: Multidisciplinary Challenges and Opportunities." Environmental Science & Technology **52**(4): 1681-1689.

Lu, L.-W., Y.-P. Peng and C.-N. Chang (2018). "Catalytic ozonation by palladium–manganese for the decomposition of natural organic matter." Separation and Purification Technology 194: 396-403.

Nicholson, B. C., J. Rositano and M. D. Burch (1994). "Destruction of cyanobacterial peptide hepatotoxins by chlorine and chloramine." Water Research **28**(6): 1297-1303.

Orr, P. T., G. J. Jones and G. R. Hamilton (2004). "Removal of saxitoxins from drinking water by granular activated carbon, ozone and hydrogen peroxide—implications for compliance with the Australian drinking water guidelines." Water Research **38**(20): 4455-4461.

Petrovic, M. (2003). "Analysis and removal of emerging contaminants in wastewater and drinking water." TrAC Trends in Analytical Chemistry **22**(10): 685-696.

Petrovic, M., E. Eljarrat, M. J. Lopez de Alda and D. Barcelo (2004). "Endocrine disrupting compounds and other emerging contaminants in the environment: A survey on new monitoring strategies and occurrence data." Analytical and Bioanalytical Chemistry **378**(3): 549-562.

Schlüter-Vorberg, L., Prasse, C., Ternes, T. A., Mückter, H., & Coors, A. (2015). Toxification by Transformation in Conventional and Advanced Wastewater Treatment: The Antiviral Drug Acyclovir. *Environmental Science & Technology Letters, 2*(12), 342-346. doi:10.1021/acs.estlett.5b00291

von Gunten, U. (2018). Oxidation Processes in Water Treatment: Are We on Track? *Environ Sci Technol, 52*(9), 5062-5075. doi:10.1021/acs.est.8b00586

Zoumpouli, G. A., Scheurer, M., Brauch, H.-J., Kasprzyk-Hordern, B., Wenk, J., & Happel, O. (2019). COMBI, continuous ozonation merged with biofiltration to study oxidative and

microbial transformation of trace organic contaminants. *Environmental Science: Water Research & Technology, 5*(3), 552-563. doi:10.1039/c8ew00855h

CHAPTER 3: Co-culturing of *in-situ* bacteria and MC-LR-degraders in dynamic and static biofilter

BRIDGE-2

BRIDGE: From the previous chapter (chapter 2, part 1 and part 2), the role and significance of bacterial co-culture in biodegrading MC-LR were evident. Also, toxic-free filter water was obtained using a co-culture approach using known MC-LR-degraders and native bacteria isolated from DWTP. Hence, the next step was to study the MC-LR as well as other water pollutant removal using biosand filter. It was also necessary to make a distinction between biodegradation and physical adsorption for the removal of MC-LR and other water pollutants. Also, the co-culture aspect was explored to find the significance of three known MC-LR-degraders with the native bacterial community to understand the behavior of each MC-LR-degraders in removing MC-LR. Hence, part 1 of this chapter is based on a dynamic bed filter where a moving bed biofilm reactor is studied while part 2 discusses the study on static bed (or sand) filter.

PART 1

Novel Fluidized-Bed Biofilm Reactor for concomitant removal of Microcystin-LR and organics

Pratik Kumar [a], Krishnamoorthy Hegde [a], Satinder Kaur Brar [a*], Maximiliano Cledon[b], Azadeh Kermanshahi-pour[c], Audrey Roy-Lachapelle[d,e], Rosa Galvez-Cloutier[f]

[a] - INRS-ETE, Université du Québec, 490, Rue de la Couronne, Québec, Canada G1K 9A9

[b] - Instituto de Investigaciones Marinas y Costeras (IIMyC-CONICET), Funes 3350, Mar del Plata 7600, Argentina

[c] – Biorefining and Remediation Laboratory, Department of Process Engineering and Applied Science, Dalhousie University, 1360 Barrington Street, Halifax, Nova Scotia B3J 1Z1, Canada

[d]- Department of Chemistry, Université de Montréal, Montréal, QC, Canada

e- Environment and Climate Change Canada, 105 rue McGill, H2Y 2E7, Montréal, QC, Canada

f- Faculté des Sciences et Génie, Département de génie civil et génie des Eaux, Université Laval, Québec (Québec), Canada.

[*]- Corresponding author, E-mail: satinder.brar@ete.inrs.ca (S.K. Brar)

Corresponding author. Tel.: +1 418 654 3116; Fax: +1 418 654 2600.

***Chemical Engineering Journal*, 359, 99-111 (2019) DOI: 10.1016/j.cej.2018.11.119**

Résumé

Un réacteur à biofilm à lit fluidisé (FBBR) a été évalué pour l'élimination de la microcystine-LR (MC-LR) des boues d'eau potable (0,3% p / v). Le biofilm formé à l'intérieur des supports solides (bioporteurs) a été étudié pour la dégradation du MC-LR dans les FBBR via des dégradeurs MC-LR connus: *Arthrobacter ramosus* (réacteur A: RA) et *Bacillus* sp. (réacteur B: RB), ainsi que la communauté bactérienne hétérogène (HBC) déjà présente dans la boue de sédimentation (comme matrice de fond). Leur capacité à former un biofilm à l'intérieur des bioporteurs immobilisés a été périodiquement quantifiée pendant plus de 300 jours pour déterminer la durée de croissance du biofilm mature, l'événement de décroissance puis la rematuration. La performance du bioréacteur a été principalement évaluée en termes de MC-LR, de nitrate, de nitrite, d'élimination de l'ammoniac et d'élimination de la demande chimique en oxygène soluble (s-COD). La dégradation biologique de MC-LR a montré un rôle significatif sur l'adsorption physique, car l'efficacité d'élimination a augmenté d'environ 30% et 26% respectivement pour RA et RB, par rapport au bioréacteur témoin RD (sans cellules bactériennes) et une augmentation de plus de 15% et 11% par rapport au réacteur RC (ne contenait que du HBC). L'analyse des spectres de masse pour RA, RB et RC renforce la possibilité d'un mécanisme de dégradation non toxique. Globalement, la RA a montré la meilleure efficacité d'élimination du MC-LR d'environ 93,7%, qui ne comprenait pas de MC-LR dans la phase surnageant et d'environ 3 µg / L dans la phase de mélange des boues. L'évaluation de la toxicité d'un échantillon biodégradé (à l'aide d'un bioindicateur) a en outre révélé la nature non toxique de l'AR avec une élimination de plus de 80% pour l'ammoniac, le nitrate et le nitrite. La mise à l'échelle du FBBR (2 L) à l'échelle du laboratoire est également proposée pour traiter 200 m^3 d'eau d'alimentation par jour sur la base d'un coefficient de transfert de masse volumétrique (kLa) similaire afin d'étudier les aspects économiques réalisables du procédé.

Mots-clés: réacteur à lit fluidisé, eau potable, cyanotoxine, microcystine, biofilm, scale-up

Abstract

Fluidized bed biofilm reactor (FBBR) was evaluated for the removal of microcystin-LR (MC-LR) from drinking water-sludge (0.3 % w/v). Biofilm formed inside the solid media carriers (biocarriers) were studied for the MC-LR degradation in FBBRs via known MC-LR degraders: *Arthrobacter ramosus* (reactor A: RA) and *Bacillus sp.* (reactor B: RB), along with the heterogeneous bacterial community (HBC) already present in the sedimentation-unit sludge (as a background matrix). Their ability to form biofilm inside the immobilized biocarriers was periodically quantified for over 300 days to determine the duration of mature biofilm growth, sloughing event and then re-maturation. The bioreactor performance was mainly evaluated in terms of MC-LR, nitrate, nitrite, ammonia removal, and soluble-chemical oxygen demand (s-COD) removal. Biological degradation of MC-LR showed significant role over the physical adsorption, as the removal efficiency increased by around 30 % and 26 % for RA and RB respectively, as compared to the control bioreactor RD (without any bacterial cells) and an increase by over 15 % and 11 % when compared to reactor RC (contained only HBC). The mass spectra analysis for RA, RB, and RC strengthen the possibility of a toxic-free degradation mechanism. Overall, RA showed the best MC-LR removal efficiency of around 93.7 %, which comprised no MC-LR in the supernatant phase and around 3 µg/L in the sludge-mixture phase. Toxicity assessment of biodegraded sample (using bioindicator) further revealed the toxic-free nature by RA with more than 80% removal for ammonia, nitrate, and nitrite. Scale-up of laboratory scale FBBR (2 L) is also proposed to handle 200 m^3 of feed water per day based on a similar volumetric mass transfer coefficient (kLa) to study the feasible process economics.

Keywords: Fluidized-bed reactor, drinking water, cyanotoxin, microcystin, biofilm, scale-up

Introduction

Cyanotoxins produced by cyanobacteria is a global problem that affects the water quality of various sources such as rivers, lakes, ponds, etc. They can be a year-round problem, which poses a serious threat to the diverse living species including humans. These secondary metabolites (cyanotoxins) remain persistent and stable for a long period (sometimes > 90 days) in the environment and hence their form remains unchanged by the time it enters a drinking water treatment plant (DWTPs) [1]. DWTPs deriving water from a cyanotoxin-affected source need to be extra careful as their treatment becomes a challenge for an existing conventional treatment system. The most prominent and commonly available cyanotoxin in various natural water bodies is microcystin (MCs), especially MC-LR which is the most toxic variant among all MCs [2].

Several physicochemical treatments, such as photocatalysis, ozonation, chlorination, Reverse Osmosis membrane, etc. have been tested so far for the MCs removal. However, problems including operational difficulties, energy intensiveness, excessive cost, and formation of the toxic by-products often limits and challenges their commercial viability [4]. On the other hand, biological treatment methods not only promise effective treatment but also are more sustainable, economical and free of toxic by-products generation [4]. Many laboratory-scale studies have been successfully performed for studying the cyanotoxins biodegradation, under both modes of bacterial growth: suspended as well as the attached growth. The attached growth biofilm processes are "static" in nature and hence it might be very interesting to observe how they behave under "fluidized" mode where the attached biofilm over the support surface is continuously under motion. Under fluidized state, better mass transfer of oxygen and less nutrient limiting conditions is expected to prevail, which might enhance the overall MCs removal.

Present work will further improve the understanding of behavioral dynamics and important role of the biofilm under fluidized mode in treating cyanotoxin (in form of MC-LR) and other organics in form of nitrite, nitrate and ammonia. Higher biodegradation of MC-LR is expected in the fluidized bed reactor due to an enhancement in mass transfer properties when compared to the suspended growth conditions. Also, the risk posed by the cyanobacterial-laden sludge due to coagulation in the drinking water treatment system is further marked by the release of cyanotoxins to the supernatant, which might eventually limit the downstream efficiency of the filtration unit (immediate treatment unit to coagulation/flocculation). Sedimentation unit sludge in a DWTP have

even been found to contain as high as 90 μg L^{-1} of microcystins whose release can be controlled and degraded through biofilm-based supports under fluidized mode (pretreatment) [5]. Hence, a 50 μg L^{-1} of MC-LR has been spiked (current study) to mimic the situation of secondary metabolite release from these cyanobacterial-laden sludges in FBBR containing biofilm-developed carriers (biocarriers).

This kind of bioreactors (FBBRs) can be employed as the pretreatment aspects in the drinking water treatment system (Xiangyang et al. 2012) [6]. Biological pretreatment processes in form of FBBRs can further strengthen the efficiency of the conventional treatment units/process, by removing organic carbon (chemical oxygen demand removal: COD), nitrate, nitrite, and ammonia along with MC-LR thereby ensuring safe drinking water. FBBRs and other biofilm-based reactors have also shown to be effective in mineralizing other toxic pollutants such as polychlorinated biphenyls, 2, 4, 6-trichlorophenol, etc. [7].

In this study, MC-LR-degraders in the form of *Arthrobacter ramosus* (Kormas et al. 2013) [4]; Manage et al. 2009) [8] and *Bacillus sp.* (Hu et al. 2012) [9] has been used as the biofilm forming opportunist along with other heterogeneous bacteria present in the sedimentation unit sludge. For the first time, MC-LR degraders have been used in an FBBR to study MCs degradation. The work also encompasses successful biofilm life-cycle, comprising all three important phases viz. biofilm formation, sloughing and re-maturation along with their periodical quantification in terms of organic carbon removal (COD), ammonia, nitrate, and nitrite removal (for over 300 days), followed by its potential to eventually degrade MC-LR during the re-maturation phase. A toxicity assessment (using bioindicator) of the final degraded broth has also been analyzed to report for any harmful effects to the humans. Based on the best performing laboratory scale study of FBBRs, a possible scale-up model is also proposed considering a similar superficial velocity and volumetric mass transfer coefficient (k_La value), to understand its feasibility and process economics.

Materials and Methods

Reagents and chemicals

K1 Kaldness media used as the bio-carrier was purchased from Cz Garden supply (Canada). Microcystin-LR was purchased from Cayman Chemicals, (Ann Arbor, Michigan, USA). To prepare the trace metal solution and feed for bacteria, $CaCl_2.2H_2O$, $MgSO_4.7H_2O$, $MnCl_2.4H_2O$, $ZnSO_4.H_2O$, $FeCl_3$, $CuSO_4.5H_2O$, $CoCl_2.6H_2O$, $Na_2MoO_4.2H_2O$, Yeast Extract, dextrose ($C_6H_{12}O_6$), KH_2PO_4, $(NH_4)_2SO_4$ were purchased from Fisher Scientific, (Ontario, Canada). Millipore system (Milford, MA, USA) Milli-Q/Milli-RO was used to prepare a trace metal solution. Sodium chloride (NaCl), peptone and yeast extract were purchased from Fisher Scientific (Ottawa, ON, Canada) to prepare Luria-Bertani medium for bacterial culture. $K_2Cr_2O_7$, $HgSO_4$, and H_2SO_4 were purchased from Fisher Scientific, (Ontario, Canada) to prepare a reagent for Chemical Oxygen Demand (COD). Saturate phenol (pH 6.6/7/9, Liq.), NaOH and ethanol (86.6%) were bought from Fisher Scientific, (Ontario, Canada) for total saccharide and EPS quantification. For the toxicity assay: Tris-HCl buffer (pH 7.5) was prepared using Tris-buffer and 6N HCl (Merck, US) and 3-(4, 5-dimethylthiazol-2-yl)-2, 5-diphenyltetrazolium bromide (MTT) was used for determining cell viability, bought from Sigma Aldrich, (Ontario, Canada).

Microorganisms

Arthrobacter ramosus (NRRL B-3159), *Bacillus sp.* (NRRL B-14393), *Sphingomonas sp.* (NRRL B-59555), and *Rhizobium meliloti* (NRRL L-84) were purchased from NRRL Agricultural Research Service (ARS) culture collection. *R. meliloti* was used as the bioindicator, whereas other listed microorganisms were used as the MC-LR-degraders [8,9]. *Staphylococcus epidermidis*: a potential biofilm-forming microorganism was used as the positive control to compare and screen MC-LR degrading bacteria capable of forming biofilm [10].

Sample collection and microbial culture

Sedimentation-unit sludge mixture was collected from the DWTP at Chemin Ste-Foy, (Quebec City, Canada) in 4-L plastic bottles. These bottles were properly rinsed 2-3 times with sludge-mixture before the final sample collection. After packing, it was transported to the laboratory, on the same day, and stored at 4°C, until further use.

All three MC-LR-degraders viz., *A. ramosus, Bacillus sp., Sphingomonas sp*. and positive control for biofilm former: *S. epidermidis* were sub-cultured (5% v/v) twice from their lyophilized state, spread-plated and finally streaked on to the LB-agar plate to review the bacteria. A loopful of the single bacterial colony was cultured until mid-exponential growth phase was reached, to get the most active form of bacteria. They were centrifuged at 8000 x g at room temperature for 20 minutes to obtain the bacterial pellets. Obtained pellets were rinsed 3 times with sterilized tap water to remove any residual carbon and then were used for spiking the FBBRs as MC-LR degraders.

Screening of biofilm-forming bacteria

A. ramosus, Bacillus sp. and Sphingomonas sp. were subjected to pre-screen test to check their biofilm-forming ability inside the biocarrier media (reactor named RA, RB and RS). *S. epidermidis* was used as the positive control. Around 9 x 10^9 bacterial cells of each of these microorganisms were spiked individually to a 3L-plexiglass batch reactor containing diluted sedimentation sludge with suspended solid: 3 g/L (0.3 % w/v); operational volume: 2L and K1 media (55%-60% as the media fill fraction of the operational volume).

Figure 3.1.1 shows an overview of the reactor configuration with details of the biocarriers used. For a quick biofilm development, microorganisms were fed at high COD concentration of 800 mg/L along with the trace metal-nutrients every 48 hours till 50 days (composition of feed and trace metal-nutrient solution. Dextrose, potassium dihydrogen phosphate, and ammonium sulfate were used as the carbon, phosphorus and nitrogen source, respectively as the feed composition. MC-degraders at the concentration of 6 x 10^6 cells/100 mL was fed every 15 days to maintain the established bacterial population in the biofilm formed over the carrier surface.

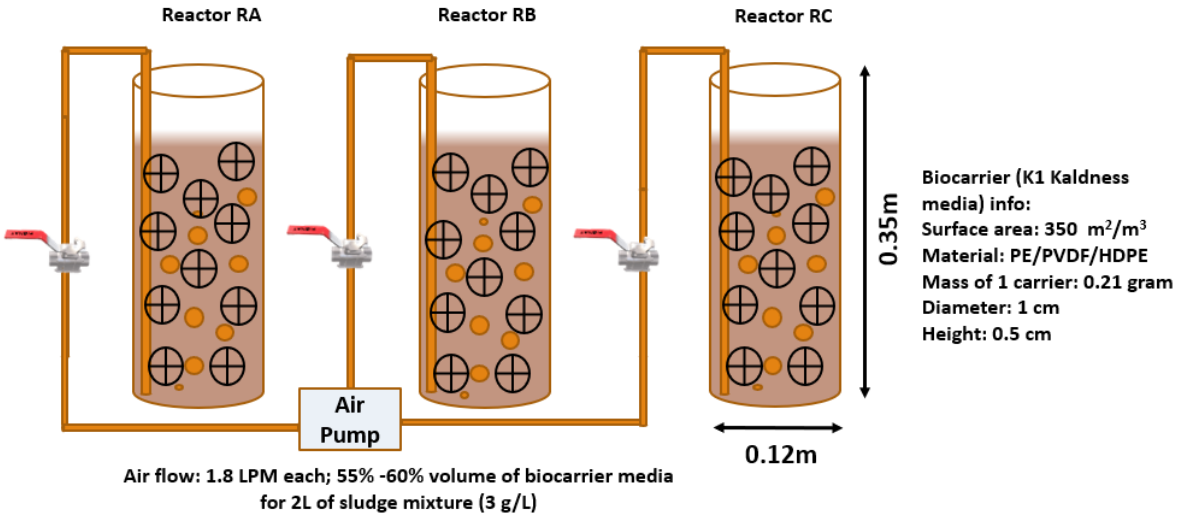

Figure 3.1.1: Set-up for the Fluidized bed biofilm reactor and biocarrier details

A constant air supply (1.8 liters/min) was provided to maintain the fluidity of the bio-carriers as well as to provide uniform and constant oxygen supply for the effective breakdown and utilization of food (dextrose) by the microorganism. Similar conditions were maintained for all the reactors including the positive control.

For the screening purpose, both, cell biomass and cell viability were determined for each of the biofilm-forming cases. Ten biocarriers were drawn out from each reactor after 10 days, 20 days, 40 days and 50 days for the biofilm quantification in terms of total biomass (live + dead cells using crystal violet assay) as well as the cell viability (only live cells using MTT assay). For sample preparation (for both these assays), excess water was first drained off by placing these biocarriers over the tissue paper. Then, the developed biofilm was scrapped off completely and suspended in a 15 mL-centrifuge tube containing 10 mL of sterile tap water to make a biofilm-broth sample (more details on assay is discussed in later section).

Reactor set-up and operational parameters

Same reactors were continued after the screening test to evaluate for the long-term performance of the bioreactors. However, bioreactor spiked with *Sphingomonas sp.* (RS) was rejected based on the screen test results (discussed in detail in result section). For the negative control, similar bioreactor but without MC-LR-degrading bacteria was installed (referred to as RC hereafter). All these reactors viz. RA, RB, and RC contain 3 g/L (0.3 % w/v) of sedimentation-unit sludge as the

matrix. A separate reactor RD was set-up along with RA, RB, and RC just before the MC-LR degradation phase (biofilm re-maturation phase) to report for the adsorption of MC-LR on the media carriers. Reactor RD contains only the fresh carrier media without any biofilm formed inside it. All the reactors were tested periodically with a thermometer to determine the operating temperature and averaged in the range of 15 °C -19 °C.

Chemical Oxygen Demand, nitrate, nitrite and ammonia removal

Chemical oxygen demand (COD) was determined to understand the effective carbon (dextrose) utilization by the active bacteria present in the bioreactor. It was determined according to the Standard Methods (1998) [11] for each reactor after every 2 days. Based on the calculated COD removal, fresh feed along with trace metal nutrients was fed accordingly.

For the nitrate, nitrite and ammonia detection, a similar method was followed as mentioned in Naghdi et al. (2017) [12]. In brief, the colorimetric titration method was employed for all three of them. Ammonium, nitrite, and nitrate were determined by indophenol method (phenol with hypochlorite combined to form indophenol in presence of ammonia), diazotization method (4-aminobenzensulfonic acid reacts with nitrite to form red shades) and reduction method (Nutrafin TM), respectively. The stock solution of nitrate (100 ppm), nitrite (10 ppm) and ammonia (10 ppm) were prepared using sodium nitrate, sodium nitrite, and ammonium sulfate, respectively.

pH, dissolved oxygen (DO) and Mixed liquor suspended solids (MLSS) measurements

Every 2nd day, just before feed supply, pH, DO, MLSS and COD were measured. DO was measured using a portable F4-Standard probe (Mettler Toledo Inc). On the other hand, Mixed liquor suspended solids (MLSS) and COD was measured in accordance with the standard methods (AWWA, 1998) where the former range was kept in between 3-4 g/L to maintain the right balance between the food and the microorganisms (ratio).

Biofilm quantification

Biofilm comprises many complex ingredients including water, protein, saccharides, etc. To quantify the successful development and nature of the biofilm, extracellular polymerase substance (EPS), total protein, total saccharides, cell biomass, and viable cells were determined.

EPS, total protein, and total saccharides analysis

To quantify the biofilm formed inside the biocarriers, three important elements comprising: EPS, total protein, and total saccharides were determined. Also, the dry and wet mass of the formed biofilm were found (not shown here). The EPS production by the bacterial cells in the biofilm (formed inside the biocarrier surface) were obtained by ethanol precipitation method as previously described by Boon et al. (2008) [13] with some modifications. The scrapped biofilm (from ten biocarriers) were resuspended in sterile tap water (10 mL) kept at 4 ± 1°C and quickly vortexed to give cell-shock to initiate cell lysis. Afterwards, the solution was spiked with 5 mL of cell-lysis buffer solution to further lyse the cells. Then, the mixture was centrifuged to 8000 x g at room temperature for 15-20 minutes. The supernatant was derived and mixed with twice the volume of ethanol (86.6% v/v) and incubated at -20 °C overnight. The precipitated EPS was dry weighted (in µg) and reported per mg of the dry biomass. The total saccharides content in EPS was quantified by the phenol-sulphuric method (Dubois et al. 1956) [14] with dextrose as the standard, and total protein content was measured by the Bradford assay (Bradford, 1976) [15] using bovine serum albumin as the standard.

Crystal Violet assay

Staining assay, such as crystal violet assay provides valuable information about the live/dead cells. It provides a good estimation of the formed biofilm as it stains both bacterial cells as well as the extracellular matrix. For the CV assay, a similar protocol was followed by Feoktistova et al. (2016) [16] with some modifications. 100 µL of suspended biofilm solution/supernatant (as discussed in later section) was seeded and stained with 100 µL of crystal violet dye (0.1% w/v) in a 96-well plate, followed by incubation at 35 ± 2°C. Care was taken not to let the stained biomass dry out completely and the wells were washed carefully with a phosphate buffer solution to remove any loose-attached biomass. After that, 200 µL of DMSO was added in each well to solubilize the stains and the absorbance was noted at 590 nm using BioTek's Epoch Micro-Volume Spectrophotometer System instrument.

(3-(4,5-dimethylthiazol-2-yl)-2,5-diphenyltetrazolium bromide (MTT) assay

MTT assay was used to evaluate the viability of bacterial cells present in the biofilm. A similar protocol was followed as described by Traba et al. (2011) [17] with some modifications. Biofilm

suspension was incubated at 35 ± 2°C with MTT (3-(4,5-dimethylthiazol-2-yl)-2,5-diphenyltetrazolium bromide at the concentration of 7 mg/10 mL. After 4h of incubation, the supernatant was carefully removed and the formazan (blue precipitate) was dissolved in 200 µL DMSO solution to measure the absorbance at 500 nm using BioTek Epoch Micro-Volume Spectrophotometer System instrument.

Stability test of the formed biofilm at different pHs

To understand the stability and change in the biofilm surface, the microscopy visuals were obtained for discrete pH values of 3,5,7,9,11 and 13. This test was done after a re-mature biofilm has formed over the surface of the biocarriers for RA, RB and RC bioreactors, post-sloughing event (after 200 days of FBBRs operation). A total of six different biocarriers for six different pH were taken and dipped individually in 20 mL of the solution adjusted to a required pH with 0.1 N HCl and 0.1 M NaOH solution. After 4h of standing, the biocarriers were placed over the tissue paper to drain out excess water retained in and around the biocarriers. Thereafter, they were kept at 60 ± 2 °C for a period just enough to dry it, as over-drying can cause crack within the biofilm surface. After drying, they were cut in the longitudinal shape (as shown in Figure B1, Appendix B) and analyzed for its surface visual under the microscope. Also, before and after MC-LR degradation study (in re-maturation stage), Scanning Electron Microscopy (SEM) images were taken to distinguish between the morphology of the biofilm for all the three FBBRs. Biocarrier was cut longitudinally and was gold-plated (15 nm thickness) using a sputter coater prior to imaging. Micrographs were captured at 10 kV accelerating voltage on an SEM (Zeiss EVO ® 50 Smart SEM system).

Kinetics measurement for observing the change in pH and dissolved oxygen

To understand the change in the behavioral dynamics of the biofilm formed inside the biocarriers, kinetics measurements were performed. This analysis was done in two different phases viz. before and after the MC-LR degradation study. The relation between simultaneous change in pH and DO was studied for each reactor: RA, RB, and RC. At discrete time interval, pH and DO was measured simultaneously till stable readings were achieved.

MC-LR degradation, mass spectra analysis and toxicity assessment of the degraded broth

MC-LR was spiked at an initial concentration of 50 µg/L in each of the reactors during the re-maturation phase of biofilm. Because this research study was done with the MC-LR-degraders for the first-time, hence, a proper long-term study on biofilm forming phase was understood and consistency was confirmed for the same before studying MC-LR degradation that included biofilm development (0-70 days), sloughing phase (71-170 days) and the consistent re-maturation phase (171-310 days). Nitrate, nitrite, and ammonia removal efficiencies were back on track after 220 days[1], as its performance used to be during the initial biofilm development phase (Figure 3.1.3 (A, B, C). At this point, MC-LR degradation was studied. Around 10 mL samples were drawn from each reactor after 36 hours, 2, 3, 4- and 6-days post-MC-LR spike. Samples were prepared in two parts considering MC-LR partitioning in the sludge-supernatant matrix.

Collected sample was centrifuged at 8000 x g for 15 minutes at room temperature, where supernatant was filtered via 0.45 µm filter membrane and an aliquot of 1 mL was stored in the amber vial at -20°C for HPLC analysis. On the other hand, to extract the MC-LR present in sludge, it was diluted with 10 mL of methanol followed by sonication at 25KHz for 1h. Afterwards, the sludge mixture was centrifuged at 8000 x g for 10 minutes to prepare supernatant aliquots of 1 mL as done for water matrix sample preparation. Hence, MC-LR removal was reported based on the partitioning of MC-LR in water as well as sludge components. A preliminary test to determine the extraction efficiency in sludge sample was also performed. Table 3.1.1 shows the overall performance of the FBBRs in terms of all the output parameters discussed, until now.

By-product fragments formed during biodegradation were analyzed by mass spectroscopy. MC-LR was used as an internal standard (1 mg/L) along with mobile phase of 50:50 (v/v) MeOH (A) and water (B) with 0.1 % formic acid. Capillary and vaporizer temperature of 350 °C and 450 °C, respectively along with sheath gas, aux gas and sweep gas pressure of 35, 10 and zero arbitrary units, respectively were used to maximize the signal intensity for final parameters. The scan time was kept at 0.02 s, where second quadrupole collision gas pressure was at 1.5 mTorr with first and third quadrupole operating at the unit resolution. Overall, this method represents an optimized

[1] Not every points for ammonia, nitrate and nitrite removal has been shown between 190th day and 220th day

rapid chromatographic method (on-line solid-phase extraction) for the determination of seven different cyanotoxins including MC-LR.

For toxicity test carried for the biodegraded sample, a similar method was followed as discussed in Kumar et al. (2018) [18] using a bioindicator: *Rhizobium meliloti*. The use of bioindicator is preferred to the PP1 inhibition assay as the latter responds to some other protein phosphatase inhibitors as well (such as okadaic acid, calyculin A, and tautomycin) that might be present in the sample. Moreover, the PP1 inhibition assay does not provide information on the toxicity of microcystins or nodularin variants (Metcalf et al. 2001) [19].

In brief, 3 mL of a mixture comprising bioindicator stock solution (*R. meliloti*), Tris-buffer (pH=7.5) and sample (1 mL each) was prepared. To them, 350 µL of MTT solution (7 mg/10 mL) was added and left for around 5 minutes to observe for the change in colour from yellow to yellow or blue (measured spectrophotometrically: λ_{max}= 500 nm). Blue colour signifies more cell viability and represents non-toxicity of the sample whereas more yellow colour signifies less cell viability and represents a toxic sample. Based on the established standard relationship between the various concentration of MC-LR and surrogate toxic solution dimethyl sulfoxide (DMSO; 10% v/v – 100% v/v), absorbance at 500 nm was correlated (Figure B2, Appendix B). The toxicity of the biodegraded-broth from each reactor was reported positive if it was found to be > 1 % v/v DMSO and non-toxic if the value is < 0.5-1.0 % v/v DMSO (for more details refer to result section).

Scale-up of lab-scale FBBR and its application in DWTP

Aeration and agitation in the aerobic bioreactor are important for promoting the effective mass transfer of oxygen from the gas phase to the liquid phase. In relation to this, the oxygen transfer coefficient, kLa value plays a significant role in the scale-up, design and overall process economics (Arjunwadkar et al.1998) [20]. Almost 30 % of the industries use kLa parameter for the scale-up operation of aerobic bioreactors (Oosterhuis et al. 1984) [21].

For the determination of kLa value, following equation 5 is used (dynamic method: Garcia-Ochoa et al. (2009) [22]):

$$dC/dt = kLa \cdot (C* - C) - q_{O2} \cdot C_X \qquad \textit{Equation 5}$$

Where, dC/dt is the accumulation of oxygen in the liquid media used, the first term on the right-hand side is the oxygen transfer rate (OTR) and the second term is the oxygen uptake rate (OUR). This last term can be expressed by the product $q_{O2} \cdot C_X$; where C_x is the microorganism concentration and q_{O2} is the oxygen utilization constant. C* is defined as the equilibrium or saturation concentration of oxygen in liquid under a particular temperature and pressure conditions in the bioreactor. It must be noted that the above equation (equation 5) is based on certain assumptions related to the mass transfer properties of oxygen molecule from the gaseous phase to the liquid-solid (bulk liquid to cell mass) interface. Also, the saturation value is obtained under gas-liquid thermodynamic equilibrium where a proper mixing of the liquid phase is ensured. The resistance of oxygen in the gaseous phase is assumed to be negligible compared to the bulk liquid phase and thus the parameter: '$C* - C$' plays an important role in driving the air flow for an efficient oxygen mass transfer.

Statistical Analyses

All statistical analyses comprising standard deviation, average, student t-test, p-value comparison, and all graphical presentations were performed in ORIGIN software (Version 8.5; OriginLab).

Results and discussion

Screening of biofilm-forming bacteria

Figure 3.1.2 (A) and Figure 3.1.2 (B) shows the CV and MTT assay results, for all the three reactors RA, RB, and RS. It was observed that the biomass (CV assay), as well as the cell viability (MTT assay) in the developed biofilm,was highest for the positive control strain (*S. epidermidis*) followed by strains in the order: *A. ramosus* > *Bacillus sp.* > *Sphingomonas sp*. Assay results of RA, RB and RS were compared to the *S. epidermidis* (positive control: biofilm forming strain) in terms of both biomass: as well as cell viability. Biomass growth was determined to be around 80 %, 80 % and 22 % of the positive control (absorbance value: Figure: 3.1.2 (A)) for RA, RB and RS, respectively, whereas the cell viability was found to be around 80 %, 60 % and 25 % of the positive control (absorbance value: Figure 3.1.2 (B) for RA, RB, and RS, respectively.

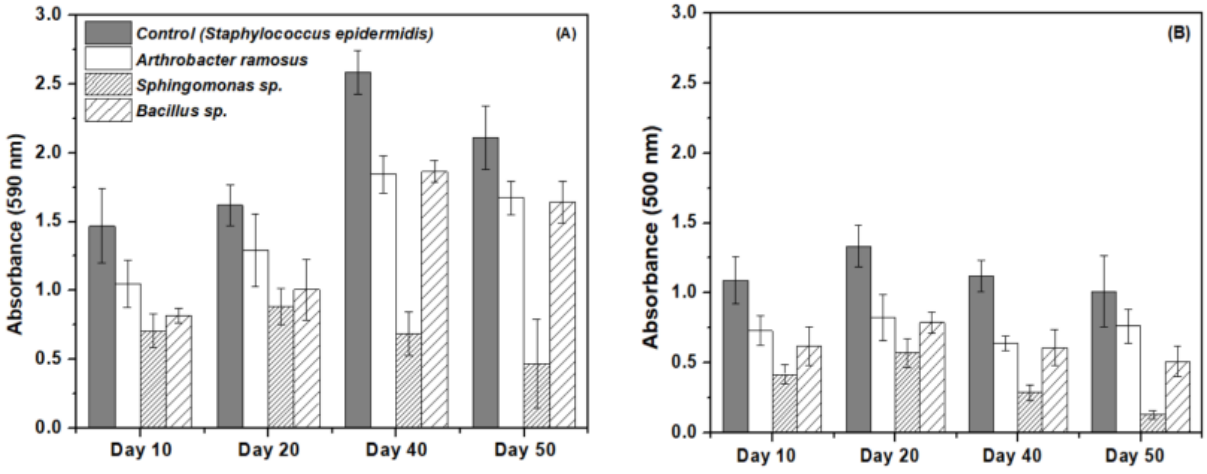

Figure 3.1.2: A) Crystal Violet assay and, B) MTT assay of different bacteria studied for quantifying biofilm formation

Cell biomass and viable cells form an integral part of the biofilm system (conditioning layer) where the latter is responsible for the maintenance of biofilm activity in removing various environmental contaminants. Poor viability (25 %) and continuous low biomass (22 %) quantified for *Sphingomonas sp.* (RS) depicts low biofilm formation ability inside the biocarriers. The reason could be the poor attachment property of this strain on the biocarrier surface. Azeredo et al. (2000) [23] shown that exopolymers have a determinant role for the *Sphingomonas sp.* to form biofilm and thus low biofilm formation in RS could be attributed to the low exopolymer formation marked by weak cell-to-cell adhesion property which led to detachment of biocells before much colonization has occurred. On the other hand, other stains hold long-term (50-70 days) promise in terms of biofilm attachment and thus the possible secretion of MC-degrading enzymes viz. *mlrA, mlrB* and *mlrC* encoded by *mlr* gene cluster (which is often responsible for the effective breakdown of the complex MCs structure), may have been effectively processed in the EPS matrix (Dziga et al. 2016) [24]. Hence, on this pretext, the RS reactor was rejected and not studied further. However, reactor RC was continued, as it was the negative control to study for the removal of MC-LR and other organics (COD removal, nitrate, nitrite, and ammonia removal) without the involvement of MC-LR degraders.

COD removal, pH, DO, MLSS analysis

Average COD removal of 72 ± 7%, 68 ± 6 % and 48.7 ± 6.7 % was obtained for RA, RB, and RC, respectively (for over 300 days). This indicated that the MC-LR-degraders present in FBBR: RA

and RB enhanced the carbon matter (organics) removal by around 24 % and 20 % ($p_{ra/rc}$=0.003; $p_{rb/rc}$ < 0.001) respectively as compared to RC where no MC-LR-degrader was present. The statistical term $p_{ra/rc}$ and $p_{rb/rc}$ indicate the p-value obtained by comparing the mean of COD removal values for reactor RA with RC (control reactor) and RB with RC, respectively. It may be linked to the enhancement in the activity of the sedimentation-unit bacterial community (HBC) due to the intrusion of the MC-LR-degraders. This phenomenon might have been responsible for an effective carbon breakdown and its utilization following better nutrient uptake

Similarly, DO level for RA and RB showed a significant difference (lower) with RC ($p_{ra/rc}$=0.00006; $p_{rb/rc}$=0.0002) while RA and RB showed no significant difference to each other ($p_{ra/rb}$=0.60). This can be related to the higher average COD removal for reactor RA and RB than RC (as mentioned above). Also, the lower DO values for RA and RB (3.27 ± 0.31 mg/L and 3.31 ± 0.4 mg/L) bioreactors as compared to RC (3.62 ± 0.45 mg/L) might be attributed to an enhanced biological activity due to biofilm developed inside the biocarriers marked by an increase in the removal efficiency of the carbonaceous/organic matter (as discussed above) using MC-degraders. Nevertheless, most of the times, the DO level remained above 3 mg/L for all the three bioreactors, thereby indicating good oxygen quality considering the drinking water aspects. The pH values were almost stable and similar for all the three reactors (averaging around 6.55). MLSS was maintained between 3-4 g/L in the reactors during the overall operational period.

Figure 3.1.3 (A), (B) and (C) shows the nitrate, nitrite, and ammonia removal efficiency for RA, RB and RC, respectively. The removal efficiency for these organics was checked periodically during the 320 days FBBRs run and samples were analyzed after 3 h of initial exposure. During the re-maturation phase, the average removal efficiency of nitrate, nitrite, and ammonia was > 80 %, ~80 %, and > 98 %, respectively, for all three FBBRs. With high nitrite presence, both as a combination of intermediate product formed during ammonia oxidation and the added stock concentration, the removal efficiency remained low and close to 80 % (Table 3.1.1).

It must be noted that the optimum bulk DO concentration is an important parameter in achieving proper nitrification. Li et al. (2016) [25] studied that in a similar kind of bioreactor, a minimum DO concentration of 4 mg/L is required for maximum nitrification. In reactor RA and RB, due to the presence of MC-degraders, DO level remained lower in the range 3-3.5 mg/L as compared to a value close to 4 mg/L in RC. However, nitrification (ammonia removal) in former reactors were

approximately 5 % more than the latter. This suggests that there could be an ammonia limited diffusion in reactor RA. In other biofilm reactor system (membrane aerated biofilm), it is stated that both ammonia and oxygen loading rate must be well controlled in order to achieve at least 80 % of total nitrogen removal [26]. In the present study, a special study for optimizing the oxygen load rate and ammonia level is not done. However, all three-nitrogen parameters, i.e., ammonia, nitrite, and nitrate for all three FBBRs, showed over 80 % removal.

Table 3.1.1: Overall performance of FBBRs[2]

Reactor	RA	RB	RC	Control (RD)[3]
Parameters				
Dry mass (mg/10 Biocarriers)	367 (+16.40)	245 (+13.20)	177 (-11.50)	NA
Moisture content (%)	80-85	80-85	80-85	NA
COD removal (%)	72 ± 7	68 ± 6	48.7 ± 6.7	< 20[2]
COD removal (sloughing phase)	60 ± 4	58 ± 3	37 ± 2	
TS (mg/mg EPS)	0.19 ± 0.04 (-8.36)	0.21 ± 0.04 (-6.84)	0.236 ± 0.04 (+22.46)	NA
TP (mg/mg EPS)	0.39 ± 0.07 (-9.95)	0.36 ± 0.09 (3.03)	0.43 ± 0.11 (15.91)	NA
TS/TP	0.49 ± 0.03	0.61 ± 0.07	0.56 ± 0.06	NA
OUR_before_MC-LR (g O_2/g-COD/hr)	0.134	0.155	0.201	NA
OUR_after_MC-LR (g O_2/g-COD/hr)	0.147	0.212	0.364	NA
MC-LR (Supernatant) (µg/L)	ND	1.72	6.52	> 15
MC-LR (Sludge) (µg/L)	3.12	3.15	4.29	NA
pH	6.48 ± 0.32	6.55 ± 0.20	6.56 ± 0.20	6.8-7.0
Dissolved Oxygen (ppm)	3.17 ± 0.29	3.22 ± 0.34	3.50 ± 0.52	5.0-6.0
EPS (ug/mg dry mass)	422 (+4.9)	381 (-16.4)	326 (-13.2)	NA

[2] Values in bracket indicates the change occurred (in %) in the parameter after MC-LR degradation phase
[3] RD only operated during the MC-LR degradation study phase as a negative control

Reactor	RA		RB		RC		Control (RD)[3]	
Parameters								
Nitrate removal during MC-LR degradation phase % (2h and12h)	58	89	46	79	37	81	24	42
Nitrite removal during MC-LR degradation phase % (2h and12h)	51	87	31	83	29	74	16	38
Ammonia removal during MC-LR degradation phase % (2h and12h)	65	97	54	89	63	93	21	35
Nitrate (Three phases of biofilm developemnt)[4]	65.5 ± 21.9; 57.9 ± 12.3; 89.3 ± 0.7		60.1 ± 2.8; 53.8 ± 2.8; 85 ± 2.7		54.7 ± 22.2; 47.6 ± 16.3; 82 ± 2.7		NA	
Nitrite (Three phases of biofilm developemnt)	67.4 ± 11.3; 63 ± 5.5; 83 ± 1.8		63.7 ± 16; 57 ± 9; 77 ± 1.8		56.8 ± 16; 47.5 ± 8.5; 74.9 ± 1.7		NA	
Ammonia (Three phases of biofilm developemnt)	94.5 ± 7,8; 91.3 ± 5; 99.7 ± 0.2		93.7 ± 8.8; 89.7 ± 6.1; 99.4 ± 0.2		89.5 ± 13.4; 85.4 ± 8.6; 98.8 ± 1		NA	

COD: Chemical oxygen demand, OUR: Oxygen utilization rate, EPS: Extracellular polymeric substances

[4] Three phases: biofilm growth phase, sloughing phase, re-maturation phase

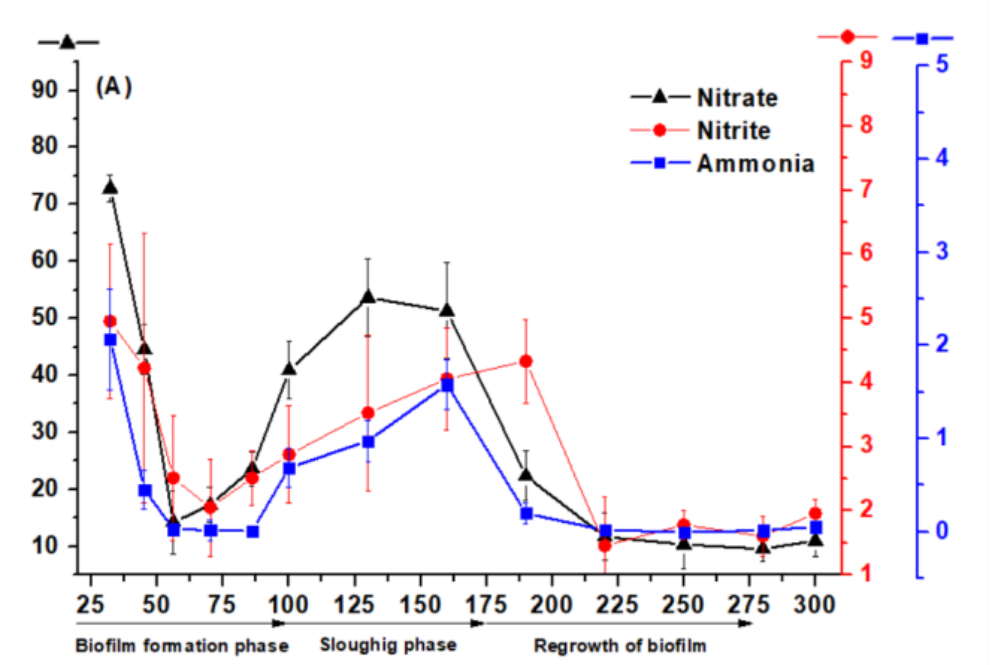
(A)
Nitrate
Nitrite
Ammonia
Biofilm formation phase
Sloughig phase
Regrowth of biofilm
Days

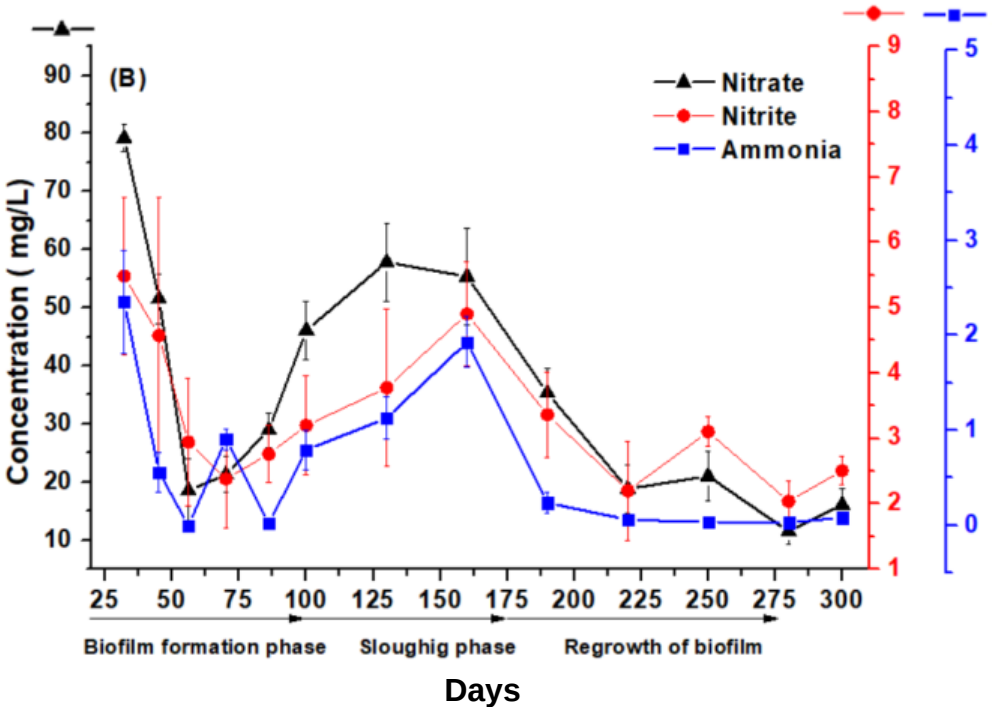
(B)
Concentration (mg/L)
Nitrate
Nitrite
Ammonia
Biofilm formation phase
Sloughig phase
Regrowth of biofilm
Days

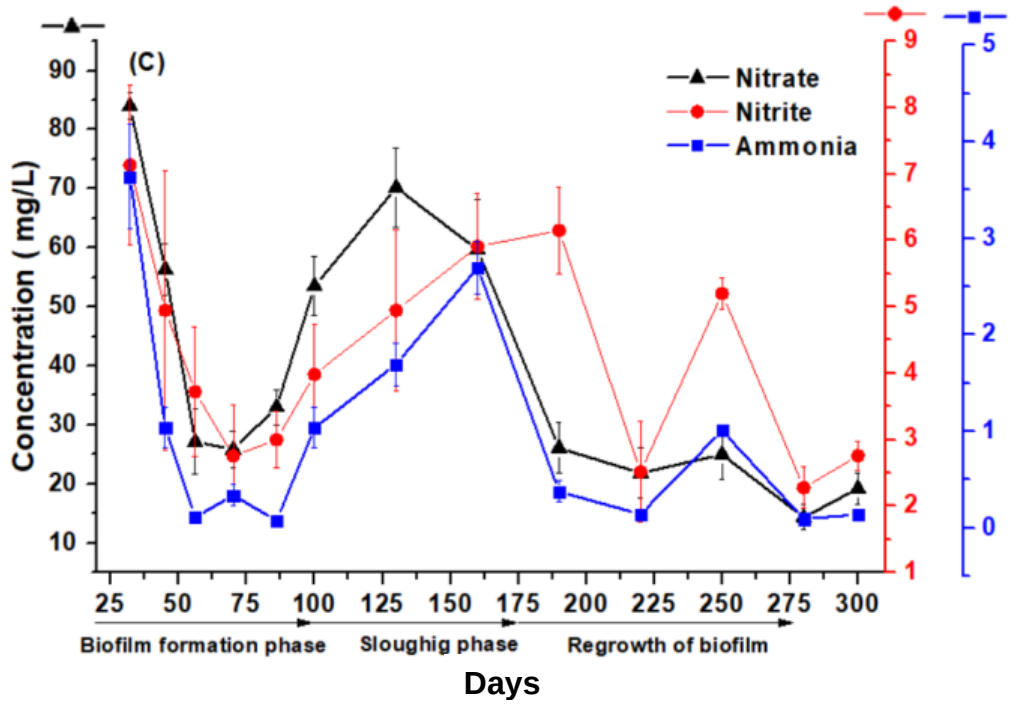

Figure 3.1.3: Nitrate, Nitrite and ammonia concentration profile for A) Fluid bed biofilm reactor (spiked with Arthrobacter ramosus) RA, B) RB (spiked with Bacillus sp.) and C) RC (no microcystin-LR degraders)

Post MC-LR degradation study (i.e., after 230 days), evaluation of FBBRs in terms of nitrate, nitrite and ammonia removal was further continued and stagnant performance in RA was observed (Figure 3.1.3 (A)). However, RB and RC showed relatively higher nitrate, nitrite and ammonia concentration in the reactor post-MC-LR degradation study. This could be due to the disintegration of the biofilm as is evident from the SEM images too (Figure B3 (A), Appendix B). However, the performance went back to normal again after 250 days (Figure 3.1.3 (B), (C)). RA reactor is shown better resilience than RB and RC, not only towards the MC-LR (discussed more in detail in later section) but also remained consistent in the removal of nitrate, nitrite, and ammonia. SEM images after MC-LR degradation too confirmed intact biofilm surface inside the biocarriers for RA (Figure B3 (A), Appendix B) highlighting the importance of an active attached biofilm surface.

Overall, for all three FBBRs, a definite trend was observed for all the mentioned parameters in terms of performance during various phases of the biofilm development: sloughing phase < initial biofilm growth phase < re-maturation phase (Table 3.1.1). Elenter et al. 2007 [27] too found that the sloughing phenomenon was responsible for the decrease in the substrate removal rate. Hence, carbon, ammonia, etc. as a substrate showed comparatively lesser removal efficiency during the sloughing phase (Table 3.1.1). A rise in average performance for reactor RA and RB as compared

to RC after the sloughing phenomenon (and in general) might be due to the enhanced microbial activity of HBCs which is supported by the soluble microbial products released by the ammonia oxidizers (which may be the MC-LR-degraders here) as suggested by Kindaichi et al. 2004 [28].

In brief, the MC-LR in the system (FBBRs) did not hamper the removal efficiency of nitrate, nitrite, and ammonia which also indicates no occurrence of the nutrient imbalance in the system and is resilient in tackling MC-LR up to 50 μg/L (discussed more in detail in later section). Also, the high nitrification rate in all the three FBBRs can be attributed to a consistency in DO level of > 2 ppm, which ensured that the DO diffusion through the biofilm was not the rate-limiting step as also observed by Glen et al. (2018) [29]. It further narrows down the research gap where suspended carrier biofilm process involves the need of higher DO level (> 6 ppm as compared to > 3 ppm in the present study) to maintain the nitrification rate (Sriwiriyarat et al. 2008) [30].

3.3 Biofilm quantification and microscopic observance

Figure 3.1.4 shows the components of the biofilm in terms of total protein (TP), total saccharides (TS) and EPS formed inside the biocarriers. EPS overall acts as a protective diffusive barrier for the bacterial cells inside the biofilm by maintaining their structural as well as the functional integrity. The total length of each individual bar (Figure 3.1.4) represents EPS while its comprising components TS and TP are shown along with other biomass component calculated as EPS - (TS+TP). It can be observed that the EPS production for RA always remained greater than RB and RC (order: RA > RB > RC) which can be related to a better stability and structure of the formed biofilm.

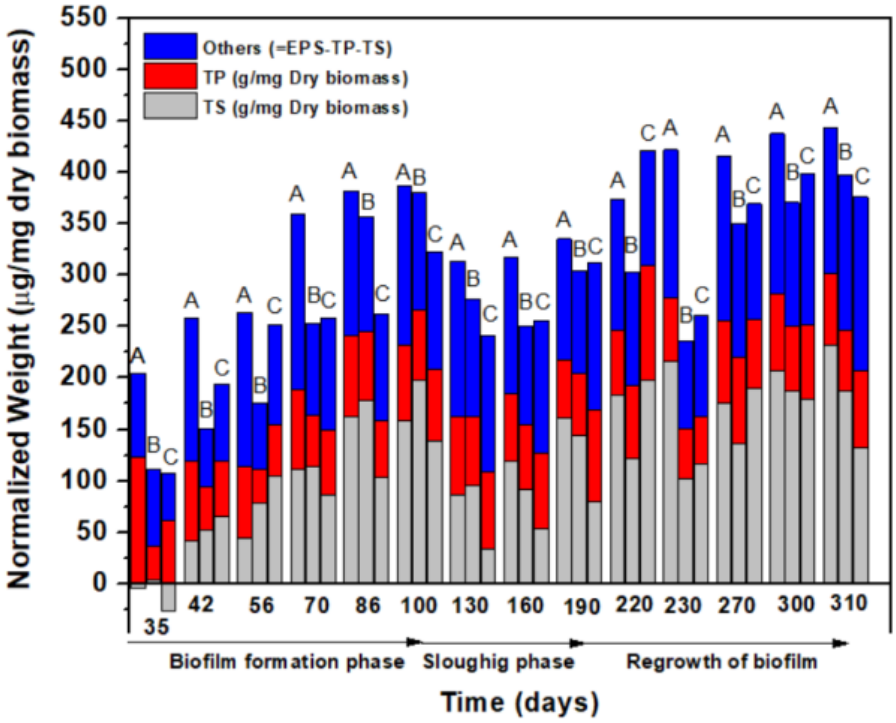

Figure 3.1.4: Total protein (TP), Total saccharides (TS) and Extra Polymerase Substance (EPS=TS+TP) shown for all three reactors viz. A) Bioreactor spiked with Arthrobacter ramosus; B) Bioreactor spiked with Arthrobacter ramosus and C) Bioreactor only with sludge-mixture.

It was observed that the EPS production in RA enhanced by 4.96 % after MC-LR degradation whereas it showed a healthy decrease of 22.3 % and 38 % for RB and RC, respectively (Table 3.1.1; Figure 3.1.4). This can be linked to the dry weight of the biofilm as observed to get enhanced by over 16 % for RA whereas it marked a decrease by over 17 % and 11 % for RB and RC, respectively. It clearly seemed that MC-LR degradation had affected the biofilm integrity in RB and RC, as both dry mass and the EPS weight decreased significantly (Table 3.1.1). SEM images before and after the MC-LR degradation phase can further give visual proof of the same showing stable biofilm structure for RA, as compared to the dismantled biofilm structure for RB and RC (Figure B3 (A), Appendix B).

Also, a stability test was performed after a stable and re-mature biofilm formation period (200th days) to know the nature of the developed re-matured biofilm. Figure B6 (B) show visuals of the biofilm under different pH environment. It can be observed that under the extreme basic/acid environment (pH: 1 & 13), the biofilm loses its texture or coverage completely. However, under pH environment of 6 and 7 and 8 (expected pH of raw water in a DWTPs), the biofilm showed

intact attachment and nice surface coverage for RA and RB when compared to RC. Overall, *A. ramosus* held the biofilm integrity (EPS mainly) intact even after the MC-LR degradation.

Degradation of MC-LR and toxicity assessment

Figure 3.1.5 (A) shows the degradation profile of MC-LR for all the four reactors viz. RA, RB, RC, and RD. It can be observed that the maximum effective (considering both in supernatant and sludge mixture) MC-LR degradation efficiency of 93.75% is achieved by bioreactor RA followed by 90.24 %, 78.37 % and 63.99 % for RB, RC, and RD. After 6 days of degradation study, RA showed the even non-detectable concentration of MC-LR in the supernatant phase as compared to just over 3 µg/L in the sludge mixture. On the contrary, other reactors still had residual MC-LR in the supernatant phase (Figure 3.1.5 (A)). MC-LR content in the sludge-biomass mixture was found to be 3.12 µg/L, 3.15 µg/L and 4.29 µg/L for RA, RB and RC respectively, which is still is above the WHO guideline values (1 µg/L). This indicates that the reactor is safe to bypass the supernatant to the next treatment unit in a DWTP, but its sludge biomass needs further treatment and strict regulatory disposal. It may also be inferred that akin to *Microcystis aeruginosa*, which contains microcystin as long as their cells remain integrated, there can be a possibility that the HBC and MC-degraders in the FBBRs also have the inherited ability (in presence of MC-LR) to store and release toxins after the flocs are stacked-up for long period [31].

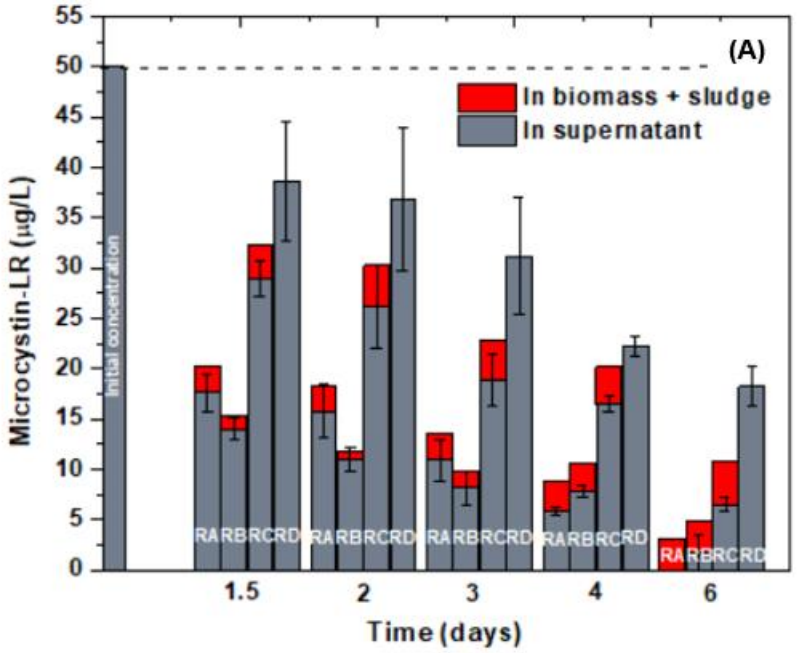

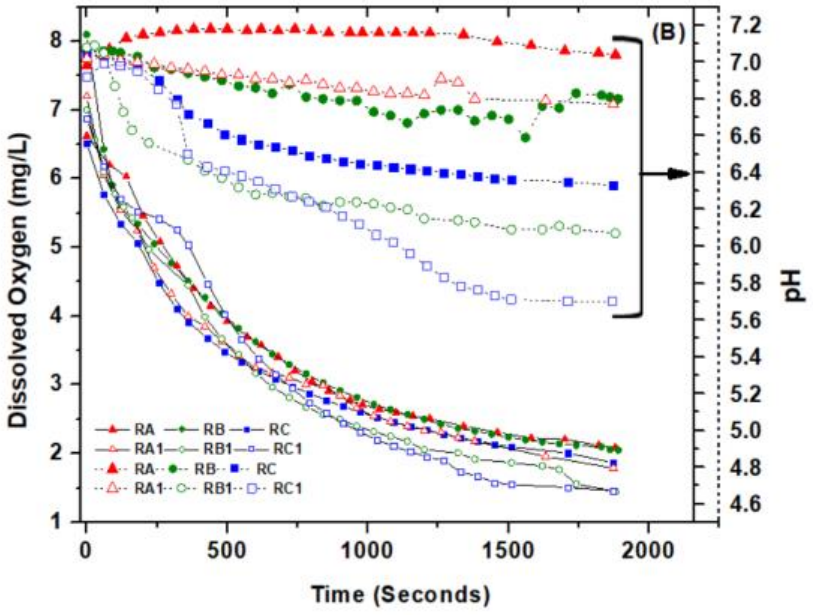

Figure 3.1.5: A) Microcystin-LR (MC-LR) degradation study for all the three bioreactors; concentration of MC-LR in supernatant (grey bar), concentration of MC-LR in sludge (pattern bar) for day 1.5, 2, 3, 4 and 6; B) Kinetics study depicting measurement of pH and Dissolved oxygen

(RA, RB and RC represent experiment before MC-LR test and RA1, RB1 and RC1 represents test after MC-LR degradation test). RA) Fluid bed biofilm reactor (spiked with *Arthrobacter ramosus*); RB (spiked with *Bacillus* sp.) and RC (no microcystin-LR degraders).

Control reactor RD showed a high concentration of undegraded MC-LR (> 18 µg/L) even after 6 days of operation. This shows that the biological activity (particularly the MC-degraders) enhanced the MC-LR removal. MC-LR removal efficiency followed the order: RA (93.7 %) > RB (90.24 %) > RC (78.37 %) which was 30 %, 26 % and 15 % more than RD (< 64 %). A similar study by Xiangyang et al. (2012) [6] showed the use of a fluidized bed reactor which achieved over 87 % of MC-LR degradation in 12 h and nearly complete removal by 73 h. In the present study, around 65 % of MC-LR degradation occurred after 36 h (for RA) and complete degradation in the supernatant phase by 144 h. However, the former study highlighted the treatment of raw water which has been previously pre-treated by two-stage grit chambers whereas the current study did not undergo any pre-treatment. Moreover, the background matrix was more complex in the current study (3 g/L of suspended solids). Thus, high diffusive resistance posed by the sludge media as compared to the raw water could be the reason accounting for relatively slower degradation rate.

The current study (RA) shown comparable degradation rate to other studies (8 μg/L/day) and even better than several studies involving suspended growth bacterial methods (Somdee et al. 2013) [32]. Same bacterial strain as present in RB (*Bacillus sp*.) showed < 50 % of MC-LR degradation at 30 °C in 12 days, in spite of the higher initial concentration of MC-LR (220 μg/L) in the mineral salt medium. In contrast, the present study (average temperature: 20-25 °C), the presence of *Bacillus sp*. enhanced the degradation efficiency of MC-LR in a fluidized biofilm system indicating better degradation behaviour under biofilm system. Though a higher temperature (37 °C) in the former study showed complete MC-LR degradation after 12 days, it may not be practical considering the operation carried in a DWTPs especially during winter time where the temperature is relatively much less.

Toxicity test performed for the degraded broth showed equivalent DMSO concentration of 0.08 %, 0.24 %, 2.32 % and 6.36 % (all values in v/v) for RA, RB, RC and RD respectively (Figure B2, Appendix B). Many researchers have used DMSO as the reference solution to observe the toxic effects on human cells as well as other species. DMSO concentration of 1% v/v, 0.6 % v/v, 0.5 % - 2 % v/v has shown to affect the neuronal cell line of rats, vascular endothelial and platelet cells, and significantly suppressed the expression of many pro-inflammatory cytokines/chemokines respectively. Considering the above scenarios, biodegraded broths for RA was found to be relatively safer than RB and RC.

Understanding MC-LR degradation mechanism through mass spectra analysis

Like any other cyanotoxin, toxicity is mainly governed by a structural fragment or moiety. For example, in cylindrospermopsin, toxicity is characterized by the "Uracil" moiety (Banker et al. 2001) [33]. Similarly, in an MC-LR, toxicity is governed by the "Adda" moiety. The Adda moiety is present in all the MCs variant and is found critical to the MCs activity (Tsuji et al. 2002) [34]. Also, the conjugated diene structure of Adda in MC-LR shows inhibition of the protein phosphatases 1 and 2A where the peptide residues without the Adda moiety is expected to be detoxified. Not only that, but the hydroxylation in Adda side chain also eliminate the overall toxicity (Barford et al. 1994, Wei et al. 2017) [35]. Figure 3.1.6 shows the possible mechanism of the MC-LR degradation interpreted according to the m/z values obtained by analyzing the mass spectra results. All the three samples for RA, RB, and RC were considered for MS result on day 3. Based on different and common peptide fragments characterized by the m/z value (for all three

cases), various possible reaction pathways have been obtained (Figure 3.1.6). Hydroxylation, mainly by oxidative cleavage of Adda side chain and isomerization is involved in the MC-LR breakdown mechanism [36]. The isomerization steps are depicted too apart from the initial hydroxylation breakdown steps to determine the involvement of Adda group that determines the toxicity [37]. Out of three pairs of isomers, isomer I_{11} and I_{12} depicts the next intermediate product after microcystin hydroxylation. Isomer I_{11} is formed due to cleavage of Adda-Arginine (Arg) bond, also eliminating the Benzene-methoxy compound, while I_{12} is formed due to cleavage of the Arg-Masp (*erythro*-β-methylaspartic acid) bond. Isomer I_{11} is basically formed when "microcystinase" enzyme (commonly known as *mlrA*) attacks the Adda-Arg bond which has been proven to have 160-fold less toxicity than the parent MC-LR compound (followed by elimination of Adda moiety) (Ho et al. 2007) [,38]. On the other hand, breakage of Adda-Masp bond in Isomer I_{12} undergoes subsequent degradation with Adda moiety intact (Figure 3.1.6) and hence this degradation pathway could account for relatively more toxicity in RC as compared to RA and RB. Most of the degradation pathway shown in Figure 3.1.6 undergoes further breakdown to m/z = 155 (Y) or 212 (X) with the inclusion of no-adda moiety, further strengthening the possibility of reduced toxicity and effective MC-LR breakdown.

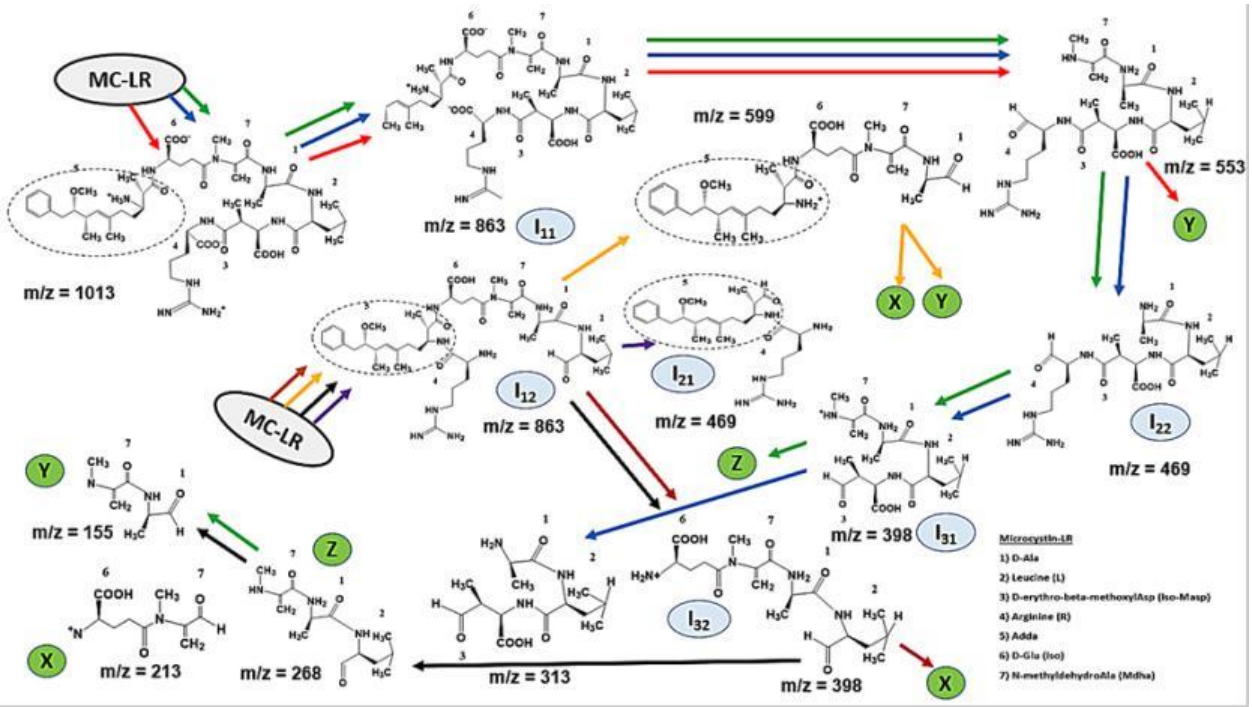

Figure 3.1.6: Possible MC-LR degradation mechanism pathway for RA, RB and RC (common by-product fragments).

RA) Fluid bed biofilm reactor (spiked with *Arthrobacter ramosus*); RB (spiked with *Bacillus* sp.) and RC (no microcystin-LR degraders)

Kinetics behaviour of biocarriers in terms of change in pH, COD and dissolved oxygen

Kinetic analysis before and after the MC-LR degradation experiments was carried out for all the three FBBRs. Figure 3.1.5 (B) shows the change in DO level and pH noted for a period of approximately 30 minutes (initial COD concentration during the start of test =1900 mg/L). After the kinetics test, which lasted for 30 minutes, final COD was determined and noted for all the three reactors. Oxygen required per gram of substrate consumption per unit time (OUR reported: g O_2/g-COD/hr), was calculated to be maximum for RC biocarriers (0.201 g O_2/g-COD/hr) before MC-LR degradation and it increased to 0.364 g O_2/g-COD/hr which was 145% and 72% more than RA and RB biocarriers, respectively (Table 3.1.1). This shows that a significantly larger amount of oxygen is required per unit substrate consumption for RC biocarriers than RA and RB biocarriers.

On the other hand, due to MC-LR degradation, change in OUR for RA and RB was just 9 % and 36 % as compared to 81 % for RC biocarriers (Table 3.1.1). It can possibly be due to the biofilm disintegration (as shown in Figure B6 (A), Appendix B) for RC biocarriers after the MC-LR degradation phase study that might have disrupted the diffusive oxygen transfer mechanism. This may have demanded more oxygen transfer to the bacteria in solution (rather than biofilm) for effective utilization of MC-LR. Also, the pH change (decrease) for RA, RB and RC was in the order: RA (0.12) < RC (0.44) < RC (0.52) before MC-LR degradation and in the order RA (0.22) < RC (0.64) < RB (0.82) post MC-LR degradation (Figure 3.1.5 (B)). This indicated the stability of the formed biofilm inside biocarrier RA that undergoes a small change in pH even under MC-LR degradation environment.

Scale-up of lab-scale FBBR and its application in DWTP

Figure 3.1.7 shows the DO response for the dynamic measurement of OUR and OTR (kLa) during bioreactor operation for RA. Since RA performed better among all the three FBBRs, hence, the scale-up study was done for this reactor. From the graph obtained, the value of $q_{O2}.C_x$ = 0.18 % O_2 s^{-1} (OUR) and kLa was determined by solving the integral equation A1 which came out to be 0.00967 s^{-1} (Appendix B). The value of the saturated oxygen level was determined as 6.99 mg/L

as shown in Figure 3.1.7. It can be observed that as the air is turned "ON", the DO level keeps rising from 1375 second mark till 2200 second mark which ultimately reaches a stagnant level and continues to be the same from there onwards, which depicts the saturation oxygen level. Cooper at al., (1944) [39] proposed equation 6 for the relationship between k_La value and the P_g/V ratio, where Pg is the power consumption and V is the volume of the broth in the bioreactor. However, for the bubble column reactor (FBBR), Rubio et al. (1999) [40] proposed a modified equation (equation 7 as follows (in next page):

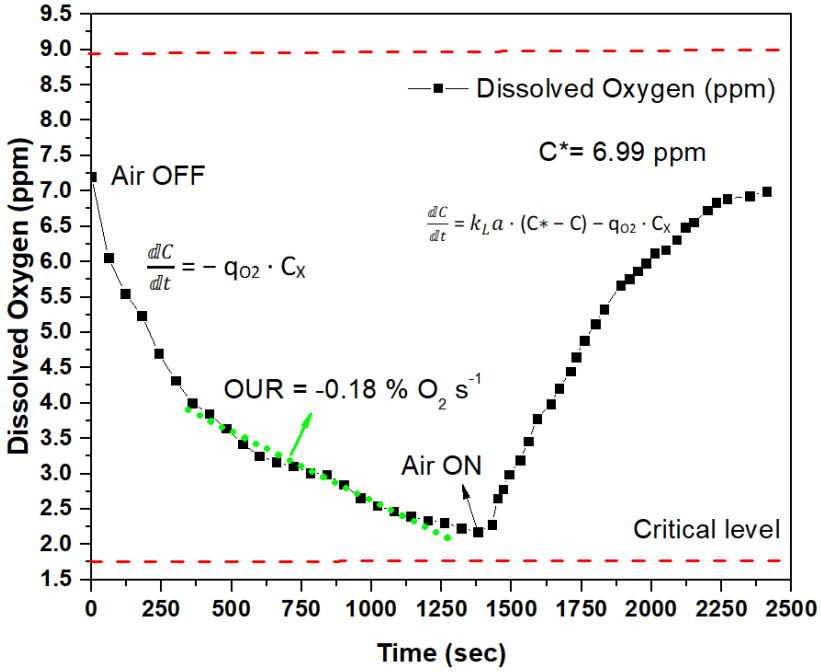

Figure 3.1.7: Simulation of Dissolved Oxygen response for the dynamic measurements of oxygen utilization rate (OUR) and oxygen transfer rate (OTR) in RA

***Arthrobacter ramosus* spiked fluidized bed biofilm reactor (RA)**

$kLa = a(Pg/V)^b (v_s)^c$ Equation 6

$kLa = 2.39 \times 10^{-4} (P_g/V_L)^{0.86}$ Equation 7

Considering same superficial velocity (justification discussed later) and kLa value for the scale-up FBBR, the value of P_g for scale-up FBBR came out to be around 14.8 kW (for V = 200m^3 and Pg/V value of 74 W/m^3 (calculation is shown in Appendix B). All the parameters used for studying the scale-up operation is mentioned in Table B1 (Appendix B). However, it must be noted that

Rubio et al. (1999) [40] derived the simulated model for the gas-liquid (G-L) equilibrium condition where the mass transfer of oxygen is studied between the gas (bubble) and the liquid phase. In contrast, this study has solid media carriers too which makes the mass transfer of oxygen under G-L-Solid equilibrium. It must also be understood that these media carriers break the bubbles into smaller sizes by creating a turbulence region around them which even shown to enhance the oxygen capacity and kLa value by around > 70 % (40-50 % carrier stuffing). Hence, the estimation of kLa here may be underestimated. For detailed discussion, Appendix B can be referred.

Significant points to be considered for the scale-up study

1.) The superficial velocity v_s = 13.75 m/h calculated for the lab-scale FBBR (refer Appendix B). This value was found to be in close agreement with a study done by Kamstra et al. (2017) [41]. They found that the superficial velocity and media fill percentage is an important parameter for the performance of a FBBR. It was shown that for 50 % media fill condition (close to this study: 55 %), the best performance of their reactor (in terms of organic and ammonium removal) is achieved at the similar superficial velocity as found above (~ 13 m/h).

On another note, same superficial velocity $v_s1 = v_s2$, in the scale-up bioreactor is needed too, and can be explained considering two cases as follows:

a) If $v_s2 < v_s1$: Under this condition, the biocarriers will not be effectively fluidized and similar oxidative environment/condition to that of lab-scale FBBR will not be matched. This will change the k_La value apart from the change in the microbial growth characteristics (q_{O2} value of biofilm) inside the biocarriers. Such condition can further deteriorate the performance of the scale-up FBBR which is anticipated to be as close as possible to the lab-scale FBBR.

b) If $v_s2 > v_s1$: Under this condition, the flow speed inside the scale-up FBBR will be too high, which will lead to an increase in the shear stress near the biofilm surface due to a turbulent flow regime inside the biocarrier cavity. This will scrape out the developed biofilm or will lead to delay in the biofilm formation (if $v_s2 > v_s1$ condition is maintained right from the start).

2.) The volume of the scale-up factor was assumed to be 200 m^3 (Hydraulic retention time: HRT = 1 day). This retention time is high considering the DWTPs perspective. However, this study is for the first time delivering the importance and possibility of such reactors for the microcystin removal along with other organics, A more specific biodegradation pathway can become more

effective in future. A more practical assumption of this chosen value also lies in the economy of the operation. It has been calculated that for a minimum of 57 % MC-LR removal and treatment of 200 m^3 raw water/day around $ 35.5 CAD is required per day for the scale-up FBBR operation (small-scale treatment). Based upon the calculated diameter of the scale-up FBBR (based on equal v_s: details in Appendix B) and volume assumed (per day of treatment: 200 m^3), the height of the cylindrical tank was found to be 5 m.

Scale-up FBBR and comparative scenarios in DWTP application

Considering similar kLa and superficial velocity of scale-up FBBR as compared to lab-scale FBBR, they have certain advantages over other pretreatment aspects discussed below:

1.) As an effective pre-treatment unit, scale-up FBBR will not just be able to remove > 57 % MC-LR (HRT = 1 day) but will also ensure > 70 % COD removal. These figures are quite promising, considering challenges that incur from the organic carbon removal in the downstream treatment units. Pre-ozonation, UV-irradiation, UV/H_2O_2 and Fenton-oxidation as a possible pre-treatment steps (which are expensive too) has shown < 20 % - 35 % of COD removal and that too under longer contact time (25 minutes) than usual (Muhammad et al. 2008; Mischopoulou et al. 2016) [42,43].

2.) The scale-up FBBR (considering similar kLa value), can remove 58 %, 51 % and 65 % of nitrate, nitrite, and ammonia, respectively within 2 h of their operation (Table 3.1.1). In the longer run (12 h), more than 80 % of removal for all the three mentioned parameters is achievable. A study by Khuntia et al. (2013) [44] showed < 55 % ammonia removal by ozonation in around 2 h. Fan et al. (2014) [45] studied just 14 % of ammonia removal after ozonation/ultrafiltration step (as a pre-treatment). Thus, scale-up FBBR can initially be very vital to deal with high carbon content (organic as well as inorganic), MC-LR, nitrite, nitrate, and ammonia. However, high HRT is a concern which can be improved by an effective degradation pathway.

3.) Improving bacterial activity and future work on eradicating operational loopholes especially improving the HRT can even lead to the replacement of the pre-ozonation unit in the treatment train. Improving HRT to 6 h can compromise on MC-LR removal (from 57 % to 26 %), but the treatment flow will be maintained more smoothly. These FBBRs can thus be directly linked to the coagulation/flocculation step minimizing subsequent dose for post-chlorination, post-ozonation

due to > 70 % or COD removal and will ensure longer durability of biological sand filter as much organics, MC-LR, ammonia, nitrite, and nitrate is already removed in the proposed preliminary unit in form of FBBR.

4.) Mogadham and Dore (2012) [46] highlighted that the ozonation operation for the treatment of high-volume water (> 30 m^3 per day) is around $ CAD 1.34 whereas according to the fact sheet released by waterrf.org [22] on advanced water treatment, annual cost of operation (for the design flow of around 400 m^3) came out to be > 93,800 USD. Table B1 tabulates pricing for scale-up FBBR where the annual cost of handling 200 m^3 and 400 m^3 came out to be $CAD 12,964 and 25,929 $CAD, respectively, which is < 25 % cost of the ozonation. It is true that ozonation has feed system, contractor, ozone destruction equipment, associated expensive controllers, etc. which makes the overall system costlier. However, they provide faster oxidation of contaminants and organics which cannot be overlooked. But, when it comes to the process economics and treatment objectives simultaneously, FBBR cannot as well be ignored, making it a feasible treatment system.

Conclusion

Fluidized bed biofilm reactor showed potential for the microcystin-LR (MC-LR) removal. Bioreactor spiked with *Arthrobacter ramosus* (RA) *and Bacillus sp.* (RB) as the MC-LR degraders have shown good long-term (over 300 days) biofilm development despite the sloughing event. Bioreactor RA and RB showed higher MC-LR removal (93.75 % and 90.24 %) than the bioreactor with just the sludge-mixture (78.37%: without MC-LR degrading bacteria: RC). The final concentration of MC-LR in supernatant for RA and RB bioreactor was non-detectable and above 1.7 µg/L, respectively. However, MC-LR concentration present in the sludge component for RA bioreactor was above 3 µg/L, which is still above the recommended WHO guidelines. Thus, effective treatment of sludge-mixture is required before its disposal. Nevertheless, biodegradation had a role to play in all the three reactors as the degradation efficiency enhanced by 30 %, 26 % and 15 % for RA, RB, and RC respectively as compared to the reactor without any bacterial activity (RD). Toxicity analysis using bioindicator revealed non-toxic nature of biodegraded broth to human cells in reactor RA. Kinetic study revealed that the oxygen utilization rate/g-COD removal, for RA and RB bioreactor, was around 145% and 72% less than RC (0.364 g O_2/g-COD/hr). Average chemical oxygen demand removal was around 70% for RA and RB reactors, which hold

the potential to simultaneously remove organic carbon apart from the MC-LR. Nitrate and nitrite removal was found to be more than 80 % on an average for RA, RB, and RC whereas ammonia was almost completely removed from the system for all FBBRs. Also, the Scanning Electron Microscopy showed stable and persistent biofilm morphology for RA after MC-LR degradation study. A scale-up study using constant volumetric mass transfer coefficient (kLa) provided a possibility to propose a pre-treatment option (economically feasible) effective in removing MC-LR, organic carbon, nitrate, nitrite, and ammonia.

Conflict of interest: None

Acknowledgment

The authors are sincerely thankful to the Natural Sciences and Engineering Research (Discovery Grant 23451), Genome Québec, Genome Canada) and ATRAPP (Algal blooms, treatment, risk assessment, prediction, and prevention) for financial support. Special thanks to Prof. Sébastien Sauvé for allowing the sample receipt and analysis in his laboratory. Authors would also like to thank the team for constant support and timely suggestions. Also, special thanks to the plant operator Mr. Guy Desgroseilliers, Ville de Quebec for availing the sedimentation-unit sludge from the drinking water treatment plant, Chemin Ste-Foy, Quebec City, Canada. The views or opinions expressed in this article are exclusively those of the authors.

References

[1] Mohamed, Z. A., Deyab, M. A., Abou-Dobara, M. I., El-Sayed, A. K., & El-Raghi, W. M. (2015). Occurrence of cyanobacteria and microcystin toxins in raw and treated waters of the Nile River, Egypt: implication for water treatment and human health. *Environmental Science and Pollution Research, 22*(15), 11716-11727. doi:10.1007/s11356-015-4420-z

[2] Fastner, J., Erhard, M., & von Dohren, H. (2001). Determination of Oligopeptide Diversity within a Natural Population of Microcystis spp. (Cyanobacteria) by Typing Single Colonies by Matrix-Assisted Laser Desorption Ionization-Time of Flight Mass Spectrometry. *Appl Environ Microbiol, 67*(11), 5069-5076. doi:10.1128/aem.67.11.5069-5076.2001

[3] Tak, S.-Y., Kim, M.-K., Lee, J.-E., Lee, Y.-M., & Zoh, K.-D. (2018). Degradation mechanism of anatoxin-a in UV-C/H 2 O 2 reaction. *Chemical Engineering Journal, 334*, 1016-1022. doi:10.1016/j.cej.2017.10.081

[4] Kormas, K. A., & Lymperopoulou, D. S. (2013). Cyanobacterial Toxin Degrading Bacteria: Who Are They? *Biomed Res Int, 2013*, 1-12. doi:10.1155/2013/463894

[5] Ho, L., Dreyfus, J., Boyer, J., Lowe, T., Bustamante, H., Duker, P., Newcombe, G. (2012). Fate of cyanobacteria and their metabolites during water treatment sludge management processes. *Science of The Total Environment, 424*, 232-238. doi:10.1016/j.scitotenv.2012.02.025

[6] Xiangyang, S. (2012). Enhanced treatment of polluted surface water from Yellow river (China) with biooxidation as pretreatment: Pilot scale studies. *Desalination and Water Treatment, 9*(1-3), 59-65. doi:10.5004/dwt.2009.753

[7] Borja, J. Q., Auresenia, J. L., & Gallardo, S. M. (2006). Biodegradation of polychlorinated biphenyls using biofilm grown with biphenyl as carbon source in fluidized bed reactor. *Chemosphere, 64*(4), 555-559. doi:10.1016/j.chemosphere.2005.11.047

[8] Manage, P. M., Edwards, C., Singh, B. K., & Lawton, L. A. (2009). Isolation and Identification of Novel Microcystin-Degrading Bacteria. *Appl Environ Microbiol, 75*(21), 6924-6928. doi:10.1128/aem.01928-09

[9] Hu, L., Zhang, F., Liu, C., & Wang, M. (2012). Biodegradation of Microcystins by Bacillus sp. strain EMB. *Energy Procedia, 16*, 2054-2059. doi:10.1016/j.egypro.2012.01.312

[10] Chusri, S., Sompetch, K., Mukdee, S., Jansrisewangwong, S., Srichai, T., Maneenoon, K.,.. Voravuthikunchai, S. P. (2012). Inhibition of Staphylococcus epidermidis Biofilm Formation by Traditional Thai Herbal Recipes Used for Wound Treatment. *Evidence-Based Complementary and Alternative Medicine, 2012*, 1-8. doi:10.1155/2012/159797

[11] Standard Methods for the Examination of Water and Wastewater, 20th ed; APHA, AWWA, WEF, Washington DC, 1998.

[12] Naghdi, M., Cledon, M., Brar, S. K., & Ramirez, A. A. (2017). Nitrification of vegetable waste using nitrifying bacteria. *Ecological Engineering*. doi:10.1016/j.ecoleng.2017.07.003

[13]Boon C.,Deng,Y.,Wang,L.H.,He,Y.,Xu,J.L.,Fan,Y.,etal.(2008).Anovel DSF-likesignalfrom*Burkholderiacenocepacia* interfereswith *Candidaalbicans* morphologicaltransition. *ISMEJ.* 2,27–36.doi:10.1038/ismej.2007.76

[14] DuBois, M., Gilles, K. A., Hamilton, J. K., Rebers, P. A., & Smith, F. (1956). Colorimetric Method for Determination of Sugars and Related Substances. *Anal Chem, 28*(3), 350-356. doi:10.1021/ac60111a017

[15] Bradford M.M. (1976), A rapid and sensitive method for the quantitation of microgram quantities of protein utilizing the principle of protein-dye binding, Anal. Biochem. 72, 248–254.

[16] Feoktistova, M., Geserick, P., & Leverkus, M. (2016). Crystal Violet Assay for Determining Viability of Cultured Cells. *Cold Spring Harbor Protocols, 2016*(4), pdb.prot087379. doi:10.1101/pdb.prot087379

[17] Traba, C., & Liang, J. F. (2011). Susceptibility of Staphylococcus aureusbiofilms to reactive discharge gases. *Biofouling, 27*(7), 763-772. doi:10.1080/08927014.2011.602188

[18] Kumar, P., Hegde, K., Brar, S. K., Cledon, M., Kermanshahi-pour, A., Roy-Lachapelle, A., & Galvez-Cloutier, R. (2018). Biodegradation of microcystin-LR using acclimatized bacteria isolated from different units of the drinking water treatment plant. *Environmental Pollution, 242*, 407-416. doi:10.1016/j.envpol.2018.07.008

[19] Metcalf, J. S., Bell, S. G., & Codd, G. A. (2001). Colorimetric Immuno-Protein Phosphatase Inhibition Assay for Specific Detection of Microcystins and Nodularins of Cyanobacteria. *Appl Environ Microbiol, 67*(2), 904-909. doi:10.1128/aem.67.2.904-909.2001

[20] Arjunwadkar, S. J., Sarvanan, K., Kulkarni, P. R., & Pandit, A. B. (1998). Gas-liquid mass transfer in dual impeller bioreactor. *Biochemical Engineering Journal, 1*(2), 99-106. doi:10.1016/s1385-8947(97)00083-1

[21] Oosterhuis, N. M. G. and Kossen, N. W. F. (1984) Dissolved oxygen concentration profiles in a productionscale bioreactor. Biotechnol. Bioeng. 26, 546–550

[22] Garcia-Ochoa, F., & Gomez, E. (2009). Bioreactor scale-up and oxygen transfer rate in microbial processes: An overview. *Biotechnology Advances, 27*(2), 153-176. doi:10.1016/j.biotechadv.2008.10.006

[23] Azeredo, J., & Oliveira, R. (2000). The Role of Exopolymers Produced bySphingomonas paucimobilisin Biofilm Formation and Composition. *Biofouling, 16*(1), 17-27. doi:10.1080/08927010009378427

[24] Dziga, D., Zielinska, G., Wladyka, B., Bochenska, O., Maksylewicz, A., Strzalka, W., & Meriluoto, J. (2016). Characterization of Enzymatic Activity of MlrB and MlrC Proteins Involved in Bacterial Degradation of Cyanotoxins Microcystins. *Toxins (Basel), 8*(3), 76. doi:10.3390/toxins8030076

[25] Li, B., Qiu, Y., Zhang, C., Chen, L., & Shi, H. (2016). Understanding biofilm diffusion profiles and microbial activities to optimize integrated fixed-film activated sludge process. *Chemical Engineering Journal, 302*, 269-277. doi:10.1016/j.cej.2016.05.048

[26] Liu, Y., Ngo, H. H., Guo, W., Peng, L., Pan, Y., Guo, J., . . . Ni, B.-J. (2016). Autotrophic nitrogen removal in membrane-aerated biofilms: Archaeal ammonia oxidation versus bacterial ammonia oxidation. *Chemical Engineering Journal, 302*, 535-544. doi:10.1016/j.cej.2016.05.078

[27] Elenter, D., Milferstedt, K., Zhang, W., Hausner, M., & Morgenroth, E. (2007). Influence of detachment on substrate removal and microbial ecology in a heterotrophic/autotrophic biofilm. *Water Research, 41*(20), 4657-4671. doi:10.1016/j.watres.2007.06.050

[28] Kindaichi, T., Ito, T., & Okabe, S. (2004). Ecophysiological Interaction between Nitrifying Bacteria and Heterotrophic Bacteria in Autotrophic Nitrifying Biofilms as Determined by Microautoradiography-Fluorescence In Situ Hybridization. *Appl Environ Microbiol, 70*(3), 1641-1650. doi:10.1128/aem.70.3.1641-1650.2004

[29] Glen, T. D., & Joshua, P. B. (2017). Oxygen Transfer in Moving Bed Biofilm Reactor and Integrated Fixed Film Activated Sludge Processes. *Water Environment Research*. doi:10.2175/106143017x15054988926596

[30] Sriwiriyarat, T., Ungkurarate, W., Fongsatitkul, P., & Chinwetkitvanich, S. (2008). Effects of dissolved oxygen on biological nitrogen removal in integrated fixed film activated sludge (IFAS) wastewater treatment process. *Journal of Environmental Science and Health, Part A, 43*(5), 518-527. doi:10.1080/10934520701796481

[31] Sun, F., Pei, H.-Y., Hu, W.-R., & Ma, C.-X. (2012). The lysis of Microcystis aeruginosa in AlCl3 coagulation and sedimentation processes. *Chemical Engineering Journal, 193-194*, 196-202. doi:10.1016/j.cej.2012.04.043

[32] Somdee, T., Thunders, M., Ruck, J., Lys, I., Allison, M., & Page, R. (2013). Degradation of [Dha7]MC-LR by a Microcystin Degrading Bacterium Isolated from Lake Rotoiti, New Zealand. *ISRN Microbiology, 2013*, 1-8. doi:10.1155/2013/596429

[33] Banker, R., Carmeli, S., Werman, M., Teltsch, B., Porat, R., & Sukenik, A. (2001). Uracil Moiety is Required for Toxicity of the Cyanobacterial Hepatotoxin Cylindrospermopsin. *Journal of Toxicology and Environmental Health, Part A, 62*(4), 281-288. doi:10.1080/009841001459432

[34] Tsuji, K., Naito, S., Kondo, F., Ishikawa, N., Watanabe, M. F., Suzuki, M., & Harada, K.-i. (2002). Stability of microcystins from cyanobacteria: effect of light on decomposition and isomerization. *Environ Sci Technol, 28*(1), 173-177. doi:10.1021/es00050a024

[35] Wei, G., Quan, X., Fan, X., Chen, S., & Zhang, Y. (2017). Carbon-nanotube-based sandwich-like hollow fiber membranes for expanded microcystin-LR removal applications. *Chemical Engineering Journal, 319*, 212-218. doi:10.1016/j.cej.2017.02.125

[36] Chang, J., Chen, Z.-l., Wang, Z., Kang, J., Chen, Q., Yuan, L., & Shen, J.-m. (2015). Oxidation of microcystin-LR in water by ozone combined with UV radiation: The removal and degradation pathway. *Chemical Engineering Journal, 276*, 97-105. doi:10.1016/j.cej.2015.04.070

[37] Park, J.-A., Yang, B., Park, C., Choi, J.-W., van Genuchten, C. M., & Lee, S.-H. (2017). Oxidation of microcystin-LR by the Fenton process: Kinetics, degradation intermediates, water quality and toxicity assessment. *Chemical Engineering Journal, 309*, 339-348. doi:10.1016/j.cej.2016.10.083

[38] Ho, L.; Hoefel, D.; Saint, C.P.; Newcombe, G. Isolation and identi-fication of a novel microcystin-degrading bacterium from a bio-logical sand filter. Water Res. 2007,41(20), 4685-4695

[39] Cooper, C. M., Fernstrom, G. A., & Miller, S. A. (1944). Performance of Agitated Gas-Liquid Contactors. *Industrial & Engineering Chemistry, 36*(6), 504-509. doi:10.1021/ie50414a005

[40] Rubio, F. C., Garcia, J. L., Molina, E., & Chisti, Y. (1999). Steady-state axial profiles of dissolved oxygen in tall bubble column bioreactors. *Chemical Engineering Science, 54*(11), 1711-1723. doi:10.1016/s0009-2509(98)00540-5

[41] Kamstra, A., Blom, E., & Terjesen, B. F. (2017). Mixing and scale affect moving bed biofilm reactor (MBBR) performance. *Aquacultural Engineering, 78*, 9-17. doi:10.1016/j.aquaeng.2017.04.004

[42] Muhammad, A., Shafeeq, A., Butt, M. A., Rizvi, Z. H., Chughtai, M. A., & Rehman, S. (2008). Decolorization and removal of cod and bodfrom raw and biotreated textile dye bath effluent through advanced oxidation processes (AOPS). *Brazilian Journal of Chemical Engineering, 25*(3), 453-459. doi:10.1590/s0104-66322008000300003

[43] Mischopoulou, M., Naidis, P., Kalamaras, S., Kotsopoulos, T. A., & Samaras, P. (2016). Effect of ultrasonic and ozonation pretreatment on methane production potential of raw molasses wastewater. *Renewable Energy, 96*, 1078-1085. doi:10.1016/j.renene.2015.11.060

[44] Khuntia, S., Majumder, S. K., & Ghosh, P. (2013). Removal of Ammonia from Water by Ozone Microbubbles. *Industrial & Engineering Chemistry Research, 52*(1), 318-326. doi:10.1021/ie302212p

[45] Fan, X., Tao, Y., Wang, L., Zhang, X., Lei, Y., Wang, Z., & Noguchi, H. (2014). Performance of an integrated process combining ozonation with ceramic membrane ultra-filtration for advanced treatment of drinking water. *Desalination, 335*(1), 47-54. doi:10.1016/j.desal.2013.12.014

[46] Mogadham A.K., Dore M. (2012), "Cost and efficacy of water disinfection practices: Evidence from Canada", Review of Economic Analysis 4, 209-223

[47] Waterrf.org "Advance Treatment" (Factsheet),http://www.waterrf.org/knowledge/advanced-treatment/FactSheets/advanced-treatment_ozone_factSheet.pdf (Date Accessed: 1st June, 2018)

BRIDGE-3

BRIDGE: Hence, from the previous study on dynamic bed biofilter, it was evident that MC-LR removal rate was slow and cannot be practiced efficiently in a DWTP. Hence, the co-culture aspect (as discussed in the link from the previous chapter) was studied using the **static bed filter** or biosand filter. The empty bed contact time of each filter used in the next study was in between 15 minutes to maximum of 1.5 hours.

PART 2

Co-culturing of native bacteria from Drinking Water Treatment Plant with known degraders to accelerate Microcystin-LR removal using biofilter

Pratik Kumar [a], Krishnamoorthy Hegde [a], Satinder Kaur Brar [a,b*], Maximiliano Cledon[c], Azadeh Kermanshahi-pour[d], Audrey Roy-Lachapelle[e,f], Sébastien Sauvé[e], Rosa Galvez-Cloutier[g]

[a] - INRS-ETE, Université du Québec, 490, Rue de la Couronne, Québec, Canada G1K 9A9

[b-] Department of Civil Engineering, Lassonde School of Engineering, York University, North York, Toronto M3J 1P3, Ontario, Canada

[c] - CIMAS (CONICET, UnComa, Rio Negro), Güemes 1030, San Antonio Oeste, Rio Negro, Argentina

[d] – Biorefining and Remediation Laboratory, Department of Process Engineering and Applied Science, Dalhousie University, 1360 Barrington Street, Halifax, Nova Scotia B3J 1Z1, Canada

[e]- Department of Chemistry, Université de Montréal, Montréal, QC, Canada

f- Environment and Climate Change Canada, 105 rue McGill, H2Y 2E7, Montréal, QC, Canada

g- Faculté des Sciences et Génie, Département de génie civil et génie des Eaux, Université Laval, Québec (Québec), Canada.

[*]- Corresponding author, E-mail: satinder.brar@ete.inrs.ca; Satinder.Brar@lassonde.yorku.ca (S.K. Brar)

***Chemical Engineering Journal*, 383 (2020), DOI:10.1016/j.cej.2019.123090**

Résumé

La biorestauration du biofilm par médiation de la source d'eau potable pour la dégradation de la microcystine-LR a été étudiée à l'aide d'un filtre à sable avec des genres bactériens dégradeurs de MC-LR connus: *Arthrobacter* (A), *Bacillus* (B) et *Sphingomonas* (S), individuelle (A, B et S) ainsi que les conditions de co-culture (A + X, B + X et S + X) avec dans des souches bactériennes natives (*Pseudomonas fragi* et *Chryseobacterium* sp. = X). Ces souches bactériennes natives ont été isolées de l'unité de filtration d'une usine de traitement d'eau potable (DWTP). Avant de commencer l'opération de filtration, la capacité de formation de biofilm des dégradeurs MC-LR a été évaluée à l'aide d'une configuration expérimentale unique. L'étude a montré que l'élimination du MC-LR était améliorée de 38% en utilisant un filtre S + X par rapport au filtre non inoculé (contrôle). À l'exception de *Bacillus* sp., les dégradeurs de MC sousforme d*'Arthrobacter ramosus* et *Sphingomonas* sp. ont augmenté le potentiel d'élimination de MC des souches bactériennes natives (X) de 10% et 17%, respectivement. Un plan central composite a été utilisé pour obtenir des valeurs optimisées des paramètres d'entrée (pH, température, turbidité initiale et temps de rétention) pour le fonctionnement du filtre. Divers paramètres de sortie, dont le carbone organique dissous (COD), les coliformes totaux, la turbidité, l'oxygène dissous, la toxicité MC-LR et l'ammoniac ont été analysés pour former un modèle bien généralisé avec un indice de désirabilité de 0,638. Dans l'ensemble, le filtre S + X a atteint une concentration de MC non détectable dans certains cycles et a montré une moyenne de > 30% de COD et > 80% de l'élimination totale des coliformes ainsi qu'une élimination sous-réglementée des nitrites, des nitrates et de l'ammoniac. Cependant, le développement du MC-LR s'est produit après 8 semaines de fonctionnement du filtre. Ces études ont démontré l'efficacité de l'inoculation de dégradeurs de MC dans une unité de filtration existante d'un STEP pour éliminer la présence saisonnière de MC dans la source d'eau.

Mots-clés: Biofiltre, co-culture, microcystine, qualité de l'eau, eau potable, filtre à sable

Abstract

The biofilm-mediated bioremediation of drinking water source for Microcystin-LR degradation was investigated using sand filter with known MC-LR-degrading bacterial genera: *Arthrobacter* (A), *Bacillus* (B) and *Sphingomonas* (S), both under individual (A, B and S) as well as co-culture condition (A+X, B+X and S+X) with the native bacterial strains (*Pseudomonas fragi* and *Chryseobacterium* sp. = X). These native bacterial strains were isolated from the filtration unit of a drinking water treatment plant (DWTP). Before starting the filter operation, the biofilm-forming ability of MC-LR-degraders was evaluated using a unique experimental set-up. The study showed that the MC-LR removal was enhanced by 38% using S+X filter as compared to the uninoculated filter (control). Except for *Bacillus* sp., MC-degraders in the form of *Arthrobacter ramosus* and *Sphingomonas* sp. enhanced the MC removal potential of the native bacterial strains (X) by 10% and 17%, respectively. The central composite design was used to obtain an optimized input parameter (pH, temperature, initial turbidity and retention time) for the filter operation. Various output parameters including dissolved organic carbon (DOC), total coliform, turbidity, dissolved oxygen, MC-LR toxicity and ammonia were analyzed to form a well-generalized model with a desirability index of 0.638. Overall, filter S+X achieved a non-detectable MCs concentration in some cycles and showed an average of > 30% DOC and > 80% of total coliform removal along with an under-regulated removal of nitrite, nitrate and ammonia. However, MC-LR breakthrough occurred after 8 weeks of filter operation. These studies demonstrated the effectiveness of inoculating MC-degraders in an existing filtration unit of a DWTP to remove the seasonal occurrence of MCs in the water source.

Keywords: Biofilter, co-culture, Microcystin, water quality, drinking water, sand filter

Introduction

Cyanotoxins are the secondary metabolites which are produced by cyanobacteria. Microcystin-LR is a cyanotoxin which is prominent in most cyanobloom-affected water bodies. Microcystins (MCs) are stable in the water bodies and sunlight alone is insufficient in their degradation as it also needs photosensitizers. Even the rate of photosensitized degradation was found to be rather low ($0.34 \times 10\text{-}3$ (kJ m^{-2})$^{-1}$) where *in-situ* half-life for MC-LR was estimated to be around 90-120 days per meter depth of the water column [1]. WHO has set a preliminary guideline for MC-LR in drinking water as 1 μg/L [2].

Most of the Drinking Water Treatment Plants (DWTPs) procuring raw water from such sources, take little to no preventive measures to remove MC-LR. Microcystins are stable and recalcitrant during the conventional water treatment processes [3]. For example, during ozone treatment, the presence of natural organic matter (NOMs) reduces the dosed-ozone concentration (as ozone also degrades NOMs) and hence reduces the MCs removal efficiency [4]. In addition, conventional coagulation/flocculation treatment is partially effective as the long-term flocs stacking releases microcystin from *Microcystis aeruginosa* [5], and pre-chlorination creates a redistribution problem of toxins in free water solution [6]. On the other hand, the post-chlorination process demands a high chlorine dose to cope up with the presence of high microcystin level in the filtered water [7,8]. Moreover, such chemical treatment processes may cause the formation of toxic or harmful metabolites, e.g.: disinfection by-products from chlorination [9,10], whereas physical bioadsorption treatment, such as bio-sand filtration, not only promises effective removal of microcystin but also reduces the number of toxic by-products [11,12].

Few studies have shown an effective removal of MCs through biosand filter while some studies have reported less efficiency and slow degradation rate [13,14,15]. Biofilters are becoming a more acceptable form of water treatment both under commercial scale (DWTPs) as well as for the smaller communities. They involve no electricity, requires less maintenance and no additional chemicals which otherwise could promote the production of toxic metabolites. Many bacterial strains isolated from water sources where the previous history of cyanotoxin presence was observed, showed successful MCs removal. Such bacteria were inoculated in a sand filter column to successfully study the MCs degradation [16,17]. Biological degradation of MC-LR using *in-situ* cultured bacteria has also been found to proceed with non-toxic by-products formation [18-

20]. However, to the best of the authors knowledge, exploration of these known or unknown microcystin-degraders, co-cultured with the native bacterial strains isolated from a DWTP-sand filter has not been studied so far. Such co-culturing technique is hypothesized to further enhance the MC-LR removal.

In the present study, three different MC-LR-degraders of genera[5]: *Arthrobacter* (A), *Bacillus* (B) and *Sphingomonas* (S) are individually co-cultured (A+X, B+X and S+X) and inoculated with the combination of native bacterial strains (X) to check for the MC-LR degradation using biosand filter. These MC-LR-degraders are also evaluated individually (A, B and S) to depict the MC-LR removal and the results are compared with the uninoculated filter (C) and their co-cultured counterparts (A+X, B+X, and S+X). Following three hypotheses form the backbone of this research work:

1) The native bacterial strains (X) could be potent enough to carry out an effective MC-LR degradation.

2) The native bacterial strains need more assistance in the form of MC-LR degraders to carry out MC-LR removal.

3) The MC-LR-degraders can co-exist with the native bacterial population to enhance the degradation of MC-LR.

The most dominant native strains isolated from the collected biofilm sample of the sand filtration unit in DWTP, are identified as *Chryseobacterium* sp. and *Pseudomonas fragi* using NCBI BLAST service in our previous study [21]. They were identified using 16S rDNA and deposited in NCBI GenBank with Acc No. MH150821 and MH150822, respectively. From our previous study, they have also been identified as a good MC-LR degrader (overall 97% and individually > 80% MC-LR degradation within ten days of incubation). Hence, throughout this study, filter X represents a "modified" model filter[6] for DWTP filtration unit (Chemin Ste-Foy, Quebec City, Canada). This study also evaluates the performance of sand filtration in terms of various water quality parameters

[5] Not all the species of the same genera are Microcystin-degraders
[6] Sand media is grinded (as obtained from DWTP, hence the word modified), and the dominant microbial community was opted

such as: turbidity, coliform, nitrate, nitrite, ammonia, total organic carbon, dissolved oxygen (DO), pH, conductivity and MC-LR toxicity assay.

Material and methods

Chemicals and microorganisms

Microcystin-LR was purchased from Cayman Chemicals (Ann Arbor, Michigan, MI, USA). 3-(4, 5-dimethylthiazol-2-yl)-2,5-diphenyltetrazolium bromide (MTT) was purchased from Sigma Aldrich, (Ontario, Canada) for the MTT assay.

Arthrobacter ramosus (NRRL B-3159), *Bacillus* sp. (NRRL B-14393), *Sphingomonas* sp. (NRRL B-59555), *Rhizobium meliloti* and *Staphylococcus epidermidis* were purchased from the NRRL Agricultural Research Service (ARS) culture collection. The last two strains were used as the bioindicator to measure the toxicity of the filtered effluent and as a positive control representing the biofilm forming strain, respectively. All the analytical reagents used in preparing nutrient and culture media were brought from Fisher Scientific, (Ontario, Canada).

Screening of the bacterial strains

Screening of the bacterial strains (three of them: A, B, and S) was performed to investigate their ability in forming biofilm over the sand media. Figure 3.2.1 shows the schematic representation of the unique set-up prepared for this objective (laboratory set-up shown in Figure C1, Appendix C). A model reactor of plastic material consisting of 10-gram sand media was placed in replica for each inoculum source (Figure 3.2.1 and Figure C1). After every 4-h, 20 mL (charge volume[7] greater than the pore space) of inoculum (6×10^7 cells/mL) was passed through the model reactors pre-set by the automatic dosage pump. The nutrient water of high chemical oxygen demand (800 mg/L) served as the matrix for the inoculum (to assist fast and active biofilm formation[8]). The operation was continued in a recirculation mode for 19 days to reach a conclusive evidence of mature biofilm formation. The assay results were compared with the negative control (without

[7] Charge volume is defined as the volume of inoculum passage in the model filter compared to its bulk capacity
[8] For the first five days COD: 800 mg/L was maintained, thereafter the COD was gradually decreased to 190 mg/L by the end of 12 days (quite close to Lake water COD). Hence nutrients were replenished each time COD was changed (2 days interval).

inoculated cells) and positive control (*Staphylococcus epidermidis*: known to be a good biofilm former) [22].

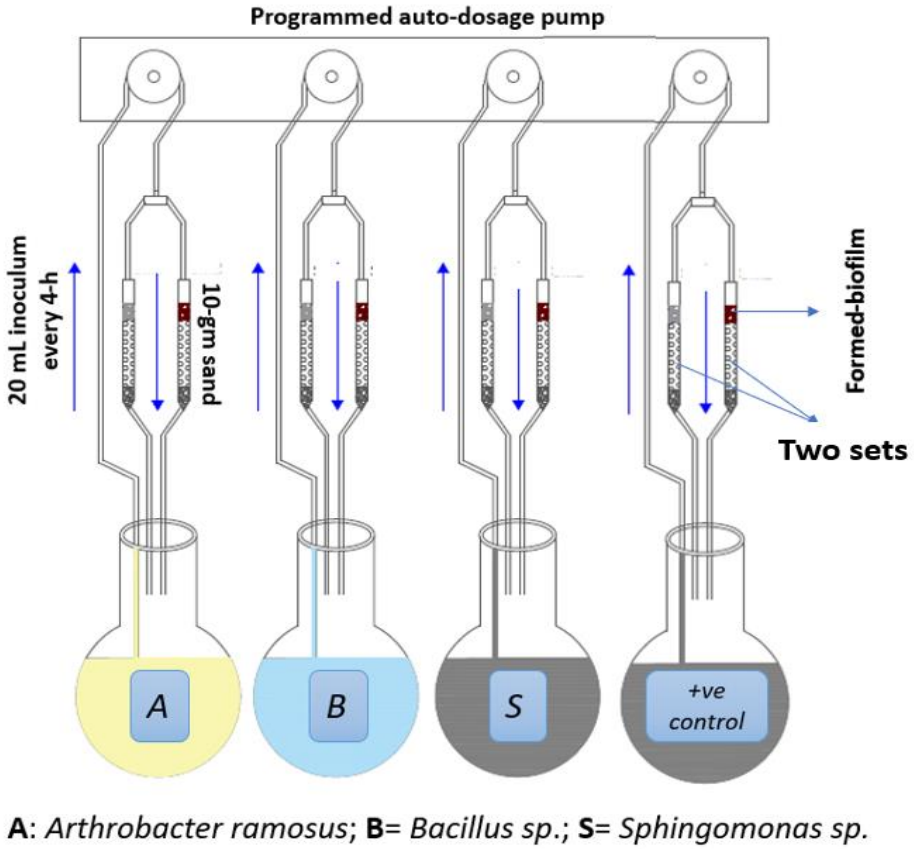

Figure 3.2.3: Arrangement/set-up to study the screening of the biofilm-forming bacteria

After every 3, 7, 11, 16 and 19 days[9], a little portion of sand media (around 0.3 g) was taken from the top layer and was suspended in 1.5 mL of tap water[10] and vortexed (to draw out the attached bacterial cells and biomass into the solution). Post-vortex, the liquid portion was drawn in a 200 µL volume to seed the wells of a 96-well plate (6 wells per sample). Biomass in three wells was stained using 100 µL of 0.1% (w/v) crystal violet (CV) and 100 µL of MTT solution (7 mg/10 mL) was injected into the leftover three wells. Similarly, the process was carried out for the samples of other strains. Afterwards, the plate was incubated overnight at 35 ± 2°C for crystal violet (CV)

[9] First set of model filter was used exclusively for day 3 and day 7 sample, while 2nd set for day 11, day 16 and day 19 sample in order to avoid underestimation of biofilm quantification each time sample is being taken out.
[10] Tap water was chosen instead of milli-Q or distilled water to allow bioactivity of cells to be intact or otherwise bacterial cells can die due to shock (no conductivity in milli-Q water)

assay and 4 h at 35 ± 2°C for MTT assay. For CV assay, the wells were carefully washed with phosphate buffer solution (pH 7.4) to remove any loosely attached biomass followed by the addition of 300 µL dimethyl sulfoxide (DMSO) solution to solubilize the stained biomass. While for MTT assay, the formed precipitate (formazan: blue colour) after drying was dissolved using 300 µL of DMSO solution. Spectrophotometric reading[11] was taken at 550 nm and 590 nm for MTT and CV assay, respectively, to quantify the cell viability (MTT assay) and cell biomass (CV assay). This experiment provided more information to assess the ability of the bacterial strain to form biofilm and not directly the biofilm formed on the sand grain. A pictorial representation of the sampling chronology is presented in appendix C (Figure C2).

Optimization of input parameters using central composite design

Before the onset of filter operation, optimization experiment was performed to understand the strength and best initial working conditions of sand filter media (for the physical parameters) comprising initial turbidity, pH, critical standby period (retention time) of filter run and temperature. Three/four levels of inputs were designed for each parameter: pH of 6, 7, and 8; initial turbidity of 10 NTU, 20 NTU and 30 NTU; temperature of 10 °C, 20 °C and 30 °C, while critical standby period (CSTI[12]) of 1h, 2h, 3h and 4h. The lake water (Lake Sainte-Anne (47.262879N, -71.665158W) was used as a solution matrix with suitable adjustments of turbidity (mimicking with turbid-hydrated clay suspension kept overnight), pH (hydrochloric acid/sodium hydroxide base) and temperature (heating[13]). Table 3.2.1 lists the details and necessary information derived from the optimization experiment. Based on the limited number of the glass columns available, the whole optimization experiment was divided into two parts: a) 3-level of temperature and 3-level of pH (9 combinations); b) 3-level initial turbidity and 4-level critical time charge period (12 combinations). Hence, a total of 21 combinations of initial parameters were designed.

To optimize these initial conditions, the output parameters (analyzed for filtered samples) in the form of total coliform removal, turbidity removal, MC-LR assay (toxicity determination), dissolved oxygen-carbon removal (DOC), flow rate, change in pH, dissolved oxygen, electrical

[11] For MTT assay: maximum absorbance was reported as 550.5 nm and for CV assay, it was 590.9 nm (as determined from the spectrum run)
[12] CSTI: It is defined as the minimum time period for which a filter should be run for a consecutive (or successive) operation without much affecting the output variables tested (to get more desirable filter operation).
[13] For obtaining water at temperature 10°C, 20°C and 30°C, the lake water stored in the cooling chamber was heated over the hot plate.

conductivity were determined. The weighted importance for each output parameter was set according to the preference of the experimental objective. For instance, MC-LR assay, total coliform removal, DOC removal, and turbidity removal were set at high priority weights of 5, 5, 4 and 4, respectively (other parameters set to 2 or 3 based on importance). With the help of central composite design (Design-Expert 7.0) and weighted importance of all the output parameters, a definite and critical solution (in coded value), i.e., the optimized value of initial turbidity, temperature, pH and filter standby period was determined.

Sand column experiment and filter maintenance

After the screening test and the optimization experiment, the glass columns were installed in a top-down flow arrangement as shown in Figure 3.2.2. Sand media was obtained from the filtration unit of the drinking water treatment plant (Chemin Ste-Foy, Quebec City, Canada). A total of eight glass columns (diameter: 25 mm, thickness 2mm, height: 650 mm) were installed, packed with the ground sand particles of effective diameter: D_{10} = 180 μm and coefficient of uniformity: C_u = 2.32 for about 490 mm height. About 40 mm of drainage was provided using sand particle size in the range: 2 -4 mm. Rest 120 mm was used as the headspace for allowing the influent water. Grain size-distribution analysis and related calculations for the sand particles are detailed in the appendix file (Figure C3, Appendix C).

Table 3.2.2 shows details of the strains used in the column filters and characteristics of the source water used as an influent to the filters. A good filter should be capable of handling other water quality parameters as well apart from MCs. The purpose of each filter was defined to evaluate the potential of individual MC-LR-degraders and when they are co-cultured with the native bacterial strains (X) present in the filtration unit of the DWTP, in removing MC-LR and other water quality parameters (WQPs). One column filter was used as the negative control (without any bacterial strain, control filter (C) to differentiate for the MC-LR removal due to adsorption and biodegradation (Table 3.2.2). Knowing the importance of the control filter[14], a replica column was installed too in parallel where the results were verified with each other in order to remove any ambiguous experimental error (over/under estimation of results). Also, one filter inoculated with the native bacterial strains isolated from the DWTP filtration unit (filter X), was simulated to

[14] To discriminate the removal of MC-LR by adsorption from biodegradation.

represent a DWTP sand filter. The result obtained from this filter (X) further allowed to evaluate for the difference in MC-LR degradation and other WQPs when X was co-cultured with MC-LR-degraders (A+X, B+X and S+X).

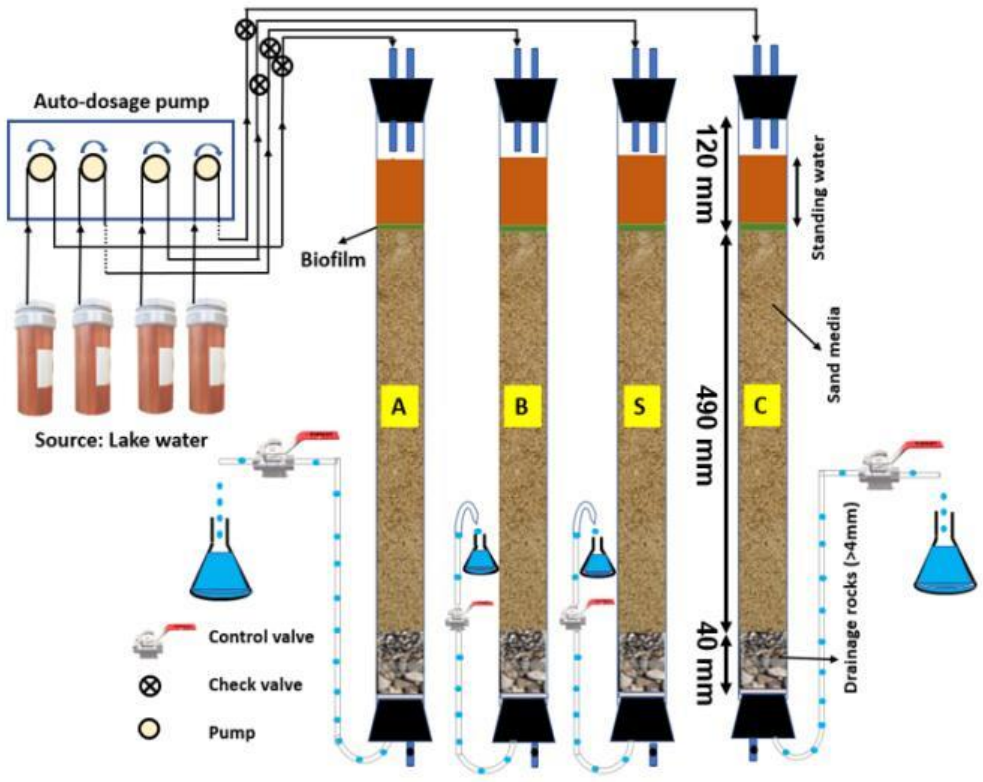

Figure 3.2.4: Detailed schematic representation of laboratory column-setup

Before the filter operation, the plug-flow condition was ensured (no air bubble and initial head loss) by determining the Morrill dispersion index (all filter showed MDI of near 2.5[15]). Each filter was separately inoculated with the respective strains for a continuous period of 2 weeks (Table 3.2.2). The inoculum was prepared in the nutrient water of 800 mg/L-COD (recipe details provided in the chapter 2 part 1), to allow for a quick establishment of the biofilm over the sand media (as done for screening test). About 50 mL of inoculum was passed every 4-h (recirculation mode) allowing substantial contact time between the bacteria and the sand media to form quick microcolonies. The inoculum was replenished with nutrients every two days, each time reducing

[15] MDI= Morrill Dispersion Index (MDI=1 for ideal plug flow condition, MDI= 23 for the completely stirred reactor)

COD by 100 mg/L to obtain 190 mg/L[16] by day 12. As compared to the model reactor that was used for the screening purpose, the inoculation during the filter column operation was performed with 10 times more concentration of biocells, i.e., 6 x 10^8 cells/mL (because 10 times more sand media was used).

The biofilm formed over the sand media was periodically quantified by analyzing parameters, such as the flow rate, DOC removal, protein concentration and cell viability. After the successful biofilm formation, all eight filters were run continuously for 8 cycles with each cycle comprising 7 days using lake water. The flow rate was measured by maintaining a constant head of 5 cm of standing water each time the measurement was recorded. Protein concentration was determined by a method similar to the CV assay, except that the sand sample was vortexed in the cell-lysis buffer to extract complete protein. The sample was centrifuged at 10000 *x* g for 2 min and the supernatant was measured for the protein concentration by Bradford assay [23]. Cell viability was measured through MTT assay as mentioned in previous section.

No previous history of microcystin or cyanobacterial bloom was reported for the lake water (result details of various microcystin and other cyanotoxin analysis are provided in the Appendix C: Table C1). Table 3.2.2 lists the environmental parameters of the lake water. Based on the empty bed contact time (EBCT), all the filters were run continuously during the day and evening time (9 AM to 10 PM). During the night hours (11 PM to 8 AM), influent uptake was auto-programmed such that during any time, the gap between two influent charges did not exceed the critical filter charge period or CSTI (2.16h ~ 135 min) as obtained from the optimization experiment.

The backwash operation was performed once, after the end of the 4th cycle, at 10% bed expansion for 5 min. This was conducted to simulate the DWTP filters that are routinely backwashed to remove any algal growth and air-bubbles (can increase the head loss thereby affecting the removal of contaminants). All pipelines and connectors were washed every 2 cycles to remove any deposited particles/biofilm.

[16] To get closer to lake water COD, otherwise bacteria can get shock during filter operation once biofilm gets formed.

Water quality parameter analysis

Coliform removal, Turbidity removal, DOC removal, nitrate, nitrite, and ammonia

Total coliforms in the effluent or filtered water were determined using the membrane filtration technique every 3 days (twice/cycle) according to the Standard Methods (APHA, 1998) [24]. The number of coliforms present in the effluent of each filter was reported as CFU/100 mL and compared with the total coliform present in the influent water (lake water). The average CFU/100 mL observed for the source water (averaging 9 samples) was 2401 ± 312 CFU/100 mL. The percentage removal of total coliform was calculated by Equation 8 as follows:

$$\frac{((2401 \pm 312 \text{ CFU/100 mL} - \text{Total coliform in filtered water sample/ 100 mL})}{(2401 \pm 312 \text{ CFU/100 mL})} \times 100 \quad \text{Equation 8}$$

The turbidity of the filtered water was determined every day using HACH instrument 2100 model. To mimic the optimized initial turbid condition (13 NTU from optimization study), the lake water was appropriately mixed using turbid concentration of hydrated clay solution as described by Asrafuzzaman et al. (2011) [25]. It must be noted that the initial turbidity of the lake water was lower (6 NTU) than the optimized turbidity value (13 NTU) and hence the above activity was performed. The average turbidity of the filtered effluent for each cycle was reported in NTU and the removal was calculated by Equation 9:

$$((13 \pm 2.2 \text{ NTU} - \text{turbidity of filtered water sample (NTU)})/(13 \pm 2.2 \text{ NTU}) \times 100 \quad \text{Equation 93}$$

Around 30 mL of the sample before and after filtration was filtered using 0.45 µm glass-fiber filter. DOC of the resultant solution was determined using a Shimadzu 5000A analyzer (Shimadzu, Japan). DOC was estimated twice a cycle and was reported in mg/L. Based on the DOC value and the UV 254 value (UVA), specific UV absorbance value termed as SUVA was reported (UVA 254/DOC) to give an indirect estimation of the NOMs removal.

Nitrate, nitrite, and ammonia were determined in the effluent sample as described by Naghdi et al. (2017) [26]. An influent lake water solution was prepared to contain 100 mg/L of nitrate, 10 mg/L of nitrite and 2 mg/L of ammonia-N at the end of each cycle[17], where the filtered sample was

[17] Stock solution of sodium nitrate, sodium nitrite and ammonium sulphate were prepared based on the stoichiometric equation for nitrate, nitrite and ammonia-N, respectively.

determined for nitrate, nitrite, and ammonia-N. Prior to the solution preparation for the required initial concentration, nitrate, nitrite and ammonia were determined in the lake water.

pH, dissolved oxygen, conductivity

The pH was measured every two days (three times a cycle) and the average value of each cycle was reported for each filter. Also, dissolved oxygen was reported every two days (thrice a cycle) using a portable F4-Standard probe (Mettler Toledo Inc) to check the water quality (no anoxic condition build-up). The electrical conductivity of the filtered effluent was measured every two days using Mettler Toledo™ S230 SevenCompact™ Conductivity Meter.

Flow rate, toxicity assay and MC-LR analysis

The flow rate of each filter was reported in m/h (or $m^3/m^2/h$) after the end of each cycle. Backwashing was done after the end of the 4^{th} cycle when the flow rate reduced to at least 35% as compared to the 1^{st} cycle. Head of the standing water during flow rate measurement was kept constant at around 115 mm.

MC-LR toxicity assay was performed on the filtered sample. A similar protocol was followed as described in Kumar et al. (2018) [21] to report on the relative toxicity of the MC-LR-spiked treated filtered samples in terms of equivalent dimethyl sulfoxide (eq. DMSO). In brief, the relationship between viability of the bioindicator cells (*Rhizobium meliloti*) and various % DMSO (v/v) solution was established. The viability was measured in terms of spectrophotometric absorbance using MTT assay. Similarly, the relationship was established for MC-LR (92- 1500 μg/L). To report the equivalent % DMSO (v/v) for the MC-LR concentration, the absorbance value of both the relationship curve was linked with each other and sample toxicity assay was reported in % equivalent DMSO. The equivalent % DMSO can be defined as the similar mortality effect on the bioindicator cells as a MC-LR solution of specific concentration will have on it. However, it must be noted that the margin of spectrophotometric absorbance values was very close to the tested MC-LR concentration range and thus the results need further validation using ELISA assay [27].

To determine the MC-LR concentration, the filtered water was collected and prepared for the ultra-high-performance liquid chromatography (UHPLC) analysis as described in Fayad et al. (2015) [28]. For every cycle, average MC-LR removal (using two replicas) was determined for each filter. Briefly, a 20-μL sample aliquot was analyzed by UHPLC coupled to a Thermo Q-Exactive

Orbitrap mass spectrometer through a positive electrospray ionization source. MC-LR was detected in full scan MS mode (resolution set at 70,000 FWHM at 200 m/z) and quantified against a matrix-matched lake water calibration curve. The limit of quantification (LOQ) was set at the lowest concentration of the calibration curve (i.e., 0.1 μg/L). To distinguish the contribution of adsorption from the biological process for the MC-LR removal, the result of filter C (which represents MC-LR removal only due to adsorption), was subtracted. To determine the MC-LR degradation exclusively due to biodegradation, this value was further subtracted from undegraded or residual MC-LR (determined from UHPLC analysis).

Bio-profiling of column filters and SEM imaging

After the end of 8 cycles of filter run (7 days/cycle), sand from each column filter was carefully dropped by gravity and collected for every 5 cm. For each of these sand samples collected, the biofilm was quantified in terms of the bioactivity (quantified as cell viability) and biomass using MTT assay and CV assay, respectively. Before and after the biofilm formation over the sand media, the SEM micrographs were captured at 10 kV accelerating voltage (Zeiss EVO ® 50 Smart SEM system).

Statistical analysis

All statistical analyses comprising standard deviation, average, student t-test, p-value comparison, and all graphical presentations were performed using ORIGIN software (Version 8.5; OriginLab).

Results and discussion

Screening of the bacterial strains

Three MC-LR-degraders (A, B and S) were subjected to biofilm formation test over the sand media (Figure 3.2.1). Positive control in the form of *S.epidermidis* was also placed in parallel with the three strains, and biofilm quantification of these stains was compared. Negative control of the experiment comprised the sand media and no passage of bacterial inoculum (only nutrient water; arrangement not shown in Figure 3.2.1). Figure 3.2.3 (A) and (B) shows the CV and MTT assay results which depict the spectrophotometric absorbance comparison among all the tested strains.

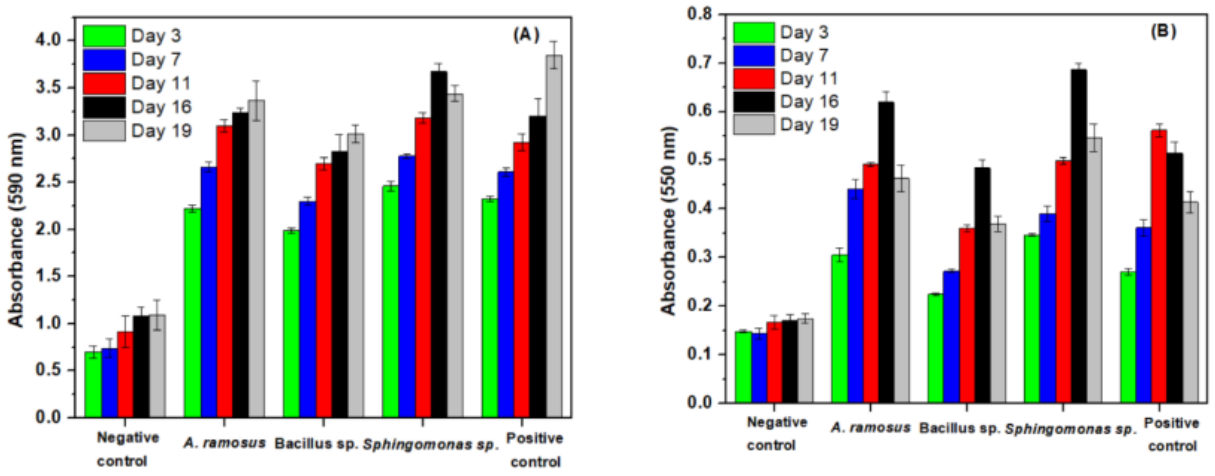

Figure 3.2.5: A) Crystal violet and; B) 3-(4,5-Dimethylthiazol-2-Yl)-2,5-Diphenyltetrazolium Bromide (MTT) assay to determine the cell biomass and cell viability of the formed biofilm

CV assay: The formed biomass (CV assay) showed a continuous increase for all the strains as the time progressed, except for the *Sphingomonas* sp. which showed an increase in the absorbance value till day 16, followed by a decrease on day 19. This decrease in biomass or the *Sphingomonas* sp. is also reflected by a decrease in the viable cells between day 16 and day 19 (Figure 3.2.3 (B)). This might indicate that apart from the decrease in the bacterial cells (live cells as observed from the MTT assay), other biological molecules, such as DNA, protein and polysaccharides present or involved in the biofilm formation ceased its formation too. As compared to the positive control, all three MC-LR-degraders showed almost similar biomass quantification (in terms of cell biomass: polysaccharides, DNA, proteins, and other biological molecules within the biofilm). However, the viability of the bacteria present in the formed biofilm was specifically observed through the MTT assay results.

MTT assay: All the three tested MC-LR-degraders showed similar or higher cell viability than the positive control (Figure 3.2.3 (B). However, the cell viability showed a decrease on day 19 (from day 16) for all the strains and can be attributed to the loss of food and nutrients.

Statistically speaking, all the three MC-LR-degraders showed comparable results to the positive control (Figure 3.2.3 (A and B)). When compared to the positive control, p-value for *A.ramosus*, *Bacillus* sp., and *Sphingomonas* sp. for CV assay was found to be 0.84, 0.22 and 0.72, respectively.

For the MTT assay, the corresponding p-values[18] were reported as 0.52, 0.19 and 0.41. Though *Bacillus* sp. showed less potential in forming biofilm as compared to the other MC-LR-degraders, still the p-value was found to be almost four times higher than the critical p-value (0.19 > 0.05). Thus, the null hypothesis was accepted (i.e., *Bacillus* sp. forms comparative biofilm to *S. epidermidis*: positive control). As a result, all three MC-LR-degraders were continued for further experiments.

Optimization of input parameters using the CCD technique

The optimized-parameter obtained using the CCD technique (Design-Expert 7.0) was found to be 7.06, 15.3 °C, 2.16 h, 13 NTU. Table 3.2.1 shows the optimization experiment results based on the obtained output parameters (desirability index = 0.638). All the significant, as well as non-significant models (compared with F-value and p-value of the model) along with the equation and desired output values, are listed in Table 3.2.1. For the input variable, turbidity (A1) and standby time (B1), all models defining the output parameters were found to be significant (Prob>F, values not shown in Table 3.2.1), except the coliform removal test. This indicates the importance of CCD to optimize and know the proper (optimized) conditions rather than choosing a random value. However, the coliform removal model showed significant p-value 0.0149 (< 0.05) for "standby time" parameter (B1) as compared to an overall p-value of the model 0.13 (> 0.05).

Table 3.2.1: Optimization results compiled in the form of the model equations using central composite design

Output Parameter	Input Parameter	Weight assigned (out of 5)	Model Equation	Significant/ No significant	Significant input co-efficient	Output value
Turbidity removal	A1= Turbidity; B1= Critical Time	4	$77.70+4.35A1-0.83B1+0.29A1B1-3.72A1^2-3.54B1^2$	SM	A1, B1, $A1^2$, $B1^2$	79.44

[18] For the p-value listed, the absorbance values obtained (including 3 replicas) for all the five points (day 3, day 7, day 11, day 16 and day 19) were compared to the positive control. It was performed for all the three MC-LR-degraders tested. Hence, all the points were covered.

Output Parameter	Input Parameter	Weight assigned (out of 5)	Model Equation	Significant/ No significant	Significant input co-efficient	Output value
	A2= pH; B2= Temperature	4	$81.29 + 0.08A2-0.19B2 + 0.08A2B2+0.15A2^2+0.12B2^2$	NSM	---	80.64
Coliform removal	A1= Turbidity; B1= Critical Time	5	$55.75+0.63A1-2.81B1-1.1A1B1-1.12A1^2$	NSM	A1, $A1^2$, A1B1	54.75
	A2= pH; B2= Temperature	5	$57.5+5.8A2=1.7B2-6.8A2B2-9.8A2^2+2.6B2^2$	NSM	---	59.55
DOC removal	A1= Turbidity; B1= Critical Time	4	$65.3-0.87A1+1.4B1-0.1A1B1-5.9A1^2-9B1^2$	SM	$A1^2$, $B1^2$	57.99
	A2= pH; B2= Temperature	4	$49.9-2A2+10.7B2-A2B2-7.3A2^2+1.7B2^2$	NSM	---	44.8
Dissolved Oxygen	A1= Turbidity; B1= Critical Time	3	$4.8-0.16A1-0.6B1+0.01A1B1-0.4A1^2-0.5B1^2$	SM	A1, B1, $A1^2$, $B1^2$	4.76
	A2= pH; B2= Temperature	3	$4.1-0.12A2-0.8B2+0.2A2B2+0.3A2^2-0.4B2^2$	SM	B2	4.44
Flow rate (m/h)	A1= Turbidity; B1= Critical Time	2	$1.26-0.1A1+0.2B1+0.02A1B1-0.05A1^2-0.06B1^2$	SM	A1, B1	1.23
	A2= pH; B2= Temperature	2	$2.21+0.4A2+0.6B2-0.03A2B2+0.08A2^2-0.4B2^2$	NSM	---	1.80
pH change	A1= Turbidity; B1= Critical Time	2	$0.05-0.04A1-0.15B1-0.04A1B1+0.02A1^2-0.11B1^2$	SM	B1	0.14
	A2= pH; B2=	2	$0.25-0.065A2-0.2A2B2-0.3A2^2-0.11B2^2$	SM	A2B2, $A2^2$	0.22

Output Parameter	Input Parameter	Weight assigned (out of 5)	Model Equation	Significant/ No significant	Significant input co-efficient	Output value
	Temperature					
MC-LR assay	A1= Turbidity; B1= Critical Time	5	$1.24-0.13B1+0.02A1B1+0.03A1^2-0.23B1^2$	SM	B1, $B1^2$	1.30
	A2= pH; B2= Temperature	5	$0.99-0.06A2-0.12B2-0.1A2B2+0.07A2^2+0.06B2^2$	NSM	---	1.06
Electrical conductivity	A1= Turbidity; B1= Critical Time	2	$235+7.6A1+0.29B1+2.3A1B1-4.3A1^2-9.8B1^2$	SM	A1, $B1^2$	222.3
	A2= pH; B2= Temperature	2	NA	NA	NA	NA
Optimized condition	Turbidity= 12 NTU	Time: 2.16 Hour	pH= 7.04	Temperature= 14.8 °C	Overall desirability: 0.638	

Turbidity level: 10 NTU, 20 NTU and 30 NTU; Critical Time: 1 hr, 2 hr and 4 hr; pH level: 6, 7 and 8; Temperature: 10 °C, 20 °C, 30°C

This observation can be simply explained by the fact that under the influent flow condition, bacteria are strongly attached when more time is allowed for the bacteria to interact with the adsorbing media and vice-versa (probably, this is the reason why parameter B1 and $B1^2$ are not in the equation). In every model defined in Table 3.2.1 for the optimization study of turbidity (A1) and time (B1), "time factor" (B1) played a crucial role. Thus, under no condition, critical stand-by time should exceed the optimized value (2.16 h) during the filter operation and care was taken for the same.

On the other hand, optimization study was done for the input parameters, pH (A2) and temperature (B2), only two output parameter models, i.e., dissolved oxygen and pH change were relevant. This meant that many output variables did not get affected by a pH range of 6-8 and temperature range of 10°C - 30°C. However, dissolved oxygen and pH form an integral aspect of drinking water treatment, and hence the optimized value was followed in any case for the rest of the experiments.

Response surface methodology plots for all the models are included in the appendix section (Figure C4, Appendix C).

Biofilm formation

All the filters were run for 8 weeks (8 cycles) post-biofilm formation over the sand media. It took 14-16 days for the mature biofilm to get formed over the sand media. As mentioned in method section, a high inoculum concentration of 6 x 10^8 cells/mL (divided equally among two or more bacterial strains for co-culture case) was used to inject the column filter. This high cell concentration allowed to attain a critical biomass concentration exceeding the level of endemic or other indigenous bacteria (present in lake water) which might have grown over the sand surface and thereby could affect the study objective. Bourne et al. (2006) [16] showed that high cell inoculation (10^7 cells/mL) aided the MC-degraders in increasing their chance of survival under the presence of the indigenous bacterial community.

Also, it was observed that MC-LR-degraders possessing the *mlrA* gene competed, even at bacterial concentration of 100 CFU/ml, with other bacteria present in the lake water.However, Bourne et al. (2006) [16] achieved enhanced biodegradation of MCs even at 10^2-10^5 cells/mL which signified that effective bacterial cell attachment is also necessary for the MCs degradation. Nevertheless, high inoculation might have increased the chance of survival of the inoculated MC-LR-degraders and lowered the acclimatization period for a filter to become mature (biofilm formation) in removing MC-LR. Also, as mentioned by Wang et al. (2007) [13], the sand particle may even take more than 6 months to establish a mature biofilm for particle size as high as 1000-1400 μm. However, in the current study, the effective diameter of the sand grain was < 200 μm, and with high inoculation, it just took 16 days to establish a mature biofilm. However, different bacterial species take a distinct period for biofilm establishment.

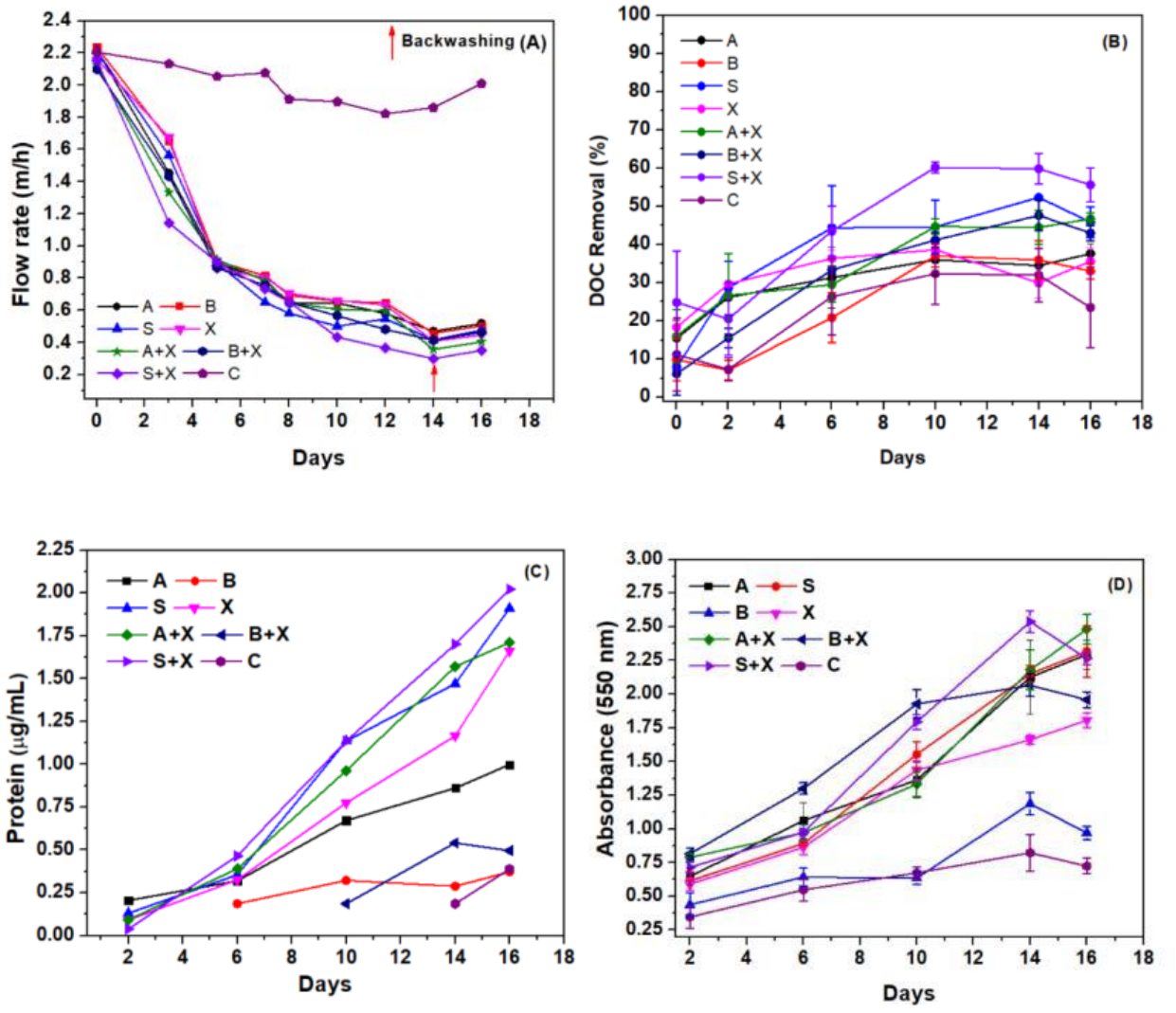

Figure 3.2.6: A) Flow rate; B) Dissolved organic carbon removal; C) Protein concentration; and D) Cell viability of/due to the biofilm formed over the sand surface of the filters studied

Figure 3.2.4 (A), (B), (C) and (D) shows the flow rate, DOC removal, protein and cell viability measure for all the filters as the biofilm starts getting formed (day 1- day 16). Successful biofilm formation was evident from the fact that DOC removal kept increasing till day 16 for all the biosand filters as compared to the control filter (filter C: only sand). As compared to the control sand filter (< 30% DOC removal), maximum DOC removal was achieved by filter S+X (~ 60%) and filter S (~ 50%), so that *Sphingomonas* sp. performed well in degrading organic carbon which is one of the primary objectives of the drinking water filter. Balkwill et al. (2006) [29] observed moderate sugar/glucose utilization (COD removal) by *Sphingomonas* sp. even under low nutrient conditions. This holds a strong prospect of utilizing and preferring such MC-LR-degrader to other

aerobic ones which showed a strong inability to survive under low nutrient conditions (filter conditions).

The formation of biofilm in each filter continuously reduced the flow rate (Figure 3.2.4 (A)). As compared to the control filter, (where a maximum reduction in the flow rate was just 13 %), filter: S+X and S showed a drastic reduction of > 70%, possibly due to more biomass production as is evident from the CV assay too (Figure 3.2.3 (A)). A very slow rate of backwashing (without much disturbing the attached biofilm) was performed on the 14th day after which the flow rate increased slightly for all filters at the expense of a decrease in the DOC removal (on an average 5 % - 10% decrease for every filter). In general, co-cultured biosand filters (A+X, B+X or S+X), enhanced DOC removal than their individual counterpart strains (A, B or S) (Figure 3.2.3 (B)). A decrease in the protein level (Figure 3.2.3 (C)) and cell viability (Figure 3.2.3 (D)) after 14 days for some filters, provided evidence of mature biofilm formation over the sand media. The biofilm formed in filter S+X and filter S showed the highest protein and cell viability among all filters, indicating the presence of a more active enzyme to carry out the MC-LR degradation.

Routine sample analysis after biofilm formation

Backwashing was performed for all the filters after the end of the 4th cycle which helped in an increase in the flow rate without compromising much of the biofilm. Lowest flow rate (0.15 ± 0.06 m/h) was observed for S+X filter and all the individual strain filters showed higher flow rate when compared to their co-cultured counterparts (Figure 3.2.4 (A)). Filter C showed the highest flow rate (1.62 ± 0.3 m/h) unsurprisingly, due to no inoculation of bacterial cells.

The lowest and highest coliform removal of 48 ± 10.7% and 81 ± 4.7% was obtained for filter C and filter S+X, respectively. Filters inoculated with co-culture strains showed higher coliform removal than their individual counterparts highlighting competition and entrapment of the coliform bacteria assisting in their removal. Filter X representing the DWTP filtration unit, achieved a moderate coliform removal of 60 ± 4%. It may be noted that the filtered water is to be further treated in the disinfection unit of a DWTP. The disinfection unit can remove 99.9 % of coliforms and hence, coliform removal of > 80% seemed promising. Also, the source water was used in the same form as it was delivered, and no further dilution was made. Thus, all load was taken by the filter unit since the source water was not subjected to any pre-treatment (pre-ozonation or coagulation/flocculation) during the experiment.

Initial DOC concentration of source water was 9.6 mg/L. Highest DOC removal of 33 ± 2.1% was achieved by filter S+X which was 19% more than the control filter C. On the other hand, other co-cultured inoculated filters (X, A+X, B+X) showed higher DOC removal than the control but not more than 29% (A+X). It must be noted that the biodegradation efficiency of MCs also depends on the biodegradable carbon source (in the form of DOC or TOC[19]) present in the influent water. Eleuterio et al. (2010) [30] demonstrated an interesting result where TOC (> 30 mg/L) acted as a hindrance to MC degradation (MC degradation started only after > 90% TOC removal happened) as the bacterial cells (isolated from biofilter of a DWTP) might prefer other carbon sources over MCs. In contrast, this study maintained a balanced removal of both DOC and MCs for every inoculated filter. Also, the lowest SUVA value for the filtered sample obtained from filter S+X as compared to other filters set-up (see Table 3.2.2) offers a good platform for the filtered water to undergo treatment in the next unit (disinfection unit). We expect that the formation of disinfection-by-products increases with increase in SUVA value (more SUVA means a higher natural organic matter is present) [31].

Table 3.2.2: Details of inoculated filters (eight) and characteristics of the source water

Filter	**A**	**B**	**S**	**X**	**C**	**A+X**	**B+X**	**S+X**
Strain inoculated	*Arthrobacter ramosus* (A)	*Bacillus* sp. (B)	*Sphingomonas* sp. (S)	*Pseudomonas fragi* + *Chryseobacterium sp.* (X)	No bacteria	A+X	B+X	S+X
MDI[20] (after 8 cycles)	2.38	2.23	2.47	2.54	2.12	2.76	2.56	2.54
Toxicity (eq. DMSO %)	8.3	13	5.8	9.1	16	0.6	6.7	0.2
Degradation contribution	17 %	14 %	21 %	21 %	0[21] %	31 %	21 %	38 %
SUVA (m^{-1}-L/mg C)	2.6	3.27	2.66	2.98	3.57	2.83	2.76	2.23
Source water characteristics								

[19] Total organic carbon
[20] MDI= Morill Dispersion Index (MDI=1 for ideal plug flow condition, MDI= 23 for the completely stirred reactor)
[21] Normalizing value of control (56 %), therefore assigned the value of MC-LR removal contribution set to zero.

pH	Alkalinity	$NH_4^+NO_2$	Al/As/Ba	NO_3^-	Conductivity	UV_{254}	DOC/COD (ppm)	SUVA
6.46	18 mg/L as $CaCO_3$	2.4 ppm/ zero	0.13/<0.01 ppm	4.4 ppm	234 µS/cm	0.465	9.6/36.3	3.52

Turbidity removal can be indirectly correlated with the bioactivity in a filter (more bioactivity and more biomass). This biomass could be responsible for the entrapment of suspended particles as is demonstrated by the control filter C which showed the highest turbidity of 3.9 NTU as compared to below guideline values (1-3 NTU) of 1.23 NTU obtained for filter S+X. The bioactivity of filter C as compared to other inoculated-filters suggests that it has always remained less effective as is evident from DOC and MC-LR removal. Also, the dissolved oxygen can be cited as an indicator of the high bioactivity in the inoculated filters (> 5 mg/L for control filter C as compared to < 3.5 mg/L for all inoculated filters).

All the filters achieved more than 90% removal of nitrite, however, only filter S+X met the final nitrite guideline value of < 3 ppm. For the nitrate removal, except for filter B, X, C, all other filters achieved the guideline value of < 45 ppm. On the other hand, for the ammonia-N removal, except for the filter S+X, none of the filters achieved the strict guideline values of < 0.121 ppm. Overall, the nitrification process was not affected by the DO limitation within the filters as the values mostly remained in the range of 2-4 mg/L [32].

MC-LR removal and toxicity assay

Figure 3.2.5 shows the stack-bar chart representation of the MC-LR removal (comprising 8 cycles) for all 8 filters, in terms of adsorption and biodegradation along with the residual MC-LR percentage in the treated (filtered) water. Highest average MC-LR removal of 87.6 ± 10% and 94.2 ± 6.8% was achieved by the co-cultured inoculated sand filter, A+X, and S+X, respectively. The reported result was compared with the control filter C (56.5 ± 9.9%), to differentiate the MC-LR removal due to biodegradation and adsorption. Co-cultured strains A+X and S+X enhanced the MC-LR removal by 31% and 38%, respectively.

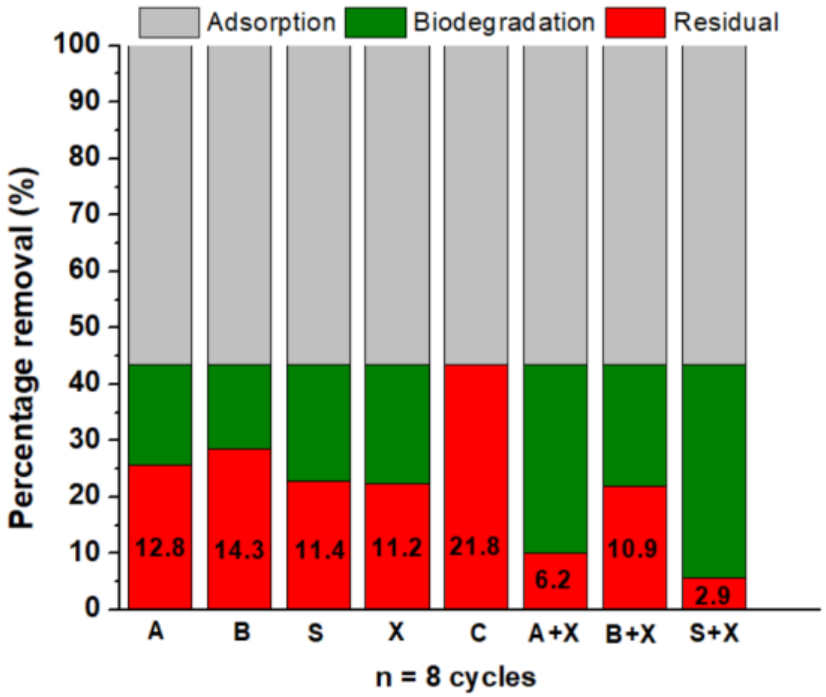

Figure 3.2.7: Stack-bar graph representing the MC-LR removal due to adsorption (in grey), biodegradation/biosorption (in green) and the residual/unremoved MC-LR (red bar)

The values inside the lower stack bar represents the MC-LR concentration (µg/L) left unremoved.

It must be noted that the MC-LR removal presented in Table 3.2.3 was accounted for only when biofilm was formed in all the filters (except filter C). Also, since the lake water was the influent matrix during the filter operation, minor biofilm formation seemed inevitable after 2 weeks (or 2 cycles), even in the control filter (filter C). This minor biofilm formation in filter C (uninoculated filter) can be attributed to the proliferation of heterogenous bacteria present in the lake water. If we compare the MC-LR removal of the control filter before the actual cycle study, it showed < 35 % of MC-LR removal (not shown in Figure 3.2.5).

Table 3.2.3: Performance evaluation of output parameters for all the tested filters

Filter	Turbidity (NTU)	Flow rate (m/h)	pH	Dissolved Oxygen (ppm)	DOC removal (%)	Coliform removal (%)	MC-LR removal %	Nitrate (ppm)	Nitrite (ppm)	Ammonia (ppm)
A	2.1 ± 0.2	0.34 ± 0.06	6.7	3.3 ± 0.1	21 ± 10	52 ± 16.7	74.3 ± 5 (7.1)	31.5	7.18	0.21
B	3.2 ± 0.6	0.39 ± 0.04	6.7	3.4± 0.1	22 ± 7	63 ± 12.3	71.1 ± 6 (13.1)	46.8	6.81	0.14

Filter	Turbidity (NTU)	Flow rate (m/h)	pH	Dissolved Oxygen (ppm)	DOC removal (%)	Coliform removal (%)	MC-LR removal %	Nitrate (ppm)	Nitrite (ppm)	Ammonia (ppm)
S	2.1 ± 0.8	0.29 ± 0.05	7.1	2.7 ± 0.1	28 ± 7	69 ± 10.5	77.1 ± 8 (5.2)	34.0	6.46	0.21
X	2.3 ± 0.6	0.27 ± 0.07	6.7	3.2 ± 0.2	22 ± 8	73 ± 10	77.5 ±8 (9.2)	49.4	4.75	0.14
A+X	1.9 ± 0.9	0.23 ± 0.06	6.8	3.1 ± 0.3	29 ± 3	68 ± 10.3	87.6 ± 10.4 (ND)	26.3	4.27	0.31
B+X	2.1 ± 0.8	0.28 ± 0.05	6.7	2.9 ± 0.3	26 ± 5	71 ± 10.8	78.1 ± 5 (8.3)	26.3	3.96	0.15
S+X	1.2 ± 0.8	0.16 ± 0.06	7.1	2.7 ± 0.2	33 ± 2	81 ± 4.9	94.2 ± 7 (ND)	18.6	2.84	0.11
Control	3.6 ± 0.5	1.63 ± 0.29	7.2	5.3 ± 0.2	14 ± 7	45 ± 15.3	56.6 ± 10	59.7	7.11	1.18
Guidelines	<1 not more than 3 NTU	SSF: 0.1-0.4	7-10.5	2-4 ppm	NA	100%	<1 µg/L	<45 mg/L	<3 mg/L	<0.121 mg/L

--- Values in bracket means the least effluent MC-LR concentration detected, --- DOC removal is calculated based on the initial lake water condition

Extracellular polymeric substance (EPS)[22] production, which is known to be an important criterion for an initial bacterial attachment to the surface and its subsequent resistance to shear flow which is very important with filtration system perspective [33], was found to be in order: *Bacillus* sp. (18 mg/g biomass) < *Arthrobacter ramosus* (98 mg/g biomass) < *Sphingomonas* sp. (138 mg/g biomass). This could explain the fact that *Bacillus* sp. maintained less integrity in their EPS matrix and could also explain the reason as to why, the filters inoculated with *Bacillus* sp. (filter B and B+X) did not contribute well to the biodegradation of MC-LR (less coverage of the green bars indicating biodegradation, Figure 3.2.5). Once a proper bacterial attachment occurred, MC-LR removal increased, as is evident from the MC-LR removal results of filter A+X and S+X (Figure 3.2.5). It can be seen fromFigure C5 (Appendix C) that a relatively weaker biofilm was formed for B+X as compared to A+X and S+X.

[22] Determined using ethanol precipitation method by sampling biofilm formed over the top layer of sand-filter during bioprofiling step

Even the individual MC-LR-degraders (A, B and S) showed an enhancement of 18%, 15% and 21%, respectively in the overall MC-LR removal when compared to the control filter (C). The native bacterial strains (X) also increased the MC-LR removal by 21%. Likewise, McDowall et al. (2009) [34] reported that biodegradation played a pivotal role in the removal of a secondary cyanobacterial metabolite: geosmin, by an additional 38%. Interestingly, co-cultured *Bacillus* sp.-native bacterial strains filter (B+X), showed no improvement (0 - 0.5% difference) when compared to filter X, rightly justifying the effect of lower EPS formation by *Bacillus* sp. which suggested the weak attachment of *Bacillus* sp. to the sand surface.

It is interesting to observe that the backwashing event (end of the 4^{th} cycle) might have retained the more resistant and better-attached bacteria in S+X and A+X and showed fast growth in the next cycle (5^{th}) to allow complete MC-LR removal in the last three cycles (see cycles 6-8 in Figure 3.2.5). However, a breakthrough of MC-LR was observed after the 8^{th} cycle in both these filters (not shown here). Also, the ability of MC-LR-degraders to survive in conjugation with the native bacterial strains (X) can be a contributing factor enhancing the biodegradation. Likewise, filter B+X showed 10% and 16% less MC-LR biodegradation potential as compared to A+X and S+X, respectively, and an early breakdown (after 5^{th} cycle) as compared to the consistent performance of A+X and S+X where breakdown phenomenon occurred after the 8^{th} cycle. The initial breakthrough of MC-LR in filter A+X and S+X (cycle 1, post-biofilm establishment) shows evidence of acclimation period followed by a consistent decrease in MC-LR concentration in the filtered sample which suggested that the majority of degradation had been achieved through the biological process [15]. However, the acclimation period in this study was comparatively lower (1 cycle or 7 days) than other studies [16,18]. Ho et al. (2006) [14] also observed a very short initial breakthrough period of just 4 days. Many studies also attribute the presence of more advanced bacterial community in a biofilm for a quick acclimation of MCs which reduces the initial breakthrough period and advanced the biodegradation period, once the bacteria adhered well to the surface [36,37].

At the end of each cycle, the filtered samples were assayed for toxicity. The toxicity of the sample was determined by the percentage equivalent of DMSO (tested as a surrogate toxic chemical to MC-LR) for the same absorbance values offered by MC-LR which was eventually related to the cell viability of the bioindicator. Maximum average equivalent DMSO value of 16% and 12%

were reported for sample filtered from control filter C and filter B, respectively, indicating toxic effects to human cells. MC-LR-degraders co-cultured with X showed comparatively lower DMSO equivalent value than the individual strain counterparts. The least toxic sample was reported for filter S+X (0.19% eq. DMSO) followed by A+X (0.6% eq. DMSO). Many researchers have reported the toxic effects of DMSO on human cells and other species. At 1% (v/v), 0.6 % (v/v), 0.5 % - 2 % (v/v) of DMSO, an effect on the neuronal cell line of rats, vascular endothelial and platelet cells on humans, and suppressing action on the expression of many pro-inflammatory cytokines/chemokines, respectively was reported [38-40]. Considering the above statement, filtered samples from filter inoculated with S+X and A+X can be assumed safer than other filters. Also, the degraded by-products as obtained from the mass spectra analysis showed m/z values of 155, 213, 268, 315, 375, 553, 862.5. These seven major by-products were similar to the degraded by-products as reported in our previous research work, where MC-LR removal was studied using moving bed biofilm reactors (MBBR) [41]. It may be because same MC-LR-degraders were bioaugmented individually in separate MBBR reactor for the development of the biofilm over the K1 Kaldness adsorbents. In the previous study, the proposed mechanism of MC-LR degradation from the obtained by-products with these m/z values directed the possibility towards a toxic-free transformation mechanism (devoid of ADDA peptide) [41,42]. However, as mentioned in previous section that the toxicity assay needs further validation using ELISA assay kits which are specific tools for measuring toxicity.

Bio-profiling of column filters

To quantify cell biomass and cell viability for the entire depth of the filter column, bio-profiling of each filter was performed as discussed in method section. Figure 3.2.6 (A) and (B) shows the cell biomass bio-profile whereas Figure 3.2.6 (C) and (D) shows cell viability bio-profile of each filter. Most active bacteria were found within the top 15 cm of the filter column. Control filter (C) showed a linear profile as compared to other filters, indicating less to no bioactivity throughout the column depth. Filter S+X showed highest cell biomass and almost constant bio-profile for cell viability up to 15 cm depth (Figure 3.2.6 (D)). This could be the reason for filter S+X accounting for the highest MC-LR degradation among all filters. This may be linked to an effective attachment (not sheared away easily) of the bacterial strains (S+X) over the sand particle which can also be seen from the SEM images (Figure C5: Appendix C). Ho et al. (2006) [14] too observed high

biomass density at the filter top where they identified the same bacterial species, i.e., '*Sphingomonas*' (91% similarity to *Sphingomonas* sp. CM-3962) as used in filter S+X. As discussed by Ho et al. (2006) [14], the biomass at the top portion of the column was around 6-8 times higher than the bottom and had higher enzyme activity (2 times using peptidase assay) than the latter. In the present study, MTT assay was used as a marker of viable cells to measure the enzymatic activity that showed similar behaviour (2.5 times higher bioactivity at the top than at the bottom). In general, *Sphingomonas* sp. (filter S or S+X) showed the higher bioactivity and cell biomass (Figure 3.2.6) as compared to other MC-LR-degraders, i.e., *Bacillus* sp. and *Arthrobacter ramosus,* which could be related to the high MC-LR degradation [14].

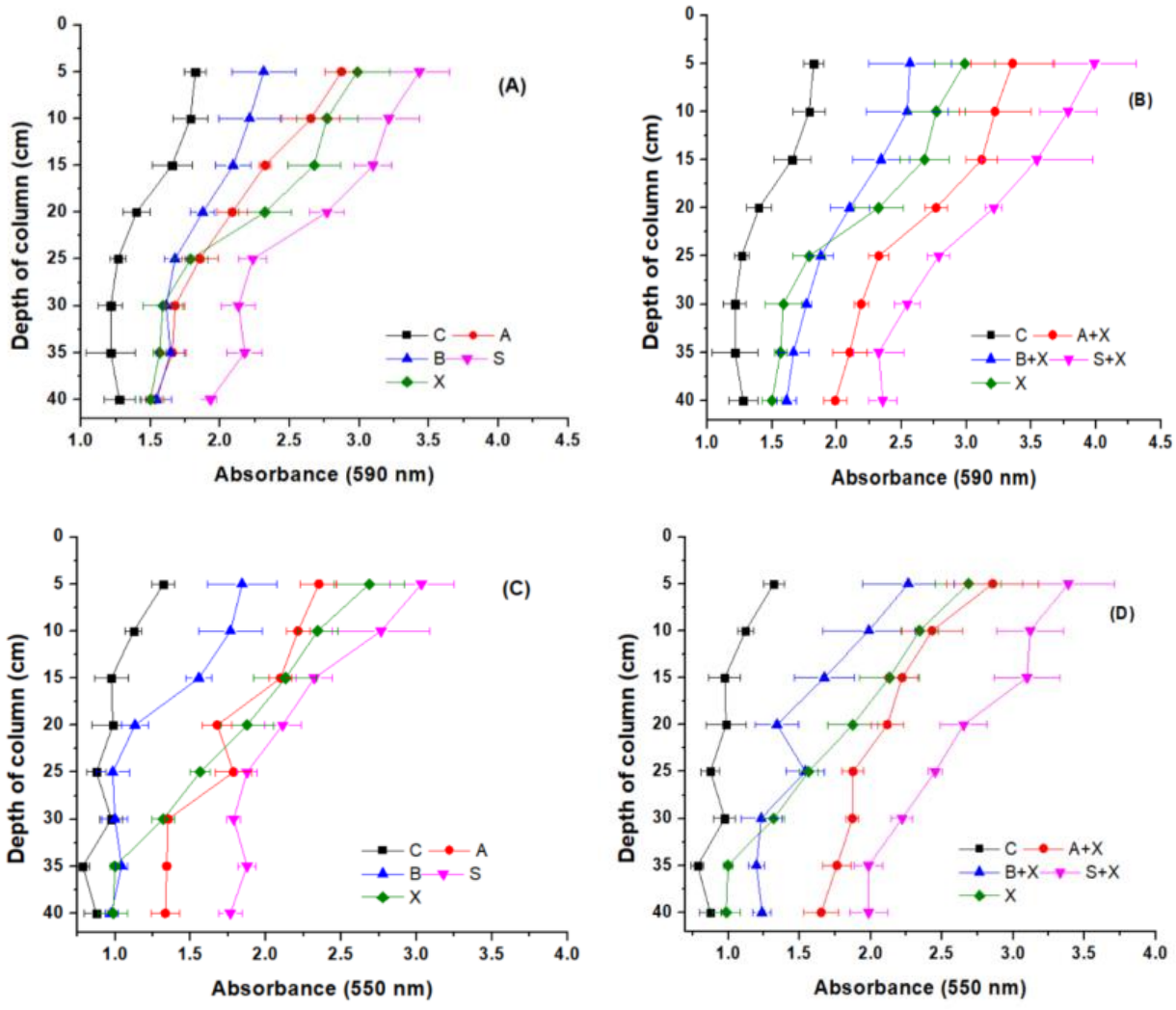

Figure 3.2.8: A) and B): Cell biomass bioprofile of the filters; C) and D) Cell viability bioprofile of the filters

Known MC-LR-degrader species in the form of *Arthrobacter, Bacillus* and *Sphingomonas* was co-cultured with the native bacterial strains residing over the filtration unit of a DWTP. It may be inferred that the source water in DWTP (St. Lawrence River) consists of these microorganisms (native: X) that had built up over the years through the continuous influent discharge in the filtration unit, showing attached growth, eventually becoming potent in degrading microcystin.

From our previous study, their ability to degrade the MC-LR was slower under suspended growth method (19.4 μg/L/d) as compared to the attached growth degradation rate (2-log increase in the present study). However, it may also be noted that the former had 6 x 10^6 cells/mL of initial inoculum concentration (IIC) and latter had IIC of 6 x 10^8 cells/mL. Nevertheless, owing to the retention time (15 - 45 min) of the filtration unit of a typical DWTP, the best-evaluated filter in the current study (retention time of 64 min), i.e., S+X, may not be promising to remove MCs below WHO guidelines (1 μg/L for human and 0.3 μg/L for children) within 25 min. Table 3.2.3 shows the overall evaluation of filters used in this study and it can be observed that S+X met other drinking water quality parameters such as, turbidity, total coliforms, nitrate, nitrite and ammonia removal. Table 1.4 shows some filtration column studies that were performed for the removal of microcystin. The bacterial genera: *Sphingomonas* was found to be a potential MC degrader for the active biological filter studies [14,16].

Also, in past, the referred native bacterial community (dominant) of genera *Chryseobacterium* and *Pseudomonas*, has also shown capability in removing other secondary cyanobacterial metabolites including geosmin and 2-methylisoborneol (MIB) [43-45]. Some studies have shown promising biological treatment of other cyanotoxins apart from MCs, such as cylindrospermopsin and nodularin via bacterial of genera used in this study viz. *Arthrobacter*, *Bacillus*. and *Sphingomonas* [46-48]. For the first time, the potential of these three listed bacteria (non-pathogenic to human as well) were studied in conjugation with the identified and dominant native bacteria residing in the filtration unit of a DWTP. Hence, in future, proper seeding method of these MC-LR degraders (also capable of handling other cyanotoxins) can be performed to tackle the toxicity posed by various cyanotoxins. DWTP operators may also utilize the backwashing facility to recirculate the MC-LR-degraders as a seeding technique to tackle the MCs removal challenge occurring for a shorter period of the year [33].

However, some research gaps, such as achieving lower retention time or empty bed contact time (EBCT), can be overcome by decreasing the IIC that will enable higher flow rate (higher penetration of fluid because of lower cell biomass growth) and will possibly help in MC-LR removal within the retention period of 15-25 min. Other common microcystin congeners such as Microcystin-RR needs to be evaluated too as they have different adsorption characteristics [49]. Also, exploring more MC-LR-degraders along with the other native bacterial strains isolated from the filtration unit of other DWTP can further help the plant operators to accomplish the degree of MC treatment required.

Conclusion

Microcystin (MC)-degraders of genera, *Sphingomonas* (S) and *Arthrobacter* (A), inoculated with the already present bacterial strains in the filtration unit (X= *Pseudomonas fragi* and *Chryseobacterium* sp.) of the drinking water treatment plant (DWTP), enhanced removal of MC-LR. Bacterial co-culturing helped in improving MC-LR removal by almost 17% (to 94% in S+X case). The presence of MC-LR in the filtration system showed no negative effect on the removal/treatment of other drinking water quality parameters such as ammonia, nitrate, nitrite, coliform removal, among others. Toxicity assessment determined in terms of equivalent DMSO concentration showed less to no toxicity (reduced from 9 % to 0.19% and 0.6% for S+X and A+X, respectively) to human cells when MC-LR-degraders was co-cultured with the native bacterial strains of the filtration unit of a DWTP. Such a treatment method can also promise to assure safe drinking water to the small communities in the form of biosand filters, especially where source water is affected by cyanobacterial bloom secreting MCs.

Future gap and research implications:

a) Filter A+X and S+X showed promise in MC-LR removal for a few cycles. However, the toxin breakthrough after backwashing was evident from the analysis and hence future experiments need to be performed to understand the long-term stability of the filter media (for e.g.: modification in the sand media)

b) An experiment related to the optimization of the bacterial inoculum can be performed for an effective biofilm formation over the sand media.

c) Also, an adsorption isotherm needs to be developed for the sand media with and without the inoculated bacterial cells to understand the kinetics of the MC-LR removal at various concentrations.

d) Native bacteria found in DWTPs can be different and hence simple co-culturing MC-degraders to accelerate MCs degradation cannot be extrapolated.

Acknowledgments

The authors are sincerely thankful to the Natural Sciences and Engineering Research (Discovery Grant 23451), Genome Québec, Genome Canada) and ATRAPP (Algal blooms, treatment, risk assessment, prediction and prevention) for financial support. Special thanks to Dana Simon for coordinating the sample receipt and analysis. Authors would also like to thank the team for constant support and timely suggestions. We would like to thank Genome Quebec for timely sequencing for the bacterial identification. The views or opinions expressed in this article is exclusively those of the authors.

Conflict of interest

None

References

1. Welker, M., & Steinberg, C. (2000). Rates of Humic Substance Photosensitized Degradation of Microcystin-LR in Natural Waters. *Environ Sci Technol, 34*(16), 3415-3419. doi:10.1021/es991274t

2. World Health Organisation. Public Health and the Environment. WHO; Geneva: 2009.Guidelines for drinking water quality policies and procedures used in updating the WHO Guidelines for Drinking Water Quality

3. Ramani, A., Rein, K., Shetty, K. G., & Jayachandran, K. (2011). Microbial degradation of microcystin in Florida's freshwaters. *Biodegradation, 23*(1), 35-45. doi:10.1007/s10532-011-9484-y

4. Chang, J., Chen, Z.-l., Wang, Z., Kang, J., Chen, Q., Yuan, L., & Shen, J.-m. (2015). Oxidation of microcystin-LR in water by ozone combined with UV radiation: The removal and degradation pathway. *Chemical Engineering Journal, 276*, 97-105. doi:10.1016/j.cej.2015.04.070

5. Sun, F., Pei, H.-Y., Hu, W.-R., & Ma, C.-X. (2012). The lysis of Microcystis aeruginosa in AlCl3 coagulation and sedimentation processes. *Chemical Engineering Journal, 193-194*, 196-202. doi:10.1016/j.cej.2012.04.043

6. Clancy J.L. and Hargy T.M., Waterborne: Drinking Water (ch. 11), In: R. Fayer and L. Xiao, eds., Cryptosporidium and cryptosporidiosis, 2nd ed., CRC Press, Boca Raton, 2008.

7. Lee J. and Walker H.W., Mechanisms and factors influencing the removal of microcystin-LR by ultrafiltration membranes, J. Membr. Sci., 320 (2008) 240–247.

8. Sun, J., Bu, L., Deng, L., Shi, Z., & Zhou, S. (2018). Removal of Microcystis aeruginosa by UV/chlorine process: Inactivation mechanism and microcystins degradation. *Chemical Engineering Journal, 349*, 408-415. doi:10.1016/j.cej.2018.05.116

9. Zhang, Y., Shao, Y., Gao, N., Chu, W., & Sun, Z. (2016). Removal of microcystin-LR by free chlorine: Identify of transformation products and disinfection by-products formation. *Chemical Engineering Journal, 287*, 189-195. doi:10.1016/j.cej.2015.10.111

10. Zong, W., Sun, F., Pei, H., Hu, W., & Pei, R. (2015). Microcystin-associated disinfection by-products: The real and non-negligible risk to drinking water subject to chlorination. *Chemical Engineering Journal, 279*, 498-506. doi:10.1016/j.cej.2015.05.048

11. Bourne, D. G., Jones, G. J., Blakeley, R. L., Jones, A., Negri, A. P., & Riddles, P. (1996). Enzymatic pathway for the bacterial degradation of the cyanobacterial cyclic peptide toxin microcystin LR. *Appl Environ Microbiol, 62*(11), 4086-4094.

12. Sovadinova, I., Babica, P., Adamovský, O., Alpatová, A., Tarabara, V., Upham, B. L., & Bláha, L. (2017). Chlorination and ozonation reduce microcystin content and tumour promoting activity of complex cyanobacterial extract. *Advances in Oceanography and Limnology, 8*(1). doi:10.4081/aiol.2017.6342

13. Somdee, T., Wibuloutai, J., Somdee, T., & Somdee, A. (2014). Biodegradation of the cyanobacterial hepatotoxin [Dha7] microcystin-LR within a biologically active sand filter. *Water Science and Technology: Water Supply, 14*(4), 672-680. doi:10.2166/ws.2014.024

14. Ho, L., Meyn, T., Keegan, A., Hoefel, D., Brookes, J., Saint, C. P., & Newcombe, G. (2006). Bacterial degradation of microcystin toxins within a biologically active sand filter. *Water Research, 40*(4), 768-774. doi:10.1016/j.watres.2005.12.009

15. Ho, L., Hoefel, D., Saint, C. P., & Newcombe, G. (2007). Degradation of Microcystin-LR through Biological Sand Filters. *Practice Periodical of Hazardous, Toxic, and Radioactive Waste Management, 11*(3), 191-196. doi:10.1061/(asce)1090-025x(2007)11:3(191)

16. Bourne, D. G., Blakeley, R. L., Riddles, P., & Jones, G. J. (2006). Biodegradation of the cyanobacterial toxin microcystin LR in natural water and biologically active slow sand filters. *Water Research, 40*(6), 1294-1302. doi:10.1016/j.watres.2006.01.022

17.Phujomjai,Y.,&Somdee,T.(2013)http://www.jolst.net/index.php?m=content&c=index&a=show&catid=34&id=66. *Journal of Life Sciences and Technologies*, 220-222. doi:10.12720/jolst.1.4.220-222

18. Yang, F., I. Y. Massey, J. Guo, S. Yang, Y. Pu, W. Zeng and H. Tan (2018). "Microcystin-LR degradation utilizing a novel effective indigenous bacterial community YFMCD1 from Lake Taihu." Journal of Toxicology and Environmental Health, Part A 81(7): 184-193.

19. Yang, F., J. Guo, F. Huang, I. Massey, R. Huang, Y. Li, C. Wen, P. Ding, W. Zeng and G. Liang (2018). "Removal of Microcystin-LR by a Novel Native Effective Bacterial Community Designated as YFMCD4 Isolated from Lake Taihu." Toxins 10(9).

20. Massey, I. Y., X. Zhang and F. Yang (2018). "Importance of bacterial biodegradation and detoxification processes of microcystins for environmental health." Journal of Toxicology and Environmental Health, Part B 21(6-8): 357-369.

21. Kumar, P., Hegde, K., Brar, S. K., Cledon, M., Kermanshahi-pour, A., Roy-Lachapelle, A., & Galvez-Cloutier, R. (2018). Biodegradation of microcystin-LR using acclimatized bacteria isolated from different units of the drinking water treatment plant. *Environmental Pollution, 242*, 407-416. doi:10.1016/j.envpol.2018.07.008

22. Chusri, S., Sompetch, K., Mukdee, S., Jansrisewangwong, S., Srichai, T., Maneenoon, K., Voravuthikunchai, S. P. (2012). Inhibition ofStaphylococcus epidermidisBiofilm Formation by Traditional Thai Herbal Recipes Used for Wound Treatment. *Evidence-Based Complementary and Alternative Medicine, 2012*, 1-8. doi:10.1155/2012/159797

23. Bradford, M. M. (1976). A rapid and sensitive method for the quantitation of microgram quantities of protein utilizing the principle of protein-dye binding. *Analytical Biochemistry, 72*(1-2), 248-254. doi:10.1016/0003-2697(76)90527-3

24. APHA, AWWA, WPCF. 1998. Standard methods for the examination of water and wastewater,19th Ed., Washington, D.C.

25. Asrafuzzaman, M., Fakhruddin, A. N. M., & Hossain, M. A. (2011). Reduction of Turbidity of Water Using Locally Available Natural Coagulants. *ISRN Microbiology, 2011*, 1-6. doi:10.5402/2011/632189

26. Naghdi, M., Cledon, M., Brar, S. K., & Ramirez, A. A. (2017). Nitrification of vegetable waste using nitrifying bacteria. *Ecological Engineering*. doi:10.1016/j.ecoleng.2017.07.003

27. Mountfort, D. O., Holland, P., & Sprosen, J. (2005). Method for detecting classes of microcystins by combination of protein phosphatase inhibition assay and ELISA: comparison with LC-MS. *Toxicon, 45*(2), 199-206. doi:10.1016/j.toxicon.2004.10.008

28. Fayad, P. B., Roy-Lachapelle, A., Duy, S. V., Prévost, M., & Sauvé, S. (2015). On-line solid-phase extraction coupled to liquid chromatography tandem mass spectrometry for the analysis of cyanotoxins in algal blooms. *Toxicon, 108*, 167-175. doi:10.1016/j.toxicon.2015.10.010

29. Balkwill, D. L., Fredrickson, J. K., & Romine, M. F. (2006). Sphingomonas and Related Genera. 605-629. doi:10.1007/0-387-30747-8_23

30. Eleuterio, L., & Batista, J. R. (2010). Biodegradation studies and sequencing of microcystin-LR degrading bacteria isolated from a drinking water biofilter and a fresh water lake. *Toxicon, 55*(8), 1434-1442. doi:10.1016/j.toxicon.2010.02.020

31. Lu, J., Zhang, T., Ma, J., & Chen, Z. (2009). Evaluation of disinfection by-products formation during chlorination and chloramination of dissolved natural organic matter fractions isolated

from a filtered river water. *J Hazard Mater, 162*(1), 140-145. doi:10.1016/j.jhazmat.2008.05.058

32. Li, B., Qiu, Y., Zhang, C., Chen, L., & Shi, H. (2016). Understanding biofilm diffusion profiles and microbial activities to optimize integrated fixed-film activated sludge process. *Chemical Engineering Journal, 302*, 269-277. doi:10.1016/j.cej.2016.05.048

33. Jayathilake, P. G., Jana, S., Rushton, S., Swailes, D., Bridgens, B., Curtis, T., & Chen, J. (2017). Extracellular Polymeric Substance Production and Aggregated Bacteria Colonization Influence the Competition of Microbes in Biofilms. *Front Microbiol, 8*. doi:10.3389/fmicb.2017.01865

34. McDowall, B., Hoefel, D., Newcombe, G., Saint, C. P., & Ho, L. (2009). Enhancing the biofiltration of geosmin by seeding sand filter columns with a consortium of geosmin-degrading bacteria. *Water Research, 43*(2), 433-440. doi:10.1016/j.watres.2008.10.044

35. Miller, M. J., & Fallowfield, H. J. (2001). Degradation of cyanobacterial hepatotoxins in batch experiments. *Water Sci Technol, 43*(12), 229-232.

36. Holst, T., Jørgensen, N. O. G., Jørgensen, C., & Johansen, A. (2003). Degradation of microcystin in sediments at oxic and anoxic, denitrifying conditions. *Water Research, 37*(19), 4748-4760. doi:10.1016/s0043-1354(03)00413-5

37. Christoffersen, K., Lyck, S., & Winding, A. (2002). Microbial activity and bacterial community structure during degradation of microcystins. *Aquatic Microbial Ecology, 27*, 125-136. doi:10.3354/ame027125

38. Galvao, J., Davis, B., Tilley, M., Normando, E., Duchen, M. R., & Cordeiro, M. F. (2014). Unexpected low-dose toxicity of the universal solvent DMSO. *The FASEB Journal, 28*(3), 1317-1330. doi:10.1096/fj.13-235440

39. Yi, X., Liu, M., Luo, Q., Zhuo, H., Cao, H., Wang, J., & Han, Y. (2017). Toxic effects of dimethyl sulfoxide on red blood cells, platelets, and vascular endothelial cells in vitro. *FEBS Open Bio, 7*(4), 485-494. doi:10.1002/2211-5463.12193

40. Proost, P., Elisia, I., Nakamura, H., Lam, V., Hofs, E., Cederberg, R., . . . Krystal, G. (2016). DMSO Represses Inflammatory Cytokine Production from Human Blood Cells and Reduces Autoimmune Arthritis. *PLoS One, 11*(3), e0152538. doi:10.1371/journal.pone.0152538

41. Kumar, P., Hegde, K., Brar, S. K., Cledon, M., Kermanshahi-pour, A., Roy-Lachapelle, A., & Galvez-Cloutier, R. (2019). Novel fluidized-bed biofilm reactor for concomitant removal of microcystin-LR and organics. *Chemical Engineering Journal, 359*, 99-111. doi:10.1016/j.cej.2018.11.119

42. Harada, K.-i., Imanishi, S., Kato, H., Mizuno, M., Ito, E., & Tsuji, K. (2004). Isolation of Adda from microcystin-LR by microbial degradation. *Toxicon, 44*(1), 107-109. doi:10.1016/j.toxicon.2004.04.003

43. Egashira, K., Ito, K., & Yoshiy, Y. (1992). Removal of Musty Odor Compound in Drinking Water by Biological Filter. *Water Science and Technology, 25*(2), 307-314. doi:10.2166/wst.1992.0066

44. Eaton, R. W., & Sandusky, P. (2009). Biotransformations of (+/−)-geosmin by terpene-degrading bacteria. *Biodegradation, 21*(1), 71-79. doi:10.1007/s10532-009-9282-y

45. Zhou, B., Yuan, R., Shi, C., Yu, L., Gu, J., & Zhang, C. (2011). Biodegradation of geosmin in drinking water by novel bacteria isolated from biologically active carbon. *J Environ Sci (China), 23*(5), 816-823.

46. Kato, H., Imanishi, S. Y., Tsuji, K., & Harada, K.-i. (2007). Microbial degradation of cyanobacterial cyclic peptides. *Water Research, 41*(8), 1754-1762. doi:10.1016/j.watres.2007.01.003

47. Lawton, L. A., Welgamage, A., Manage, P. M., & Edwards, C. (2011). Novel bacterial strains for the removal of microcystins from drinking water. *Water Science and Technology, 63*(6), 1137-1142. doi:10.2166/wst.2011.352

48. Mohamed, Z. A., & Alamri, S. A. (2012). Biodegradation of cylindrospermopsin toxin by microcystin-degrading bacteria isolated from cyanobacterial blooms. *Toxicon, 60*(8), 1390-1395. doi:10.1016/j.toxicon.2012.10.004

49. Sathishkumar, M., Pavagadhi, S., Vijayaraghavan, K., Balasubramanian, R., & Ong, S. L. (2011). Concomitant uptake of microcystin-LR and -RR by peat under various environmental conditions. *Chemical Engineering Journal, 172*(2-3), 754-762. doi:10.1016/j.cej.2011.06.058

50. Wang, H., Ho, L., Lewis, D. M., Brookes, J. D., & Newcombe, G. (2007). Discriminating and assessing adsorption and biodegradation removal mechanisms during granular activated carbon filtration of microcystin toxins. *Water Research, 41*(18), 4262-4270. doi:10.1016/j.watres.2007.05.057

51. Grützmacher, G., Böttcher, G., Chorus, I., & Bartel, H. (2002). Removal of microcystins by slow sand filtration. *Environ Toxicol, 17*(4), 386-394. doi:10.1002/tox.10062

52. Terin, U. C., & Sabogal-Paz, L. P. (2019). Microcystis aeruginosa and microcystin-LR removal by household slow sand filters operating in continuous and intermittent flows. *Water Research, 150*, 29-39. doi:10.1016/j.watres.2018.11.055

BRIDGE-4

BRIDGE: After evaluating the co-culture aspect in static bed biofilter, it was evident from the result that the MC-LR breakthrough in the filtered water happened just after few weeks of operation. This clearly indicated a low or poor adsorbent capacity of sand used as an adsorbent material. Not only that, but the planar sand surface could be held responsible for the washout of the attached bacteria cells after few weeks of operation (turbidity increase) which could also be attributed to low bioactivity prevailing in the biosand filter. Hence, to enhance the biofilm activity, the use of agro-residue fibers as a 'top-cover' filter material was applied over the sand filter media to report the MC-LR removal and other water pollutants.

PART 3

Agro-industrial residues as a unique support in a sand filter to enhance the bioactivity to remove Microcystin-LR and organics

Pratik Kumar[a], Heidi Dayana Pascagaza Rubio[b], Krishnamoorthy Hegde[a], Satinder Kaur Brar[a,c*], Maximiliano Cledon[d], Azadeh Kermanshahi-pour[e], Sébastien Sauvé[f], Audrey Roy-Lachapelle[f,g], Rosa Galvez-Cloutier[h]

[a]- INRS-ETE, Université du Québec, 490, Rue de la Couronne, Québec, Canada G1K 9A9

[b]- Facultad de Ingeniería Departamento de Ingeniería Civil y Agrícola Universidad Nacional de Colombia Bogotá - Colombia

[c]-Department of Civil Engineering, Lassonde School of Engineering, York University, North York, Toronto, Ontario, Canada, M3J 1P3

[d]- CIMAS (CONICET, UnComa, Rio Negro), Güemes 1030, San Antonio Oeste, Rio Negro, Argentina

[e-] Biorefining and Remediation Laboratory, Department of Process Engineering and Applied Science, Dalhousie University, 1360 Barrington Street, Halifax, Nova Scotia B3J 1Z1, Canada

[f]- Department of Chemistry, Université de Montréal, Montréal, QC, Canada

[g]- Environment and Climate Change Canada, 105 rue McGill, H2Y 2E7, Montréal, QC, Canada

[h-] Faculté des Sciences et Génie, Département de génie civil et génie des Eaux, Université Laval, Québec (Québec), Canada.

[*]- Corresponding author, E-mail: Satinder.Brar@lassonde.yorku.ca; satinder.brar@ete.inrs.ca

***Science of The Total Environment,* 670, 971-981 (2019) DOI: 10.1016/j.scitotenv.2019.03.260**

Résumé

Dans le passé, la polyvalence d'un filtre biosable a été vérifiée avec succès pour contrer les solides en suspension, les métaux, le carbone organique dissous (DOC), les coliformes et d'autres paramètres de qualité de l'eau (WQP) provenant des sources d'eau potable. Dans cette étude, la cyanotoxine sous forme de microcystine-LR (MC-LR) ainsi que les WQP mentionnés ci-dessus, y compris le nitrate, le nitrite et l'ammoniac, sont analysés pour leur élimination à l'aide de filtres biosables à base d'agro-résidus (ARSF) pendant 49 jours (7 cycles). Trois différents matériaux agro-résidus (ARM) à savoir, les boues de désencrage (DSF), les fibres de chanvre (HFF) et les boues sèches de pâte à papier (PPF) ont été utilisées comme matériau de support (5 cm supérieurs) avec du sable (49 cm) comme susbtrat filtrant principal pour améliorer la bioactivité globale. Cette amélioration de la bioactivité est supposée éliminer plus de MC-LR, DOC, coliformes et permettre une nitrification / dénitrification plus efficace. Une communauté bactérienne native isolée de l'unité de filtration d'une usine de traitement d'eau potable (*Chryseobacterium* sp. et *Pseudomonas fragi* = X) avec le dégradeur de MC-LR connu: *Arthrobacter ramosus* (qui a été sélectionné comme le meilleur ancien biofilm parmi deux autres MC -LR-dégradeurs testés) ont été utilisés pour inoculer les filtres (les trois ARSF). Dans l'ensemble, le DSF a obtenu les meilleurs résultats parmi tous les ARSF par rapport au filtre à sable (SFI) inoculé avec les mêmes souches bactériennes (A + X). Une augmentation de la bioactivité des ARSF, en particulier du DSF, a été mise en évidence par l'élimination du DOC (44 ± 11%, 15% de plus que le SFI), l'élimination des coliformes (92,7 ± 12,8%, 24% de plus que le SFI), l'élimination du MC-LR (87 ± 14%, 13% de plus que SFI) et une nitrification / dénitrification efficace, réduisant le niveau d'ammoniac, de nitrate et de nitrite en dessous des valeurs recommandées. Une évaluation de la toxicite à l'aide d'un bioindicateur (Rhizobium meliloti) 'a révélé que seul le treatment DSF permelt de produire unde eau filtree sans toxicite

Mots-clés: Microcystine, agro-résidus, filtre à sable, qualité de l'eau, bioaugmentation

Abstract

In the past, the versatility of a biosand filter has been successfully checked to counter suspended solids, metals, dissolved organic carbon (DOC), coliforms and other water quality parameters (WQPs) from the drinking water sources. In this study, cyanotoxin in the form of microcystin-LR (MC-LR) along with above-mentioned WQPs including nitrate, nitrite, and ammonia are analyzed for their removal using agro-residue based biosand filters (ARSFs) for 49 days (7 cycles). Three different agro-residue materials (ARMs) viz. deinking sludge (DSF), hemp fiber (HFF) and paper-pulp dry sludge (PPF) were used as the support material (top 5 cm) along with sand (49 cm) as the primary filter media to enhance the overall bioactivity. This enhancement in bioactivity is hypothesized to remove more MC-LR, DOC, coliform along with efficient nitrification/denitrification. Native bacterial community isolated from the filtration unit of a drinking water treatment plant (*Chryseobacterium sp.* and *Pseudomonas fragi* = X) along with the known MC-LR-degrader: *Arthrobacter ramosus* (which was screened as the best biofilm-former among two other MC-LR-degraders tested) were used to inoculate the filters (all three ARSFs). Overall, DSF performed the best among all the ARSFs when compared to the sand filter (SFI) inoculated with the same bacterial strains (A+X). An increase in the bioactivity for ARSFs, particularly DSF was evident from the DOC removal (44 ± 11 %, 15 % more than SFI), coliform removal (92.7 ± 12.8 %, 24 % more than SFI), MC-LR removal (87 ± 14 %, 13 % more than SFI) and an effective nitrification/denitrification, reducing ammonia, nitrate and nitrite level to below guideline values. Toxic assessment using bioindicator (*Rhizobium meliloti*) revealed safe filter water only in case of DSF.

Keywords: Microcystin, agro-residues, sand filter, water quality, bioaugmentation

Introduction

Toxin-producing cyanobacterial harmful algal blooms (CHABs) are increasing annually and creating havoc in the drinking water system. The most common cyano(toxin) released by these CHABs is microcystins (MCs), where MC-Leucine aRginine is its most prominent variant. Drinking water treatment plant (DWTP) deriving raw water from such sources, if left untreated, can cause liver and nerve disorders in humans, if consumed for a longer period (Falconer et al. 1999). WHO recommends a critical safe concentration of MC to be < 1 μg/L in the drinking water for adults and < 0.3 μg/L for the children (US EPA, 2018).

Various conventional treatment processes have been practiced till date for the MCs-LR removal including ozonation, chlorination, flocculation, etc. with most of the time found effective as well (Nicholson et al. 1994, Pelaez et al. 2011). However, the presence of various environmental components in source water such as natural organic matter (NOMs), metals ions and other recalcitrant compounds makes the overall treatment of MCs ineffective. At different stages of the water treatment process, MCs becomes competitive (with other byproducts) mainly because of the different kinds of bacteria present in the respective units (Kumar et al. 2018 a). Especially the (pre-)ozonation and chlorination byproducts in the form of bromide, formaldehyde and microcystin-chlorinated compounds renders treated water toxic (He et al. 2014). Amidst these, filtration unit holds a great responsibility in MCs removal as it is preceded by pre-ozonation and succeeded by chlorination.

Some studies have shown promise in the MCs removal through a sand filter system (Grützmacher et al. 2002). With the involvement of the biological factor (biofilter), the removal efficiency significantly improved (up to 38 %) for some cyanobacterial metabolites such as geosmin (Mcdowall et al. 2009). Biodegradation process (biosand filter) over adsorption studies (sand filter) has the advantage to produce toxic free MCs degradation too. However, it may be considered that the presence of NOMs and the presence of other recalcitrant carbon compounds in the influent water, may hinder the bioactivity in a sand filter responsible for the biodegradation of MCs. Several studies on MC removal involving a suspended growth mechanism of bacterial cells found a negative correlation with the presence of NOMs as well as other carbon sources (Kelley et al. 2017). Thus, there is a need to enhance the bioactivity of the sand material to prolong the activism of the bacterial cells residing in the sand (filtration) media to cope up with the MCs removal along

with the presence of other competitive compounds. An increase in the bioactivity will counter for the excess effect posed by different contaminants other than MCs. To the best of author`s knowledge, there is no study carried out involving any support/hybrid material with any common or primary media (sand) that assisted in enhancing the bioactivity, thereby promoting more MC-LR biodegradation (regarding rate, efficiency or breakthrough).

In this study, the use of agricultural waste residue in the form of deinking sludge, hemp fibers[23], and pulp and paper waste (microwave treated) (Laadila et al. 2017) have been used as the "top-over" support material in a sand filter. The idea is to utilize these agricultural waste and provide a platform for the bacterial cells to captivate and offer fast biofilm growth that will be prolonged and be more effective than the biofilm formed over sand media in degrading MC-LR and organics. The global idea is to enhance the bioactivity of the existing filtration unit of the DWTP at Ste-Foy, Quebec City, Canada. To achieve this, the native bacterial strains already existing over the sand media of plant filter along with the MC-degraders were co-cultured and inoculated (discussed in detail in later section) to check the possibility of an enhanced MC-LR removal than the normal process. The idea of using agro-residue materials (as discussed above) is to enhance and prolong the bioactivity of the existing sand filter model.

Material and methods

Chemicals and microorganisms

Microcystin-LR was purchased from Cayman chemicals, (Ann Arbor, Michigan, USA). For measuring the cell viability, 3-(4,5-dimethylthiazol-2-yl)-2,5-diphenyltetrazolium bromide (MTT) was brought from Sigma Aldrich, (Ontario, Canada). All the analytical reagents and chemicals used in preparing the culture media and other nutrient solutions were brought from Fisher Scientific, (Ontario, Canada).

Three known MC-LR degraders: *Arthrobacter ramosus* (NRRL B-3159), *Bacillus sp.* (NRRL B-14393) and *Sphingomonas sp.* (NRRL B-59555), positive control for the biofilm forming microorganism: *Staphylococcus epidermidis* (NRRL: B-14901) and bioindicator used for the

[23] For the treatment procedure of deinking sludge and the hemp fiber, refer to supplementary file

toxicity assessment: *Rhizobium meliloti* (NRRL L-84), were brought from the NRRL Agricultural Research Service (ARS) culture collection.

Screening of the bacterial strains

Bacterial strains with a potential of MC-LR degradation (experimental details shown in Kumar et al. 2018) were isolated from the native bacterial strains of the filtration unit of drinking water treatment plant (Chemin-Ste-Foy, Quebec City, Quebec). They were identified as *Pseudomonas fragi* and *Chryseobacterium sp.* (combination represented as X) using NCBI BLAST service in our previous study (Kumar et al. 2018 (a)) and deposited in NCBI GenBank with Acc No. MH150822 and MH150821, respectively. They were also identified as a potent MC-LR degrading microorganism (> 80 % degradation within ten days).

These native bacterial strains (X) were combined individually with the bacterial strains of genera *Arthrobacter* (A+X), *Bacillus* (B+X) *and Sphingomonas* (S+X) and subjected to screening test in understanding their ability to form biofilm over the agro-residues (as discussed above). Figure 3.3.1 (A) shows the schematic representation of the unique set-up that was installed for the same. Sand media was obtained from the filtration unit of the DWTP (Chemin Ste-Foy, Quebec City, Quebec, Canada), finely grinded to obtain an overall effective diameter (D_{10}) of 181 μm and coefficient of uniformity (C_u) as 2.18 (to minimize any risk of clogging, $C_u < 4$) (Achak et al. 2009). Around 10 gm of sterile-sand material was filled inside the model column and was supported (not mixed) with respective agro-residues (~ 1 gm) viz. dry deinking sludge (DS), Hemp fiber (HF) and Paper and pulp dried-sludge (PPS) (Figure 3.3.1 (A) shows arrangement for DSF only, for others same arrangement was made). 25 mL of inoculum with initial cell concentration of 6 x 10^7 cells/mL[24] in the nutrient media, adjusted to final chemical oxygen demand (COD) concentration of 800 mg/L (nutrient solution recipe mentioned in previous chapter) was passed through each model reactor every 6 hours using an auto-dosage pump. The inoculum of three different MC-degraders was passed individually through respective agro-residue supported sand material as described above (total 9 combinations). A replica model column for each of the hybrid material was installed too, as can be seen from Figure 3.3.1 (A).

[24] X= MC-degrader, *Chryseobacterium sp*. and *Pseudomonas fragi* was taken as 2 x 10^6 cells/mL (total 6 x 10^6 cells/mL).

To quantify the cell biomass and cell viability that has grown over the support material, crystal violet (CV) assay and MTT assay was performed, respectively. In brief, after every 2 days, 4 days and 7 days, the agro-residue material was carefully taken out from each model column and mixed well in an aluminum dish to finally draw out 0.1 gram of sample (for experimental pictures, refer appendix C, Figure C2). The drawn sample is suspended in 1.5 mL of tap water and vortexed for 1-2 minutes to detach the biofilm from the material. The supernatant of 200 μL (containing biocells) was placed inside the well of a 96-well plate in octuplicates (4 each from replica). For CV and MTT assay (4 wells each), 0.1 % w/v CV and 7 mg/10 mL MTT was put inside the designated wells. After an overnight incubation, the stained cells (post-phosphate buffer wash to remove loose cells in case of CV assay) and the formed precipitate (formazan: in case of MTT assay-wells) was dissolved using 300 μL dimethyl sulphoxide (DMSO) to produce a uniform colour (blue for CV assay and brown for MTT). Finally, the spectrophotometric reading was obtained at 550[25] nm and 590[26] nm for MTT and CV assay wells to quantify the cell viability and cell biomass, respectively.

Optimization of input parameters using central composite design

Overall, A+X was found to be the most compatible bacterial strains, as it achieved better biofilm quantification level (both regarding cell biomass and cell viability, for details, refer to the result section for all the three agro- residues. Optimization step was further carried to understand the behaviour of the column filter under the best possible input physical parameters viz. pH, a critical standby time interval (CSTI)[27] and the initial turbidity. Three levels for each input parameters were chosen, pH[28]: 6,7 and 8; initial turbidity: 10 NTU, 20 NTU and 30 NTU (± 0.5 -1.0 NTU); and CSTI: 1-hour, 2-hour, 4-hour. The desirability for the above experimental design was obtained by simulating several output parameters viz. turbidity removal, total coliform removal, pH change, total organic carbon (TOC), flow rate, dissolved oxygen (DO), MC-LR assay, electrical

[25] Maximum absorbance was found at 550.9 nm for MTT assay
[26] Maximum absorbance was found at 590.3 nm for CV assay
[27] CSTI is defined as the maximum time interval of the filter run where different output parameters studied, deliver the best desirability through design of experiment (Design-Expert 7.0). In simple words, it may be considered equivalent to the residence time of filter operation (for more significance of CSTI: refer supplementary section).
[28] Refer to supplementary section to understand the significance of optimizing pH parameter.

conductivity. Design-Expert 7.0 was used for deriving the model equation based on the output results obtained.

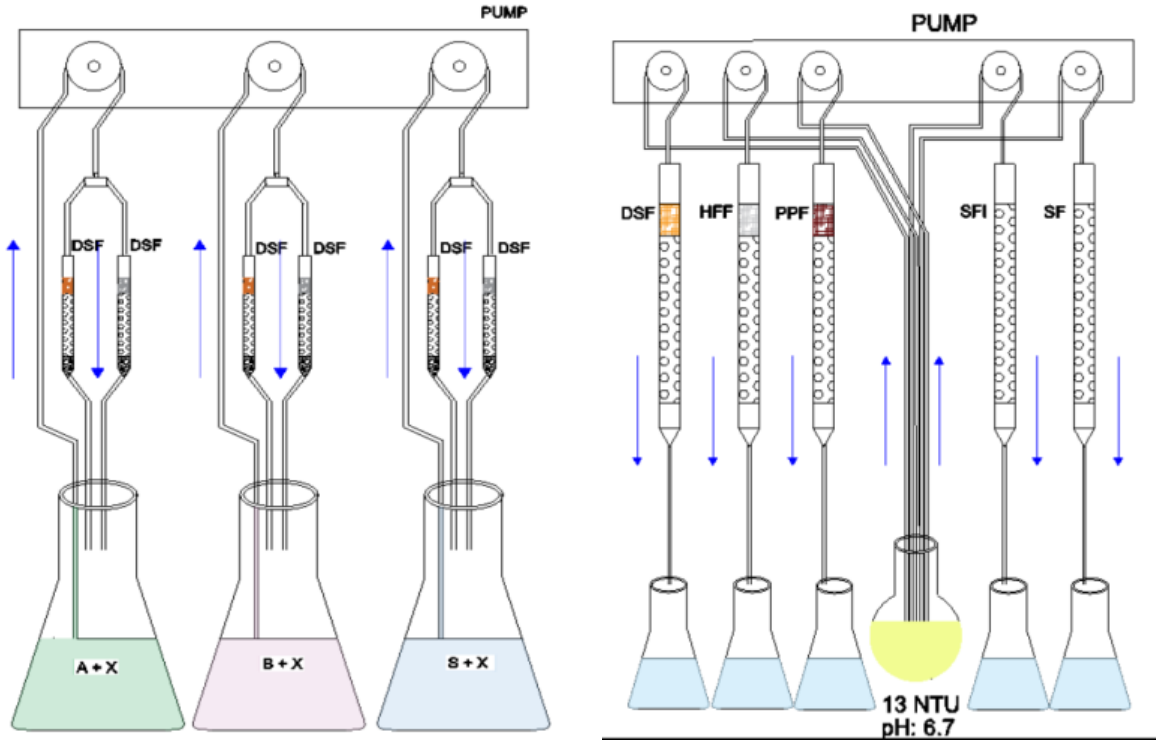

Figure 3.3.1: Schematic representation of: A) Model sand filter used for biofilm screening test

***Chryseobacterium* sp. and *Pseudomonas fragi* = X): A: Arthrobacter ramosus, B = Bacillus sp., S = *Sphingomonas* sp. (This figure represents only the set-up for deinking sludge filter in replica, similar set-up for other tested filters. B) Agro-residue sand filters (as a support material for sand filter) and sand filter with A+X (SFI) and sand filter without any inoculum (SF)**

Sand column experiment

After optimizing the physical input parameters, five different column filters (diameter: 25 mm, thickness: 2 mm and height: 650 mm) were installed in a top-down flow arrangement. Figure 3.3.1 (B) shows the schematic representation of the set-up. The filters were named according to the support material that was put at the top of the sterile-sand media (sterile 4-gram dry weight covering 2 cm height). From here on, dry deinking sludge, hemp fiber, and pulp and paper sludge supported over the sand media will be named as DSS filter, HFS filter and PPS filter, respectively. The other two filter column consists only of sand media (no agro-residue as support material inoculated with and without the screened bacterial strains, SFI and SF, respectively). SFI filter can

be assumed as a model filter representing the modified[29] filtration unit in a drinking water treatment plant (Chemin Ste-Foy, Quebec City, Canada). About 120 mm height was kept for the influent water to stand over the filter media and 40 mm was used for the drainage system at the bottom of the filter column, comprising bigger sand particle size in the range: 2 mm- 4 mm. Rest 480-500 mm height (including 20 mm for agro-residue material) was used as the filter media. A detailed grain size distribution analysis and related calculations for preparing the sand media is mentioned in the appendix D (Figure D1).

For a rapid biofilm development over the top layer of the filter material, high COD nutrient media of 800 mg/L suspended with high inoculum (6×10^8 cells/mL) was recirculated for about 12 days (30 mL every CSTI and adjusted accordingly based on biofilm growth[30]) where after 5 days, COD of the nutrient solution was readjusted to 800 mg/L. For tracking the biofilm development, TOC removal, protein concentration, flow rate and cell viability (MTT assay) was determined after 2 days, 6 days, 9 days and 12 days.

Before and after the biofilm development (day zero and day 12), Morrill dispersion index[31] (MDI) was determined as well to understand the behaviour of influent passage (degree of plug-flow condition) through the filter media and was found to be in the range of 2.25-2.52 for all the reactors. Generally, biofilm growth affects the flow passage and thus to ensure filter media void of air entrapment, this test was required.

Post-matured biofilm formation, all filters were run for 7 cycles (7 days each) using Lake Sainte-Anne (47.262879N, -71.665158W) as influent water. Approx. volume of 30 mL was fed into the filters after optimized CSTI (1 hour). Table 3.3.1 shows the characteristics of the lake water used along with other filter properties. According to lake history, there were no presence of cyanobacteria and cyanotoxin reported so far and the MC-LR analysis too shows no presence of it (< 0.03 µg/L, reports not shown herefor other microcystin variants). The filter was run continuously during the daytime (10 AM- 8 PM) and was appropriately auto-programmed (during night hours, based on average empty bed contact time, EBCT of each filter) to discharge water

[29] Sand as obtained from the filtration unit was further grinded to bring down D_{10} value close to 180 µm from 875 µm. Also, two bacterial: *Chryseobacterium sp.* and *Pseudomonas fragi* (X) were isolated from the filtration unit have been used as an inoculum.

[30] Biofilm growth hinders the flow rate and thus readjustment of CSTI is performed from time to time using an auto-dosage pump

[31] MDI of 1 represents an ideal plug flow reactor whereas MDI of 23 represents a complete stirred reactor.

into the filter such that CSTI is appropriately maintained. All the filters during the operation were backwashed with sterile tap water (bed expansion of around 10 % - 15 %) at the end of the 4th cycle. The airline tubing, check valves, and other accessories were washed at the end of every cycle to remove any deposited/built-up particles.

Water quality parameter analysis

The effluent collected from the filters were periodically analyzed for various water quality parameters comprising total coliform removal, turbidity removal, DOC removal, nitrate, nitrite, ammonia removal, dissolved oxygen content, flow rate, electrical conductivity, change in pH.

Table 3.3.1: Filter details and lake water characteristics

Filter	**DSF**	**HFF**	**PPF**	**SFI**	**SF**
Strain inoculated	*Arthrobacter ramosus* (A), *Chryseobacterium sp. and Psuedomonas fragi* (A+ X)	*Arthrobacter ramosus* (A), *Chryseobacterium sp. and Psuedomonas fragi* (A+ X)	*Arthrobacter ramosus* (A), *Chryseobacterium sp. and Psuedomonas fragi* (A+ X)	*Arthrobacter ramosus* (A), *Chryseobacterium sp. and Psuedomonas fragi* (A+ X)	No bacteria
MDI[32] (after 7 cycles)	2.45	2.77	2.88	2.38	2.12
Toxicity (eq. DMSO %)	2.3	9.2	14.3	7.6	22.1
Degradation contribution	22 %	17 %	13 %	9 %	0[33] %
EPS (µg/mg)	170 ± 13	142 ± 32	83 ± 21	67 ± 29	NA
SUVA (m^{-1}-L/mg C)[34]	2.88	3.05	3.25	3.24	3.21
SUVA removal (%)	17.1	12.2	6.4	6.7	7.5
Alkalinity after 4 cycle and after 7	46; 36	48; 39	51; 41	44; 43	34; 33

[32] MDI= Morill Dispersion Index (MDI=1 for ideal plug flow condition, MDI= 23 for the completely stirred reactor)
[33] Normalizing value of control (65 %), therefore assigned the value of MC-LR removal contribution set to zero.
[34] Initial SUVA of the raw lake water is 3.47 m^{-1}-L/mg C

Filter	**DSF**	**HFF**	**PPF**	**SFI**	**SF**
Strain inoculated	*Arthrobacter ramosus* (A), *Chryseobacterium sp. and Psuedomonas fragi* (A+ X)	*Arthrobacter ramosus* (A), *Chryseobacterium sp. and Psuedomonas fragi* (A+ X)	*Arthrobacter ramosus* (A), *Chryseobacterium sp. and Psuedomonas fragi* (A+ X)	*Arthrobacter ramosus* (A), *Chryseobacterium sp. and Psuedomonas fragi* (A+ X)	No bacteria
cycle (as $CaCO_{3)}$					
Lake water characteristics					
pH	**Alkalinity**	**$NH_4^+NO_2$**	**Al/As/Ba**	**NO_3^-**	**Conductivity**
6.59	23 mg/L as $CaCO_3$	1.4 ppm/ zero	0.13/<0.01 ppm	4.2 ppm	231 µS/cm

DSF: Deinking sludge filter, HFF: Hemp fiber filter, PPF: Pulp and paper sludge filter, SFI: sand filter without above state agro material as a support but with inoculation, SF: sand filter without agro materials.

Total coliform removal, DOC removal, nitrate, nitrite, ammonia, and turbidity removal

Total coliform removal was determined by the membrane filtration technique as discussed in the standard methods (APHA, 1998). The total coliform removal was reported as CFU/100 mL and determined at the end of every cycle. The initial coliform concentration reported in the influent-fed water (Lake Sainte-Anne, Quebec, Canada) was 451 ± 32 CFU/ 100 mL (averaging five tests). Based on this initial CFU value, total coliform removal was calculated (in %).

DOC of the influent and the effluent was determined using a Shimadzu 5000A analyzer (Shimadzu, Japan). Initial DOC was found to be 5 mg/L and its removal was reported in %. The optimized value for the initial turbidity was found to be 13 ± 1.1 NTU[35]. Effluent turbidity was measured after every two days of the cycle (twice/cycle) using HACH instrument 2100 model and the total turbidity removal was calculated in %. At the end of each cycle, initial concentration of 50 mg/L for nitrate (sodium nitrate), 10 mg/L nitrite (sodium nitrite) and 10 mg/L solution of ammonia (ammonium sulphate) was passed through the filter column and their final concentration in the effluent was determined using the method described in Naghdi et al. (2017) and reported in mg/L.

pH, dissolved oxygen and flow rate

[35] Initial turbidity of the lake water was 6 NTU and was increased using hydrated kaolin solution to mimic the optimized condition (13 NTU).

The pH of the effluent filtered sample was analyzed at the end of every cycle. Also, the dissolved oxygen of the effluent was measured using a portable F4-Standard probe (Mettler Toledo Inc) to check for any anoxic condition build-up and the biological activity (more activity more DO consumption and vice-versa). Initial DO of the lake water (aerated 30 minutes before each feed) was found to be 6.77 O_2-mg/L. The flow rate was measured for each filter at a constant (stand-by water) head of 7.5 cm from the top layer of the filter bed material every day at 17:00 PM. The value was reported in m/h($m^3/m^2/h$).

MC-LR assay and MC-LR degradation

MC-LR assay was performed to understand the relative toxicity of the effluent water based on the survival rate of the bioindicator cells (*Rhizobium meliloti*). A similar protocol as described in Kumar et al. (2018 a) was followed for this assay where MTT was used as a reagent at the concentration of 7 mg/10 mL. For this test, a surrogate and known toxic compound: dimethyl sulfoxide (DMSO) was used and the absorbance of the formazan[36] solution was spectrophotometrically analyzed at λ_{max}= 550nm to indirectly quantify the survived bacterial cells (rest killed by the degree of toxicity in the tested sample). The absorbance of the formazan solution at different concentration (0 % - 100 % v/v) of DMSO was related to the absorbance value of the formed formazan solution due to MC-LR (up to 900 µg/L) denoting the same degree of bioindicator mortality.

At day 3 and day 6 of each cycle, the column was passed with 50 µg/L of MC-LR (same matrix: lake water, pulse concentration). The effluent sample was collected and measured via ultra-high-pressure liquid chromatography (uHPLC) as described by Fayad et al. (2015). The MC-LR removal was reported as percent (%) removal (Table 3.3.2) discriminated into four different sections viz. removal due to 1.) Sand media only (physical removal by SF); 2.) Bacterial activity in the sand (represented as Bio 1, removal difference between SFI and SF); 3.) Support material (Agro residues) and bioactivity in only that region where agro-residual material is placed (indicated by Agro-material + Bio 2); 4.) remained undegraded.

Extra polymeric substance (EPS) and protein analysis

[36] Formazan is the term given to the bacterial cell precipitate formed when MTT is added to the live bacterial cells

The EPS quantification in the biofilm formed over the agro-residue was performed (after cycle 7, before filter column dismantling) by ethanol precipitation method as previously described by Boon et al. (2008). In brief, top 10 mm or around 2-gram of the agro material (sand in case of SFI) was carefully removed from the column filter and suspended in 10 mL of tap water to initiate cell lysis (cell-shock). A cell-lysis buffer solution was spiked (5 mL) to further lyse the cells. Afterwards, the solution was vortexed for 2-3 minutes and centrifuged at 7000 x g at room temperature for 20 minutes. The derived supernatant was mixed with twice the volume of ethanol (around 25 mL) and kept at -20 °C overnight. The precipitated EPS was reported in µg/mg of the dry mass of the agro residue taken initially.

For the protein analysis, approx. 0.1 gm of agro-residue from the top of each column filter (DSF, HFF, PPF) was carefully taken and suspended in 1.5 mL of distilled water (microcentrifuge tube). After 2 minutes of vortex and centrifugation (8000 x g) at room temperature for 3 minutes, the supernatant was analyzed for the total protein analysis by Bradford assay and reported as µg/mL (Bradford, 1976).

Bio-profiling of column filters and SEM imaging

To understand the distribution profile of the bacterial cells (cell proliferation) in each biosand filters, samples were carefully isolated for every 2 inches (approx. 50 mm) of the glass column. Each sample was appropriately mixed and around 0.5 gram was dipped in 1.5 mL of tap water to carry the CV assay (biomass distribution profile) and MTT assay (viable cell distribution profile) as described in previous section. Since higher bioactivity was expected in the top layer of the filter media (agro-residue + some sand material), the contribution of the top 5 cm of the filter material in terms of cell biomass and cell viability was calculated as per the Equation 10 below:

$$\% \text{ change in biomass/cell viability} = \frac{(\text{Absorbance at first sampling point (at 0.75 cm)} - (\text{Absorbance at 5 cm})}{\{\text{Absorbance at 0.75 cm} - \text{Absorbance at last point of sampling (at 40 cm)}} \quad \text{Equation 10}$$

SEM images for the agro-residues (support material used in the biosand filters) were obtained both before and after the biofilm formation. The structure of the agro-residual fiber after the biofilm formation was observed closely for its integration with biocells (EPS). Such integration where these fibers can play the role of an architectural element is necessary for the long-term adhesion of the bacterial cells and hence the biofilms (Serra et al. 2013). The micrographs were captured

between 12-15 kV accelerating voltage (Zeiss EVO ® 50 Smart SEM system). Before obtaining the images, the materials were gold plated (15 nm thickness) using a sputter coater.

Statistical analysis

All statistical analyses comprising standard deviation, average, student t-test, p-value comparison, and all graphical presentations were performed in ORIGIN software (Version 8.5; OriginLab).

Results and discussion

Screening of the bacterial strains

Figure 3.3.2 (A) and (B) shows the absorbance values results for CV assay and MTT assay used for the quantification of cell biomass and cell viability, respectively for all three bacterial strains inoculated (A+X, B+X, and S+X) and different materials (DS, HF, PP, Sand). Among the three tested bacterial strains, *Bacillus sp.* (with X) showed the least affinity towards all the three agro-residue support materials (least absorbance by CV and MTT assay as compared to A+X and S+X (Figure 3.3.2 (A, B). However, there was a close competition for screening between *Arthrobacter ramosus* and *Sphingomonas sp.*, with both showing a similar affinity towards the tested materials. To further resolve this deadlock, an MC-LR assay (initial MC-LR concentration: 50 μg/L) was performed at the end of day 7, to quantify the degree of toxicity in the filtered sample from each filter (detailed results shown in Table D1, Appendix D).

The biomass formed by A+X on DS, HF, and PP was comparatively 1 %, 9.4 %, 22 % higher than S+X case (calculated by taking mean absorbance values for day 2, day 4 and day 7). On the other hand, the viability of bacterial cells over DS, HF, and PP was 1.1 %, 8.3 % and 4.5 % higher for A+X as compared to S+X[37]. Also, the relative toxicity of the filtered sample at the end of day 7 was found to be 8.4 % less toxic for A+X case as compared to S+X (for all three agro-residue material[38]). Thus, *Arthrobacter ramosus* (with the native bacterial strains: A+X) was finally screened for all the three agro-residue as it was found to be the most desirable biofilm forming MC-degrader as well as producing relatively less toxic filtered sample than others.

[37] B+X was not compared as the assay results show that the quantification for biomass and cell viability has always remained lower when compared with A+X and S+X.
[38] Also individually too, each agro-residue material gave less toxic effect by A+X case.

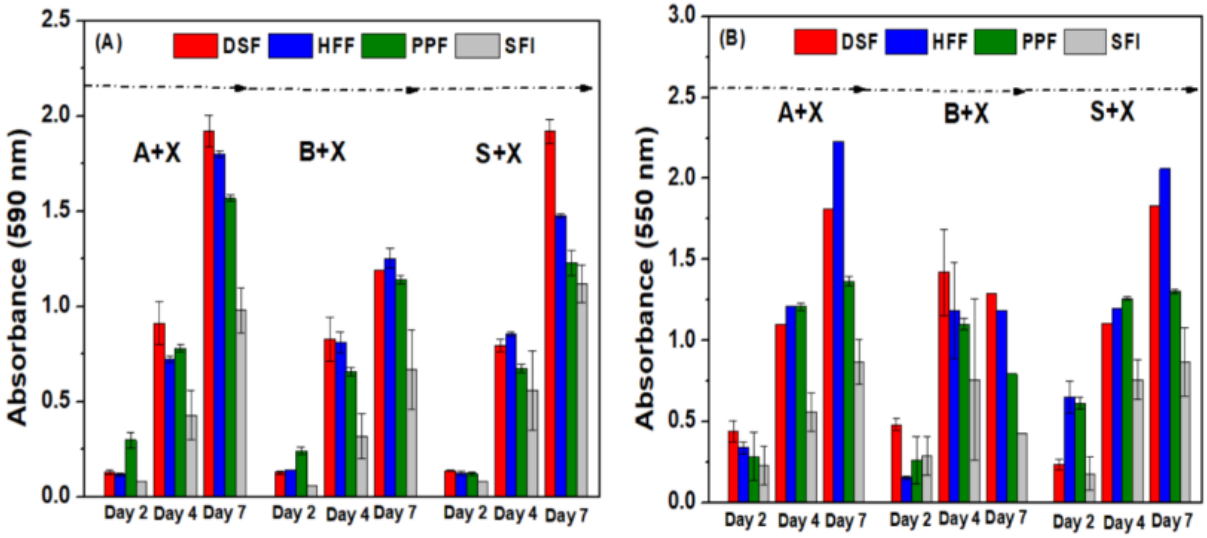

Figure 3.3.2: A) Crystal violet assay and B) MTT assay for agro-residue model sand filters and sand filter

DSF: Deinking sludge filter, HFF: Hemp fiber filter, PPF: Pulp and paper sludge filter, SFI: sand filter without above state agro material as a support but with inoculation, SF: sand filter without agro materials; Chryseobacterium *sp. and* Pseudomonas fragi = *X): in combination with three microcystin-degraders viz. A:* Arthrobacter ramosus, *B* = Bacillus *sp., S* = Sphingomonas *sp. (individually).*

Optimization of input parameters using CCD technique

Physical parameters viz. initial turbidity, pH and CSTI were evaluated using the central composite design of an experiment, analyzing output desirability via response surface methodology (RSM). Various RSM plots were obtained for each of the output parameters (all plots are shown in the appendix D: Figure D2). A desirability index of 0.685 was obtained based on the goal set-up for an input-output relation. The optimized pH, initial turbidity and CSTI obtained were 6.8, 13 NTU and 3 hours, respectively. Except for two models (pH change: prob> F; 0.96, and turbidity removal: prob > F; 0.32), rest all five output models were found to be significant to the three inputs (at three different levels. Coliform removal was found to be significantly dependent upon all the three input parameters (pH (A): p-value= 0.002 (A^2); CSTI (B): p-value= <0.0001 (B^2); Turbidity (C), p-value= 0.006 (C^2)). It is obvious that with an increase in the value of parameter B, shows a positive impact on the total coliform removal (+ 17.44 B^2). For the effective DOC removal, RSM model shows an obvious negative correlation with turbidity (-3.9 C^2) and positive relation with CSTI

(+14.4 B), indicating low influent turbidity and high retention time increases filter performance in terms of DOC removal.

Model equation for MC-LR assay depicted a necessary inference that when pH decreases, the toxicity of the filtered sample decreases too (-0.23 A^2, p-value: 0.006), which agrees to the fact that MC-LR adsorbs to the surface better at low pH (Teixeirra et al. 2012). In a DWTP, where disinfection is next to the filtration system, a low pH can favour both treatment units delivering MC-LR maximum adsorption followed by effective disinfection (Ward et al. 1984). The flow rate is an important parameter too providing quick and effective filtration at the same time without compromising the water quality parameters (Mallongi et al. 2016). Model equation showed sensitive and significant (p-value < 0.0001 for a C^2 variable, $-0.64C^2$) relation with the initial turbidity resulting in to be operated at 13 NTU for an optimum filter run. It may be noted that the present system working at 13 NTU (initial turbidity), needed backwash after an active filter run of 28 days (from mid-cycle 2- cycle 6) agrees in good agreement with Gottinger et al. (2011) for the effective treatment of Canadian rural prairie water using SSF[39] where backwashing needed after 40 days.

Biofilm formation

To verify the development of a mature biofilm, various parameters such as flow rate, DOC, protein content and cell viability were analyzed. Figure 3.3.3 (A, B, C, D) shows the analysis for the above parameters in the same order. Filter DSF, HFF, and PPF start off with a reduced flow rate of 0.78 m/h, 0.82 m/h, 0.67 m/h as compared to 1.45 m/h for SF because of the less density and fineness property of the agro-residues being used as the support material. On day 9, backwashing (at a slow flow rate) was performed because the hydraulic conductivity shall in no case reduce to $1/4^{th}$ the initial value (around 2.4 m/h). Users/researchers are directed to maintain the filters (backwashing/harrowing) when flow rate becomes too slow; thus, our designation of $¾^{th}$ reduction in flow rate is a subjective minimum.

[39] SSF= slow sand filter (Filter DSF, HFF and PPF is a kind of slow sand filter as flow rate range: 0.1 m/h – 0.4 m/h)

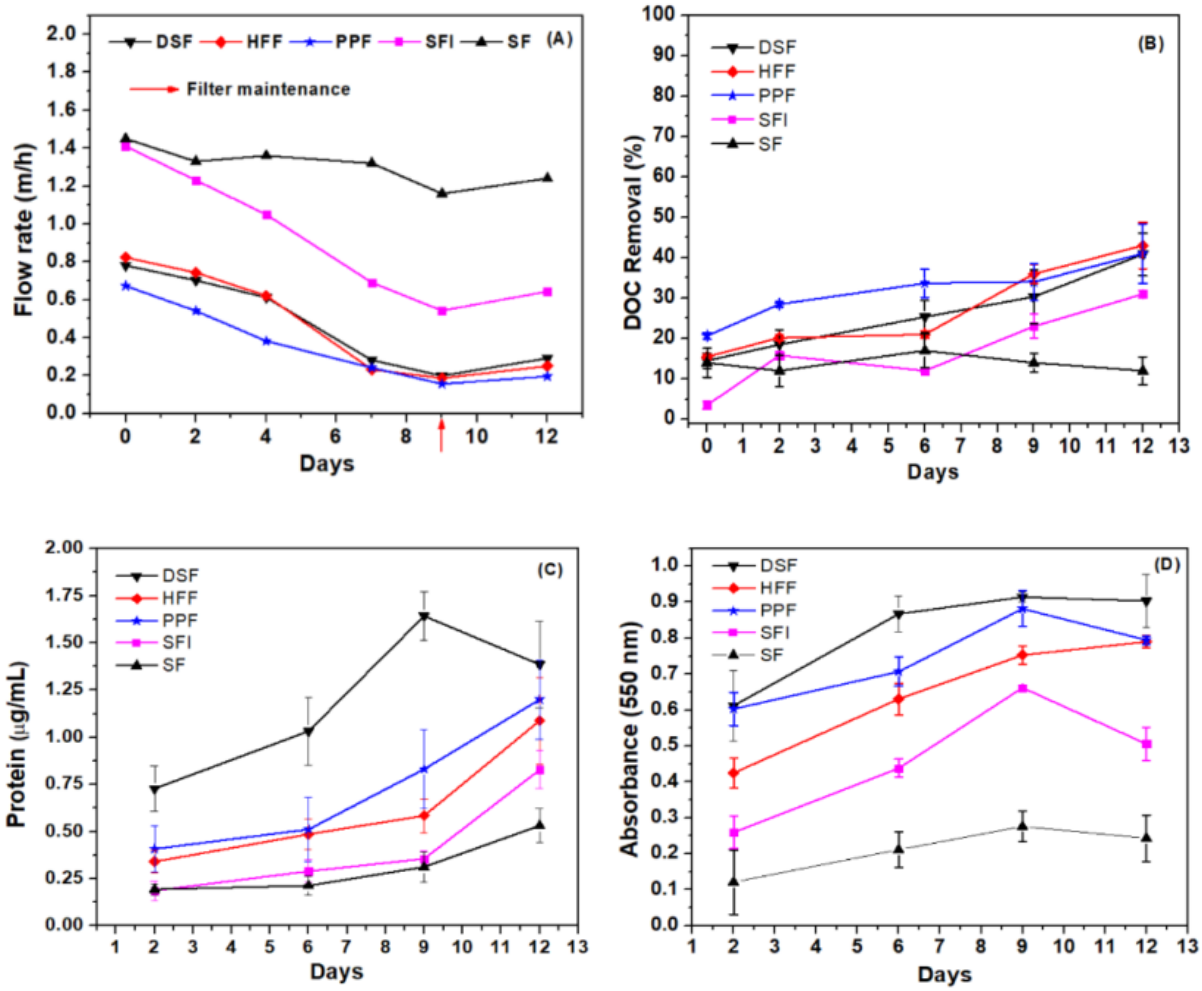

Figure 3.3.3: A) Flow rate; B) Dissolved organic carbon; C) Protein content and; D) cell proliferation of biofilm sample obtained for all the filters tested during the biofilm development phase

DSF: Deinking sludge filter, HFF: Hemp fiber filter, PPF: Pulp and paper sludge filter, SFI: sand filter without above state agro material as a support but with inoculation, SF: sand filter without agro materials.

The increase in the protein concentration and the DOC removal might be attributed to the colonization of the inoculated bacterial strains (A+X). After day 12, both the above parameter showed a constant behaviour till day 18 (not shown in Figure 3.3.3 (A) and (B)), highlighting the mature growth inside the pores of the filter media (sand). More confirmatory evidence of the same was derived from the MTT assay, performed for the top layer of the filter media (around 0.4 g mass, process details in method section) showing the constant amount of viable cells even after the backwashing event at 0.06 m/h and 15 % bed expansion.

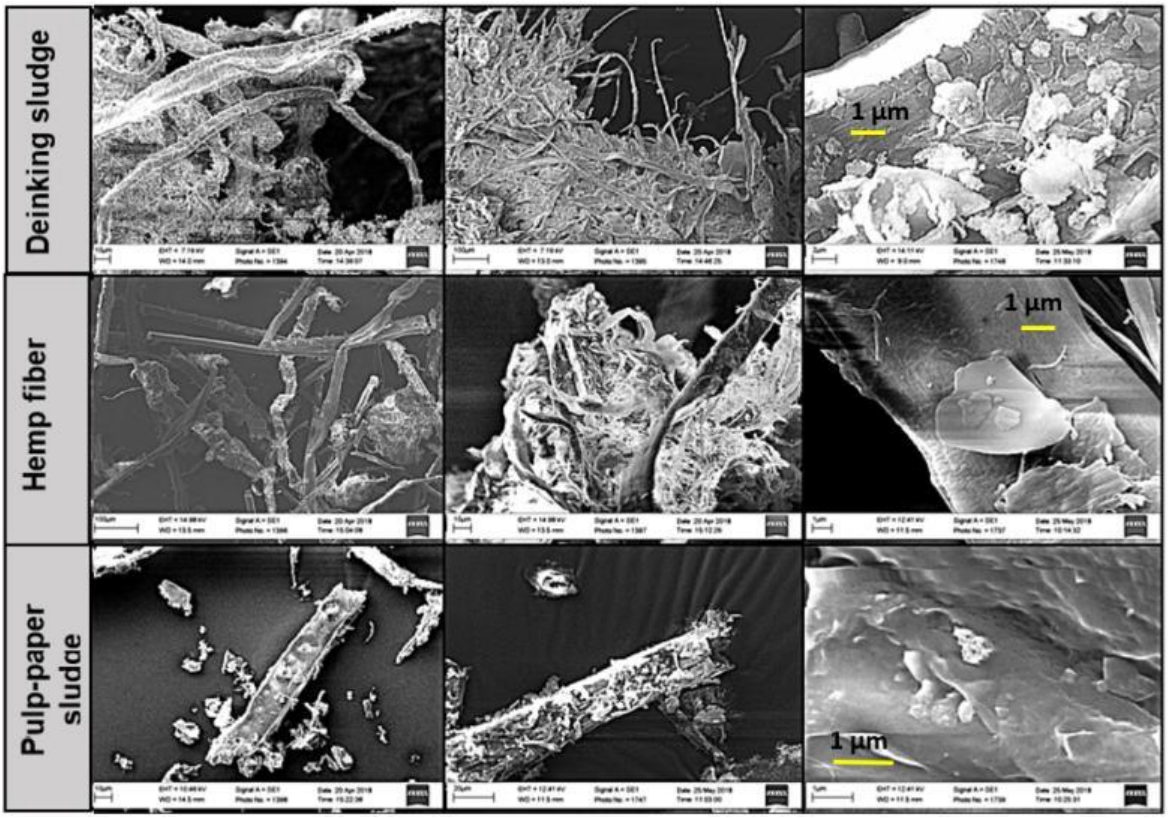

Figure 3.3.4: Scanning electron microscopy images of agro-residue materials viz deinking sludge, hemp fiber and paper-pulp sludge both before (A, D, G) and after (B, E, H) biofilm formation. A closer look (indicated by yellow colour (length of 1 µm)) is also provided (C, F, I).

Routine sample analysis after biofilm formation

Post-biofilm formation, all filters were primed for about 80-bed volume for 3 days every hour to remove excess turbidity in the effluent due to loosely attached biomass within the column. Table 3.3.2 shows various water quality and other filtration parameters that were analyzed after the priming event. Maximum coliform removal of 92.7 ± 12.8 was achieved by DSF followed by HFF and PPF (around 83 % each, Table 3.3.2) and were > 30 % higher than SF. This observation reveals that agro-residue as the support material enhanced the pathogenic bacteria entrapment due to their less pore volume behaviour as compared to sand particle (not mentioned) where further colonization of bacterial strains enhanced the bacterial activity in ARSFs to allow a substantial degree of predation. Predation mechanism, top-down trophic interaction, and adsorption to biomass could be the reason for high coliform removal as mentioned above (Haig et al 2014). Wand et al. (2007) too revealed enhanced coliform removal (3-4 log removal) in a sand filter due to the predation mechanism which can be linked to the effective microbial colonization.

Table 3.3.2: Filter performance for water quality parameters

Filter	Coliform removal (%)	Turbidity (NTU)	DOC removal (%)	NO_3^- (mg/L)	NO_2^- (mg/L)	NH_3-N (mg/L)	Flow rate (m/h)	pH	DO (mg-O_2/L)	MC-LR removal (%)
DSF	92.7 ± 12.8	0.9 ± 0.3	44 ± 11	3.25	2.5	0.04	0.3 ± 0.1	6.4 ± 0.4	4.3 ± 1.2	87 ± 14
HFF	83.1 ± 11.3	0.8 ± 0.4	35 ± 3	18.6	3.4	0.21	0.25 ± 0.1	6.5 ± 0.3	4.85 ± 1	82 ± 7
PPF	84.1 ± 11.8	1.0 ± 0.3	31 ± 7	18.7	4.6	0.23	0.19 ± 0.1	6.6 ±0.3	4.6 ± 0.9	78 ± 4
SFI	68.5 ± 17.8	2.5 ± 1.4	29 ± 5	26.1	7.1	0.32	0.62 ± 0.2	6.9 ±0.3	4.5 ± 1	74 ± 5
SF	54.8 ± 11.7	4.1 ± 0.7	26 ± 9	39.9	8.1	1.19	1.06 ± 0.1	7.2 ± 0.2	5.3 ± 0.2	65 ± 4
Guide lines	100%	<1 not more than 3 NTU	NA	<45 mg/L	<3 mg/L	<0.121 mg/L	SSF[40]: 0.1-0.4	7-10.5	2-4 ppm	<1 µg/L

Effluent turbidity for the agro-residue sand filters showed similar (range: 1-1.4 NTU) response to each other. However, the turbidity of the effluent for ARSFs was better than SFI (2.53 ± 1.4 NTU) and SF (4.0 ± 0.7 NTU). Relative low turbidity in ARSFs as compared to SF or SFI can be attributed to the enhanced particle staining due to biolayer formation and change in the media particle/surface. Like the current study, Napotnik et al. (2017) too found a positive correlation between turbidity and coliform (*E.coli*) removal in the long term operated biosand filter. WHO recommends turbidity of < 1 NTU for efficient chlorination (WHO, 2004).

Inoculated sand filter (SFI) without agro-residue achieved an average DOC removal of 29 ± 5 %, very similar to what Campos et al. (2002) achieved (23 % – 25 %). On the other hand, DOC removal in ARSFs: DSF, HFF, and PPF were 15 %, 6 %, 2 % and 18 %, 9 %, 5 % higher than SFI and SF, respectively. This indicates higher bioactivity in the agro-residue filters (especially DSF) as compared to the inoculated sand filter (SFI) possibly because of the higher surface area of the support material (low void ratio) and higher biomass growth within the filter column. Collins et al

[40] SSF: Slow sand filter

(1994) too observed an increase in organic carbon removal with an increase in the biomass concentration in the sand.

This phenomenon can also be backed up by the reduction of pH and DO in the filtered effluent of the inoculated filters (SFI, PPF, DSF, HFF) when compared to SF (Table 3.3.2). Agro-residue supported sand filters (ARSFs) were also able in removing ammonia from the influent feed water to close to the guideline values (0.121 mg/L), which indicated a healthy behaviour of a mature filter (Ellis et al. 2009). Also, the denitrification property of ARSFs filters (especially DSF) was found to be significantly higher than SFI (> 55 % for NO_3^- as well as NO_2^- removal), achieving below guideline values of 3.25 mg-NO_3^-/L and 2.5 mg- NO_2^-/L. Sun et al. (2018) too observed the enhanced performance in denitrification (NO_3^- to N_2) using agro-residues in the form of corncob and wheat straw. In general, SSF shows an increase in the nitrate removal once the bacterial colonization captivates as also studied by Adeniran and Akanmu (2013) which showed an increase in the nitrate removal from 25 % (day 1) to 74 % (day 27). In the current study, SF achieved nitrate removal of 21 % which increased to 48 % due to bacterial inoculation (SFI) and further to 64 % each for HFF and PPF and 93 % for DSF.

It must also be noted that the agro-residues usually has a high C/N ratio which can cause NO_3^- limitation for the denitrifiers (lower depth of the material), thereby promoting N_2 conversion (Her et al. 1995). Hence, the denitrifiers present at the lower region of the filter will face lower concetration of nitrates to be broken effectively into nitrogen. However, if the amount of liable carbon is more (due to the high C/N ratio), it may further enhance the rate of denitrification as inferred from Miller et al. (2008). Thus, deinking sludge may consist more liable carbon as compared to HF and PP agro-residues raising the C/N ratio (not determined) and making their surface more available for the denitrifiers. However, no particular study was performed to know the stability of the DS material as they are more prone to biodegradation which might need periodical replacement as a support material to the sand filter. Moreover, higher DOC removal of 44 ± 11 % achieved in DSF as compared to 35 ± 3 % and 31 ± 7 % in HFF and PPF may be linked to the high liable carbon present within the filter (HFF and PPF) which might be responsible for hindering the denitrification (ineffective nitrite and nitrate removal for HFF and PPF as compared to DSF, Table 3.3.2). These discussions also led to an interesting conclusion that a large portion of denitrification might have happened within the ARMs in the ARSFs.

MC-LR removal and MC-LR assay (toxicity) analysis

Figure 3.3.5 shows the bar graph representation of the MC-LR removal, discriminated into four categories as discussed in the method section. Maximum MC-LR removal of 87 ± 14 % was achieved by DSF comprising all seven cycles of the filter run. Other ARSFs viz. HFF and PPF achieved MC-LR removal of 82 ± 7 % and 78 ± 4 %, respectively. As compared to the inoculated sand filter (SFI), ARSFs enhanced the overall MC-LR removal by 13 % (DSF), 8 % (HFF) and 4 % (PPF). The contribution of the agro-materials (and bioactivity they possess: Bio 2) for MC-LR removal can be observed from the graph (black bar coverage), being more prominent for DSF. The consistency of their share in degrading MC-LR became more sound towards the latter part of the cycles (cycle 4-cycle 7) especially for DSF which achieved almost complete MC-LR removal (Figure 3.3.5). Mcdowall et al. (2009) too showed that biodegradation plays a key role in the filter system where cyanobacterial metabolites: geosmin got removed by an extra 38 %.

The mutual property of bacterial cells and their interaction with the surface (to be attached) plays a key role too. If the bacterial strains are not properly acclimatized (immature and weak) and attached to the surface (agro-residue material here), it may lead to low degradation of the contaminants. Likewise, as can be observed from Figure 3.3.5, degradation of MC-LR during initial few cycles was low for DSF and HFF. However, once the acclimatization of bacteria with MC-LR have occurred, the overall percentage degradation increased too (Figure 3.3.5). Even the breakthrough period prolongs for the filter if proper acclimation has occurred. However, for PPF, as can be seen from the SEM images, that the bacterial attachment is not too dense and captivating over the surface. This might be the reason for less enhancement in the bioactivity for PP material which eventually leads to similar MC-LR removal as that of SFI (74 % -78 %). Holst et al. (2003) and Christoffersen et al (2002) too studied acclimation activity of bacterial community with MC-LR and found to be an impactful event in its removal.

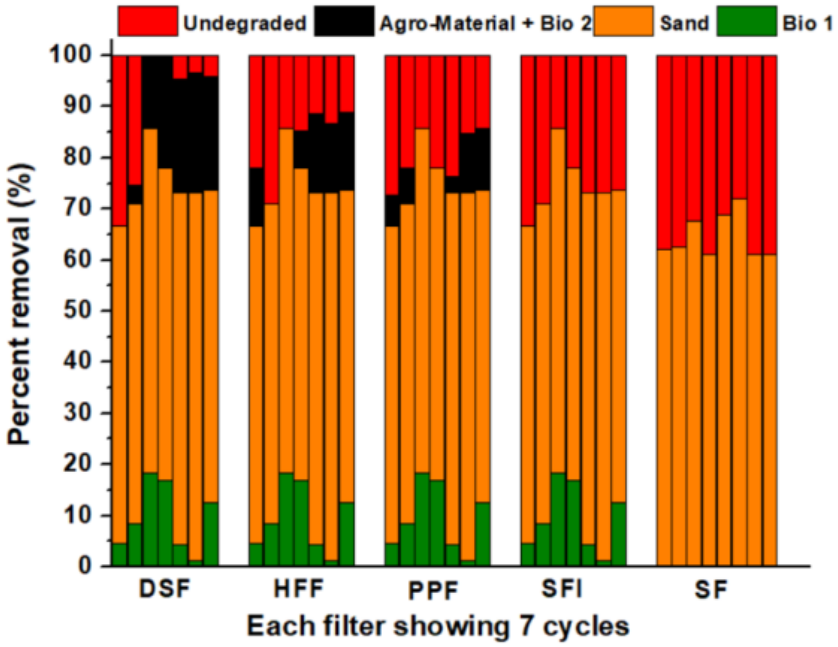

Figure 3.3.5: Microcystin-LR removal contribution due to: a) sand only (orange bar); b) bioactivity (bio 1) within sand media (green bar); c) Agro-material and bioactivity within it (black bar) and d) undegraded portion (red bar)

Backwashing was performed after cycle 1 for DSF and HFF and after cycle 2 for PPF. The phenomenon had a negative effect on HFF and PPF while a positive effect on DSF in terms of MC-LR removal. It might be due to the persistent, more stable and potential biofilm that colonized the DS material. Figure 3.3.4 (A to I) shows the SEM images for the three agro-residues, before and after the biofilm formation. It can be observed that the fibers present in the DS became more attached like a 'cloth' structure (Figure 3.3.4 (B)) after the biofilm formation which PP material lacked (Figure 3.3.4 (H)). HF material too exhibited binding of fibers (Figure 3.3.4 (E)). The effective binding might be due to the extra polymeric substance (EPS) which is an integral part of the biofilm development. To confirm this, EPS was quantified at the end of cycle 7. The reported EPS was found to be in order: DSF (170 ± 13 µg/mg) > HFF (142 ± 32 µg/mg) > SFI (83 ± 21 µg/mg) > PPF (67 ± 29 µg/mg). Thus, it may be possible that the production of EPS during biofilm maturation helped in an effective binding of the fibers in DS and HF material which was around 2.5 and 2.1 times higher than PP material. However, it is very interesting to observe that the EPS production in SFI was more than PP material which can be related to the less bioactivity (less EPS) that might be the cause for just 4 % increase in MC-LR removal (Table 3.3.2). In two cycles (cycle

3 and cycle 4), DSF even showed potential in achieving below detection level concentration of MC-LR in the effluent filtered water.

Due to the difficulty in culturing bioindicator (*Rhizobium meliloti*) for the initial few cycles of the filter operation, toxicity assessment of the filtered samples for each filter was performed only for the last three cycles. Equivalent DMSO concentration of the filtered sample from DSF, HFF, PPF, SFI and SF was reported as 1.19 ± 0.18 %, 3.16 ± 1.38 %, 7.49 ± 1.62 %, 8.36 ± 1.8 % and 17.1 ± 0.81 %, respectively. In some literature, > 1 % - 2% DMSO (v/v) has been reported to affect the human cells such as epithelial cells, vascular endothelial and platelet cells, suppressing the expression of inflammatory cytokines, etc. (Proost et al. 2016, Yi et al. 2017, Cao et al. 2007). According to the mentioned facts, only filter DSF qualifies based on the toxicity assessment. As mentioned by Koechler et al. (2015), attached growth system with high protein, EPS (diffusion barrier reduces the toxic concentration) and nutrient around bio cells helps them to survive under the toxic environment (toxic compound resisting mechanism). With this context, in the present study, maximum protein estimated in the supernatant solution during biofilm development for DSF was around 1.50 μg/mL as compared to < 0.80 μg/mL for SFI (Figure 3.3.3 (C)). Also, the EPS quantified (as discussed above) in case of DSF was significantly higher than SFI.

Bio-profiling of column filters

Bio-profiling of the filter revealed that most of the biomass and viable cells resided in top 10-15 cm of the filter. Figure 3.3.6 (A) and (B) show the quantification (indirect) of cell biomass and cell viability (based on the absorbance values) for DSF and followed in the order: DSF > HFF > PPF > SFI > SF. Biomass and viable cell activity in the top 5 cm of the filter material were calculated according to the equation mentioned in method section. A decline of around 39 % and 35 % in the activity of the cell biomass and cell viability was found for DSF (comparing to the absorbance at 0.75 cm sampling point), highlighting a major portion of the bioactivity lying within the DS material. Similarly, for HFF and PPF, these values were: 25 %, 27 % and 16 %, 15 %, respectively and in the range 8 % - 11 % for SFI and SF[41], respectively.

[41] Bioactivity in the uninoculated filter (SF) had come from the bacterial community present in lake water (influent as feed)

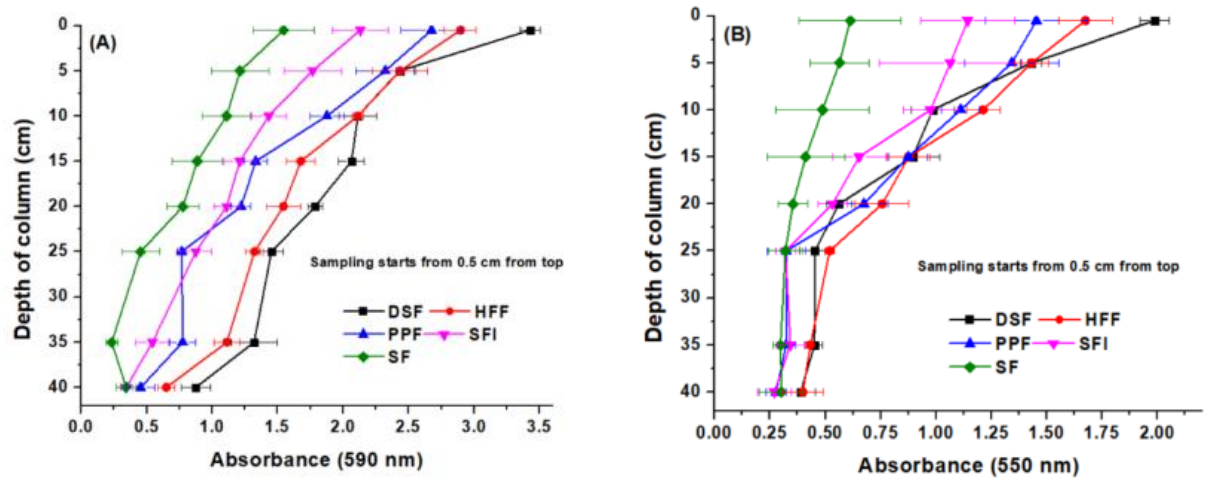

Figure 3.3.6: Bio-profile of all five sand filters based on the quantification of A) cell biomass (crystal violet assay) and; B) cell proliferation (viability by MTT assay).

High bacterial activity at the top part of the filter may be responsible for the effective ammonia removal (nitrification) in case of DSF (reducing NH_3^- concentration to below guideline value, Table 3.3.2) as compared to HFF and PPF. No special experiment was done for the quantification of the adsorbed MC-LR within the support material and thus physical adsorption of the same was not analyzed. Campos et al. (2002) and Duncan et al (1988) too observed the same trend (decrease in biomass as depth increase) in the biomass growth over the sand media and highlighted the importance of major microbial growth over the top layer of the filter media contributing significantly to the water purification. In this study, the influence of higher microbial community growth (both in terms of cell biomass and viability) observed at the top 10 cm of filter media rightly suggests the versatility of ARSFs, especially DSF, which showed 13 % more MC-LR and 15 % more DOC removal than SFI.

Bioaugmentation of sand filters with microcystin degraders: an asset

Bioaugmentation of sand filters in a DWTP using MC-degraders can be an asset for an effective removal of microcystins. However, care must be taken during inoculation that it should be enough to compete with the native or indigenous bacterial community residing over the sand media. In this work, the purpose of high inoculation of the specific bacterial strains, i.e., A+X, was to maximally counter the growth of any opportunistic bacterial strains present in the lake water (used as a feed) that might have grown over the agro-residue and the sand media present inside the filter column. The plate count method reported the heterogenous bacterial cell count present in the lake

water to be around 2.8 x 10^5 cells/mL (averaged for 4 media plates used for the experiments). This value is around 2000 times less as compared to the inoculated strains (A+X). It has been mentioned by Bourne et al. 2006, that the high cell inoculation (as high as 10^7 or 10^8 cells/mL) not only helped in forming quick biofilm but also ensured that the level of microcystin degrading strains always exceeded the level of indigenous bacteria which resulted in an increased chance of survival of the former in the biological filtration systems.

The optical density value (OD λ_{600} nm) was derived from the growth-curve at 25 °C for A+X (2 colonies each of *Arhtrobacter, Chryseobacterium and Pseudomonas fragi* to start with) and heterogeneous bacterial species (picked 6 different individual colonies from the growth plate). The maximum OD value of former (A+X) has always remained on the higher (2.7-3 times) side as compared to the latter case till stationary phase of the growth was reached.

To further confirm the dominance of A+X bacterial strains for a longer period of time over the top layer of the sand filter, MC-LR removal was analyzed after 32 days from the completion of the last cycle (cycle 7). The removal percentage of MC-LR was reported as 75 %, 67 % and 64 % for DSF, PPF and HF as compared to < 45 % for SF. Here, it must be understood that the filter after 7 cycles was kept under minimum maintenance condition and hence the reported MC-LR removal values are almost 5-10 % lesser than the average of 7 cycles (Table 3.3.2). But, still, the trend of MC-LR removal was similar as it was during the filter operation from cycle 1 to cycle 7 (DSF > HF > PPF > SFI).

Also, a very interesting finding in the same research paper was that the microcosm experiment demonstrated the enhanced microcystin removal when the MC-degrading bacteria (MJ-PV) were inoculated with just 100 cells/mL (Bourne et al. 2006). This suggested that the inoculated bacteria, i.e., MJ-PV which contains the *mlrA* genes, is quite powerful when it comes to tackling the indigenous bacterial community that might have tried to overpower the microcystin degraders. In our work too, the inoculated strains in the filter were of the genus: *Arthrobacter ramosus* (which expresses *mlrA* gene, Manage et al. 2009) and X which is a combination of *Pseudomonas fragi* and *Chryseobacterium sp.* which has been proven to be a good MC-degrader in our previous study (Kumar et al. 2018). Thus, considering a high inoculation (6 x 10^8 cells/mL) of the potential strains capable of MC degradation in the current study is significantly higher than the critical cell concentration (10^2 cells/mL) needed for the enhanced microcystin degradation (from above

discussion). Likewise, the performance of filter followed the same trend even after 32 days of major filter operation (cycle 7), which indicated the prolonged, proactive behaviour of the inoculated strains (A+X). However, a taxonomical study is still required to confirm the presence of inoculated bacteria for a longer duration.

Conclusion

Agro-residue material (ARMs) in the form of deinking sludge (DS), hemp fiber (HF) and paper and pulp dried-sludge (PP) was utilized as a support material to enhance the bioactivity of the sand filter (DSF, HFF and PPF). Overall, as compared to the normal inoculated sand filter (no agro-residue as a support material: SFI), DSF performed better among other agro-residue supported sand filters (ARSFs). DSF showed enhanced dissolved organic carbon removal (15 % more than SFI, and 9 %, 13 % more than HFF and PP, respectively), microcystin-LR removal (13 % more than SFI and > 5-10 % when compared to HFF and PPF), nitrification (to below guideline level), and maintaining pH and dissolved oxygen well within the guideline values (pH: 7- 10.5 and dissolved oxygen: 2-4 mg/L). Water quality parameters were improved using the ARSFs. DSF, HFF, and PPF removed > 83 % of total coliform on an average as compared to 69 % in SFI. Also, the turbidity of the filtered water remained in the range: 0.8 – 1.0 NTU for ARSFs while it remained 2.5 ± 1.4 NTU and 4.1 ± 0.7 NTU for SFI and sand filter (SF) filter, respectively. Scanning electron microscope images showed high extra polymerase substance (EPS) with DSF: 170 ± 13 μg/mg > HFF 142 ± 32 μg/mg > SFI 83 ± 21 μg/mg, that might have been responsible for effectively binding the fibers of DS and HF material forming stable biofilm surface. Bio-profile of the ARSFs showed most bioactivity present within the top 10 cm of the filter media which included 5 cm of ARMs. Morrill dispersion index for ARSFs, even after 7 cycles of filter operation remained in the range 2.4-2.9 as compared to 2.12 for SF providing evidence of persistence plug flow condition. However, the stability of these agro-residue needs further study as they can be degraded over time. Following are some research gaps/ research implications:

a) More in-depth analysis for the nitrification/denitrification needs to be studied by increasing the ARMs depth in a column filter. Such filters will be effective and essential for the surface water polluted with fertilizers (high ammonia).

b) Long-term stability of the ARMs is crucial for the plant operators to understand the frequency of material change-over.

c) Breakthrough period of the filter should be determined for the MC-LR compound or otherwise, the formation of toxic microcystin-chloride compound (resulting from the disinfection step) will be received at the tap source by the consumers.

Acknowledgment

The authors are sincerely thankful to the Natural Sciences and Engineering Research (Discovery Grant 23451), Genome Québec, Genome Canada (Grant 6116548-2015) and ATRAPP (Algal blooms, treatment, risk assessment, prediction, and prevention) for financial support. Special thanks to Dana Simon for coordinating the sample receipt and analysis. Authors would also like to thank the team for constant support and timely suggestions. We want to thank Genome Quebec for timely sequencing for the bacterial identification. The views or opinions expressed in this article is exclusively those of the authors.

Conflict of interest

None

References

Achak, M., Mandi, L., & Ouazzani, N. (2009). Removal of organic pollutants and nutrients from olive mill wastewater by a sand filter. *J Environ Manage, 90*(8), 2771-2779. doi:10.1016/j.jenvman.2009.03.012

Adeniran, A. E., and Akanmu, J. O. (2013). The Efficiency of Slow Sand Filters in the Treatment of Secondary Effluent from a Water Hyacinth Domestic Sewage Plan. NSE Technical Transactions, 47(2).

APHA, AWWA, WPCF. 1998. Standard methods for the examination of water and wastewater, 19th Ed., Washington, D.C.

Boon, C., Deng, Y., Wang, L.-H., He, Y., Xu, J.-L., Fan, Y., Zhang, L.-H. (2007). A novel DSF-like signal from Burkholderia cenocepacia interferes with Candida albicans morphological transition. *The ISME Journal, 2*(1), 27-36. doi:10.1038/ismej.2007.76

Bradford, M. M. (1976). A rapid and sensitive method for the quantitation of microgram quantities of protein utilizing the principle of protein-dye binding. *Analytical Biochemistry, 72*(1-2), 248-254. doi:10.1016/0003-2697(76)90527-3

Bourne, D. G., Blakeley, R. L., Riddles, P., & Jones, G. J. (2006). Biodegradation of the cyanobacterial toxin microcystin LR in natural water and biologically active slow sand filters. *Water Research, 40*(6), 1294-1302. doi:10.1016/j.watres.2006.01.022

Cao, X.-G., Li, X.-X., Bao, Y.-Z., Xing, N.-Z., & Chen, Y. (2007). Responses of Human Lens Epithelial Cells to Quercetin and DMSO. *Investigative Opthalmology & Visual Science, 48*(8), 3714. doi:10.1167/iovs.06-1304

Campos, L. C., Su, M. F. J., Graham, N. J. D., & Smith, S. R. (2002). Biomass development in slow sand filters. *Water Research, 36*(18), 4543-4551. doi:10.1016/s0043-1354(02)00167-7

Christoffersen, K., Lyck, S., & Winding, A. (2002). Microbial activity and bacterial community structure during degradation of microcystins. *Aquatic Microbial Ecology, 27*, 125-136. doi:10.3354/ame027125

Collins MR, Eighmy TT, Fenstermacher JM, Spanos SK, Malley JP, Morgan DF, Royce J.Removal of natural organic material by slow sand filtration.In: Collins MR, Graham NDJ, editors.Slow sand filtration.Denver, CO: AWWA, 1994.p.190–216

Duncan A.The ecology of slow sand filters.In: Graham NJD, editor.Slow sand filtration: recent development in water treatment technology.Chichester, UK: Ellis Horwood, 1988.p.163–80

Ellis, K. V., & Wood, W. E. (2009). Slow sand filtration. *Critical Reviews in Environmental Control, 15*(4), 315-354. doi:10.1080/10643388509381736

Falconer, I. R. (1999). An Overview of problems caused by toxic blue-green algae (cyanobacteria) in drinking and recreational water. *Environ Toxicol, 14*(1), 5-12 doi:10.1002/(sici)1522-7278(199902)14:1<5::Aid-tox3>3.0.Co;2-0

Fayad, P. B., Roy-Lachapelle, A., Duy, S. V., Prévost, M., & Sauvé, S. (2015). On-line solid-phase extraction coupled to liquid chromatography tandem mass spectrometry for the analysis of cyanotoxins in algal blooms. *Toxicon, 108*, 167-175. doi:10.1016/j.toxicon.2015.10.010

Gottinger, A. M., McMartin, D. W., Price, D., & Hanson, B. (2011). The effectiveness of slow sand filters to treat Canadian rural prairie water. *Canadian Journal of Civil Engineering, 38*(4), 455-463. doi:10.1139/l11-018

Grützmacher, G., Böttcher, G., Chorus, I., & Bartel, H. (2002). Removal of microcystins by slow sand filtration. *Environ Toxicol, 17*(4), 386-394. doi:10.1002/tox.10062

Guidelines for drinking-water quality; World Health Organization: Geneva, 2004.

Haig, S.-J., Schirmer, M., D'Amore, R., Gibbs, J., Davies, R. L., Collins, G., & Quince, C. (2014). Stable-isotope probing and metagenomics reveal predation by protozoa drives E. coli removal in slow sand filters. *The ISME Journal, 9*, 797. doi:10.1038/ismej.2014.175

Her, J.-J., & Huang, J.-S. (1995). Influences of carbon source and C/N ratio on nitrate/nitrite denitrification and carbon breakthrough. *Bioresour Technol, 54*(1), 45-51. doi:10.1016/0960-8524(95)00113-1

He, X., Zhang, G., de la Cruz, A. A., O'Shea, K. E., & Dionysiou, D. D. (2014). Degradation Mechanism of Cyanobacterial Toxin Cylindrospermopsin by Hydroxyl Radicals in Homogeneous UV/H2O2 Process. *Environ Sci Technol, 48*(8), 4495-4504. doi:10.1021/es403732s

Holst, T., Jørgensen, N. O. G., Jørgensen, C., & Johansen, A. (2003). Degradation of microcystin in sediments at oxic and anoxic, denitrifying conditions. *Water Research, 37*(19), 4748-4760. doi:10.1016/s0043-1354(03)00413-5

Kelley, T., G. Abulikemu, D. Dionysiou, and J. Pressman (2017). Evaluating removal of microcystin-LR from drinking water using Granular Activated Carbon with various amounts of NOM Preloading. American Water Works Association Water Quality Technology Conference, Portland, OR, November 12 - 16, 2017

Koechler, S., Farasin, J., Cleiss-Arnold, J., & Arsène-Ploetze, F. (2015). Toxic metal resistance in biofilms: diversity of microbial responses and their evolution. *Res Microbiol, 166*(10), 764-773. doi:10.1016/j.resmic.2015.03.008

Kumar, P., Hegde, K., Brar, S. K., Cledon, M., Kermanshahi-pour, A., Roy-Lachapelle, A., & Galvez-Cloutier, R. (2018 a). Biodegradation of microcystin-LR using acclimatized bacteria isolated from different units of the drinking water treatment plant. *Environmental Pollution, 242*, 407-416. doi:10.1016/j.envpol.2018.07.008

Kumar, P., Hegde, K., Brar, S. K., Cledon, M., & Kermanshahi pour, A. (2018 b). Physico-chemical treatment for the degradation of cyanotoxins with emphasis on drinking water treatment—How far have we come? *Journal of Environmental Chemical Engineering, 6*(4), 5369-5388. doi:10.1016/j.jece.2018.08.032

Laadila, M. A., Hegde, K., Rouissi, T., Brar, S. K., Galvez, R., Sorelli, L., Abokitse, K. (2017). Green synthesis of novel biocomposites from treated cellulosic fibers and recycled bio-plastic polylactic acid. *Journal of Cleaner Production, 164*, 575-586. doi:10.1016/j.jclepro.2017.06.235

Mallongi, A., Daud, A., Ishak, H., Ane, R. L., Birawida, A. B., Ibrahim, E., . Rahman, S. A. (2016). Clean Water Treatment Technology with an Up-flow Slow Sand Filtration System from a Well Water Source in the Tallo District of Makassar. *Journal of Environmental Science and Technology, 10*(1), 44-48. doi:10.3923/jest.2017.44.48

Manage, P. M., Edwards, C., Singh, B. K., & Lawton, L. A. (2009). Isolation and Identification of Novel Microcystin-Degrading Bacteria. *Appl Environ Microbiol, 75*(21), 6924-6928. doi:10.1128/aem.01928-09

McDowall, B., Hoefel, D., Newcombe, G., Saint, C. P., & Ho, L. (2009). Enhancing the biofiltration of geosmin by seeding sand filter columns with a consortium of geosmin-degrading bacteria. *Water Research, 43*(2), 433-440. doi:10.1016/j.watres.2008.10.044

Miller, M. N., Zebarth, B. J., Dandie, C. E., Burton, D. L., Goyer, C., & Trevors, J. T. (2008). Crop residue influence on denitrification, N2O emissions and denitrifier community abundance in soil. *Soil Biology and Biochemistry, 40*(10), 2553-2562. doi:10.1016/j.soilbio.2008.06.024

Naghdi, M., Cledon, M., Brar, S. K., & Ramirez, A. A. (2018). Nitrification of vegetable waste using nitrifying bacteria. *Ecological Engineering, 121*, 83-88. doi:10.1016/j.ecoleng.2017.07.003

Napotnik, J. A., Baker, D., & Jellison, K. L. (2017). Effect of Sand Bed Depth and Medium Age on Escherichia coli and Turbidity Removal in Biosand Filters. *Environ Sci Technol, 51*(6), 3402-3409. doi:10.1021/acs.est.6b05113

Nicholson, B. C., Rositano, J., & Burch, M. D. (1994). Destruction of cyanobacterial peptide hepatotoxins by chlorine and chloramine. *Water Research, 28*(6), 1297-1303. doi:10.1016/0043-1354(94)90294-1

Pelaez, M., de la Cruz, A. A., O'Shea, K., Falaras, P., & Dionysiou, D. D. (2011). Effects of water parameters on the degradation of microcystin-LR under visible light-activated TiO2 photocatalyst. *Water Research, 45*(12), 3787-3796. doi:10.1016/j.watres.2011.04.036

Proost, P., Elisia, I., Nakamura, H., Lam, V., Hofs, E., Cederberg, R., Krystal, G. (2016). DMSO Represses Inflammatory Cytokine Production from Human Blood Cells and Reduces Autoimmune Arthritis. *PLoS One, 11*(3), e0152538. doi:10.1371/journal.pone.0152538

Serra, D. O., Richter, A. M., & Hengge, R. (2013). Cellulose as an Architectural Element in Spatially Structured Escherichia coli Biofilms. *J Bacteriol, 195*(24), 5540-5554. doi:10.1128/jb.00946-13

Sun, Z., Zheng, T., Xin, J., Zheng, X., Hu, R., Subhan, F., & Shao, H. (2018). Effects of alkali-treated agricultural residues on nitrate removal and N 2 O reduction of denitrification in unsaturated soil. *J Environ Manage, 214*, 276-282. doi:10.1016/j.jenvman.2018.02.078

Teixeira, M. R., & Rosa, M. J. (2012). How does the adsorption of microcystins and anatoxin-a on nanofiltration membranes depend on their co-existence and on the water background matrix. *Water Science and Technology, 66*(5), 976-982. doi:10.2166/wst.2012.265

USEPA, Nutrient policy and data (2018), Guidelines and Recommendations, https://www.epa.gov/nutrient-policy-data/guidelines-and-recommendations, Date Accessed: 11th November, 2018.

Wand, H., Vacca, G., Kuschk, P., Krüger, M., & Kästner, M. (2007). Removal of bacteria by filtration in planted and non-planted sand columns. *Water Research, 41*(1), 159-167. doi:10.1016/j.watres.2006.08.024

Ward, N. R., Wolfe, R. L., & Olson, B. H. (1984). Effect of pH, application technique, and chlorine-to-nitrogen ratio on disinfectant activity of inorganic chloramines with pure culture bacteria. *Appl Environ Microbiol, 48*(3), 508-514.

Yi, X., Liu, M., Luo, Q., Zhuo, H., Cao, H., Wang, J., & Han, Y. (2017). Toxic effects of dimethyl sulfoxide on red blood cells, platelets, and vascular endothelial cells in vitro. *FEBS Open Bio, 7*(4), 485-494. doi:10.1002/2211-5463.12193

CHAPTER 4: Modification of sand media to enhance its adsorption capacity and breakthrough time

BRIDGE-5

BRIDGE: Agro-residue fibers did enhance the biofilm activity as compared to its non-usage as a 'top-cover' material in a biosand filter. However, the filtration rate slowed down which often needed backwashing. Moreover, the leaching of MC-LR in filter water remained the challenge. So, the 'limit of biodegradation' was understood, and more idea was explored towards the physical adsorption. For this, sand grain was modified and coated using various 'potential' compounds. Part 1 of this chapter discusses various such compounds that were used to coat sand, such as graphitized sand using brewery sugar, graphitized sand using sucrose, manganese dioxide coated sand and a combination of graphitized sand and manganese dioxide. Whilst part 2 of this chapter discuss the use of carbon submicron particles such as graphene oxide and reduced graphene oxide to coat sand. In amidst of exploring the physical adsorption strength, the biodegradation purpose was not kept aside as all the material presented above, was also tested for the biodegradation of MC-LR using known MC-LR-degraders and native bacteria (co-culture aspect).

PART 1

Physical and biological removal of Microcystin-LR and other water contaminants in a biofilter using coated sand composites

Pratik Kumar [a], Hadji Rehab[b], Krishnamoorthy Hegde [a], Satinder Kaur Brar [a,c*], Maximiliano Cledon[d], Azadeh Kermanshahi-pour[e], Sung Vo Duy[f], Sébastien Sauvé[f], Rao Y. Surampalli[g]

[a-] INRS-ETE, Université du Québec, 490, Rue de la Couronne, Québec, Canada G1K 9A9

[b-] Sorbonne Université, 4 Place Jussieu, 75005 Paris

[c-] Department of Civil Engineering, Lassonde School of Engineering, York University, North York, Toronto M3J 1P3, Ontario, Canada

[d-] CIMAS (CONICET, UnComa, Rio Negro), Güemes 1030, San Antonio Oeste, Rio Negro, Argentina

[e-] Biorefining and Remediation Laboratory, Department of Process Engineering and Applied Science, Dalhousie University, 1360 Barrington Street, Halifax, Nova Scotia B3J 1Z1, Canada

[f-] Department of Chemistry, Université de Montréal, Montreal H3C 3J7, Canada

[g-] Dept. of Civil Engineering, Univ. of Nebraska–Lincoln, N104 SEC PO Box 886105, Lincoln, NE 68588-6105

[*]Corresponding author, E-mail: satinder.brar@ete.inrs.ca; satinder.brar@lassonde.yorku.ca (S.K. Brar)

***Science of The Total Environment,* 703 (2020), DOI:10.1016/j.scitotenv.2019.135052**

Résumé

Le sable comme milieu filtrant est souvent mis à l'épreuve par la presenc de matière organique naturelle, d'ions métalliques et de divers micropolluants dans l'eau de source. Cela est principalement dû à la présence de sites d'adsorption actifs limités et à une faible surface spécifique qui cause un potentiel d'adsorption inefficace du matériel sableux. Ici, du sable graphite a été synthétisé pour surmonter les limites ci-dessus en utilisant deux sources de solution sucrée : a) effluent de brasserie (en tant que solution à bas coût) (GS1) et b) une solution de saccharose (GS2). GS1 a montré une constante d'adsorption maximale (qmax) plus élevée de 68%, 60%, 99% pour les ions métalliques divalents : fer, cuivre et manganese respectivement en comparaison avec le sable brut (RS). Le revêtement du sable graphité avec du MnO_2 (les GSM : GS1M et GS2M) a également aidé à la degradation de MC-LR (3% - 9%) lorsqu'il a été inoculé avec des dégradeurs de MC-LR, mais n'était pas aussi efficace pour éliminer les métaux, le carbone organique et l'azote en comparant au sable graphité sans revêtement au MnO_2 (GS1 ou GS2). L'inoculation de GS et des GSM (pour les deux sources de sucre) a non seulement contribué à une élimination plus élevée des MC-LR (10% - 15% de plus) mais a également augmenté l'élimination d'autres contaminants de l'eau notamment les métaux, l'azote organique et le carbone. GS1 a montré une élimination supérieure en MC-LR de 20% et 50% par rapport au matériel sableux testé à une concentration initiale faible et élevée en MC-LR (de 5 µg/L et 50 µg/L). Le plus grand temps de traversée a été obtenue pour le filtre GS1 en utilisant 1mg/L de colorant Rhodamine-B, soit 12 fois (48 minutes) plus que le filtre à sable brut et presque 2,5 fois plus (deuxième meilleur, 21 minutes) que GS1M. Après trois cycles de régénération et de réutilisation du filtre GS1, une diminution de seulement 14% de la capacité d'adsorption saturante a indiqué son aspect de réutilisation élevée.

Mots-clés: Sable revêtu de manganese, sable graphène, biofilter, microcystine, analyse en composantes principales, eau potable

Abstract

Sand as a filter media is often challenged by the presence of natural organic matter, metal ions, and various micropollutants in the source water. It is mainly due to the presence of limited active adsorption sites and low surface area that governs an ineffective adsorption potential of the sand material. Herein, graphitized sand was synthesized to tackle the above limitations using two sugar solution sources: a) brewery effluent (as a low-cost solution) (GS1) and b) sucrose solution (GS2). GS1 showed 68%, 60%, and 99% higher maximum adsorption constant (q_{max}) for divalent metal ions: iron, copper, and manganese, respectively as compared to raw sand (RS). Coating of MnO_2 over the graphitized sand (GSMs: GS1M and GS2M) further helped in MC-LR (3% - 9%) when inoculated with MC-LR-degraders, but was not as effective in removing metals, organic carbon and nitrogen when compared to just graphitized sand (GS1 or GS2). Inoculating GS and GSMs (for both sugar sources) not only helped in higher MC-LR removal (10%- 15% more) but also enhanced the removal of other water contaminants including metals, organic nitrogen, and carbon. GS1 showed 20% and 50% more MC-LR removal than the sand material when tested at a low and high initial concentration of MC-LR (5 µg/L and 50 µg/L). The highest breakthrough period was obtained for GS1 filter using 1 mg/L Rhodamine-B dye, which was 12 times (48 minutes) more than the raw sand filter and almost 2.5 times (second best, 21 minutes) than GS1M. After three cycles of regeneration and reuse of GS1 filter, a decrease of just 14% in saturation adsorption capacity indicated its high reusability aspects.

Keywords: Manganese-coated sand, graphene sand, biofilter, microcystin, principal component analysis, drinking water

Introduction

The excess presence of various chemical pollutants, nutrients and organic matter in drinking water sources is mainly attributed to the unregulated anthropogenic activities and climate change (Basheer et al. 2018a; Basheer et al. 2018b). This leads to a behavioral change in certain microorganisms which impact their growth and physiological activities. For example, under a high nutrient environment and rise in Carbon dioxide solubility in surface water, cyanobacteria tend to release more cyanotoxins (a secondary metabolite), especially Microcystin-LR: MC-LR (Boopathi et al. 2014). Primary pollutants, which are generally present at the macro-scale such as metal ions, natural organic matter (NOMs) and other carbonaceous compounds, are being effectively treated in a drinking water treatment plant (DWTP). However, emerging contaminants, such as cyanotoxins, if not treated, cause acute human exposure to the nerve (neurotoxins) and liver (hepatotoxins) cells at the micro-scale or at very low concentration (as low as 1 μg/L).

The most prominent cyanotoxin found in the source water is MC-LR (Falconer et al. 2005). The persistent and stable behaviour of MC-LR makes its removal challenging, in terms of high energy requirement and chemical dosage using conventional treatment methods, such as chlorination, ozonation and physical adsorption (Falconer et al. 1999; Haider et al. 2003; Ali et al. 2013; Ali et al. 2015; Ali et al. 2016). However, several studies have shown an effective removal of MC-LR or other pollutants using sand filters and other adsorbing materials such as activated carbon and nanoparticles (Bartel et al. 2002; Ali et al. 2015; Ho et al. 2006; Drogui et al. 2012; Ali et al. 2018a; Ali et al. 2018b). Common adsorbents, such as granular activated carbon, powdered activated carbon have been evaluated earlier for the removal of MC-LR (Huang et al. 2007; Keijola et al. 1988; Ho et al. 2011). These adsorbents were effective; however, they incur competitive adsorption due to the presence of NOM in the source water and thus leads to a variation in their dosage making treatment process challenging and complex. Use of agro-industrial waste, such as lentil husk and deinking sludge has been reported to adsorb various pollutants that demonstrates the impact and importance of porosity and increase in surface area of the adsorbents (Mo et al. 2018; Kumar et al. 2019). However, the leaching/breakthrough of adsorbed pollutants into the treated water increases the health risk of the consumers. Hence, this work aims to provide an increase in porosity and surface area for a longer period of filter operation.

Due to low operational cost, easy maintenance, and low chemical input, sand filtration is an acceptable treatment approach in DWTPs for natural organic matter (NOMs), metal ions, coliforms, and micro-pollutants. However, complex matrix ingredients present in source water blocks the surface area of the sand particles in a fight for effective and competitive adsorption that leads to a lesser organics and micropollutants removal than expected. This leaves little to no space for the micropollutants, such as MC-LR to get effectively adsorbed on to the sand surface. Thus, modifications in the sand surface can minimize this limitation. Rahman et al. (2016) reported that graphene-coated sand enhanced the metal removal by 10-fold when compared with activated carbon, which they attributed to the enhanced surface property (area and roughness) of the sand particles. Other studies also reported an increase in the removal of organics, dyes, metals, and pollutants by graphene-sand composites (Zularisam et al. 2017; Dubey et al. 2015).

In the past, various forms of metal oxides (iron, manganese) have shown effective functionalization over the sand particles which delivered better removal of metals and organic pollutants as compared to sand (Lai et al. 2001; Rachmawati et al. 2013). Also, MC-LR carries a negative charge (pH: 2.1-10.2) in water and is expected to get attracted towards metal oxide surface because of the possible positive charge interface. Thus, modulating the specific surface area (SSA) of sand by graphene coating and functionalization of metal oxide over it was hypothesized to effectively remove MC-LR and other organic pollutants. The use of commercial sugar in the form of sucrose has been tested by some researchers but may prove costly for scale-up operations and hence it can reduce the remarkability of the graphene-sand materials as a powerful, stable and effective adsorbent media (Gupta et al. 2012; Achazhiyath Edathil et al. 2019). Hence, in this study, two different sugar sources were used: a) Brewery effluent (excluding hop) as a low-cost solution and commercial sucrose as a high-cost solution (for comparison), to obtain the graphene-sand composite. For the metal oxide coating, manganese dioxide was functionalized over raw and graphitized sand (obtained from both sugar solution sources).

To further strengthen the hypothesis that inoculating the sand filter (biofilter) may enhance the removal of metal ions, organic carbon or nitrogen and especially emerging contaminants, such as MC-LR reported in few studies (Ho et al. (2006,2007); Bartel, H. and G. Grützmacher, (2002); Bourne et al. (2006); Hallé et al. (2015); Zhang et al. 2017), all the prepared sand composites were inoculated with a combination of MC-LR-degrader and native bacterial strains isolated from the

filtration unit of a DWTP. The choice of the MC-degrader was strictly based on their biofilm forming-ability. In total, three MC-LR-degraders viz. *Arthrobacter ramosus*, *Bacillus* sp. and *Sphingomonas* sp. were used for the screening process of respective sand composites. This study for the first time reported the preparation of combined manganese oxide-graphene sand composite in general, and the use of low-cost brewery effluent as a sugar source for the synthesis of graphene-sand composite (GSC). To the best of the authors' knowledge, no study has been done earlier for the removal of MC-LR using such sand composites either as physical adsorption or biofilter operation (using graphitized or manganese-impregnated sand). More than 13 WQPs were monitored for over 70 days of biofilter operation in two stages comprising physical adsorption and the biological mode to also report for any major variation in a long-term filter operation.

Material and methods

Chemicals and microorganisms

Microcystin-LR (MC-LR) was purchased from Cayman Chemicals (Ann Arbor, Michigan, MI, USA) and a stock solution of 50 mg/mL was made by diluting 100 μg lyophilized film of MC-LR (as supplied) using 2 mL of methanol, stored at -20 °C. Crystal violet and 3-(4, 5-dimethylthiazol-2-yl)-2,5-diphenyltetrazolium bromide (MTT) were purchased from Sigma Aldrich, (Ontario, Canada). Various reagents for preparing the stock solution of iron, magnesium and copper (divalent form) including: ferrous ammonium sulphate hexahydrate (iron source), o-phenanthroline, magnesium sulphate (magnesium source), o-cresolphthalein, barium chloride, ethylenediamine tetraacetate, potassium cyanide, and copper sulphate pentahydrate (copper source), were purchased from Sigma Aldrich, (Ontario, Canada). Quartz sand used as the filter media was obtained from Chemin Ste-Foy DWTP, Quebec City, Canada.

MC-degraders: *Arthrobacter ramosus* (NRRL B-3159), *Bacillus* sp. (NRRL B-14393) and *Sphingomonas* sp. (NRRL B-59555) were purchased from NRRL Agricultural Research Service (ARS) culture collection. All the analytical reagents used in preparing nutrient and culture media, LC-MS grade solvents and reagents used to prepare analytical mobile phases, were purchased from Fisher Scientific, (Ontario, Canada).

Property of sand grains used for the preparation of different sand composites

Various sizes of sand grain in the range 125 - 1000 μm were used to formulate an overall filter media with an effective diameter (D_{10}) of 200 μm and coefficient of uniformity of 2.18. Hence, for the preparation of GSC and MnO_2 coated sand (MOCS) (as discussed in the next section), 200 gram of the formulated sand mixture was used.

Preparation of filter media material

Preparation of manganese dioxide coated sand (MOCS)

MOCS was prepared according to the optimized method by Jia et al. (2015) with some modifications. Briefly, 200 gram of formulated sand mixture was soaked overnight in 140 mL of 9 % (w/v) NaOH solution (base activation increases specific surface area and allows more MnO_2 to coat over the sand particles). Afterwards, sand was washed and soaked overnight in 7 % (w/v) $KMnO_4$ solution and later calcinated at 250 °C for 4 hours. The obtained sand mixture was washed until neutral pH, where excess manganese pellets were removed, and it was finally dried at 120 °C overnight to obtain MOCS.

Preparation of sugar (graphene) coated sand or graphene sand composite

Two different sources of sugar: a) brewery effluent; and b) commercial sucrose, were used to graphitize sand particles. Reducing sugar content of the former was found to be 50 g/L. Accordingly, around 0.1 gram-sugar/gram-sand was used as the final optimized recipe for preparing the sugar-sand mixture (for both cases) after several experiments' outcomes in terms of no leaching phenomenon and effective coating as observed from the compound microscope (Appendix E: Figure E1). The leaching was determined using the supernatant of the sand composite prepared after giving it a short spin. The optical density was compared to that of distilled water to understand the clarity of the filtered water. Briefly, 400 mL (equivalent to 0.1 gram-sugar/gram-sand) of brewery effluent was mixed with 200-gram quartz sand in one beaker (1000 mL size) and 20-gram sucrose with 200-gram sand in another beaker. Both mixtures were stirred and heated at 90 ± 10 °C to obtain a concentrated sugar-coated sand mixture. Later, the mixture was placed in a crucible. and kept inside the muffle furnace under reduced atmospheric condition and heated to 100 °C for first 30 minutes, followed by a gradual increase in temperature until 190 °C (sugar melting point: 186 °C) where it was kept for an hour (to allow the sugar to melt and form a uniform coating). Thereafter, the temperature was ramped to 450 °C in the next 1 hour and it was

maintained for another two hours to ensure complete graphitization of sand. The sample mixture was dried at room temperature and it was later activated using 0.5 M sulphuric acid (2 mL/gram of GSC) for 30 minutes. The sand mixture was washed until neutral pH. Finally, the GSC was obtained after an overnight drying at 120 °C.

Characterization of the prepared materials

Scanning electron micrographs (SEM) of the prepared sand composites were recorded using Zeiss Evo®50 Smart SEM system between 5-15 kV. Fourier-Transform Infrared Spectroscopy (FTIR) of the prepared adsorbents media were recorded using Perkin Elmer, Spectrum RXI, FT-IR instrument fitted with lithium tantalate ($LiTaO_3$) detector. Energy dispersive X-ray (EDX) analysis was performed for confirming the atomic and weight percentage of the impregnated elements (manganese, oxygen, silica or carbon) over the sand surface.

Metal adsorption studies

The prepared sand composites were analyzed for their potential in removing the common divalent metal cations that are usually found in the drinking water sources. For the metal adsorption experiment, model columns of 15 cm^3 each, were used to place various sand composites. A solution of copper, magnesium, and iron (divalent metal cations) at different initial concentrations of 5, 10, 50, 100, 200, 250, 300 and 350 mg/L was added to each column. The final equilibrium concentration of copper, magnesium, and iron in the filtered sample was determined spectrophotometrically as detailed by Mehlig et al. (1941), Tesfaldet et al. (2004) and Fortune et al. (1938), respectively. In this study, the adsorption isotherm model which best fitted to the observed values (discussed in detail in the result section) was Langmuir isotherm. This model assumes monolayer adsorption onto a surface that contains a finite number of adsorption sites assuming no transmigration of the adsorbate in the plane surface (Hameed et al. 2007). The isotherm is represented by Equation 11 as follows:

$$Ce/qe = 1/bqmax + Ce/qmax \qquad \text{Equation 11}$$

The linear plot of (Ce/qe) vs qe (as represented by equation 11) obeyed Langmuir model where constants b and q_{max} signifies the energy of adsorption and the maximum adsorption capacity, respectively, obtained from the intercept and slope.The essential characteristics of the parameter obtained from the Langmuir adsorption isotherm can be used to predict the sorbate-sorbent affinity

using a dimensionless constant, R_L (separation factor). This is expressed by the following Equation 12:

$R_L = 1/(1+bCi)$ Equation 12

where, Ci is the initial sorbate concentration. The shape of the isotherm and nature of the adsorption is indicated by the range of R_L values presented as under:

$R_L > 1$, Unfavorable; $R_L = 1$ Linear; $0 < R_L < 1$, Favorable; $R_L = 0$, Irreversible

Biofilm forming ability of different microcystin-degraders over various sand composites

Biofilm formation in a biosand filter is a prerequisite. Three different MC-degraders in form of *Arthrobacter ramosus* (A), *Bacillus* sp. (B) and *Sphingomonas* sp. (S) (Manage et al. 2009; Hu et al. 2012, Alamri et al. 2012; Somdee et al. 2013) were co-cultured with the native bacterial community that were isolated from the biofilm sample of the filtration unit in a DWTP (Chemin Ste-Foy, Quebec City, Canada). The dominant bacterial strains present in the collected biofilm sample were identified as *Pseudomonas fragi* and *Chryseobacterium* sp. (combinedly represented as X from hereon) in our previous study (Kumar et al. 2018). These strains were also found to be potent in degrading MC-LR. In another study done in parallel (data not shown), the co-culturing of MC-degraders with these native bacterial strains were found to enhance their potential in degrading MC-LR. Hence, in the current study, the co-culture model was adopted for the screening process. In a real scenario, it would be more rational to choose the co-culture mode too (A+X, B+X, and S+X) for the screening process. Figure 4.1.0 shows the schematic representation of the unique set-up prepared for this objective. Two sets for each sand composite (fixed particle size: 300 μm, 10 gram) were placed horizontally in a model column. The columns were operated by the auto-dosage pumps.

Figure 4.1.0: Biofilm forming setup to screen the best MC-LR-degrader

Luria-Bertani was used as the culture media to grow the bacterial cells which were centrifuged and rinsed thrice to obtain the bacterial pellets. Thereafter (determining their count/mL), it was suspended in the nutrient buffer to prepare the inoculum source for the filter media. After every 6 hours, 20 mL (6 x 10^7 cells/mL) of inoculum source (A+X, B+X, and S+X, separately) were pumped to all the six sand composites allowing enough time for the bacteria to proliferate and form the biofilm. The process was continued for 10 days and after 2-day, 4-day, 7-day, and 10-day, sand composites from top layer was taken partially (~0.1 gram for all cases). This sample was suspended in 1.5 mL of tap water in a microcentrifuge tube and vortexed to detach the biofilm formed over the sand composite particles. The supernatant consisting of biomass and live cells were seeded in 96-well microplates in triplicates to quantify the biofilm using crystal violet (CV) assay and MTT assay. CV assay and MTT assay were performed to quantify the biomass and live cells present in the biofilm, respectively. The protocol for the same is mentioned in our previous study (Kumar et al. 2019). Negative control comprised the sand composite materials passed using tap water (not the nutrient-biocell solution) and positive control comprised *Staphylococcus epidermidis* which is known as a good biofilm former (Chusri et al. 2012). The result obtained from the positive control was used to compare the biofilm quantification (for both cell viability as well as cell biomass) of other bacteria.

Optimization of the input parameters using Central Composite Design

For optimizing the physical parameters of the Lake water, used as an influent matrix in the sand composite columns, three input parameters with different levels were chosen: a) pH (3-levels, 6, 7, and 8); b) initial turbidity (3-levels, 10 NTU (Nephelometric Turbidity Units), 20 NTU, and 30 NTU); and c) retention time (4-levels, 1-h, 2-h, 3-h, and 4-h). Hence, a total of 36 input combinations were tested for each sand composite. The optimization test before commencing the filter operation was considered as an important aspect as it brought out the working strengths and limitations of the initial parameters. The output of the responses was recorded in terms of total coliform removed, total turbidity removed, pH change, dissolved oxygen content, conductivity, total organic carbon (TOC) removal, flow rate, and ammonia removal. The model column used for the optimization step was of internal diameter 22 mm and a total height of 650 mm (490 mm for the media, 120 mm for the headspace, 40 mm for drainage). All the responses obtained were analyzed using Design-Expert 7.0 software by central composite experimental design and critical solutions were obtained through response surface methodology. The desirability index was reported for all six sand composites and found to be in the range of 0.3-0.4.

Column experiment and setup details

Similar column dimensions were used for the main filter operation too as discussed in the previous section. Figure 4.1.1 shows the schematic diagram of biofilter under operation. The filter operation was conducted in three stages: stage a) No bacterial inoculation stage (for six cycles: 1 cycle equivalent to 7 days); stage b) biofilm formation stage, and stage c) post-biofilm operation (for additional six cycles).

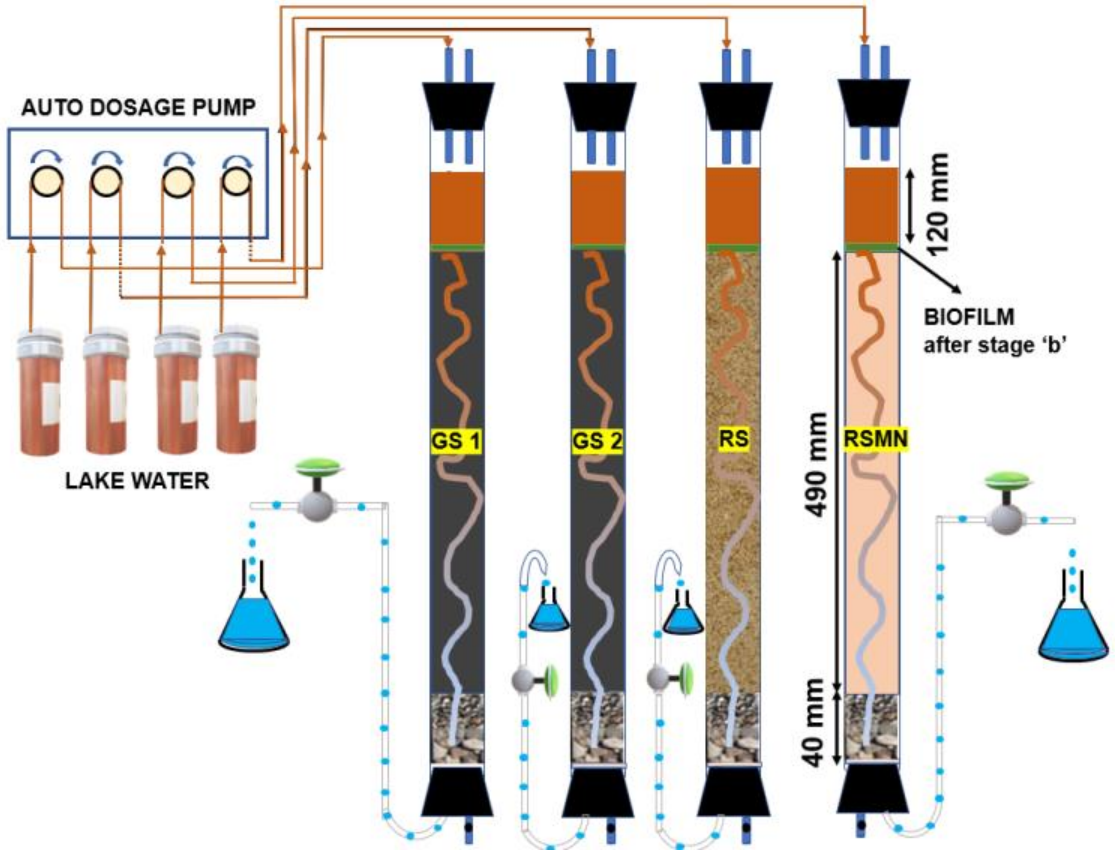

Figure 4.1.1: Schematic representation of the filter operation (other filters: GS1MN and GS2MN are not shown here)

Stage operations 'a' and 'c' were carried out for every sand composite filters to distinguish the physical and biological degradation performance for various water quality parameters (WQPs). The respective screened-co-culture bacterial strains as obtained from the screening process were inoculated (6 x 10^8 cells/mL) for each sand composite filter. After every 6h, the inoculum was passed through the filter column using an auto-dosage pump and was continued for ten days. A decrease in the flow rate, increased protein concentration and cell viability of the formed biofilm, along with an enhanced TOC removal indicated the successful biofilm formation over the sand composites (not shown here). Later, the filter columns were run for additional six cycles (stage 'c') to evaluate various water quality parameters viz, total coliform removal, total turbidity removal, dissolved oxygen, metal removal, flow rate, conductivity, pH, TOC removal and ammonia removal.

Analysis of Water Quality Parameters (WQPs)

Coliform removal, Turbidity removal, DOC removal, and ammonia removal

Total coliform removal was determined twice a cycle (every 3rd and 6th day of a 7-day cycle) in the filtered water sample by membrane filtration technique according to the standard method APHA (1998). Total coliform was reported in CFU/100 mL and removal percentage was determined based on the initial coliform content present in the lake water. The average count of the total initial coliform was found to be 1581 ± 342 CFU/100 mL (average from 9 plates count).

The initial turbidity of the lake water was 6 ± 0.9 NTU, which was less than the maximum limit value as obtained from the optimized conditions for each sand composite. Hence, to operate the filters under the worst exposure, very fine hydrated clay particles (< 25 μm soaked overnight) was used to mimic and increase the turbidity of the influent water. The final turbidity of the filtered sample was observed every day using HACH instrument 2100 model and it was reported in NTU. DOC of the effluent sample was determined using a Shimadzu 5000A analyzer (Shimadzu, Japan). In brief, around 30 mL of the filtered sample was filtered using a 0.45 μm glass-fibre filter. Initial DOC of the influent water (Lake water) was observed to be 9 ± 1.7 mg/L.

Ammonia-N, nitrite-N, and nitrate-N were determined in the filter sample as per the method described by Naghdi et al. (2017). Initial ammonia-N, nitrite-N and nitrate-N concentration in the lake water was determined to be 1.3 mg/L, 2.1 mg/L, and 0.5 mg/L, respectively and was made up to corresponding 5 mg/L, 10 mg/L and 50 mg/L using the stock solution: ammonium sulfate (source of ammonia), sodium nitrite (for nitrite) and sodium nitrate (for nitrate).

pH, dissolved oxygen, metals removal, conductivity

pH and DO measurement of the filtered water provided the information about bacterial activity within the column. DO was measured using a portable F4-Standard probe (Mettler Toledo Inc). A working solution of metals in the form of magnesium, copper, and iron were prepared in lake water matrix at an initial concentration of 20 mg/L for both stages (‘a’ and ‘c’). The conductivity of the filtered sample was measured using Mettler Toledo™ S230 SevenCompact™ Conductivity Meter.

Flow rate and MC-LR removal studies of filter columns

The flow rate was reported in m/h ($m^3/m^2/h$) for each filter after the end of each cycle. During the flow rate measurement, stagnant water head was maintained at around 80 mm measured from the top layer of sand composite media. Backwashing was performed for each filter (during stage 'c' filter operation) because of a continuous decrease in the flow rate due to the biomass formed inside the column filter. The flow rate at no point should decrease to $1/4^{th}$ the initial flow rate at which the column was designed. This was just considered as the subjective minimum throughout the experiment.

The appropriate volume of MC-LR from stock solution was spiked in the lake water (matrix) to obtain an initial MC-LR concentration of 50 μg/L. For the MC-LR analysis, the filtered sample from each sand composite column was collected and the samples were processed using a method adapted from Fayad et al. (2015). Briefly, a 20-μL sample aliquot was analyzed by ultra-high-performance liquid chromatography coupled to a Thermo Q-Extractive Orbitrap mass spectrometer through a positive electrospray ionization source. MC-LR was detected in full-scan MS mode (resolution set at 70,000 FWHM at 200 m/z) and quantified against a matrix-matched lake water calibration curve. The method limit of quantification (LOQ) was set at the lowest concentration level of the calibration curve (i.e. 0.1 μg/L). Also, after the end of stage 'c' operation, all the filters were passed with three different MC-LR concentration: 5 μg/L (low), 20 μg/L (medium) and 40 μg/L (high), to better understand the limitation of the biofilters.

Regeneration and reuse studies

Regeneration and reusability of the column is an important aspect to understand the behaviour of the adsorbent filter media and overall economic feasibility of the column. For this, Rhodamine-B solution was used as the model dye-adsorbate (initial concentration, Co: 1 mg/L) for each adsorbent (various sand composites). A continuous flow rate of 4 mL/minute was chosen for a material bed depth of 7.5 cm. After each throughput volume of 40 mL, OD_{550} was determined (using a 96-well plate) in triplicates to quantify the amount of Rhodamine-B adsorbed on to the material. After the exhaustion of the bed material (C/Co ~1), the adsorbents were regenerated via acetone solution and reused for a total of three cycles to understand the reusability potential of the adsorbent. The saturated adsorption capacity (Wsat: mg/g) of each material was calculated using Equation 13:

$W_{sat} = (\int(U_o C_o)(1-c/c0))/ (g\text{-adsorbent})$ Equation 13

Where, Uo is the flow velocity in L/minute, Co is the initial adsorbate concentration in mg/L and t (integrated from 0 to t) is the breakthrough time in minutes.

Statistical analysis and graphics

All statistical analyses comprising standard deviation, average, student t-test, p-value comparison, Principal Component Analysis (PCA) and all graphical presentations were performed in ORIGIN software (Version 8.5; OriginLab).

Results and discussion

Characterization of sand composites

FT-IR: Figure 4.1.2 (A) shows the absorbance spectra for RS, GS1 and GS2 and Figure 4.1.2 (B) shows the absorbance spectra for RS, GS1M, and GS2M. The only absorbance peak for RS at 560 cm^{-1} indicated Si-O-Si bond while spectra for GS1 and GS2 showed additional and characteristic graphene absorbance peak at 1050 cm^{-1}, 1125 $cm^{-1,}$ and 1610 cm^{-1} attributing to C-O bond, C-O-C linkage, and C=C bond, respectively. This ensured complete graphitization of sugar onto the sand particles (Dubey et al. 2015). The C-O-C linkage in sucrose (GS2) is a glycosidic bond other mono sugars (glucose or fructose).

Figure 4.1.2 (B) showed the absorbance FTIR-spectra for the manganese coated graphitized-sand composites (GS1M and GS2M). Absorbance peaks around wavenumber 1125 cm^{-1}, 1750 cm^{-1}, 2360 cm^{-1}, 2750 cm^{-1} and 3300 cm^{-1} -3700 cm^{-1} were observed. The peak at 1125 cm^{-1} can be attributed to the Mn-OH functionalization group that might have generated due to the base treatment step that was performed before the calcination step, indicating activation of surface area (Chaudhry et al. 2016). The absorption peak at 1750 cm^{-1} in case of GS1M and GS2M indicated vibrational stretch of Mn-OH bond that may be due to the link between manganese atom and the graphitized carbon atoms. The peak at 2360 cm^{-1} might indicate -OH bound manganese oxide, while the peak at 2750 cm^{-1} and 3300-3700 cm^{-1} indicates -OH bond functionalized at the sand surface.

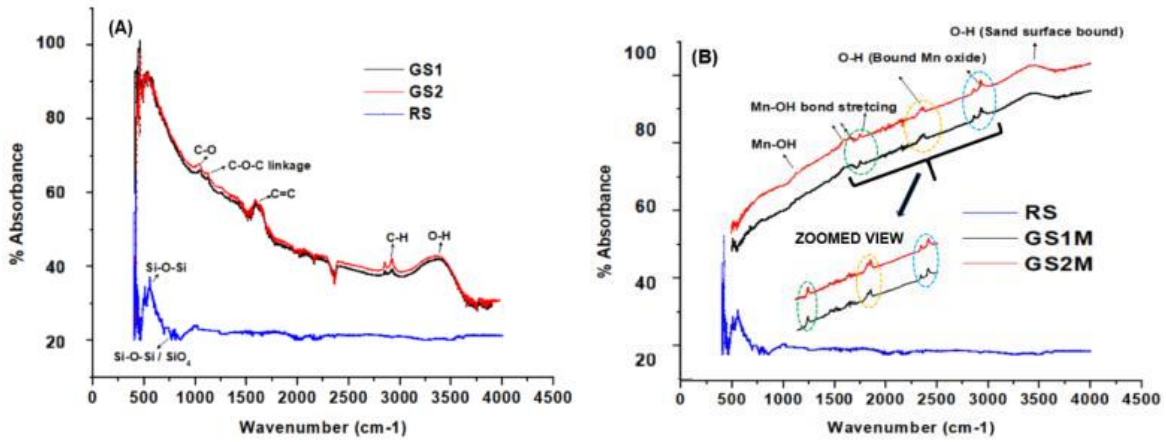

Figure 4.1.2: Fourier-transform infrared spectroscopy spectra for the sand composites: A) raw sand: graphitized sand 1 and graphitized sand 2 and; B) manganese impregnated graphitized sand 1 and 2.

RS: Raw sand; RSMN: Raw sand manganese; GS1: Brewery solution sugar-coated sand; GS2: Sucrose solution coated sand; GS1M and GS2M: Manganese dioxide-coated graphitized sand from respective sugar sources.

EDX: The elemental composition of the coated sand composites was further confirmed by EDX (quantitively). Table 4.1.1 shows the elemental composition in terms of atomic % and weight % for all the sand composites.

Table 4.1.1: EDX analysis of all the sand composites in terms of weight and atomic %

	RS		RSMN		GS1		GS2		GS1M		GS2M	
Element	W	A	W	A	W	A	W	A	W	A	W	A
O	68.2	78.7	45.7	70.1	31.0	26.2	33.8	40.4	22.1	22.6	30.1	39.4
Si	30.8	20.2	13.3	10.6	0.9	0.4	11.5	0.3	0.2	0.2	0.8	0.6
Mn	0	0	40.9	18.2	0	0	0	0	23.8	6.8	44.4	16.9
C	0	0	0	0	64.1	71.9	54.6	58.3	52.4	70.2	23.6	41.9
Others	1	1	0.01	1	3.9	1.4	0.1	0.9	0.8	0.2	1	1

W%: Weight percentage; A%: Atomic percentage

Uncoated sand (RS) showed a ratio of 1:4 for silica atoms (20%) and oxygen atoms (80%) which indicated a general SiO_4 structure (tetrahedron) of the quartz sand. GS1 and GS2, both showed < 1% atomic composition of silica as also observed by Zularisam et al. (2017), while > 70%/ > 20 % and > 55%/ > 40% carbon/oxygen atoms for GS1 and GS2, respectively. This further ensured complete graphitization of sugar onto the sand surface. More manganese dioxide compounds were

coated over GS2 (17%) as compared to GS1 (7%). This might be due to the morphological differences occurred due to graphitization of pure sugar (sucrose) in case of GS2 as compared to brewery sugar in case of GS1. Herein, the sugar media (brewery effluent) consisted of a mix of many sugars including xylose and galactose (GS1) that may have changed the property of the final graphitized surface thereby allowing attachment of fewer manganese dioxides.

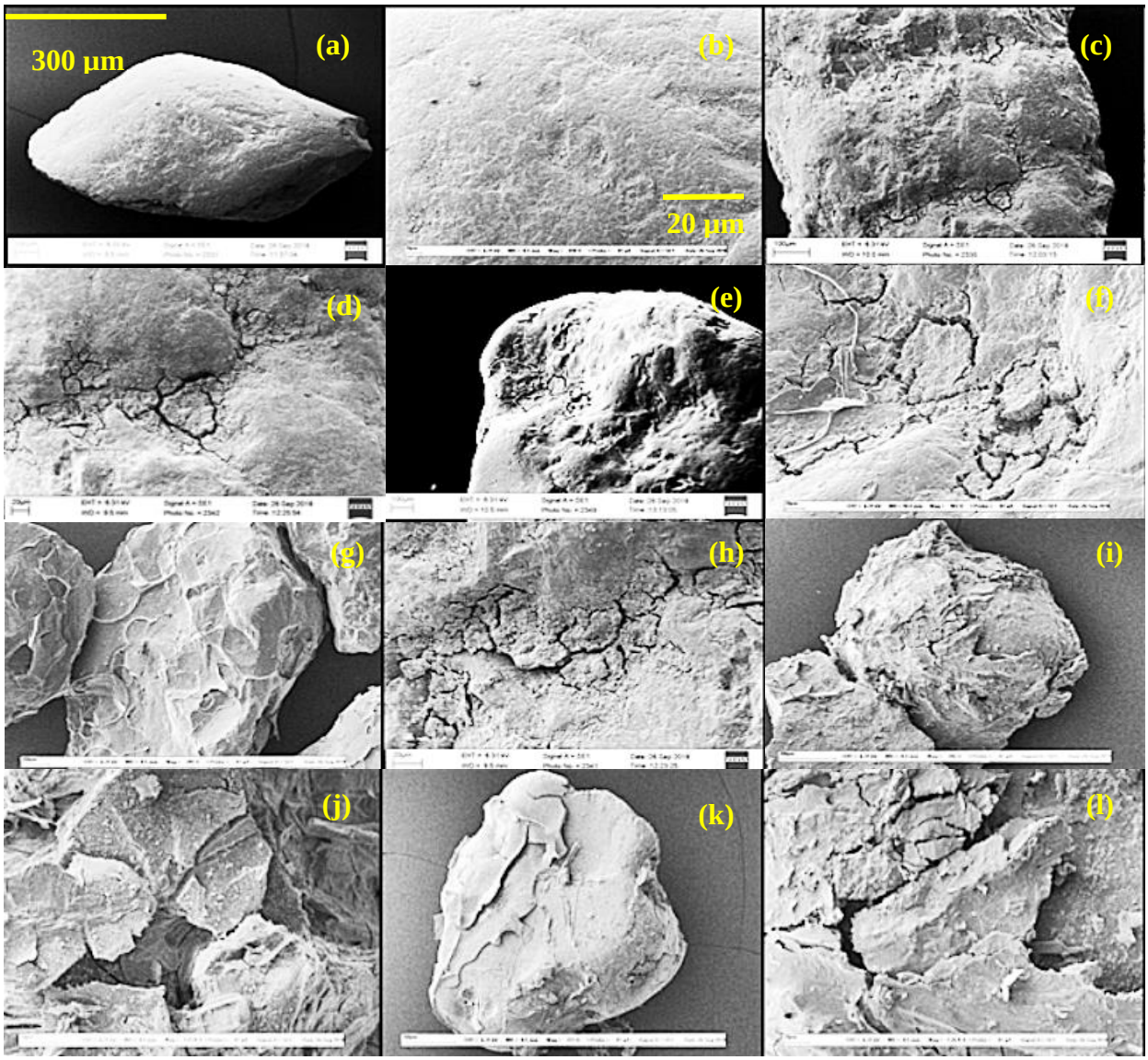

(RS: Raw sand; RSMN: Raw sand manganese; GS1: Brewery solution sugar-coated sand; GS2: Sucrose solution coated sand; GS1M and GS2M: Manganese dioxide-coated graphitized sand from respective sugar sources. Figure b,d,f,h,j and l are the zoomed-in view of a, c, e, g, i and k and scale is shown as a reference by figure *4.1.*3 (a and b for full and zoomed view, respectively)

Metal adsorption studies

For all the three divalent metal ions tested, the observed equilibrium points (C_e vs C_e/q_e) fit the Langmuir isotherm model as represented by Equation 11. The linearity of the curve revealed the applicability of these isotherms for the adsorption. Figure 4.1.4 (A), (B) and (C) represents the Langmuir isotherm of iron, copper, and magnesium for all the six sand composites.

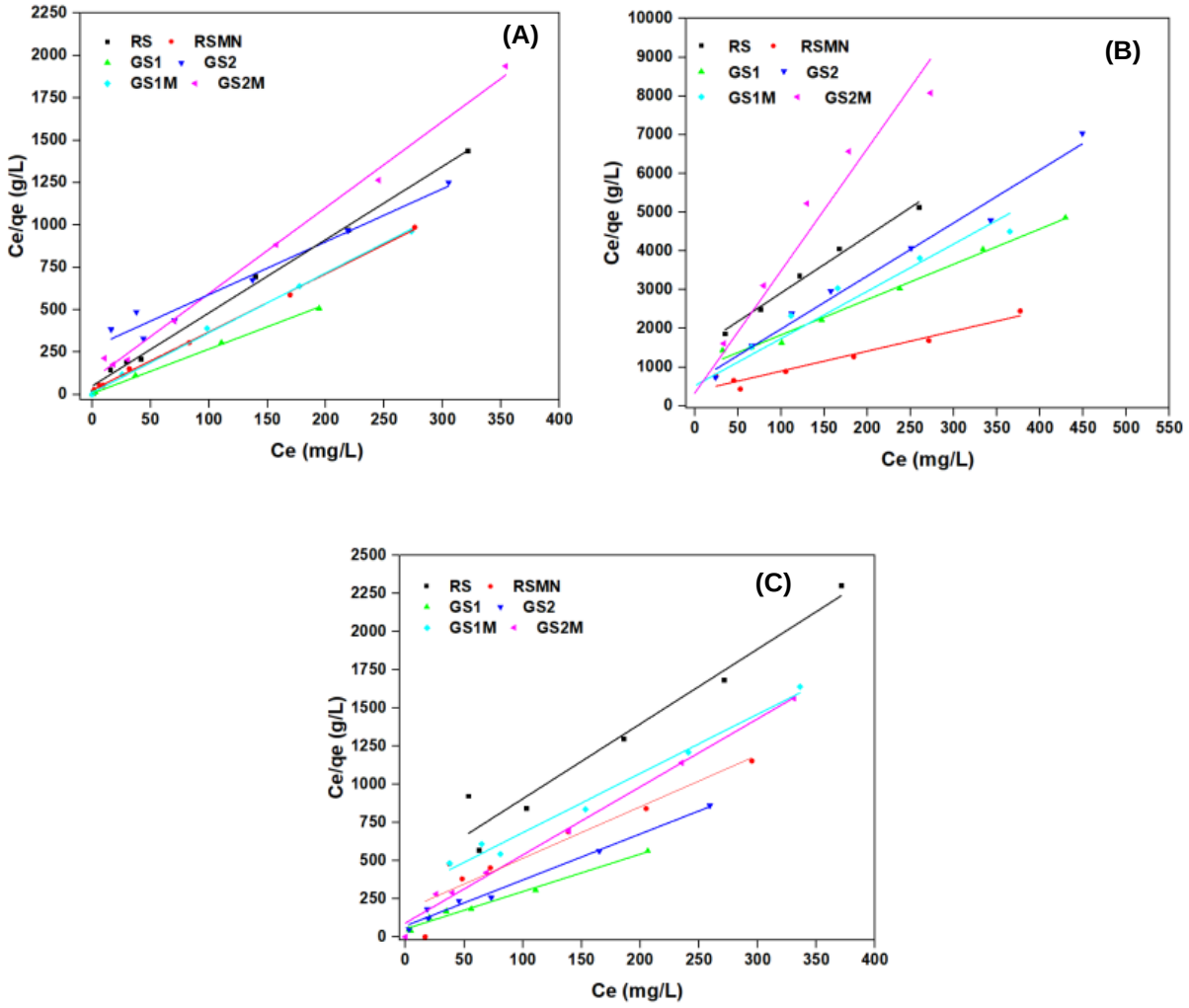

Figure 4.1.4: Linear Langmuir isotherm adsorption curve for all the sand composites for the adsorption of a) iron; b) copper and; c) magnesium.

(RS: Raw sand; RSMN: Raw sand manganese; GS1: Brewery solution sugar-coated sand; GS2: Sucrose solution coated sand; GS1M and GS2M: Manganese dioxide-coated graphitized sand from respective sugar sources)

Table 4.1.2 presents the estimated isotherm parameters for all the sand composites. R_L value indicated the favourable nature of the adsorption for all the three metal ions onto the sand

composites (Table 4.1.2). From the q_{max} values, it can be inferred that iron (range: 0.195 mg/g - 0.380 mg/g) and manganese (range: 0.204 mg/g - 0.408 mg/g) are more adsorbed on sand composites (all six adsorbent material studied) as compared to the copper ions (range: 0.031 mg/g - 0.193 mg/g). Highest adsorption capacity (q_{max}) for iron, copper, and manganese was shown by GS1, RSMN, and GS1, respectively. RS performed the worst in terms of adsorption capacity for all the three divalent metal ions (Table 4.1.2). In general, MnO_2 coating over the graphitized sand (GS1M or GS2M) did not really enhance the metal adsorption capacity (as compared to GS1 or GS2) while MnO_2 coating onto the raw sand (RSMN) has helped in enhancing the sorption capacity of raw sand (Table 4.1.2). Also, RSMN mostly performed at par with the graphitized sand (GS1 or GS2) in terms of maximum adsorption capacity (q_{max}) for all the three divalent metal ions indicating graphitization may not be necessary to remove more metal ions.

Table 4.1.2: Metal adsorption parameters obtained from the Langmuir adsorption curve

Metal Ions	Isotherm parameters	RS	RSMN	GS1	GS2	GS1M	GS2M
Iron (Fe^{2+})	q_{max} (mg/g)	0.226	0.286	0.380	0.268	0.281	0.195
	b (L/mg)	0.162	0.133	0.466	0.013	0.300	0.058
	R^2	0.996	0.998	0.998	0.966	0.997	0.994
	R_L range	0.10 - 0.55	0.10-0.60	0.10-0.30	0.13-0.94	0.10-0.40	0.10-0.76
Copper (Cu^{2+})	q_{max} (mg/g)	0.068	0.193	0.109	0.068	0.073	0.031
	b (L/mg)	0.042	0.013	0.009	0.010	0.022	0.094
	R^2	0.957	0.950	0.990	0.990	0.982	0.969
	R_L range	0.05- 0.83	0.13-0.94	0.18-0.96	0.16-0.95	0.08-0.90	0.02-0.68
Magnesium (Mg^{2+})	q_{max} (mg/g)	0.204	0.363	0.408	0.332	0.257	0.224
	b (L/mg)	0.011	0.008	0.047	0.041	0.013	0.048
	R^2	0.951	0.968	0.987	0.987	0.985	0.991
	R_L range	0.15- 0.947	0.20-0.96	0.04-0.81	0.05-0.82	0.08-0.94	0.04-0.81

RS: Raw sand; RSMN: Raw sand manganese; GS1: Brewery solution sugar-coated sand; GS2: Sucrose solution coated sand; GS1M and GS2M: Manganese dioxide-coated graphitized sand from respective sugar sources.

Biofilm forming ability

As discussed in the method section, three MC-degraders A, B, and S were co-cultured with X (A+X, B+X, and S+X) and distributed equally in terms of cell concentration (6 x 10^8 cells/mL).

This combination of bacterial co-culture was passed through the sand composites to quantify the formed biofilm. Figure E2 shows the schematic representation of the setup (Appendix E). Figure 4.1.5 (A) and (B) shows the MTT and CV assay absorbance values for four different day sampling: 2nd day, 4th day, 7th day and 10th day. It can be observed that the biomass (CV) and cell viability (MTT) showed a positive correlation (for every sand composites) which means more cell viability, more is the cell biomass and vice-versa. A general trend of increasing absorbance values can be observed for both the assays as time progressed. In almost every sand composite, the MTT assay (Figure 4.1.5 (A)) showed a decrease in cell viability after 7 days which indicated that the bacterial cell activity remained intact for 7 days before they died due to nutrient limitation or other reasons.

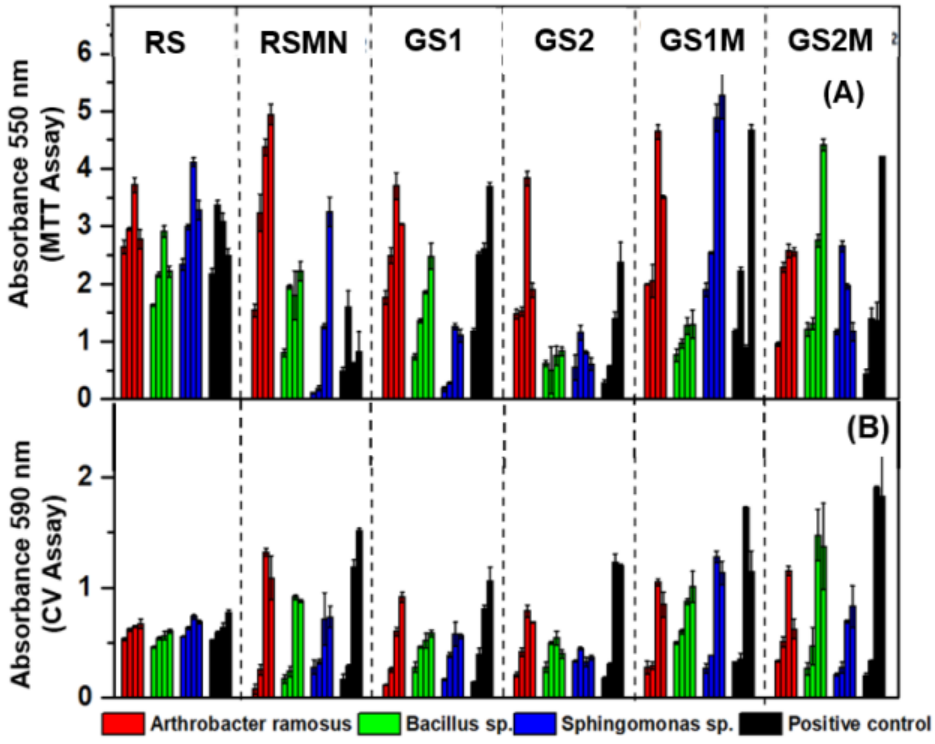

Figure 4.1.5: Absorbance bar chart for the quantification of biofilm in terms of: a) biomass (CV assay); and b) cell viability (MTT assay)

RS: Raw sand; RSMN: Raw sand manganese; GS1: Brewery solution sugar-coated sand; GS2: Sucrose solution coated sand; GS1M and GS2M: Manganese dioxide-coated graphitized sand from respective sugar sources)

Based on the highest absorbance values achieved for MTT as well as CV assay, the MC-degrader-co-culture screened for RS, RSMN, GS1, GS2, GS1M, GS2M were S+X, A+X, A+X, A+X, S+X, and B+X, respectively (Figure 4.1.5). Statistically, for RS, both A and S performed well in comparison to the positive control (PC). However, lower p-value for pair {S+X}:{PC} (0.75) as

compared to pair {A+X}:{PC} (0.93), made S+X the better choice in terms of the statistical significance. For RSMN, GS1, and GS2, A+X showed better biomass and cell viability quantification, while it was B+X which performed well for GS2M. For GS1M, both A+X and S+X performed equally well in comparison to the PC and thus once again based on the p-value between pair: {A+X}:{PC}(0.83) and {S+X}:{PC} (0.48), S+X was preferred over A+X.

Optimization of the input parameters

For every sand composite, the optimized results as obtained through the CCD analysis using RSM were decoded (from the experimental code values) of each input parameter studied. Table 4.1.3 presents the optimized value of variables and other operational characteristics used during the optimization experiment. Except for GS2M, other sand composites showed desirable output at pH 7.3 as compared to 7.13 for the former. Whilst optimum turbidity was found in between 13-15 NTU for all the sand composites, the residence time was found to be around 20 minutes for all the sand composite except GS2M (over 18 minutes). This meant, if residence time at any stage of the filter operation exceeded 20 minutes and turbidity > 15 NTU, it might show a decline in its performance. The filters are operated under no-forced flow condition (free fall under steady water head level). The time to filter 40 mL of standing water (TFSW) for all the filters were less than 20 minutes for the stage ‘a' operation (no biofilm condition). However, under biofilm conditions (stage ‘c’), the TFSW increased for all the sand composite filters. Hence, it was ensured that the flow rate was put back to around same initial linear flow velocity through backwashing operation as it was during the start of stage ‘c’ operation (for the filters crossing TSFW of 20 minutes). The influent water was fortified with hydrated-clay particles to achieve initial turbidity of not more than the optimized value (between 13-15 NTU) whereas the pH was ensured to be in the optimized range (7.13-7.30).

Table 4.1.3: Operational characteristics of the sand composite filters

Filter	**Density (kg/m^3)**	**Pore volume (mL)**	**Surface area (cm^2/g)**	**Optimized conditions (Input parameters)**			**Screened MC-LR-degrader**	**Time to filter 40 mL standing water (minutes)**	
				pH	Turbidity (NTU)	Residence time (min)	Stage ‘c’	Stage ‘a’	Stage ‘c’
RS	2.50	44.7	80	7.3	13.1	20	*Sphingmonas* sp.	3.4 ± 0.6	8.3 ± 1.9

Filter	**Density (kg/m^3)**	**Pore volume (mL)**	**Surface area (cm^2/g)**	**Optimized conditions (Input parameters)**			**Screened MC-LR-degrader**	**Time to filter 40 mL standing water (minutes)**	
				pH	Turbidity (NTU)	Residence time (min)	Stage 'c'	Stage 'a'	Stage 'c'
RSMN	2.45	42.8	82	7.3	13.35	20	*Arthrobacter ramosus*	4.4 ± 0.7	9.7 ± 1.4
GS1	2.17	46.2	93	7.3	15	20	*Arthrobacter ramosus*	5.1 ± 0.6	14.7 ± 1.5
GS2	2.26	48.1	88	7.3	14.85	20	*Arthrobacter ramosus*	5.7 ± 1.2	17.6 ± 2.9
GS1M	2.12	45.7	94	7.3	15	20	*Sphingmonas* sp.	6.6 ± 0.8	20.6 ± 2.6
GS2M	2.13	44.3	93	7.13	15.1	18.8	*Bacillus* sp.	7.3 ± 1.3	20.3 ± 3.1

(RS: Raw sand; RSMN: Raw sand manganese; GS1: Brewery solution sugar-coated sand; GS2: Sucrose solution coated sand; GS1M and GS2M: Manganese dioxide-coated graphitized sand from respective sugar sources)

Water Contaminants (WCs) removal

Table 4.1.4 presents the overall result of the WCs for both the stages: 'a' and 'c'. It can be observed that ammonia, nitrite and nitrate removal increased during stage 'c' operation for all the filters attributing the capability of the MC-LR-degraders in each filter to nitrify ammonia. Highest ammonia (60%), nitrite (55%) and nitrate (86%) removal were observed in filter GS1. In general, graphitization of sugar enhanced the ammonia (25% & 15% for GS1 and GS2), nitrite (19% & 8% for GS1 and GS2) and nitrate (30% & 26% for GS1 and GS2) removal capacity as compared to the raw sand material (RS) while coating of MnO_2 over graphitized sand (GS1M and GS2M) failed to further enhance the potential of graphitized sand (GS1 or GS2) in removing ammonia, nitrate, and nitrate. Enhanced removal potential by graphitized sand filters may be attributed to the biological conversion of ammonia, denitrification process, and effective cell-synthesis as described by Healy et al. (2007) due to an increase in cell biomass of the screened MC-LR-degraders in conjugation with X. Also, an increase in the surface area of the graphitized sand (Table 4.1.3) allowed effective nitrification which got further elevated because of the active biofilm growth (stage 'c' compared to stage 'a') (Davidson et al. 2008).

Table 4.1.4: Water Quality Parameters (WQPs) for all the sand composites during filter operation for both stages

Water Quality Parameters	Stage	RS	RSMN	GS1	GS2	GS1M	GS2M
Conductivity	Stage a	208 ± 8	186 ± 11	192 ± 8	180 ± 13	206 ± 17	219 ±18
	Stage c	223 ± 6	214 ± 7	215 ± 4	218 ± 15	217 ± 7	238 ± 10
DO (mg/L)	Stage a	4.8 ± 0.3	4.6 ± 0.4	4.5 ± 0.2	3.1 ± 0.2	2.9 ± 0.3	2.9 ± 0.3
	Stage c	3.9 ± 0.1	3.7 ± 0.2	3.5 ± 0.2	2.82± 0.2	2.8 ± 0.3	2.6 ± 0.2
Time to filter 40 mL standing water (min)	Stage a	3.4 ± 0.6	4.4 ± 0.7	5.1 ± 0.6	5.7 ± 1.2	6.6 ± 0.8	7.3 ± 1.3
	Stage c	8.3 ± 1.9	9.7 ± 1.4	14.7 ± 1.5	17.6 ± 2.9	20.6 ± 2.6	20.3 ± 3.1
NH_3-N (mg/L)	Stage a	6.86 ± 0.58	6.83 ± 0.65	6.14 ± 0.64	6.29 ± 0.11	6.25 ± 0.19	6.42 ± 0.54
	Stage c	6.43 ± 0.32	6.37 ± 0.43	4.01 ± 0.48	5.02 ± 0.23	4.21 ± 0.21	4.45 ± 0.29
NO_2^--N (mg/L)	Stage a	6.9 ± 0.3	5.6 ± 0.3	4.6 ± 0.3	6.3 ± 0.3	4.5 ± 0.3	4.9 ± 0.2
	Stage c	6.4 ± 0.2	5 ± 0.18	4.5 ± 0.4	5.4 ± 0.5	4.7 ± 0.4	4.4 ± 0.6
NO_3^--N (mg/L)	Stage a	20.7 ± 0.7	17.9 ± 0.5	7.7 ± 0.9	14.3 ± 1.7	8.9 ± 1.6	11.3 ± 0.3
	Stage c	22.2 ± 0.7	15.1 ± 0.9	6.7 ± 0.1	8.5 ± 0.9	8.2 ± 0.7	7.7 ± 1.6
pH	Stage a	6.8 ± 0.1	6.6 ± 0.1	6.6 ± 0.1	6.4 ± 0.1	6.4 ± 0.1	6.4 ± 0.2
	Stage c	6.7 ± 0.1	6.6 ± 0.2	6.5 ± 0.1	6.5 ± 0.1	6.4 ± 0.1	6.5 ± 0.1
Total Coliform (per 100 mL)	Stage a	31.2 ± 4.4	23.5 ± 5.1	10.8 ± 1.7	11.3 ± 3.2	10.2 ± 2.9	10 ± 3.8
	Stage c	24.1 ± 6.7	19.6 ± 5.4	10.2 ± 3.3	9 ± 3.1	8 ± 3.3	8.3 ± 5.7
Turbidity (NTU)	Stage a	2.6 ± 0.8	1.5 ± 0.4	0.8 ± 0.2	0.8 ± 0.3	0.9 ± 0.3	0.9 ± 0.4
	Stage c	2.2 ± 0.9	1.3 ± 0.6	0.8 ± 0.2	0.9 ± 0.4	0.9 ± 0.3	1.4 ± 0.3
Mg (mg/L)	Stage a	9 ± 0.3	4.2 ± 0.04	3.4 ± 0.4	5 ± 0.4	9 ± 0.3	12.2 ± 0.2
	Stage c	10.8 ± 0.5	4.1 ± 0.2	2.4 ± 0.15	4.4 ± 0.5	7.3 ± 0.8	10 ± 1.1
Cu (mg/L)	Stage a	14.8 ± 1.8	10.1 ± 1.6	13.9 ± 0.5	14.3 ± 1.2	13.9 ± 2.1	15.6 ± 1.7
	Stage c	11 ± 0.9	7.4 ± 0.6	8.8 ± 0.8	10.9 ± 0.9	9.2 ± 0.65	11.2 ± 0.9
Fe (mg/L)	Stage a	8.2 ± 1.2	7.4 ± 0.35	6.4 ± 0.14	7.9 ± 0.9	6.1 ± 0.4	8.9 ± 1.1
	Stage c	6.6 ± 0.4	6.2 ± 0.3	5.9 ± 0.2	5.8 ± 1.1	6.4 ± 0.2	6.8 ± 0.6
MC-LR removal (%)	Stage a	39.3 ± 7	68.0 ± 12.3	79.9 ± 6.3	77.9 ± 4.6	78.1 ± 7.7	71.0 ± 8.8
	Stage c	48.1± 11.7	77.6 ± 12.7	93.9 ± 9.4	81.2 ± 7.9	96.7 ± 1.7	90.1 ± 6.8

Water Quality Parameters	Stage	RS	RSMN	GS1	GS2	GS1M	GS2M
DOC removal (%)	Stage a	27.5 ± 6.3	35.6 ± 7.2	49.9 ± 4.8	47.4 ± 5.3	49.1 ± 6.2	47.1 ± 4.5
	Stage c	33.8 ± 0.8	33.6 ± 0.6	45.5 ± 0.8	36.8 ± 2	47.5 ± 1.5	48 ± 1.3

Initial NH_3-N, NO_2^--N, NO_3^--N, Iron, Copper and Magnesium, MC-LR and TOC concentration were: 10 mg/L, 10 mg/L, 50 mg/L, 20 mg/L, 20 mg/L, 20 mg/L, 60 mg/L and 9 mg/L[42], respectively. (RS: Raw sand; RSMN: Raw sand manganese; GS1: Brewery solution sugar-coated sand; GS2: Sucrose solution coated sand; GS1M and GS2M: Manganese dioxide-coated graphitized sand from respective sugar sources)

Both coliform and turbidity removal for graphitized filters (GS1, GS2, GS1M, and GS2M) were found to be 10% - 15% more than the RS filter. This might be due to an increased surface area of the graphitized sand (Table 4.1.3) that led to the availability of more attachment sites and hence allowed an effective entrapment of the coliforms between the sand composites (Jenkins et al. 2011). Also, coliform removal was observed to be 15% - 20% more during the stage 'c' operation as compared to stage 'a' operation. This might be due to the predation mechanism by the active MC-LR-degraders co-cultured with X acting as protists (Unger et al. 2008). GS2 and GS2M showed a slight turbid effluent during stage 'c' operation (cycle 7 - cycle 12) that indicated quick maturation of the attached biomass that led to its detachment carrying away the mimicked clay particles along with it.

Highest iron (70%) and magnesium (89%) removal were observed for GS1 filter, while copper removal was maximally removed by RSMN filter (63%). On an average, magnesium, copper and iron removal for all the filters were further enhanced during the stage 'c' operation as compared to stage 'a' operation by around 5% - 10%, 20% -30% and 10% - 15%, respectively. Increased removal of metal ions (by up to 20%) in RSMN filter as compared to the manganese dioxide-coated graphitized sand composite filter (GS1M or GS2M) may be explained due to the fact that a significant amount of free surface was occupied by the manganese dioxide particles along with the cage-like C-O-C bond structure (as shown in Figure E3, Appendix E) thereby allowing less attachment of the metal ions. Out of all the four graphitized sand composites (GS1, GS2, GS1M or GS2M), only GS1 showed better or comparable metal removal to RSMN filter. This can further be explained because of the availability of more free sites for the metal ions (iron, copper or magnesium) to attack the oxygen atom (negatively charged) as compared to GS1M and GS2M where the oxygen atom is already attached to the manganese atoms (Figure E3). However, the

[42] TOC = 26.5 mg/L and DOC ~ 9 mg/L

reason GS1 performed better in the removal of metal ions as compared to GS2 may be attributed to a more porous and rough structure of the former as can be seen from the SEM images: Figure 4.1.3) which allowed better metal ion pore diffusion and hence more attachment before exhaustion or equilibrium is reached (Bajpai et al. 2017).

Removal of Microcystin-LR

An average of 10% - 15% increase in MC-LR removal under stage ‘c’ operation was observed for all the filters (except GS2, only 4-5% increase) indicating that the screened-MC-LR-degrader contributed to the MC-LR removal. Their activity and increase in the biomass concentration were evident from the fact that pH/DO decrease further during stage ‘c' operation (Table 4.1.4) and TSFW significantly increased (2-3-fold due to increasing biomass) for all the filters. As compared to RS filter, RSMN, GS1, GS2, GS1M, and GS2M showed an enhancement of 29.5%, 45.8%, 33.1%, 48.6%, and 42%, respectively for the removal of MC-LR. It may be possible that other MC-LR-degraders that was not selected after the screening process (as discussed in detail in earlier section) could have performed better. However, the screening was done based on an important prerequisite of the bacterial strains that are required for the successful operation of any biofilters, i.e. cell viability and cell biomass. It was very interesting to observe that during stage ‘a’ filter operation, GS1 performed the best in terms of MC-LR removal (close to 80%) among all the filters and filter GS1M and GS2M underperformed (despite having 3% - 6% more surface area, Table 4.1.3) or were at par with the former.

In general, graphitized sand showed enhanced MC-LR removal as compared to the RS in both the stages (Table 4.1.4). However, manganese coating over the graphitized sand has not really helped in further removal of MC-LR (stage ‘a’ result accounting 2% - 7% decrease in value). Thus, in stage ‘c’ operation, an increase of 3% and 9% in MC-LR removal for GS1M as compared to GS1M and GS2 as compared to GS2M, respectively, indicate the prominent contribution of biodegradation. In the last four cycles (cycle 8-12), filter GS1 and GS1M during stage ‘c’ operation showed complete removal of MC-LR (data in appendix E, Table E1) indicating that the brewery effluent used as the low-cost sugar solution performed better than the commercial sugar (sucrose). The surface composition, roughness and other morphological details of GS1 were key factors responsible for the MC-LR removal, and not the manganese dioxide impregnation factor.

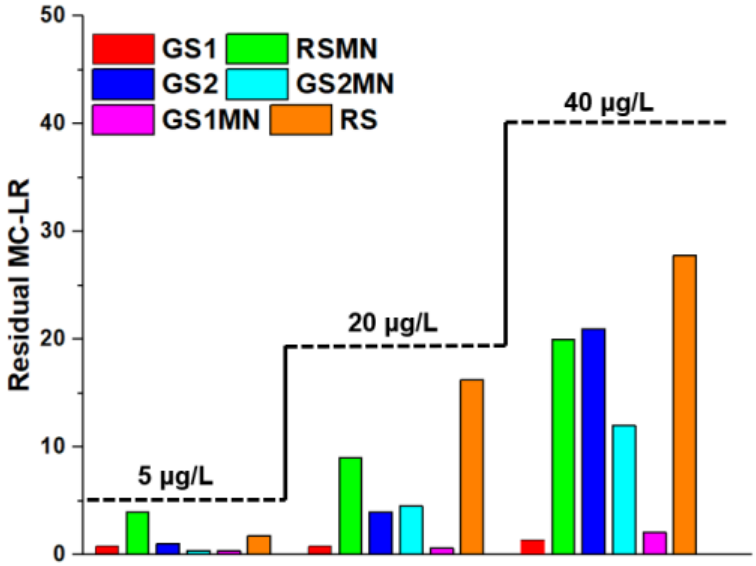

Figure 4.1.6: Residual MC-LR concentration tested for all the sand composites in a column study for three different initial MC-LR concentration: 5 µg/L, 20 µg/L and 40 µg/L.

Figure 4.1.6 shows the residual MC-LR concentration for all the biofilters when tested at three different initial MC-LR levels after stage 'c' operation was finished. GS1 continued to perform well and showed <1 µg/L of residual MC-LR concentration at low MC-LR levels (5 and 20 µg/L) while the MC-LR concentration just exceeded (~ 1.8 µg/L) the critical limit as set by the WHO (1 µg/L). Among other biofilters, the residual MC-LR concentration was found to be in order: GS1MN < GS2MN < RSMN < GS2 < RS.

Interpretation of the WCs removal using PCA analysis

Figure 4.1.7 shows the PCA biplot graph for the observation variables in the form of filters used and Water Quality Parameters (WQPs) as the variables. Based on the cluster of variables around the principal components (PC1 and PC2), WQPs can be mainly divided into two groups: a) metals ion removal (WQP1) and; b) organic carbon and nitrogen, MC-LR and coliform/turbidity removal (WQP2). For the stage 'a' filter operation, PC1, and PC2 accounted for 61% and 25% of the total variation in data, respectively, for a total of 86% (Figure 4.1.7 (A)). Metal removal variables are closely aligned with PC2 while other variables are closely aligned with PC1. This indicated a strong correlation among the WQP1 and WQP2 variables (correlation matrix is shown in the Appendix E, Table E2, E3). Both RS and RSMN showed less correlation towards the WQPs

(WQP1 or WQP2) except copper removal (as is also evident from results, Table 4.1.4). Filter GS1, GS1M, and GS2M are on the right side of the biplot graph, where GS1 and GS1M are closely spaced with the WQP2 variables indicating a positive correlation with each other and hence also signifies better filter potential resulting in a high removal of WQP1 and WQP2 variables. The clustering of WQP2 variables was mostly orthogonal to copper removal variable indicating no correlation with each other.

On the other hand, PCA biplot for the stage ‘c' operation (Figure 4.1.7 (B)) accounted for 64% and 24% for PC1 and PC2, respectively, for a total of 88% variation in data (Figure 4.1.7 (B)). Akin to stage ‘a' operation, the WQP1 are clustered together around PC2 (though less as compared to stage ‘a' PCA biplot) while WQP2 are clustered around PC1. Also, RS and RSMN were once again present on the left side of the biplot graph indicating weak correlation for the WQPs (WQP1 or WQP2) removal as is also evident from their results (Table 4.1.4). The observation variable (filters) on the same side of the WQPs represented a high correlation between each other (correlation matrix in the Appendix section (appendix E)). For stage ‘c' PCA biplot, WQP1 and WQP2 variables are on the same side (right) of the observation variables: GS1, GS2, GS1M, and GS2M. Among WQP1 variables, Cu, Mg, and Fe showed high correlation (Table E2) with each other while, among WQP2 variables, TOC, MC-LR, NO_2^- and NO_3^- showed a very strong correlation with each other (Figure 4.1.7 (B). Higher correlation (correlation coefficient: 0.90) between TOC removal and MC-LR removal is generally found seldom because of the competition between the organic carbon compound and MC-LR as the primary choice of substrate for the bacterial cells. This can be framed as a very positive research inference as most of the time the high competition is reported in other studies (Dixit et al. 2018). However, under stage ‘a' operation, the competition was observed between TOC removal and MC-LR removal, as they were poorly correlated with each other (correlation coefficient: 0.67).

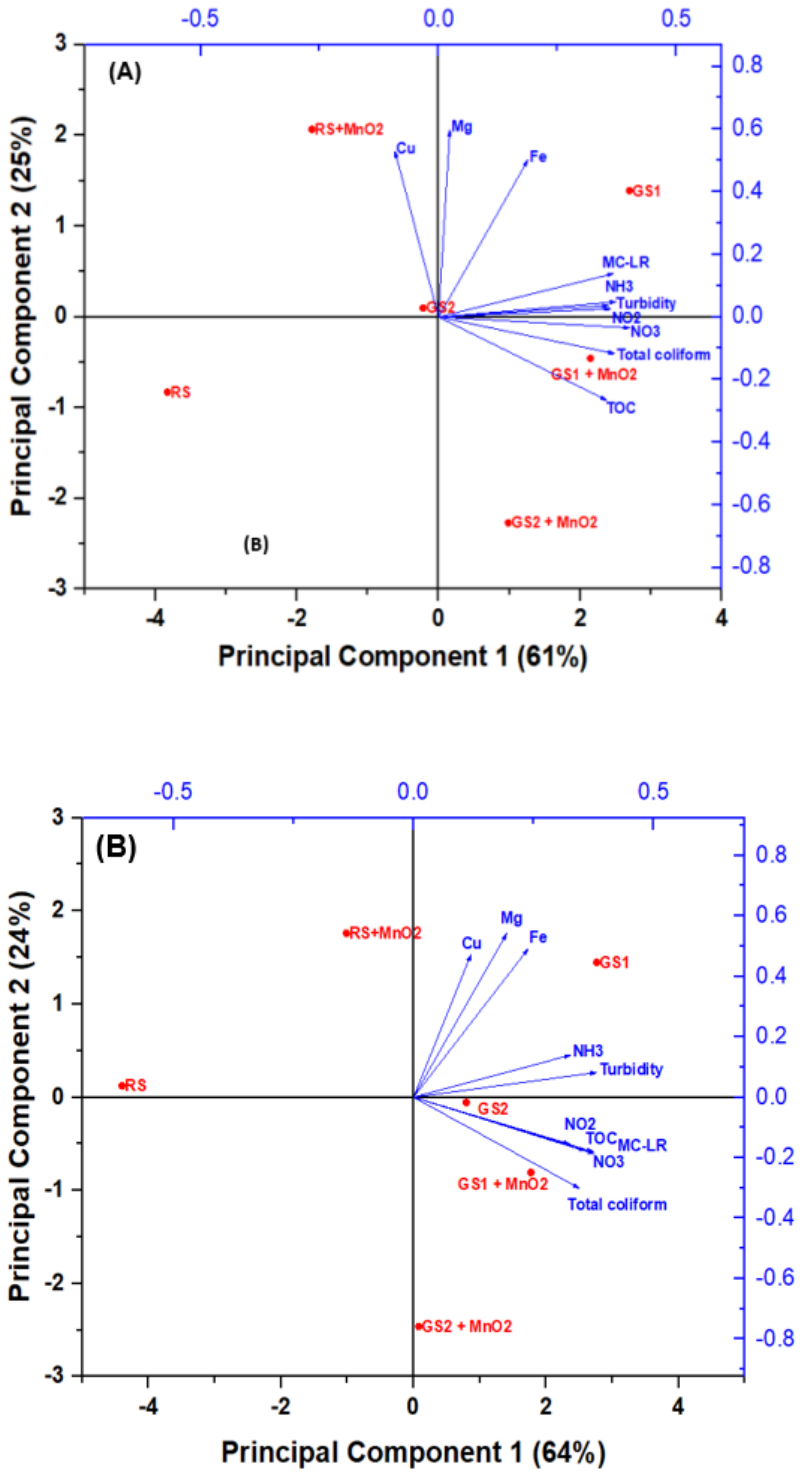

Figure 4.1.7: Principal component analysis (PCA) for the WQPs obtained under filter operation for stage A) stage 'a' and; B) stage 'b'

RS: Raw sand; RSMN: Raw sand manganese; GS1: Brewery solution sugar-coated sand; GS2: Sucrose solution coated sand; GS1M and GS2M: Manganese impregnated graphitized sand from respective sugar sources.

In short, the sand composite filters (especially, RS and RSMN) were found to face a tough challenge when metal ions were present in the source water as is evident from the PC2 loading of more than 24% for both stages of filter operation. GS2 and GS2M (especially GS2M) were quite far from PC1 loading as compared to GS1 and GS1M observation variables indicating the effectiveness of brewery sugar-coated sand in the removal of WQPs. For instance, GS2 was found to be just on the left side of the PCA biplot under stage ‘a' operation and GS2M occupied a much lower or farther position from the PC1 axis. In contrary, GS1 is nicely positioned with WQP1 and WQP2 and is less orthogonal to the variable vectors. WQP1 under stage ‘c' operation was found to be more oriented towards the PC1 axis and hence less orthogonal and closer to the WQP2 variables indicating the importance of biofilm (or biodegradation) in removing the metal ions (as for the removal of WQP2 it enhanced quite substantially, refer to Table 4.1.4).

Regeneration and reuse of filter media

Figure 4.1.8 (A, B and C) shows the breakthrough curves of each sand composites for three cycles (two cycles of regeneration). Table 4.1.5 shows the breakthrough curve parameters for all the sand composite filters. The breakthrough time (C/Co = 0.05) for RS, RSMN, GS1, GS2, GS1M, and GS2M was found to be around 3.67 minutes, 4.1 minutes, 50 minutes, 4.67 minutes, 21 minutes, and 5 minutes, respectively.

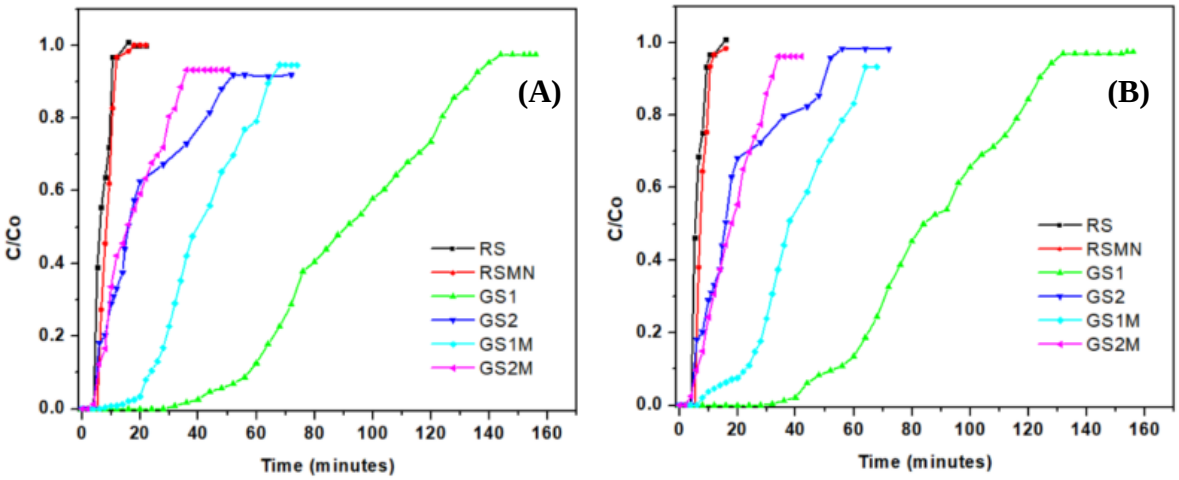

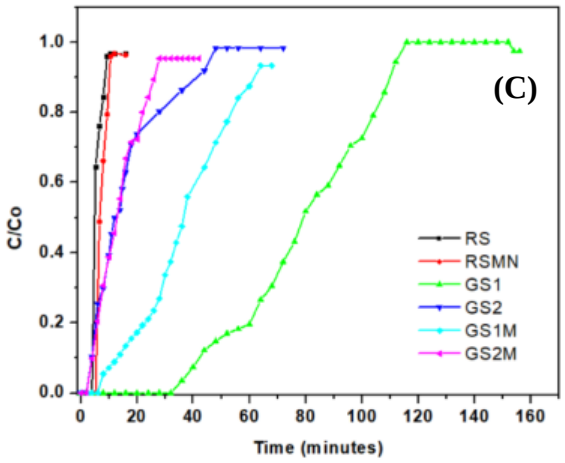

Figure 4.1.8: Breakthrough curve for all the six sand composites after A) cycle 1, B) cycle 2 and C) cycle 3.

RS: Raw sand; RSMN: Raw sand manganese; GS1: Brewery solution sugar-coated sand; GS2: Sucrose solution coated sand; GS1M and GS2M: Manganese impregnated graphitized sand from respective sugar sources.

The breakthrough time for GS1 and GS1M was found to be significantly higher (5-12 times) than the rest filter materials as can be depicted from the above-stated values. The saturated adsorption capacity (W_{sat}) for all the sand composites are shown in Table 4.1.5 and has been compared for a total of three cycles of regenerated material. The W_{sat} value for GS1 and GS1M was found to be 18.6 mg/kg and 8.6 mg/kg while others showed the value of < 5 mg/kg. In the second and third cycle of the regenerated material, W_{sat} values decreased for all the materials where the best performance was still carried by GS1 (reduced only by 14%). The reusability of the sucrose (sugar) graphitized sand was found to be poor as the adsorption capacity decreased by 40 % after 3 cycles of reuse (Table 4.1.5). All the six filters followed the bed-depth service time model (not shown here).

Table 4.1.5: Breakthrough curve parameters for all the sand composite material for 3 cycles of reuse

Filter	Breakthrough time at C/Co = 0.05 (in minutes)			Throughput volume at breakthrough (mL)			Wsat (mg/kg)		
	Cycle 1	Cycle 2	Cycle 3	Cycle 1	Cycle 2	Cycle 3	Cycle 1	Cycle 2	Cycle 3
RS	3.6	3.4	2.8	37	32	31	1.41	1.25	1.11
RSMN	4.1	3.8	3.4	43	39	36	1.7	1.54	1.44
GS1	50	44	40	504	454	412	18.61	17.54	15.89
GS2	4.7	4.2	3.9	49	43	44	4.5	4.2	2.74

Filter	Breakthrough time at C/Co = 0.05 (in minutes)			Throughput volume at breakthrough (mL)			Wsat (mg/kg)		
	Cycle 1	Cycle 2	Cycle 3	Cycle 1	Cycle 2	Cycle 3	Cycle 1	Cycle 2	Cycle 3
GS1M	21	14	9	219	145	98	8.49	8.11	7.44
GS2M	5	4.6	4.2	58	51	46	3.65	3.47	2.72

-----RS: Raw sand; RSMN: Raw sand manganese; GS1: Brewery solution sugar coated sand; GS2: Sucrose solution coated sand; GS1M and GS2M: Manganese impregnated graphitized sand from respective sugar sources.

Overall, the graphitized sand showed a contrast in the adsorption characteristics for the source of sugars used for their synthesis. The adsorption parameters can also be related to an average MC-LR removal efficiency showed by GS2 (Figure 4.1.6) as compared to GS1 where the latter was effective in nearly achieving the WHO guidelines. However, some future considerations must be accounted for the present study such as:

a) A rigorous kinetics study for all the biofilters needs to be performed to know the adsorption behaviour of MC-LR or other cyanotoxins.

b) An experiment to explore the relationship between the surface charge of the adsorbents and pH can be performed to better understand the adsorbent properties.

c) Other MC-LR-degraders, such as *Rhodococcus* sp., *Brevibacterium* sp., and *Stenotrophomonas* sp. must be tested for the bioaugmentation of the filters.

Conclusion

Brewery effluent used as a sugar source for sand graphitization performed better than the commercial sugar (sucrose) for most of the water contaminants (WCs) including organic carbon, nitrogen, and micropollutant: microcystin-LR (MC-LR). Coating of manganese dioxide over raw sand increased the removal efficiency of various WQPs as compared to raw sand filters. In contrast, coating manganese oxide over the graphitized-sand (MOGS) was unable to enhance the removal efficiency of most WQPs including metals and MC-LR. Inoculation of screened MC-LR-degraders and native bacterial strains (isolated from drinking water plant: filtration unit) to different sand composite filters (graphitized or raw or MOGS) further enhanced the removal of the WQPs. Filter operation during inoculation stage showed 10% - 15% higher MC-LR removal thereby suggesting favourable surface for the bacterial cells to proliferate and degrade MC-LR.

All the sand composites were found to follow the Langmuir isotherm model and bed depth service time model for metal adsorption and breakthrough curve, respectively. Regeneration and reuse experiment showed fourteen times more breakthrough time for graphitized sand obtained from brewery effluent. The future application of the graphitized sand can be a household filter or as a replacement or conjugation of the sand media in a DWTPs. However, for the DWTP application, further work on the filtration rate and scale-up parameters needs to be performed adsorption before it can be applied.

Acknowledgments

The authors are sincerely thankful to the Natural Sciences and Engineering Research (Discovery Grant 23451), and ATRAPP (Algal blooms, treatment, risk assessment, prediction, and prevention) for financial support (Genome Québec, Genome Canada; Grant 6116548-2015). Special thanks to Dana Simon for coordinating the sample receipt and analysis. Authors would also like to thank the team for constant support and timely suggestions. We want to thank Genome Quebec for timely sequencing of the bacterial identification. The views or opinions expressed in this article is exclusively those of the authors.

Conflict of interest

None

References

Achazhiyath Edathil, A., Hisham Zain, J., Abu Haija, M., & Banat, F. (2019). Scalable synthesis of an environmentally benign graphene–sand based organic–inorganic hybrid for sulfide removal from aqueous solution: an insight into the mechanism. *New Journal of Chemistry, 43*(8), 3500-3512. doi:10.1039/c8nj05301d

Alamri, S. A. (2012). "Biodegradation of microcystin-RR by Bacillus flexus isolated from a Saudi freshwater lake." Saudi Journal of Biological Sciences **19**(4): 435-440.

Ali, I., Z. A. Al-Othman, A. Alwarthan, M. Asim and T. A. Khan (2013). "Removal of arsenic species from water by batch and column operations on bagasse fly ash." Environmental Science and Pollution Research **21**(5): 3218-3229.

Ali, I., Z. A. Alothman and M. M. Sanagi (2015). "Green Synthesis of Iron Nano-Impregnated Adsorbent for Fast Removal of Fluoride from Water." Journal of Molecular Liquids **211**: 457-465.

Ali, I., Z. A. Al-Othman and A. Al-Warthan (2015). "Removal of secbumeton herbicide from water on composite nanoadsorbent." Desalination and Water Treatment **57**(22): 10409-10421.

Ali, I., Z. A. Al-Othman and O. M. L. Alharbi (2016). "Uptake of pantoprazole drug residue from water using novel synthesized composite iron nano adsorbent." Journal of Molecular Liquids **218**: 465-472.

Ali, I. (2018a). "Microwave assisted economic synthesis of multi walled carbon nanotubes for arsenic species removal in water: Batch and column operations." Journal of Molecular Liquids **271**: 677-685.

Ali, I., O. M. L. Alharbi, Z. A. Alothman and A. Alwarthan (2018b). "Facile and eco-friendly synthesis of functionalized iron nanoparticles for cyanazine removal in water." Colloids and Surfaces B: Biointerfaces **171**: 606-613.

APHA, AWWA, WPCF. 1998. Standard methods for the examination of water and wastewater,19th Ed., Washington, D.C.

Asrafuzzaman, M., Fakhruddin, A. N. M., & Hossain, M. A. (2011). Reduction of Turbidity of Water Using Locally Available Natural Coagulants. *ISRN Microbiology, 2011*, 1-6. doi:10.5402/2011/632189

Bajpai, A. K., Dubey, R., & Bajpai, J. (2017). Synthesis, Characterization, and Adsorption Properties of a Graphene Composite Sand (GCS) and Its Application in Remediation of Hg(II) Ions. *Water, Air, & Soil Pollution, 228*(9). doi:10.1007/s11270-017-3511-5

Bartel, H., & Grützmacher, G. (2002). Elimination of Microcystins by Slow Sand Filtration at the UBA Experimental Field. In *Riverbank Filtration: Understanding Contaminant Biogeochemistry and Pathogen Removal* (pp. 123-133).

Basheer, A. A. (2018a). "Chemical chiral pollution: Impact on the society and science and need of the regulations in the 21st century." Chirality **30**(4): 402-406.

Basheer, A. A. (2018b). "New generation nano-adsorbents for the removal of emerging contaminants in water." Journal of Molecular Liquids **261**: 583-593.

Boopathi, T., & Ki, J.-S. (2014). Impact of Environmental Factors on the Regulation of Cyanotoxin Production. *Toxins (Basel), 6*(7), 1951-1978. doi:10.3390/toxins6071951

Bourne, D. G., R. L. Blakeley, P. Riddles and G. J. Jones (2006). "Biodegradation of the cyanobacterial toxin microcystin LR in natural water and biologically active slow sand filters." Water Research **40**(6): 1294-1302.

Chaudhry, S. A., Khan, T. A., & Ali, I. (2016). Adsorptive removal of Pb(II) and Zn(II) from water onto manganese oxide-coated sand: Isotherm, thermodynamic and kinetic studies. *Egyptian Journal of Basic and Applied Sciences, 3*(3), 287-300. doi:10.1016/j.ejbas.2016.06.002

Chusri, S., Sompetch, K., Mukdee, S., Jansrisewangwong, S., Srichai, T., Maneenoon, K., Voravuthikunchai, S. P. (2012). Inhibition ofStaphylococcus epidermidisBiofilm Formation by Traditional Thai Herbal Recipes Used for Wound Treatment. *Evidence-Based Complementary and Alternative Medicine, 2012*, 1-8. doi:10.1155/2012/159797

Davidson, J., Helwig, N., & Summerfelt, S. T. (2008). Fluidized sand biofilters used to remove ammonia, biochemical oxygen demand, total coliform bacteria, and suspended solids from an intensive aquaculture effluent. *Aquacultural Engineering, 39*(1), 6-15. doi:10.1016/j.aquaeng.2008.04.002

Dixit, F., Barbeau, B., & Mohseni, M. (2018). Characteristics of competitive uptake between Microcystin-LR and natural organic matter (NOM) fractions using strongly basic anion exchange resins. *Water Research, 139*, 74-82. doi:10.1016/j.watres.2018.03.074

Drogui, P., R. Daghrir, M.-C. Simard, C. Sauvageau and J. F. Blais (2012). "Removal of microcystin-LR from spiked water using either activated carbon or anthracite as filter material." Environmental Technology **33**(4): 381-391.

Dubey, R., Bajpai, J., & Bajpai, A. K. (2015). Green synthesis of graphene sand composite (GSC) as a novel adsorbent for efficient removal of Cr (VI) ions from aqueous solution. *Journal of Water Process Engineering, 5*, 83-94. doi:10.1016/j.jwpe.2015.01.004

Falconer, I. R. (2005). Is there a Human Health Hazard from Microcystins in the Drinking Water Supply? *Acta hydrochimica et hydrobiologica, 33*(1), 64-71. doi:10.1002/aheh.200300551

Falconer, I. R. (1999). An Overview of problems caused by toxic blue-green algae (cyanobacteria) in drinking and recreational water. *Environ Toxicol, 14*(1), 5-12. doi:10.1002/(sici)1522-7278(199902)14:1<5::Aid-tox3>3.0.Co;2-0

Fortune, W. B., & Mellon, M. G. (1938). Determination of Iron with o-Phenanthroline: A Spectrophotometric Study. *Industrial & Engineering Chemistry Analytical Edition, 10*(2), 60-64. doi:10.1021/ac50118a004

Haider, S., Naithani, V., Viswanathan, P. N., & Kakkar, P. (2003). Cyanobacterial toxins: a growing environmental concern. *Chemosphere, 52*(1), 1-21.

Hallé, C., P. M. Huck and S. Peldszus (2015). "Emerging Contaminant Removal by Biofiltration: Temperature, Concentration,and EBCT Impacts." Journal - American Water Works Association **107**(7): E364-E379.

Hameed, B., Din, A., & Ahmad, A. (2007). Adsorption of methylene blue onto bamboo-based activated carbon: Kinetics and equilibrium studies. *J Hazard Mater, 141*(3), 819-825. doi:10.1016/j.jhazmat.2006.07.049

Healy, M. G., Rodgers, M., & Mulqueen, J. (2007). Performance of a stratified sand filter in removal of chemical oxygen demand, total suspended solids and ammonia nitrogen from high-strength wastewaters. *J Environ Manage, 83*(4), 409-415. doi:10.1016/j.jenvman.2006.03.005

Ho, L., Meyn, T., Keegan, A., Hoefel, D., Brookes, J., Saint, C. P., & Newcombe, G. (2006). Bacterial degradation of microcystin toxins within a biologically active sand filter. *Water Research, 40*(4), 768-774. doi:10.1016/j.watres.2005.12.009

Ho, L., Hoefel, D., Saint, C. P., & Newcombe, G. (2007). Degradation of Microcystin-LR through Biological Sand Filters. *Practice Periodical of Hazardous, Toxic, and Radioactive Waste Management, 11*(3), 191-196. doi:10.1061/(asce)1090-025x(2007)11:3(191)

Ho, L., P. Lambling, H. Bustamante, P. Duker and G. Newcombe (2011). "Application of powdered activated carbon for the adsorption of cylindrospermopsin and microcystin toxins from drinking water supplies." Water Research **45**(9): 2954-2964.

Huang, W.-J., B.-L. Cheng and Y.-L. Cheng (2007). "Adsorption of microcystin-LR by three types of activated carbon." Journal of Hazardous Materials **141**(1): 115-122.

Hu, L., F. Zhang, C. Liu and M. Wang (2012). "Biodegradation of Microcystins by Bacillus sp. strain EMB." Energy Procedia **16**: 2054-2059.

Jenkins, M. W., Tiwari, S. K., & Darby, J. (2011). Bacterial, viral and turbidity removal by intermittent slow sand filtration for household use in developing countries: Experimental investigation and modelling. *Water Research, 45*(18), 6227-6239. doi:10.1016/j.watres.2011.09.022

Jia, H., Liu, J., Zhong, S., Zhang, F., Xu, Z., Gong, X., & Lu, C. (2015). Manganese oxide coated river sand for Mn(II) removal from groundwater. *Journal of Chemical Technology & Biotechnology, 90*(9), 1727-1734. doi:10.1002/jctb.4524

Keijola, A. M., K. Himberg, A. L. Esala, K. Sivonen and L. Hiis-Virta (1988). "Removal of cyanobacterial toxins in water treatment processes: Laboratory and pilot-scale experiments." Toxicity Assessment **3**(5): 643-656.

Kumar, P., Hegde, K., Brar, S. K., Cledon, M., Kermanshahi-pour, A., Roy-Lachapelle, A., & Galvez-Cloutier, R. (2018). Biodegradation of microcystin-LR using acclimatized bacteria isolated from different units of the drinking water treatment plant. *Environmental Pollution, 242*, 407-416. doi:10.1016/j.envpol.2018.07.008

Kumar, P., Rubio, H. D. P., Hegde, K., Brar, S. K., Cledon, M., Kermanshahi-pour, A., . . . Galvez-Cloutier, R. (2019). Agro-industrial residues as unique support in a sand filter to enhance the bioactivity to remove microcystin-Leucine aRginine and organics. *Science of The Total Environment, 670*, 971-981. doi:10.1016/j.scitotenv.2019.03.260

Lai, C. H. and C. Y. Chen (2001). "Removal of metal ions and humic acid from water by iron-coated filter media." Chemosphere **44**(5): 1177-1184.

Manage, P. M., C. Edwards, B. K. Singh and L. A. Lawton (2009). "Isolation and Identification of Novel Microcystin-Degrading Bacteria." Applied and Environmental Microbiology **75**(21): 6924-6928.

Mehlig, J. (1941). Colorimetric Determination of Copper with Ammonia. *Industrial & Engineering Chemistry Analytical Edition, 13*(8), 533-535. doi:10.1021/i560096a006

Mo, J., Q. Yang, N. Zhang, W. Zhang, Y. Zheng and Z. Zhang (2018). "A review on agro-industrial waste (AIW) derived adsorbents for water and wastewater treatment." Journal of Environmental Management **227**: 395-405.

Mohan, D., & Pittman, C. U. (2007). Arsenic removal from water/wastewater using adsorbents—A critical review. *J Hazard Mater, 142*(1-2), 1-53. doi:10.1016/j.jhazmat.2007.01.006

Rachmawati, S., C. Tizaoui and N. Hilal (2013). "Manganese Coated Sand for Copper (II) Removal from Water in Batch Mode." Water **5**(4): 1487-1501.

Rahman, S., & Praseetha, P. K. (2016). Analysis of Water Purification Efficiency of Graphene Sand Nanocomposite. *International Journal of Engineering Research in Africa, 24*, 17-25. doi:10.4028/www.scientific.net/JERA.24.17

Somdee, T., M. Thunders, J. Ruck, I. Lys, M. Allison and R. Page (2013). "Degradation of [Dha7]MC-LR by a Microcystin Degrading Bacterium Isolated from Lake Rotoiti, New Zealand." ISRN Microbiology **2013**: 1-8.

Tesfaldet, Z. (2004). Spectrophotometric determination of magnesium in pharmaceutical preparations by cost-effective sequential injection analysis. *Talanta, 64*(4), 981-988. doi:10.1016/j.talanta.2004.04.026

Unger, M., & Collins, M. R. (2008). Assessing Escherichia coli removal in the schmutzdecke of slow-rate biofilters. *Journal - American Water Works Association, 100*(12), 60-73. doi:10.1002/j.1551-8833.2008.tb09799.x

Zhang, Y., H. Zhu, U. Szewzyk, S. Lübbecke and S. Uwe Geissen (2017). "Removal of emerging organic contaminants with a pilot-scale biofilter packed with natural manganese oxides." Chemical Engineering Journal **317**: 454-460.

Zularisam, A. W., Wahida, N., & Alfian, A. (2017). Comparison on characteristic of Mesoparticle Graphene Sand Composite (MGSC) using different types of sugar to remove methylene blue. *IOP Conference Series: Materials Science and Engineering, 217*. doi:10.1088/1757-899x/217/1/012005

PART 2

Removal of Microcystin-LR and other water quality parameters using sand filter media coated with bio-optimized carbon submicron particles

Pratik Kumar[a], José Alberto Espejel Pérez[b], Maximiliano Cledon[c], Satinder Kaur Brar[a,d], Sung Vo Duy[e], Sébastien Sauvé[e], Émile Knystautas[f]

[a-] INRS-ETE, Université du Québec, 490, Rue de la Couronne, Québec, Canada G1K 9A9

[b-] Facultad de Ciencias Quimicas, Universidad La Salle Mexico, Benjamin Franklin 45, Cuauhtemoc, Mexico City 06140, Mexico

[c-] CIMAS (CONICET, UnComa, Rio Negro), Güemes 1030, San Antonio Oeste, Rio Negro, Argentina

[d-] Department of Civil Engineering, Lassonde School of Engineering, York University, North York, Toronto M3J 1P3, Ontario, Canada

[e-] Department of Chemistry, Université de Montréal, Montreal H3C 3J7, Canada

[f]-Department of Physics, Physical Engineering and Optics, Laval University, 1045 Avenue de la Médecine, Québec, Canada G1V 0A6

[*]Corresponding author, E-mail: satinder.brar@ete.inrs.ca; satinder.brar@lassonde.yorku.ca (S.K. Brar)

Journal of *Chemical Engineering Journal*; 397, p-125398; DOI: 10.1016/j.cej.2020.125398

Résumé

Le sable est un milieu filtrant largement utilisé dans les usines de traitement des eaux (STEP). Cependant, la présence de divers composés aqueux tels que les métaux, la matière organique naturelle, le carbone organique total, l'ammoniaque ou les micropolluants tels que la microcystine-LR (MC-LR), peut limiter son efficacité en tant qu'adsorbant. Dans cette étude, le sable a été enduit d'oxyde de graphène (GO) et d'oxyde de graphene réduit (rGO) synthétisés en laboratoire pour améliorer ses propriétés de surface en termes d'hydrophilie, de rugosité et de surface spécifique, permettant une meilleure adsorption des macropolluants tout comme un micropolluant unique en tant qu'étude de cas (MC-LR). Une surface plus électropositive sous forme de sable revêtu d'oxydes de fer (IOCS ou Fe) et sa combinaison avec GO (FeGO) a été testé pour valider l'hypothèse d'une adsorption accrue de MC-LR en raison de l'attraction électrostatique puisque MC-LR porte une charge négative à pH 7. Deux dégradeurs de MC-LR connus (*Arthrobacter ramosus* and *Bacillus* sp.) ont été examinés avant la bioaugmentation, basé sur le potentiel de formation de biofilm pour chaque composite de sable revêtu. De plus, leur dose a été bio-optimisée avant le revêtement de GO et rGO sur les grains de sable, pour obtenir un effet non toxique et non perturbateur (maintenant au moins 60% de viabilité cellulaire) des bio-cellules pendant qu'elles forment le biofilm. La plus grande élimination de MC-LR de 91% a été obtenue en phase de biodégradation (opération de biofiltre de 6 semaines) en utilisant du sable enduit de rGO qui a montré une augmentation de 47,2% de l'élimination des MC-LR par rapport à la phase d'adsorption physique (opération de 6 semaines). De façon inattendue, le filtre Fe a sous-performé pour l'élimination des MC-LR (max: 33,6% d'élimination) pour les deux phases de fonctionnement du filtre par rapport au filtre à sable (max: 54,7% d'élimination). La bioaugmentation des dégradeurs de MC-LR examinés a montré une amélioration de 14,6%, 32,4%, 38,4%, 3,5% et de 47,2% dans l'élimination des MC-LR pour les filtres FeGO, Fe, sable, GO et rGO, respectivement. L'Analyse en Composantes Principales (PCA) a montré que rGO et GO étaient les meilleurs filtres parmi tous, compte-tenu également des autres variables des paramètres de qualité de l'eau (WQP). Les capacités maximale d`adsorption adsorbantes saturantes les plus élevées de 8,5 mg/kg et de 7,2 mg/kg ont été obtenues pour les milieux de sable revêtus GO et rGO, respectivement, ce qui était 5 à 6 fois plus élevé que celle du sable non revêtu.

Mots-clés: Biofiltre, MC-LR, Qualité de l'eau, Eau potable, Polluant, Adsorption

Abstract

Sand is a widely used filter media in drinking water treatment plants (DWTPs). However, the co-occurrence of various waterborne components such as metals, natural organic matter, total organic carbon, ammonia or micropollutants such as Microcystin-LR (MC-LR), may limit its effectiveness as an adsorbent. In this study, sand was coated using laboratory-synthesized graphene oxide (GO) and reduced graphene oxide (rGO) to enhance its surface properties in terms of hydrophilicity, roughness and specific surface area, allowing enhanced adsorption of macro pollutants as well as one target micropollutant as a case-study (MC-LR). A more electropositive surface in form of iron oxide coated sand (IOCS or Fe) and its combination with GO (FeGO) was tested to validate the hypothesis of enhanced MC-LR adsorption due to electrostatic attraction as MC-LR bears negative charge at pH 7. Two known MC-LR degraders (*Arthrobacter ramosus* and *Bacillus* sp.) were screened before bioaugmentation, based on the biofilm forming potential for each coated sand composite. Additionally, their dose was bio-optimized before GO and rGO coating over the sand grains, to obtain a non-toxic and non-disruptive effect (maintaining at least 60 % cell viability) of bio-cells while they form the biofilm. A highest MC-LR removal of 91% was obtained under biodegradation phase (6-weeks biofilter operation) using rGO coated-sand that showed an increase of 47.2 % in MC-LR removal when compared to physical adsorption phase (6-weeks operation). Unexpectedly, the Fe filter underperformed in removing MC-LR (max: 33.6% removal) for both phases of filter operation as compared to sand filter (max: 54.7% removal). Bioaugmentation of screened MC-LR-degraders showed an enhancement of 14.6%, 32.4%, 38.4%, 3.5% and 47.2% in MC-LR removal for FeGO, Fe, sand, GO and rGO filter, respectively. Principal Component Analysis (PCA) showed rGO and GO as the best filters among all, considering other water quality parameters (WQPs) variables as well. The highest saturation adsorbent constants of 8.5 mg/kg and 7.4 mg/kg were obtained for GO and rGO coated sand media, respectively, which was 5-6 times higher than the uncoated sand.

Keywords: Biofilter, MC-LR, Water Quality, Drinking water, Pollutant, Adsorption

Introduction

The filtration unit forms a major treatment module in the drinking water treatment plant (DWTPs) chain. The majority of the DWTPs consists of sand as the primary filter media which adsorbs metals ions, sediments and organic matter, thus providing an economical and quick treatment solution (Elbana et al. 2012). However, sand as a filter media presents certain limitations, mainly because of its low adsorption capacity, and may only provide partial removal of water pollutants, especially the emerging contaminants. The stringent water quality guidelines set for some highly toxic emerging contaminants such as the hepatotoxic Microcystin-LR at <1 µg/L (WHO), makes sand media questionable in the context of the modern drinking water treatment aspects. A low surface area and planar morphology of sand is often responsible for the low water pollutant removal (Nageeb, 2013; Kumar et al. 2020a). In this study, use of graphene oxide (GO) and reduced graphene oxide (rGO) submicron particles is explored to enhance the adsorption performance of quartz sand by thermal coating. Various studies have shown the potential of these sub-micron materials for the removal of diverse water contaminants (Ali et al. 2019, Frage et al. 2019, Yousefi et al. 2018). Commercialized carbon source adsorbents such as granulated activated carbon have shown less contaminant removal (~60%) for pharmaceutical mixtures as compared to GO (96%) (Rizzo et al. 2015). However, use of only GO could be uneconomical and time-consuming, delivering a high empty bed contact time during the filter operation in a DWTPs. Hence, coating them over bigger size particles such as sand, could be a suitable alternative.

Graphene oxide coated over sand was shown to effectively remove metal ions, natural organic matter: NOMs and organic carbon (Ding et al. 2014, Hou et al. 2015). However, the removal of cyanotoxins has not been explored to date. How these modified sand surfaces behave for cyanotoxin removal when co-occurring water constituents are present, is an important research question to address. MC-LR is a deadly algal toxin released mainly by a most prominent cyanobacteria: *Microcystis Aeruginosa* in water ecosystems. Lake Erie has repeatedly hit the headlines in recent years due to large outbreaks of harmful algal blooms (HABs). The extent of pollution prompted the DWTPs across the lake basin to rethink about the existing treatment facilities (www.stuff.co.nz/environment/117561856).

Owing to the antibacterial property of GO and rGO and concept of biofilter, these materials were first bio-optimized for their coating dose at which they showed at least 60% survivability rate of the MC-LR-degraders potent in forming biofilm. In the current study, to hypothesize the surface charge influence on the MC-LR removal (as it bears negative charge for the wider pH range: 3.5-10.4), a more electropositive surface was proposed. To achieve this, iron oxide was coated over the sand (IOCS or Fe filter) owing to a high pZC (>7.5) of the former than the latter (pH: 3-4) (Stenkamp et al. 1994). Submicron carbon particles (in form of graphene oxide) owing to their high adsorption capacity was also introduced in the above hypothesis to further investigate any rise in the adsorption performance of WQPs, especially MC-LR, when coated on electropositive surface (Fe sand) in the form of FeGO filter media (Fe + GO). It should be noted that Fe + rGO was not considered as an option in this study, due to unsuccessful coating over the sand surface despite showing high electropositive surface of rGO particles (-14.3 ± 3.5 mV) when compared with GO particles (-37.5 ± 6.8 mV). Thus, in total, five filters were tested for the above presented problems and hypothesis including one control: uncoated sand media.

To the best of authors knowledge, this is the first time that an iron oxide coated sand filter (herein after referred to as Fe filter), GO-coated filter (GO filter), and rGO-coated filter (rGO filter), are tested for their adsorption and biodegradation of any cyanotoxin (MC-LR), in conjunction with MC-LR-degraders. To mimic a real treatment scenario, native bacterial species isolated from the filtration unit of a DWTP were co-cultured along with the MC-LR-degraders to study the overall biodegradation of MC-LR. Additionally, the FeGO sand media was synthesized for the first time and tested for any water pollutant.

Material and methods

Chemicals and reagents

Microcystin-LR (MC-LR) was bought from Cayman Chemicals (Ann Arbor, Michigan, MI, USA) and a stock solution of 50 µg/mL was made by diluting 100 µg lyophilized film of MC-LR (as provided by the supplier) using 2 mL of HPLC-grade methanol and stored at -20 °C. Crystal violet and 3-(4, 5-dimethylthiazol-2-yl)-2,5-diphenyltetrazolium bromide (MTT) were purchased from Sigma Aldrich, (Ontario, Canada). Quartz sand was obtained from the filtration unit of the drinking water treatment plant (DWTP) from Chemin Ste-Foy DWTP, Quebec City, Canada. *Arthorobacter ramosus* (NRRL B-3159) and *Bacillus* sp. (NRRL B-14393) were purchased from NRRL

Agricultural Research Service (ARS) culture collection. All the analytical reagents used in preparing nutrient and culture media, LC-MS grade solvents and reagents used to prepare analytical mobile phases, were purchased from Fisher Scientific, (Ontario, Canada).

Synthesis of graphene oxide and reduced graphene oxide

Around 6 gm of graphite flake (mesh size 10) was mixed with 160 mL of concentrated sulphuric acid. To avoid explosive reaction, 15 mL of orthophosphoric acid was used along with 3 gm of $NaNO_3$. After 2 hour of reaction, 20 gm of potassium permanganate was added to further oxidize the reaction. The reaction was left for 4-6 hours. After that, 75 mL of distilled water was added very slowly into the reaction mixture followed by a quick addition of 350 mL of distilled water. The reaction was stirred for half an hour and then 15-20 mL of 30% hydrogen peroxide was added to terminate the reaction. The reaction mixture was centrifuged at 5000 x g for 30 minutes at room temperature obtaining the solid pellets which were washed with distilled solution until neutral. The neutral washed solution was dried at 60 ± 3 °C overnight to obtain solid graphite oxide. To obtain graphene oxide, various batches of 50 mg of graphite oxide were mixed with 100 mL distilled water and sonicated for 4 hours until a uniform dispersion was obtained. The obtained mixture was dried at 60 ± 3 °C overnight to obtain solid graphene oxide (GO). The particle size distribution of GO showed a mean size of 298 nm.

To synthesize reduced graphene oxide in various batches, around 300 mg of ascorbic acid was added to 100 mL of graphene oxide (concentration: 0.5 mg/mL). The solution was stirred for three time periods viz. 20 mins, 40 mins and 70 mins. The solution pH was alkaline (pH 10.5) to keep the material stable via electrostatic repulsion. The temperature of the set-up was maintained between 60-70 °C. The obtained mixture was then dried at 60 ± 3 °C overnight to obtain solid reduced graphene oxide (rGO). Based on the material characterization results, single time period among the above three (reduction process time of 40 min) was chosen. The particle size distribution of rGO showed a mean size of 193 nm.

Bacterial activity test for the synthesized rGO and GO

From a stock solution of prepared GO solution (3330 mg/L), concentrations of 100 mg/L, 300 mg/L, 400 mg/L, 540 mg/L and 620 mg/L of GO were prepared in different Erlenmeyer flasks containing 10 mL of Luria Bertani media (Appendix F: Figure F1). One flask without GO served

as the negative control. After eight hours of incubation at 150 rpm at 30 ± 1°C (16 time more than generation time), cell enumeration was reported based on survival % for both the MC-LR-degraders at various GO concentrations (as mentioned above). Cell enumeration value obtained for the control case was assigned a 100% survival rate. Each flask was inoculated with 4 x 10^7 cells/mL of respective MC-LR-degraders. A subjected minimum of 60% survivability value was chosen as the criterion for selecting the optimum dose in order to justify for the GO/rGO coated surface favouring the biofilm formation. However, the above experiment was dynamic (shaking incubator) as compared to the static bed system (biofilter operation) for the rGO/GO coated sand. Hence, the relationship to estimate the real GO/rGO dose per gram sand was balanced based on the static-dynamic factor as explained in the Appendix F (Figure F2). For the rGO material also, the same experimental method was executed as discussed above and survivability % was reported for each dose concentration.

Synthesis of GO-coated, rGO-coated, Iron oxide-coated (Fe) and FeGO-coated sand

According to the static-dynamic relationship, the real dose of GO and rGO with respect to the survivability rate was found to be 5 mg GO/gm-sand and 6.5 mg rGO/gm-sand, respectively. To effectively coat GO and rGO over sand (individually), distilled water and ethylene glycerol was chosen, respectively as the base solution to get a uniform dispersion (screened based on 5 different polar solvents tested) after sonication. For coating, the dispersed solution (100 mL of GO/rGO per 100-gm sand) was mixed well with sand and later calcinated at 400 °C for about 4 hours in a muffle furnace. The coated material was left to dry at room temperature overnight followed by activation using 0.1 M sulphuric acid for 30 minutes, neutralized and dried again before using it as the filter media.

Iron oxide coated sand (Fe-sand) was synthesized to understand the change in the adsorption behaviour of WQPs occurring when Fe-sand was formulated with GO (FeGO). To coat iron oxide over the sand, crystalline ferric nitrate was chosen as the iron oxide source and was prepared according to the method described by Hansen et al. (2001). For FeGO-sand coating, GO at the concentration of 5mg/gm of Fe-sand was chosen and was calcinated at 400 °C for 4 hours and similar protocol for activation and drying was followed as mentioned above for GO/rGO.

Characterization of the synthesized materials and coated sand grains

Scanning electron micrographs (SEM) of the synthesized GO/rGO and prepared coated sand materials were recorded using Zeiss Evo®50 Smart SEM system between 5-15 kV. Also, the Fourier-Transform Infrared Spectroscopy (FTIR) data were recorded using a Perkin Elmer, Spectrum RXI, FT-IR instrument fitted with a lithium tantalate ($LiTaO_3$) detector. Energy dispersive X-ray (EDX) analysis was performed for confirming the atomic percentage of oxygen and carbon atoms in the synthesized GO/rGO and to determine the proportion of iron, carbon and oxygen in the Fe and FeGO coated sand surface. The zeta potential of the obtained coated grains was compared with the uncoated sand grains to report the degree of relative (as compared to uncoated sand grain) electro-positive surface obtained after the coating process. Pulverized sand grains (coated and uncoated) were suspended using ultrapure water in DTS1060 disposable cells, used as the zeta potential cells for Malvern Instruments according to the manufacturer instructions.

Screening the MC-LR-degraders for different sand composite

For screening the most potent MC-LR-degrader among *Arthrobacter ramosus* (A) and *Bacillus* sp. (B), a unique experimental set-up was prepared as mentioned in our previous work (Kumar et al. 2020a).. For this, two sets of model reactor (10 gm coated sand, fixed size: 300 μm for each A and B) were placed horizontally. To inoculate the coated sand media, the influent solution of A and B was separately discharged through them at an intermittent rate of 30 mL (6×10^7 cells/mL) every 4 hours (using an auto-dosage pump) to allow enough time for the biocells to proliferate in between two discharges. The cells were harvested in Luria-Bertani media and was centrifuged at 9000 x g at room temperature to obtain the pellets which was mixed with lake water (Lake Sainte-Anne, (47.262879 N, −71.665158 W)) to obtain the discharge inoculum solution as mentioned above. As a control, uncoated sand media was also kept in the experimental set-up for comparison purposes. The process was continued for 8 days and a sample was taken every 1-day, 4-day, 6-day and 8-day. For this purpose, a small amount of the material (~0.1 gram for all cases) was taken from the top surface (as more biofilm is expected in this zone) and was suspended very quickly in 1.5 mL saline-buffer prepared in tap water to hydrate the living biocells (attached to sand) . The sample was vortexed for 2 minutes at high speed to detach the biocells from the sand grains. The supernatant consisting of biomass and live cells were analyzed for the Crystal Violet (CV) assay and MTT assay as per the protocol mentioned in our previous study (Kumar et al. 2020a). The CV

assay quantified the degree of biomass (live + dead cells) in a biofilm whereas the MTT assay quantified the live cells in the biofilm. The results were compared with the results of the negative control (uncoated sand media). Flow rate was also estimated to determine the rate of biomass formation within the sand grains.

Column experiment and setup details

Figure 4.2.1 shows the schematic representation of the filter set-up used for the experiment (actual set-up figure: Figure F3, Appendix F). The cylindrical glass rods of height 650 mm with an inner diameter of 20 mm and thickness of 1.5 mm were used for the column study. Around 490 mm of adsorbent media (coefficient of uniformity: 2.32) was put inside the dry column underlain by the drainage section (120 mm length) which comprised larger sand grains (4-8 mm size). The adsorbent media comprised of mixture of various sand grain sizes (range 125 µm-1000 µm) that eventually characterized the overall media for an effective diameter (D_{10}) of 210 µm.

The column experiment was run for 3 stages. A) Stage 1: Physical adsorption studies of water quality parameters including MC-LR removal for 5 weeks (1 week = 1cycle). B) Stage 2: Biofilm formation phase, wherein the column was fed intermittently using an auto-dosage pump with lake water. The lake water was inoculated (9×10^8 cells/mL) with the screened MC-LR-degrader for the respective adsorbing filter media co-cultured with the native bacterial cells isolated from the filtration unit of the DWTP (discussed in detail in next section). Every hour, 40 mL per intermittent discharge was carried out using an auto-dosage pump. Stage 2 filter operation was continued for a total of 11 days until conclusive evidence of substantial biofilm formation was reported (detail in the result section), C) Stage 3: Biodegradation phase study of water quality parameters for 6 weeks. For the daytime hours (10 am to 6 pm), the filters were operated every hour and during nighttime hours, the auto-dose pump was set to run every 4 hours where sampling for the WQPs was done at 2 pm every 2^{nd} and 5^{th} day of a 7-day cycle. For stage 1 and stage 3 filter operation, water pollutant-spiked lake water (details in later section) was discharged intermittently every hour (40 mL volume) for the analysis of various water quality parameters viz, total coliform removal, total turbidity removal, dissolved oxygen, metal removal (copper and iron), flow rate, conductivity, pH, TOC removal and ammonia removal. The initial concentration of these WQPs are mentioned in later section.

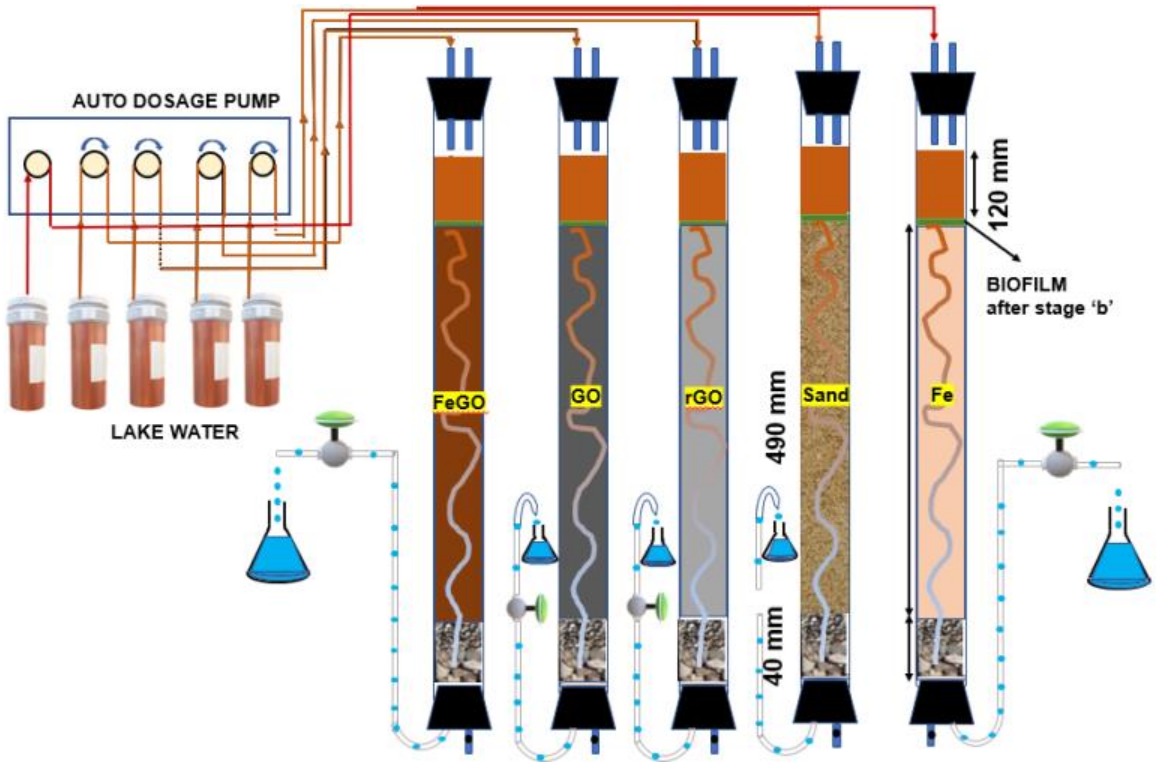

Figure 4.2.1: Schematic representation of the column experiment using five filter media

rGO: reduced graphene oxide, GO: Graphene oxide, FeGO: Iron coated on graphene oxide coated sand

Biofilm characterization for the stage 2 filter operation

For the stage 3 filter operation, a healthy biofilm formation was a pre-requisite to understand the effect of inoculation (bioaugmentation) on MC-LR removal. Each filter column was inoculated using the screened MC-LR-degraders for respective sand composite along with the native bacterial cells isolated from the DWTP (Kumar et al. 2018). This co-culturing aspect of MC-LR-degrader with the native bacterial community (combination of *Chryseobacterium* sp. and *Pseudomonas fragi* = X, from here on) was proven to accelerate the MC-LR biodegradation (Kumar et al. 2020a). Also, considering the real scenario of the filtration unit in the DWTP and for improvement of MC-LR biodegradation, co-culture practice seemed more rational. A total cell concentration of 6 x 10^7 cells/mL (as mentioned before) was inoculated where each bacterial species was divided equally (2 x 10^7 cells/mL each). The columns were fed every 6 hours with the inoculum and given enough time between the next discharge for the biocells to adhere to the sand composite and proliferate. After every 3 days for a total of 12 days, sampling for the biofilm quantification was done in a similar manner (CV assay, MTT assay) as discussed in the earlier section.

Analysis of Water Quality Parameters (WQPs)

pH, DO and conductivity

During the filter operation, change in pH and DO value for the influent/effluent indicates the activity of biofilm formation and water quality. The effluent (or filtered) water was duly checked for DO value measured using a portable F4-Standard probe (Mettler Toledo Inc), to check for any anoxic environment built-up in the drainage zone of the column (< 2mg/L-O_2). Also, the pH information was important to understand the degree of alkalinity that is needed to maintain for the next treatment step, i.e., disinfection, if the results are to be applied. The conductivity of the sample was measured using a Mettler Toledo™ S230 SevenCompact™ Conductivity Meter. The change in conductivity was primarily used to test for any micro-leaching phenomenon that had happened from the coated sand.

DOC, Ammonia, Nitrite, Nitrate, Iron, Copper, Magnesium removal

In general, the primary objective of the filter unit is to remove the organic matter from the source water. Hence, in this study, the DOC removal study was done where the initial DOC of the lake water was found to be around 6 ± 0.9 mg/L. All the measurements were done using a Shimadzu 5000A analyzer (Shimadzu, Japan). In brief, around 30 mL of the effluent sample was filtered using a 0.45 µm glass-fiber filter and analyzed for the DOC.

Ammonia-N, nitrate-N and nitrite-N removal studies was performed by spiking ammonium sulfate, sodium nitrate and sodium nitrite, respectively, in the lake water matrix to reach an initial concentration of 5 ppm, 10 ppm and 50 ppm of NH_4-N, NO^{2-} and NO^{3-}, respectively. Initial ammonia-N, nitrite-N and nitrate-N concentration in the lake water was determined to be 1.3 mg/L, 2.1 mg/L, and 0.5 mg/L, respectively, and the spiking was done accordingly. The analysis was done by a similar method as discussed in Kumar et al. (2020a).

To evaluate the filter performance for the removal of metal ions, Fe^{2+} and Cu^{2+} was chosen as the metal indicators in lake water where $FeSO_4.7H_2O$, $CuSO_4.5H_2O$ was used as the metal source to spike it (stoichiometric equivalent) at an initial concentration of 10 ppm and 20 ppm respectively. When copper test was reported, it was made sure that there was no ammonia in the water and vice-versa, because of the likely interference of these compounds to form a complex with each other,

thereby incurring overestimation in reporting the ammonia/Cu^{2+} removal. The detailed method for estimating copper and iron are mentioned in Mehlig et al. (1941) and Fortune et al. (1938), respectively.

Turbidity, Total Coliform, Specific UV254 removal

Initial turbidity of the lake water was around 13.2 ± 4 NTU. All the filters were tested for their efficiency in removing suspended particles from the lake water using HACH instrument 2100 model where the effluent turbidity was reported in Nephelometric Turbidity Unit (NTU).

Total coliform removal test was performed twice a cycle (every 2^{nd} and 5^{th} day of the week or cycle) for the filtered water sample by membrane filtration technique according to a standard method APHA (1998). Initial total coliform present in the lake water was determined to be 56 CFU ± 14 /100 mL. To report the degree of natural organic matter removal, an indirect measurement using specific UV254 (SUVA) was done, where the change in SUVA for the influent and effluent was reported for the organic matter removal.

Flow rate and MC-LR removal

The flow rate for each filter was reported in m/h ($m^3/m^2/h$) after the end of each cycle. A stagnant water head of 70 ± 5 mm was maintained (from top layer of sand composite media) throughout the measurement process. The flow rate for any filter should not decrease to $1/4^{th}$ of the initial flow rate during any stage of the biofilter operation which was kept as the subjective minimum criterion. If the flow falls below $1/4^{th}$ the initial flow rate value, backwashing was performed for the filter at the flow rate low enough to not fluidize the bed and should not cause more than 15% bed expansion.

MC-LR from the stock solution was diluted appropriately to the lake water (lake water had no detectable MC-LR) to obtain an influent MC-LR concentration of 50 µg/L. The effluent was analyzed for MC-LR twice a cycle (or week) using a method adapted from Roy-Lachapelle et al. (2019). Briefly, a 20-µL sample aliquot was analyzed by ultra-high-performance liquid chromatography coupled to high-resolution mass spectrometry (Thermo Q-Exactive Orbitrap) through a positive electrospray ionization source. The chromatographic column was a Thermo Hypersil Gold with C18 selectivity (100 x 2.1 mm, 1.9 µm particle size). MC-LR was detected in full-scan MS mode (resolution set at 70,000 FWHM at 200 m/z) and quantified against a matrix-

matched lake water calibration curve (Roy-Lachapelle et al. 2019). The analytical method was validated for linearity, accuracy, and precision; the performance was compliant with acceptance criteria (Roy-Lachapelle et al. 2019). The method limit of quantification (LOQ) was set at the lowest concentration level of the calibration curve (i.e. 0.1 µg/L). At the end of stage 2 and stage 3 filter operation, all the filters were subjected to three different MC-LR influent concentration of 5 µg/L, 20 µg/L and 50 µg/L to better understand the limitation of each filters.

Regeneration and reuse studies

A regeneration and reusability study for all the filter media was performed to understand the behaviour of adsorption and to envisage the economic feasibility of using each filter medium. The adsorbate used for the study was Rhodamine-B dye which represented the coloured and model contaminant. The dye-adsorbate was used at an initial concentration (C_o has an optical density of 0.21) of 1 mg/L for each adsorbent. A continuous flow rate of 4mL/min was maintained using a peristaltic pump and the effluent OD at 550 nm (C_e) was taken after every bed volume (25 mL) to estimate the adsorption of dye material on to the sand composites. A column height of 7.5 cm for each adsorbent was taken. The breakthrough period was determined at $C/C_o = 0.05$) for each of the sand composites. After the exhaustion of bed material ($C/C_o \sim 1$), the adsorbent media was regenerated using acetone solution and was reused again for the dye-adsorption study. The saturation adsorption capacity (Wsat) of the bed media was reported for each filter media for 3 regenerated cycles to understand the reusability aspect of each adsorbent. The following equation (Equation 14) was used for calculating the Wsat (mg/g) value:

$$W_{sat} = \left(\int_0^t U_o\, C_o \left(1 - \frac{c}{c_0}\right)\right) / \text{(g-adsorbent)} \qquad \ldots\text{Equation 14}$$

Where, Uo is the flow velocity in L/minute, Co is the initial adsorbate concentration in mg/L and t is the breakthrough time in minutes.

Statistical analysis and graphics

All statistical analyses comprising standard deviation, average, student t-test, p-value comparison, Principal Component Analysis (PCA) and all graphical presentations were performed using the ORIGIN software (Version 8.5; OriginLab).

Results and Discussions

Bacterial activity test for the synthesized rGO and GO

Table 4.2.1 shows the cell enumeration results of two MC-LR-degraders viz. *Arthrobacter ramosus* and *Bacillus* sp. for GO and rGO at various dose concentrations (mentioned in method section). A high GO/rGO dose was required to provide high surface area for coated sand, hypothesizing a better MC-LR adsorption on the coated surface and at least a 60% survivability of the MC-LR-degraders was also required to proceed with the screening experiment as the biofilm formation was a pre-requisite for biofilter operation. However, a high dose of GO/rGO were found antibacterial (Table 4.2.2) and thus the maximum dose was restricted to 640 mg/L. It was observed that 400 mg/L of GO showed 62% and 61% survivability while 520 mg/L of rGO showed survivability of 62% and 64% for *Arthrobacter ramosus* and *Bacillus* sp., respectively. As the dose of GO and rGO was increased beyond 400 mg/L for GO and 540 mg/L for rGO, the survivability % also decreased and hence the above values, i.e., 400 mg/L and 520 mg/L for GO and rGO, were selected. To convert this dynamic value to static value, 5mg/g-sand and 6.5 mg/g-sand was chosen as the coating dose for GO and rGO, respectively. The rationale for the static-dynamic calculation is shown in Figure F2 (Appendix F).

Table 4.2.1: Cell-enumeration to study the survivability rate of Microcystin-LR-degraders

Case	*Arthrobacter ramosus#*	% survival	*Bacillus* sp.#	% survival
Zero	32 ± 7	100	51 ± 12	100
100 mg/L GO	28 ± 5	87	42 ± 13	82
300 mg/L GO	25 ± 8	78	36 ± 8	71
400 mg/L GO	20 ± 3	62	31 ± 9	61
520 mg/L GO	14 ± 6	44	18 ± 6	35

640 mg/L GO	12 ± 9	38	14 ± 4	27

Case	***Arthrobacter ramosus#***	**% survival**	***Bacillus* sp.#**	**% survival**
Zero	32 ± 6	100	51 ± 6	100
100 mg/L rGO	29 ± 2	92	48 ± 2	94
300 mg/L rGO	24 ± 7	81	41 ± 7	80
400 mg/L rGO	22 ± 8	75	37 ± 6	73
520 mg/L rGO	19 ± 4	62	33 ± 3	64
640 mg/L rGO	16 ± 6	51	18 ± 5	35

The count of bacterial colonies was done for the 10^5 dilution LB-media agar plates; rGO: reduced graphene oxide, GO: Graphene oxide, FeGO: Iron coated on graphene oxide coated sand

Characterization of the synthesized materials: GO/rGO

To characterize the obtained graphene oxide, an FT-IR interferogram was generated and analyzed for the presence of the oxygen-functionalized groups to validate the oxygen atoms intrusion in synthesized graphene oxide. Figure 4.2.2 (A) shows the FT-IR spectra for the graphite flake and graphite oxide. From the FT-IR, spectra, -COOH, -OH and C-O-C groups was completely absent for the graphite flake while these groups were observed at the characteristic wavenumbers: 1719 cm^{-1}, 3200 cm^{-1} and 1351-1390 cm^{-1}, respectively. The FT-IR spectra also showed the evidence of skeletal vibration of the graphene plane at wave number of around 1560 cm^{-1}. This suggested that the exfoliation of the graphite oxide happened in form of graphene oxide. Figure 4.2.2 (B) shows the FT-IR spectra for the graphene oxide prepared at three different pH: 3, 7 and 10. Figure 4.2.3 (A) shows the SEM images of the graphite flake and synthesized GO at pH 3, 7 and 10. Skeleton vibration of the graphene plane which occurs at the characteristic peak of 1560 cm^{-1}, was chosen as the main criterion to distinguish the degree of exfoliation in graphene oxide. It was observed from the FT-IR spectra that the peaks were more pronounced for the graphene oxide at pH 10. Also, the SEM demonstrated that the synthesized GO showed more exfoliation on its surface under alkaline condition.

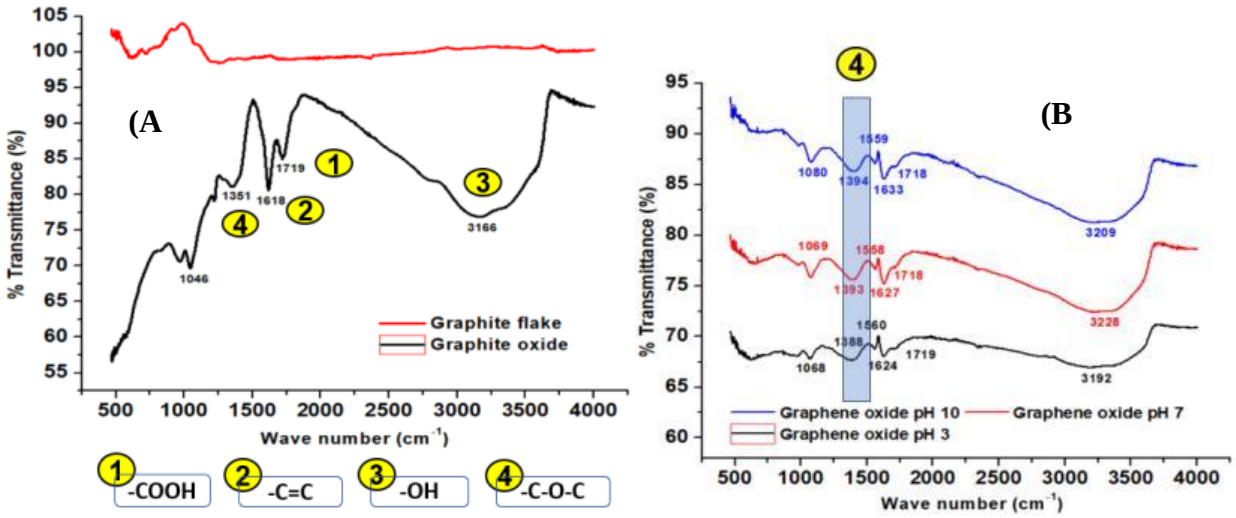

Figure 4.2.2: FT-IR spectra for the A) graphite flake and synthesized graphite oxide, B) Graphene Oxide at different pH

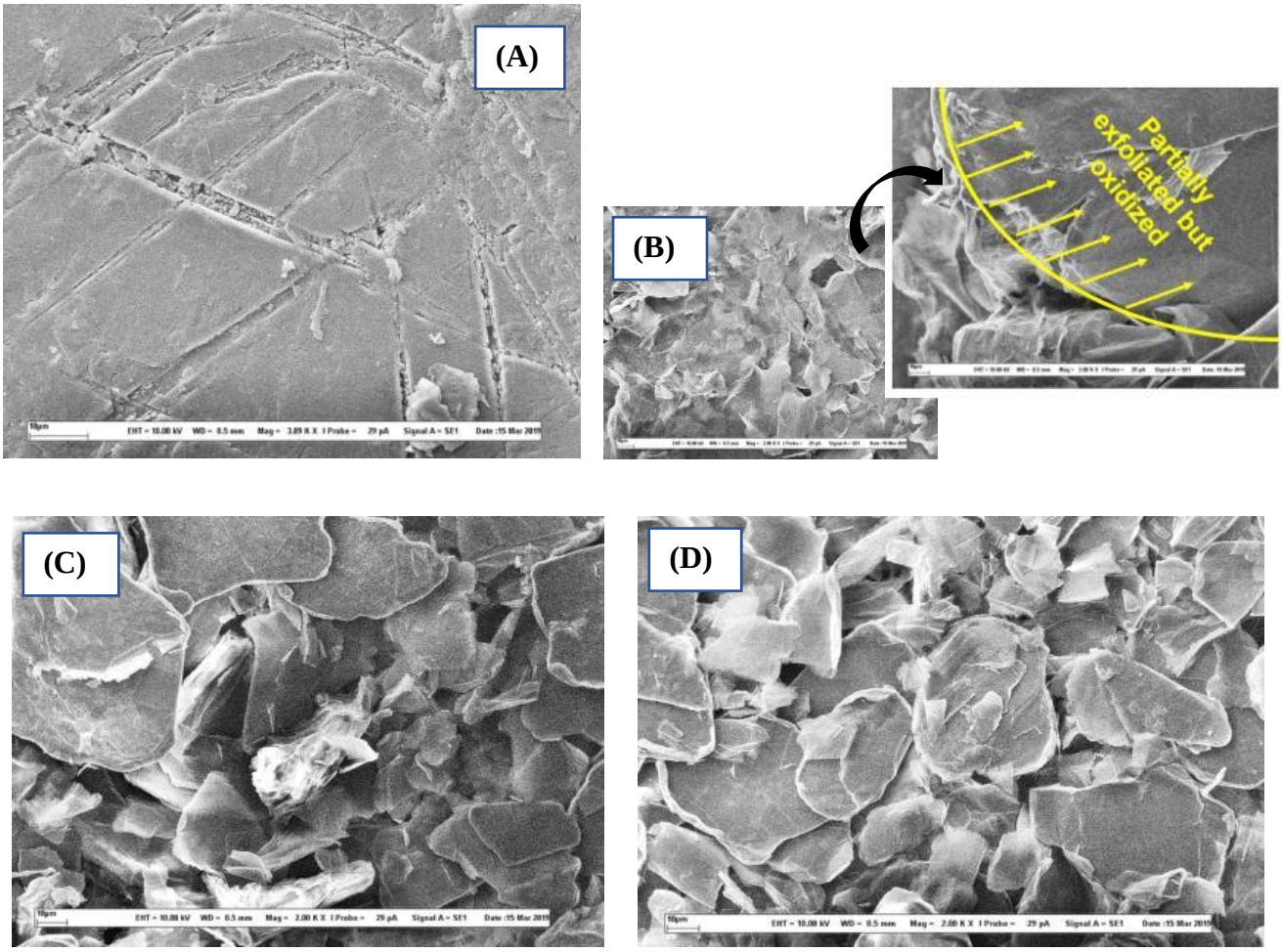

Figure 4.2.3: SEM images of the A) graphite flake, Exfoliated graphene oxide at B) pH 3, c) pH 7 and D) pH 10.

To further validate the synthesis of graphene oxide, EDX analysis was carried out to determine the ratio of C/O in terms of the atomic percentages. EDX spectra showed that the ratio of C/O for graphite flake was more than 75 while it reduced to 2.1 due to the oxidation of graphite into graphite oxide. Sonication of graphite oxide to graphene oxide at different pH increased the C/O ratio to 2.5, 2.8 and 2.2 at pH of 10, 7 and 3, respectively. The minimum ratio among all was at pH 10 which attributed to more oxygen atom intrusion into the graphene sheet as compared to pH 3 and 7. Thus, for the sand thermal coating, alkaline environment was chosen for dispersing the GO compound. To characterize the rGO compound, FT-IR spectra was obtained (Figure in Appendix F: Figure F4). It was observed that rGO after 40 min of reaction time (40 min reduction of GO) showed the maximum oxygen reduction (especially of the -OH peak at 3200-3300 cm^{-1}).

Characterization of the coated sand composite

Table 4.2.1 shows the EDX analysis for all the synthesized filter media. A high percentage of carbon was found to be coated in GO (~70%) and FeGO (52%) coated-sand grains whereas, maximum atomic Fe % of 43% and 6% was found for the iron-coated grains viz. Fe and FeGO, respectively. This ensured high iron oxide coating in case of Fe grains while a balance of carbon and iron oxide for FeGO grains. According to the atomic percentage values (Table 4.2.1) the chemical formula obtained for Fe and FeGO sand grains was $SiFe_{18}O_{22.5}$ and $SiFe_{7.5}C_5O_8$, respectively. The surface zeta potential measured for Fe, FeGO, GO and rGO was -21.3 mV, -13.4 mV, -22.3 mV and -18.7 mV, respectively. As compared to the zeta potential of uncoated sand grain, all the surfaces were found to be more electro-positive, especially the Fe grain.

Table 4.2.2: EDX analysis for all the synthesized filter media

Filter Media	Atomic% C	Atomic% O	Atomic% Si	Atomic% Fe	Color	Figure	Zeta potential (mV)
Iron oxide coated sand (Fe)	NA	53.97	2.40	43.05	Orange		-21.3
FeGO (Fe+GO)	22.4	36.93	4.60	34.5	Brownish black		-13.4
GO	69.87	24.56	4.87	NA	Black		-22.3

Filter Media	Atomic% C	Atomic% O	Atomic% Si	Atomic% Fe	Color	Figure	Zeta potential (mV)
rGO	29.67	59.87	8.75	NA	Light black		-18.7
Sand	0.00	72.30	26.70	NA	Yellowish white		-43.2

rGO: reduced graphene oxide, GO: Graphene oxide, FeGO: Iron coated on graphene oxide coated sand

Screening the MC-LR-degraders for each sand composite

Figure 4.2.4 (A) and Figure 4.2.4 (B) present the bar chart graphs for the CV assay and MTT assay, respectively for all the sand composite adsorbents.

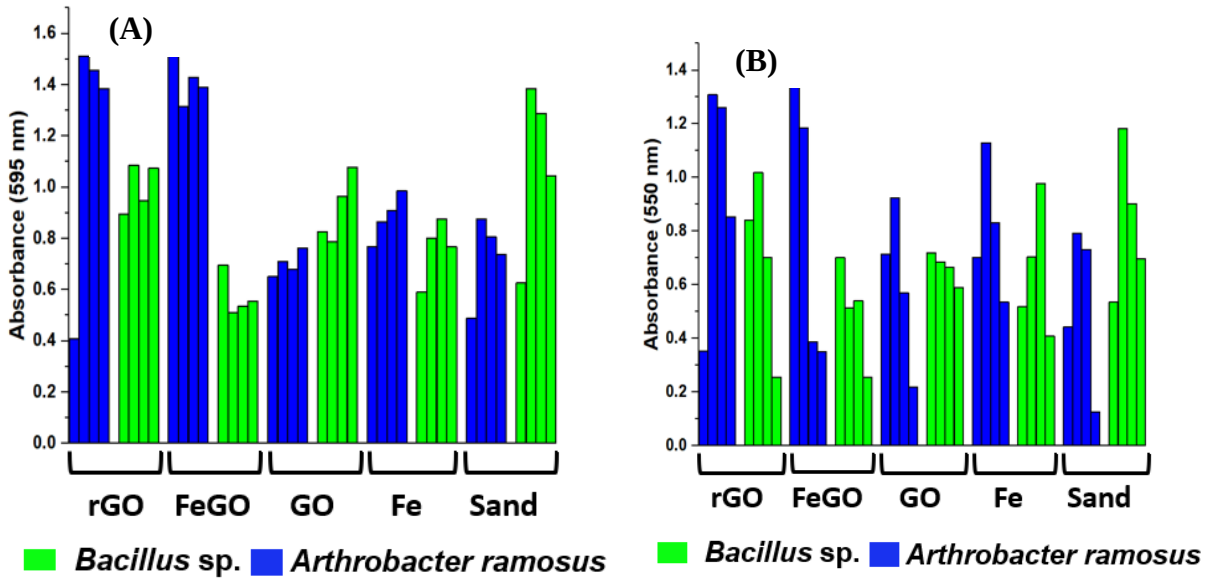

Figure 4.2.4: Biofilm screening test for all the synthesized filter media quantified as A) CV assay and B) MTT assay.

rGO: reduced graphene oxide, GO: Graphene oxide, FeGO: Iron coated on graphene oxide coated sand

For rGO and FeGO, *Arthrobacter ramosus* (AR) showed higher optical density than *Bacillus* sp. (BS), for both CV as well as MTT assay. The observed mean difference for rGO and FeGO between the data set for AR and BS was 0.19/0.24 and 0.84/0.32 for CV and MTT assay,

respectively. For GO and Fe, the OD value between AR and BS data set was similar. The statistical analysis showed p-value of 0.11 for GO case (CV assay data sets for AR and BS) and p-value of 0.15 for Fe case (CV assay). The mean difference of OD between AR and BS for CV and MTT assay was -0.11 and 0.06, respectively. From the above two statistical considerations, AR and BS seemed the most appropriate choice for GO and Fe, respectively. For sand, as can be observed, BS was the preferred choice over AR.

Biofilm formation study: Stage 2 filter operation

After the stage 1 filter operation, each filter was inoculated with their respective screened MC-LR-degraders (along with native bacterial co-culture: 'X' as mentioned in method section). Figure 4.2.5 (A), (B) and (C) represents the CV assay, MTT assay and flow rate (m/h) for each filter. All filters showed an increase in biomass production especially for the sand surface (uncoated) as compared to other sand composite materials (average CV assay OD of 0.78 as compared to next best OD of 0.59 for rGO). The rGO/GO coated-sand material still showed better biomass formation (average CV assay OD of 0.59/0.51) on its surfaces as compared to Fe and FeGO sand composites (average CV assay OD of 0.26/0.36). The choice of the 60% survivability principle corresponds well with the biomass growth. This can also be perceived from the MTT assay result too (Figure 4.2.4 (B)) where it can be observed that the biofilm adhered to rGO/GO sand composites (average MTT assay OD of 0.43/0.36) surface had better cell viability only next to the uncoated sand surface (average MTT assay OD of 0.49).

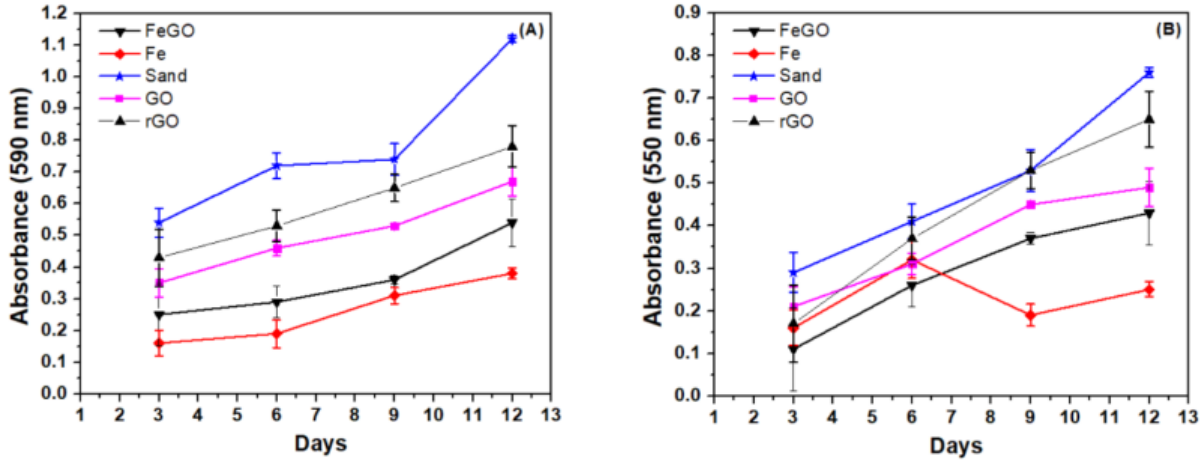

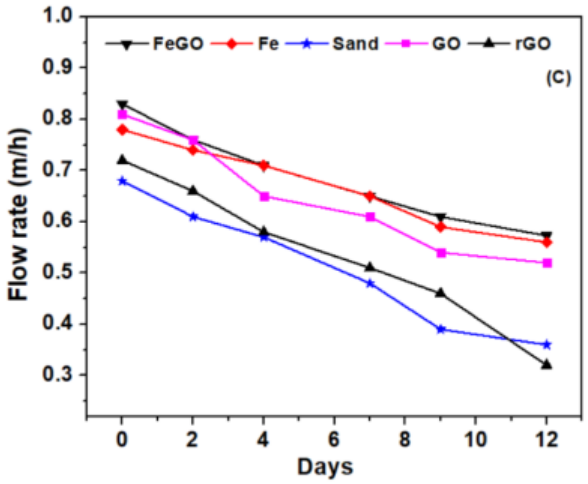

Figure 4.2.5: Biofilm forming phase study for A) biomass formation (CV assay), B) cell viability (MTT assay) and C) Flow rate (m/h).

rGO: reduced graphene oxide, GO: Graphene oxide, FeGO: Iron coated on graphene oxide coated sand

Flow rate for all the filter decreased as was expected because of the tortuosity resistance in flow due to the biomass formation between the sand grains. The maximum decrease in the flow rate was measured for sand filter (43%) followed by rGO (36%) and GO (33%) coated sand filter. These results go in coordination with the biofilm formation for both CV as well as MTT assay (all showed a correlation of ~ -0.9).

Water Quality Parameters (WQPs)

Table 4.2.3 presents various WQP of all the sand composite media for both the phases of filter operation. Maximum NH_4-N removal was observed for the FeGO filter (56%) in both the stages where bioaugmentation improved the removal efficiency by 12% (44% to 56%) whereas the GO filter showed the maximum improvement of 24%. The second-best filter for ammonia removal was the Fe filter which showed removal of 46% in stage 3 indicating that it was iron more than GO that was responsible for high ammonia adsorption in case of FeGO. In contrast, for the oxidized form of nitrogen, i.e., nitrate, FeGO was the third best filter that showed 45% removal next to the rGO/GO filter (each showed over 60% nitrate removal). The Fe filter was the least effective with just over 12% removal indicating the contrasting nature of iron for ammonia and nitrate adsorption.

Maximum average total coliform removal of over 80% was observed for the GO and rGO filters followed by 68%, 47%, and 14% for the FeGO, Fe and sand filters, respectively. This indicated that GO mixed with Fe (for the FeGO filter) enhanced the total coliform removal by 21%. The GO surface might have created a physical disruption of the bacterial cells or created oxidative stress environment for the coliforms (Hu et al. 2010). Bioaugmentation of MC-LR degraders and native bacterial species did not enhance the total coliform removal by much (maximum of 9% in the rGO filter) which clearly illustrates that the predation mechanism was not prevalent in these biofilters (Li et al. 2012). Hence, modification in the surface of sand directly affected the coliform removal by other mechanisms such as trapping, oxidative stress or physical disruption as mentioned above.

Table 4.2.3: Water Quality Parameters (WQPs) for all the filter media

Water Quality Parameter	Stage	FeGO	Fe	Sand	GO	rGO
Conductivity	Stage 1	107 ± 16	110 ± 14	90 ± 32	212 ± 12	209 ± 23
	Stage 3	114 ± 13	116 ± 12	87 ± 17	211 ± 32	232 ± 21
DO (mg/L) [5.7 mg-O_2/L)	Stage 1	5.31 ± 0.34	5.48 ± 0.13	5.2± 0.40	5.6 ± 0.32	5.4 ± 0.17
	Stage 3	4.56 ± 0.18	4.43± 0.26	4.1 ± 0.22	4.7 ± 0.15	4.4± 0.32
Time to filter 40 mL standing water (min)	Stage 1	10.5 ± 1.5	9.1 ± 0.6	13.3 ± 1.7	10.76 ± 1.6	13.3 ± 2.9
	Stage 3	15.4 ± 1.2	13.3 ± 1.7	25.6 ± 2.7	13.7 ± 1.1	29.1 ± 3.3
NH_3-N (mg/L) [5 mg/L]	Stage 1	2.8 ± 0.5	3.1 ± 0.6	3.3 ± 0.7	4.2 ± 0.3	3.3 ± 0.4
	Stage 3	2.2 ± 0.2	2.7 ± 0.4	3.72 ± 0.6	3.0 ± 0.5	3.2 ± 0.5
NO_2^--N (mg/L) [10 mg/L]	Stage 1	7.8 ± 0.2	7.9 ± 0.8	6.2 ± 0.5	5.5 ± 0.6	6.1 ± 0.5
	Stage 3	7.5 ± 0.3	7.5 ± 0.8	5.8 ± 0.4	4.9 ± 0.4	5.8 ± 0.5
NO_3^--N (mg/L) [50 mg/L]	Stage 1	30.6 ± 1.9	44.4 ± 6	31.9 ± 4	20.9 ± 4.1	21.9 ± 4.3
	Stage 3	27.5 ± 2	43.7± 3	29.9± 4	19.76 ± 2	19.32 ± 3
pH	Stage 1	5.87 ± 0.3	6.17 ± 0.2	6.18 ± 0.4	5.99 ± 0.1	6.16 ± 0.1
	Stage 3	5.99 ± 0.1	6.11± 0.2	5.78 ± 0.4	5.76± 0.7	6.43 ± 0.3
Total Coliform (per 100 mL) [56 CFU]	Stage 1	17 ± 5	19 ± 4	47 ± 6	14 ± 3	16 ± 6
	Stage 3	16 ± 3	27 ± 4	44 ± 5	10 ± 2	11 ± 2
Turbidity (NTU) [13.2]	Stage 1	2.82 ± 0.39	3.55 ± 0.76	3.12 ± 0.16	1.34 ± 0.47	1.66 ± 0.28
	Stage 3	2.45 ± 0.38	3.44 ± 1.14	4.27 ± 0.35	1.28 ± 0.53	1.61 ± 0.41
Cu (mg/L) [20 mg/L]	Stage 1	6.2 ± 2.7	14.1 ± 2.3	15.4 ± 2.9	11.4 ± 3.1	13.1 ± 2.4
	Stage 3	5.9 ± 0.9	11.8 ± 1.4	15.7 ± 1.9	8.4 ± 3.3	9.2 ± 1.6
Fe (mg/L) [10 mg/L]	Stage 1	0.18 ± 0.14	6.3 ± 0.4	6.7 ± 1.43	0.18 ± 0.12	0.21 ± 0.12
	Stage 3	0.26 ± 0.15	6.2 ± 0.3	5.6 ± 0.70	0.34 ± 0.19	0.41 ± 0.32

Water Quality Parameter	Stage	FeGO	Fe	Sand	GO	rGO
MC-LR removal (%) [50 µg/L]	Stage 1	71.2 ± 8.1	1.15 ± 9.4	16.3 ± 20.3	79 ± 19.4	44.2 ± 10.6
	Stage 3	85.8 ± 11.7	33.5 ± 17	54.6 ± 14	82.5 ± 6.8	91.4 ± 6.5
DOC removal [6 mg/L]	Stage 1	3.7 ± 0.1	4.8 ± 0.2	4.6 ± 0.2	3.1 ± 0.3	4.4 ± 0.1
	Stage 3	3.4 ± 0.23	4.5 ± 0.1	4.8 ± 0.2	2.3 ± 0.4	2.2 ± 0.2

Initial concentration of each WQP is given in bracket; rGO: reduced graphene oxide, GO: Graphene oxide, FeGO: Iron coated on graphene oxide coated sand

The maximum DOC removal of 62% each was obtained for the GO and rGO filters whereas the Fe and sand filters performed worst with just 23% and 17%, respectively. DOC removal enhanced maximally during the biodegradation phase (stage 3) for the rGO filter (50%) followed by the GO filter (26%). Highest DOC removal by the GO filter can mainly be attributed to an enhanced hydrophilicity of the sand surface due to the GO coating leading to more interaction with the chemical contaminant in aqueous media (here lake water) at the nanometer level (Singh et al. 2011). After a long usage of the GO filter (13 weeks including all the stages) there was no evidence of any surface peel-off. In addition, hydrogen bonding and π–π interaction could also be responsible for high DOC removal/adsorption on GO-coated sand media (Hou et al. 2015).

Maximum copper removal was observed for FeGO (71%) followed by 54% and 58% for the rGO and GO filters, respectively as compared to <25% for the sand filter and 40% for the iron coated sand filter. On the other hand, FeGO, GO and rGO showed >95% Fe^{2+} ions removal for both stage 1 and 3 of filter operation whereas the sand filter and the iron coated sand filter showed < 50% adsorption.

High adsorption of metal ions (copper and iron) for FeGO can be linked to low pH effluent among all the filters (Table 4.2.3). This removal mechanism involves the leaching of H^+ ions when already sorbed-metal surface is exposed to the cationic metal ions (Benjamin et al. 1996). However, a possible desorption mechanism occurs when the sorbed-surface becomes alkaline and meets the diffused H^+ ions to release back the sorbed metal ions. Hence, any alkaline pretreatment of raw water before filtration may make these filters less efficient. On the other hand, high metal adsorption can be linked to the multi-layered and rough surface GO coating over the planar sand surface (SEM image, refer Figure F5, Appendix F) which allowed more adsorption of metal ions. Gao et al. (2011) suggested a core-shell structure of GO that formed over the sand surface

responsible for 5-times more Hg^{2+} ions adsorption as compared to sand media. Also, in the above study, the coating of GO per gram of sand was quite close (3.5 mg/g-sand) to the present study (5 mg/g-sand) and hence intergranular diffusion resistance can be almost similar that formed the basis for comparison of GO-coated sand in the former study with more commercialized filter media: activated carbon.

Understanding the Water Quality Parameters (WQPs) removal using PCA and deciding the best filter

Figure 6 (A) and Figure 6 (B) represents the PCA biplot graph for stage 1 and stage 3 filter operation. The biplots comprises of filters as the observation variables and various WQP (based on their removal %) as the main variables. Principal component 1 (PC1) and Principal component 2 (PC2) accounted for 57% and 29% of the total variation in data while its 66% and 25% for stage 1 PCA and stage 3 PCA, respectively.

Since PC1 showed a high variable load in both the cases, hence, the loading scores obtained on PC1 axis was primarily used to determine the overall filter (observation variables) performance and their % improvement from stage 1 to stage 3. The overall best and worst loading score (LS) for stage 1 was -2.98 and +2.67 and for stage 3 it was -2.92 and +2.43, respectively. From the LS data, the best filter in stage 1 was GO (LS: +2.67) followed by rGO (LS: +1.58), FeGO (+0.70), Sand (LS: -1.97) and Fe (LS: -2.98). In stage 3 filter operation, the rank followed: rGO (+2.43) > GO (+2.20) > FeGO (+0.86) > Sand (-2.56) > (-2.92). A major improvement in the filter performance was observed for rGO (53%) after the biofilm formation followed by sand (30%) and FeGO (23%). A high improvement for rGO was mainly contributed from the enhanced removal of copper, DOC and nitrite by 36%, 28% and 14%, respectively. The poor performance of the uncoated sand filter and Fe filters in both the stages (1 and 3) was evident from the PCA biplot which shows their position (red dot) in the far end 3rd and 2nd quadrant, respectively and no proximity with PC1 or eigenvectors of any WQPs. However, if an overall PCA biplot is investigated, there does not exist much difference between both the stages of the filter performance.

Except for the ammonia eigenvector, all other WQP showed a positive correlation (> 0.5) with MC-LR for both the filter operation stages (correlation matrixnot shown here). Proximity of FeGO

with the ammonia eigenvector was justified owing to its best ammonia removal performance (55%) as compared to other filters (especially uncoated sand: 25% only).

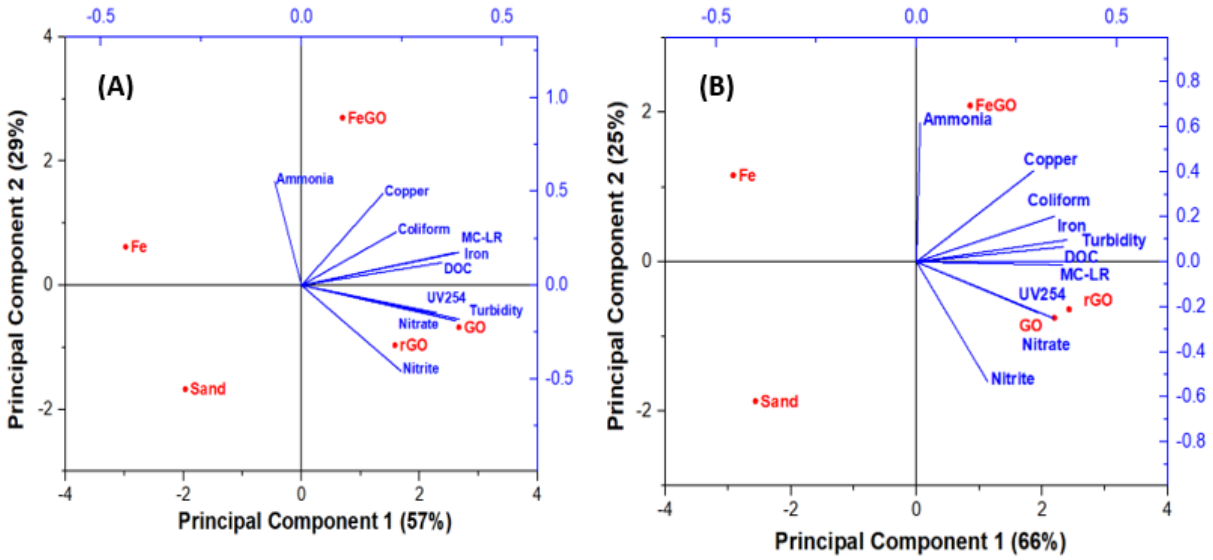

Figure 4.2.6: Principal component analysis for water Quality Parameters (WQPs) as the main variables and the filters as observation variables: (A) Physical adsorption stage (stage 1), B) Bio-adsorption stage (stage 3).

rGO: reduced graphene oxide, GO: Graphene oxide, FeGO: Iron coated on graphene oxide coated sand

Copper was the closest eigenvector to ammonia and best related to the latter with a correlation factor of 0.64. This can be attributed to the complexation of the two compounds which lead to their removal simultaneously. In this study, there was no specific study done to analyze their complex and thus it would be interesting to study this parameter by the plant operator in DWTPs as it may lead to health problems in humans such as digestive problem, collapse and vomiting if not removed.

Microcystin-LR removal

The average mean MC-LR removal for stage 1 was 71.2%, 1.15%, 16.3%, 79%, 44% for FeGO, Fe, Sand, GO and rGO, respectively. The poor removal efficiency of MC-LR in the Fe filter can be attributed to a planar surface morphology of Fe grains (refer to SEM image: Figure F5, Appendix F). Despite a high electropositive surface (Table 4.2.1), Fe grains could not adsorb MC-LR molecules and performed below par even to the control filter. In contrast, the FeGO and GO filters performed quite well achieving >70% MC-LR removal which can mainly be due to

roughness (functionalized groups of graphene oxide layers) on their surface as observed from the SEM images (Figure F5). The functionalized groups containing more oxygen atoms could be the reason for making the surface more hydrophilic that might had allowed more surface attachment of the hydrolyzed MC-LR molecules (Doepke et al. 2012).

On the other hand, less hydrophilic surface in case of rGO-coated sand media, due to functionalization of compounds containing fewer oxygen atoms might be the reason for less MC-LR attachment (for physical adsorption phase). Also, the BET isotherm showed a high mesoporous surface with specific surface area of 33.8 m^2/g for GO-coated sand as compared to 5.5 m^2/g for uncoated sand, respectively (BET isotherm in appendix F: Figure SA6). Teixidó et al. (2011) too showed strong sorption (10^6 L/kg) of hydrophilic compounds (sulfamethazine) on the carbon surface (biochar) that mainly found electron donor-acceptor (EDA) interaction (due to ring structure in sulfamethazine) with π-electron-rich graphene surface responsible for the adsorption. However, MC-LR consists of small fraction of such EDA (ADDA group) in their whole macromolecule and thus such possibility of adsorption could be highly unlikely as compared to the surface groups contribution on FeGO and GO coated sand surfaces. Also, Coulombic attraction between negatively charged MC-LR and more electropositive charged surface of FeGO (-13.4 mV) and GO (-22.3 mV) sand media as compared to uncoated-sand surface (-43 mV) could possibly be responsible for high MC-LR removal in case of GO and FeGO. However, the same theory does not hold true for Fe and rGO sand grains, especially Fe which showed almost the same degree of electropositive surface (-21.3 mV) as GO-coated sand. Hence, the meso-porous surface layer of GO could be the main contributor to high MC-LR adsorption (Wang et al. 2019). Apart from performing MC-LR analysis twice a cycle, all the filters were tested for the residual MC-LR concentration in filtered water at the end of stage 1 (6^{th} Week) and stage 3 (14^{th} Week). The experiment was performed for three different initial MC-LR concentration viz. 5 µg/L, 20 µg/L and 50 µg/L.

Figure 7 (A) and Figure 7 (B) shows the residual MC-LR obtained in form of bar chart for both the stages of filter operation. GO filter performed best among all the filter media even at the highest initial MC-LR concentration of 50 µg/L, removing 77% and 91% MC-LR in stage 1 and stage 3, respectively.

On an average, the mean removal efficiency of 71.2 ± 8.1 % and 86.0 ± 11.7 % was observed for FeGO filter when GO was coated over Fe-coated sand for stage 1 and stage 3 filter operation (Table 2), respectively. From this, it can be inferred that the GO coating over Fe-coated sand has remarkably enhanced the MC-LR adsorption by > 70% and > 50% in stage 1 and stage 3 filter operation. This further strengthens the factor of 'pi-pi interaction' and 'C-O-C group interaction' with -COOH and NH_2 group of MC-LR molecule that can be held responsible for a higher MC-LR adsorption or molecule transformation (discussed more in detail in next section). An overall average enhancement of 14.8%, 32%, 38%, 3.5% and 47% in MC-LR removal due to bioaugmentation (stage 3) was observed for FeGO, Fe, Sand, GO and rGO, respectively. It shows that except GO, rest all adsorbents shown enhanced performance in MC-LR removal, possibly by biodegradation.

In general, it can be inferred that the carbon atom coated over sand material such as GO, not only enhanced the MC-LR removal but also maintained a good adsorption rate (> 80% MC-LR removal at a residence time < 25 minutes). This could also be related from the results of our previous study where graphitized sand (> 65 % carbon atoms based on atomic percentage value), synthesized using the brewery effluent sugar solution achieved a similar removal efficiency to GO [27]. A comparative study of various sand filters is presented in our previous published work (Kumar et al. 2020a). Though, the removal efficiency achieved by carbon sub-micron particles coated sand (GO) for MC-LR and other water pollutants is higher (Table 4.2.3) than uncoated sand, the cost of synthesis can be an issue in future. However, a strong saturation adsorption capacity (discussed in later section) and hence a higher breakthrough period can further improve the service life of sand material which can then be made techno-economically feasible. A preliminary technoeconomic study was done based on the MC-LR adsorption capacity of GO-coated sand and sand adsorbent for the household purpose filter (according to Center for Affordable Water and Sanitation Technology or CAWST biofilter specification version 10.0). It was found that the GO-coated sand filter was economical (¾ th price to that of sand household filter (~ 2800 CAD/annum)). The frequency change in the filter media as calculated for the sand filter was just 6 days as compared to over 70 days for the GO filter.

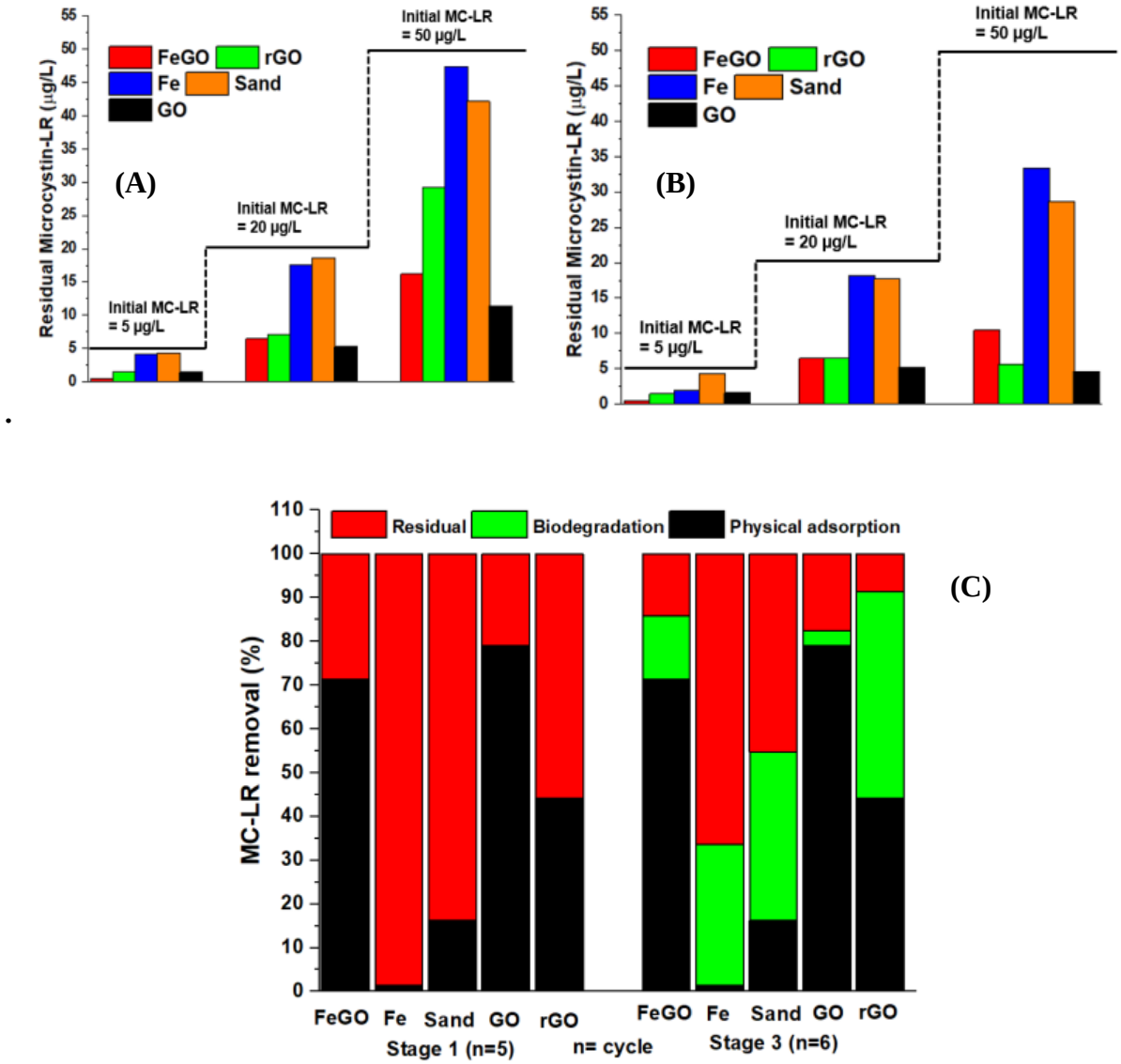

Figure 4.2.7: Microcystin-LR removal by different synthesized filter media tested at three different concentration for A) stage 1 and B) Stage 3, and C) Microcystin-LR removal by different synthesized sand media

rGO: reduced graphene oxide, GO: Graphene oxide, FeGO: Iron coated on graphene oxide coated sand

In the current study, only two MC-LR degraders: *Arthrobacter ramosus* and *Bacillus* sp. were chosen and co-cultured with the native bacterial species isolated from the filtration unit of DWTP and hence, any inferences on the possibility of more MC-LR biodegradation that could have been achieved otherwise is always subjective and most likely. Nevertheless, the highest MC-LR improvement due to bioaugmentation was reported for the rGO filter (by 47%) which was also

evident from the PCA analysis (Figure 6 (B)) where rGO point variable moved more closer to the MC-LR removal eigenvector in stage 3 filter operation. Since the GO and FeGO grains were tested for the biofilm formation and survivability test for GO particles before coating them over sand, it could be interpreted that the MC-LR and other water quality parameters were responsible for the decrease in cell viability in the formed biofilm resulting in a low MC-LR removal performance. Another possibility could be the incompatibility issues of co-culture growth mode for MC-LR-degraders with native bacterial species that outcompeted the former. The toxicity and the degradation mechanism were not deciphered in the current study and hence it would be very interesting to understand the by-product toxicity.

MC-LR interaction with the adsorbents: A chemistry point of view

Figure 4.2.8 depicts a Venn diagram showing common chemical interaction factors for every adsorbent material that could be held responsible for the MC-LR adsorption. Table 4 shows the chemical interaction factors and their evidence with the reference code to study Figure 4.2.8. Fe-coated sand adsorbent performed extremely poor (< 5 % MC-LR removal in phase 1) as compared to other adsorbents. The only contributing factor that could be held responsible for the MC-LR adsorption is electrostatic interaction due to electropositive surface properties (MC-LR molecule is negatively charged at pH 7). The reason for an average performance of rGO-coated sand adsorbent in terms of MC-LR removal (< 45% MC-LR removal) as compared to its oxidized form (GO-coated sand: 79 % MC-LR removal) could be attributed to the lack of C-O-C group due to less oxygen atom in the chemical structure of the former (refer EDX results: Table 2). Since, the MC-LR molecule in its native form shows two -COOH groups and one -NH_2 group, and the fact that C-O-C group assists in the transformation of above two chemical groups to other products (as shown in supplementary figure S10), could be held responsible for the above difference in MC-LR removal.

Table 4.2. 4: Type of chemical interaction responsible for MC-LR adsorption

Reference code	Type of interactions	Evidence
A	Hydrophobic interaction	Zeta potential
B	Epoxy/Ether group (C-O-C)	FT-IR

C	Pi-Pi interaction	FT-IR and comparison of result for MC-LR removal between GO/rGO and Fe/Sand
D	Electrostatic interaction	Zeta analysis

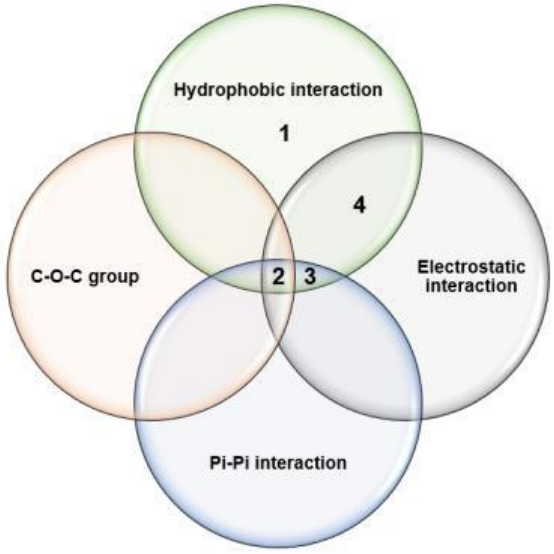

Adsorbent	**Designated number**	**Combination**
Sand		No
Fe	1	A
GO	2	A+B+C+D
rGO	3	A+C+D
FeGO	4	A+D

Figure 4.2. 8: Venn- diagram showing common chemical interaction factors for every adsorbent material

The common factor for GO and rGO that can be held responsible for the removal of MC-LR include electrostatic interaction, pi-pi interaction and hydrophobic interaction. On the other hand, FeGO shows the most electropositive surface among all the synthesized adsorbent material and due to more hydrophobic in nature, the combined factor showed strong factor in MC-LR removal as FeGO achieved more than 71% MC-LR removal during stage 1 filter operation. However, among all the four factors as depicted in Table 4.2.4, electrostatic interaction could be the weakest among all for the promotion of MC-LR adsorption as sand surface was found to be less electropositive than Fe-coated sand and yet the latter showed 30% less MC-LR removal than the former. Equally, the factor of BET surface area cannot be ignored as the physical adsorption also depends on the surface area available for the pollutant adsorption through Van der Waals` force (BET value of GO vs. Sand discussed earlier).

Regeneration and reusability study of the filter media

Figure 4.2.9 shows the breakthrough curve obtained for all the filters using Rhodamine-B as an adsorbate. The highest breakthrough time was observed for GO filter (30 minutes) followed by rGO (23 minutes), FeGO (22 minutes), Fe (7 minutes) and sand (7.3 minutes). The highest saturation adsorption (Wsat) was determined for the GO filter (10.4 mg/kg) followed by rGO (7.4 mg/kg) which was 7.4 and 5.3 times more than the sand filter. After three cycles of regeneration, GO filter media still retained the Wsat of 8.7 mg/kg, declining by just 16% as compared to a maximum decrease of 54% for Fe followed by 38% for FeGO and 24% for rGO coated sand media. The above results suggest high reusability aspects of GO filters that can be sustained for a longer period (operational time) as compared to the sand media.

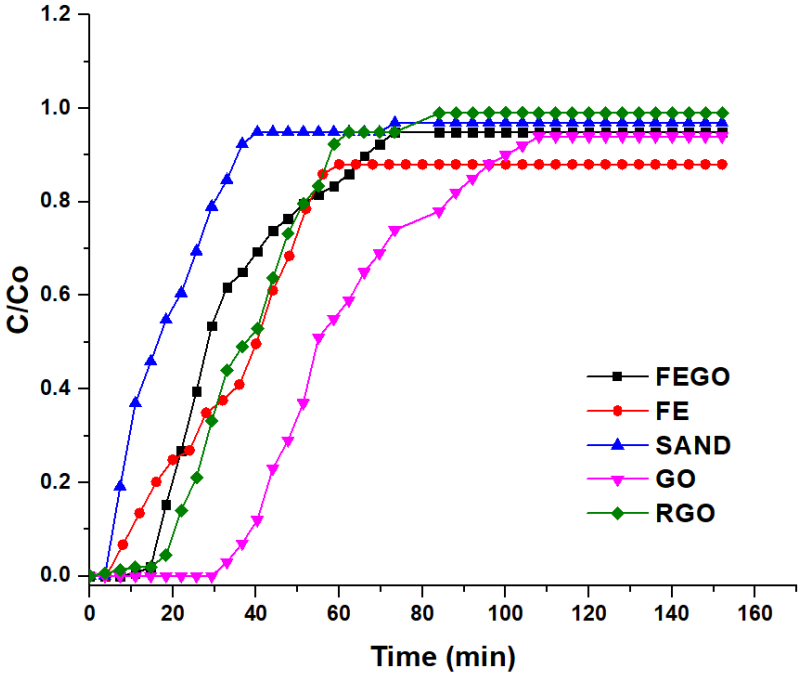

Figure 4.2.9: Breakthrough time curve for all the synthesized filter media

rGO: reduced graphene oxide, GO: Graphene oxide, FeGO: Iron coated on graphene oxide coated sand

Conclusion

Carbonization in form of graphene oxide (GO) and reduced graphene oxide (rGO) over sand grains improved the physical adsorption of Microcystin-LR (MC-LR) by 63% and 28%, respectively. Removal of other water quality parameters (WQPs) including metal ions, dissolved organic carbon and organic nitrogen components (NH_4-N, NO_2-N and NO_3-N) enhanced by coating GO and rGO over the sand media. The synthesized GO and rGO dose was optimized as 420 mg/L and 540 mg/L, respectively, before coating them over sand that maintained a survivability rate of at least 60% for the tested MC-LR-degraders: *Arthrobacter ramosus* and *Bacillus* sp. Under both phases of filter operation, the most efficient filter according to the Principal Component Analysis (PCA Loading scores) was the rGO-coated sand filter which was potent in removing most of the WQPs, including MC-LR by up to 91% (initial MC-LR: 50 µg/L). Regeneration of GO filter media showed around 7 times better saturation adsorption capacity (10.4 mg/kg) than the uncoated sand media. The more electropositive surface as compared to uncoated sand surface was found to be effective in MC-LR adsorption with enhanced performance (except iron oxide coated sand media). Presence of hydrophilic groups on mesoporous graphene oxide planes were found responsible for active adsorption of MC-LR on GO and FeGO (Fe + GO) coated sand media. Bioaugmentation of MC-LR-degraders further elevated the performance of WQPs removal where the MC-LR removal efficiency increased by 14.6%, 32%, 38%, 3.5% and 47% for filters: FeGO, Fe, sand, GO and rGO, respectively. Overall, the water treatment study using bio-optimized GO/rGO-coated sand media, carried by integrating various WQPs in real source water (lake water), has the potential to break frontiers for the biofiltration studies providing a modern approach to drinking water treatment facilities.

Acknowledgments

The authors are sincerely thankful to the Natural Sciences and Engineering Research (Discovery Grant 23451), and ATRAPP (Algal blooms, treatment, risk assessment, prediction, and prevention) for financial support (Genome Québec, Genome Canada; Grant 6116548-2015). Special thanks to Dana F. Simon (Université de Montréal) for coordinating the sample receipt and analysis. Authors would also like to thank the team for constant support and timely suggestions. We want to thank Genome Quebec for timely sequencing of the bacterial identification. The views or opinions expressed in this article is exclusively those of the authors.

Conflict of interest

None

References

Benjamin, M. M., Sletten, R. S., Bailey, R. P., & Bennett, T. (1996). Sorption and filtration of metals using iron-oxide-coated sand. *Water Research, 30*(11), 2609-2620. doi:10.1016/s0043-1354(96)00161-3

Stenkamp, V. S., & Benjamin, M. M. (1994). Effect of iron oxide coating on sand filtration. *Journal - American Water Works Association, 86*(8), 37-50. doi:10.1002/j.1551-8833.1994.tb06236.x

Li, L., Qiu, Y., Huang, J., Li, F., & Sheng, G. D. (2014). Mechanisms and Factors Influencing Adsorption of Microcystin-LR on Biochars. *Water, Air, & Soil Pollution, 225*(12). doi:10.1007/s11270-014-2220-6

Ali, I., Basheer, A. A., Mbianda, X. Y., Burakov, A., Galunin, E., Burakova, I., . . . Grachev, V. (2019). Graphene based adsorbents for remediation of noxious pollutants from wastewater. *Environ Int, 127*, 160-180. doi:10.1016/j.envint.2019.03.029

Fraga, T. J. M., Carvalho, M. N., Ghislandi, M. G., & Motta Sobrinho, M. A. d. (2019). Functionalized Graphene-Based Materials as Innovative Adsorbents of Organic Pollutants: A Concise Overview. *Brazilian Journal of Chemical Engineering, 36*(1), 1-31. doi:10.1590/0104-6632.20190361s20180283

Yousefi, N., Wong, K. K. W., Hosseinidoust, Z., Sørensen, H. O., Bruns, S., Zheng, Y., & Tufenkji, N. (2018). Hierarchically porous, ultra-strong reduced graphene oxide-cellulose nanocrystal sponges for exceptional adsorption of water contaminants. *Nanoscale, 10*(15), 7171-7184. doi:10.1039/c7nr09037d

Ding, Z., Hu, X., Morales, V. L., & Gao, B. (2014). Filtration and transport of heavy metals in graphene oxide enabled sand columns. *Chemical Engineering Journal, 257*, 248-252. doi:10.1016/j.cej.2014.07.034

Hu, W., Peng, C., Luo, W., Lv, M., Li, X., Li, D., . . . Fan, C. (2010). Graphene-Based Antibacterial Paper. *ACS Nano, 4*(7), 4317-4323. doi:10.1021/nn101097v

Singh, V., Joung, D., Zhai, L., Das, S., Khondaker, S. I., & Seal, S. (2011). Graphene based materials: Past, present and future. *Progress in Materials Science, 56*(8), 1178-1271. doi:10.1016/j.pmatsci.2011.03.003

Gao, W., Majumder, M., Alemany, L. B., Narayanan, T. N., Ibarra, M. A., Pradhan, B. K., & Ajayan, P. M. (2011). Engineered Graphite Oxide Materials for Application in Water Purification. *ACS Appl Mater Interfaces, 3*(6), 1821-1826. doi:10.1021/am200300u

Wang, Y., Li, Z., Tang, C., Ren, H., Zhang, Q., Xue, M., . . . Jiang, J. (2019). Few-layered mesoporous graphene for high-performance toluene adsorption and regeneration. *Environmental Science: Nano, 6*(10), 3113-3122. doi:10.1039/c9en00608g

Doepke, A., Han, C., Back, T., Cho, W., Dionysiou, D. D., Shanov, V., Heineman, W. R. (2012). Analysis of the Electrochemical Oxidation of Multiwalled Carbon Nanotube Tower Electrodes in Sodium Hydroxide. *Electroanalysis, 24*(7), 1501-1508. doi:10.1002/elan.201200105

Elbana, M., Ramírez de Cartagena, F., & Puig-Bargués, J. (2012). Effectiveness of sand media filters for removing turbidity and recovering dissolved oxygen from a reclaimed effluent used for micro-irrigation. *Agricultural Water Management, 111*, 27-33. doi:10.1016/j.agwat.2012.04.010

Nageeb, M. (2013). Adsorption Technique for the Removal of Organic Pollutants from Water and Wastewater. In *Organic Pollutants - Monitoring, Risk and Treatment*.

Kumar, P., Hegde, K., Brar, S. K., Cledon, M., Kermanshahi-pour, A., Roy-Lachapelle, A., & Galvez-Cloutier, R. (2018). Biodegradation of microcystin-LR using acclimatized bacteria isolated from different units of the drinking water treatment plant. *Environmental Pollution, 242*, 407-416. doi:10.1016/j.envpol.2018.07.008

Kumar, P., Hegde, K., Brar, S. K., Cledon, M., Kermanshahi-pour, A., Roy-Lachapelle, A., . . . Galvez-Cloutier, R. (2020a). Co-culturing of native bacteria from drinking water treatment plant with known degraders to accelerate microcystin-LR removal using biofilter. *Chemical Engineering Journal, 383*. doi:10.1016/j.cej.2019.123090

Kumar, P., Rehab, H., Hegde, K., Brar, S. K., Cledon, M., Kermanshahi-pour, A., . . . Surampalli, R. Y. (2020b). Physical and biological removal of Microcystin-LR and other water contaminants in a biofilter using Manganese Dioxide coated sand and Graphene sand composites. *Science of The Total Environment, 703*. doi:10.1016/j.scitotenv.2019.135052

Rizzo, L., Fiorentino, A., Grassi, M., Attanasio, D., & Guida, M. (2015). Advanced treatment of urban wastewater by sand filtration and graphene adsorption for wastewater reuse: Effect on a mixture of pharmaceuticals and toxicity. *Journal of Environmental Chemical Engineering, 3*(1), 122-128. doi:10.1016/j.jece.2014.11.011

Hansen, B. Ø., Kwan, P., Benjamin, M. M., Li, C.-W., & Korshin, G. V. (2001). Use of Iron Oxide-Coated Sand To Remove Strontium from Simulated Hanford Tank Wastes. *Environ Sci Technol, 35*(24), 4905-4909. doi:10.1021/es0108990

Li, Y. L., Deletic, A., Alcazar, L., Bratieres, K., Fletcher, T. D., & McCarthy, D. T. (2012). Removal of Clostridium perfringens, Escherichia coli and F-RNA coliphages by stormwater biofilters. *Ecological Engineering, 49*, 137-145. doi:10.1016/j.ecoleng.2012.08.007.

Fortune, W. B., & Mellon, M. G. (1938). Determination of Iron with o-Phenanthroline: A Spectrophotometric Study. *Industrial & Engineering Chemistry Analytical Edition, 10*(2), 60-64. doi:10.1021/ac50118a004

Mehlig, J. (1941). Colorimetric Determination of Copper with Ammonia. *Industrial & Engineering Chemistry Analytical Edition, 13*(8), 533-535. doi:10.1021/i560096a006

Roy-Lachapelle, A., Duy, S. V., Munoz, G., Dinh, Q. T., Bahl, E., Simon, D. F., Sauvé, S. (2019). Analysis of multiclass cyanotoxins (microcystins, anabaenopeptins, cylindrospermopsin and anatoxins) in lake waters using on-line SPE liquid chromatography high-resolution Orbitrap mass spectrometry. *Analytical Methods, 11*(41), 5289-5300.

BRIDGE-6

BRIDGE: It was evident from the study so far, that the adsorbent GS1 performed quite well, especially if the performance is ranked based on the adsorption capacity that delayed the leaching phenomenon of MC-LR for more than 20 weeks as compared to second-best filter: rGO that only delayed it for 5 weeks. However, if performance needs to be ranked out, in terms of the water pollutant removal, the decision was still to be made. Hence, in the next study, the use of principal component analysis was performed to select the best performing filter adsorbent which will ultimately qualify for the scale-up study.

PART 3

Selection of the best filter adsorbent using principal component analysis from the available data on water quality parameters

Pratik Kumar[a], Maximiliano Cledon[b] Satinder Kaur Brar[a,c]

[a]- INRS-ETE, Université du Québec, 490, Rue de la Couronne, Québec, Canada G1K 9A9

[c]-Department of Civil Engineering, Lassonde School of Engineering, York University, North York, Toronto, Ontario, Canada, M3J 1P3

[d]- CIMAS (CONICET, UnComa, Rio Negro), Güemes 1030, San Antonio Oeste, Rio Negro, Argentina

[*]- Corresponding author, E-mail: Satinder.Brar@lassonde.yorku.ca; satinder.brar@ete.inrs.ca

Résumé

L'Analyse en Composantes Principales est un outil statistique multivarié qui peut être utilisé pour évaluer la performance des variables d'observation en fonction de la réponse des paramètres associés. Ici, dans cette étude, les variables observées sont les filtres comprenant différents milieux adsorbants, synthétisés en laboratoire et évalués pour l'élimination de plusieurs contaminants de l'eau (paramètres de qualité de l'eau: WQP) dont l'ammoniac, le nitrite, le nitrate, le magnésium, le cuivre, le fer, les coliformes totaux, la turbidité, le carbon organique total et la microcystine-LR. Le pointage de charge PC (Composant Principal) a été obtenu pour tous les filtres à différentes étapes de l'opération à savoir: la phase d'adsorption physique (PAP) et la phase de bioadsorption (BAP). Les résultats obtenus pour divers filtres adsorbants compte-tenu des paramètres mentionnés ci-dessus (discutés en détail dans le chapitre 4 partie 1 et partie 2), le meilleur filtre adsorbant a été jugé en utilisant PCA. La PCA a aidé à classer les filtres en 3 grandes catégories : Groupe 1 : filtre à sable et filtre à sable enduit de fer (filtres à faible performance). Groupe 2 (filtres à sable graphité) et Groupe 3 (filtres à sable à revêtement submicronique en carbone). Pour les deux, PAP et BAP, GS1 (filtre à sable graphité à base d'effluents de brasserie) a obtenu les meilleurs résultats, obtenant un pointage de charge PC de +3,01 et +2,54, respectivement. Un score de charge PC inférieur pour GS1 sous PAP par rapport à BAP a souligné que l'élimination majeure des WQP s'est produite en raison de l'adsorption physique et qu'il restait peu de place pour la biodégradation. D'autre part, une amélioration du pointage de charge PC de +1,08 (BAP sur PAP) pour le filtre à sable enduit d'oxyde de graphène réduit, a signifié l'importance de la biodégradation pour l'élimination de divers polluants de l'eau. Le score de charge PC a également aidé à révéler qu'un revêtement d'oxyde de graphène sur du sable enduit de fer n'est pas nécessaire (en termes de performances) et a également révélé qu'un revêtement en dioxyde de manganèse sur du sable brut peut améliorer considérablement les performances du filtre à sable.

Mots-clés: Analyse en composantes principales, Score de charge, Paramètres de qualité de l'eau, Traitement de l'eau potable

Abstract

Principal Component Analysis (PCA) is a multivariate statistical tool that can be used to evaluate the performance of the observation variables based on the response of associated parameters. Herein, in this study, the observed variables are the filters comprising different adsorbent media, synthesized in the laboratory and assessed for the removal of several water contaminants (water quality parameters: WQPs) including ammonia, nitrite, nitrate, magnesium, copper, iron, total coliform, turbidity, total organic carbon and microcystin-LR. The PC (principal component) load score was obtained for all the filters under the different stage of the operation viz. physical adsorption phase (PAP) and bioadsorption phase (BAP). The results obtained for various filter adsorbents considering above-mentioned parameters (discussed in detail in chapter 4 part 1 and part 2), the best filter adsorbent was judged using PCA. PCA assisted in categorizing the filters broadly into three groups: Group 1: sand and iron-coated sand filter (low-performance filters). Group 2 (graphitized sand filters) and Group 3 (carbon submicron coated sand filters). For both, PAP and BAP, GS1 (graphitized sand filter using brewery effluent) performed the best, securing a highest PC load score of +3.01 and +2.54, respectively. A lower PC load for GS1 under PAP as compared to BAP highlighted that major WQPs removal occurred due to physical adsorption and little scope was left for the biodegradation. On the other hand, an improvement in PC load score of +1.08 (BAP over PAP) for reduced graphene oxide coated-sand filter, signified the importance of biodegradation for the removal of various water pollutants. PC load score also helped to reveal that coating of graphene oxide over iron-coated sand is not necessary (performance-wise) and also revealed that manganese dioxide coating on raw sand can greatly improve the sand filter performance.

Keywords: Principal component analysis, load score, water quality parameters, drinking water treatment

Introduction

PCA is a tool to analyse multi-variables which helps in the judgement of observation variables. PCA reveals and categorize the key parameters involved in an overall input data where output variables are observed to highlight the importance of any change in the process variables. Udayakumar et al. (2009) illustrated a real picture of the quality environmental variables to observe for the monitoring programme where interpretation and evaluation were easier, utilizing a wide scope of PCA. A standard algorithm of process execution comprises: a) parameter selection, b) weight assignment of parameters screened and c) final aggregation of weighted parameters to define an index that indicates the overall process assessment. PCA as a multivariate statistical tool was found to help in the initial parameter selection where Tripathi et al. (2019) showed the importance of PCA in finding the critical water quality parameters (9 of them) among 28 variables studied that reduced the selection parameters by retaining the maximum variance in the data set and projecting only the important water quality parameters.

PCA helps in making the process more feasible and economical by reducing the time and effort to monitor the samples of less importance, especially when larger parameters are under question. The application of the PC load score can be beneficial to judge the range of worst to best performing observation variables (here various filters). For example, in this study, more than 11 WQPs were assessed for 10 filters which make a total of 110 output data. Hence, to interpret these data to judge the best filter that performs well for every variable, may sound a cumbersome task. Use of PCA loading score has made the evaluation less bias and concise making the result or judgement more objective in nature. Also, the load score comparison for physical adsorption phase and bioadsorption phase revealed that coating of graphene oxide (GO) over iron-coated sand, i.e, FeGO is unnecessary as the performance of GO-coated sand remained very similar to FeGO (discussed in detail in results and discussion section). The use of PC load score can also be helpful in determining the essential WQPs from multi-sources along with many sampling done at different time order. For example, Alves et al. (2018) found that from 23 WQPs for 12 sampling stations (averaging 4 sampling campaigns in different seasons), only 16 were found essential for the water quality assessment when sampling was done in the dry season while 17 were found essential during the rainy season. A more advanced assessment can also be thought by integrating cluster analysis

with PCA where further subgroups can be observed thereby opening a new dimension to how the data can be looked into.

PCA also becomes handy in categorizing the observation variable (for example, here various filters) in relation to the output behaviour of the major variables (here, WQPs). For example, Gvozdić et al. (2012) categorized the degree of pollution level for three different sources into a low, medium and high genre by utilizing 15 major WQP variables. In this study too, three different groups of filters were categorized: Group 1 (sand and iron coated sand filter), Group 2 (submicron carbon-coated sand filter) and Group 3 (graphitized sand filter) (discussed more in detail in the result and discussion section). Such classification can be useful for the field engineers or plant operators assisting in taking measures to advance for preventing the water contaminants in the treated water. Mahapatra et al. (2012) too assessed the water quality index to classify the water quality. However, the accuracy of an overall assessment depends on the judicious screening of the process variables.

This chapter discusses the Principal Component Analysis (PCA) for the potential filters capable of removing MC-LR as discussed in chapter 4 (part 1 and part 2). The filters were the observation variables while all the water quality parameters (WQPs) formed as the main variable in a PCA analysis. Different WQPs comprises ammonia, nitrite, nitrate, total coliform, turbidity, iron, copper, magnesium, UV254, MC-LR and TOC while 10 filter named: RS + MnO2 (MnO2 coated over raw sand), GS1 (Graphitized sand using brewery sugar), GS2 (Graphitized sand using sucrose), GS1+MnO2 (MnO2 coated over GS1), GS2+MnO2 (MnO2 coated over GS2), GO (Graphene oxide coated sand), rGO (reduced graphene oxide coated sand), FeGO (Iron oxide coated over GO -coated sand), Fe (Iron oxide coated sand) and sand filter (no coating).

Material and methods

PCA analysis graphics and data: Multivariate Principal Component Analysis (PCA) and all graphical presentations were performed using the ORIGIN software (Version 8.5; OriginLab). The data on water quality parameters are mentioned in chapter 4 (part 1 and part 2).

Principal Component (PC) load score analysis

The load score was calculated based on the eigenvector projection on the principal axes: PC1 and PC2 axis. The load score obtained for both the axes was summed and assigned to each observation variables (various filters).

Figure 1 (A) and Figure 1 (B) show the PC biplot load score for the PAP and BAP, respectively.

1.) For the PAP, the filters were scored from -5.7 (worst performing filter) to + 3.02 (best performing filter) based on the biplot loading score.

2.) For the BAP, the filters were scored from -6.23 (worst performing filter) to + 2.53 (best performing filter) based on the biplot loading score.

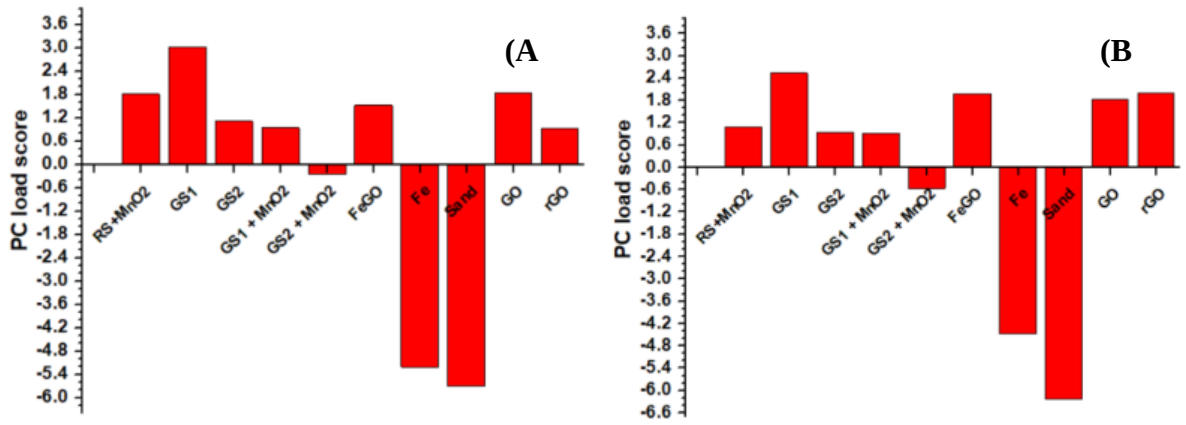

Figure 4.3.1: PC biplot load score for (A) physical adsorption phase, (B) bioadsorption phase

RS + MnO2 (MnO2 coated over raw sand), GS1 (Graphitized sand using brewery sugar), GS2 (Graphitized sand using sucrose), GS1+MnO2 (MnO2 coated over GS1), GS2+MnO2 (MnO2 coated over GS2), GO (Graphene oxide coated sand), rGO (reduced graphene oxide coated sand), FeGO (Iron oxide coated over GO -coated sand), Fe (Iron oxide coated sand)

Results and Discussion

Principal Component: Biplot analysis

Figure 2 and Figure 3 represents the PCA biplot of the physical adsorption phase (PAP) with and without eigenvectors, respectively. On the other hand, Figure 4 and Figure 5 represents the PCA biplot of the bioadsorption phase (BAP) with and without the eigenvectors, respectively. It can be observed from Figure 3 and Figure 5 that all the tested filters can be grouped together into three categories or clusters: Group 1, Group 2 and Group 3. Group 1 comprises lower-performing filters

named: Sand and Fe. Group 2 comprises graphitized-sand filters (GS1, G2, GS1 + MnO_2, GS2 + MnO_2) while Group 3 comprises carbon sub-micron-coated sand filters (rGO and GO).

Physical adsorption phase PCA: It can be observed from Figure 2 that Fe and Sand filters (Group 1 filters) occupy the 3rd quadrant of the biplot and projects a negative loading score on both the principal axes (Principal component axis 1 (PC1) and Principal component axis 2 (PC2)). The combined load score (PC1 + PC2) for Sand and Fe filter was found to be -5.2 and -5.7, respectively. These scores by Group 1 filter forms the worst scores for the PAP. On the other hand, Group 2 filters scored 1.51, 1.83 and 0.91 for FeGO, GO and rGO filters. This highlighted that the graphene oxide coating over and improved the performance of the sand filter and coating of iron over GO (FeGO) was really not needed.

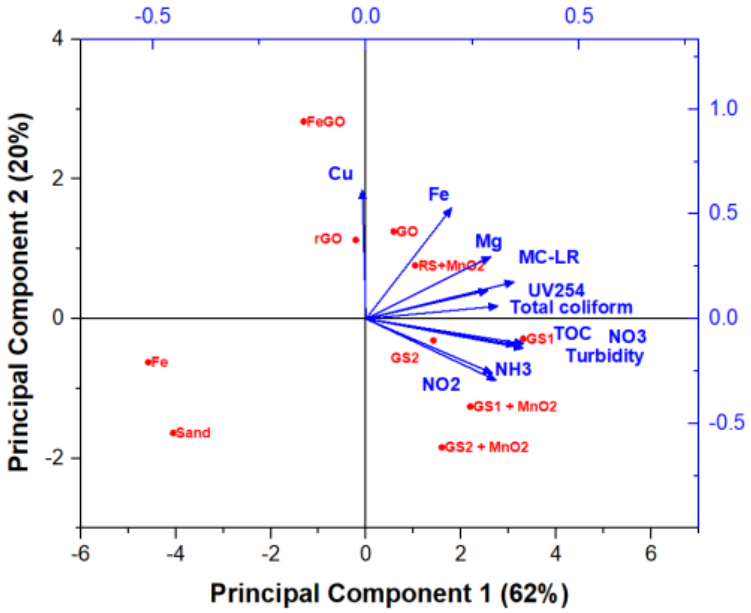

Figure 4.3.2: Principal component analysis for physical adsorption phase

RS + MnO2 (MnO2 coated over raw sand), GS1 (Graphitized sand using brewery sugar), GS2 (Graphitized sand using sucrose), GS1+MnO2 (MnO2 coated over GS1), GS2+MnO2 (MnO2 coated over GS2), GO (Graphene oxide coated sand), rGO (reduced graphene oxide coated sand), FeGO (Iron oxide coated over GO -coated sand), Fe (Iron oxide coated sand)

Whilst, rGO-coated sand filter performed averagely. This was attributed to the fact that rGO-coated sand filter performed well for metal removal and not quite effective for other WQP such as ammonia, nitrite, nitrate, TOC and coliform (refer chapter 4 for more detail). As compared to Group 1 and 2 filters, Group 3 filters performed relatively better where all the filters except GS2+MnO2 showed a positive loading score of at least 0.9. The best filter turned out to be GS1

with a maximum loading score of +3.02 which had a huge margin as compared to the second-best filter, i.e., +1.83 for GO-coated sand filter and +1.8 for RS+MnO_2. This also suggests that coating manganese dioxide over sand can be as influential as coating GO over sand when overall filter performance is considered. Overall, GS1 performed best among all the filters for the physical adsorption phase.

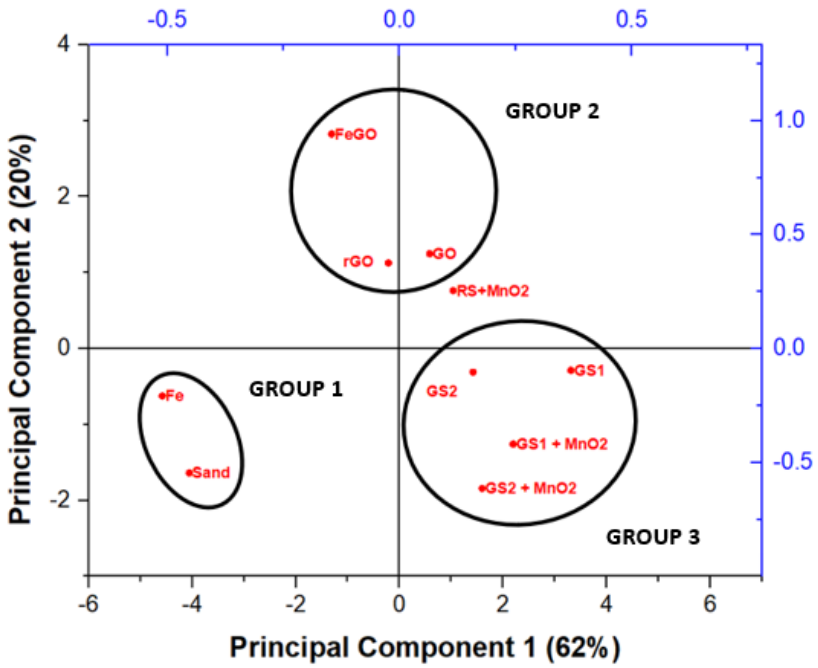

Figure 4.3.3: Principal component analysis for physical adsorption phase (without eigenvector)

RS + MnO2 (MnO2 coated over raw sand), GS1 (Graphitized sand using brewery sugar), GS2 (Graphitized sand using sucrose), GS1+MnO2 (MnO2 coated over GS1), GS2+MnO2 (MnO2 coated over GS2), GO (Graphene oxide coated sand), rGO (reduced graphene oxide coated sand), FeGO (Iron oxide coated over GO -coated sand), Fe (Iron oxide coated sand)

Bioadsorption phase PCA: It can be observed from Figure 4 that Group 3 filters: Sand and Fe filter occupy the 3rd quadrant of the biplot akin to PAP and projected a negative loading score of -6.23 and -4.47. An improvement in the loading score of around +0.73 (from -5.7) for Fe filter is attributed to better metal removal and other WQPs (refer chapter 4 for details) while sand performed even worse than the PAP declining the PC loading by -0.53. On the other hand, the performance of Group 2 filters improved as indicated by the PC load scores. GO-coated sand filter performed nearly the same when compared to the physical adsorption phase while FeGO and rGO showed an escalating PC score of +0.46 and +1.08, respectively.

Such a significant improvement for rGO-coated filter points that biodegradation played a pivot role in removing WQPs that mainly attributed to the high surface area, roughness (for details refer to chapter 4) and reducing surface (less oxygen atom as compared to GO) which improved the biofilm formation proving an effective bacterial colonization over the rGO-coated surface. The performance of rGO-coated sand filter was second (based on PC biplot score) that fell only short to GS1 filter.

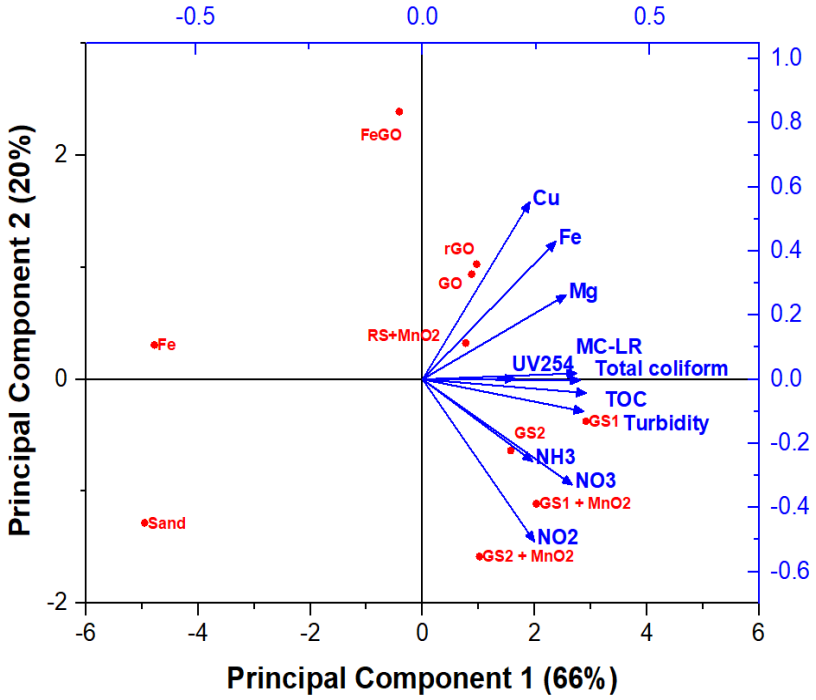

Figure 4.3.4: Principal component analysis for bioadsorption phase

RS + MnO2 (MnO2 coated over raw sand), GS1 (Graphitized sand using brewery sugar), GS2 (Graphitized sand using sucrose), GS1+MnO2 (MnO2 coated over GS1), GS2+MnO2 (MnO2 coated over GS2), GO (Graphene oxide coated sand), rGO (reduced graphene oxide coated sand), FeGO (Iron oxide coated over GO -coated sand), Fe (Iron oxide coated sand)

Group 3 filters declined (though not by much) in performance as compared to the PAP. The highest load score was still accounted for by GS1 filter that showed the highest PC load score of +2.54 highlighting that GS1 filter achieved much of the WQP removal during the PAP and bioaugmentation really did not help much in improving the pollutant removal. A common inference from PCA biplot of both the phases indicates that Group 2 filters performed better for the metals ion removal (eigenvectors proximity to these filters) while Group 3 filters showed better removal of ammonia, nitrite nitrate, turbidity and total coliform removal.

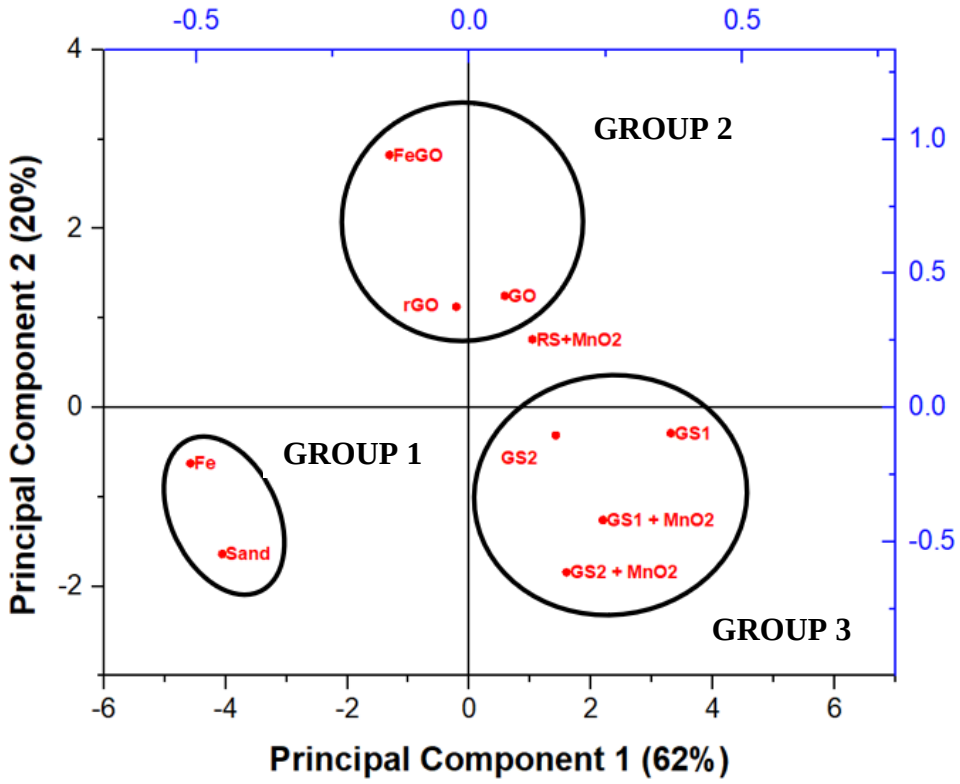

Figure 4.3.5: Principal component analysis for bioadsorption phase (without eigenvector)

RS + MnO2 (MnO2 coated over raw sand), GS1 (Graphitized sand using brewery sugar), GS2 (Graphitized sand using sucrose), GS1+MnO2 (MnO2 coated over GS1), GS2+MnO2 (MnO2 coated over GS2), GO (Graphene oxide coated sand), rGO (reduced graphene oxide coated sand), FeGO (Iron oxide coated over GO -coated sand), Fe (Iron oxide coated sand)

Conclusion

From the Principal Component (PC) biplot load score, GS1 outperformed other filters with a score of +3.02 and +2.53 in the physical adsorption phase (PAP) and bioadsorption phase (BAP), respectively. Second best filter was found to be GO for PAP and rGO for BAP, securing a PC load score of +1.83 and +1.99, respectively. Physical adsorption factor was principally held responsible for the water pollutants removal in case of GS1 while rGO-coated sand filter showed a significant difference in PC load score for PAP and BAP (score of +1.99 for BAP as compared to <0.95 PAP) highlighting the positive influence of bioaugmentation on water pollutants removal. Sand and iron-coated sand filter showed worst performances for both PAP and BAP securing a PC load score of -5.7 & -5.2 and -6.24 & -4.47, respectively.

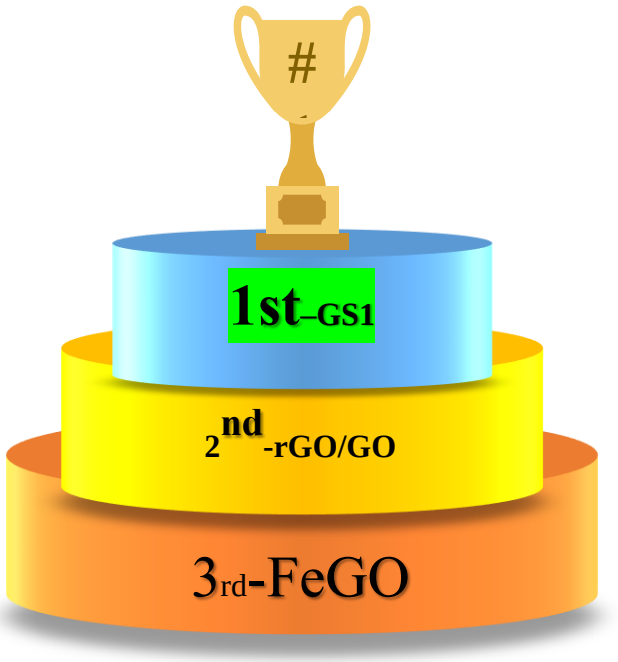

Figure 4.3.6: Rank podium for the top 3 filters based on Principal Component Analysis

GS1 (Graphitized sand using brewery sugar), GO (Graphene oxide coated sand), rGO (reduced graphene oxide coated sand), FeGO (Iron oxide coated over GO -coated sand).

References

Gvozdić, V., Brana, J., Malatesti, N., & Roland, D. (2012). Principal component analysis of surface water quality data of the River Drava in eastern Croatia (24 year survey). *Journal of Hydroinformatics, 14*(4), 1051-1060. doi:10.2166/hydro.2012.063

Mahapatra, S. S., Sahu, M., Patel, R. K., & Panda, B. N. (2012). Prediction of Water Quality Using Principal Component Analysis. *Water Quality, Exposure and Health, 4*(2), 93-104. doi:10.1007/s12403-012-0068-9

Alves, J. d. P. H., Fonseca, L. C., Chielle, R. d. S. A., & Macedo, L. C. B. (2018). Monitoring water quality of the Sergipe River basin: an evaluation using multivariate data analysis. *Rbrh, 23*(0). doi:10.1590/2318-0331.231820170124

Tripathi, M., & Singal, S. K. (2019). Use of Principal Component Analysis for parameter selection for development of a novel Water Quality Index: A case study of river Ganga India. *Ecological Indicators, 96,* 430-436. doi:10.1016/j.ecolind.2018.09.025

Udayakumar, P., Abhilash, P. P., & Ouseph, P. P. (2009). Assessment of water quality using principal component analysis--a case study of the Mangalore coastal region, India. *J Environ Sci Eng, 51*(3), 179-186.

CHAPTER 5: Scale-up using best performing filter media

BRIDGE-7

BRIDGE: From the PCA, it was clear and evident that GS1 filter adsorbent outperformed other filter adsorbents by some margin. Now, the next target was to scale-up. But, before that, the hydrodynamics has to be studied out that can help in selecting a 'subjective minimum scale-up dimension' (SMS) such that the module system is devoid of short circuit phenomenon (the main cause of building negative pressure inside the filter). Hence, in the next study, computational fluid dynamics was used to study the bench-scale filter to find out the SMS.

PART 1

Can ANSYS-CFX be Used to Predict the Scale-up Dimension of a Filter Column? A Computational Fluid Dynamics Approach

Pratik Kumar[a], Maximiliano Cledon[b], Satinder Kaur Brar[a,c]

[a-] INRS-ETE, Université du Québec, 490, Rue de la Couronne, Québec, Canada G1K 9A9

[b-] CIMAS (CONICET, UnComa, Rio Negro), Güemes 1030, San Antonio Oeste, Rio Negro, Argentina

[c-] Department of Civil Engineering, Lassonde School of Engineering, York University, North York, Toronto M3J 1P3, Ontario, Canada

[*]Corresponding author, E-mail: satinder.brar@ete.inrs.ca; satinder.brar@lassonde.yorku.ca (S.K. Brar)

Draft (to be submitted)

Abstract

A bench-scale filter consisting of sand media was tested for the hydrodynamic parameters (velocity and pressure) using ANSYS-CFX to determine the 'subjective minimum scale-up' (SMS) filter dimension devoid of 'poor flow regime'. No specific study is usually performed by the researchers to understand what an ideal minimum scale-up dimension of their working bench-scale filter column could be. In this study, the poor flow regime was assumed to occur due to a high variance in the pressure gradient obtained for a plane perpendicular to the direction of fluid flow. The flow regime pattern was analyzed by structural modelling and in-built programming: ANSYS-CFX solver using the concept of computational fluid dynamics (CFD). This could sort the operational issues caused due to pressure-velocity parameters which mainly accounts for an ideal flow dynamic., CFD model was validated using two intrinsic properties of the porous media (sand): a) permeability constant and b) loss coefficient. The pressure drop across the porous media filter was found using the Kozeny-Carman equation and was incorporated to the programming using pre-CFX solver. Subsequently, the simulation was obtained for the scale-up reactors using the intrinsic properties to validate the model using CFD. After few hit and trials (n =71), SMS dimension of 9 cm x 9 cm and a height of 30 cm delivered a radial pressure gradient distribution (contour mapping) on the plane orthogonal to the linear flow velocity.

Keywords: ANSYS-CFX, pressure-velocity, filter, simulation, flow regime

Introduction

Bench-scale filter column provides a base study for any adsorbent material to understand its feasibility for the removal of pollutants before progressing towards a scale-up study. Bench-scale filters have shown an effective removal in the past for various water pollutants such as organic matter, dyes, metals and pharmaceutical compounds (Callery et al. 2016; Vijayaraghavan et al. 2004). Bench-scale columns have even proven to accurately predict the hydrodynamic behavior of the fluid flow (Biglari et al. 2016). However, the boundary conditions and wall effects in a small diameter column are majorly responsible for a non-uniform flow regime in a continuous fluid flow condition as compared to a larger dimension column where latter possess an insignificant wall effect. These non-uniform flow regimes could possibly be linked to a change in the adsorption

efficiency of the contaminant removal. Hence, it is required to understand the hydrodynamics of a bench-scale filter before it can be applied at a higher scale.

The head loss parameter plays an important role in an overall filter operation which is mainly responsible for the change in the flow rate and hence flow regime (Sedgh-Asl et al. 2013). In particular, for a biofilter operation studied using small diameter column, problems such as clogging, air-entrapment (due to biofilm growth), often escalate maintenance issues and requires frequent backwashing (Lim et al. 2012). Due to a limited degree of freedom for the fluid movement in a bench-scale filter column (generally water), and a persisting capillary action due to low diameter column, the velocity and pressure distribution does not follow a smooth head loss pattern. This leads to an unavoidable consequence of misjudgment during filter dimensioning for the scale-up study. Many researchers even perform a scale-up study by choosing a random column diameter without assessing the hydrodynamic behavior of the fluid. In such cases, adsorption efficiency may show an underperformance when translated to a higher scale than bench-scale. Hence, proper flow regime must be understood for a chosen bench scale column to determine the degree of 'poor flow regime' and then a step forward to eradicate it.

Herein, the bench-scale column filter dimensioning 22 mm square side, 650 mm length and 1 mm thickness was chosen out of 71 other chosen dimensions (not mentioned here) and was studied for the sand-based porous media to understand the flow regime using two governing parameters: pressure and velocity. Computational fluid dynamics (CFD) was used to evaluate the numerical analysis involved in the fluid flow with respect to the adsorbent properties (porous sand media) including density, porosity, head loss coefficient, permeability constant, etc. After analyzing the contour mapping (flow regime) for the bench-scale columns based upon the pressure gradient values, various scale-up dimensions were hit and trialed (n=71) to determine a radial and more uniform distribution pattern of the pressure gradient for a plane chosen perpendicular to the direction of the fluid flow. For simplicity, only one scale-up dimension was shown in this study out of 71 trailed simulation that offered a good flow regime.

Material and methods

Materials

A column dimensioning 22 mm square sides, 650 mm length and 1 mm thickness was used as the representative bench-scale filter column. Sand was used as the porous filter adsorbent based on the grain size distribution as described in the supplementary section. For the analysis of hydrodynamic conditions, computational fluid dynamics was studied using ANSYS 2019 R2 software.

Column set-up and operation

A glass column was set-up (vertically) similar to what is represented in Figure 5.1.1 and was continuously fed with lake water at a linear velocity equal to 0.00025 m/sec (0.9 m/h) which is approx. 40 mL discharge in 8.5 minutes under constant flow rate and at a constant water head of 12.5 cm above the filter bed media. A constant head of 12.5 cm was chosen to determine the experimental flow velocity of the fluid in a bench-scale column. It is to be noted that the velocity can further be increased by changing the pressure head up to some extent, depending on the quality of water to be delivered at the expense of compromising the water quality. However, in the current study, flow velocity was determined at a fixed water head (i.e., 12.5 cms) based on a nominal water quality of the effluent.

Morrill Dispersion Index or MDI

The Morrill dispersion index or MDI is a widely used parameter to determine the amount or degree of diffusion and mixing in the contact system (Teixeira and do Nascimento, 2008). It was calculated based on the residence time distribution analysis where KCl was used as the tracer compound. 200 mg/L KCl was found equivalent to 67.7 μS/cm. MDI was calculated based on the following equation:

$MDI = T_{90}/T_{10}$ *Equation 15*

Where,

T_{90} = time taken to reach 90% of the conductivity value (proportional to tracer element concentration)

T_{10} = time taken to reach 10% of the conductivity value (proportional to tracer element concentration)

MDI value close to 1 defines a perfect plug flow condition while value of 23 defines a completely mixed/stirred reactor (Fia et al. 2016). Hence, for a porous packed bed column, value closer to 1 was more desirable.

Details on ANSYS-CFX and velocity-pressure determination

The effluent flow (in mL) of the bench scale column was measured experimentally and converted to m/sec. After that, the flow velocity was crosschecked with the flow velocity value obtained from modelling and simulation program using ANSYS-CFX solver. The simulation program came in-built in the software for example: steady-state flow condition, isotropic loss model to name a few while the user inputs related to fluid and adsorbent properties such as fluid density porosity of the adsorbent media (here sand), head loss coefficient (L) and permeability constant (P) were fed to the program. Some trials were done using L and K values to land up to a flow velocity near to the experimental value. Table 1 tabulate these values which were used to achieve a similar observation flow velocity. The error in velocity was reported by the Equation as follows:

(Experimental velocity – Velocity observed after ANSYS-CFX simulation)/ Experimental velocity) x 100% Equation 16

Volume porosity was calculated experimentally using a fixed volume column (approximately 10 cm^3) where distilled water was used to fill the void space until brim (V_w). The bed porosity was then calculated using the formula as below:

Bed porosity = volume of void/volume of column (fixed) Equation 17

where the volume of the void is V_w and the volume of the fixed column was determined by the graduation marked outside the column, which was approximately 10 cm^3.

Table 5.1.1: Input and Output Parameters for the ANSYS/CFX solver

Parameters	**Value**
Volume porosity	0.43
Loss model	Isotropic loss
Permeability constant (m^2)	10,145,873,265 m^2
Loss coefficient	11,500,000 m^{-1}
Heat transfer coefficient	1.0 $W/m^2/K$
Pressure drop (from equation 18)	

Parameters	Value
	176 Pa
Velocity from the experiment (m/s)	0.000265 m/s
Velocity from modelling and ANSYS-CFX simulation (m/s)	0.000254 m/s (4.1% error)

The value of permeability constant and loss coefficient was known from the loop trial (as discussed above) based on the error reported in experimental velocity and velocity obtained after ANSYS/CFX solver for the bench-scale filter. The error of less than 5% was desired to confirm the model preciseness) and hence the value of 4.1% error reported in this study was accepted. The permeability constant and loss coefficient value were determined by few trials (5-10)(at error < 5% as mentioned above) and reported to be 1.01e10 m^2 and 1.15e7 m^{-1}, respectively (Table 1). The pressure loss calculated with the Kozeny-Carman equation was found to be 302 Pa as mentioned below.

$\Delta P = (kVs\mu\ (1-\varepsilon)^2 L)/\emptyset s^2 Dp^2 \varepsilon^3$ Equation 18

Where, ΔP is the pressure loss or head loss

k is a parametric value inversely proportional to $(6/D_p^2)$

L is the length of filter bed media in a column

Vs is the superficial velocity

μ is the viscosity of the fluid

ε is the bed porosity

Φ_s is the sphericity of the particles in the packed bed

D_p is the diameter of the spherical particle (here sand)

Based on the head loss reported, the 'flow regime' needed to be analyzed in order to obtain the '*minimum subjective scale-up dimension'* free of wall effect and capillary action. For this, another module (CFX-post) of the software was used which programmed all the data obtained from CFD simulation from CFX solver manager and created a flow regime contour plot (based on the pressure

gradient values). This contour plot was obtained only after validating the velocity and head loss (pressure) response. Figure 5.1.1 and Figure 5.1.2 depict the velocity and pressure distribution along the length of the bench-scale filter.

After obtaining the velocity (at <5% error) and head loss distribution inside the column, the pressure gradient was obtained using post-CFX solver. To remove any effect of sudden pressure change (fluid flow inside the column to atmospheric pressure at the exit), the plane (orthogonal to fluid flow direction) was chosen at an offset height of 10% from the bottom (at 600 mm) and not exactly at the bottom of the filter column. All the trials were simulated for no less than 25 iterations or root mean square error of <0.001, whichever was reached first (latter preferable though).

Results

ANSYS-CFX contour mapping

After crosschecking the experimental flow velocity of the fluid for the bench-scale filter with one obtained from ANSYS-CFX simulation, the CFX-post was run to get the contour plot of the pressure distribution along the length of the filter (as mentioned above). Figure 5.1.2 shows the pressure distribution along the length of the bench-scale filter. As can be observed, the effluent pressure was set to 101001 Pa (atmospheric pressure) while the pressure at the influent to the column was set to 101302 Pa (difference was calculated using equation 1 as discussed above). On the other hand, velocity distribution was maximum (2.6 e-4 m/s) at the top and minimum (2.09 e-4 m/s) at the bottom. However, at the bottom, a sudden decrease in the pressure flow to atmospheric pressure, the velocity peaked a bit (2.54 e-4 m/s) and was reported as the effluent linear flow velocity. It was obvious from the velocity pressure relation (relationship curve not shown here), that higher the pressure head, more is the flow velocity and vice-versa.

Figure 5.1.3 shows the pressure gradient contour at the defined plane (as mentioned in material and method section). It can be clearly observed that a non-uniform flow pattern existed where the pressure gradient (can be related to velocity of water flow) changes dynamically within the same plane as indicated by a dashed arrow (Figure 5.1.2). Each color depicts an arc-shaped flow line with different pressure gradient and could possibly be because of a restricted degree of freedom caused due to wall resistance and high capillary condition. Since the diameter of the column is small (20 mm), the eddy current in the flow rise towards one end of the plane (shown by red color

in Figure 5.1.2). The MDI value of the bench-scale column was found to be >3 (for graph, refer supplementary figure, Figure F1 (A)) which might raise and be responsible for some issues such as air entrapment, negative pressure built-up and reduced flow through velocity than normal.

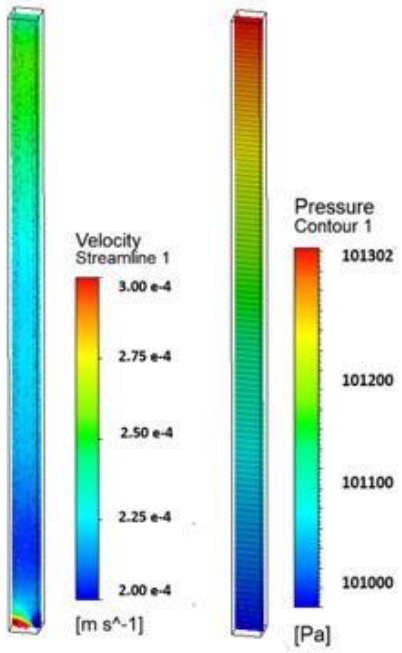

Figure 5.1.1: Velocity and Pressure distribution along its length in bench-scale filter column

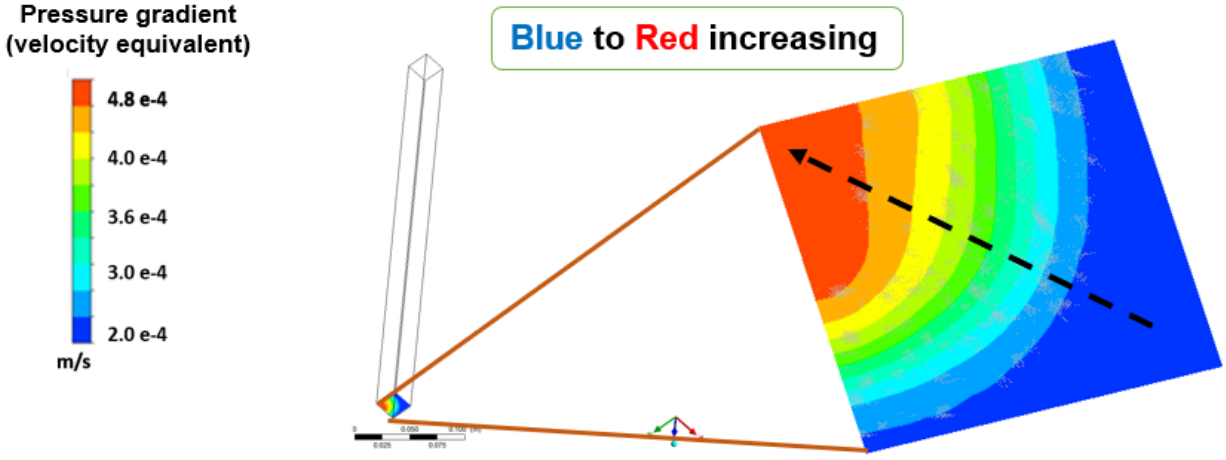

Figure 5.1.2: Velocity contour of bench-scale filter taken at an orthogonal plane at 600 mm height

Finding minimum subjective scale-up dimension

The next objective was to use the derived parameters from ANSYS-CFX, i.e., permeability constant and loss coefficient, to determine the 'subjective minimum scale-up' dimension (SMS) which could eradicate the poor flow regime condition (Figure 5.1.2) and develop a more channelized and radial pressure gradient pattern so that more bed surface can be utilized for the fluid flow. Different dimensions were trialed and simulated (not shown here) for sand media and the SMS was found to be 9 cm x 9 cm x 30 cm. This filter dimension was judged based on the flow-through velocity value which was meant to be at least similar if not lower than what was obtained experimentally for the bench-scale column. However, it should be noted that the requirement of a similar velocity value for the scale-up filter is less desirable than obtaining a uniform pressure gradient pattern. Figure 5.1.3 shows the obtained pressure gradient plot for the trialed scale-up dimension (9 cm x 9 cm x 30 cm) which offered a radial distribution pattern of the pressure gradient on the plane (chosen at 10% offset from the bottom and orthogonal to the fluid direction).

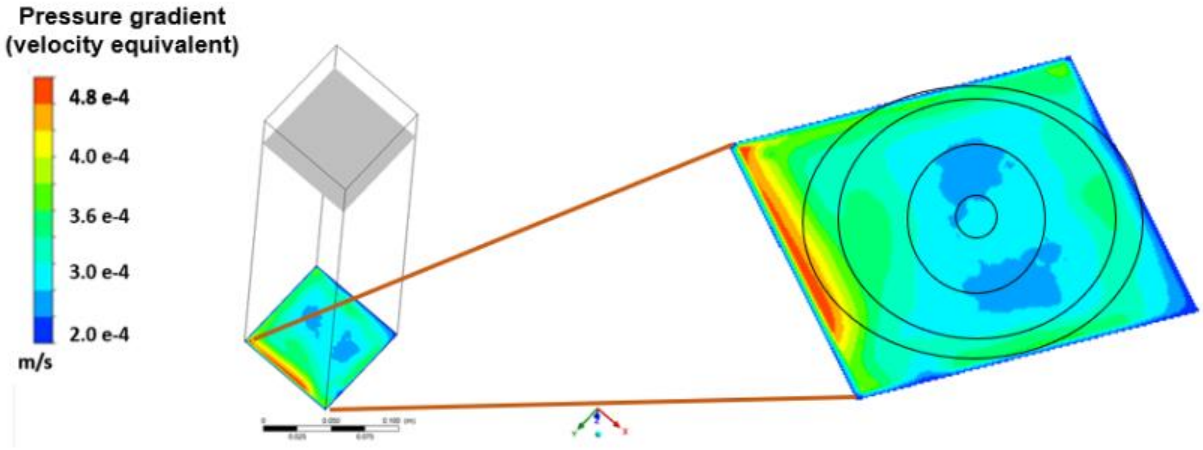

Figure 5.1.3: Velocity contour of scale-up filter taken at an orthogonal plane at 270 mm height

As can be observed from Figure 5.1.3, the flow regime on the selected plane is much more radial and uniform in the pattern which allowed a better plug flow condition too (MDI <2.2, refer supplementary section, Figure F1 (B)) as compared to bench-scale case (MDI >3). The experiment to determine the MDI value for the chosen SMS dimension was done using plexi-glass column. A lower MDI value (> 26%) for the scale-up filter column signifies a better plug-flow condition as compared to the bench-scale filter. This change was obvious because of a better flow regime

condition (Figure 5.1.3) that was developed in the scale-up column filter. It should be noted that a higher MDI value for the scale-up filter as compared to the bench-scale filter can be compromised only if a radial flow regime is obtained for the former. However, an ideal condition would be to obtain a lower MDI as well as better pressure gradient (flow regime) distribution. Figure 5.1.4 summarizes the overall process (8-step) that was performed to determine the SMS dimension from bench-scale column filter that depicted a radial and uniform pressure gradient pattern.

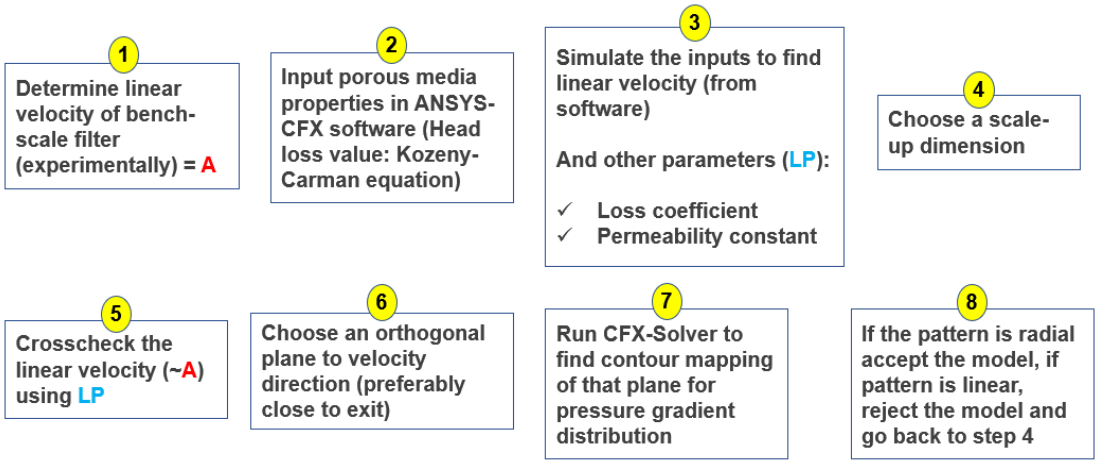

Figure 5.1.4: A 8-step approach to determine subjective minimum scale-up dimension.

Discussion

Previous studies on CFD have shown the importance of hydrodynamics in a column reactor (Baten and Krishna 2004, Dhotre and Joshi 2004). An important benefit of the CFD approach to the column reactors is that the geometry and scale effects are automatically accounted for simulation. However, the success of the scale-up strategy depends on proper modelling of the fluid and media properties (Baten et al. 2003). In the present study, CFD model was validated using only two intrinsic properties of the porous media (sand): permeability constant and loss coefficient. After that, the simulation was obtained for the scale-up reactors. Though the above-mentioned studies failed to form a discussion on the scale-up size limit, a scale-up ratio of 20 was found to demonstrate a strong influence on the column hydrodynamics (Baten et al. 2003). Such influence was confirmed even at the scale-up factor of 4.5 in present study. This was attributed mainly due to the boundary limit at low scale columns which was evident from the flow pattern as observed from the planer contour diagram (Figure 5.1.2 and Figure 5.1.3). This was also confirmed by a decrease in the MDI value suggesting a better plug-flow condition regime when the reactor was

scale-up. Such flow regime becomes an important aspect when it comes to an actual scale-up practice. Above mentioned idea may formulate a user desirable approach using a prototype or model (pilot scale) filters. However, for the technological feasibility this study still needs some important validation as the flow regime was only understood using two variables (pressure and velocity) and two intrinsic properties in form of head loss coefficient and permeability constant.

Nevertheless, the flow regime pattern is required to understand so as to not allow the excess pressure to build up inside a big or actual scale-up filter unit. Only after a successful scale-up validation based on the flow regime, a scale-up feasibility should be made rather than prioritizing the importance of other follow-up objectives. For example, adsorption of contaminant 'X' using adsorbent media 'Y' can be studied later but first thing first is to assure that the hydrodynamics of the matrix fluid is validated. In general, this could also account for a lower adsorption efficiency when translating any bench-scale condition to a scale-up condition. Many studies have also successfully predicted the breakthrough time of a bench-scale packed bed column (da Rosa et al. 2015). However, the scale-up reactor could possess a different hydrodynamics property as compared to the bench-scale reactor, making all these matching experimental and simulation data null and void. Hence, the CFD application can form a preliminary approach for the bench-scale filters to understand their scale-up feasibility and deciphering a SMS dimension that can avoid any hydrodynamic issues during the filter operation.

Conclusion

The use of computational fluid dynamics (CFD) using ANSYS-CFX (software) can help to understand the hydrodynamic fluid properties such as pressure and flow velocity for a porous adsorbent filter media in a tubular column. A non-uniform and non-radial asymmetric flow condition were observed for the bench-scale filter from the pressure gradient contour plot. It helped in understanding the limitation of the bench-scale filter with respect to the flow regime producing a low plug-flow condition inside the filter (Morrill dispersion index, MDI > 3). The derived properties comprising permeability constant and loss coefficient from bench-scale computational analysis helped to find the scale-up dimension at which the flow regime showed a more radial and uniform pressure gradient contour. Also, a better plug-flow condition (MDI = 2.2) was observed as compared to the bench-scale filter that suggested the importance and significance of CFD for

determining the scale-up dimension of a filter column. In future, CFD approach may be beneficial to lay a foundation for the scale-up studies.

Conflict of interest: None

Acknowledgement

The authors are sincerely thankful to the Natural Sciences and Engineering Research (Discovery Grant 23451). A Special thanks to the plant operator Mr. Guy Desgroseilliers, Ville de Quebec for availing the quartz sand from the filtration unit of the drinking water treatment plant, Chemin Ste-Foy, Quebec City, Canada.

References

Biglari, M., Liu, H., Elkamel, A., & Lohi, A. (2016). Application of Scaling-Law and CFD Modeling to Hydrodynamics of Circulating Biomass Fluidized Bed Gasifier. *Energies, 9*(7). doi:10.3390/en9070504

Callery, O., Healy, M. G., Rognard, F., Barthelemy, L., & Brennan, R. B. (2016). Evaluating the long-term performance of low-cost adsorbents using small-scale adsorption column experiments. *Water Research, 101*, 429-440. doi:10.1016/j.watres.2016.05.093

da Rosa, C. A., Ostroski, I. C., Gimenes Meneguin, J., Gimenes, M. L., & Barros, M. A. S. D. (2015). Study of Pb2+ adsorption in a packed bed column of bentonite using CFD. *Applied Clay Science, 104*, 48-58. doi:10.1016/j.clay.2014.11.021

Dhotre, M. T., & Joshi, J. B. (2004). Two-Dimensional CFD Model for the Prediction of Flow Pattern, Pressure Drop and Heat Transfer Coefficient in Bubble Column Reactors. *Chemical Engineering Research and Design, 82*(6), 689-707. doi:10.1205/026387604774195984

Fia, F. R. L., Fia, R., Campos, C. M. M., & Oliveira, L. F. C. d. (2016). Hydrodynamic behaviour of a combined anaerobic-aerobic system employed in the treatment of vinasse. *Ciência e Agrotecnologia, 40*(6), 718-729. doi:10.1590/1413-70542016406010416

Lim, T.-T., Jin, Y., Ni, J.-Q., & Heber, A. J. (2012). Field evaluation of biofilters in reducing aerial pollutant emissions from a commercial pig finishing building. *Biosystems Engineering*, *112*(3), 192-201. doi:10.1016/j.biosystemseng.2012.04.001

Sedghi-Asl, M., Rahimi, H., & Salehi, R. (2013). Non-Darcy Flow of Water Through a Packed Column Test. *Transport in Porous Media*, *101*(2), 215-227. doi:10.1007/s11242-013-0240-0

Teixeira, E. C., & do Nascimento Siqueira, R. (2008). Performance Assessment of Hydraulic Efficiency Indexes. *Journal of Environmental Engineering, 134*(10), 851-859. doi:10.1061/(asce)0733-9372(2008)134:10(851)

Van Baten, J. M., & Krishna, R. (2004). Scale Effects on the Hydrodynamics of Bubble Columns Operating in the Heterogeneous Flow Regime. *Chemical Engineering Research and Design, 82*(8), 1043-1053. doi:10.1205/0263876041580703

Van Baten, J. M., Ellenberger, J., & Krishna, R. (2003). Scale-up strategy for bubble column slurry reactors using CFD simulations. *Catalysis Today, 79-80*, 259-265. doi:10.1016/s0920-5861(03)00048-8

Vijayaraghavan, K., Jegan, J., Palanivelu, K., & Velan, M. (2004). Removal of nickel(II) ions from aqueous solution using crab shell particles in a packed bed up-flow column. *J Hazard Mater*, *113*(1-3), 223-230. doi:10.1016/j.jhazmat

BRIDGE-8

BRIDGE: After finding the SMS, the scale-up study was to be performed. However, the scale-up was done using an integrated mass balance approach. It meant, creating a micro-model of the DWTP in the laboratory (named: SAP-1©). More than 10 water quality parameters were studied including MC-LR removal using both: a) commercially available MC-LR and b) algal biomass-release MC-LR. This study successfully highlighted the importance of filter unit in a DWTP chain and versatility of GS1 filter adsorbent as a household application too.

PART 2

A low-cost graphitized sand filter to deliver MC-LR-free drinkable water: A mass balance approach using laboratory-made Drinking Water Treatment Plant micro-model (SAP-1©)

Pratik Kumar[a], Maximiliano Cledon[b], Satinder Kaur Brar[a,c]

[a-] INRS-ETE, Université du Québec, 490, Rue de la Couronne, Québec, Canada G1K 9A9

[b-] CIMAS (CONICET, UnComa, Rio Negro), Güemes 1030, San Antonio Oeste, Rio Negro, Argentina

[c-] Department of Civil Engineering, Lassonde School of Engineering, York University, North York, Toronto M3J 1P3, Ontario, Canada

[*]Corresponding author, E-mail: satinder.brar@ete.inrs.ca; satinder.brar@lassonde.yorku.ca (S.K. Brar)

Science of the Total Environment

Résumé

Après une étude réussie de l'élimination de Microcystine-LR au niveau de la paillasse, la faisabilité à grande echelle a été testé en utilisant la dynamique des fluides computationnelle (CFD). A partir de CFD (à l'aide du logiciel ANSYS-CFX), un filtre à "echelle minimale subjective" (SMS) a été conçu sur la base du régime d'écoulement radial et uniforme obtenu, éliminant la possibilité de court-circuit pendant la condition d'écoulement du bouchon trouvé dans les colonnes du filtre à échelle de la paillasse. A l'aide du filtre SMS, une étude de bilan massique a été réalisée à l'aide de la configuration du modèle DWTP en laboratoire nommée : SAP-1. Parallèlement à MC-LR, divers autres WQP (paramètres de qualité de l'eau) ont été étudiés, notamment les ions métalliques, les coliformes totaux, la turbidité et le carbone organique dissous. L'efficacité d'élimination de ces contaminants de différentes unités de traitement a été rapportée. La chaine de traitement comprend : un décanteur d'eau brute, un reservoir de pré-oxydation complété par un oxydant (permanganate de potassium), suivi par un réservoir de coagulation/floculation (alun), un réservoir de sédimentation, un filtre (média de sable graphité) et enfin un réservoir de désinfection alimenté par une solution d'hypochlorite. La majeure partie de l'élimination a eu lieu dans l'unité de filtration, soulignant son importance dans une chaîne de traitement. Une étude d'élimination du MC-LR à une concentration initiale de 50 µg/L a été réalisée en utilisant deux sources a) le MC-LR commercial, b) le MC-LR libéré par la biomasse algale. Pour le MC-LR commercial, l'unité de pré-oxydation a éliminé plus de 50% de MC-LR par rapport à <20% pour le MC-LR libéré par la biomasse algale. L'unité de filtration a pu réduire davantage le MC-LR résiduel entrant de 12,1 µg/L et 25,4 µg/L (provenant de l'unité précédente: unité de sédimentation) pour se conformer avec succès aux directives de l'OMS (<1 µg/L) pour les cas « a » et le cas « b », respectivement. Une concentration initiale de MC-LR de 50 µg/L (les deux sources MC-LR) alimentée directement à travers le filtre a montré une élimination complète, mettant en évidence l'application de l'unité de filtre comme module de traitement autonome également.

Mots-clés: Filtre à grande échelle, MC-LR, Bilan massique, Chaine de traitement, Eau potable, Adsorption

Abstract

A scale-up feasibility of the graphitized sand filter (GS) pertaining to Microcystin-LR (MC-LR) and its impact on other water pollutants (WPs) was assessed through a mass-balance study, using a laboratory-based drinking water treatment plant (DWTP) micromodel named: SAP-1©. The treatment chain comprised: raw water tank, pre-oxidation tank supplemented with potassium permanganate oxidant, followed by coagulation/flocculation tank (alum supplemented), sedimentation tank, filtration module and finally disinfection tank (dosed with hypochlorite solution). Two filter modules were studied: a) graphitized-sand media + sand media = ½ GS1 + ½ sand (FM1) and ½ sand + ½ sand (FM2). MC-LR removal study was performed using two sources: a) commercial MC-LR, b) algal-biomass released MC-LR, each at an initial concentration of 50 µg/L each. Along with MC-LR, other WPs were also evaluated that includes metal ions (Fe^{2+} and Cu^{2+}), total coliform, turbidity, ammonia-N and dissolved organic carbon. The removal efficiency of these contaminants for each treatment units was reported. FM1 was able to reduce the inflow residual MC-LR of 12.1 µg/L and 25.4 µg/L for commercial and algal-cell MC-LR source, respectively (coming from the preceding unit: sedimentation unit) to < 0.61 µg/L and hence successfully complying to the WHO guidelines (<1 µg/L). PP1A toxicity assay confirmed a much safer and more toxic-free filtrate (by 40%-50%) for FM1 as compared to filtrate obtained from FM2. The technoeconomic evaluation showed that for a household filter application, 91 CAD needs to be spent on one GS-based filter (prepared using sustainable sugar or carbon source) as compared to 2800 CAD (equivalent price) for the conventional sand-based filter to provide MC-LR-free water, based on an expected average seasonal outbreak concentration of MC-LR (up to 10 µg/L) in source water.

Keywords: Scale-up filter, MC-LR, graphitized sand, treatment chain, drinking water, adsorption

Introduction

Microcystin-LR (MC-LR) is the most prominent cyanotoxin which is commonly found in the cyanobloom-affected aquatic ecosystem, polluting the drinking water sources such as lakes, rivers and ponds. Since the WHO guidelines for MC-LR micropollutant in drinking water is < 1 µg/L, the need to treat them in a drinking water treatment plant (DWTPs) or household filters (that use direct source water) becomes very essential (WHO, 2009). Apart from the aquatic organisms, MC-LR has a profound impact on human health too. MC-LR is a hepatotoxin and attacks the liver cells which causes acute to chronic health effects, damaging the immune system, liver, kidney and sometimes multiple organ failure too.

Most of the treatment methods commonly practiced in a typical DWTP has shown an effective MC-LR removal. The oxidation processes such as ozonation and chlorination have shown even complete MC-LR removal (Lawton et al. 1999; Keijola et al. 1988). However, the oxidant dose is highly dependent on the MC-LR concentration to be treated and also depends on pH, natural organic matter, and presence of other contaminants in the source water (Ma et al. 2012). Hence, a high MC-LR concentration demands higher oxidant dosage which produce toxic by-products in the treated water after complexing with the hydrolyzed or fragmented MC-LR molecules. Moreover, a longer contact time than normal is required to completely remove the MC-LR. Hence, to keep the dose under regulation and toxicity under check, along with a strict residence time operation, treatment unit should be less chemical dependent, less energy intensive and economical. One such treatment unit in a DWTP chain is sand filter unit which has shown potential in adsorbing MC-LR and can render toxic-free treated water if bioaugmented with MC-LR degraders (Kumar et al. 2020). The major advantage of using sand filter is that it is not an energy-intensive treatment unit, require no chemical addition and is economical too. Many studies have shown successful bio sand filter operation for the MC-LR removal too (Ho et al. 2006, Ho et al. 2007, Somdee et al. 2013). However, most of these studies were experimented at the bench-scale which does not necessarily expect to perform the same at a higher scale. Not only that, but sand-based filters without bioaugmentation has performed poor pertaining to the MC-LR adsorption (20%-30% adsorption capacity). A promising result obtained at the bench-scale using graphitized-sand adsorbent for various water pollutants including MC-LR (> 90% removal) from our previous study (Kumar et al. 2019), prompted to further check the adsorbent feasibility at the pilot-scale. The

graphitization of sand was performed using sustainable sugar solution in form of brewery effluent (0.1g-sugar/g-sand). This study not only highlights the importance of graphitized-sand filter in the treatment chain but as a stand-alone treatment unit as well. However, this study only focuses on the physical adsorption and not the biodegradation aspect of MC-LR removal.

During the plant operations, it is important to understand the mass balance of contaminant that defines the water quality at each stage of treatment. These include primary water pollutants such as metals (copper, iron), dissolved organic matter, turbidity, total coliform, ammonia-N. Herein, in this study, a mass balance approach is presented for the above mentioned WQPs including MC-LR from two different sources (commercial as well as algal cells-derived). For this, a DWTP micromodel was set-up in the laboratory comprising raw water tank, pre-oxidation, coagulation/flocculation, sedimentation, filtration module, and disinfection treatment unit. Two filter modules were studied viz. sand filter module (½ sand + ½ sand: control) which represents the existing DWTP treatment chain whereas a hybrid filter module (½ GS1 + ½ Sand) to understand the impact of graphitized sand module as a 'modified' DWTP treatment chain.

To the best of the author's knowledge, it is the first time a mass balance approach is studied to report various WQPs using a laboratory-made DWTP micromodel that includes MC-LR using two different sources (as mentioned above). The set-up is fully automatic which was modelled to treat 2 liters of lake water as per the residence/treatment time involved in the treatment module of a typical DWTP. This study also comprises toxicity assessment of the filtrate water from both filter modules and technoeconomic evaluation of the standalone graphitized-sand filter for household purpose.

Material and methods

Reactor fabrication, chemicals and reagents

Plexiglass column reactors for filters were fabricated by Poly Alto, Quebec City, Canada, dimensioning 9 cm x 9 cm x 33 cm with a thickness of 8 mm from all sides. To stir the coagulant at a defined vortex gradient speed, a compact digital mixer system was bought from Cole-Parmer (Ontario, Canada). Water Quality Parameter (WQP) kit for Cu^{2+}, Fe^{2+} and ammonia-N, aerator pumps, pipelines, check valves, barbed connectors, fitters and other accessories were bought from Amazon.ca, Canada. The oxidants: potassium permanganate and alum: aluminum sulphate, were

bought from Sigma Aldrich, (Ontario, Canada). For the PP1A assay, enzyme and substrate: Protein Phosphatase-1 Catalytic Subunit (α-Isoform from rabbit) and p-nitrophenyl phosphate (pNPP), respectively were purchased from Sigma Aldrich (Ontario, Canada). Quartz sand used as the filter media was obtained from Chemin Ste-Foy DWTP, Quebec City, Canada.

Preparation of lake water

Lake Sainte-Anne (47.262879N, -71.665158W) water was used as an influent matrix solution. The contaminants were spiked to reach the final concentration as follows: NH_4-N: 5 mg/L, Cu^{2+} 20 mg/L, Fe^{2+} 10 mg/L, MC-LR: 50 µg/L (both commercial as well as one released from laboratory-cultured algal biomass). Before spiking the above contaminants, the background concentration of each pollutant was determined and then accordingly the final solution was prepared.

API freshwater master test kit-800 was used for ammonia-N, Cu^{2+} and Fe^{2+} calibration and sample analysis experiment. The colour produced by the kit reagent and sample was calibrated spectrophotometrically where absorbance was measured at the characteristic wavelength as obtained from the scan kinetic using UV Cary 300 spectrophotometer instrument. Ammonium sulphate was used as the ammonia-N source and was spiked in the lake water according to the stoichiometric calculations to prepare a final concentration of 5 mg/L NH_4-N (final volume: 2 liter).

Dissolved organic carbon (DOC) was estimated using Shimadzu 5000A analyzer (Shimadzu, Japan). In brief, around 50 mL of the effluent sample was filtered using a 0.45 µm glass-fiber filter and analyzed for the DOC. The average DOC in lake water was found to be 4.1 ± 0.6 mg/L which was further increased to 14.8 ± 1.1 mg/L using dextrose (relationship of dextrose dose and DOC is mentioned in the supplementary section). In general, DOC in lake water remains < 6 mg/L but in this study DOC level was enhanced to represent the source water during peak (monsoon) season.

Total coliform was determined by membrane filtration technique according to the standard method APHA (1998). The average total coliform in lake water was reported to be 121 ± 37 CFU/100 mL.

Fe^{2+} and Cu^{2+} metal ions were chosen as the metal ion indicator in lake water where $FeSO_4.7H_2O$ and $CuSO_4.5H_2O$ were used as the respective metal source. The initial Fe^{2+} and Cu^{2+} concentration of 10 mg/L and 20 mg/L was chosen based on the stoichiometric equivalent of the metal sources (as mentioned above) and measurement was done spectrophotometrically. The background

concentration of ammonia-N and Cu^{2+} in lake water ranged 0.1-0.3 mg/L and 1.3-2.3 mg/L and thus prepared copper concentration of 20 mg/L (spiked) did not formed ammonia-Cu complex in a significant amount and vice-versa. Thus, only for ammonia-N analysis (for initial concentration: 5 mg/L), it was made sure that the raw water (prepared lake water) does not contain spiked copper ions and vice-versa as otherwise it could have interfered in the colorimetric analysis. Hence, two separate lake water influent was prepared where second batch was used every day only for the analysis of Cu^{2+}/NH_4-N.

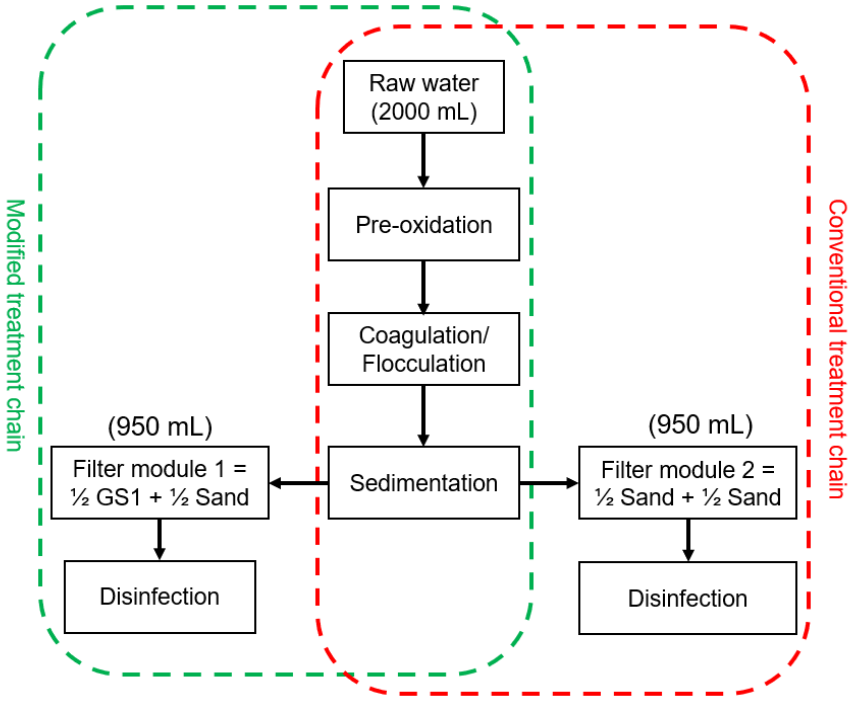

Figure 5.2. 1: Flowchart of the treatment chain for both the filter modules; GS1: Graphitized sand

Finally, the turbidity of the prepared lake water was measured using HACH instruments 2100A which averaged 42.5 ± 5.2 NTU. Figure 5.2.1 shows the flowchart diagram of the treatment chain being studied in the current study where filter module 1 comprised graphitized-sand filter (as half filter with sand filter as another half), while filter module 2 comprised only sand filter representing modified and conventional treatment chain, respectively. Turbidity, total coliform, Fe^{2+} and Cu^{2+} analysis was done each day for 41-days experiment while NH_4-N, DOC and MC-LR (both sources) were done 16 times, 6 times and 5 times at regular period for a total of 41 days, respectively.

DWTP model SAP-1© set-up

Figure 5.2.2 shows the set-up model representing a typical DWTP, named as SAP-1©.It represents a typical plant operation comprising the raw water tank, pre-oxidation tank, coagulation/flocculation tank, followed by sedimentation tank, filter module (here only filter module 1 is shown = ½ GS1 + ½ Sand) and disinfection unit. Filters consisted of sand/graphitized sand (GS) media (depending on FM1/FM2) for a height of 22 cm followed by the drainage section (particles size >2 mm and <5 mm). Graphitized sand was synthesized using brewery effluent liquid containing sugar as detailed in our previous study (Kumar et al. 2019). The effective diameter of the filter grain in filters was around 0.26 mm with a coefficient of uniformity <2.4. The raw water tank was filled with 2-litre lake water (preparation as discussed above) and the feed influent was immediately transferred to the pre-oxidation tank using an auto-dosage pump where potassium permanganate was used as an oxidant (dose: 1.5 mg/L). After 10 minutes of pre-oxidation (aerated continuously using air pump), the treated water was pumped into the next treatment unit: flocculation tank, where alum (90 mg) was dosed for the oxidized raw water. The stirring was done at 225 ppm for 2 minutes (to allow a uniform dispersion of alum) followed by slow stirring at 50 rpm (flocculation) for 10 minutes.

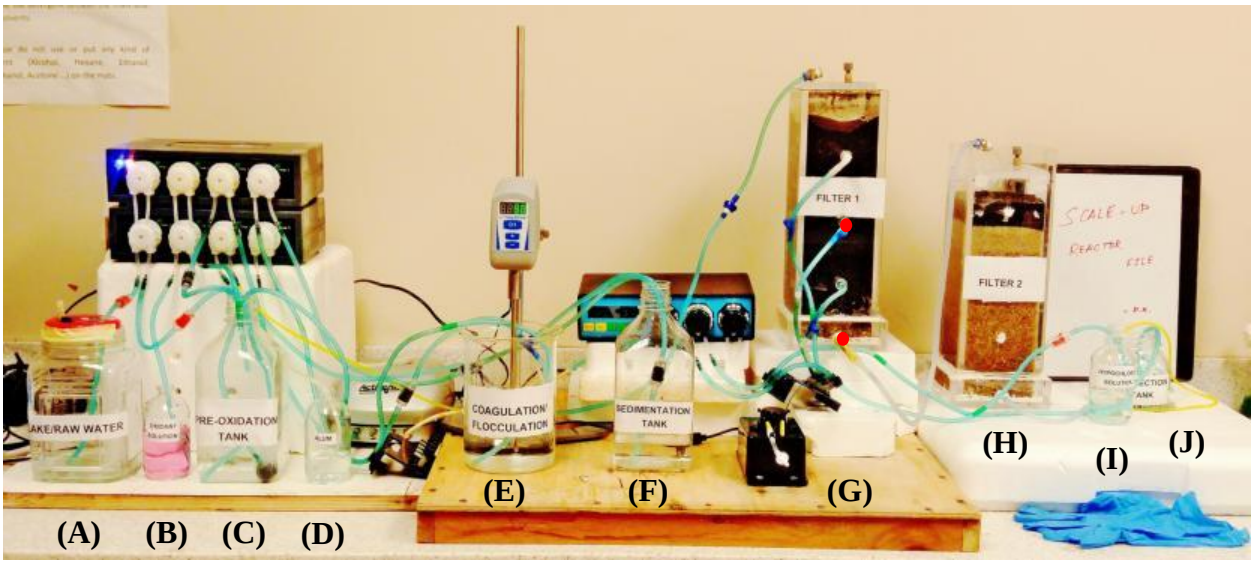

Figure 5.2. 2: Drinking water treatment plant micro-model (SAP-1©); the red dot shows the mid and end sampling port of the GS1 filter; GS1: Graphitized sand

After this step, the supernatant (around 1.95 liters) was discharged to the sedimentation tank allowing a settling time of 45 minutes (typically expected in a real sedimentation tank present in

DWTPs). Afterwards, the supernatant (1.95 L) was pumped to both the filter modules equally (950 ml each) which filtered water at an overall rate of 100 ml per minute (0.75 m/h). The filter rate was measured at the effluent port that opened to the disinfection unit. The disinfection unit was dosed with 4 drops or 0.15 ml @ 6% hypochlorite solution (bleach) for approx. 1.8 liter of filtered water.

The disinfection tank was aerated for 1 minute and then left undisturbed for 5 minutes to complete the process. Table 5.2.1 shows the treatment chain unit with their residence time, chemicals used and their respective dosage. All the transfer of influent/effluent was done through the auto-dose pump, set at the defined run time according to the residence time of the influent as described in Table 5.2.1. Overall, the process took 110 minutes starting from the raw water tank to disinfection tank. Before commencing the actual study, the set-up was run for 3 days with each day 6 liters of lake water treated before starting the WQPs testing and analysis. This was performed to adjust the influent-effluent conditions in the set-up chain and calibrating the auto-dosage pump with precision. In total 8 pump channels were used to make the operation fully automatic and convenient for the operator.

Table 5.2.1: Treatment module details and characteristics

Name	Treatment unit	Residence time (min)	Chemical added (if any)	Remarks
A	Raw water/Lake water tank	0	NA	NA
B	Oxidant solution	NA	Potassium permanganate	Stock solution of PP: 60 ppm, dose vol.: 50 mL.
C	Pre-oxidation tank	10 min	Oxygen bubble (aeration)	Final dose: 1.5 ppm
D	Alum	NA	Alum	Stock solution of PP: 1125 ppm, dose vol.: 80 mL.
E	Coagulation/Flocculation	10 min	Alum	Final dose: 45 ppm
F	Sedimentation tank	45 min	NA	NA
G	Filter 1 (GS1 filter for FM1 and sand filter for FM2)	10 min	NA	Main filter
H	Filter 2 (Sand filter for FM1 and sand filter for FM2)	5 min	NA	Extension filter
I	Hypochlorite dose	NA	Bleach in our lab (6% NaOCl)	Stock sol of 8.25% hypochlorite sol., dose vol: 0.15 mL
J	Disinfection tank	6 min		NA

NA: not applicable; FM1 and FM2: Filter module 1 and 2; GS1: Graphitized sand

Justification for pre-oxidant and coagulant dose

Justification for potassium permanganate dose

Potassium permanganate (PP) has been widely used as the point-of-entry treatment for many years. One major advantage of using PP is that it oxidizes the metal contaminant and converts them into the oxide form which is filtered and hence easy to remove later. Also, it removes taste and odor problems even after it combines with the chorine molecules later in the treatment. 1-1.5 ppm dose of PP for 10-15 minutes was found suitable for the pre-oxidation purpose (Welch, 1963). Hidayah et al. (2018) tested a range of PP dose from 0.25 to 4 ppm and found major changes happened in terms of disinfection by-product (DBPs) formation. The least DBPs formed at a dose of 1.8 ppm (reduced by 23% from peak value). Hence, for this study, a dose of 1.5 ppm was chosen for the treatment.

Study for alum coagulant dose

Iron-based coagulants are expensive as compared to alum (for a similar equivalent dose) and reduce the alkalinity of raw water which degrades the water quality (Gebbie, 2006). Also, iron-based coagulants generate fluffier flocs that takes time to settle. Hence, in this study, crystalline potassium aluminum sulphate $KAl(SO_4)_2 \cdot 12H_2O$ was used to counter above challenges. Alum dose of 45 mg/L was selected based on the literature review of some studies based on the jar test experiment (Ebeling et al. 2003, Kamel et al. 2018).

Toxicity analysis using protein phosphatases inhibitory assay (PP1A assay)

Protein phosphatase 1 (PP1) belongs to a protein serine/threonine phosphatases class and is related to the control of glycogen metabolism in liver. Since MC-LR is a hepatotoxin, it inhibits the kinetic activity of PP1 protein. Many researchers have specified PP1A assay to report the toxicity of the MC-LR samples. In this study, PP1A assay was performed following a developed protocol for MC-LR by Moore et al. (2016) with some modifications.

This assay was performed in a 96-well plate. In a 300 µL well, 20 µL of sample or known MC-LR (to prepare the standards), 40 µL of PP1 enzyme (well concentration of 0.85 U/mL), and 240 µL of pNPP substrate (final well concentration of 115 mM) were mixed to initiate the enzyme-substrate reaction. A blank was also prepared with substrate blank which represented the baseline activity of PP1 to normalize the effect of MC-LR in a PP1 activity. The PP1A activity rate was determined based on the optical density (OD) at λmax: 405 nm after every 2 minutes for 1 hour. After 1080 seconds, the plateau region was reached for the substrate blank from where change in OD/min was calculated until 3480 seconds. More the hydrolysis of pNPP by PP1A enzyme, lesser

the OD observed and lesser the PP1A inhibition and hence more the PP1A activity. All measurements were done in triplicates.

Culture of *Microcystis aeruginosa* and MC-LR analysis

Microcystis aeruginosa was received as a kind gift from Dr. Jerome Compte (Professor, INRS-ETE, Quebec City, Canada) in a 30 ml culture tube. BG-11 media was used for culturing M.*aeruginosa* as mentioned by Rippka et al. (1979). A fluorescent light was installed to provide a constant source of light (8h/16h; light/dark phase) to the growing culture. Every week for up to 12 weeks, 10 ml of prepared BG-11 media was added to the growing culture in a 250 ml Erlenmeyer flask and optical density at λ_{max} = 700 nm was noted down (not shown here). After 12 weeks of culture growth, for up to 6 more weeks, MC-LR toxin was analysed in the growing medium. For this, 3 ml of culture was filtered using a 0.45 µm HA filter where cells were retained over the filter and filtrate was further used for the MC-LR analysis (only extracellular MC-LR was analysed) using uHPLC using a method adapted from Roy-Lachapelle et al. (2019). Briefly a 20-µL sample aliquot was analyzed by ultra-high-performance liquid chromatography coupled to high-resolution mass spectrometry (Thermo Q-Exactive Orbitrap) through a positive electrospray ionization source. The chromatographic column was a Thermo Hypersil Gold with C18 selectivity (100 x 2.1 mm, 1.9 µm particle size). MC-LR was detected in full-scan MS mode and quantified against distilled water. The analytical method was validated for linearity, accuracy, and precision; the performance was compliant with acceptance criteria (Roy-Lachapelle et al. 2019). The method limit of quantification (LOQ) was set at the lowest concentration level of the calibration curve (i.e. 0.1 µg/L). At the end of 6-weeks of MC-LR analysis, a final mean concentration of 8255 µg/L was obtained from a 150 ml culture which was sufficient to prepare 2-liter lake water at a final MC-LR concentration of 50 µg/L for more than 10 times using dilution.

Results and discussions

pH and DO analysis

Figure 5.2.3 shows the trend of pH and DO in different treatment units of the set-up: SAP-1©. In total, pH and DO measurement was taken 7 times during the 41-day experiment. Initial raw water pH and DO were 7.12 ± 0.06 and 4.65 ± 0.1 mg-O_2/L, respectively. After pre-oxidation, the DO increase to 5.45 ± 0.21 mg-O_2/L as it was continuously aerated during the process, while pH

remained almost the same (7.01 ± 0.16). The coagulation step further elevated the DO content of the influent water and could be accounted due to mixing during the flocculation stage (Figure 5.2.3).

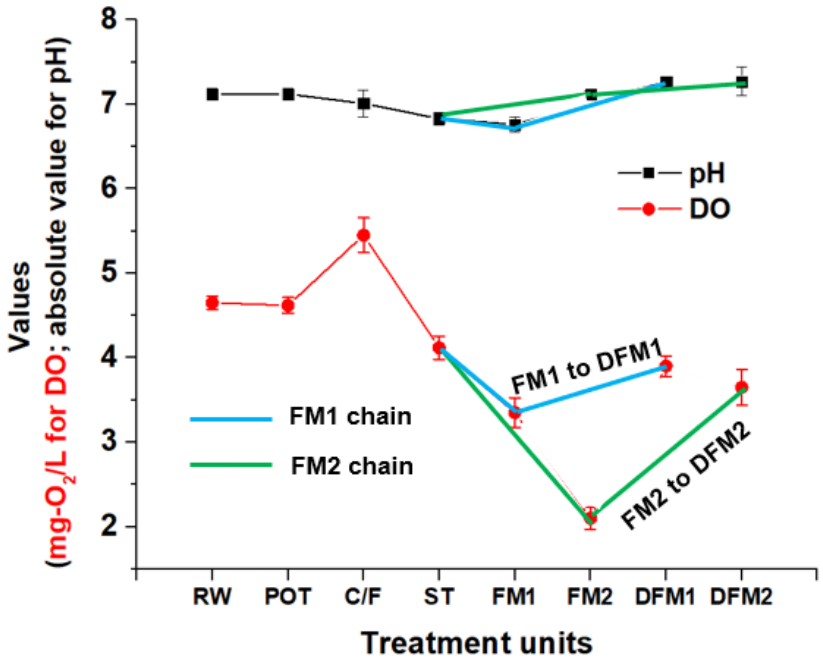

Figure 5.2.3: pH and Dissolved oxygen (DO) trend in different treatment modules (x-axis); RW: Raw water; POT: Pre-oxidation tank; C/F: Coagulation/Flocculation; FM1: Filter module 1; FM2: Filter module 2; DFM1/DFM2: disinfection tank of FM1/FM2.

However, after the sedimentation, the DO decrease to 4.12 ± 0.14 mg-O_2/L from 5.45 ± 0.21 mg-O_2/L which could be due to non-mixing condition during the 45 min long-standing. The pH of the influent water kept on decreasing and fall to its minimum value of 6.76 (-0.36 than raw water) for FM1 module filtrate but remained same for the filtrate obtained from FM2 (7.1 ± 0.1). Overall, the pH of the filtrate did not change by much which clearly attributed the working of PP as an oxidant (not reduced the alkalinity by a significant amount: just 0.36 change in pH value).

However, filter module 1 and filter module 2 majorly reduce the DO of the incoming water from sedimentation tank, especially FM2 filtrate that showed an average DO of < 3 mg-O_2/L. This could be due to less dissolution of oxygen within the sand grains (full sand filter equivalent) as compared to filter module 1 that consists of graphitized sand where more diffusion of water happened due to more pore volume as derived from the BET analysis (7.1 cm^3/g as compared to 3.2 cm^3/g for sand).

Also, the pH of filtrate from FM1 was lower than (6.76 ± 0.2) the filtrate obtained from FM2 (7.1 ± 0.3). This could be due to more DOC removal by FM1, from 6.5 ± 0.2 to 1.88 ± 0.3 mg/L, as compared to FM2, from 6.5 ± 0.2 to 4.1 ± 0.4 mg/L (more details are provided in later section). However, consumption of DO by the heterogenous bacteria (grown within filter column) in FM1 was found to be more effective in utilizing dissolved carbon than that of FM2 as the change in DO/mg-DOC removal for the latter was comparatively higher (0.83 mg-O_2 utilized/mg DOC removed) than the former (0.16 mg-O_2 utilized/mg DOC removed). This strengthens the fact that the population of heterogenous bacteria in graphitized sand grains (part of FM1) is relatively more productive than that attached over the sand grains in terms of organic carbon removal. However, a more long-term evaluation and genomic analysis of the formed biofilm could lead to a more definite conclusion on the relative abundancy of high carbon utilizing bacterial species and their identification as well.

Turbidity, total coliform, and total organic carbon (TOC)

Table 5.2.2 shows the data of water quality parameters tested for the treatment chain comprising two different filter modules. The initial turbidity of the raw water was 42.5 ± 5.2 NTU and can be attributed to a high organic component (DOC: 15 mg/L) present in it along with the suspended solids. This value represents a season-peak turbidity of the lake water during the monsoon season when more organic compounds leach and mix with the surface water bodies. After pre-oxidation, the turbidity reduced to 32.2 ± 4.8 NTU, but a major change was observed after coagulation step when turbidity reduced to 18 ± 3.2 NTU followed by settling of suspended particles in the sedimentation tank which further reduced it to 8.1 ± 2.3 NTU. After filtration (filter module 1), the turbidity dropped down to 0.6 ± 0.3 NTU which complies with the Canadian drinking water guidelines. On the other hand, it can be observed that filter module 2 still showed an average turbidity of 2.3 ± 0.9 NTU. Initial total coliform present in the raw water was 121 ± 37 CFU/100 mL and reduced drastically after pre-oxidation to 42 ± 16 CFU/100 mL. Filter 1 further reduced this count to 2 ± 1 CFU/100 mL and disinfection showed almost complete removal. Both the filter modules were found equally efficient in removing the total coliforms. Considering the utility of filter modules for a household purpose, both filters (FM1 and FM2) performed equally well for the total coliform removal, achieving an almost complete removal.

Table 5.2.2: Water Quality Parameters along the treatment chain

Water Quality Parameters	Raw water	Pre-oxidation	C/F	Sedimentation	½ GS1 + ½ Sand filter	Disinfection
Turbidity (NTU)	42.5 ± 5.2	32.2 ± 4.8	18 ± 3.2	8.1 ± 2.3	0.6 ± 0.3	0.3 ± 0.1
					½ Sand + ½ Sand filter	**Disinfection**
					2.3 ± 0.9	1.5 ± 0.6
NH4-N (mg/L)	5 ± NIL	4.6 ± 0.3	4.2 ± 0.4	4.1 ± 0.3	1.1 ± 0.1	ND
					½ Sand + ½ Sand filter	**Disinfection**
					3.3 ± 0.4	ND
MC-LR commercial (µg/L)	50 ± NIL	23.8 ± 2.3	13.2 ± 1.4	12.1 ± 0.9	< 0.1	<0.1
					½ Sand + ½ Sand filter	**Disinfection**
					8.2 ± 0.4	4.1 ± 1.1
MC-LR Algae cell (µg/L)	55.8 ± 1.2	45.9 ± 1.7	28.7 ± 2.7	25.2 ± 1.2	<0.1	<0.1
					½ Sand + ½ Sand filter	**Disinfection**
					20.9 ± 0.9	14.2 ± 1
DOC (mg/L)	14.8 ± 1.1	11.2 ± 1.5	8.3 ± 0.6	6.5 ± 0.2	1.8 ± 0.3	ND
					½ Sand + ½ Sand filter	**Disinfection**
					4.1 ± 0.4	ND
Fe2+ (mg/L)	10 ± NIL	7.95 ± 0.4	4.7 ± 0.55	3.1 ± 0.5	0.95 ± 0.4	ppt
					½ Sand + ½ Sand filter	**Disinfection**
					2.3 ± 0.4	ppt
Cu2+ (mg/L)	20 ± NIL	15.2 ± 1.1	13.4 ± 1.4	11.9 ± 1.2	2.6 ± 1.1	ppt
					½ Sand + ½ Sand filter	**Disinfection**
					6.6 ± 0.6	ppt
Total coliform (CFU/100 mL)	121 ± 37	42 ± 16	21 ± 7	24 ± 4	2 ± 1	1 ± 1
					½ Sand + ½ Sand filter	**Disinfection**
					3 ± 3	2 ± 1

Ppt: Precipitation formed in most of the analysis; CFU: Coliform forming unit; C/F: Coagulation/Flocculation; NTU: Nephelometric Turbidity unit

Dissolved organic carbon present in raw water was 14.8 ± 1.1 mg/L, which after pre-oxidation did not got removed by much and the value remained on the higher side (> 11 mg/L). However, a major change occurred after the treatment from filter module 1, which reduced DOC value of the

supernatant coming from the sedimentation tank from 6.53 ± 0.2 mg/L to 1.89 ± 0.3 mg/L. After disinfection, the value reduced to non-detection level. On the other hand, DOC still needed a better removal efficiency when filter module 2 was used, as any organic matter present during disinfection (here: 4.1 ± 0.4 mg/L) can combine with chlorine to form disinfection by-products (DBPs) such as THM4, dihaloacetic acids (DHAAs) and trihaloacetic acids (THAAs), especially for DOC level exceeding 4 mg/L (Bond et al. 2014). The formation of DBPs was not investigated in this study.

Ammonia-N removal

Initial ammonia-N present in raw water was 5 mg/L and its removal was noted for each treatment module. Due to high solubility of ammonia-N in water, there was hardly any change observed until sedimentation (4.1 ± 0.3 mg/L). Even pre-oxidation did not remove the dissolved ammonia-N. However, a maximum change was observed during filtration from filter module 1, where ammonia-N decreased from 4.1 ± 0.3 mg/L to 1.1 ± 0.1 mg/L. On the other hand, filter module 2 showed poor adsorption of ammonia-N as the filtrate showed 3.3 ± 0.4 mg/L of DOC. The major change observed for filter 1 could be attributed to an effective adsorption due to a high mesoporous surface of the graphitized sand as a BET isotherm of type IV was obtained (supplementary file). Not surprisingly, the level of ammonia-N analyzed after the disinfection in either cases (filter 1 or filter 2) showed no trace due to the possible reaction of ammonia with hypochlorite ion (present in bleach) forming chloramine vapour.

Iron, copper and MC-LR

Initial Fe^{2+} and Cu^{2+} concentration present in the raw water was 10 mg/L and 20 mg/L (spiked according to the background concentration). Surprisingly, there was not much decrease in either of the metal ions after pre-oxidation (Table 2). For Fe^{2+}, coagulation removed a major portion by decreasing its concentration from > 8 mg/L to less than 5 mg/L. After sedimentation, some Fe^{2+} ions may have settled along with the suspended solids that formed flocs after coagulation (4.7 ± 0.55 mg/L to 3.1 ± 0.5 mg/L). After filtration from filter module 1, the concentration decreased to < 1 mg/L while the filtrate of filter module 2 showed 2.3 ± 0.4 mg/L. Hence, the final Fe^{2+} concentration remained more than the Canadian guidelines value (< 0.3 mg/L) for both these cases. However, it is to be noted that the initial concentration of Fe^{2+} was more than the normal concentration found in the source water (1-5 mg/L). On the other hand, copper (Cu^{2+}) showed a

distinct removal by filter module 1 as the residual Cu^{2+} concentration after sedimentation (12 mg/L) decreased to 2.6 ± 1.1 mg/L as compared to filter module 2 (6.6 ± 0.6 mg/L). A high removal of both metal ions highlighted the versatility of GS1 media filter for the household purpose. As the treatment was analyzed each day for the iron and copper ions, initial few days showed a non-detectable concentration after disinfection. However, after few days, a precipitate was seen building at the bottom of the disinfection bottle suggesting a possible residual metal ion after reacting with the hypochlorite ions present in bleach.

Initial MC-LR concentration for the commercial (MC1) and one extracted from algal cells cultured in the laboratory (MC2) were kept nearly the same at 50 µg/L and 56.8 µg/L in the prepared lake water influent. It was difficult to anticipate before the extraction process, the amount of dilution required for the MC-LR extracted from the algal cells to reach a target concentration of 50 µg/L, as cells continue to produce toxins offsetting the rise between two sets of analysis. Hence, the starting MC-LR concentration was obtained slightly greater than 50 µg/L. It was observed that the MC1 removal was more than MC2 after pre-oxidation (Table 2). However, coagulation and sedimentation treatment modules kept the degree of MC1 and MC2 removal almost similar. A major change was observed after filtration from filter module 1, where the residual MC1 and MC2 coming from the sedimentation tank, 12.1 ± 0.9 µg/L and 25.4 ± 1.2 µg/L, respectively, further decreased the MC-LR concentration to < 0.6 µg/L (both cases) complying WHO guidelines (< 1.0 µg/L). This attributes to the remarkable adsorption capacity of graphene-sugar sand (GS1) which is capable to adsorb high concentration of the MC-LR present in the influent raw water.

To further test the strength of the adsorbent, 50 µg/L of MC1 and MC2 were directly fed to GS1 filter block (1/2 GS1 filter of filter module 1) and checked for its filtrate concentration from mid-port as well as end port (shown in Figure 2 by red dot), before it enters the other half filter of the same module (i.e., ½ sand filter). A complete removal of MC-LR (~ 0.6 µg/L) was observed from both the ports which might suggest that $1/4^{th}$ GS1 filter was enough to remove a high degree of MC-LR (50 µg/L). Though, this concentration is rarely found in any natural water bodies, except the peak cyanobloom season. However, these results need to be further verified in terms of longevity of the filters as the current study only reported five runs of MC-LR at regular interval of a 41-day experiment (five each for commercial and algal cell derived MC-LR). However, from our previous study on graphitized sand filter adsorbent at the bench scale (110 gram), a 16 week

operation of the filter (3 times water discharge per day @ 50 µg/L: 40 mL each), did not showed any breakthrough of MC-LR in the filtered water.

Impact of filter module 1 (½ GS1 filter + ½ Sand filter) in the treatment chain

Figure 5.2.4 shows the heat map of different WQPs analyzed for the treatment chain comprising filter module 1 (FM1) and filter module 2 (FM2). The common heat map for both treatment chains is raw water tank, pre-oxidation tank, flocculation/coagulation and sedimentation tank. The green zone, light green zone, yellow zone, orange zone and red zone indicate high, mid-high, average, low and poor range of WQP guideline values for different treatment units (designated as 1-6 on the y-axis of the heat mapping).

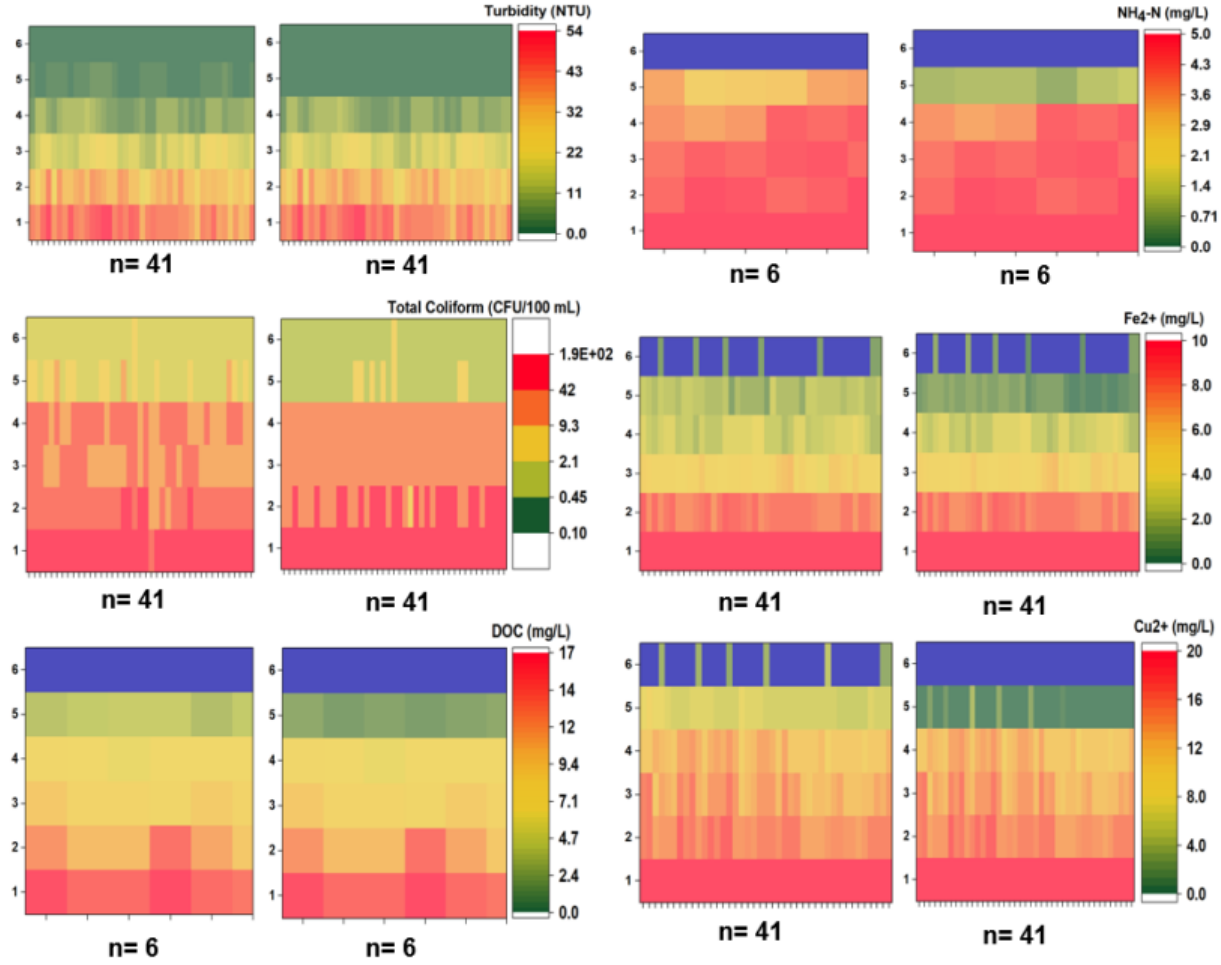

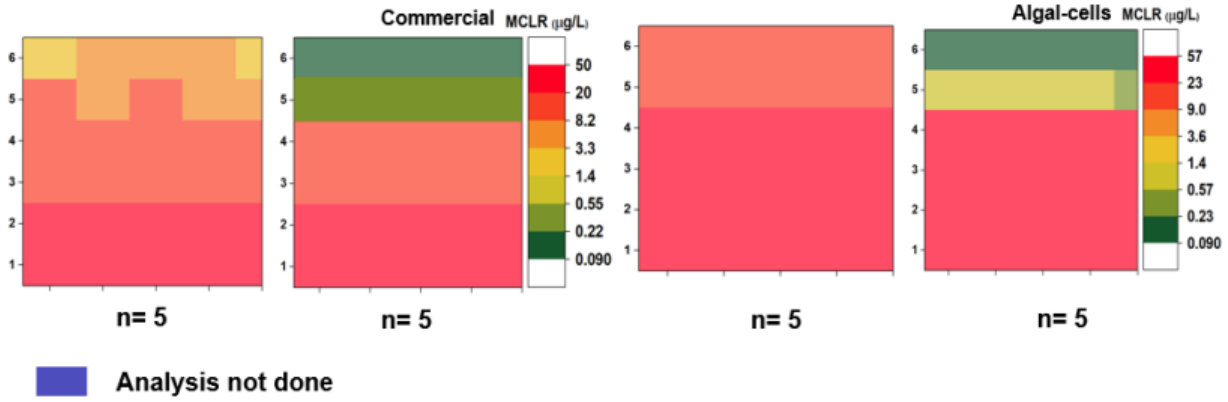

Figure 5.2.4: Heat map of different treatment units 1) Raw water; 2) Pre-oxidation; 3) Coagulation/Flocculation; 4) Sedimentation; 5) Filter module 1 and 2 (left/right) and 6) Disinfection (these numbers are indicated on the y-axis of each heat map). Guideline values for turbidity <1 NTU, total coliform = NIL, ammonia-N is 0.121 mg/L, Fe^{2+} and Cu^{2+}: 0.3 mg/L and < 1 mg/L, respectively; MC-LR: < 1 µg/L; DOC: NIL (typically). The blue region depicts no sample done for that day.

These guideline values are mentioned in the caption of Figure 5.2.4. The right-hand side and left-hand side of the heat mapping for a WQP represents the analysis results of treatment chain containing FM1 and FM2, respectively (though 1-4 remains same as discussed above and in Figure 1). The importance of FM1 for the removal of particular water pollutant can be observed via heat map when compared with FM2 (control). For turbidity and total coliform removal, a greener zone in the heat map can be observed after sedimentation unit for FM1 than FM2. However, the major contrast between treatment step 4 and step 5 (or sedimentation effluent and filter effluent) was observed for the DOC and ammonia-N parameter for FM1 as compared to FM2 heat map. Filtered effluent from FM1 showed safer and cleaner water quality (greener mapping) for over 41 days of experiment, ensuring the applicability of FM1 for a longer period. Also, the metals, iron and copper showed a contrast heat mapping where FM2 treatment showed yellow to feeble green color as compared to the FM1 treatment where heat map showed green to dark green color zone.

Heat map for two sources of MC-LR was also plotted to get a fair idea of the public safety in terms of cleaner looking but a possible toxic-laden potable water. The heat map for the treatment chain comprising FM1 showed remarkable contrast to the FM2 treatment for both sources of MC-LR where latter remained orange even after the disinfection treatment as compared to former which showed green heat map. Among the sources of MC-LR, algal cells-derived MC-LR was found

more difficult to remove as compared to the commercial MC-LR until sedimentation unit, which remained common for FM2 (as discussed above).

An impact factor was calculated considering the average score obtained for each WQP for both the filter modules. Table 5.2.3 tabulates the color (characteristic) obtained by averaging the color mapping of each sampling points (n=41 or 6 or 5 as shown in the heat map: Figure 3 for different WQP) with their average score calculated based on proximity achieved to the guideline value (calculation not shown here). Overall, the average impact ratio of > 0.9 for FM1 as compared to < 0.6 for FM2 shows the impact of FM1 that consists of ½ GS1 filter. This further highlights a poor adsorption property of sand especially for the MC-LR water pollutant justifying the need for graphitized sand filter module in the drinking water treatment system or for the household purpose.

Table 5.2.3: Average map color of the water quality parameter (WQPs) for filter module 1 and filter module 2

Water Quality Parameter (WQPs)	Average color mapping		Average score FM1	Average score FM1
	FM1	FM2	FM1	FM2
NH_4-N			75	35
Cu^{2+}			90	70
Fe^{2+}			92	75
Total coliform			90	90
Turbidity			90	75
DOC			90	80
Commercial MC-LR			100	30
Algal MC-LR			95	20
Total impact score			722	475
Impact ratio			0.91	0.59

DOC: Dissolved organic carbon; MC-LR: Microcystin-LR; FM1: Filter module 1 and FM2: Filter module 2

Toxicity assessment of filtrate from both filter modules

Figure 5.2.5 (A) and Figure 5.2.5 (B) shows the bar chart of the PP1A activity (%) assay for filter module 1 and filter module 2, respectively. A higher PP1A activity was obtained for the filtrate sample obtained from FM1 (71.4 ± 2.9 % and 66.2 ± 4.2 %, calculated as mean of the means) as compared to FM2 (29.2 ± 1.5 % and 15.9 ± 2.4 %) for commercial MC-LR as well as algal cells-

derived MC-LR. Also, the PP1A activity of the filtrate obtained for commercial MC-LR (red bar) was significantly higher than the algal cells-derived MC-LR (green bar) for both the filter modules which were tested individually. The p-value for FM1 observations was 0.09 as compared to the p-value of 0.003 for FM2 filtrate. Overall, it strengthens the fact that graphitized sand filter media is better than sand media for providing safe and drinkable water free of MC-LR and its toxic by-products.

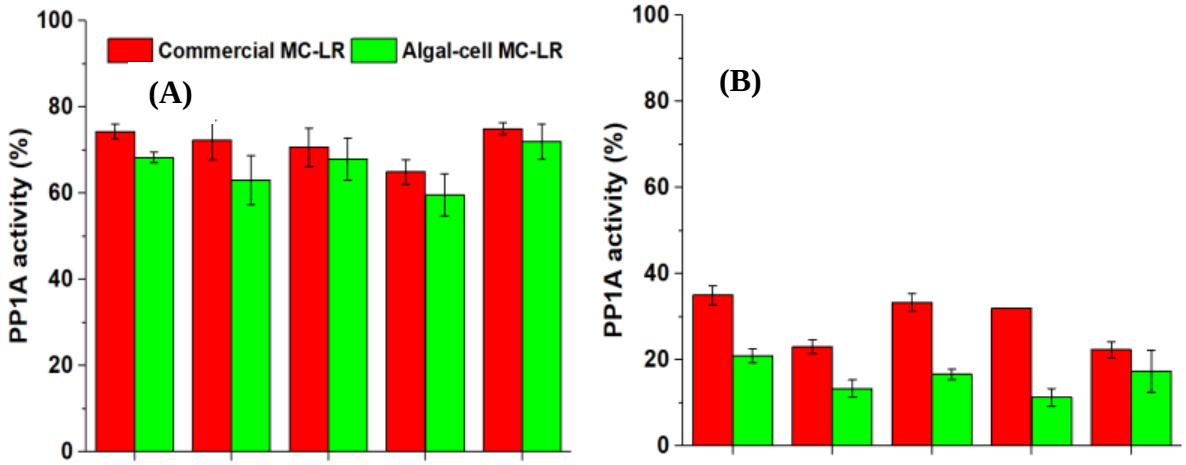

Figure 5.2. 5: PP1A % activity of the filtered sample from Filter Module 1 (½ GS1 + ½ sand) and Filter module 2 (½ sand + ½ sand); GS1: Graphitized sand

For both the filter module, algal-cell derived MC-LR showed more relative toxicity as compared to the commercial MC-LR. As a comparison, blank showed an activity of 87 ± 5 %. This shows that though filter module 1 attained a complete MC-LR removal with over 70% and over 65% of PP1A activity, tested using commercial and algal-cells derived MC-LR, respectively, a fair amount of toxicity persists in the filtered water. However, a better inference can only be made to the final toxicity through the degradation mechanism of the filtered sample to report for molecules or fragments containing adda moiety (responsible for toxicity in MC-LR degraded sample). In this study, no separate study was done pertaining to the exploration of MC-LR by-products or its degradation mechanism. However, this conclusion can be taken with two possibilities: a) 15-20% less PP1A activity shown by filtrate of FM1 as compared to the control can be due to the presence

of other water pollutant present along with MC-LR or b) a need for bioaugmentation of filter which can form a research gap (biofilter concept) to this study and can be studied in future to report if the PP1A activity of the filtrate reaches a value close to the control. Many studies on bacterial degradation of MC-LR explored for the reduced toxicity in the treated water where bacterial strain showed the presence *mlrA* gene which was mainly responsible for reducing the toxicity of the MC-LR (by up to 200 times) (Bourne et al. 1996, Dziga et al. 2012).

Application feasibility of the filter module at household level

This section discusses an overview of the technoeconomic feasibility of the filter modules at the household scale. Instead of assessing two half filters (one module), the technoeconomic study was done considering standalone sand and GS1 filter based on the household filter version as suggested by the Center for Affordable Water and Sanitation Technology (CAWST). Figure 5 shows the model of the household filter with dimension and other details. Table 3 enlists all the materials and cost parameters estimated to produce filter material for both sand and graphitized sand filter. The cost calculation suggested that at large scale material production (material for 2200 sand filters and 2900 GS1 filters), one unit of GS1 filter costs 65 CAD as compared to 46 CAD for sand filter. All the necessary details and calculations are presented in Table 3.

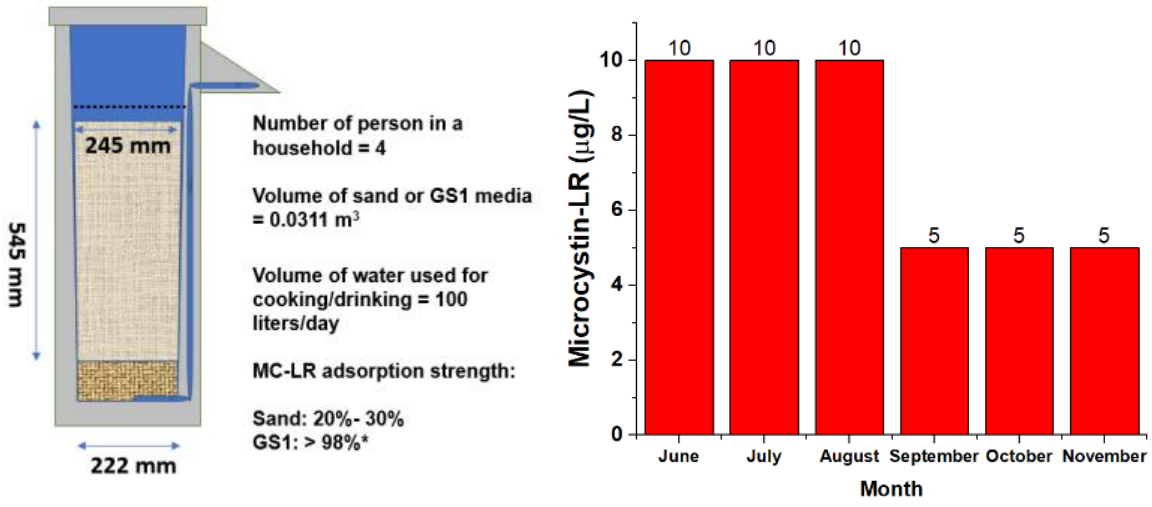

Figure 5.2.6: A) Schematic of biosand filter according to the guidelines of Center for Affordable Water and Sanitation Technology (CAWST) and B) Bar chart of the seasonal outbreak of MC-LR (with expected concentration) for 6 month with their expected concentration present in the source water

The technical performance of the filter was mainly judged based on the ability of the adsorbent material to remove MC-LR. From the results obtained in the current study and our earlier study using sand media (Kumar et al. 2020), the average removal percent of MC-LR at an initial concentration of 50 µg/L stands at 20%-30% (no bioaugmentation case) and >98% for sand and graphitized sand material, respectively. For calculation, following assumptions were made:

1) A household comprise 4 people where 100 liters of water is utilized for cooking and drinking purpose.

2) From June to August (peak cyanobloom season) and September to November, the concentration of MC-LR in source water is assumed to be 10 µg/L and 5 µg/L, respectively (as shown in Figure 5.2.6).

Based on the adsorbent efficiency and saturation capacity (obtained from previous experiments, more detail in supplementary section and Table 3), the calculation showed that sand filter needed a change (based on the MC-LR breakthrough) in the adsorbent media every 6 days as compared to 261 days for graphitized sand filter (Table 3)**.** This means that on a yearly basis, around 90 CAD is required for GS-based household filter as compared to around 2800 CAD (equivalent) for sand-based filter. It must also be noted here that the MC-LR adsorbent capacity of sand filter is 20%-30% and hence the calculated estimates are based on equivalent basis unlike GS-based filter which ensures >98% MC-LR removal each time it filters raw water.

Table 5.2.4: Techno-economic parameters and assessment of both adsorbent filters (household-level according to Center for Affordable Water and Sanitation Technology (CAWST)

Properties/items of cost	**Sand**	**GS1**
Economic performance parameters		
Density (Bulk) [gm/cc]	1.36	1.05
Density (Solid) [gm/cc]	2.68	2.16
Filter material volume (m3)	0.0311	0.0311
Material required per filter (kg)	42.3	32.7
a) Cost of raw sand (@ 0.548 CAD/kg)	23.1804	17.9196
Cost of sand per batch	512.9	512.9
b) Coating solution	NA	NIL
c) Other cost such as fittings, concrete mix, etc.	100	100
Processing time (operation)	1-2 hour	6 hours

Properties/items of cost	**Sand**	**GS1**
Labour cost (100 CAD/hour)	200-400	1200
Number of labours per batch of muffle/washing operation	2	2
Cost of muffle furnace (capital cost in CAD)	9800	9800
Power of muffle furnace	70 kW	70 kW
Electricity cost (0.1 CAD/kWh)	0	42
Number of filters per batch	22	29
Cost of 1 batch operation (including instrument cost) in CAD	10,713	11,555
Cost of 100 batches of operation in CAD	1,01,093	1,85,293
Cost of 1 filter in CAD	46	65

Technical performance parameters		
MC-LR adsorption performance	20%-30%	> 98%
Volume to be treated per day (in liters)	100	100
MC-LR adsorption capacity (µg/g)	0.11	5.99
MC-LR (June-August) cumulative adsorption (µg)	90,000	90,000
MC-LR (September-November) cumulative adsorption (µg)	45,000	45,000
Total target in 6 months (µg)	1,35,000	1,35,000
Adsorption capacity for 1 filter (µg)	4,522	1,95,772
Change filter every (days)	6.03	261.03
Annual service cost (based on providing MC-LR free water#	2,800 CAD	91 CAD

 # It is calculated on equivalent basis as GS-based filter assured >98% MC-LR removal as compared to sand-based filter which achieves just 20%-30% MC-LR adsorption at any given time

Conclusion

A micro-model drinking water treatment plant (DWTP) set-up (named: SAP-1©) was evaluated for the removal of various water quality parameters (WQPs) including micropollutant: Microcystin-LR (MC-LR) using two filter modules in the same chain individually. Filter module 1 comprised of graphitized sand filter as a half filter along with sand filter as the other half whereas two half sand filter together constitute filter module 2. FM1 performed well for most of the WQPs where a mean difference of 20%- 40% was observed in the final treated value as compared to FM2. In brief, metal pollutants in the form of copper and iron, dissolved organic carbon, ammonia-N,

turbidity, and total coliform was almost completely removed by FM1 to follow the norms of Canadian drinking water guidelines. Graphitized sand filter module showed 40%-50% more PP1A activity than sand filter module that ensures a toxic-free MC-LR filtrate and hence fit for the public consumption. The standalone graphitized sand filter can be practiced commercially to offer a low-cost solution (90 CAD/year) as compared to a conventional sand filter (>2800 CAD/year) for a household purpose for an effective removal of most WQPs during the seasonal or year-round outbreak of MC-LR in surface water if used directly as a source for drinking water.

Acknowledgement

The authors are sincerely thankful to the Natural Sciences and Engineering Research (Discovery Grant 23451). A special thanks to the plant operator Mr. Guy Desgroseilliers, Ville de Quebec for availing the quartz sand from the filtration unit of the drinking water treatment plant, Chemin Ste-Foy, Quebec City, Canada.

Conflict: None

References

APHA, AWWA, WPCF. 1998. Standard methods for the examination of water and wastewater,19th Ed., Washington, D.C.

Bond, T., Huang, J., Graham, N. J. D., & Templeton, M. R. (2014). Examining the interrelationship between DOC, bromide and chlorine dose on DBP formation in drinking water — A case study. *Science of The Total Environment, 470-471*, 469-479. doi:10.1016/j.scitotenv.2013.09.106

Bourne, D. G., G. J. Jones, R. L. Blakeley, A. Jones, A. P. Negri and P. Riddles (1996). "Enzymatic pathway for the bacterial degradation of the cyanobacterial cyclic peptide toxin microcystin LR." Appl Environ Microbiol **62**(11): 4086-4094.

Campos, A., & Vasconcelos, V. (2010). Molecular Mechanisms of Microcystin Toxicity in Animal Cells. *Int J Mol Sci, 11*(1), 268-287. doi:10.3390/ijms11010268

Davidson, J., Helwig, N., & Summerfelt, S. T. (2008). Fluidized sand biofilters used to remove ammonia, biochemical oxygen demand, total coliform bacteria, and suspended solids from

an intensive aquaculture effluent. *Aquacultural Engineering, 39*(1), 6-15. doi:10.1016/j.aquaeng.2008.04.002

Duan, X., Sanan, T., de la Cruz, A., He, X., Kong, M., & Dionysiou, D. D. (2018). Susceptibility of the Algal Toxin Microcystin-LR to UV/Chlorine Process: Comparison with Chlorination. *Environ Sci Technol, 52*(15), 8252-8262. doi:10.1021/acs.est.8b00034

Dziga, D., B. Wladyka, G. Zielińska, J. Meriluoto and M. Wasylewski (2012). "Heterologous expression and characterisation of microcystinase." Toxicon **59**(5): 578-586.

Ebeling, J. M., Sibrell, P. L., Ogden, S. R., & Summerfelt, S. T. (2003). Evaluation of chemical coagulation–flocculation aids for the removal of suspended solids and phosphorus from intensive recirculating aquaculture effluent discharge. *Aquacultural Engineering, 29*(1-2), 23-42. doi:10.1016/s0144-8609(03)00029-3

Fearing, D. A., Jarvis, P. R., Goslan, E. H., Jefferson, B., & Parsons, S. A. (2004). Natural organic matter – the relationship between character and treatability. *Water Supply, 4*(5-6), 43-48. doi:10.2166/ws.2004.0091

Gebbie P., "An operator's guide to water treatment coagulants", 31st Annual QLD Water Industry Workshop – Operations Skills, University Central Queensland, Australia (2006), pp. 14-20

Healy, M. G., Rodgers, M., & Mulqueen, J. (2007). Performance of a stratified sand filter in removal of chemical oxygen demand, total suspended solids and ammonia nitrogen from high-strength wastewaters. *J Environ Manage, 83*(4), 409-415. doi:10.1016/j.jenvman.2006.03.005

Hidayah, E. N., & Yeh, H. H. (2018). Effect of Permanganate Preoxidation to Natural Organic Matter and Disinfection by-Products Formation Potential Removal. *Journal of Physics: Conference Series, 953*. doi:10.1088/1742-6596/953/1/012218

Ho, L., Meyn, T., Keegan, A., Hoefel, D., Brookes, J., Saint, C. P., & Newcombe, G. (2006). Bacterial degradation of microcystin toxins within a biologically active sand filter. *Water Research, 40*(4), 768-774.

Ho, L., Hoefel, D., Saint, C. P., & Newcombe, G. (2007). Isolation and identification of a novel microcystin-degrading bacterium from a biological sand filter. *Water Research, 41*(20), 4685-4695.

Kamel S. ,Z, Zouheir, Kassim J., (2018). The Effectiveness of Psophocarpus Tetragonolobus's Seed as Turbidity Removal. *International Journal of Engineering & Technology, 7*(3.11). doi:10.14419/ijet.v7i3.11.15949

Keijola, A. M., Himberg, K., Esala, A. L., Sivonen, K., & Hiis-Virta, L. (1988). Removal of cyanobacterial toxins in water treatment processes: Laboratory and pilot-scale experiments. *Toxicity Assessment, 3*(5), 643-656.

Kumar, P., Hegde, K., Brar, S. K., Cledon, M., Kermanshahi-pour, A., Roy-Lachapelle, A., Galvez-Cloutier, R. (2019). Co-culturing of native bacteria from drinking water treatment plant with known degraders to accelerate microcystin-LR removal using biofilter. *Chemical Engineering Journal*. doi:10.1016/j.cej.2019.123090

Kumar, P., Pérez, J. A. E., Cledon, M., Brar, S. K., Duy, S. V., Sauvé, S., & Knystautas, É. (2020a). Removal of microcystin-LR and other water pollutants using sand coated with bio-optimized carbon submicron particles: Graphene oxide and reduced graphene oxide. *Chemical Engineering Journal, 397*. doi:10.1016/j.cej.2020.125398

Kumar, P., Rehab, H., Hegde, K., Brar, S. K., Cledon, M., Kermanshahi-pour, A., Surampalli, R. Y. (2020b). Physical and biological removal of Microcystin-LR and other water contaminants in a biofilter using Manganese Dioxide coated sand and Graphene sand composites. *Science of The Total Environment, 703*. doi:10.1016/j.scitotenv.2019.135052

Lawton, L. A., & Robertson, P. K. J. (1999). Physico-chemical treatment methods for the removal of microcystins (cyanobacterial hepatotoxins) from potable waters. *Chemical Society Reviews, 28*(4), 217-224

Ma, M., Liu, R., Liu, H., & Qu, J. (2012). Chlorination of Microcystis aeruginosa suspension: Cell lysis, toxin release and degradation. *J Hazard Mater, 217-218*, 279-285. doi:10.1016/j.jhazmat.2012.03.030

Moore, C., J. Juan, Y. Lin, C. Gaskill and B. Puschner (2016). "Comparison of Protein Phosphatase Inhibition Assay with LC-MS/MS for Diagnosis of Microcystin Toxicosis in Veterinary Cases." Marine Drugs **14**(3).

Rippka, R., Stanier, R. Y., Deruelles, J., Herdman, M., & Waterbury, J. B. (1979). Generic Assignments, Strain Histories and Properties of Pure Cultures of Cyanobacteria. *Microbiology, 111*(1), 1-61. doi:10.1099/00221287-111-1-1

Roy-Lachapelle, A., Duy, S. V., Munoz, G., Dinh, Q. T., Bahl, E., Simon, D. F., Sauvé, S. (2019). Analysis of multiclass cyanotoxins (microcystins, anabaenopeptins, cylindrospermopsin and anatoxins) in lake waters using on-line SPE liquid chromatography high-resolution Orbitrap mass spectrometry. *Analytical Methods, 11*(41), 5289-5300.

Somdee, T., Thunders, M., Ruck, J., Lys, I., Allison, M., & Page, R. (2013). Degradation of [Dha7]MC-LR by a Microcystin Degrading Bacterium Isolated from Lake Rotoiti, New Zealand. *ISRN Microbiology, 2013*, 1-8.doi:10.1155/2013/596429

Sovadinova, I., Babica, P., Adamovský, O., Alpatová, A., Tarabara, V., Upham, B. L., & Bláha, L. (2017). Chlorination and ozonation reduce microcystin content and tumour promoting activity of complex cyanobacterial extract. *Advances in Oceanography and Limnology, 8*(1). doi:10.4081/aiol.2017.6342

US EPA (2007), "Cost evaluation of point-of-use and point-of-entry treatment units for small systems: cost estimating tool and user guide", https://www.epa.gov/sites/production/files/2015-04/documents/epa815b07001.pdf (Date accessed: 12 July, 2020).

Welch, W. A. (1963). Potassium Permanganate in Water Treatment. *Journal - American Water Works Association, 55*(6), 735-741. doi:10.1002/j.1551-8833.1963.tb01082.x

Welten, R. D., Meneely, J. P., & Elliott, C. T. (2019). A Comparative Review of the Effect of Microcystin-LR on the Proteome. *Exposure and Health, 12*(2), 111-129. doi:10.1007/s12403-019-00303-1

Wezernak, C. T., & Gannon, J. J. (1967). Oxygen-nitrogen relationships in autotrophic nitrification. *Appl Microbiol, 15*(5), 1211-1214. Retrieved from https://www.ncbi.nlm.nih.gov/pubmed/6077417

World Health Organisation. Public Health and the Environment. WHO; Geneva: 2009. Guidelines for drinking water quality policies and procedures used in updating the WHO Guidelines for Drinking Water Quality

Zhao, H., Wang, L., Zhang, H., Wu, X., Zhao, B., & Han, F. (2018). Effect of potassium permanganate dosing position on the performance of coagulation/ultrafiltration combined process. *Chinese Journal of Chemical Engineering, 26*(1), 89-95. doi:10.1016/j.cjche.2017.03.037

CONCLUSIONS, RECOMMANDATIONS ET REMARQUES

CONCLUSIONS

Les conclusions suivantes peuvent être terees a paites de le projet de recherche

8.1 Deux nouveaux dégradeurs in situ du MC-LR ont été isolés de l'échantillon du biofilm de l'unité de filtration d'une usine de traitement des eaux potables. Il s'agissait principalement du *Chryseobacterium* sp. et *Pseudomonas fragi* (collectivement nommé « X »). En comparant avec les autres espèces bactériennes, isolées au sein de l'unité de sédimentation et de l'eau brute, ces nouvelles espèces ont été bien acclimatées sous un milieu MC-LR et ont pu dégrader plus que 97 % dans 10 jours. Il a révélé de même que les bactéries attachées (obtenues à partir de l'unité de filtration) étaient plus efficaies dans la dégradation de la MC-LR que les espèces bactériennes présentes en suspension. Du plus, ces espèces bactériennes se sont révélées aptes à dégrader la MC-LR sans formation de sous-produits toxiques. Cela a été confirmé par des résultats obtenus à partir de la spectrométrie de masse et un bioindicateurs : *Rhizobium meliloti.*

8.2 Les bactéries indigènes ont été inoculées avec les dégradeurs MC-LR connus *: Arhrobacter ramosus* (A) et *Bacillus sp*. (B) dans un filtre à sable à l'échelle du banc. Une telle procédure de coculture a révélé une toxicité faible (dosage PP1A) dans l'eau de lac enrichie en MC LR traitée. L'expérience a également exploré la faisabilité d'un système hybride de traitement par filtre ozonation-biosable pour contrôler la dose d'ozone sous la limite tout en traitant MC-LR en présence de prolifération d'algues et de matière organique naturelle.

8.3 La performance de la co-culture a été davantage explorée en utilisant un filtre biosable statique ainsi qu'un biofiltre à lit mobile. Les réacteurs à biofilm à lit mobile ont montré un enlèvement efficace du MC-LR (> 93%) dans l'eau et les boues enrichies en MC-LR. Cependant, la dégradation a pris du temps (5-6 jours) pour atteindre une telle efficacité d'élimination et principalement attribuée à la mauvaise élimination de la MC-LR dans un bioréacteur à écoulement en suspension. D'autre part, le biofiltre a biomasse fixee sous forme de filtre de biosable a montré > 90% de degradation de la MC-LR pour un temps de contact sur lit vide (EBCT) allant de 1,15 à 2 heures en utilisant la communauté bactérienne native (X) co-cultivée avec Sphingomonas sp. (S + X) et Arhtorbacter ramosus (A + X), montrant ainsi un meilleur potentiel que le bioréacteur en suspension (comme mentionné ci-dessus). Cependant, la lixiviation de MC-LR dans l'eau filtrée

était fréquente et inévitable après 8 semaines de fonctionnement du filtre, ce qui pourrait être attribuée à une faible bioactivité à l'intérieur du filtre ou à une mauvaise propriété d'adsorption du sable.

8.4 Afin d'améliorer la bioactivité dans le filtre biosable, les agro-résidus : fibre de boues de désencrage (DSF), fibre de pates a papiers, fibre de chanvre, ont été étudiés comme matériau de couverture supérieure (2 cm au-dessus du sable). Le DSF comme étant un milieu adsorbant de couverture a formé un biofilm à maturité rapide en seulement 8 à 10 jours d'inoculation continue (A+X : communauté bactérienne criblée, pour plus de détails, reportez-vous au chapitre 3, partie 3), contre 19 à 21 jours sans lui (chapitre 3 partie 2). Une élimination de MC-LR d'environ 90 % a également été obtenue. Cependant, le défi de percée persistait, ce qui a nécessité la modification des grains de sable pour renforcer sa capacité d'adsorption.

8.5 Parmi une variété de grains de sable modifiés recouverts d'oxyde de fer, d'oxyde de graphène, d'oxyde de graphène réduit, d'oxyde de graphène réduit en oxyde de fer, de dioxyde de manganèse, il s'agissait de sable revêtu d'oxyde de graphène réduit qui ont pu atteindre 90 % d'elimation du MC-LR. Une limination de la MC-LR et autres paramètres de qualité de l'eau en moins de 60 minutes de période de filtration. En outre, une meilleure période de percée de plus de 10 semaines a été observée. Alors que le filtre à sable enduit de rGO a fonctionné principalement sous la phase de biodégradation (BAP) (> 40% d'élimination du MC-LR par rapport à la phase d'adsorption physique, PAP), le filtre à sable enduit de GO a fonctionné principalement pendant le PAP (> 80% d'élimination de la MC-LR).

Le sable de sucre graphité produit en utilisant deux sources, le saccharose (GS1) et l'effluent de la brasserie (GS2) a également bien performé pour l'élimination de la MC-LR et d'autres paramètres de qualité de l'eau avec une moyenne de plus de 90% d'élimination de la MC-LR. Cependant, c'est GS1 qui a montré une meilleure capacité adsorption qui a non seulement éliminé plus de 90% de MC-LR (dans certains cycles, même 100%), mais n'a également montré aucune lixiviation de MC-LR dans l'eau filtrée pendant 20 semaines. De plus, tous les adsorbants testés ont montré 10 à 15% de plus d` élimination desWQP et MC-LR lorsqu'ils ont été inoculés avec des dégradeurs MC-LR et des espèces bactériennes indigènes (X), soulignant l'importance de la bioaugmentation de la co-culture.

8.6 L'étude de la dynamique des fluides (EDF) pour le filtre GS1 à l'échelle du banc a montré un régime d'écoulement non uniforme et non radial en raison de l'effet de canalisation provoqué par une colonne de faible diamètre. À l'aide du logiciel ANSYS-CFX, une dimension « d'échelle minimale subjective » a été produite qui pourrait être utilisée pour créer un module de filtre à échelle exempte de problèmes mentionnés ci-dessus qui, s'il n'était pas signalé, pourrait créer un emprisonnement d'air et une perte de charge négative pendant l`adsorption du filtre . Ce phénomène de court-circuit pendant le fonctionnement du filtre pourrait conduire à un faible taux de filtration, affectant l'élimination des polluants de l'eau. Une dimension de 9 cm x 9 cm x 30 cm se sont avérées être une taille appropriée pour une étude à plus grande échelle. Le CFD a aidé à comprendre la limitation du filtre à l'échelle du banc par rapport au régime d'écoulement, produisant une faible condition de débit de bouchage à l'intérieur du filtre (déduite de la valeur de l'indice dispersion de Morrill). Les propriétés dérivées comprenant la constante de perméabilité et le coefficient de perte de l'analyse de calcul à l'échelle du banc, ont aidé à trouver la dimension de mise à l'échelle à laquelle le régime d'écoulement montrait des contours de vitesse plus radiaux et uniformes. La condition d'écoulement en prise s'est avérée inférieure au filtre à l'échelle du banc, ce qui suggère l'importance du CFD pour la mise à l'échelle du module de filtre.

Une installation de micro-modèle de station de traitement d'eau potable (DWTP) (SAP-1 ©) comprenant un module de filtrage à grande échelle (avec un support GS1) a été évaluée pour la suppression de divers paramètres de qualité de l'eau (WQP), y compris le micropolluant : MC-LR. Le filtre à plus grande échelle constituant le sable graphité comme adsorbant du filtre a bien fonctionné pendant la majeure partie de l'élimination du WQP. En bref, les polluants métalliques sous forme de cuivre et de fer, de carbone organique dissous, d'ammoniac-N, de turbidité et de coliformes totaux ont montré une élimination complète respectant les normes des lignes directrices canadiennes sur l'eau potable. L'unité de filtration a joué un rôle important dans l'élimination de la MC-LR et d'autres paramètre de qualité de l'eau (PQE) tels que l'ammoniac-N, la turbidité, les coliformes totaux et le carbone organique dissous. Le module de traitement peut être pensé pour offrir une solution durable pour une élimination efficace de divers PQE pour la dissémination saisonnière ou toute l'année de MC-LR dans les eaux de surface et en tant que module de traitement autonome à des fins domestiques.

REMARQUES

Hypothesis No.	HYPOTHESIS	REMARKS
1	A more controlled ozone treatment, utilizing less ozone dose than general (as practiced in DWTPs) could possibly lower the formation of toxic by-products.	Low ozone dose of 0.8 mg-O3.min/L removed more than 50% MC-LR exclusive of different NOM concentration or bloom intensity condition. Also, the formation of toxic by-products was reduced as can be observed from the PP1A activity results.
2	Hence, proper acclimatization of isolated bacteria might help in enhancing the MC-LR degradation. Also, the possibility of native bacteria, such as those present within DWTP units, can be explored considering their fast adaptability that might enhance the MC-LR degradation rate. Hence, bacteria from different units of the treatment plant can be isolated and evaluated for their performance in terms of MC-LR removal and if possible, can be acclimatized under MC-LR environment to offer 'even better' removal.	Acclimatization of the native bacteria isolated from different units of the drinking water treatment plant showed increase in the kinetic activity by at least 40%. As can be observed from the results presented in Chapter 2, Part 1, similar MC-LR removal (efficiency) was achieved in 10 days as compared to 15 days for non-acclimatized native bacteria.
3 a)	Thus, these known MC-LR-degraders in form of *Arthrobacter ramosus*, *Bacillus* sp., and *Sphingomonas* sp., could be explored as a possibility to co-culture	As observed from the results presented in Chapter 2, Part 2: these native bacteria not only enhanced the MC-LR removal by

Hypothesis No.	HYPOTHESIS	REMARKS
	them individually with the native bacteria isolated from the filtration unit of DWTP (assisting fast biofilm formation).	20%-30%, but also showed 30% more PP1A activity when co-cultured with the known MC-LR-degraders.
3 b)	This mode (Attached growth in form of moving bed biofilm reactor) of working is expected to provide a good oxidative environment in and around the developed biofilm where MC-LR is diffused and oxidized.	Moving bed biofilm reactor showed very poor removal rate for the MC-LR to as low as 1.6 µg/L/hour
4	The bioactivity of the sand filter could be enhanced and prolonged by laying a stable 'top-cover' composite material that could facilitate an ambient support for the biofilm formation.	Bioactivity of the sand filter improved as it achieved 10%-20% more DOC and coliform removal. Also, the biofilm was formed by the bioaugmented bacteria in less than 11 days as compared to 19 days for the normal sand filter (using same inoculum)
5	The MC-LR adsorption can be enhanced for the sand surface by making it a) more electropositive (as MC-LR possess negative charge at pH range 3.5-10.4), b) creating more hydrophilic functionalized surfaces and by c) creating mesoporous surface by thermal coating of various compounds over the sand grains. These submicron carbon particles (in the form	Increase in electropositive property did not shown to improve the MC-LR removal as can be observed from the results presented in Chapter 4, Part 1 and Part 2. Mesoporous surface in form of graphitized sand (GS1) and graphene oxide coated sand enhanced the MC-LR removal by

Hypothesis No.	HYPOTHESIS	REMARKS
	of GO and rGO) owing to their high adsorption capacity might adsorb high MC-LR, offering more breakthrough period than just sand (uncoated).	> 40% as can be observed from the results presented in Chapter 4, Part 1 and 2.
6	Graphene sugar sand can offer a large-area π–π interaction that could provide better longevity and saturation adsorption capacity than graphene submicron particles coating over the sand grains. Also, the sugar source could be derived from the waste brewery effluent which will provide a sustainable solution to the synthesis of graphene-sand as compared to a more expensive preparation of graphene oxide-sand using graphite flakes.	Evidence of pi-pi interaction was observed for both GO-coated and GS1 sand as mentioned in the result and discussion section in Chapter 4: Part 2. A sustainable solution was achieved for the removal of MC-LR and other water quality parameters.
7	The bench-scale filter could be modelled and analyzed according to the intrinsic property of the porous media: loss coefficient and permeability constant. This can help in deciphering the 'minimum subjective scale-up dimension' where flow regime is expected to be more radial and channelized that could minimize the possibility of a short circuit phenomenon during the filter operation.	Computational Fluid Dynamics was successfully used for studying the scale-up dimensions of filter by eradicating the problem of pressure gradient (achieving a uniform gradient as discussed in Chapter 5: Part 1).

LIMITATION OF THE WORK DONE:

Though the project objectives were successfully performed and disseminated in form of published articles, a list of limitations persists.

A. Global Objective 1: As listed in the objective section, global objective 1 states "Significance of bioaugmentation in a filter using native bacteria isolated from DWTP". A major limitation of this objective lies in the choice of native bacteria that were tested for the toxicity and degradation of MC-LR. Though a preliminary testing related to the MC-LR degradation potential for the screened bacteria were performed (before further step of bacterial identification), still the approached could have been better. For instance, the bacterial screening step could have been strengthened to test the degradation capacity of the isolated bacteria for other cyanotoxins as well. It is known that 90% of the times, it is MC-LR cyanotoxin that persists in a cyanobloom affected water bodies, but, a more versatile bacterial species needed to be identified that can handle at least three major cyanotoxins: Microcystin, anatoxin and saxitoxin. This limitation needs to be break before applying the bioaugmentation step in the field work or filtration unit of the drinking water treatment plant.

B. Global Objective 2: As listed in the objective section, global objective 2 states "Co-culturing of *in-situ* bacteria and MC-LR-degraders in moving bed and fixed bed biofilter". Though most of the hypotheses have been addressed through different set of experiments for this objective, a major limitation lies in the frequency of bioaugmentation that will be needed to counter the challenge of MC-LR and other water pollutants throughout the year or seasonal outbreak. Since the breakthrough period is < 1 week, there can be a major plant operation issue or even failure, considering a long-term filter operation. Also, before bioaugmentation, the bacterial cell concentration can be further optimized concerning the presence of other cyanotoxins in the source water.

C. Global Objective 3: As listed in the objective section, global objective 3 states "Modification of sand media to enhance its adsorption capacity and breakthrough time". Through this objective two major adsorbents were deciphered in form of graphitized sand and graphene oxide-coated sand that were able to remove almost complete MC-LR. However, a "possible" limitation that surround this objective is the testing of these synthesized adsorbents for other cyanotoxins. The adsorption capacity of graphitized sand (GS1 especially) seems very promising and is sustainable to produce as well. However, for commercializing it at the house-hold level or even to the drinking water

plant, further testing is required. On the other hand, graphene oxide coated sand poses a major limitation due to its cost of production. Though, in this project the cost was significantly reduced for the graphene oxide powder synthesis ($50 per 5 gram) as compared to commercial price (up to $5000). Despite of high production cost of GO, techno-economic analysis showed 3/4th cost to what conventional or sand-based filter would cost (household filter). In future, this limitation can be further addressed to make the GO-based filter more economical.

D. Global objective 4: As listed in the objective section, global objective 4 states "Scale-up study using best performing filter media". The major limitation of this objective lies in the use of ANSYS-CFX software where the bench-scale filter was considered rectangular instead of circular (cross-section) as performed experimentally in the laboratory. Though the above action is not expected to produce much of a difference, still the crosscheck needs to be done. More nodal points need to be added for the corner points or surface to get more precise and accurate results for the scale-up dimension. The second part of this objective which refers to the mass-balance study has few limitations as well which are pointed as follows:

1.The treatment chain comprised pre-oxidation tank where chemical treatment in form of potassium permanganate was preferred over ozone. Hence, the mass balance study carried out does not provide the information about the treatment plant where pre-ozonation is under operation. Similarly, this limitation applies to other chosen treatment units (micromodel).

2. Though the MC-LR study had variability in terms of source: a) commercial MC-LR and b) Algal cells-derived MC-LR, still this objective lacked the performance evaluation of treatment chain for other concentration of MC-LR (other than 50 µg/L).

RECOMMENDATIONS

Sur la base des résultats obtenus dans cette étude, les recommandations suivantes sont proposées

1. Dans cette étude, trois dégradeurs connus ont été étudiés pour l'élimination de la MC-LR et, par conséquent, davantage d'espèces bactériennes potentielles devraient être examinées pour accélérer la dégradation de MC-LR et d'autres cyanotoxines.

2. Davantage de bactéries indigènes devraient être isolées de différentes usines de traitement d'eau potable (STEP) et être explorées pour leur potentiel de biodégradation de la MC-LR. De cette

manière, comme lors de cette étude, il serait préférable de trouver la solution au sein des unités de traitement des STEP comme l'unité de filtration.

3. La quantification du biofilm doit être effectuée au niveau du gène pour comprendre la relation entre la «copie du gène» (comme les gènes mlrA si la dégradation de MC-LR doit être étudiée) et leur viabilité en cas de co-culture avec l'espèce indigène ou d'autres espèces bactériennes. . Une telle évaluation aidera à comprendre l'abondance relative des dégradeurs de MC-LR dans le biofilm formé sur le substrat filtrant.

4. Le meilleur biofiltre pour l'élimination du MC-LR et d'autres polluants de l'eau obtenu dans cette étude devrait également être testé pour d'autres cyanotoxines telles que l'anatoxine, la cylindrospermopsine et la saxitoxine.

5. Bien qu'un colorant modèle «Rhodamine-B» ait été utilisé pour obtenir les paramètres d'adsorption (constante d'adsorption et capacité de saturation) pour différents milieux filtrants, une étude plus complète sur la cinétique d'adsorption utilisant «MC-LR» devrait être effectuée afin de mieux evaluec la capacite d`adsorption des adsorbants. Cela aidera les opérateurs de STEP à juger du bon type d'adsorbant à utiliser, en particulier lorsque de nombreux adsorbants possèdent un potentiel d'élimination de MC-LR égal, testé seulement quelques fois en laboratoire.

APPENDIX

APPENDIX A

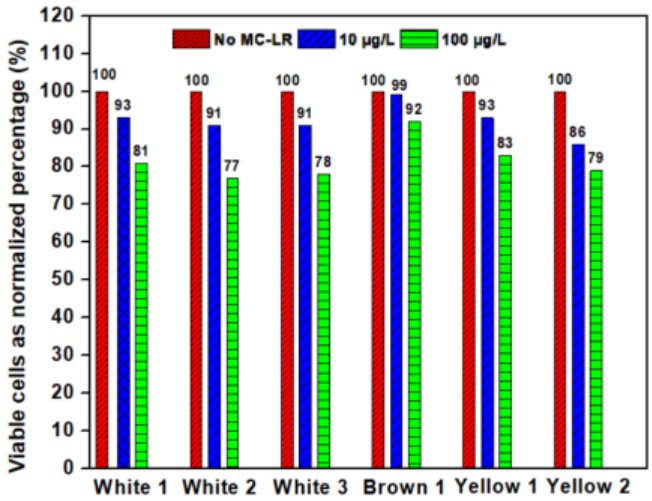

Figure A1: Viable cells comparison for isolated bacteria under no microcystin-LR (MC-LR) and with 10 and 100 µg/L MC-LR

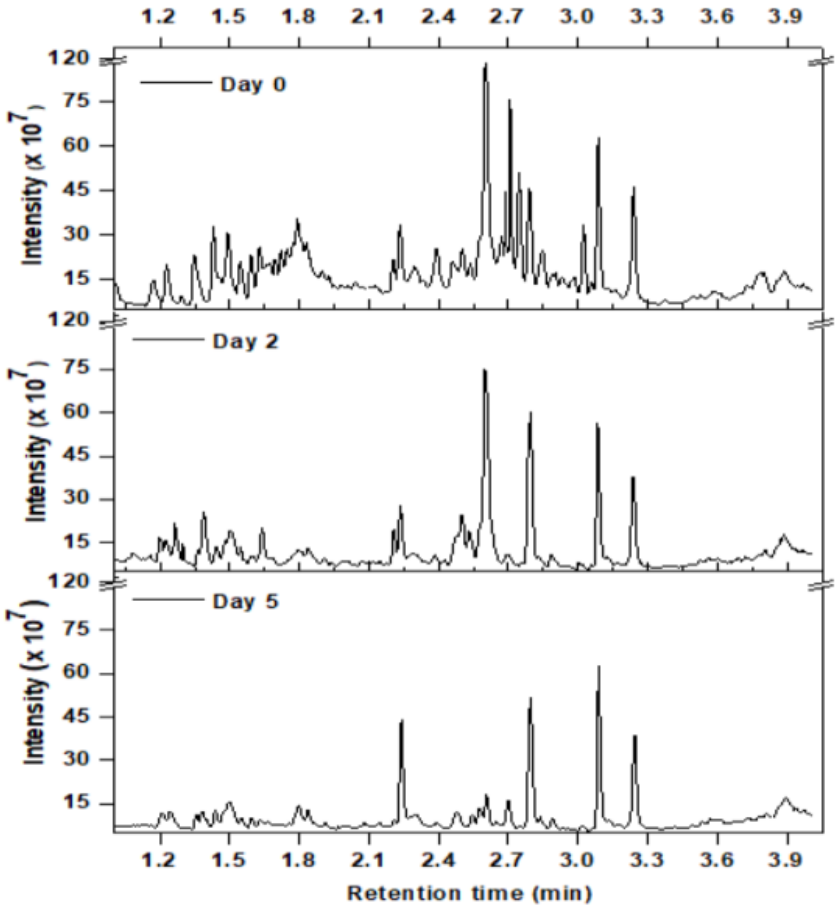

Figure A2: Chromatographs showing a decrease in peak height at retention time 2.6 minutes (Microcystin-LR compound) for Top-sand filtration unit (TSFU) sample at day 0, day 2 and 5th day

Table A1: Toxicity-shock test data

Isolated Bacteria	**Sum of all viable cells comprising 4 Exponential Points CFU_{sum} (0 MC-LR) (CFU/mL x10^6) [Normalized value]**	**Sum of all viable cells comprising 4 Exponential Points CFU_{sum} (10 µg/L) (CFU/mL x10^6)**	**Sum of all viable cells comprising 4 Exponential Points CFU_{sum} (100 µg/L) (CFU/mL x10^6)**	**Percent survival of exponential bacteria at 10 µg/L MC-LR [Normalized value]**	**Percent survival of exponential bacteria at 100 µg/L MC-LR [Normalized value]**
INRS W1	14.8 [100]	13.9	12.1	93 %	81 %
INRS W2	11.2 [100]	10.3	8.7	91 %	77 %
INRS W3	6.7 [100]	6.1	5.3	91 %	78 %
INRSB1	7.5 [100]	6.7	5.9	89 %	79 %
INRS Y1	4.3 [100]	3.9	3.6	93 %	83 %
INRS Y2	4.1 [100]	3.5	3.3	86 %	79 %

APPENDIX B

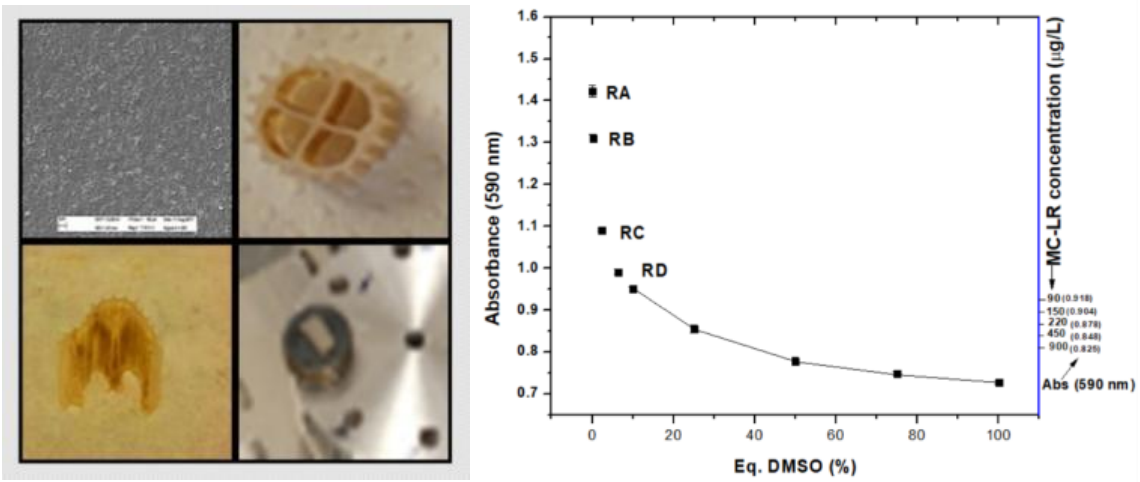

Figure B1: Biocarrier with biofilm developed (left) ; Figure A2: Equivalent DMSO toxicity for the biodegraded broth sample along with standard curve relation between DMSO (v/v) and absorbance (590 nm) value (right).

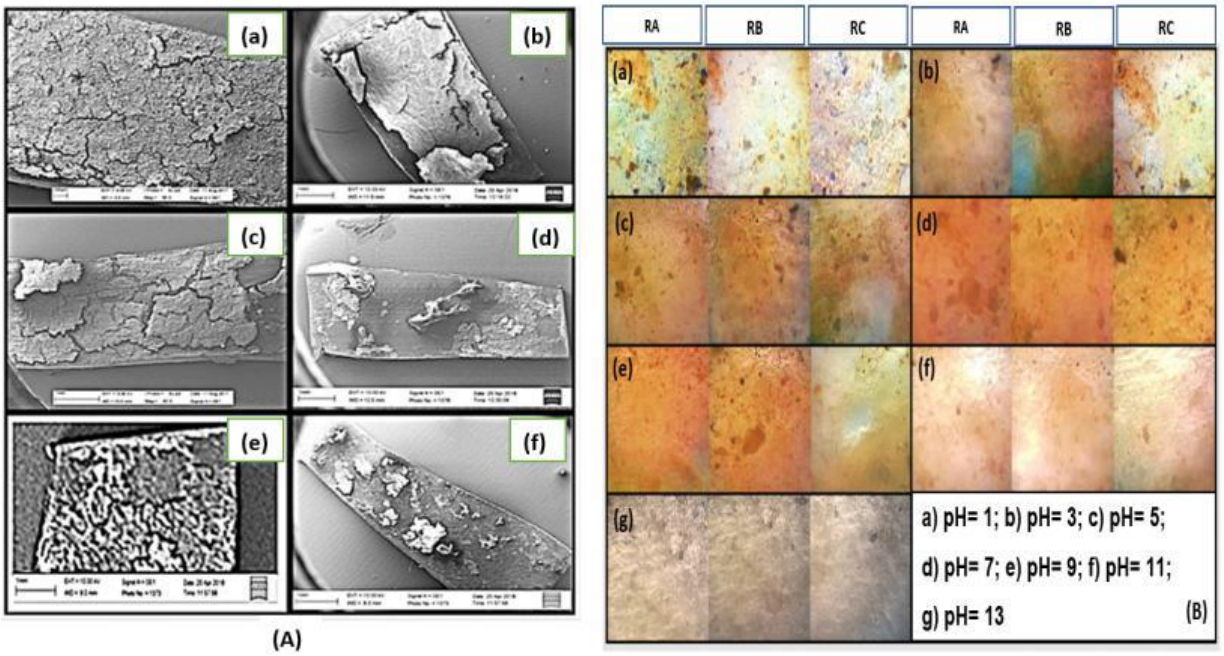

Figure B3: A) Scanning Electron Microscopy (SEM) images of biofilm developed-biocarrier surface (of all three bioreactors studied) for the case a), c) and e) before MC-LR degradation and b), d), f) after MC-LR degradation study. B) Stability test study using microscopy visuals at different pH values for all three bioreactors

Table B1: Operational parameters for laboratory scale FBBR and Up-scale FBBR based on same kLa value

Parameters	Lab-Scale	Scale-up
Flow per day[43]	2 L	200 m^3
Height	30 cm	5 m
Diameter	10 cm	7.2 m
Reynold`s number	6015	>2 x 10^5
Power number	8	8
V_L	2 L	200 m^3
V_s	13.75 m/h	13.75 m/h
kLa	0.00967 s^{-1}	0.00967 s^{-1}
$q_{O2.Cx}$	0.18 % O_2 s^{-1}	0.18 % O_2 s^{-1}

Calculation of the Reynolds number:

As specified by Doran (2013), for a suspended solids system, Rushton turbine is effective for the proper dispersion of the bubble regime, including a three-phase system (like present study). Considering the effective solid suspension and proper gas dispersion, the turbine should have an effective diameter of 4 cm for a working diameter of 0.12 m or 12 cm. Hence, according to the equation as follows:

Re (Reynolds` number) = (Ni x Di x ρ / μ)

Where Ni is the impeller speed in rpm = 100 here

Di is diameter of the impeller: 0.04 m or 4 cm here

ρ = density of the fluid in the bioreactor = 3 kg/m3.

μ= fluid viscosity = 0.00200 Pa.s

Putting these values, we get, Re = 6,015 (> 4,000)

Similarly, for scale-up bioreactor, Ni = 0.2 m (7.2 m – 1/4th clearance)/10 impellers, Re = 60,000

From the same book (reference below), it is referred that for Re > 4000, Power number is = 8.

Hence, for scale-up and laboratory bioreactor, power number is independent of the Reynolds number. Power number is a dimensionless quantity which relates the resistance force to the inertial force (which in the present case remains independent mainly due to turbulence regime condition in the bioreactor).

Pauline M. Doran (2013), Bioprocess engineering principles, 2nd Edition, Elsevier limited, doi: 10.1016/C2009-0-22348-8

kLa calculation:

[43] For lab-scale, since major portion of MC-LR degradation (> 55%) happened within 36 hours, thus operational volume (2 L) was mentioned as a flow rate for 24 hours (1 day)

Determination of kLa:

$dC/dt = kLa \cdot (C* - C) - q_{O2} \cdot C_X$

» $\int_0^{Ct} dC = \int_0^{t1} kLa \cdot (C* - C) - q_{O2} \cdot C_X)\, dt$ Integrating both sides, we get,

$C_t - 2.28 + 0.0018\, t = kLa.\ t\ (6.99 - C_t)$; [OUR = 0.18 % O_2 s^{-1} from graph shown in Figure 3.1.6]

For C_t= 6.12 (linear range value taken) and t = 580 second (580 + 1430 in actual), we get,

kLa = 0.00967 s^{-1}

Calculation of P_g/V ratio for the scale-up FBBR:

Superficial velocity in the scale FBBR is kept same as discussed in the main text

Superficial velocity in the laboratory scale FBBR = Q_1 / A_{s1} = (1.8 LPM)/(7.85 x 10^{-3} m^2) = 13.75 m/h; A_s is the cross sectional area of the bioreactor.

From an equation shown by Alam et al. (2005), for the up-scale FBBR, the flow rate required will change as per the equation mentioned below:

$Q_2 = Q_1 (D_2/D_1)^2$ where Q_1 = 1.8 LPM.

Where, D_1 = 0.1 m

This gives, $Q_2 = 1.8\ (D_2/0.1)^2$ LPM

Now, knowing, $A_{s2} = Q_2/Vs_2$

» $\Pi\ (D_2^2)/4 = 1.8\ (D_2/0.1)^2$ LPM

On solving, we get, D_2 = 7.2 m

From equation 2 (b), discussed in the main text, and keeping kLa value same for laboratory scale and scale-up FBBRs,

We get, Pg/V_L = 74 W/m^3

For V_L= 200 m^3 (assumed that the up-scale bioreactor can handle this volume of water per day based on operational characteristics and economics discussed in Table S5)

Pg = 14.8 kW.

Thus, for a volume of 200 m^3 (HRT = 1 day) and a diameter of 7.2 m, a height of approx. 5 m is calculated.

APPENDIX C

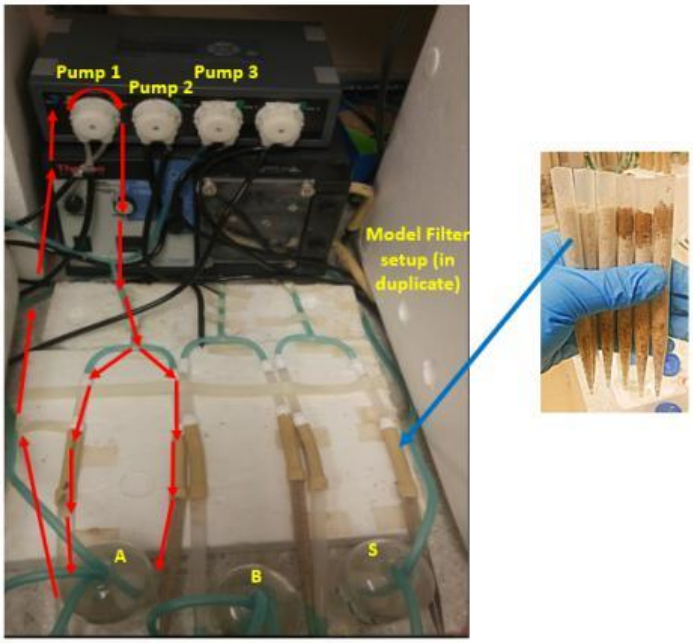

Figure C1: Model reactor set-up for the screening of the bacterial strains (Microcystin-LR degraders), A: *Arthrobacter ramosus*; B= *Bacillus* sp.; S= *Sphingomonas* sp.

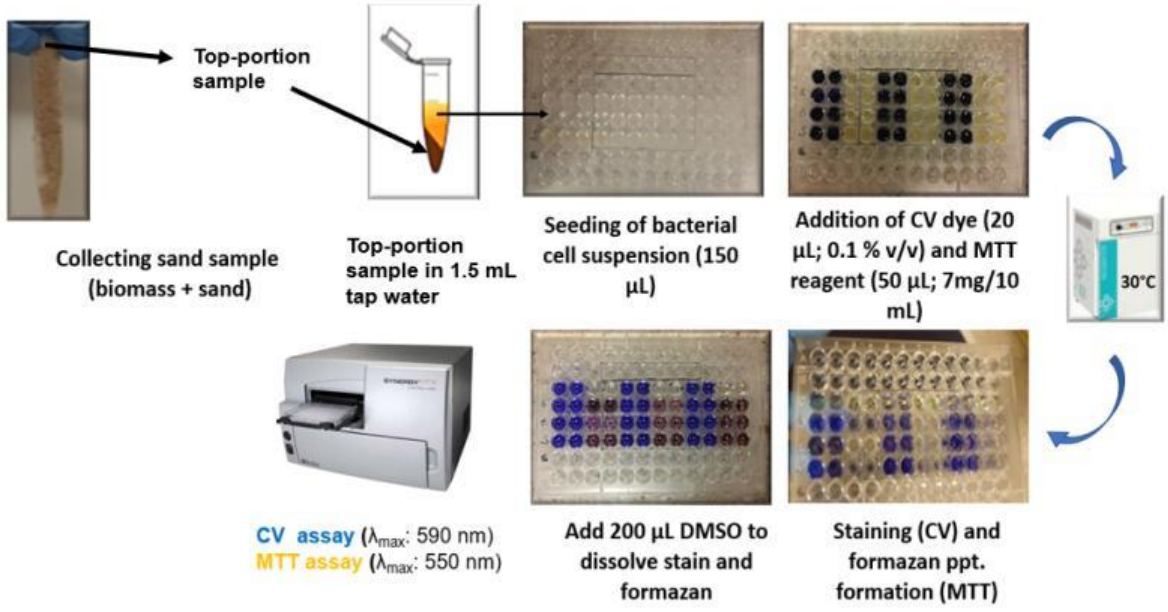

Figure C2: Sampling of the sand media for the Crystal violet and MTT assay (screen test of the bacterial strains suitable for the biofilm test)

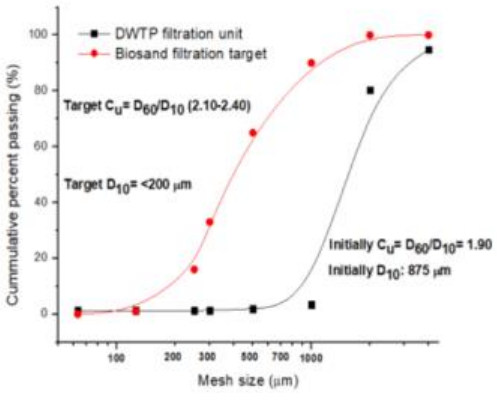

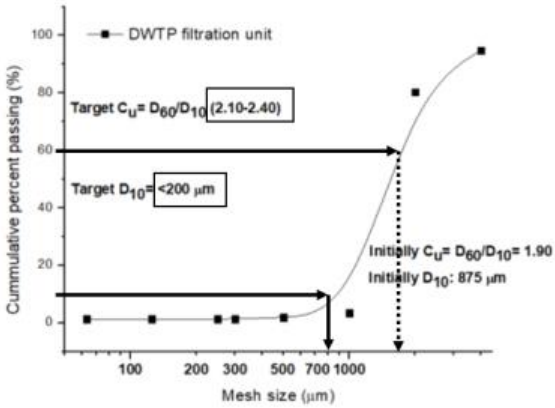

D_{10}: 10% of the sand particle is finer than this size
D_{30}: 30% of the sand particle is finer than this size
D_{60}: 60% of the sand particle is finer than this size

$C_u = D_{60}/D_{10}$

$C_c = D_{30}^2 / (D_{60} \times D_{10})$

Figure C3: Grain-size distribution curve for the modified sand media used for biofilter operation.

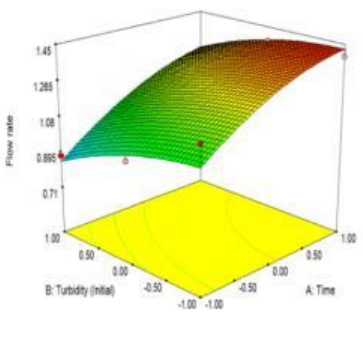

Flow rate vs Time and Initial turbidity

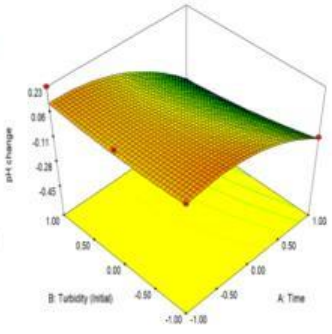

pH change vs Time and Initial turbidity

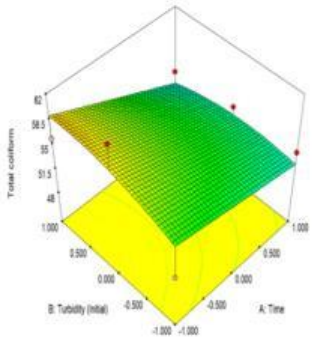

Total coliform removal vs Time and Initial turbidity

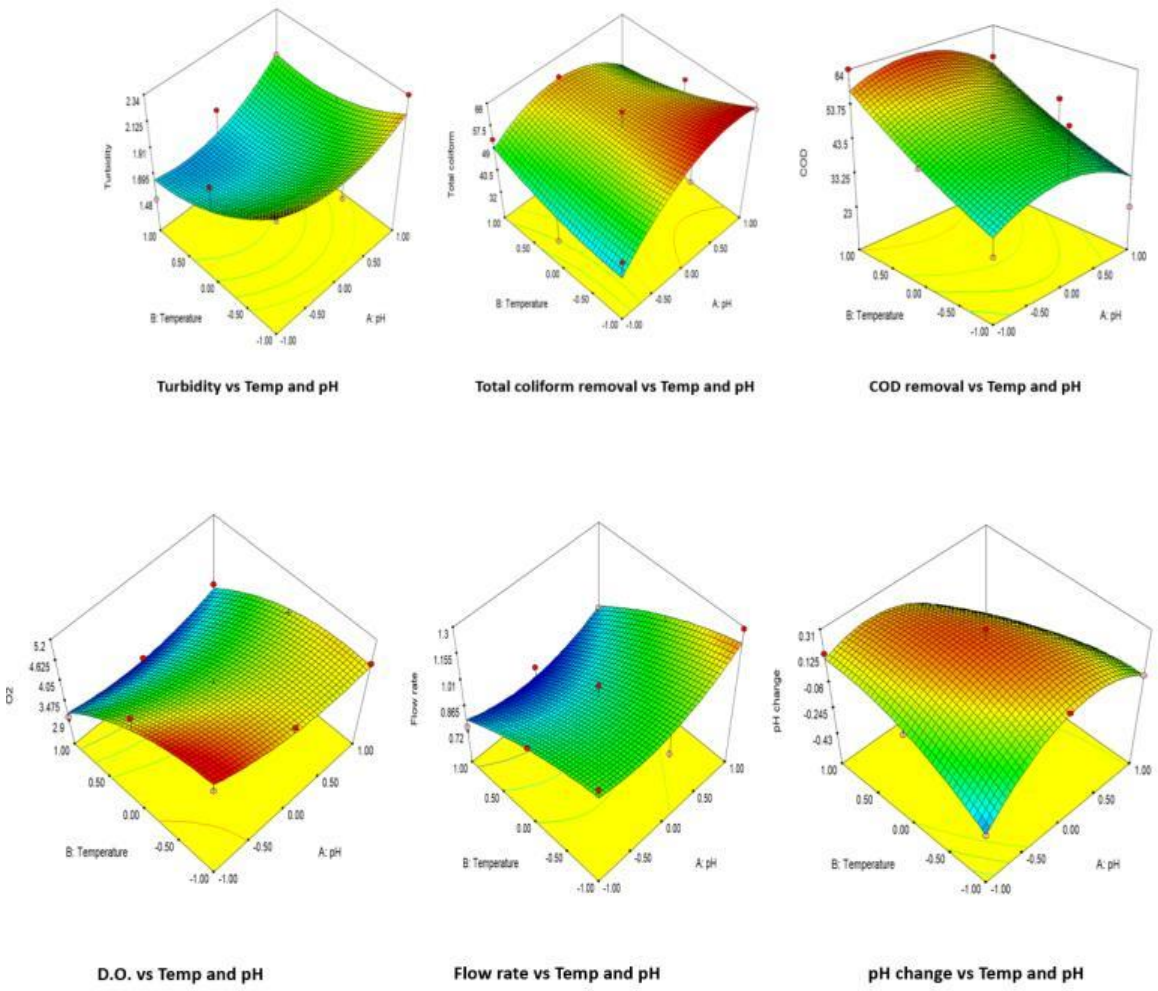

Figure C4: Response surface methodology for all the models studied to optimize the input parameters

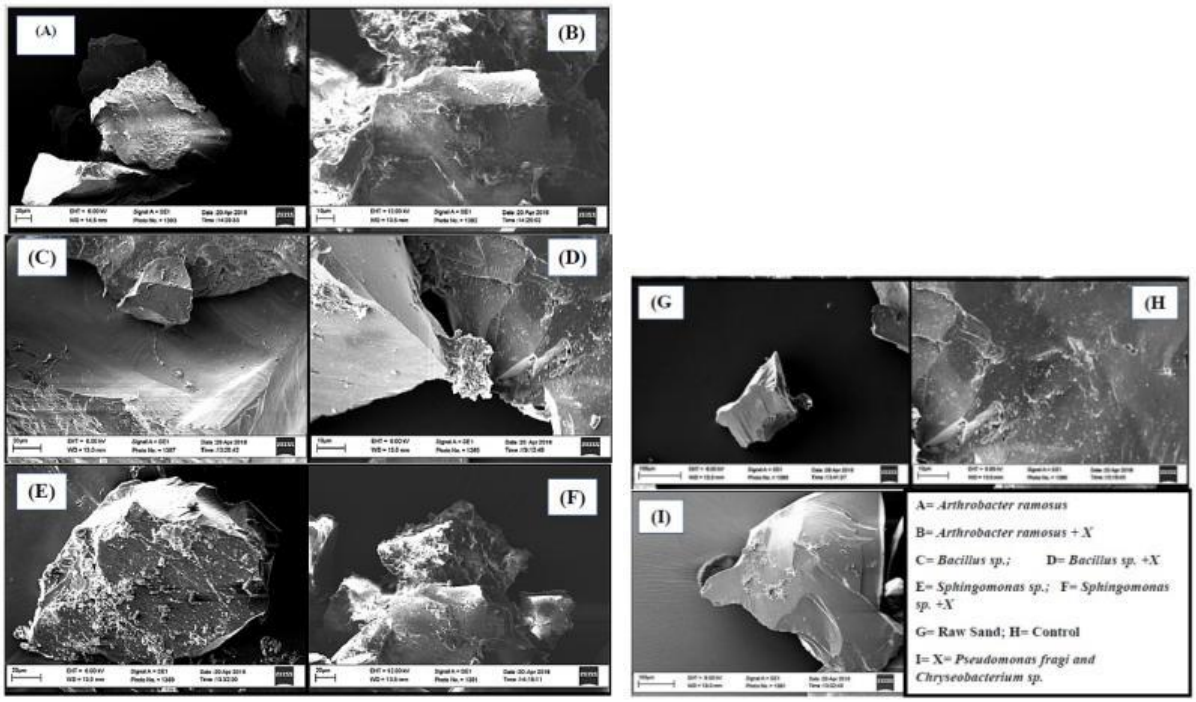

Figure C5: Scanning electron microscope (SEM) image of raw sand particle (G) and when bacterial attachment occurred (description in inset)

Table C1: Various cyanotoxin analysis for the lake water collected

Sample	CYN	ANA-a	[Asp^3]MC-RR	MC-RR	MC-YR	MC-HtyR	MC-LR	[Asp^3]MC-RR	MC-HiIR	MC-WR	MC-LA	MC-LY
Sample 1 (July 2017)	<LOD	<LOD	<LOD	<LOD	<LOD	<LOD	34.3	<LOD	<LOD	<LOD	<LOD	<LOD
Sample 2 (August 2017)	<LOD	<LOD	<LOD	<LOD	<LOD	<LOD	50.7	<LOD	<LOD	131.8	<LOD	<LOD

Units: ng/L

APPENDIX D

Table D1: MC-LR assay to break the deadlock between screening of A+X and S+X for all the materials

MC-LR assay results	SM17		SM27		SM37		
		Mean Absorbance	Std dev	Mean Absorbance	Std dev	Mean Absorbance	Std dev
A+X		3.451	0.212	3.212	0.043	3.653	0.346
B+X		2.376	0.321	2.764	0.176	2.876	0.541
S+X		2.987	0.117	3.411	0.227	3.112	0.219

SM17, SM27 and SM37 indicates different material viz. Deinking sludge, Hemp fiber and Pulp and paper waste whose toxicity assay was reported after 7 days.

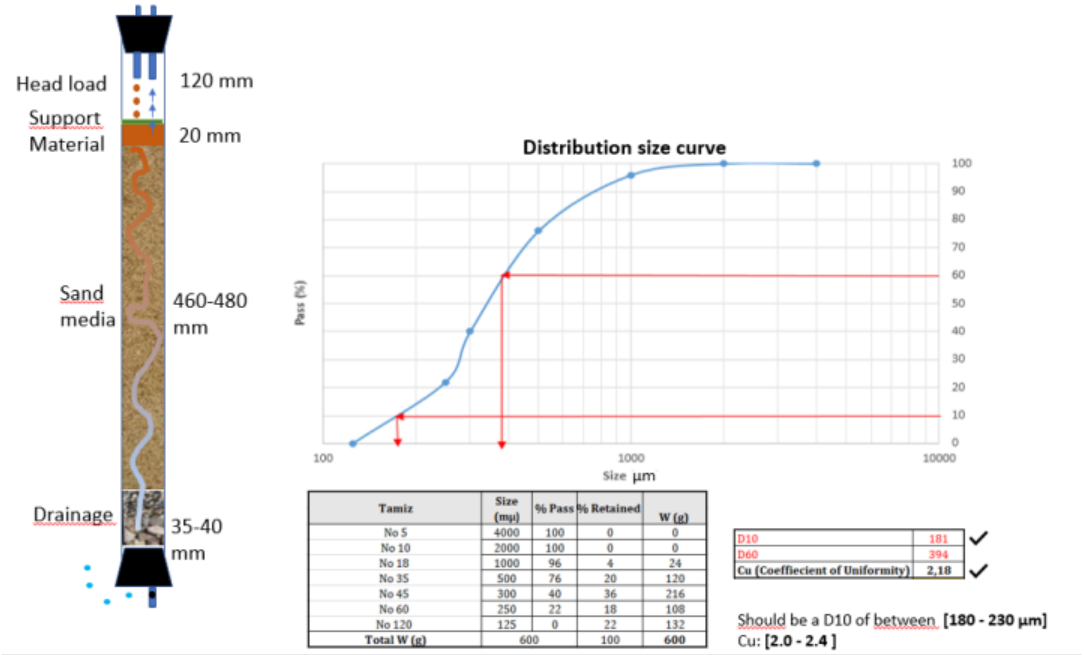

Tamiz	Size (mµ)	% Pass	% Retained	W (g)
No 5	4000	100	0	0
No 10	2000	100	0	0
No 18	1000	96	4	24
No 35	500	76	20	120
No 45	300	40	36	216
No 60	250	22	18	108
No 120	125	0	22	132
Total W (g)		600	100	600

D10	181
D60	394
Cu (Coeffiecient of Uniformity)	2,18

Figure D1: a) Sand filter column dimensions and other details b) Grain-size distribution curve obtained for the sand media used in the filter column

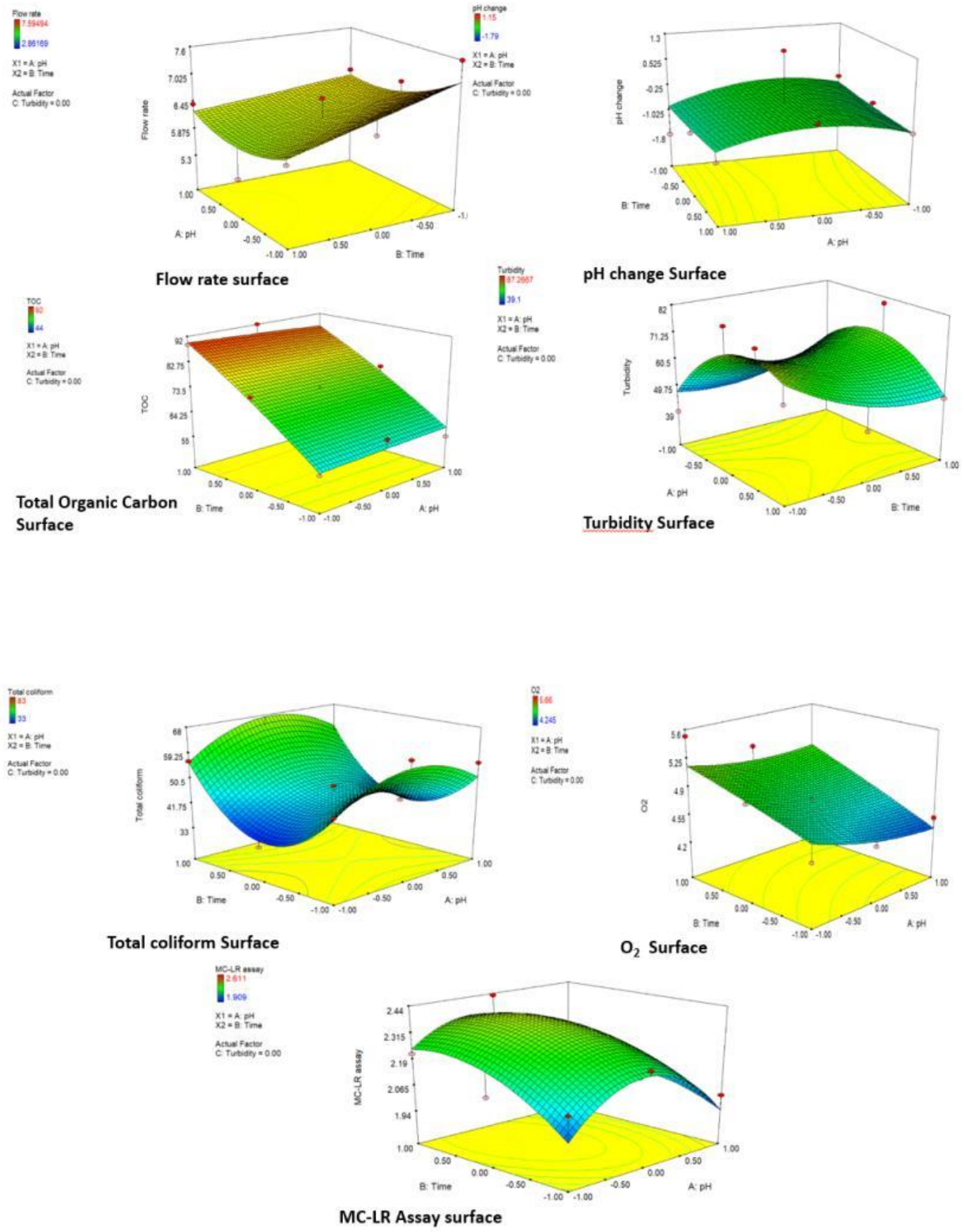

Figure D2: Response surface methodology images for the output variables (written alongside each figure/graph)

APPENDIX E

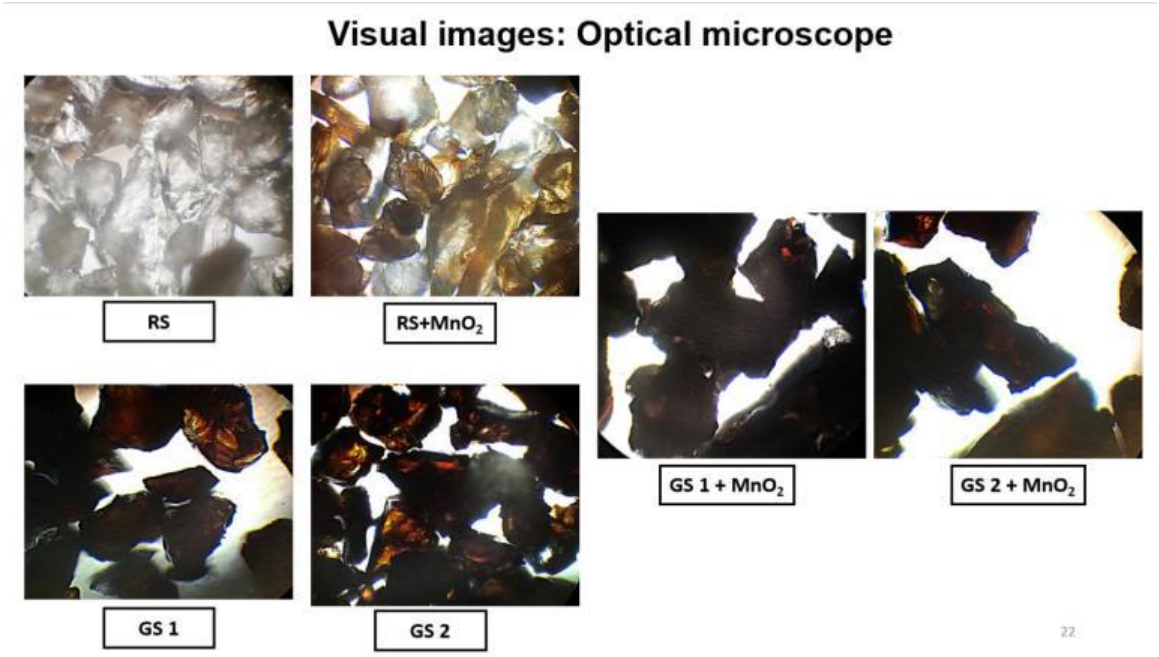

Figure E1: View of various sand composites under compound microscope

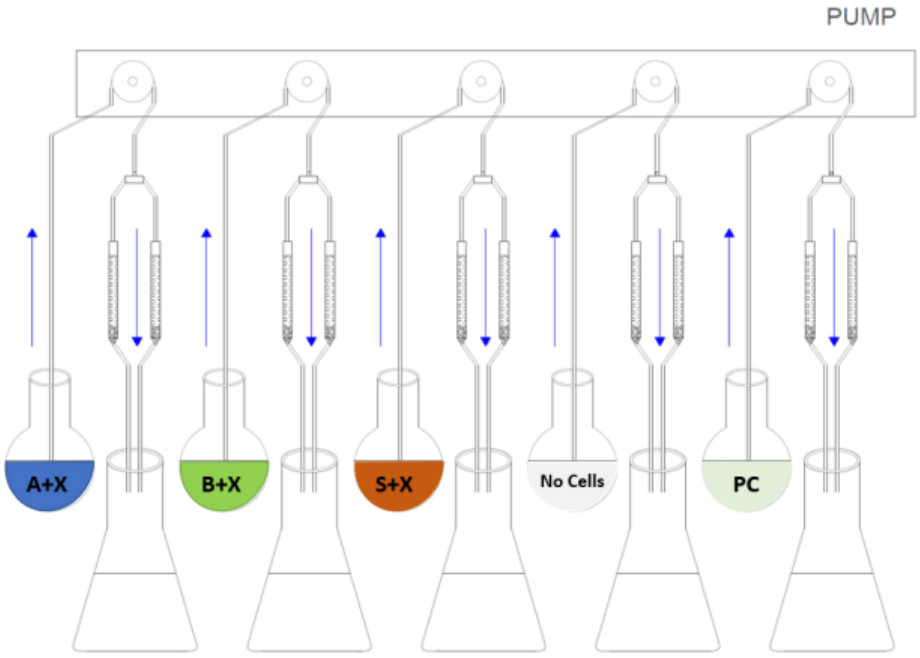

Figure E2: Schematic representation of the arrangement for studying the CV and MTT assay experiment for the quantification of the biofilm

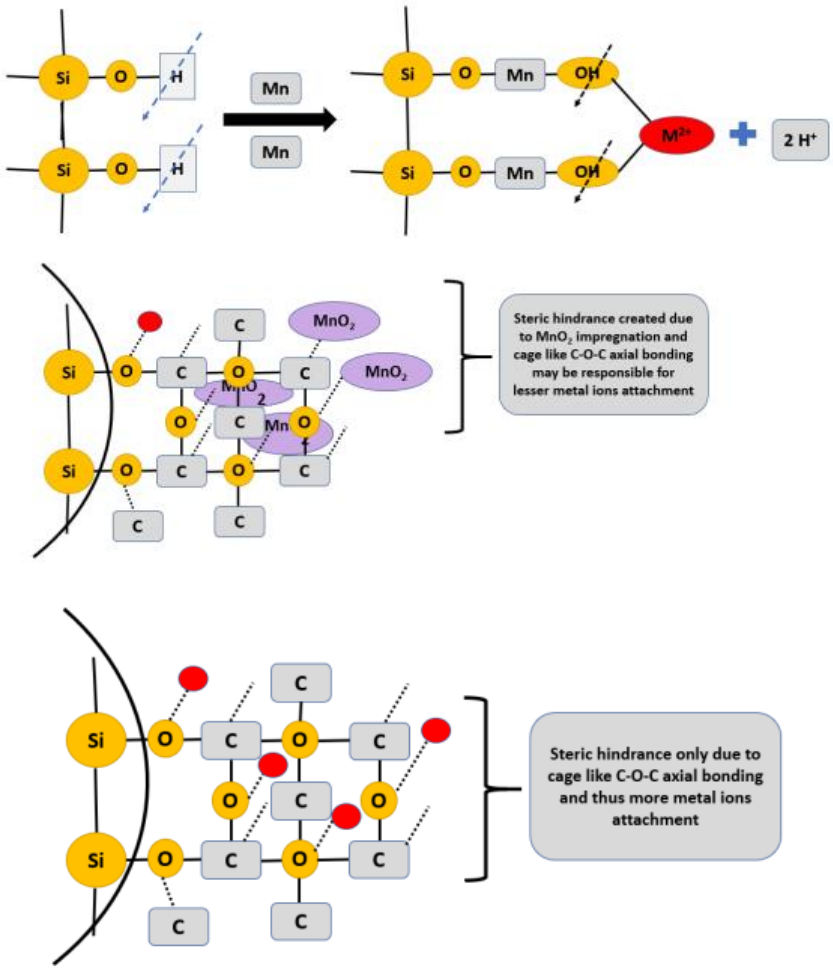

Figure E3: Metal adsorption proposed mechanism for different cases

Table A1: MC-LR results

	RS	RSMN	GS1	GS2	GS1M	GS2M
Cycle 1	30.68	33.86	17.41	13.34	20.85	21.99
Cycle 2	25.01	15.07	11.7	18.06	14.54	23.88
Cycle 3	24.12	15.62	14.98	13.70	12.80	16.42
Cycle 4	17.58	15.56	9.34	11.51	10.32	15.59
Cycle 5	24.56	15.72	6.77	9.67	7.316	9.07
Average	24.39	19.17	12.04	13.26	13.16	17.39
Std dev.	4.15	7.35	3.81	2.80	4.54	5.22
Percent removal	59.34	68.04	79.92	77.89	78.05	71.00
Cycle 7	24.48	-0.11241	14.25	7.063	1.9	-0.11241
Cycle 8	16.71	15.22	8.18	9.10	1.9	7.49
Cycle 9	27.15	14.4	0	10.1	1.9	8.06
Cycle 10	7.13	11.2	0	19.6	1.9	1.44
Cycle 11	24.8	13.71	0	13.74	1.9	11.91
Cycle 12	14.62	26	0	5.204	1.9	6.87

	RS	RSMN	GS1	GS2	GS1M	GS2M
Average	19.15192	13.40304	3.663391	10.80793	1.9	5.944337
Std dev.	7.014461	7.644106	5.619947	4.741268	1	4.090336
Percent removal	68.08014	77.6616	93.89435	81.98678	96.83333	90.09277

Table E2: Correlation matrix for the stage 'a' filter operation

Correlation Matrix

	NH3	NO2	NO3	Total coliform	Turbidity	Mg	Cu	Fe	TOC	MC-LR
NH3	1	0.87102	0.94457	0.71093	0.65479	0.096	-0.2336	0.63452	0.8363	0.79105
NO2	0.87102	1	0.88991	0.72111	0.72444	-0.05527	-0.01096	0.5114	0.86325	0.69728
NO3	0.94457	0.88991	1	0.89942	0.84629	0.00843	-0.29989	0.44951	0.90354	0.88666
Total coliform	0.71093	0.72111	0.89942	1	0.95904	-0.04937	-0.34024	0.145	0.80181	0.89764
Turbidity	0.65479	0.72444	0.84629	0.95904	1	0.16253	-0.07821	0.27918	0.6722	0.92212
Mg	0.096	-0.05527	0.00843	-0.04937	0.16253	1	0.62957	0.7266	-0.40611	0.3452
Cu	-0.2336	-0.01096	-0.29989	-0.34024	-0.07821	0.62957	1	0.46065	-0.50813	-0.07655
Fe	0.63452	0.5114	0.44951	0.145	0.27918	0.7266	0.46065	1	0.15453	0.49537
TOC	0.8363	0.86325	0.90354	0.80181	0.6722	-0.40611	-0.50813	0.15453	1	0.62801
MC-LR	0.79105	0.69728	0.88666	0.89764	0.92212	0.3452	-0.07655	0.49537	0.62801	1

Table E3: Correlation matrix for stage 'c' filter operation

Correlation Matrix

	NH3	NO2	NO3	Total coliform	Turbidity	Mg	Cu	Fe	MC-LR	TOC
NH3	1	0.39693	0.74294	0.64713	0.77414	0.65499	0.11124	0.74368	0.61594	0.7625
NO2	0.39693	1	0.79533	0.76296	0.74094	0.08955	0.37502	0.27361	0.94916	0.79472
NO3	0.74294	0.79533	1	0.96755	0.88656	0.26217	0.05497	0.33435	0.88931	0.99091
Total coliform	0.64713	0.76296	0.96755	1	0.80688	0.07203	-0.1382	0.16775	0.86445	0.97871
Turbidity	0.77414	0.74094	0.88656	0.80688	1	0.606	0.38739	0.64589	0.78465	0.88782
Mg	0.65499	0.08955	0.26217	0.07203	0.606	1	0.65226	0.92415	0.13578	0.24855
Cu	0.11124	0.37502	0.05497	-0.1382	0.38739	0.65226	1	0.64754	0.20335	0.01663
Fe	0.74368	0.27361	0.33435	0.16775	0.64589	0.92415	0.64754	1	0.35303	0.35612
MC-LR	0.61594	0.94916	0.88931	0.86445	0.78465	0.13578	0.20335	0.35303	1	0.90464
TOC	0.7625	0.79472	0.99091	0.97871	0.88782	0.24855	0.01663	0.35612	0.90464	1

APPENDIX F

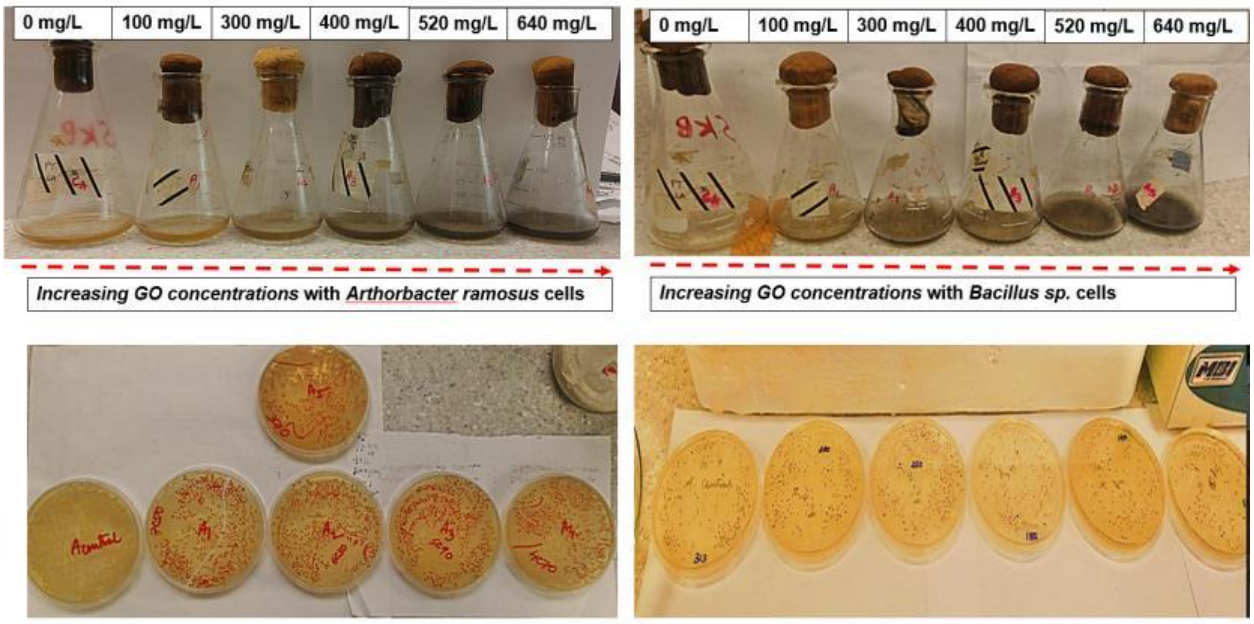

Figure F1: GO and rGO antibacterial experiment at various dose.

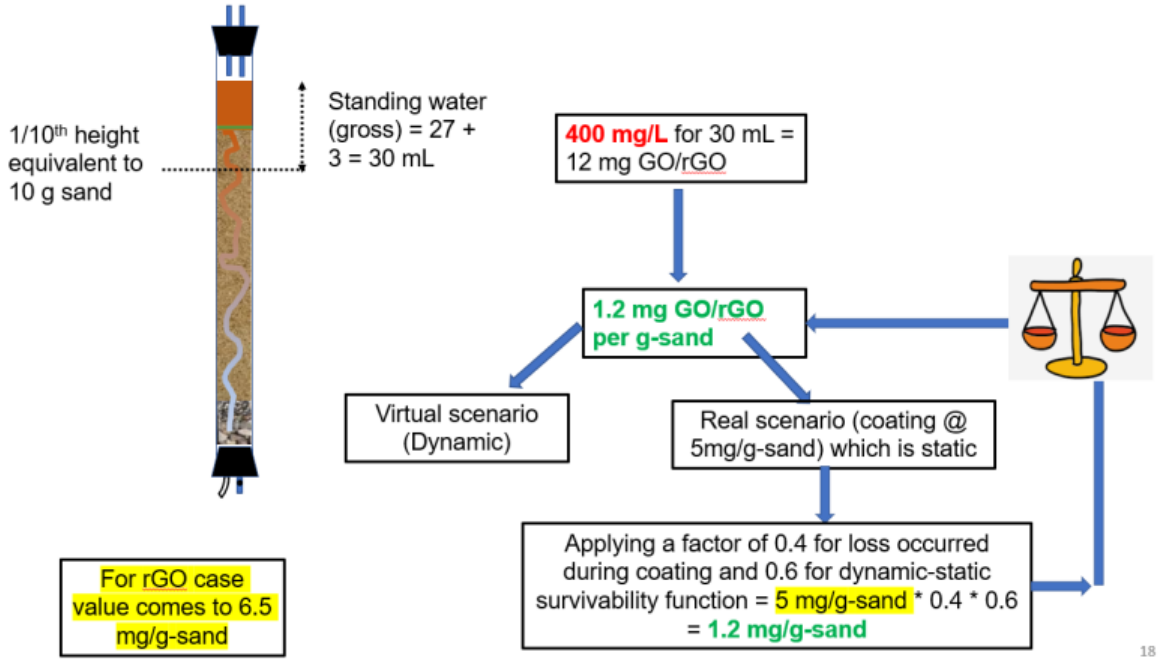

Figure F2: Static-dynamic explanation schematic for the dose of GO/rGO taken

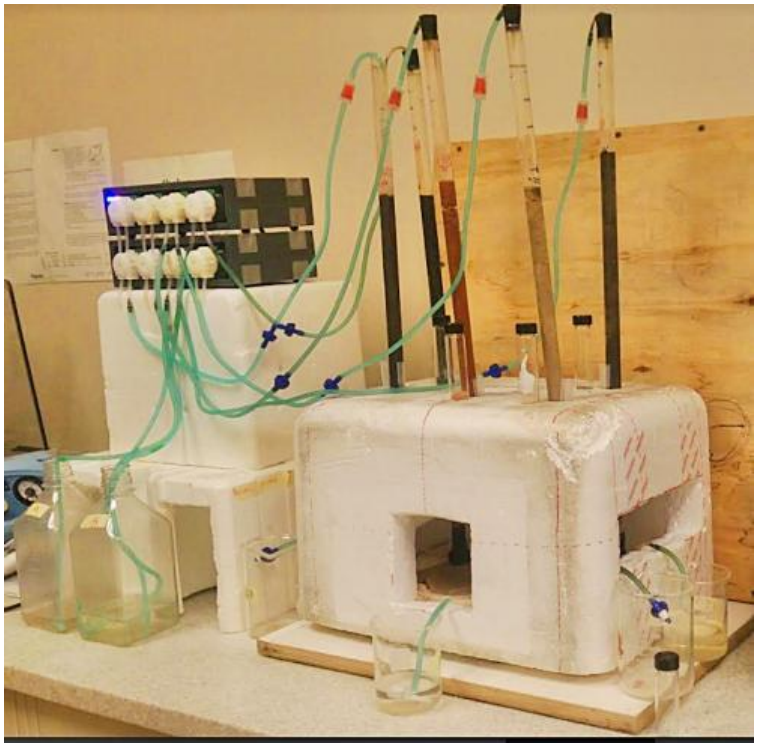

Figure F3: Set-up for the filter operation at all the three stages.

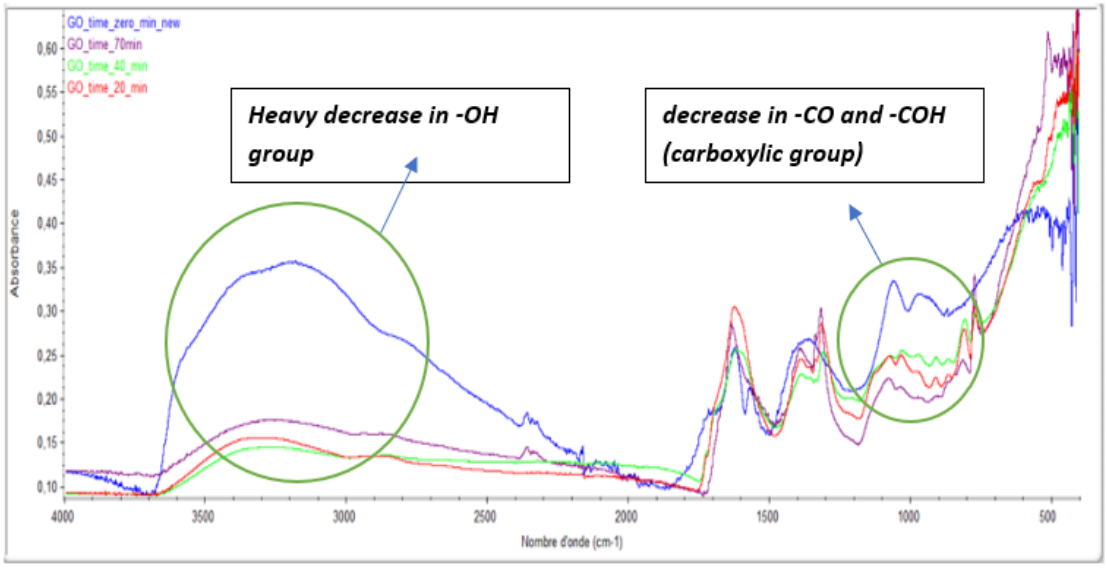

Figure F4: FT-IR spectrogram for the rGO at various temperature: 20, 40 and 70 degree Celsius.

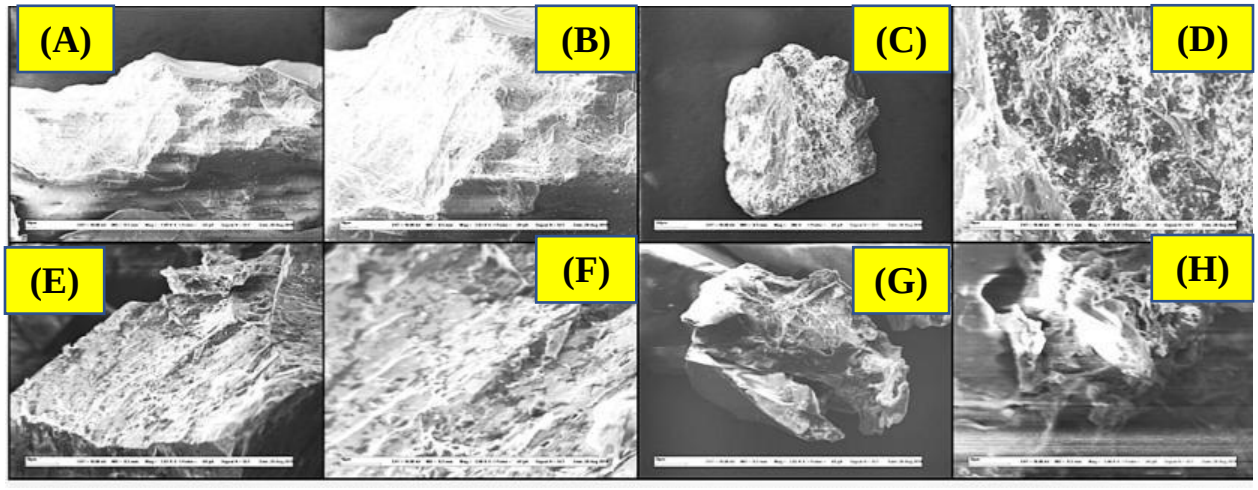

Figure F5: (A), (C), (E) and (G) are the zoom out image for Fe-coated sand, GO-coated sand, rGO-coated sand, and FeGO-coated sand, respectively while Figure Sx: (B), (D), (F) and (H) are the zoom in image for Fe-coated sand, GO-coated sand, rGO-coated sand, and FeGO-coated sand.

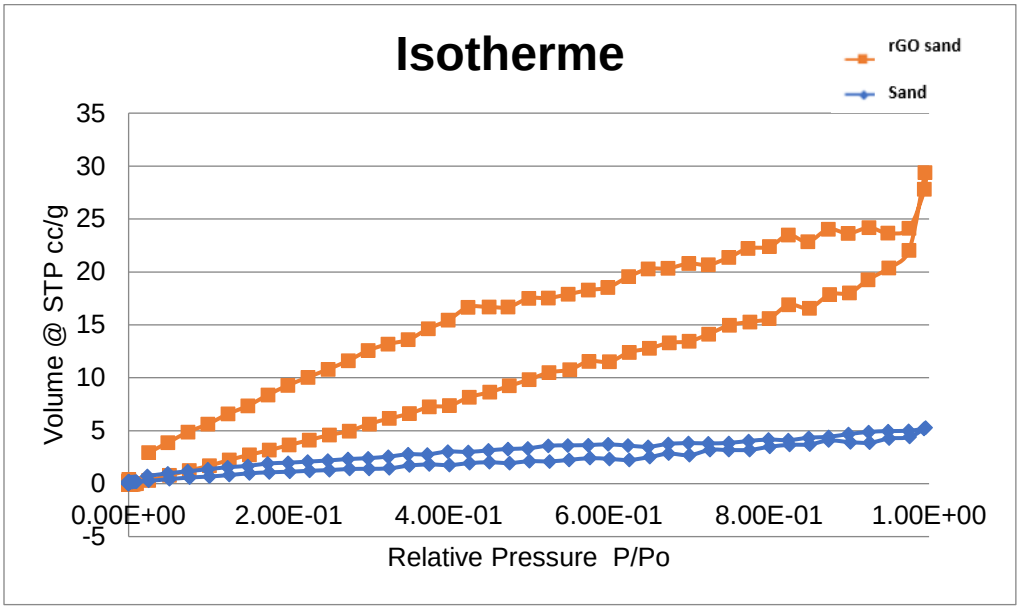

Figure F6: BET isotherm for GO-coated sand (orange) and uncoated sand (blue)

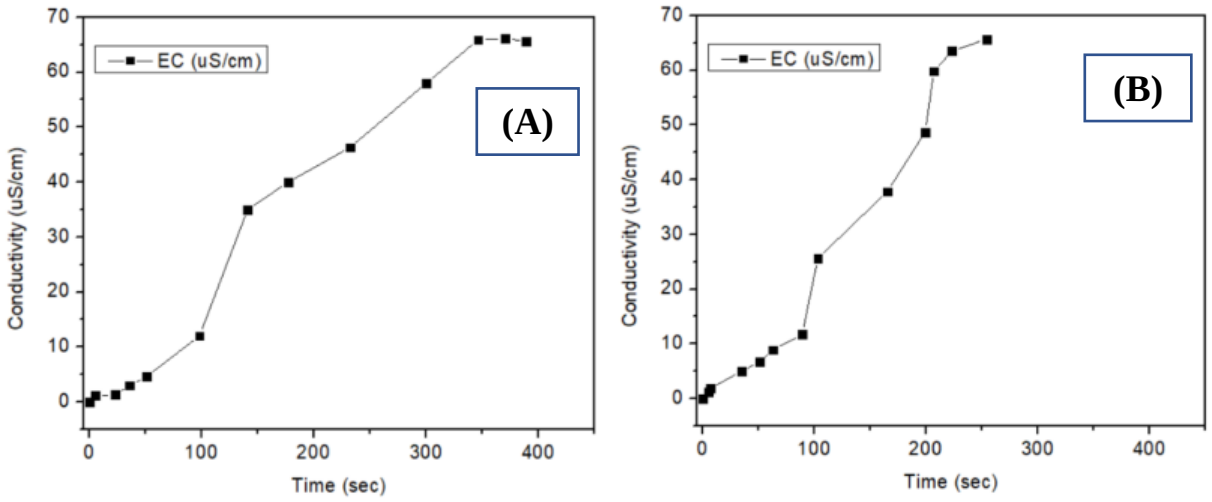

Figure F7: Conductivity vs time relationship to determine the Morrill dispersion index of the A) Bench scale filter, B) scale-up filter column